Modelling the Effects of Vegetation Change on Stormflow Hydrology

Timothy John Acton Davie

Department of Geography

A thesis submitted to the University of Bristol in accordance with the requirements of the degree of Ph.D. in the Faculty of Science.

January 1993

ABSTRACT

A study into the effects of vegetation change (particularly afforestation and reforestation) on the hydrology of an area requires a predictive investigative method. This is because empirical studies require a long time period to collate the necessary data and the results cannot be transferred to a remote site with any confidence. Physically based, distributed hydrological modelling offers a predictive capability but the use of effective parameters and lack of verification and validation casts doubts on the ability of the current generation of these models to be used in applications.

In this thesis a new modelling scheme is developed that focuses directly on simulating the effects of afforestation on the storm event hydrology of small catchments in humid temperate regions. A mixed conceptual/physically based model (*VSAS4*), is developed to act as the hydrological base model. In order to parameterise the change in vegetation for *VSAS4* a separate, pre-processing, forest growth model is developed. This model is a distance dependent, individual tree based, forest growth simulator. The combination of *VSAS4* and the forest growth model is given the name *LUCAS* (Land Use Change, Afforestation, Simulator).

Testing of *LUCAS* is carried out with verification and validation. The primary aim of these was to assess the worth of the scheme and highlight areas for future research. The difficulty of verifying a complex modelling scheme such as *LUCAS* has led to the use of a scaled down sensitivity analysis. This is designed to test the schemes robustness and the influence of forest growth on the *VSAS4* simulations. The forest growth model is verified and validated separately as an independent predictor of forest growth.

The lack of a United Kingdom hydrological data set that spans the period of a forest growth on a catchment has led to only a limited validation of the scheme. The Tanllwyth catchment in Mid Wales was adjudged to be the best available (from a choice of four sites). The scheme cannot be considered a valid predictor of the effects of vegetation change on storm hydrology in humid temperate regions due to the lack of a full data set but the results suggest it cannot be considered invalid. The assessment of *LUCAS* as a predictor of the effects of vegetation change on storm event hydrology indicates that it has considerable potential but it is not able to be used directly in applications without further development.

The validation of *LUCAS* using hydrograph reproduction and hypothetical scenarios has highlighted several avenues for future research within the study of the effects of vegetation change on stormflow hydrology. These are: the role of canopy closure in vegetation change; the need for soil water flow equations that account for more than just soil matrix flow; and the development of a probabilistic framework so that modelling schemes such as *LUCAS* can be used in applications without full verification and validation.

ACKNOWLEDGEMENTS

I am grateful to many people who have helped and encouraged me with this thesis, especially the following:

- Professor Malcolm Anderson for supervision and guidance
- Staff at the Plynlimon Research Station (Institute of Hydrology) and especially Jim Hudson for freely providing much of the data used in chapter eight
- The University of Bristol for providing the University Scholarship that has enabled me to study here
- Postgraduates and staff in the Department of Geography for much encouragement and help with computing and other problems
- Above all I thank Chris for love, understanding, and considerable encouragement over the past three years and God, the source of all inspiration and wisdom. Thank you both once again for everything

MEMORANDUM

This thesis is the original work of the candidate except where acknowledgement is given and it has not been submitted for a higher degree in this or in any other University

T.J.A. Davie
January 1993

SUMMARY OF CONTENTS

DETAILED TABLE OF CONTENTS

LIST OF TABLES

LIST OF FIGURES

LIST OF SYMBOLS

Symbol	Definition	Units
A_t	Area of triangle	m^2
a	Drainage coefficient	
$Bgap_t$	Gap area between crowns in a triangle *t*	m^2
b	Drainage coefficient	s^{-1}
CC_t	Crown cover excluding overlapping per triangle *t*	m^2
C_l	Storage capacity of triangle layer *l*	m
CPA_{it}	Crown projected area of tree *i* in triangle *t*	m^2
D	Length of segment/subsegment	m
D_l	Drainage from triangle layer *l*	m^{s-1}
dbh	Diameter of tree trunk measured at breast height	m
d_n	Distance from stream to increment *n*	m
E	Error	%
E_l	Evaporation from leaf layer	m
E_p	Potential evaporation	m
e	Exponential function	
F_i	Input parameter	
F_o	Model output	
f_t	Free throughfall coefficient per triangle *t*	
$G(\theta)$	Extinction function for the leaf angle distribution	
g	Growth ratio for potential tree growth	
h_t	Tree height	m
h_{max}	Maximum tree height	m
$K(\theta)$	Unsaturated hydraulic conductivity	m^{s-1}
K_{sat}	Saturated hydraulic conductivity	m^{s-1}
k	Proportion of maximum potential tree size	
LA_i	Leaf area of tree *i*	m^2
LAI_i	Leaf area index of tree *i*	
LAI_t	Leaf area index of triangle *t*	
N	Total number of increments in a segment/subsegment	
P'_n	Probability of a raindrop encountering *n* layers in a triangle	
P_i	Proportion of subject tree (i) crown projected area overlapped by the ZOI of tree *j*	
p_i	Proportion of tree crown *i* generating stemflow	
p_{it}	Proportion of tree crown *i* generating stemflow in triangle *t*	

Q	Rate of soil water flow	$m^3 s^{-1}$
Q_l	Input water rate for layer l minus the evaporation rate	m
q	Soil water velocity	ms^{-1}
S	Sensitivity	
S_l	Storage in triangle layer l	mm
SAI	Stem area index (see LAI for subscript notation)	
t	Time	s
V	Volume	m^{-3}
Wgap	Within crown gap area	m^2
γ	Poisson distribution weighting factor	
η	Amount of interference from neighbouring trees	
θ	Soil moisture content	$m^3 m^{-3}$
θ_{sat}	Saturated soil moisture content (porosity)	$m^3 m^{-3}$
ψ	Soil suction	m

CHAPTER 1

INTRODUCTION

The question of how a hydrological regime is altered by land use change is one that hydrologists have attempted to answer for many years. It is important for land users and planners to understand the likely effects of a proposed change in land use so that the full implications of the change can be considered and some form of cost-benefit analysis performed.

The hydrological implications of some changes in land use, and vegetation change in particular, have been understood for a considerable length of time. In the UK pioneering work by Law (1956) provided some of the first empirical evidence that a forest canopy consumes greater quantities of water than grassland and that this can be carried through to show the effects on a total catchment water balance. Since then numerous studies around the world have highlighted the critical role of vegetation within the water balance of catchments (94 of these are summarised by Bosch & Hewlett (1982)) and more detailed studies have investigated the hydrological processes contributing to these catchment scale changes (e.g. Calder & Wright (1986)). All of these studies have confirmed the important role that vegetation plays in controlling processes within the hydrological cycle but there is little consensus on actual amounts of change that could be expected for a given amount of land use change.

In general terms a large canopy (e.g. forest) causes a greater interception of rainfall, some of which may be returned to the atmosphere as interception loss (or wet leaf evaporation). When water supply is not limited forest transpiration rates (dry leaf evaporation) are similar, if not lower, than pasture and arable crops, however the deeper rooting system of larger plants give them an ability to obtain water for transpiration that smaller plants cannot. The combination of wet and dry leaf evaporation (also termed evapotranspiration) is often higher for a forested area than for a smaller vegetation cover which can lead to lower stream flows from a forested catchment. There are complicating factors though which can lead to a negative feedback effect. An example is that of fog interception by a canopy with high aerodynamic roughness, which causes greater water yield from forested area where fog is an important precipitation component. This has been illustrated by the series of studies at the Bull run municipal watershed in Oregon (e.g. Ingwersen (1985)).

Added to the complicating factor such as fog interception is the variation in hydrological regimes at different sites. The different hydrological regimes for various regions means that in some circumstances a process such as interception may be critical

(such as found by Stewart (1977) for mid Wales) while in others it may be minor compared to fog interception (e.g. Ingwersen (1985)). The inter-relationship of processes and the difference in hydrological regimes led Bosch & Hewlett (1982) to conclude from their world-wide review of vegetation change experiments that only direction and approximate magnitude of change in water yield can be estimated from the combined results, as the variation in streamflow change with increasing amounts of vegetation change is too great to derive a direct relationship.

The lack of a direct relationship between the degree of alteration in forest cover and change in water yield for a catchment means that there is no easily derivable answer to the question posed by land users and planners as to how the hydrological regime may alter with a vegetation change at a given site. Consequently an individual study needs to be carried out to ascertain the hydrological implications of a vegetation change for the site. This thesis is concerned with developing a new framework for an investigative study into the effects of vegetation change on hydrology. After further defining the type of vegetation change to be studied the remainder of this chapter is concerned with identifying possible forms that this investigative framework can take.

1.1 Forms of vegetation change

In recent years the vegetation change that has received the most world-wide attention has been deforestation, but just as important is the role of afforestation where the changes may be less dramatic but still of a similar degree. In their review of catchment experiments investigating the effects on water yield of vegetation change Bosch & Hewlett (1982) report only 12 which were concerned with afforestation (or reforestation). In the more recent review of 62 experiments investigating the effects of vegetation change on storm flows, Son (1990) found only 5 which were monitoring afforestation or reforestation.

The lack of research into implications of long term† vegetation change does not mean that it is an irrelevant issue. A good example of the importance of the consideration of long term vegetation change can be found in current engineering design techniques based on the principles of a extreme frequency analysis (probable maximum flood and flood recurrence intervals). The principle of a probable maximum flood is that by using historical rainfall-runoff records for a catchment the relationship between rainfall and runoff (usually logarithmic) can be extrapolated to find the resultant runoff from a probable maximum storm. The size of the probable maximum storm is usually calculated as the maximum possible rainfall given the topography and usual synoptic conditions of the area.

† Long term is used to mean the time period of a forests growth i.e. between 30 and 200 *years*.

There has been considerable work done within engineering research as to the statistical validity of probable maximum floods, particularly when they are based upon a short length of rainfall-runoff records. What has not been considered is the change in runoff generating processes contributing to streamflow within the river catchment that may have occurred **during** the period of historical records i.e. the probable maximum flood concept assumes that the rainfall-runoff relationship is time invariant. If there has been a land use change then the rainfall-runoff relationship derived before or during the change are likely to be different from the relationship for the period after the change, as the runoff generating processes in areas that contribute to streamflow are likely to have altered. Where the land use change has been gradual, as in the case of afforestation, it may not be possible to detect the exact timing of the change in hydrological regime and the assumption of temporal invariancy is not reasonable, as opposed to a sudden change where the rainfall-runoff records can be separated to account for the change.

This flaw in one of the key underlying assumptions of extreme frequency analysis theory suggests that it may be a redundant concept with regard to catchments that have undergone a vegetation (or any land use) change. This means that engineering design may have to devise a new method of predicting the probable maximum flood that takes into account the past, present, and future land use changes within a river catchment. This highlights the importance of long term vegetation change as an important hydrological issue to be investigated.

It is ironic that the early empirical work on vegetation change of Law (1956) was concerned with afforestation but most of the work that has followed has been investigation of deforestation. This lack of data on the role of afforestation can be attributed to several factors:

- The long time scale required for field investigation (and consequent expense)
- The lack of suitable means of investigation other than empirical measurement
- The idea that an understanding of deforestation is necessary for an understanding of afforestation
- The lack of perception of afforestation as an important issue (as opposed to the extremely visible deforestation)

All of these factors have their own part to play in the lack of investigation into long term vegetation change but the first two provide the largest reasons in themselves. Whatever form an empirical monitoring of the effects of afforestation takes (see section 1.2.1) it is required to be set up and maintained for a period of between 30 and 200 *years* whereas a full study of deforestation effects could produce adequate results from only 5 to 30 *years*

monitoring. Although the deforestation monitoring study is still a large undertaking it is nowhere near the scale of an afforestation study which would normally span beyond the working life of a single researcher.

The idea that an understanding of deforestation is necessary for an understanding of afforestation is in part a response to the first two factors. If it is difficult to investigate afforestation then a sensible approach is to research a similar issue that is easier to study. This is a valid response and the generalisations of the review by Bosch & Hewlett (1982) can be applied in reverse for long term vegetation change but the conclusion, that no universal generalities apply, is also appropriate, leading to the need for individual studies into the effects of afforestation on the hydrological regime of a catchment. The difficulty with applying results from deforestation studies to afforestation is that the former represents an abrupt change from mature canopy to no canopy with nothing in between whereas afforestation is a continuous gradual change. The final point, that afforestation is not as visible a phenomena as deforestation, may be important for public perception and therefore public funding but cannot be put forward as a serious reason for not researching long term vegetation change.

Within the United Kingdom the replacement of moorland and upland pasture with coniferous forests has become an important issue over the last 2-3 decades, particularly in Scotland and Wales where extensive areas have undergone this form of land use change. This afforestation is important especially where the plantations are not considered native flora as the vegetation change is imposing hydrological conditions that have not occurred previously in the region. The effects of afforestation on many aspects of the hydrological regime is an important interest of the downstream users of the water and consequently considerable effort has been put into studying its influence particularly with regard to water quantity and quality from the afforested areas.

Although water quality is not a completely separate matter from water quantity, to investigate them both at the same time requires an extremely large scope of study. Any changes in water quality that may result from a land use change is a very important hydrological issue to consider but this thesis concentrates on looking at changes in water **quantity** that result from vegetation change. Within the field of water quantity this thesis concentrates on the impacts of long term vegetation change on **storm events in humid temperate environments** (in Great Britain in particular).

This thesis is concerned with developing a new framework for investigating the effects of long term vegetation change (afforestation and reforestation) on stormflow hydrology of humid temperate regions. Having established the need for individual investigative studies into the effects of long term vegetation change on hydrology and considered the importance of afforestation as a hydrological issue, the following section describes the two methods available for this kind of study.

1.2 Methods of investigating vegetation change

There are two methods of researching into the hydrological impact of vegetation change: field monitoring; or a numerical modelling study. The techniques are not restricted to purely vegetation change, they can be used for a study of any land use change but are discussed in the remainder of this section with direct reference to vegetation change.

1.2.1 Field monitoring

The most common method of monitoring the hydrological effects of a change in land use is to use a paired catchment study. A paired catchment study is essentially the same as any scientific paired experimental study, it is a field investigation of the effects of some change on a study catchment, with another study catchment kept as a control. The normal procedure is to choose two catchments of similar size, topography, and any other relevant feature (e.g. underlying geology) and start to monitor the runoff occurring from both of them. The initial monitoring or calibration period (usually between 3 and 10 *years*) is the time during which the differences (or similarities) in hydrological regime between the catchments can be detected and noted. After this calibration period the land use of one of the catchments is altered while the control has no land use change and consequently acts in a similar manner to the control in any scientific experiment. Any differences in runoff response between the catchments that was not observable during the calibration period is then attributed to the effects of the land use change. As with any paired experimental technique the assumption has to made that the non-controllable inputs (e.g. climate) do not change between the initial monitoring and post land use change period, thereby moving outside the range of conditions monitored during the calibration period.

There are two variations on the paired catchment study described above. The first of these is to do away with the initial calibration period, by choosing two catchments with similar physiography but different land uses. Any differences in hydrological regime between the catchments is then attributed directly to the disparity in land use. The second variation is to monitor only one catchment over a land use change period (including the pre-change calibration period) and assume that all hydrological change that results is attributable solely to the land use change. Neither of these methods are as strictly controlled as the paired catchment experiment outlined and therefore it is more difficult to draw distinct conclusions from the results. Various constraints may force these less rigo rous forms of study to be implemented (e.g. time restraints on the land use change or lack of resources to run the project for a longer period) but the results must be viewed with an understanding of the constrained methodology at all times.

Catchment experiments using all of the above designs have been implemented for

most of this century (Bosch & Hewlett (1982) report the initiation of the first catchment experiment at Wagon Wheel Gap, Colorado, U.S.A. in 1909) and have been carried out in many places world-wide. A well planned paired catchment study can give high quality data but there are several limiting factors to their effectiveness:

- Costs to set up and run are high
- The need to be run over a long time period (especially for afforestation)
- Results are always site specific
- Processes within the catchment can normally only be inferred
- Results are retrospective.

The first two of these factors severely restrict the body of researchers capable of setting up and running a paired catchment study. As a result they are often initiated and maintained by government agencies able to afford the expense and with continuity of research staff to maintain the monitoring. The time and cost involved is realistically the most likely factor to influence a researchers choice of whether or not to proceed with a paired catchment study.

The final three limiting factors are important for the scientific details of a study that is attempting to investigate the hydrological effects of a vegetation change. The data obtained from a paired catchment study are always site specific in that it is the result of a particular set of hydrological processes occurring in a unique set of controlling conditions. General trends detected from the results may be able to be inferred as occurring elsewhere but it is dangerous to try and transfer the details of change to other sites undergoing similar vegetation change where there will be another set of unique controlling hydrological conditions. There have been two recent literature reviews that reinforce this point, that the results of a field monitoring catchment study are non-transferable. Bosch & Hewlett (1982) present a review of 94 vegetation change catchment experiments from locations world-wide and conclude that only direction and approximate magnitude of change in water yield can be estimated from the combined results, as the variation in streamflow change with increasing amounts of vegetation change is too great. Similarly Son (1990) was unable to establish definite transferable results from a summary of 43 vegetation change experiments world-wide which have concentrated on changes in storm runoff.

One of the reasons for it being impossible to transfer the results from one region to another is that all the changes in hydrological processes occurring within a catchment as a result of land use change are commonly analysed through one result, i.e. streamflow. This lumping of results means that changes in processes occurring at a scale within the catchment, and consequently the effects smaller scale changes, can only be inferred.

In a similar vein to the results of paired catchment studies being site specific and the processes lumped together, it is important to note that the results are retrospective i.e.

they tell you what has happened not what might or will happen. This is critical to an issue such as afforestation where the changes occur gradually over a long time period and a wait for retrospective results is frequently beyond the scope of a single study. In this particular case some kind of predictive† tool is required, but the shortcomings of paired catchment studies mean that the results from previous experiments are non-transferable to other sites and therefore they lack predictive ability.

A well set up paired catchment study is capable of producing, and has produced, high quality data (see Bosch & Hewlett (1982)) but the limiting factors listed above, especially the first two (cost and long time scale of monitoring), make other methods of vegetation change investigation an attractive option for any study of vegetation change. This conclusion can be taken a step further in the special case of researching the hydrological effects of long term vegetation change where it is clear that a predictive method of investigation is required and that field monitoring does not offer this possibility.

1.2.2 Numerical modelling

A numerical modelling study attempts to eliminate the need for field monitoring by representing some or all of the hydrological processes occurring within a catchment as a series of mathematical relationships which can be altered to simulate a change in land use. It is based on the knowledge that the catchment output is measured as a series of numerical data (e.g. streamflow values with time) which in turn can be numerically simulated. The various process equations are usually programmed onto a computer and a model structure ascertained so that the processes interact with each other in a method that is akin to a conceptual knowledge of the catchment under study. Solving of the relationships for given inputs (normally climatological variables) gives the necessary output (e.g. streamflow) under the simulated conditions. Vegetation change can be incorporated into the model simulations by either altering the input parameters for the governing equations or else by defining a new set of relationships altogether for the altered circumstances.

All numerical models are simplifications of reality, an attempt to explain the hydrological cycle in a mathematical form, albeit with different levels of simplicity, that as mathematics stands at present cannot hope to fully explain the heterogeneity of hydrological processes and scale as they are known to occur. Consequently models selectively exaggerate the fundamental aspects of a system at the expense of incidental detail, the main aim of hydrological modelling being to assess the outputs from a hydrological system in either real time (forecasting) or with no specific time reference (prediction) (Anderson & Burt (1985)).

---

† The term *predictive* is used to mean a projection with no specific time reference as opposed to *forecasting* which is a projection within real time.

The different types of hydrological models have been categorised by various authors (e.g. Fleming (1979) and Anderson & Burt (1985)) into subdivisions based on their mathematical representation of processes and the scale of calculation. The traditional primary subdivision in numerical modelling strategies is between *deterministic* (where the system behaviour can be predicted precisely by the model) and *stochastic* models (where stochastic theory is used to provide a probability of a certain prediction occurring). The mathematical representation categories traditionally break down into three further groups:

- Black box models
- Conceptual models
- Physically based models.

Black box models are the simplest form of modelling strategy, lumping all hydrological processes into a single mathematical relationship. Anderson & Burt (1985) list four types of black box models commonly used in hydrology: the unit hydrograph; extreme frequency analysis; regression analysis; and real time forecasting models.

Within a *conceptual model* a small number of hydrological processes are represented using relationships that are perceived to be conceptually similar to the way a process is known to operate (often a linear or non-linear reservoir). The values of the parameters that govern these non-linear relationship are obtained through model calibration (i.e. by their adjustment until model output fits a measured data set). As such they have no physical meaning and therefore cannot be measured independently.

Each of the processes represented in a conceptual model are linked together by a central model framework that adds and subtracts the volumes of water involved and arrives at an output volume per timestep. The actual number of processes represented within the framework is restricted by the need to calibrate each of the parameters. The higher the number of parameters the greater the number of combinations that could yield exactly the same results. Consequently it is better to have a small number of parameters to calibrate, hence Beven (1989) suggests that the optimum number of parameters for a lumped conceptual model is between three and five.

A *physically based model* attempts to represent every known hydrological process by a mathematical relationship that is derived from physical laws (normally in the form of a partial differential equation). Because the equations driving the model have a physical basis the input parameters can be measured, there is no need for any form of calibration, and consequently there is no restriction on the number of input parameters. A physically based model has a central framework in the same manner as a conceptual model that links all the process representations together and then adds and subtracts the necessary volumes to arrive at an output per timestep. Because each process is calculated separately the model output can take many forms other than simple catchment streamflow such as soil

water distribution, rainfall below the canopy, and overland flow volumes for example.

The final categorisation of models is concerned with the scale of mathematical representation of the hydrological processes (only for conceptual and physically based models). This distinguishes between *lumped* modelling schemes where the hydrological processes are represented as one homogeneous unit at a single scale (normally the catchment) and *distributed* schemes where the processes are represented as being distributed throughout a catchment at a scale that accounts for the known natural heterogeneity.

The traditional categorisation described here consists of divisions which are not mutually exclusive, a modelling scheme will rarely fall completely within one category. For instance it is possible to have a modelling scheme that is mainly physically based and distributed but some processes can be represented in a simplified conceptual manner, while still being distributed. An example of this kind of mixed category model is the *VSAS* model described by Troendle (1985) which as well as having combined conceptual and physically based construction also unites stochastic and deterministic elements into a broadly deterministic structure. A second problem with the traditional categorisation is that it is often difficult to distinguish between categories e.g. how distributed is distributed and how physically based are physically based models? This kind of question has led to recent criticism of this type of categorisation by Beven (1989) on the basis that physically based, distributed models do not live up to their title and in fact should be considered as lumped conceptual models. This argument is taken further in chapter two. For the present these distinctions are maintained in order to establish the modelling need in the investigation of long term vegetation change on the basis of previous modelling studies that have utilised this traditional categorisation.

Rogers (1985) lists four points that must be incorporated by any model assessing the impacts of land use change, these can be summarised as:

- Multiple land use change within one catchment†
- Vegetation parameters independent of other catchment characteristics
- Land use change modelled to the correct spatial context
- Parameters capable of transfer over space and time.

The last of these factors is particularly important in the special case of long term vegetation change as it allows the model to become predictive which has already been identified as an important requirement. Black box models do not fulfil any of these criteria and cannot be seriously considered for any investigation of vegetation change. The slightly more complicated strategies such as conceptual models do not always have independent

† This consideration is not relevant when only one land use change is being considered, as in this study.

vegetation parameters, cannot usually model change at any scale less than the catchment, and do not have parameters capable of transfer over space and time. Rogers (1985) concludes that the four requirements listed above can only be fulfilled by physically based, distributed models precisely because the parameters are physically based and distributed. Similarly Betson *et al* (1985) suggests that for predictions of land use change impacts, models are needed which do not require prior calibration and validation, these criteria should only be able to be fulfilled by physically based modelling schemes.

Rogers (1985) lists the ability to transfer the physically based parameters over time but omits that these parameters can also be **transformed** over time. The physical basis of these parameters means that physical relationships can be used to transform them as a particular change occurs. This is particularly relevant for the investigation of long term vegetation change where the alteration of parameters as a forest grows will be significant but occur gradually.

Physically based modelling schemes offer a possible **predictive** tool to investigate the impacts of long term vegetation change. All of the five factors listed as restrictive to the use of field monitoring in the section 1.2.1 should be overcome by using this type of modelling scheme because any study using them is not bound by real time constraints and is able to represent processes in a distributed manner. This then appears to present an ideal framework to investigate the special case of the hydrological effects of long term vegetation change.

1.3 Summary

This chapter has identified the impacts of long term vegetation change (afforestation and reforestation) on the hydrology (particularly stormflows) of an area in a humid temperate environment as the issue of study for this thesis. It has been established that there is a need for individual studies to consider the hydrological impacts of this land use change for different regions as there is no direct empirical relationship that can be found between degree of change and altered streamflows despite numerous field studies. The two methods of investigation (field monitoring and numerical modelling) were reviewed and the conclusion drawn that physically based, distributed modelling offers the only feasible framework to study the impacts of long term vegetation change as it has a potential predictive ability which is lacking in field monitoring and the other modelling approaches. Consequently physically based, distributed modelling is the investigative method pursued in this thesis.

In very broad terms the aims of this study can be listed as:

- To review the requirements of a new predictive method of investigating long term vegetation change
- To develop a new predictive method of investigating long term vegetation change
- To assess the worth of the new method as an investigator of long term vegetation change.

The following chapter reviews the role of physically based, distributed modelling with respect to long term vegetation change in order to achieve the first aim above. These aims are reviewed and redefined into more detailed objectives at the end of chapter three once the research method has been fully established.

CHAPTER 2

DISTRIBUTED MODELLING OF VEGETATION CHANGE

In chapter one the conclusion was reached that in order to move away from the empirical method which does not provide the predictive investigative approach required to research long term vegetation change, it is necessary to use numerical models. Physically based, distributed modelling schemes are the only type of model to offer a possible predictive research method as the parameters are capable of transfer and transformation over space and time. This chapter critically examines this type of modelling as a possible predictive method for the study of long term vegetation change.

2.1 Critique of physically based, distributed modelling

Ever since the idea of being able to develop physically based hydrological models was first mooted in the 1960s one of the main justifications for their development has been a hoped for ability to predict the hydrological response to land use change within a catchment (e.g. Freeze & Harlan (1969)). This is because the physical basis of the models partial differential equations enable them to be used in a range of situations without calibration to find the values of the input parameters for a particular site. As there is no calibration involved simulations should be able to predict the effects of vegetation change on hydrology so long as the change in parameters with time is understood.

Since Freeze & Harlan (1969) submitted their "blueprint for a physically-based digitally-simulated hydrological response model" and following further pioneering work by Freeze (e.g. Freeze (1972)), several of these models have been constructed along the blueprint lines, most notably the Système Hydrologique Européen (*SHE*) and the Institute of Hydrology Distributed Model (*IHDM*), which have both been in operation since the early 1980s. Subsequent usage of these models have highlighted several areas of considerable concern.

The first major concern to be raised was to do with difficulties in their usage which can be examined on two fronts: the need for expert users with large scale computing facilities; and the large data set required to run the models. The need for large scale computing facilities is becoming less of a problem as computing technology advances

rapidly but these models still cannot be easily run by non-expert users which is a major limitation in their application beyond the research field. These points are not relevant criticisms when distributed models are used for research such as in this thesis and are therefore not considered any further.

The second point about the large data set required is illustrated by Abbott *et al* (1986a) who list 30 plus input parameters which should be measured within each grid element (for the *SHE* model). If the distributed nature of the *SHE* is to account for the known spatial heterogeneity of parameters then some, such as the soil physics inputs, should be measured at less than a *metre* scale and others, such as vegetation, at tens of metres at the very least. This huge requirement for input data led Anderson & Rogers (1987) to point out that even though the input parameters represent measurable properties the measurements are "at best very expensive and time-consuming to obtain, and at worst, so difficult to undertake as to be virtually impossible" (p40). It was recognised from the outset of development of these models that this was likely to be a constraining factor in the utilisation of physically based distributed models but it was hoped that remote sensing techniques would advance rapidly to overcome the problem of measuring the input parameters within every grid element (Abbott *et al* (1986b), p75). This has not occurred so that the problem still remains with any usage of a physically based, distributed hydrological model. The need for large data sets has been the cause of some simplifications in the modelling structure, the ramifications of which have led to severe criticisms which are reviewed below.

In a wide ranging analysis of physically based models and their usage Beven (1989) has three major areas of concern:

- Lumping of subgrid processes
- Effective parameter values
- Model calibration.

These three points are described separately below before some further criticism leading into an analysis on the future of physically based, distributed modelling.

Although the driving equations for these models are physically based the physics from which they are derived (usually of small scale homogeneous systems) is not necessarily at the same scale as that at which they are utilised. This means that the process representation has to be lumped and assumed homogeneous within the grid element when it is well known that in many cases this assumption does not hold. Beven (1989) uses the example of average capillary potential, and asks what this actually means, especially when the average capillary potential gradient is calculated over a very large plan area as in some *SHE* applications (e.g. grid squares of $250m$ x $250m$ in Bathurst (1986a); $1km$ x $1km$ in Dunn *et al* (1992)). Beven (1989) concludes that the current generation of physically

based, distributed models do not warrant their title and in effect are lumped conceptual models. This mirrors the concern in chapter one that the traditional categorisation of models does not hold as there are no distinct categories, just gradations from one to the other and that the true physically based, distributed model may not exist.

The size and shape of the grid mesh used within a distributed modelling scheme depends on the model used and its solving scheme, but ideally each grid element should be small enough to consider the smallest spatial heterogeneity of each hydrological process and measured input parameter. This is simply not possible as it would necessitate literally thousands of parameter measurements throughout a catchment and a grid scale that would require well beyond the current capacity of computational power to solve the partial differential equations. Because of this considerable effort has been put into developing effective parameters to account for the spatial variability of processes within the larger grid elements that are inevitably used, such as those given earlier for applications of the *SHE*. These effective parameters are not necessarily the value that would be obtained by going out and measuring the parameter at a set point but a value that represents the overall value for the grid element and one which it is hoped accounts for the known process heterogeneity. There are two weaknesses in this approach, the first is that the parameters no longer have a physical meaning and therefore cannot be transferred or transformed in space and time. The second problem, as Beven (1989) points out, is that previous studies investigating spatial variability have concluded that a consistent effective parameter value cannot be found to account for the tremendous heterogeneity observable in the field. Some recent work has gone into ways of overcoming this kind of problem through stochastic means within the overall deterministic model structure (e.g. Fawcett (1992)).

The final problem listed, that of calibration, stems from and is interrelated to the two previous shortcomings. Because these models have problems with the lumping of subgrid processes and require effective parameter values they require some form of calibration before application (e.g. Bathurst (1986a) for the *SHE*, Calver (1988) for *IHDM*). The calibration usually involves finding the values of some of the parameters that cannot be adequately estimated from field measurements by comparing measured and predicted hydrographs. This is directly opposed to the aims of developing such modelling schemes as espoused by Freeze & Harlan (1969) but is necessary for the reasons outlined above. Rogers (1985) suggests that:

> The use of calibration is not a major restriction for the use of distributed models for land use change applications, because the parameters are physically based and their values can therefore be extrapolated to other locations with considerably greater confidence than is possible with conceptual models. (p104)

This view cannot be upheld when the values of the parameters are obtained by calibration and the physical basis of the equations at the scale utilised remains questionable.

All of the above factors contribute to the view of Beven (1989) that the current generation of physically based distributed models are really lumped conceptual models and that if three to five is the optimum number of parameters for declared lumped conceptual models then the physically based models are grossly overparameterised (Beven (1989)). Despite this there is still effort being put into developing the schemes further using the current broad models as a base to tack on new routines (e.g. the sediment transfer routine described by Bathurst & O'Connell (1992) that makes *SHE-TRAN*) when in fact the original model structure is not providing a satisfactory base as it is not operating as was originally intended.

One area of physically based modelling that Beven (1989) touched on very lightly is the problems involved with model verification and validation when using these schemes. *Verification* is the process by which it is insured that the computer program actually carries out the logical processes expected of it and verifying that the model behaves as intended. *Validation* is any process designed to measure the correspondence between the model and the system under study and thus indicates the usefulness of the scheme for predictive applications (Miller *et al* 1976).

The difficulty with attempting to verify a physically based modelling scheme is that in trying to represent every hydrological process through a series of partial differential equations using a finite difference or finite element solving scheme an extremely complex network of process interactions is built up. A verification exercise often takes the form of a sensitivity analysis which tests the sensitivity of the model response to a change in input parameters. The large number of parameters and the complex interactions between them mean that a sensitivity analysis becomes a huge task that is realistically unfeasible to perform to its full extent. Consequently in studies using physically based models it has been necessary to perform limited sensitivity analyses (e.g. Bathurst (1986b)) that do not fully verify the modelling schemes.

The usual validation method (in conceptual and black box modelling studies) is to compare predicted and observed hydrographs. This is not adequate validation for a model that aims to predict the response of many different hydrological processes simultaneously as it is measuring the validity of the model based on a single process output: runoff. To fully validate a physically based scheme it would be necessary to have spatially distributed data for all the hydrological processes simulated (e.g. interception, soil moisture distribution, groundwater flow etc.) yet there is no realistic chance of obtaining this kind of data and because the field measurement techniques are not necessarily accurate it may well end up saying "more about the quality of data used, rather than confirming the model mechanisms themselves" (Anderson & Burt (1985), p10).

In previous applications of physically based models validation attempts have involved calibration of the initial boundary conditions involved within the validation (e.g. Calver (1988)). Stephenson & Freeze (1974) are very critical of this method arguing that the resultant flexibility from calibrating initial boundary conditions "ensures that satisfactory validation will be obtained" (p289). The justification given for this kind of model validation is that there are insufficient data to set up and validate physically based models, so simplifying measures have to be taken. Taking the examples of ground water models, which have the same type of problems as surface hydrology physically based distributed models, Konikow & Bredehoeft (1992) point out "accepting that one needs to calibrate a site specific ground-water model is tantamount to acknowledging the impossibility of validating such a model" (p77).

Konikow & Bredehoeft (1992) go on to suggest that because verification and validation are confusing terms and a true validation is impossible the labels should be abandoned in favour of model testing and model evaluation. These ideas are not pursued here because the terms testing and evaluation have less direct meaning than validation/verification and a change in terminology is likely to increase confusion rather than clarify the issues.

The importance of verification and validation within a traditional model development strategy is indicated in figure 2.1. This is a version of a diagram that appears in Sargent (1982) setting out the traditional framework for operations research modelling, it has been adapted to hydrological modelling by Howes (1985). The diagram shows that verification links the mathematical model to the actual programmed code while validation links the computerised model back to the hydrological system under study. When these links cannot be established the framework breaks down and it may be never possible to use the modelling system in an application on the original hydrological problem. This then presents a severe test to the usage of physically based models because it suggests that in their present state they cannot be used as investigative or application tools.

In broad terms the criticisms of physically based distributed modelling can be summarised in two statements:

- Physically based, distributed models are not what their name suggests
- Physically based, distributed modelling schemes cannot be adequately verified or validated and therefore cannot be used in applications.

Following the conclusion of chapter one that physically based modelling offers the only possible means of studying the special case of long term vegetation change, it now appears that there are considerable problems involved in their utilisation and that the current generation of models are not adequate to tackle the problem.

Although Beven (1989) is extremely critical of the physically based modelling

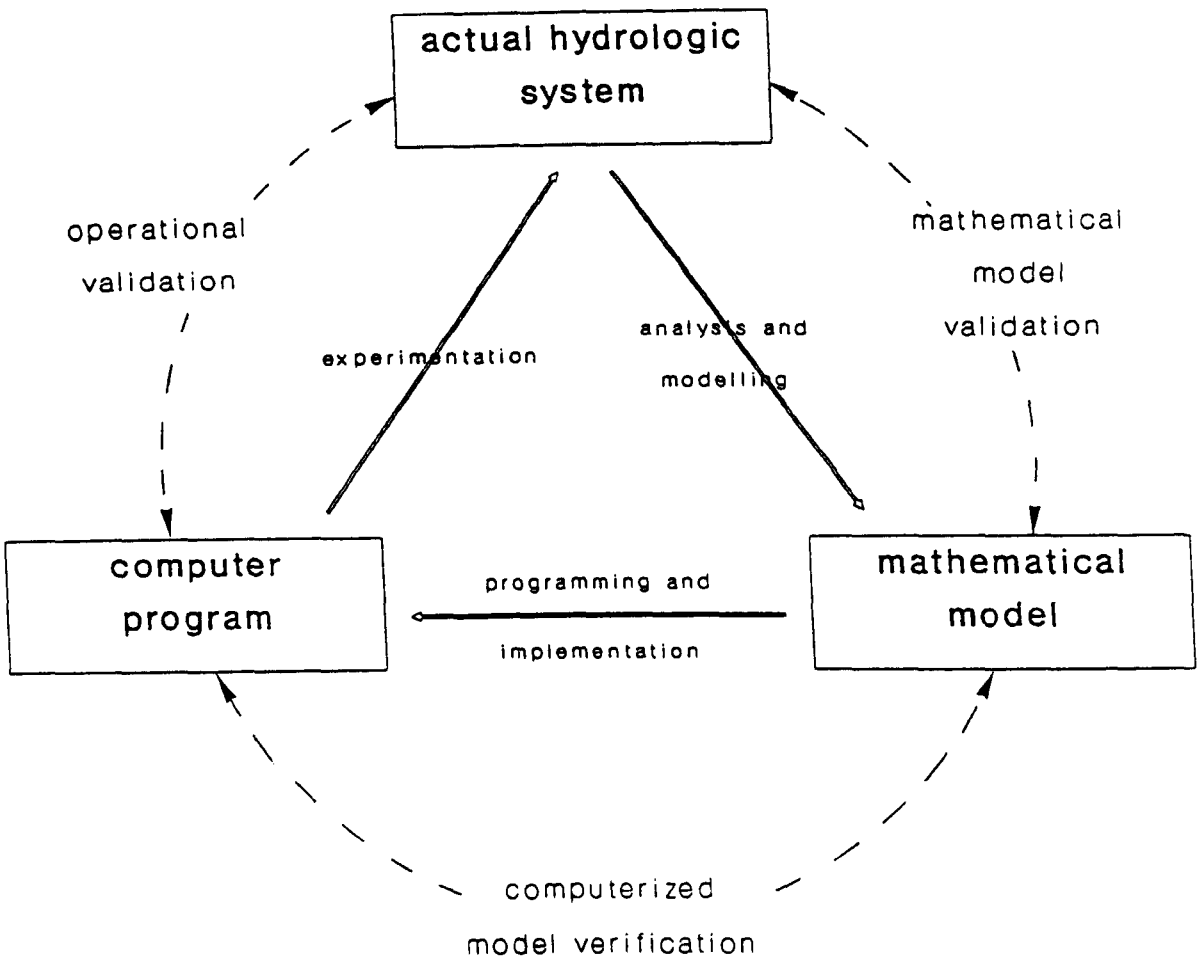

Figure 2.1: Three stage model development scheme (after Sargent (1982) and Howes (1985))

approach he does conclude "there are some hydrological problems demanding predictions which at present can only be provided by physically based models" (p168) and goes on to use the prediction of the effects of land use change as an example. This is because physically based models attempt to overcome the shortcomings of black box and lumped conceptual models and although the usage of physically based models has severe problems, it provides **the only approach available at present that should be able to make predictions beyond their calibration conditions.**

This last statement reconfirms the conclusion made at the end of chapter one that physically based, distributed modelling offers the only possible method of investigating the special case of long term vegetation change but it is obvious from this section that the current generation of physically based models have considerable problems attached with their usage. The following section takes the criticisms and introduces some ideas on the future of this type of modelling with particular reference to investigating the impacts of long term vegetation change.

2.2 Future of physically based, distributed modelling

The idea that the current generation of physically based, distributed models are in fact complicated versions of lumped conceptual models is borne out by the lumping of subgrid processes and use of effective parameter values within their structure. The use of the term physically based, distributed modelling becomes a statement of desire rather than fact i.e. it is desired that the governing equations be physically based and the processes distributed rather than they are physically based and distributed. Although it may be at first misleading it is necessary to retain the title because they are different from lumped conceptual models and crucially there are hydrological problems such as long term vegetation change which require at least some attempt at physical basis to provide predictions. The dropping of the physically based, distributed title is likely to lead to increased confusion with nomenclature within the already vast range of lumped conceptual models.

Fundamentally there are three options for the future of physically based, distributed hydrological modelling:

- Abandon the schemes altogether in favour of models that are known to work adequately
- Look to redefine the governing equations
- Redevelopment with different aims.

The first option appears rather drastic but is in fact perfectly sensible for some model applications. Beven (1989) makes the point that it is not difficult to predict streamflow from a catchment using a very simple black box approach: "all that is needed is a loss function and a routing function" (p159). Therefore, when all that is required is a streamflow prediction to fill a gap in historical data records for example, a simple model is probably perfectly adequate and is as likely to produce satisfactory results as a physically based model but at considerably less cost to the user. This approach is only possible in simple applied cases. When complex problems such as providing predictions as to the effects of long term vegetation change on stormflow hydrology are required, the simpler models have no potential compared to the admittedly flawed present generation of physically based models. This leaves one of the two other options as possibilities for this study.

The second option given above is to attempt a fundamental change to the model structure to make them what their name suggests i.e. physically based and distributed. Two of the major criticisms levelled against physically based, distributed models in section 2.1 are: that they have tried and failed to incorporate the spatial heterogeneity of hydrological processes into their structure; and that the driving physical equations were not developed at the scale at which they are now used. This leads to the inevitable conclusion that maybe a new set of governing equations can be developed that either account for the spatial heterogeneity through a greater sophistication or are not bound by problems of scale.

The process representations used during the development of the current range of these models was drawn from the most sophisticated techniques available at the time and little has changed in the intervening 10-15 years. Therefore it would appear that any redefining of process equations may have to be at a different scale rather than a more sophisticated representation. Laws that apply at any scale and which could be formed into a model structure have long been sought but in reality do not seem a possibility due to the extreme heterogeneity of natural systems. It cannot be ruled out that at some time in the future fundamental hydrological laws will be discovered and used in hydrological models but at present these do not exist. Although a redefinition of the process equations is not an impossibility it seems that without a major breakthrough in hydrological theory the models using the new equations are unlikely to be any improvement on the current range.

To examine the possibility of the third option, redevelopment of the models with different aims, it is first necessary to look at the aims set during the development of the current range of physically based, distributed models. Prior to and during the early development of these models it was envisaged that they would be broad and all encompassing simulators of a range of hydrological issues. This can be seen from the following two quotations:

> The output from the response model would provide a total picture of the hydrologic system. ..... The output would be continuous in both time and space and would incorporate surface-water, soil-water, and ground-water zones as components of a single system, not as discrete elements. (Freeze & Harlan (1969), p244)

> At the time, it was considered that only through such a system would it be possible to address many of the practical hydrological problems which were becoming increasingly pressing. (Abbott *et al* (1986b), p47)

These ideas tie in with the typical model development strategy expressed in figure 2.1 where the aim is to complete the circle by simulating "the actual hydrologic system" in full through an extremely detailed approach.

It is clear from the previous sections critique of physically based distributed models constructed with these aims, that they are not able to predict "a total picture of the hydrologic system" or address "many of the practical hydrological problems" of then and now. If these models cannot achieve what was desired for them and yet there are still issues to be investigated that require the physically based, distributed modelling approach, then a new form of model may be required.

A possible way forward for physically based modelling is to narrow the development aims and formulate the models with one specific issue of study, or one specific site of study in mind. Because the modelling categories (i.e. physically based/conceptual) have been shown to be arbitrary there is no need for the model developer to stick entirely to the strict criterion of a physical basis for all process representations as the actual implementation is likely to render much of the physical basis into purely conceptual terms. In this way it would be possible to construct a mixed conceptual/physically based model that concentrates the numerical techniques and consequent computational power on processes that are known to be critical for the issue or site under study.

This mixed category approach is not entirely new, the *VSAS* (Variable Source Area Simulator) model described by Troendle (1985) was developed along very similar lines. The model was developed by Hewlett & Nutter (1970) as a mathematical representation of the variable source area concept and concentrates computational power on the solving of Darcian soil water flow equations which are considered crucial to the variable source areas concept. Many of the other hydrological processes (e.g. canopy interception, channel flow etc.) are simulated in a simplified conceptual manner. Similarly the studies of Ross *et al* (1979) and Hillman & Verschuren (1988) are examples of physically based modelling studies investigating vegetation change where a model has been constructed with many

simplifying assumptions in order to study the one issue. The real difference between these and the new approach suggested here is that the previous work all used it as a deliberate strategy to overcome a lack of computing power. In this study it is proposed as a deliberate strategy to avoid model complexity (and consequent need for effective parameters).

The point of this approach is that an investigator wanting to study a specific issue or a particular site using a modelling approach is faced with a decision: which modelling scheme best fits my needs? If the current generation of physically based, distributed models on offer do not live up to their hoped for aims of providing a total picture of the hydrological system and at the same time are extremely difficult to verify and validate, let alone apply, then why choose to use them at all? And if the process representation is in many cases no more than lumped and conceptual why use the more complex form? Instead a user could construct a model along the lines they need, concentrating the physical basis on process representations that are known to be important in the issue or site of study. This new form of model development can be seen to lie within the broad field of expert systems. An expert user assembles a model from a base of known process representations drawing on a conceptual knowledge of the system and issue under study. What is different from the early days of physically based modelling is that the computing hardware is now available that enables relatively quick model assemblage from the already developed process representations.

A recent paper by McKim *et al* (in press) illustrates this principle within a computing software approach. A series of process representations is available to the user who simply selects the relevant icons on screen and they are then assembled into a modelling framework by a software package to produce a designer model for whatever issue is under investigation. In this case the user may not have to be a modelling expert but they do need to have a sound knowledge of the system under study so that the selection of icons is an informed choice. If this form of model construction is taken to its extreme the user could have the choice of a whole string of mathematical representations (from simple conceptual to physically based) for the same process and make their choice based on the perceived importance of that process in the system under investigation. As an example of this focussed development approach an investigator interested in sediment transport may do better to start from scratch and construct a designer model which places great emphasis on overland and channel flow and then build in sediment transport routines on those rather than use a current generation physically based, distributed model such as the *SHE* which has much additional process representation of dubious value.

The reason for continuing with any form of physical process representation within the developed model structure is that this should allow the parameters critical to long term vegetation change (or whatever the issue of study is) to be transferred and/or transformed

over space and particularly time and hence provide some predictive ability. Other parameters controlling the simpler conceptual process representations that are perceived to be less important can be assumed to be time invariant. There is no need to represent these less critical processes in the full physically based manner as the implementation is likely to render these to a conceptual degree of sophistication anyway.

The advantages of this kind of model development are that:

- The number of input parameters that need to be measured or derived prior to application is reduced
- Less time and effort has to spent finding effective parameters etc.
- Important parameters maintain their physical basis to enable them to be transformed over space and/or time in an objective manner
- The verification is a less complicated procedure.

The suggestion of developing a new physically based model with a specific issue of study or site in mind is mostly a response to the charge that physically based models are not what their title suggests, therefore there is no need to maintain the broad general structure of the current generation. Instead of this new model versions can be constructed that have some process representations that attempt to be physically based and others that are not. The second charge summarised at the end of section 2.1 was that physically based, distributed models cannot be adequately verified or validated and therefore cannot be used in normal applications. The problems might be slightly alleviated with this focussed development strategy but in general will still apply, particularly the difficulty of validating a distributed scheme when there is not enough measured data available. The acknowledgement of the need to use physically based models (in whatever form) to investigate complicated issues such as long term vegetation change means that new research methods have to be devised that account for the difficulties if not impossibilities of validating of these schemes.

In the normal validation process the main problem for distributed models is in finding the data measured at the appropriate scale, whereas in the study of long term vegetation change an extra dimension of difficulty is added in that these measurements are required for a long time period. It has already been pointed out that because of the long time scale involved with afforestation it is necessary to have a predictive modelling structure, but if the model requires validation using historical records then this calls for data covering the period of forest growth on a catchment, thereby removing the predictive element of the study. Apart from the fact that these length of records are unlikely to be available to researchers, especially in the detail required by the current generation of physically based models, the situation arises where the model is developed to overcome the lack of available empirical data but then cannot be validated because of the very same lack

of field data. Therefore new modelling study frameworks have to be devised to tackle the complicated issues. It is no longer possible to adhere to the simple model development and application design displayed in figure 2.1 because there is no likelihood of validation and hence the model cannot be applied back to the original research problem. In response to these complexities, which arise from investigating an issue such as long term vegetation change, it is necessary to design a new research structure that takes account of the difficulties of verification and impossibility of validation.

2.3 Methods of parameterising vegetation change

A physically based, distributed model in whatever form provides the basic tool to start investigating long term vegetation change. The predictive ability of these models is usually provided by the measurement of input parameters to represent the change in processes occurring. In order to have a modelling system that predicts the hydrological impacts of vegetation change it is essential to quantify how the input parameters change with time before the changes occur. This is particularly important for afforestation as the change in parameters is likely to be gradual over the period of a forests growth, therefore requiring some form of temporally dynamic parameterisation.

There are two methods available to quantify a change in input parameters that accompany a long term vegetation change:

- Measurement of the parameters at different stages of vegetation change and the use of these parameters as initial boundary conditions for the modelling scheme
- Transforming the input parameters by a modelling algorithm and using the transformed parameters as initial boundary conditions.

There are no databases available that have measured the changes in the types of parameters by a physically based model at a single site as the vegetation changes e.g. all of the empirical studies reported by Bosch & Hewlett (1982) concentrate solely on the monitoring of streamflow. The only method of measuring the numerous input parameters prior to a vegetation change would be to monitor them at different sites, each representing a stage of vegetation change and assume that the same parameters apply on the remote study site. Although the input parameters should be capable of this transfer over space and time the use of effective parameters and other practices outlined in section 2.1 mean that this is not possible for many of the parameters. Consequently the measurement of input parameters for physically based, distributed models in order to parameterise the impacts of

long term vegetation change is not a realistic option if the predictive ability is to be retained.

A transformation of the input parameters using a modelling algorithm would maintain the predictive criteria and also be feasible where the process representations, and therefore input parameters, are physically based. A knowledge of how the parameters change with time is required to develop the algorithm but not the detailed site measurements needed by the first option. The algorithm could take the form of a simple linear transformation or involve a full scale pre-processing model. Either way the entire modelling package (parameterising model and the distributed hydrology model) is offering a means of **predicting** the effects of long term land use change on hydrology.

Any addition of modelling within a study will necessarily increase the need to make simplifications of reality but in the case of long term vegetation change it is the only method available to produce a predictive investigative tool. It must be emphasised that it is only possible to consider transforming the input parameters using a modelling algorithm because they are physically based. It would not be feasible for a purely conceptual model as the transformation of the parameters could not be based on any sound reasoning. This then provides an additional reason for the use of physically based process representations within a distributed modelling structure.

Previous physically based, distributed modelling studies of vegetation change have concentrated on deforestation rather than afforestation, so that the temporal constraints are not so great, although there is still a need for prediction. Ross *et al* (1979) simulated vegetation change by altering the value of Mannings roughness coefficient (a dimensionless factor used in the calculation of channel and overland flow) and the properties of the "hydrological response units" that controlled soil moisture. Rogers (1985) modified the rainfall input and the Chézy roughness coefficient (similar to Mannings roughness coefficient) in the *IHDM* to simulate the effects of deforestation on stormflows. Hillman & Verschuren (1988) used a simple sink term to remove water from the soil water flow equations, the actual volume of water removed per timestep being kept constant. All of these studies have simply **estimated** the effect of change on input parameters rather than transform them in a deliberate manner. The use of modelling to transform the input parameters represents a significant step forward in the hydrological study of vegetation change as it points towards a temporally dynamic predictor of the effects of change.

Transforming the input parameters with a modelling algorithm ties in with the idea of model development with a specific issue of study in mind as the choice of process representation can then be based on the ability to transform the inputs. In the study of afforestation it is necessary to model the change in canopy characteristics as the forest grows so the choice of canopy interception routine is critical, and yet for another issue such as urbanisation it is less important. An application of a current generation physically based

model such as *SHE* to both of these problems would require the usage of the same 2 dimensional interception routine rather than a 3d representation for afforestation (allowing a forest growth model to be used in conjunction) and a simpler conceptual representation for the urbanisation. The 2d option of *SHE* is a compromise in both cases, not detailed enough for afforestation and over detailed for urbanisation.

The fact that a transformation of the input parameters using a model is required reflects the increasing complexity of issues being investigated using physically based, distributed models. This ties in with the ideas expressed at the end of section 2.2 that new research methods are required to investigate these complex issues. The provision of input parameter values for physically based models using a separate modelling structure is part of this new research structure. The following chapter describes the research structure used in this study in order to develop a new framework for investigating the hydrological effects of long term vegetation change and in particular the implications of afforestation.

2.4 Summary

In chapter one the point was made that physically based, distributed modelling provides the only method of investigating an issue such as long term vegetation change because it offers the possibility of predicting the effects beyond a specific time reference. In the first section of this chapter a critique of the current generation of physically based, distributed models found that there are immense difficulties in the usage and they do not live up to their title. Despite this they still offer the only investigative method for studying long term vegetation change. Therefore a new model design is required that can then be incorporated into a research framework that accounts for the difficulties in verification and impossibility of validation.

In the second section of chapter two the criticisms of the current generation of physically based, distributed models were used to describe some possibilities in the future for these models. This included the development of mixed conceptual/physically based models with one specific subject of study or site in mind and focussing the physical basis on those processes that are known to be important for this issue (or site). In the case of long term vegetation change any new model structure has to include some method of transforming the input parameters to quantify the gradual change that occurs as a forest canopy grows. The only feasible means of achieving this is to represent the change in input parameters with time in modelling algorithms and this is only possible when the parameters are physically based. The "all in" modelling package (one model feeding input to the hydrology model) is a new development in the investigation of vegetation change

and reflects the tackling of increasingly complex problems such as predicting the hydrological effects of long term vegetation change.

The following chapter details the research design used in this study in order to investigate the hydrological effects of long term vegetation change and in particular the implications of afforestation.

CHAPTER 3

RESEARCH DESIGN

The previous two chapters have identified numerical modelling as the investigative approach used in this study. The modelling requirement identified in these chapters is for a physically based, distributed hydrological model and some form of algorithm to transform the input parameters of the hydrological model in order to parameterise vegetation change. There are two modelling approaches that could be used to investigate long term vegetation change in this context:

- Use existing modelling schemes and concentrate on obtaining values for the input parameters
- Development† of a new modelling scheme.

These two approaches require different research designs, the first concentrating on field measurement of the input parameters and testing for a specific site or sites, the second concentrating on programming and testing rather than application. Both of these options represent valid investigative approaches for long term vegetation change as there has been very little previous work in this field but the first option is only possible if the available modelling schemes can be considered adequate for the task. The critique of physically based, distributed hydrological models in section 2.2 has suggested that this is not the case, therefore the option of developing a new modelling scheme has been pursued. Included in this scheme is the incorporation of new and also previously developed modelling algorithms to parameterise the degree of vegetation change at stages within the period of afforestation. This means that the emphasis of the study is on model construction and testing rather than obtaining input parameter values through measurement and/or calibration and then application. However within the development of the modelling scheme the construction effort is primarily concentrated on the transformation of the input parameters for the hydrological model using modelling algorithms. This is because the construction of a mixed conceptual/physically based model to act as a hydrological base model for the study is a relatively simple task as all the process representations have been developed previously.

The research framework outlined in this chapter includes the development of a new hydrological model designed along the lines described in section 2.2 and the transformation of input parameters using a model to provide a temporally dynamic

† The term model development is used to mean both programming and testing.

predictor of the effects of long term vegetation change on stormflow hydrology.

3.1 Modelling scheme development

In chapter two reference was made to a traditional model development strategy (see figure 2.1) as put forward by Sargent (1982) and adapted to hydrological modelling by Howes (1985). The traditional modelling study structure outlined in figure 2.1 is a three stage circle, each of the stages (the hydrologic system, the mathematical model, and the computerised model) being linked by deliberate steps. The first step (mathematical model validation) aims to confirm as valid the assumptions made about the real world in the selection of the driving equations and hydrological process representation. The next step is the production of the program code and its verification by identifying that the code is performing as intended. In model application studies these first two steps have already been performed by others during the model development and therefore do not require repetition. The final step is calibration of the model parameters (if required) and a validation of the model structure by measuring its performance against a given data set. The model is then ready, providing the validation was satisfactory to simulate the hydrological system in an applied sense.

The kind of modelling development framework shown in figure 2.1 is not valid for the investigation of long term vegetation change using a distributed model for three reasons:

- The verification and validation steps necessary to link the separate stages is not possible due to the model complexity and lack of data for validation (see in section 2.1)
- The degree of input parameter transformation has to be assessed in some manner other than measurement, therefore an extra layer of modelling is necessary within the overall structure
- The original hydrological problem (impacts of long term vegetation change) requires model predictions based on assumptions of a future change in the hydrologic system rather than a known change.

This last point means that the issue has to be investigated in a different manner than direct application to a measured data set (such as might be the case for filling in gaps in streamflow records).

The fact that a physically based, distributed model of whatever form can never be fully verified and that there are insufficient data to validate any scheme investigating long

term vegetation change does not mean that such steps should be abandoned altogether. It would be impossible to proceed in any modelling study without including some attempt at verification and validation as the model user would have no objective reason to show confidence in the model predictions. Because it is essential to use these models to investigate issues such as long term vegetation change they must be verified and validated as much as is possible given the data constraints. This means that they can never fully be used in a direct application sense, which begs the question why develop these models if they cannot be applied? Konikow & Bredehoeft (1992) suggest that application does not present the sole purpose for modelling:

> Models provide a tool for critical analysis. They are a means to organize our thinking, test ideas for their reasonableness, and indicate which are the sensitive parameters. They point the way for further investigation. (Konikow & Bredehoeft (1992), p82)

Apart from the options given above the lack of full validation does not rule out physically based, distributed models their use as investigative tools of any sort, particularly as pointed out by Fawcett (1992) when used in a probabilistic application.

In a similar vein Beven (1989) divides modelling studies into two categories distinguished by the general aims. These are:

- To explore implications of making certain assumptions about the nature of the real world system
- To predict behaviour of the real world system under a set of naturally occurring circumstances (Beven (1989), p158).

The first of these aims is broadly speaking the use of models in research, while the second is using a model for a direct application. If a modelling study is restricted to the first of these aims then there is not a serious problem with the lack of full verification and validation as this becomes one of the assumptions inherent within the model structure. It is only when the model is used in a manner adhering to the second of these aims, predicting real world behaviour (especially in a strictly deterministic sense), that the lack of full verification and validation becomes a matter for serious concern.

In more general terms Konikow & Bredehoeft (1992) question the whole philosophy of model validation by relating it to the fundamental principles of scientific research. The two schools of thought on scientific endeavour can be summarised as *positivism*, where theories are proved through experiments designed to validate them, or those following the thought of Popper (1959) who argued that you can never prove a theory, only disprove it. Positivism seems to have been the school of thought dictating model development that involves absolute validation whereas in developing models for

investigating complex issues such as long term vegetation change the ideas of Popper (1959) may be more applicable.

The need for an extra layer of modelling within the overall model structure is a direct result of the problem being investigated, the hydrological effects of long term vegetation change. It means that there are now two or more models (the parameter transformation models plus the distributed hydrological model) that need to be verified and validated within the simulation framework before the overall model structure can be used to investigate the original issue. This does not necessarily present a great problem but does mean the framework shown in figure 2.1 needs considerable amendment to account for the model interaction.

The final point listed at the start of this section is perhaps the most serious because it suggests that the circular form of figure 2.1 is not possible here as the model cannot be applied directly back to the original problem through a known data set. The predicted effects of a long term vegetation change will be based on an assumed change in input parameters (i.e. the parameterisation of model input) rather than a known change in inputs. This means that effects of the long term change have to be investigated via a series of hypothetical scenarios rather than through direct application of a data set. This is an entirely feasible method of investigation but is not the direct step back to the original problem in the hydrologic system as is suggested in figure 2.1.

In this study a new research design has been devised to take into account the changes described above. This simulation framework is shown in figure 3.1. There are two fundamental differences between figures 3.1 and 2.1, firstly the new simulation framework is not circular because the verification and validation cannot be conclusive enough to allow direct application within the actual hydrologic system to the original problem. The second point, which is derived from the first, is that the fundamental aim of the study is to form an opinion as to the worth of the model as an investigative tool for the study of long term vegetation change rather than to directly apply a model to the problem. This is in line with the first aim of Beven (1989) listed above: to explore the implications of making certain assumptions about long term vegetation change rather than to directly predict the behaviour of a certain system under this change. It can also be viewed in line with the views of Popper (1959) as trying to disprove the model as a predictive tool rather than prove it. The emphasis of this study is on development and assessment of the worth of the modelling system as a predictor of long term vegetation change, throughout the whole framework.

The first step in figure 2.1 (mathematical model validation) is not required as the process representations will have all been used previously in other model structures. This means this step is a straight choice of previously used process representations based on an *a priori* knowledge of long term vegetation change and therefore the programming of the

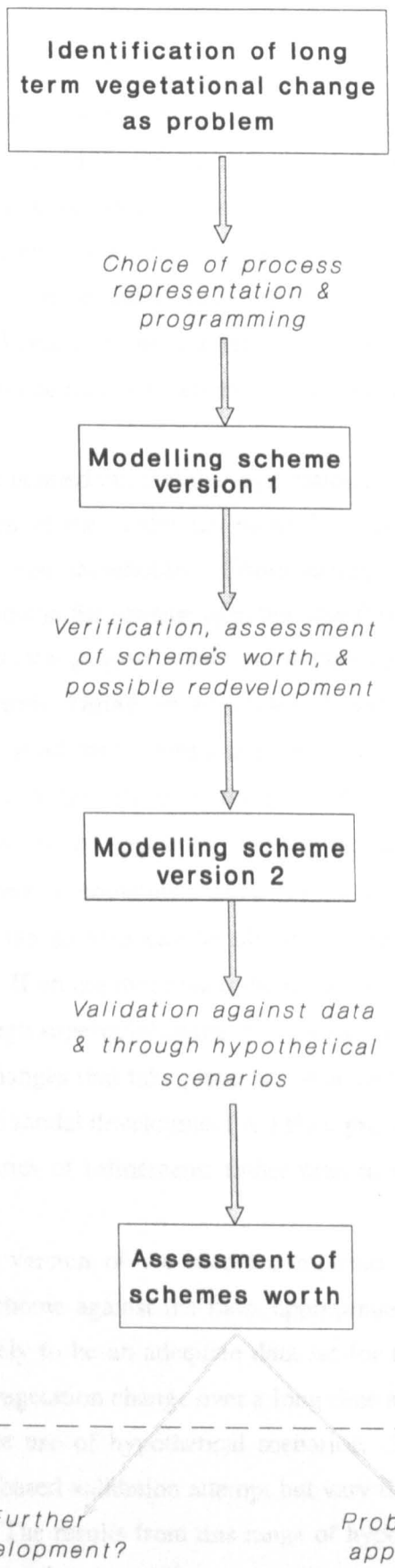

Figure 3.1: Proposed modelling scheme development plan

code providing the scheme structure can begin immediately. Consequently after this first step the initial version of the modelling scheme is produced. This version will include the two tiers of modelling (input parameters as well as catchment hydrology) and have the basic structure in place. Because the emphasis of the whole project is on model development and assessment of worth there is no need for this to be the final version of the model, improvements to the scheme can be made at any stage but as soon as any verification or validation takes place the improvements must be of a superficial nature rather than fundamental. A fundamental change would be to change the form of process representation within the overall structure whereas a superficial change would be to alter the way that the process representation performs without changing the actual model structure. If a fundamental change to the model structure was made after verification the conclusions from this testing could not be taken forward nor could the model be validated in any form.

It has already been pointed out that the verification testing that takes place between the first and second version of the model can never fully verify the scheme because the complex structure makes this impossible. Consequently the verification is primarily focussed on any new features in the scheme (e.g. the transformation of input parameters in modelling algorithms) with the primary intention of ranking their importance relative to other factors that are already known to be critical within the model structure. The secondary intention of the verification testing is to provide some assessment of the worth of the scheme as a predictor of the effects on stormflow hydrology of long term vegetation change. If at this stage the model appears to have no sensitivity to long term vegetation change in all of the different combinations tested (this would differ from all the previous empirical evidence) then the scheme can be abandoned before a major commitment in resources has been made. If on the other hand the results look encouraging the model can be developed further through superficial changes to various process representations.

The superficial changes that take place between version 1 and 2 of the modelling emphasise the fact that the model development is a fluid process that occurs throughout the whole framework as a series of refinements rather than in the one stage as suggested in figure 2.1.

With the second version of the model completed this can then be used in an attempt to validate the scheme against the most appropriate empirical data set available. Because this is never likely to be an adequate data set for the full validation of a model predicting the effects of vegetation change over a long time scale, the model then has to be tested further through the use of hypothetical scenarios. This will use the same basic inputs of the empirically based validation attempt but vary the parameters to simulate long term vegetation change. The results from this range of hypothetical scenarios can then be used to form an opinion on the worth of the modelling scheme as a long term vegetation

change predictor and to "explore implications of making certain assumptions about the nature of the real world system" (Beven (1989), p158).

The use of hypothetical scenarios to assess the models worth can be seen as a form of validation in itself when the term validation is used to mean ensuring the model is (or isn't) a valid representation of the hydrological system (rather than the stricter terminology defined in chapter two†). It is a method forced upon the study by the choice of investigating a problem such as long term vegetation change when there is always likely to be a lack of empirical data to fully validate a modelling scheme. This need not be a drawback as it still represents a significant step forward in the study of long term vegetation change by attempting to develop a predictive investigative method.

After the validation attempt an assessment of the scheme's worth can be used to highlight the future direction of this modelling scheme, whether that be towards further development, areas for future research in vegetation change, on to a application, or even abandoning the approach altogether. Any application of the modelling scheme to land use change prediction will have to be achieved using a probabilistic approach as the lack of full verification/validation and the problems associated with physically based distributed models prevent direct predictions on a deterministic basis.

In figure 3.1 the modelling system versions include the two tiers of models (parameterisation and catchment hydrology) in one step. It is important to realise that these are separate concerns and as such require separate verification and validation even though they are included within the same predictive modelling scheme.

Figure 3.2 translates the research plan of figure 3.1 into the thesis structure. The identification of long term vegetation change as the research problem has been achieved in chapter one. The choice of process representation and description of the resultant model is detailed in chapters four and five, the first of these detailing the hydrological model developed with the specific focus on vegetation change, while chapter five describes the transformation of input parameters using a model. Together these constitute a temporally dynamic predictor of the effects of long term vegetation change that is the modelling scheme version 1 in figure 3.1. Chapter six details the verification testing of the overall scheme and assessment of its worth, with chapter seven concerning some redevelopment of parts of the scheme in light of the verification results and a more detailed verification of the new modelling section which transforms the input parameters for the hydrological model. Chapter eight details the validation attempt with empirical data and the testing with hypothetical scenarios to form an overall assessment of the modelling schemes worth as a predictor of the effects of long term vegetation change. Finally in chapter nine the future options are discussed in light of all the previous chapters and conclusions drawn.

---

† Validation was defined in chapter two as any process designed to measure the correspondence between the model and the system under study.

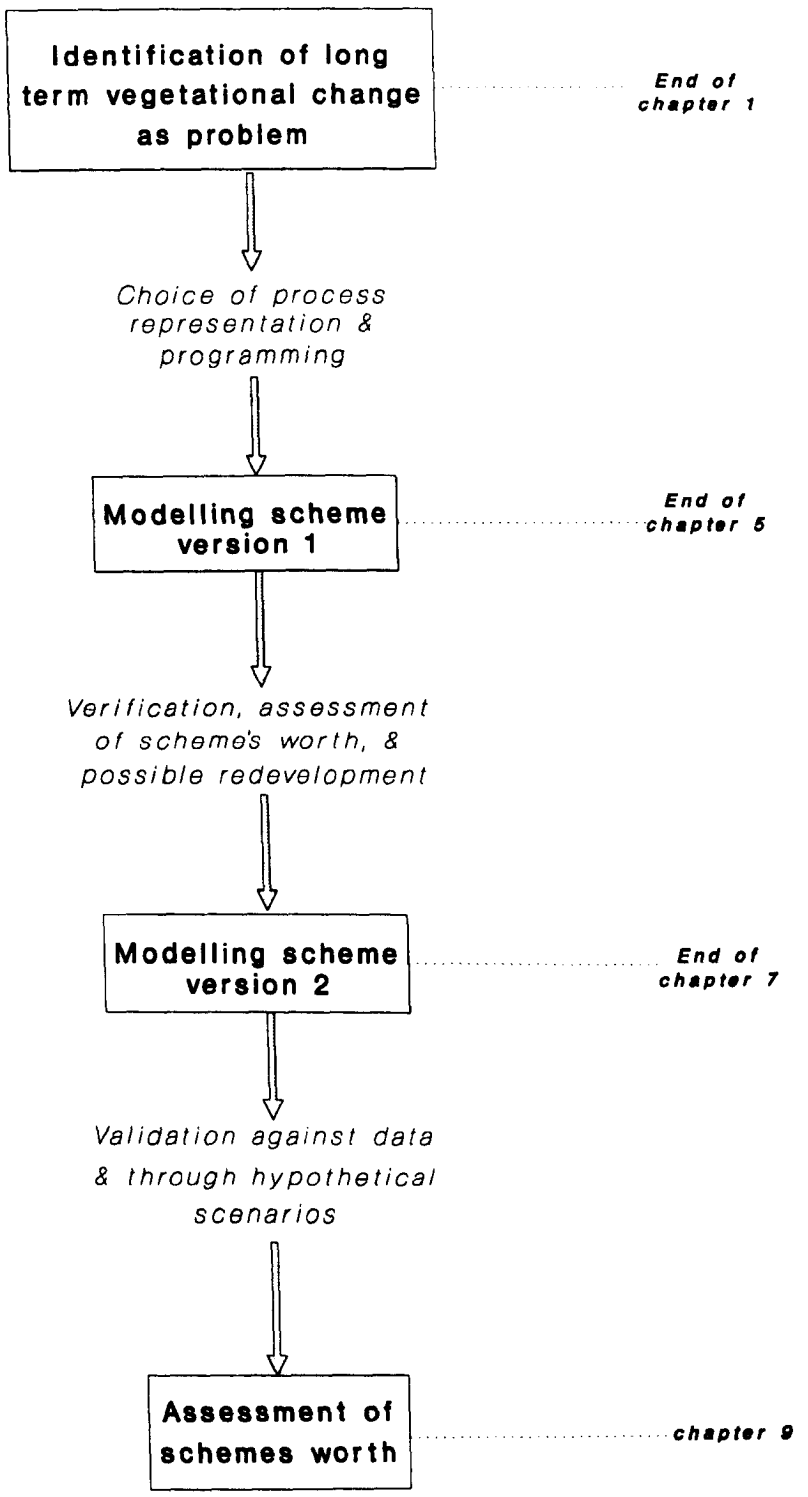

Figure 3.2: Thesis plan

3.2 Research objectives and summary

At the end of chapter one three broad aims were listed for the study. The first of these aims, a review of the requirements of a new predictive method of investigating long term vegetation change, has been achieved in chapter two. A broad outline of how the second aim (development of the new method) will be achieved has been given in this chapter along with the overall research method that encompasses both the second and third aims (assessing the worth of the new method). Now that the actual predictive method has been established the objectives can be refined further. These are:

- To design and construct a physically based, distributed hydrological model with the primary aim of investigating the effects on hydrology of long term vegetation change
- To transform the input parameters for this model using modelling algorithms so that the overall scheme is predictive and temporally dynamic
- To attempt verification and validation of the overall scheme
- To assess the modelling schemes capabilities as a predictive model investigating long term vegetation change.

The originality of this thesis can be summarised on four levels. This study accepts that there is no real distinction between the traditional categories of conceptual and physically based process representations within a distributed model structure (except in intent to be physically based) and therefore attempts to develop a new form of model that mixes these categories into a single structure that is focussed directly on solving issues of vegetation change. The method of focussing on long term vegetation change is to restrict the physical basis of process representation to those processes known to be important in long term vegetation change. This is a new approach in the field of physically based, distributed hydrological modelling.

This study represents the first attempt to transform the input parameters of a quasi-physically based, distributed hydrological model in a deliberate manner using separate modelling algorithms in order to represent the change in parameters occurring prior to a vegetation change taking place.

Problem	*Need*	*Approach used*
Long term vegetation change	Prediction	Physically based numerical model
Current generation of models are inadequate	New model designs	Mixed conceptual/physically based model; aiming physical basis at hydrological effects of vegetation change
Parameterising change	Prediction	Transformation of input parameters using a model
Model development strategies are inadequate	Strategy not dependent on full verification and validation	See figure 3.1

Table 3.1: Research problems tackled in thesis

This study represents the first attempt to develop a methodology to specifically investigate the hydrological effects of long term vegetation change in a predictive manner. Table 3.1 sets out the problems tackled in this thesis in terms of the research need and the approach taken here. The study can be summarised as the development of a predictive investigative method for the exploration of the effects of long term vegetation change on stormflow hydrology through modelling the transformation of input parameters of a new mixed conceptual/physically based, distributed hydrological model. The study is concerned with the hydrology of humid temperate environments, and Great Britain in particular.

CHAPTER 4

DESIGN AND STRUCTURE OF THE HYDROLOGICAL MODEL (*VSAS4*)

Chapter three has described the research framework used in this study highlighting two areas of new investigative approach. Firstly the development of a modelling scheme specifically designed for a particular problem (in this case to investigate the effects of long term vegetation change on stormflow hydrology) including a new mixed conceptual/physically based distributed hydrological model. Secondly the transformation of input parameters using modelling algorithms to represent vegetation change. This chapter describes the construction of the focussed physically based distributed hydrology model that forms the nucleus of the total modelling scheme envisaged to investigate the hydrological effects of long term vegetation change.

The first section of this chapter is concerned with the background within which hydrological processes can be considered to be important in the study of long term vegetation change. Section 4.2 details the background and structure of the two previously developed models that have been integrated to produce the hydrological model used in this study. Section 4.3 is a detailed description of the integrated hydrological model which is then put through initial testing in section 4.4.

4.1 Options for model design

In chapter one the point was made that physically based, distributed modelling offered the only method of investigating an issue such as the hydrological effects of long term vegetation change because it offers the possibility of prediction beyond a specific time reference. In chapter two a critique of the current generation of physically based, distributed models found that there are immense difficulties in their usage and that they do not live up to their title. Despite this they offer the only investigative method for studying the hydrological effects of long term vegetation change and therefore a new model design is required that is incorporated into a research framework that accounts for the difficulties in verification and impossibility of validation.

One of the conclusions drawn in section 2.2 was the suggestion that a possible future development is to design the models with one specific issue of study in mind. At the

same time it was suggested that, as the differences between conceptual and physically based models are blurred, there is no need to adhere to the strict criteria of having every process represented by physical, partial differential equations (as has been the case in the current generation of physically based, distributed models). This has the capability of freeing up the model structure so that the numerical techniques and computational power can be concentrated on the process representations that are known to be critical for the issue under study thereby reducing the model inputs that have to be measured or derived and lessening the need for deriving effective parameters.

There is no doubt that a distributed hydrological model is required to investigate vegetation change because real life alteration is rarely catchment wide in extent and a lumped model would severely limit the capabilities to predict any consequent effects. A distributed model should be able to simulate common vegetation change practices such as block planting and different tree spacings within a forest. The new focussed development approach suggested in section 2.2 is adhered to in this study, so that a distributed model with some physically based attributes is designed specifically to investigate the hydrological effects of long term vegetation change. The actual structure of the model is in section 4.3 but before this it is necessary to consider the important processes that occur during long term vegetation change so that the choice of process representation is based on a solid *a priori* knowledge of the system and issue under study.

There are seven main hydrological processes that need to be considered for their importance within an area undergoing long term vegetation change:

- Transpiration
- Rainfall partitioning†
- Snowmelt
- Overland flow
- Channel flow
- Soil water flow
- Groundwater flow

These are assessed here for their importance as an area is covered by forest and the canopy develops.

Transpiration is an important hydrological process to be considered for any vegetation cover and consequently is important to consider for a change in flora. To model the effects of transpiration fully it is necessary to have a root water uptake routine to simulate the extraction of soil water by the vegetation (e.g. Hoogland *et al* (1981) and Tiktak & Bouten (1992)). It is not necessarily the case that a larger canopy transpires at a

† The term *rainfall partitioning* is used throughout the remainder of this thesis to mean the subdivision of an above canopy rainfall input into interception loss, stemflow, and throughfall.

greater rate, measurements of transpiration loss above grassland have been shown to be as great and sometimes greater than above a forest canopy (McIlroy & Angus (1964)), but in times of soil moisture deficit a larger canopy such as a forest is more likely to be able to extract water for transpiration from deep sources using its root network.

The overall affect of transpiration is less during a storm event than in the intervening periods where it represents one of the few losses to a catchment system (along with open water and bare soil evaporation). This means that in a study considering the hydrological effects of long term vegetation change on low flows transpiration must be modelled in a physically based manner whereas for an investigation of the effects on stormflows the representation does not need to be so rigourous.

The role of *rainfall partitioning* and consequent interception loss in a canopy has long been seen as critical in controlling the amount of water reaching the soil surface and therefore being available for streamflow. Initially it was thought that interception merely replaced transpiration as a water balance loss during a storm (Penman (1963)) but subsequent studies have shown that interception loss can exceed transpiration rates by as much as three or four times (Stewart (1977)) in a forest canopy. Critically other studies have shown that interception loss from grass is approximately equal to the transpiration rate (McIlroy & Angus (1964)). The amount of interception loss changes as the canopy grows, a mature canopy is able to store considerably more water on its leaves which is then available for evaporation and subsequent loss to the catchment water balance. At the same time the aerodynamic roughness of the canopy will change as it grows thereby increasing the evaporative flux transfer between canopy and atmosphere. Studies such as those of Stewart (1977) and Calder & Wright (1986) have highlighted rainfall partitioning as important not only for low flows where the loss of rainfall to the soilwater is significant but also for storm events where there is often a heat flux other than solar radiation (e.g. advection within the cyclonic system) available to drive the evaporative process. It is important for any study attempting to model the impacts of long term vegetation change on hydrology that interception loss is adequately represented.

As well as interception loss, rainfall partitioning can be an important process because of the modification in timing of the rainfall reaching the soil surface. This factor is important for consideration of storm flows especially where there is known to be a predominance of overland flow in which case a modification to the rainfall input can have a large effect on the storm hydrograph. The growth of a forest canopy increases the magnitude of this effect as there are more intercepting layers to delay the rainfall falling through the trees. A detailed consideration of rainfall partitioning is critical to any attempt at modelling the impacts of long term vegetation change on hydrology.

Snowmelt is only an important process in regions where it forms a significant proportion of the rainfall. The results of studies on the amount of snow interception by

trees (summarised by Ward & Robinson (1990)) are conflicting as to whether forests do intercept more snow than smaller vegetation covers. The change in microclimate resulting at the surface where the snow melts can be altered by vegetation change affecting the rate of snowmelt but not the amount. It is only necessary to consider the modelling of snowmelt in a physically based manner in regions where it is an important component of the water balance which is not the case for much of the Great Britain.

Overland flow is an important hydrological process to consider during storm events under any vegetation cover as it contributes to much of the storm runoff. The mechanisms leading to the generation of overland flow have been the cause of much debate but it is now generally agreed that saturated overland flow is the predominant form and that Hortonian (or precipitation excess) overland flow only occurs in special circumstances such as hydrophobic or compacted soils. The simulation of the routing of overland flow in models such as the *SHE* have used two dimensional flow representations such the Mannings equation (a kinematic approximation of the continuity equation for one or two dimensional transient flow) which rely on roughness parameters to simulate the time taken between grid elements. Ross *et al* (1979) used the change in Mannings roughness parameters to model the effects of vegetation change using a finite element solution network.

For a straight storm hydrograph prediction the important part of simulation is in determining the volume of overland flow, the actual timing can be relatively easily achieved using a simple routing function. It is only in special cases such as the investigation of sediment transfer or soil erosion where the overland flow mechanism has to be modelled in great detail. The volume of overland flow is a function of the soil moisture and soil water flow representation so this should have more importance in a scheme modelling storm runoff alone than the actual representation of overland flow.

Channel flow is very similar to overland flow in that to produce a storm hydrograph the accurate simulation of the mechanisms producing the **volume** of runoff contributing to channel flow is more important than the detailed representation of how the water moves within the channel. For small basins this can be adequately simulated by simple routing functions although if the study requires more than a storm hydrograph (e.g. for channel erosion or sediment transfer analysis) then the detailed channel flow representations such as Mannings equation are required.

Soil water flow is of critical importance to any model simulating low flows (for the soil water contribution to low flows) and predicting storm hydrographs (for the controls it places on the generation of saturated overland flow). The soil structure, and consequently the soil physics controlling soil water flow, must be expected to change with the growth of a different vegetation cover, especially in the surface layer. Consequently soil water flow must be modelled in a sophisticated form in any scheme attempting to model the

hydrological effects of long term vegetation change.

The contribution of *groundwater* to low flows is well understood but there is still considerable controversy on its role in stormflows. Groundwater flow could be expected to change with an alteration in vegetation cover as the amount of water percolating through the soil layer to reach the permanent water table could be expected to change. Where there is a particularly porous bed-rock (e.g. Karst topography) and the effect of long term vegetation change on low flows is being investigated then groundwater should be represented in a physically based manner such as Darcys law. Where there is a mostly impermeable bed-rock and the study is investigating the effects on storm hydrographs then groundwater can be largely ignored.

The summary of the importance of these main hydrological processes in long term vegetation change modelling is shown in table 4.1. It is clear from this that the two most important processes for a mixed physically based/conceptual modelling scheme to represent in a physically based manner are soil water flow and canopy rainfall partitioning. The other six processes could be represented in a more simplistic manner depending on what form of study is undertaken (e.g. investigating the effects of long term vegetation change on stormflows **or** on low flows **or** both).

As well as an assessment of the importance of various hydrological processes, some practises that are associated with afforestation should be considered. The most notable of these is the use of drainage ditching where the forest is planted in upland peat bog regions (common in the UK). Robinson (1986) has shown that this can have a significant effect on the hydrology of a catchment, through a greater predominance of quickflow and also the rapid drainage of the soil near the ditches. This is a difficult practise to consider in a model as it requires both discrete rapid drainage lines and a gradation in soil moisture moving away from each ditch.

This is the first time the hydrological effects of long term vegetation change has been studied in a predictive modelling manner (previous studies such as Ross *et al* (1979) and Rogers (1985) concentrated on deforestation). Therefore it was decided to focus on making a first pass over the subject and keep the study within strict limits by investigating the effects of long term vegetation change on storm flows. This reinforces the point made in chapter three that this study has the aim of exploring the implications of making certain assumptions about the nature of the real world system rather than predicting the behaviour of this system (from Beven (1989)). The emphasis is on developing a new model form and testing it, not on applying the modelling system to immediately predict real world behaviour with its multiple complicating factors.

The new modelling design outlined in the remainder of this chapter focuses on the

Process	*Comment on role within long term vegetation change*
Transpiration	Important for analysis of low flows, not so much for storm flows. Can be coupled with root extraction model to influence soil water distribution
Rainfall partitioning	Critical importance with growth of canopy for low flows and storm flows
Snowmelt	Only important in certain environments
Overland flow	Important for erosion but volume more important than extent for storm flows
Channel flow	Important for large catchments or catchments with large floodplains
Soil water flow	Critical for the production of overland flow volume
Groundwater flow	Important for low flows, uncertain contribution to stormflow

Table 4.1: Summary of the importance of the main hydrological processes in long term vegetation change modelling

hydrological effects of long term vegetation change by having soil water flow and canopy interception represented in what is traditionally thought of as a physically based manner while representing the other processes in a simpler conceptual manner. These process representations making up the new hydrological model were not selected totally from scratch and amalgamated together, in the manner of McKim *et al* (in press). The new model is a combination of two previously separate models. The two base models are detailed mathematical representations of:

- Hillslope hydrology within a catchment (*VSAS*)
- Rainfall partitioning within a forest canopy (*INTMO*)

VSAS (Troendle (1985) was selected because it is a semi-physically based, distributed catchment model that concentrates its computational complexity on soil water flow while simplifying most other processes. *INTMO* (Durocher (1991)) was selected as a better representation of canopy interception than is already present within *VSAS*, and the three dimensional physical basis of it allows for ready transformation of input parameters to represent vegetation change. *VSAS* was chosen as the model to provide the basic structure of the scheme as it is a catchment hydrology model in its own right, therefore *INTMO* was integrated within the *VSAS* structure. Previous to this study both of these models were separate working units, having never been linked. Section 4.2 gives a brief overview of these models, section 4.3 describes the new integrated model (*VSAS4*) in detail, and section 4.4 details some initial testing of the scheme.

4.2 Background and outline of VSAS4

4.2.1 VSAS

The hillslope hydrology model used in this study is a version of the variable source area model (*VSAS*). It was originally developed by Troendle (1979), building on earlier work by Hewlett & Nutter (1970) and Hewlett & Troendle (1975). The model is called the variable source area model because it was written as a mathematical representation of the variable source area concept as proposed by Hewlett & Hibbert (1963, 1967).

Hewlett & Hibbert (1963) initially proposed an alternative runoff generating mechanism to the generally accepted infiltration excess (Hortonian) overland flow mechanism that was the dominant theory at the time. Overland flow as proposed by Horton (1933) occurs when the rainfall rate exceeds the infiltration capacity of a soil and therefore the excess rainfall travels downslope as surface runoff. Field studies by Hursh (1944) and others pointed to the fact that rainfall rate almost never exceeds measured soil infiltration capacities in a forest soil, and yet there is still a runoff peak during a storm event in a forested catchment. Hewlett & Hibbert (1963) proposed that overland flow occurs when initially all rainfall infiltrates beyond the soil surface causing the water table to rise toward the surface. When the water table reaches the surface no further rain can infiltrate the saturated soil and any water returning to the surface from the saturated zone, or further rain falling on already saturated zones, moves downslope as *saturated overland flow*.

It is now generally accepted that Hortonian overland flow occurs only under special conditions (e.g. compacted or hydrophobic soils) while saturated overland flow is the dominant runoff producing mechanism in vegetated humid environments.

Hewlett & Hibbert developed their stormflow generating ideas further into the variable source area concept which can be summarised in two basic statements:

- Overland flow is predominantly produced by saturated overland flow
- The area of a catchment producing saturated overland flow is spatially and temporally variable and acts as a "rapid extension of the channel system" (Hewlett & Hibbert 1967)

The fact that *VSAS* was written as a mathematical description of the variable source area concept makes it a good choice as the hydrological base model for this study. The main concentration of computing power is on soil water flow and the generation of saturated overland flow which are generally acknowledged as being the dominant storm runoff processes in humid, mid-latitude environments.

The original version of *VSAS* (Troendle 1979) was written to concentrate on the computation of soil water flow and the representation of topography. This incorporates the first variable source area concept statement listed above. The model was developed further by Bernier (1982, 1985) with the addition of a routine to recalculate the catchment area when the streamside regions became saturated, thus treating saturated areas as part of the channel system (the second variable source area statement listed above). Bernier named this version *VSAS2*. A recent study by Prevost *at al* (1990) has used *VSAS2* for a study of snowmelt beneath a coniferous forest in Canada. Their study used *VSAS2* as a hydrological base model incorporating a detailed snowmelt routine into the structure in a similar manner to *VSAS3* is used here.

Whitelaw (1988) developed another version of the model, *VSAS3*, the main modifications being: soil water flow is treated in a three dimensional manner; an altered topographical input; and the calculation of unsaturated hydraulic conductivity has been improved. *VSAS3* is the version of the model used as a base for *VSAS4* in this study. It is a semi-physically based, distributed hydrological model written in *FORTRAN-77* programming language. It uses a block centred finite difference scheme to solve soil water flow equations in a quasi three dimensional manner.

VSAS has three sets of inputs:

- Catchment topography and soil mantle geometry
- Soil hydrological characteristics
- Hourly rainfall

Catchment streamflow and soil moisture data are output hourly. A generalised flow diagram of *VSAS3* is shown in figure 4.1 which gives a broad overview of the model structure.

VSAS3 is a semi-physically based, distributed, hydrological model, developed for a capability to represent the variable source area concept. Computational power has been concentrated on hydrological processes that were perceived as being the most important at the time of initial model development (e.g. soil water flow), but this has been done at the expense of other processes. The representation of canopy interception, for instance, lacks any physical basis and has minimal distribution within a catchment. Whereas at the time of *VSAS* development a lack of computational power was a considerable constraining factor, this is now no longer as pressing a problem, and it is possible for *VSAS3* to be modified to better represent hydrological processes with issues of long term vegetation change kept in mind.

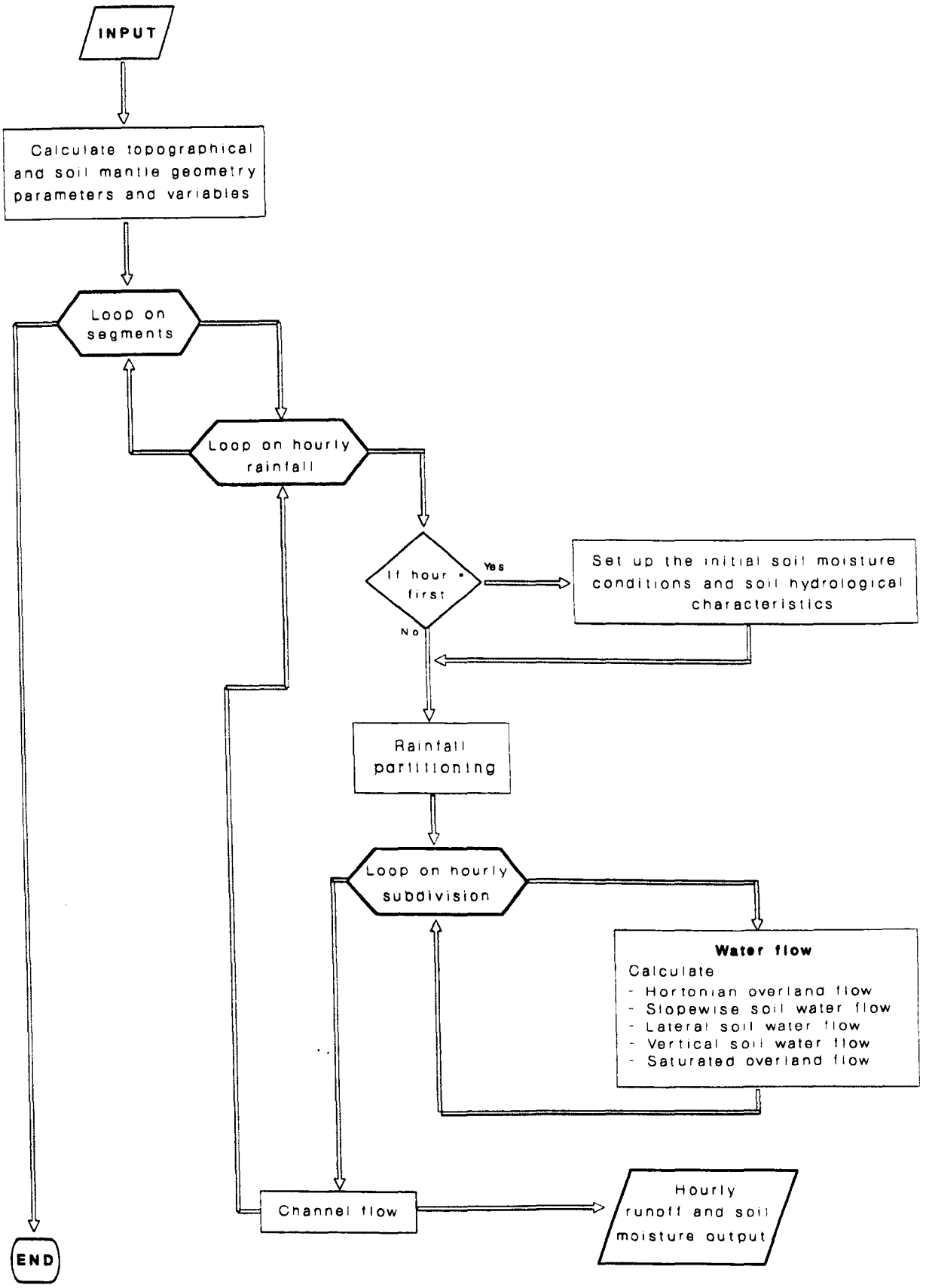

Figure 4.1: Generalised flow diagram of *VSAS* structure

4.2.2 INTMO

The canopy interception model adapted for use in this study (*INTMO*) was developed by Durocher (1991) as part of an intensive plot study investigating the importance of spatial distribution on hydrological processes within a deciduous forest plantation. *INTMO* has been used successfully by Durocher (1991) to model interception, stemflow, and throughfall using time scales ranging from hourly to monthly totals. The model has several unique features compared to standard canopy interception models (e.g. Rutter *et al* (1971) or Gash (1979)):

- Three dimensional canopy representation
- Forest hydrological processes modelled to the leaf scale
- A method of stochastically simulating a mature deciduous canopy.

These features make it an attractive model to integrate with *VSAS* so that the resultant *VSAS4* has a detailed representation of both soil water flow and canopy interception which have been identified in section 4.1 as important processes in the hydrological study of long term vegetation change.

INTMO is a model that can be divided into two distinct sections that run separately from each other:

- Stochastic generation of the canopy parameters that are used in rainfall partitioning
- Rainfall partitioning

The canopy generation part of *INTMO* is a routine which stochastically generates the structural properties that influence rainfall partitioning. Rather than deriving measured values for a spatially discrete canopy it is generated in a stochastic manner. Once these structural parameters are in place the discretisation part of *INTMO* takes the canopy generated and stochastically subdivides it into the basic units needed by the model to simulate rainfall partitioning. Because the model was developed for a deciduous forest canopy there is a temporal variation routine that accounts for the difference in canopy structure with changing seasons through the year.

The rainfall partitioning is based upon the work by Rutter *et al* (1971) but has been extended to three dimensions and a finer spatial scale. This entailed subdividing the canopy into discrete cells, each cell being the basic unit for interception computations.

INTMO uses above canopy rainfall (for a range of timesteps from seconds to hours) and produces stemflow and throughfall as output. A generalised flow diagram of *INTMO* is shown in figure 4.2.

The three dimensional nature of the interception computation makes *INTMO* an extremely flexible model to investigate rainfall distribution under a forest canopy and the

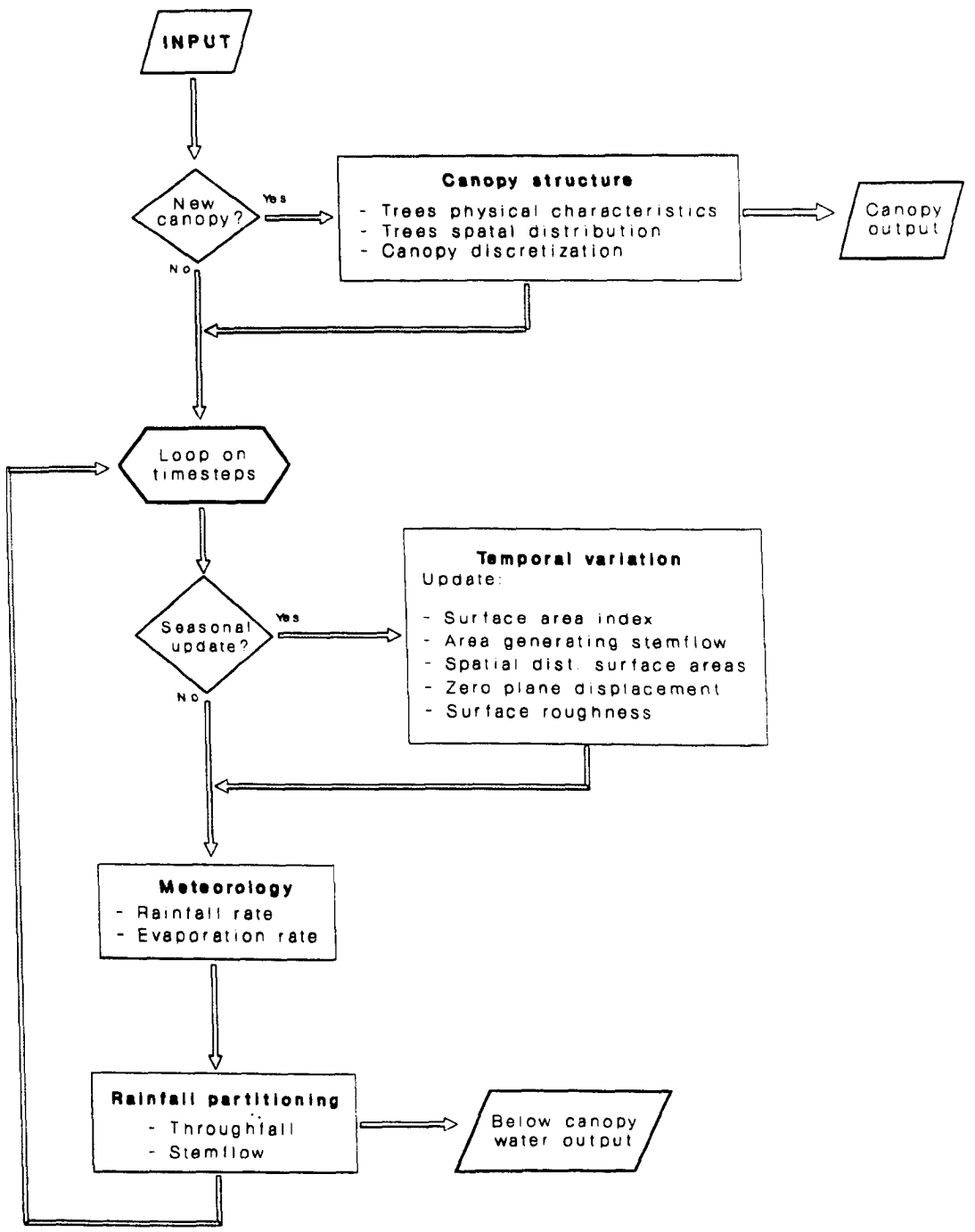

Figure 4.2: Generalised flow diagram of *INTMO* structure

effect of varying that canopy. Although the increase in scale, from a single layer canopy (as in the Rutter model) to leaf scale computation, inevitably increases the size of computer program, and power of the machine needed to run it, this is not beyond the range of present day Mainframes.

The distributed three dimensional nature of the rainfall partitioning provides a good basis to integrate *INTMO* with *VSAS* as it is a feature lacking in the current *VSAS* structure.

4.2.3 *Combined version*

VSAS4 is an integration of the rainfall partitioning model *INTMO* into the *VSAS3* structure to provide a physically based, distributed hydrological model. This will act as a storm event simulator within a modelling scheme specifically designed to investigate long term vegetation change.

The structure of *VSAS4* is illustrated in the generalised flow diagram in figure 4.3. A comparison to figure 4.1 shows that the position and nature of the main changes from *VSAS2* is in the rainfall partitioning by integrating this part of *INTMO* into the *VSAS* scheme.

The major difference is that now the rainfall partitioning is performed within the soil water flow subroutine. This is to synchronise the computation time steps for soil water flow and rainfall partitioning. Within a time step the above canopy rainfall is input, the rainfall moves through the canopy the allowed amount, and then the total below canopy output (stemflow, direct and indirect throughfall) is added to the soil surface.

The difference described above required a considerable rearrangement of both program codes (i.e. *VSAS3* and *INTMO*). Three factors had to be synchronised:

- Timing within the separate models
- Time step within the separate models
- Volumes of water passing between the two sections (canopy and catchment surface)

This integration has been achieved through a subroutine called from within the soil hydrology subroutine.

Figure 4.4 is a conceptual representation of the coupling that constitutes *VSAS4*. The separate sections of the model are semi-autonomous. **The integration of the three dimensional rainfall partitioning routine from *INTMO* into *VSAS* represents an original coupling of two previously developed models to form a distributed, physically based hydrological model with special emphasis on soil and canopy hydrology.**

The following section describes in detail the structure and process representation

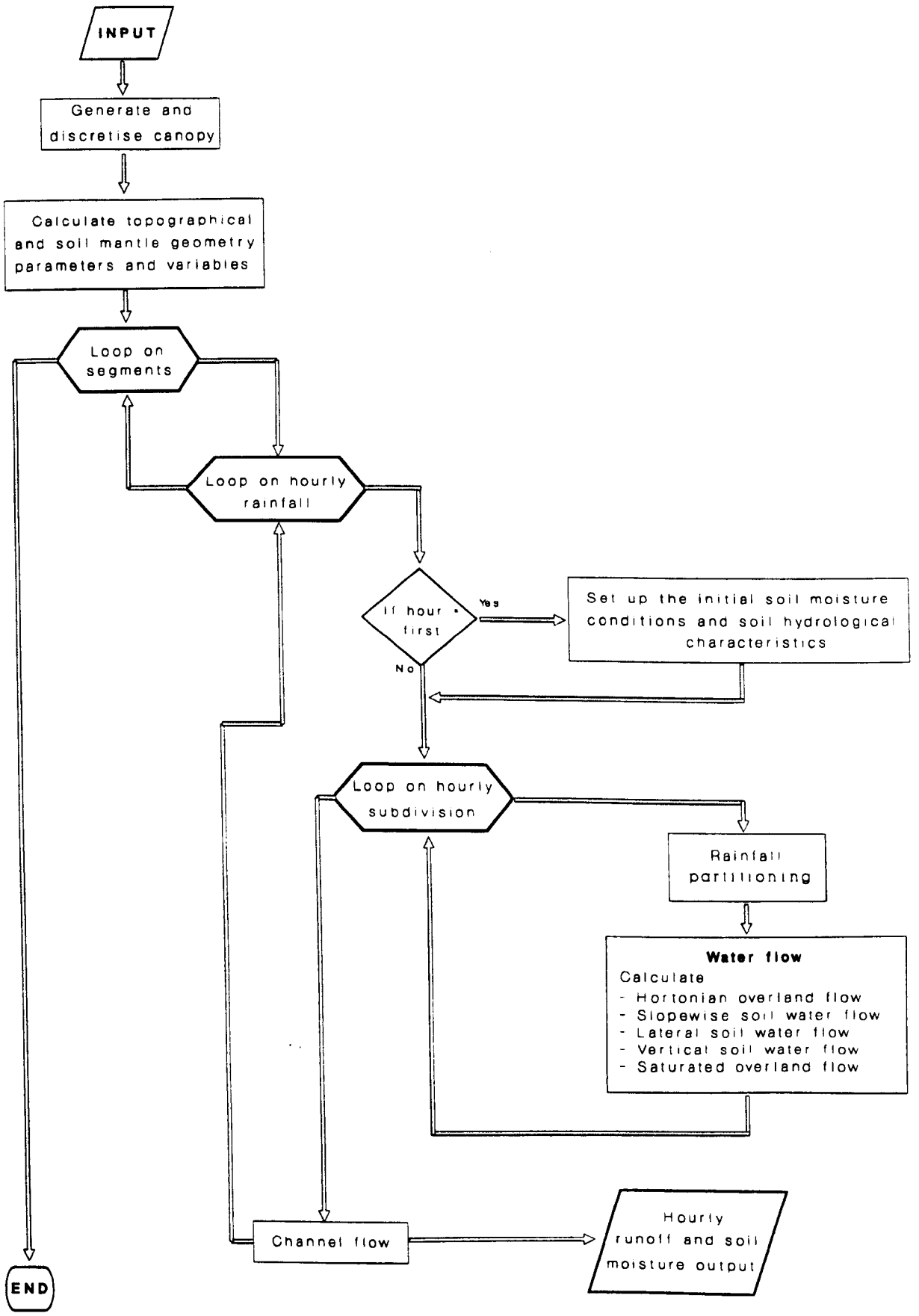

Figure 4.3: Generalised flow diagram of *VSAS4* structure

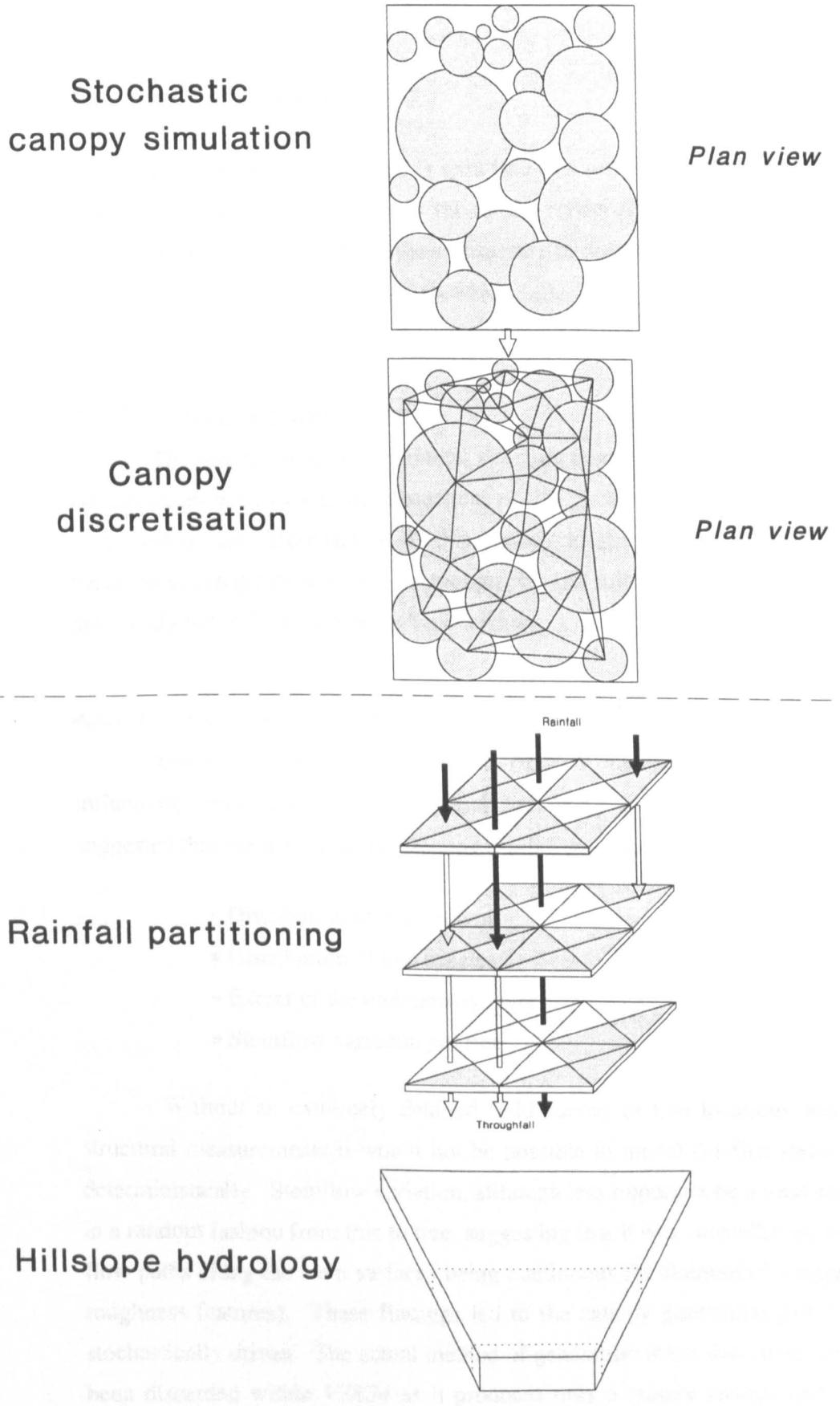

Figure 4.4: Conceptual representation of *VSAS4*

of *VSAS4*. A list of the input parameters required by the model is contained in table 4.2 at the end of section 4.3.

4.3 Structure of VSAS4

The description of *VSAS4* is split into two sections: those calculations carried out prior to any simulation in order to set up the model structure (section 4.3.1); and those calculations carried out within a preset timestep in order to provide the simulation through a series of process representations (section 4.3.2).

4.3.1 Overall structure

The setting up of the simulation structure carried out by *VSAS4* can be divided into six categories which form the subsections of this section. These are: the initial generation of a canopy; the discretisation of this canopy to the tree and leaf scale; the temporal variation in canopy parameters; the topography and soil mantle geometry of the catchment; and finally the soil hydrological characteristics.

4.3.1.1 Canopy generation

Durocher (1991) used the results from an intensive field plot study into factors influencing rainfall partitioning spatial variability to design *INTMO*. These results suggested that the main factors affecting rainfall partitioning are:

- Distribution of tree crowns
- Distribution of tree species
- Extent of the understorey layer
- Stemflow variation per tree

Without an extremely detailed field survey of tree locations and individual tree structural measurements it would not be possible to model the first three of these factors deterministically. Stemflow variation, although less important on a total stand basis, varied in a random fashion from tree to tree, suggesting that it was controlled by the probability of flow paths along the stem surfaces being continuous (or alternatively being interrupted by roughness features). These findings led to the canopy generation part of *INTMO* being stochastically driven. The actual method of generation is not described here because it has been discarded within *VSAS4* as it produces only a mature canopy and therefore cannot produce the temporally dynamic input required in a predictive study of the hydrological

effects long term vegetation change. The input that is required to run the rainfall partitioning is the point position and dimensions of all trees in a multi-specific forest. This can be generated either as a series of discrete measurements or as the output from a temporally dynamic forest growth model. This is discussed further in chapter five.

The part of canopy generation that has been retained within *VSAS4* is that each tree is assigned a proportion of the canopy surface area which generates stemflow. Durocher (1991) found in his field study that the distribution of stemflow proportion was log normal and therefore the random selection of stemflow proportion for each tree is drawn from a log normal distribution statistically described by the input mean and standard deviation of the proportion of each tree crown generating stemflow. The mean of the stemflow proportion is derived from the slope of the linear regression relationship between mean stemflow and rainfall (see Helvey and Patric (1965) for examples).

4.3.1.2 Tree scale discretisation

The stochastically generated canopy is subdivided into a set of cells that become the basic units for the calculation of interception and throughfall. The new cells are triangles with a tree trunk at each vertex (see figure 4.5). This *Delauney tessellation* (derived from Watson (1982)) of the canopy area is achieved by each triangle having as near as is possible equal internal angles and it is conserved only if no data point lies within the circumference of its *circumcircle*†. To eliminate edge effects, any triangle is excluded if two or more of its vertices (trees) are located in a border region equal to a set amount of the side length of the total area (a square).

Each triangle is the basic surface area from which interception and throughfall are simulated, stemflow is simulated on a per tree basis. It is assumed that throughfall is spatially uniform in plan within each triangle, whereas a vertical leaf/stem scale variation is considered for throughfall, stemflow, interception and canopy storage.

Within each Delauney triangle the leaf area index (*LAI*) is a fundamental parameter that is used for the computation of other triangle properties. The mean *LAI* of a triangle (t) is calculated from the input mean leaf area index for each tree (different between species), with the proportion of each crown contributing to stemflow subtracted (see equation 4.1). This assumes that no overlapping of trees occurs as long as the total of the three crown projected areas does not exceed the triangle area.

$$LAI_t = \frac{\sum_{i=1}^{3} [AI_i (CPA_{it} - p_{it} CPA_{it})]}{A_t - \sum_{i=1}^{3} (p_{it} CPA_{it})} \qquad (4.1)$$

† The circle with its circumference passing through each vertex.

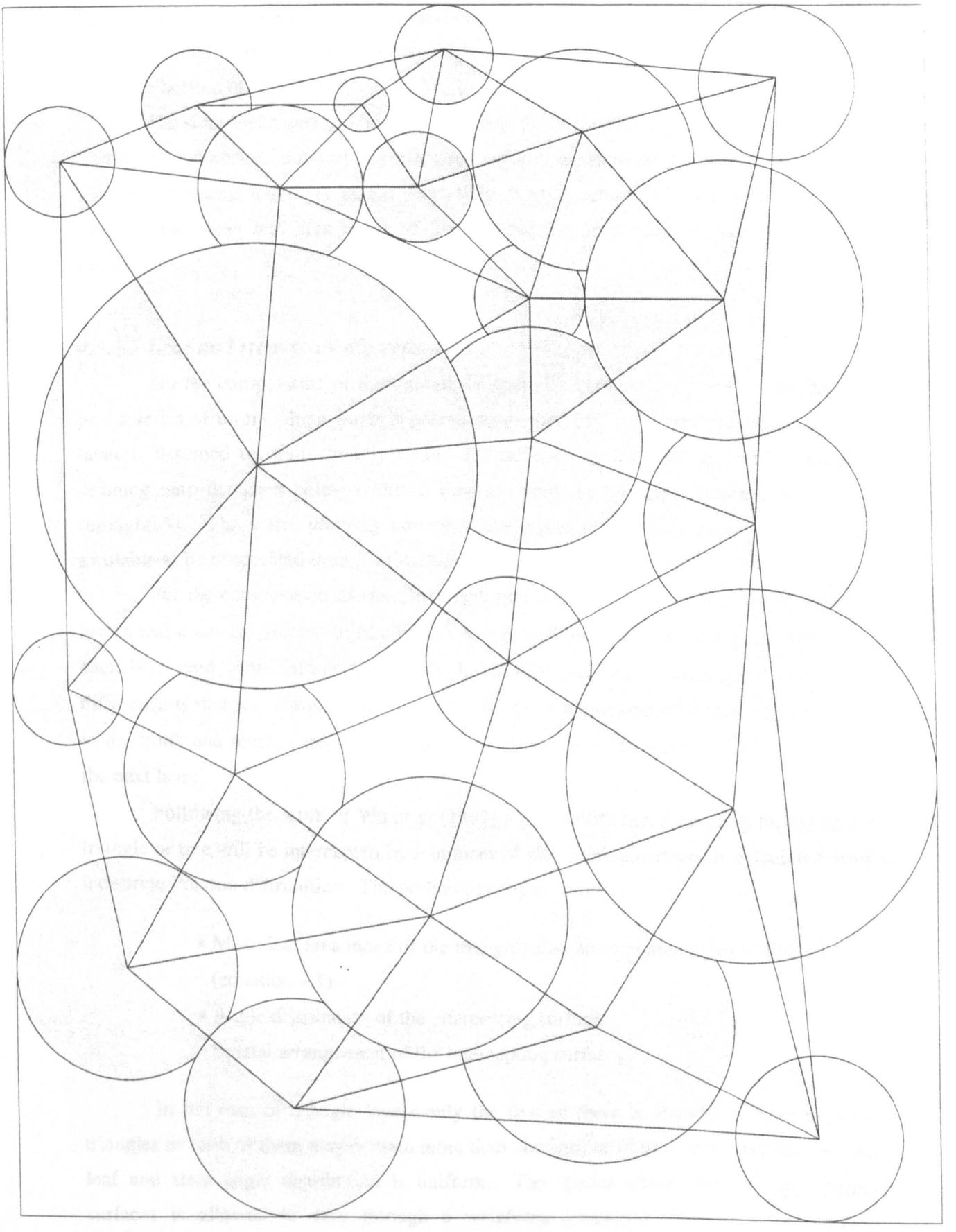

Figure 4.5: Example of a Delauney tessellation within a forest canopy

CPA_{it}	=	Crown projected area of tree *i* in triangle *t*
AI_i	=	Total surface area index of tree *i*
A_t	=	Area of triangle
p_{it}	=	Proportion of tree crown *i* generating stemflow in triangle *t*

The *LAI* is the average number of leaf layers in each triangle. This can be visualised as the average number of times an intercepting surface is touched by a plumb-line dropped from the top to bottom of a canopy.

The stem area index (*SAI*) is also required, this is the number of layers containing a continuous network of intercepting elements capable of transporting water to the trunk. The stem elements may vary in size from twig to trunk scale. It is assumed that *SAI* is equal to the mean leaf area index of the tree for the proportion of crown generating stemflow.

4.3.1.3 Leaf and stem scale discretisation

For the computation of throughfall the triangles between each tree are subdivided into a series of layers which water is passed down through. A certain proportion of each layer is assumed to drain directly to the ground (free throughfall) with the remainder draining onto the layer below within a timestep until the last layer is reached (indirect throughfall). The water draining through these layers is canopy storage and therefore available to be evaporated during a timestep.

For the computation of stemflow each tree is subdivided into a series of separate layers and a similar process to throughfall occurs with some rainfall being intercepted by each layer and some falling directly to the surface (i.e. free throughfall). The major difference is that it is assumed that when the water is intercepted by a stem layer it drains to the trunk and reaches the ground within the same timestep rather than being passed to the next layer.

Following the work of Wu *et al* (1987) a probability that a raindrop falling onto a triangle or tree will be intercepted by *n* number of intercepting surfaces is calculated using a discrete Poisson distribution. The probability depends on:

- Mean leaf area index of the triangle or mean stem area index of the tree (equation 4.1)
- Angle distribution of the intercepting surfaces
- Spatial arrangement of the intercepting surfaces

In the case of triangle layers only the first of these is allowed to vary between triangles as each of them may contain more than one species of tree. It is assumed that the leaf and stem angle distribution is uniform. The spatial arrangement of intercepting surfaces is allowed to vary through a weighting parameter (γ) within the Poisson

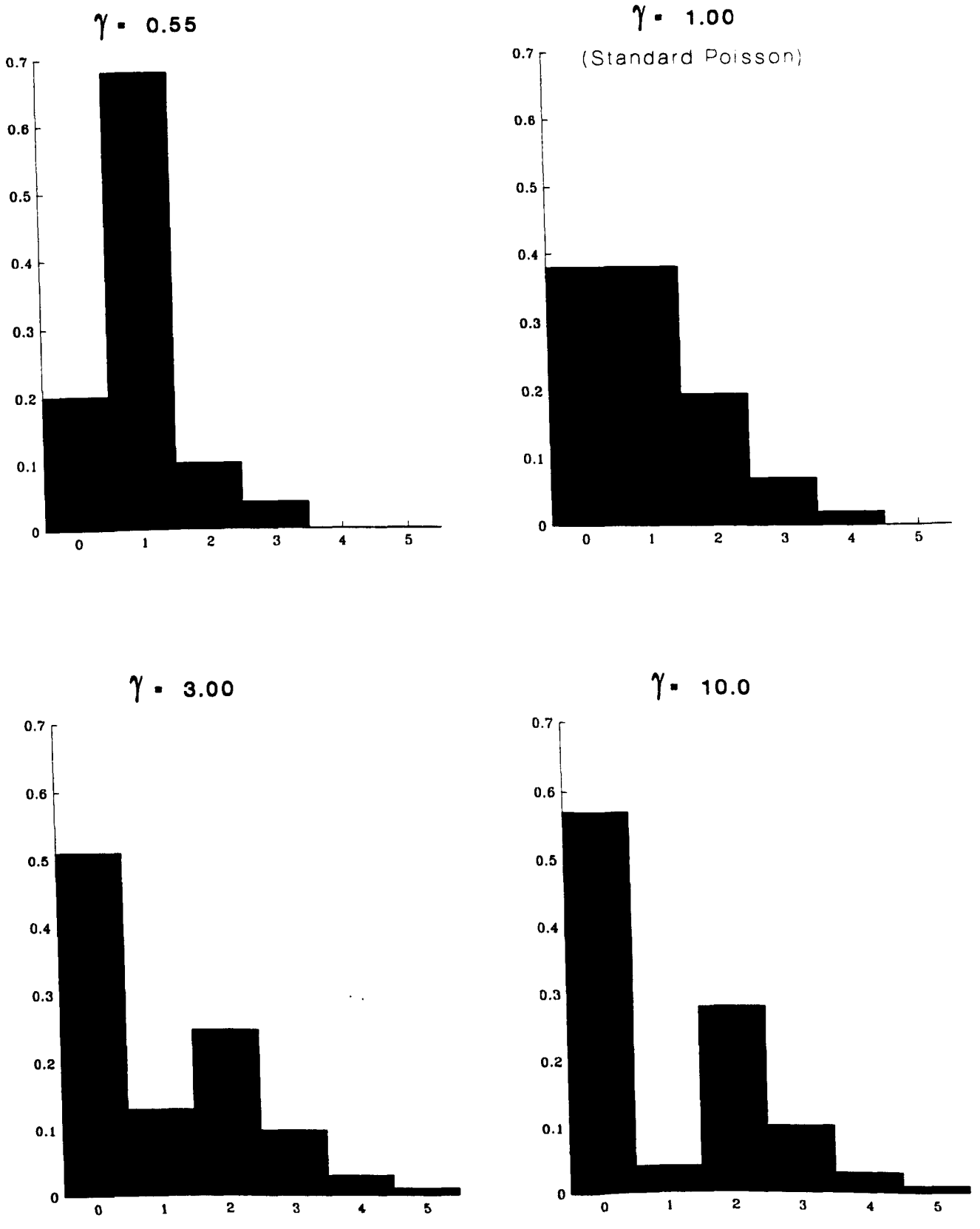

Figure 4.6: Influence of weighting factor (γ) on a Poisson distribution. Number of intercepting layers on x axis, probability on y axis. As γ increases the distribution moves from normal to bimodal

distribution. This is used to provide a varied distribution of the number of intercepting layers in a tree or triangle depending on the stand architecture (see figure 4.6 for how γ affects a Poisson distribution).

The probability of a triangle or stem layer having n layers is calculated in the manner shown in equations 4.2-4.4.

$$P'_n = \begin{cases} x - (1-x)\,P_n & (i = j) \\ (1-x)\,P_n & (i \neq j) \end{cases} \tag{4.2}$$

where:

$$x = \frac{P_n}{1 - P_n} \left[\frac{1}{\gamma} - 1 \right] \tag{4.3}$$

and:

$$P_n = \frac{[LAI_t G(\theta)]^n \; e^{-[LAI_t G(\theta)]}}{n!} \tag{4.4}$$

P'_n = Probability of a raindrop encountering n layers in a triangle
$G(\theta)$ = Extinction function for the angle distribution (equal to 1/2 for a uniform distribution)
i = Mean number of layers
j = Discrete value
γ = Weighting factor

Within each triangle the proportion area composed of at least 1 to n layers is given by the cumulative probability of equation 4.4 (see equation 4.5).

$$\sum_{x=1}^{n} P'_x = P'_1 + \ldots\ldots P'_{n-1} + P'_n \tag{4.5}$$

P'_x = Proportional area composed of $1 \rightarrow n$ layers

For each triangle the number of layers and proportion area of the triangle in each layer is calculated and stored for usage in the rainfall partitioning routine.

4.3.1.4 Temporal variation

VSAS4 allows three canopy structural properties to vary with time to replicate the change in canopy structure with different seasons. The time varying parameters are:

- Mean leaf area index for a species
- Mean proportion of a crown surface area generating stemflow
- Standard deviation of the proportion of crown surface area generating

stemflow

The variation in the above properties is input as a vector in concordance with a time vector (in Julian days). The value of the property on the simulation day is estimated by linear interpolation between the two nearest variable values with respect to the time vector.

4.3.1.5 Topography and soil mantle geometry

VSAS4 requires that a catchment be divided into a series of polygons called *segments* by the user (see figures 4.7 and 4.8). This is achieved using a a topographical map, and any *a priori* knowledge of flow paths within the catchment. A segment is an autonomous hydrological unit, stretching from the base of a slope (normally a channel) to the watershed boundary. It is assumed that the only water exiting from a segment occurs at the slope base by flowing into a stream channel. This requires the intersegment boundaries (normally a ridge or valley bottom), watershed boundary, and soil base to be impermeable. The side boundaries need not be parallel to each other, so a segment can take a rectangular, square, convergent, divergent, or skew form.

This is a similar topographic representation to the *IHDM4* model (e.g. Calver (1988)), but very different to the grid representation used in the *SHE* model (e.g. Abbott *et al* (1986b)). Figure 4.7 illustrates the difference in topographic representation between the better known *SHE* modelling scheme and *VSAS4*.

Each segment can be divided lengthwise into an odd number of *subsegments* (maximum of 5). These are effectively smaller versions of segments except that water is allowed to flow laterally between subsegments. Their incorporation by Whitelaw (1988) allows detailed topography within a segment to be better represented, especially with regard to flow convergence zones such as hillslope hollows and also allows the calculation of soil water flow in three dimensions.

Each subsegment is divided slopewise into a series of *increments*. The division is performed in the fashion shown in equation 4.6:

$$d_n = D \left[\frac{n}{N} \right]^2 \qquad (4.6)$$

d_n = Distance from stream to increment *n*
D = Length of segment/subsegment
N = Total number of increments

The number of slopewise divisions (*N*) is decided by the user, normally depending on the detail required at the segment base. As can be seen from figure 4.8b the logistic nature of this equation divides the slope into small increments at the stream side, which increase in

Figure 4.7: Comparison of topographic representation between the *SHE* and *VSAS* modelling schemes

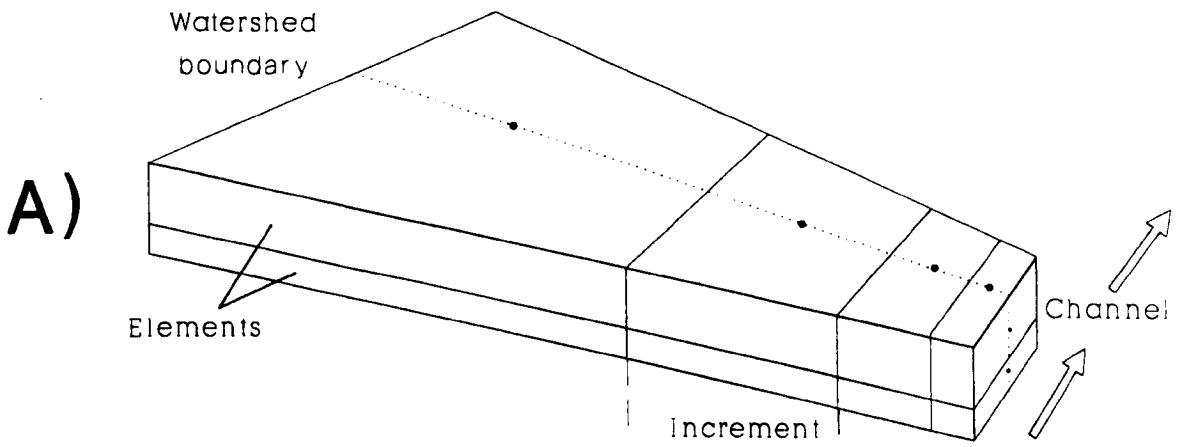

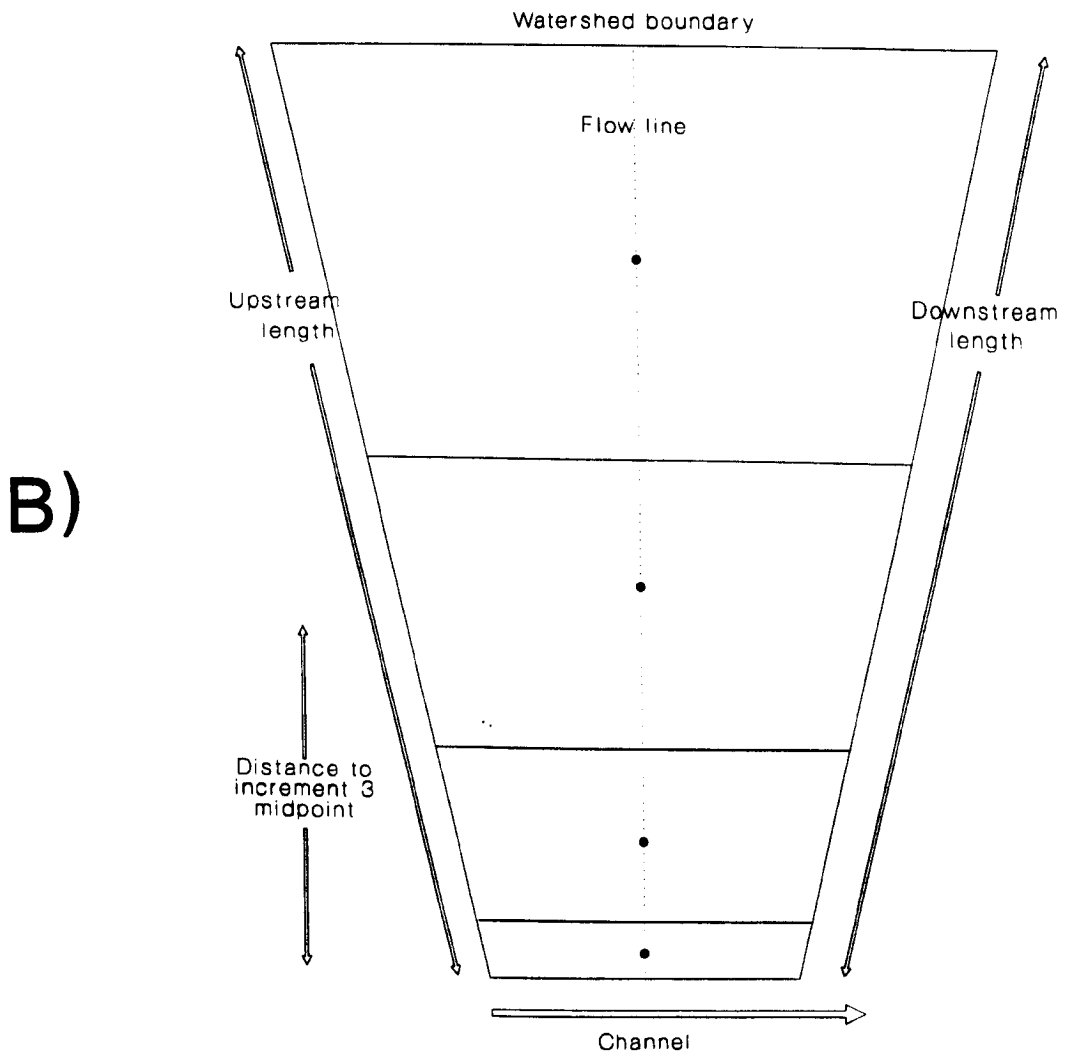

Figure 4.8: Discretisation within a *VSAS* segment. a) oblique view b) plan view

size upslope towards the watershed boundary. This gives greater model sensitivity in the region nearest the stream, which the variable source area concept predicts is the most important for runoff generation. At each increment centre point, the surface elevation, distance to stream, and soil depth to the impermeable bed-rock are input. These values are obtained from a combination of topographical map and field investigation.

Each increment is divided with depth into a series of soil *elements* (see figure 4.8a). The number and depth of these elements is uniform for each segment, the actual values being dependent on the soil heterogeneity. This is the basic unit of *VSAS4* soil water flow calculation, all soil hydrological properties are assigned to a point in the centre of the element and are assumed uniform throughout an element. The element centre point is the solution point for the *VSAS4* block centred finite difference scheme, with soil water flow being computed in three dimensions (non-simultaneously).

The linkage between the element centres is the flow line (see figure 4.8b) along which it is assumed all subsurface flow moves toward the stream. Where a segment is divided into subsegments and the central flow lines do not run parallel to each other it is necessary to measure an offset between the subsegments (see figure 4.9). This is because the soil water passed between subsegments (i.e. lateral flow) is assumed to flow at right angles to the central flow line of the subsegment it is leaving. The model calculates which element is directly orthogonal to the element centre where the water is coming from and then transfers it directly to the centre of this. At the base of the slope orthogonal flow from one element centre may be beyond the limits of the neighbouring subsegment (i.e. in the stream) so this flow is not transferred. The offset is measured from a topographical map.

For each segment a percentage of each soil depth represented as stones can be input. This is converted to a volume and is then discounted from the element volumes and surface area i.e. it is assumed that the stones are impervious and therefore the area of soil available for soil matrix flow is diminished.

VSAS4 calculates the relevant volumes, distances, and areas (e.g. element volume, distance between element centres, surface area between elements) for the soil water flow computations in a subroutine (*BLKVOL*) prior to any calculations being made.

The method of catchment discretisation used in *VSAS* deliberately places emphasis on the role of topographic convergence (and conversely divergence) to produce flow convergence zones. As water flows down a *convergent* slope the element volume decreases until either the subsurface flow reaches the channel or the element becomes saturated and any "extra" water becomes return flow. This is to emphasise the important role topographic convergence can play in runoff generation, as shown by Anderson & Burt (1978) and Anderson & Kneale (1982).

Segment area (change from VSAS3)

As part of the finite difference solution it is assumed that all flow occurring along

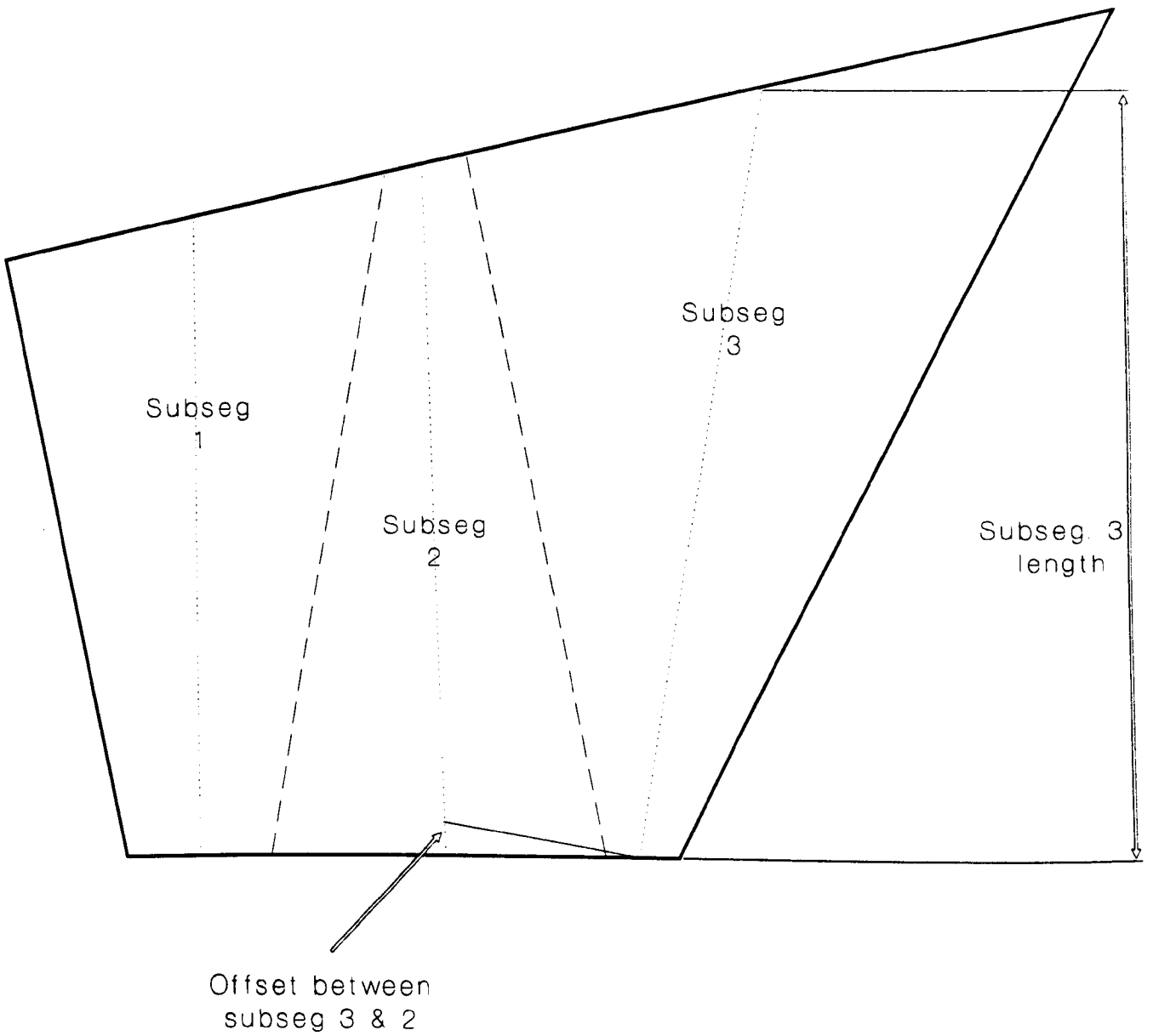

Figure 4.9: Subsegment length and offset for flow between skewed subsegments

the central flow line exits the segment at an angle orthogonal to the stream direction. To achieve the conditions of this assumption it is sometimes necessary for *VSAS4* to perceive the segment in a slightly different manner to the input measurements i.e. when the central flow line is non-orthogonal to the stream the segment is effectively straightened so that it is orthogonal whilst maintaining the same length of flow line. This is illustrated in the two examples shown in figure 4.10.

Figures 4.10a and 4.10c represent possible segments (or subsegments) where the flow line is non-orthogonal to the stream whilst figures 4.10b and 4.9c represent the way that *VSAS4* perceives them to be for computational purposes. The straightening up of both of these segments has resulted in an increase in surface area of the segment as shown by the actual surface areas shown. This discrepancy in surface area increases as the angle between the stream and the central flow line decreases i.e. greater discrepancy in surface area the further the flow line is away from orthogonal to the stream.

To overcome this discrepancy it is necessary to compromise the soil mantle geometry specifications in some manner. Within the *VSAS4* soil geometry there are five factors that in an ideal solution would be the same between the measured topographic inputs and how the model conceptualises them. These are:

- Segment area
- Flow orthogonal to the stream
- The length of central flow line
- Width of the streamside element
- All other segment dimensions.

The fact that *VSAS4* is a physically based distributed model means that the catchment area is an extremely important parameter; any model of this sort should be able to predict actual flow volumes from a catchment (and within a catchment) rather than just flow depths. To achieve this it is necessary to have the correct catchment (as the sum of segments) area when the flow calculations are being made.

As mentioned above it is necessary to have the water entering the stream at an angle orthogonal to the stream for the finite difference solution used in solving the partial differential equations for soil water flow.

The length of the central flow line is measured from streamside to watershed boundary and then is used to obtain the surface elevations of each of the increments making up the segment or subsegment i.e. the elevations are measured along the central flow line. The elevations and distances along the central flow line are critical for the definition of the slope profile and therefore cannot be altered.

The width of the streamside element is important for defining the two dimensional area that water has to drain through to enter the stream. It is also important for having the

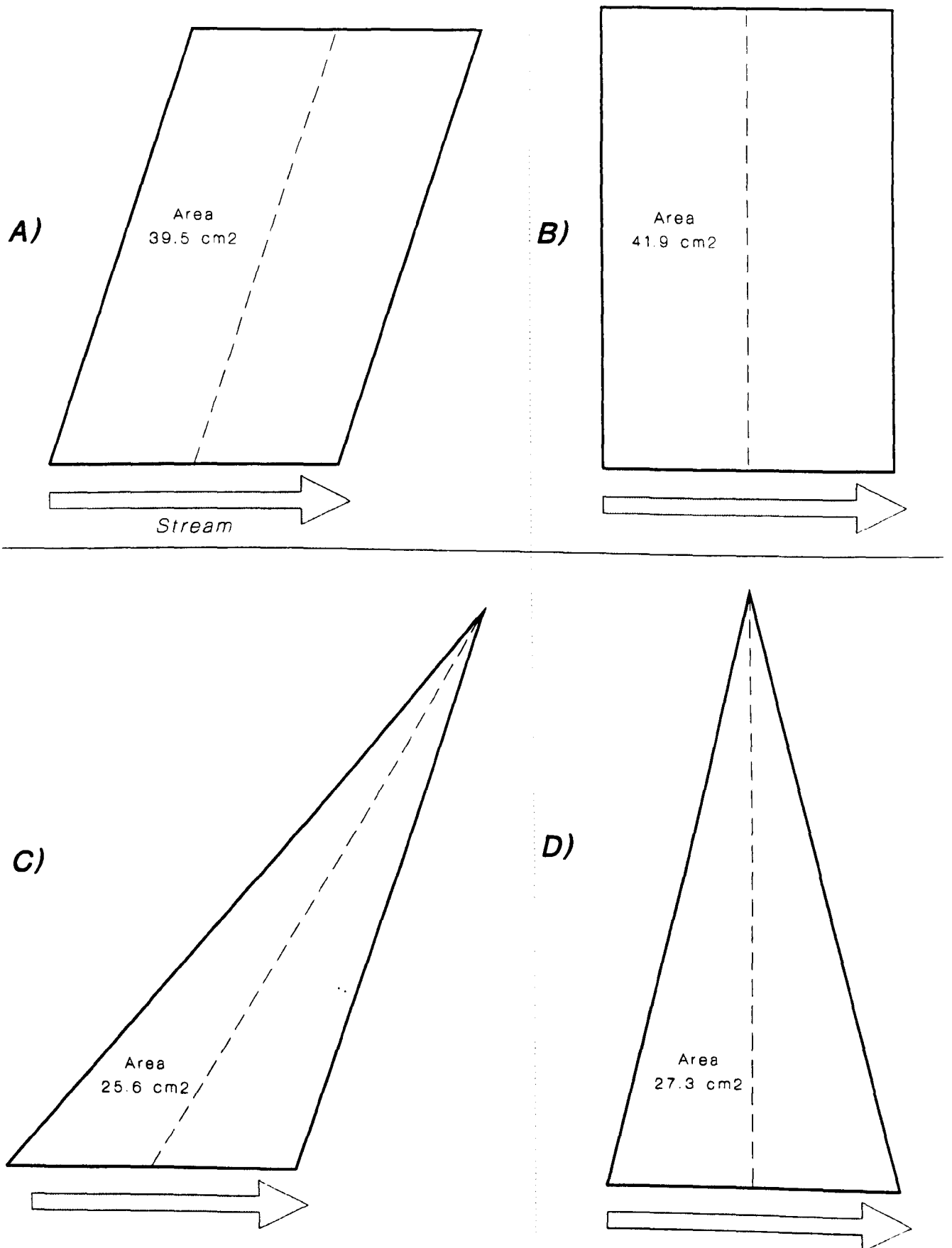

Figure 4.10: Segment and subsegment conceptualisation within *VSAS3*. a) and c) represent actual segments, c) and d) how they are conceptualised

correct area of the zones of saturation extending beyond the stream that form an integral part of the variable source area concept that was the basis for the original *VSAS* model.

It is desirable that all of the dimensions input from a topographic study of a catchment (e.g. segment widths and side lengths) are maintained by the model so that factors such as topographic convergence down a slope are not distorted by the difference between model perception and measured topography.

It is obvious from figure 4.10 that all of these conditions cannot be met simultaneously and therefore one or more of the factors has to be compromised. Segment area, orthogonal flow into the stream, and length of the central flow line are all integral parts of the model structure and therefore cannot be compromised without either reformulating the model or disregarding the basic model principles. The dimensions of each segment can be altered so long as the relative differences are maintained, although it is desirable that the original streamside length is retained.

An alteration to the model structure has been made so the original area of a segment (as input by the user) is maintained regardless of the angle between the central flow line and the stream. The alteration is in the subroutine *BLKVOL* which carries out all of the soil mantle geometry calculations. For every segment and subsegment in a catchment the user now inputs the relative coordinates of all four corners. These are relative to a fixed point, the most sensible fixed point for figure 4.10a would be the bottom left hand corner which would be assigned the coordinates *(0,0)*, all other coordinates being measured in metres from this point. From these coordinates three factors can be mathematically derived that were originally input independently:

- Segment area
- Streamside and watershed length
- Central flow line length.

Knowing the original area the segment is then straightened if necessary and the watershed width and the width of all the segments except the streamside element are reduced until the new area is exactly the same as the original. This is illustrated by figure 4.11.

The resulting segment image is distorted from the original but four of the original five factors listed above (segment area; central flow line length; flow orthogonal to the stream; and streamside length) have been maintained with the least important (other dimensions) being altered. This is a compromise but represents a viable option that causes the least disruption to the overall model structure.

4.3.1.6 Soil hydrological characteristics

Each subsegment can be divided into any number of hydrological *zones*. Zones are regions with distinct soil hydrology properties that stretch across subsegment width.

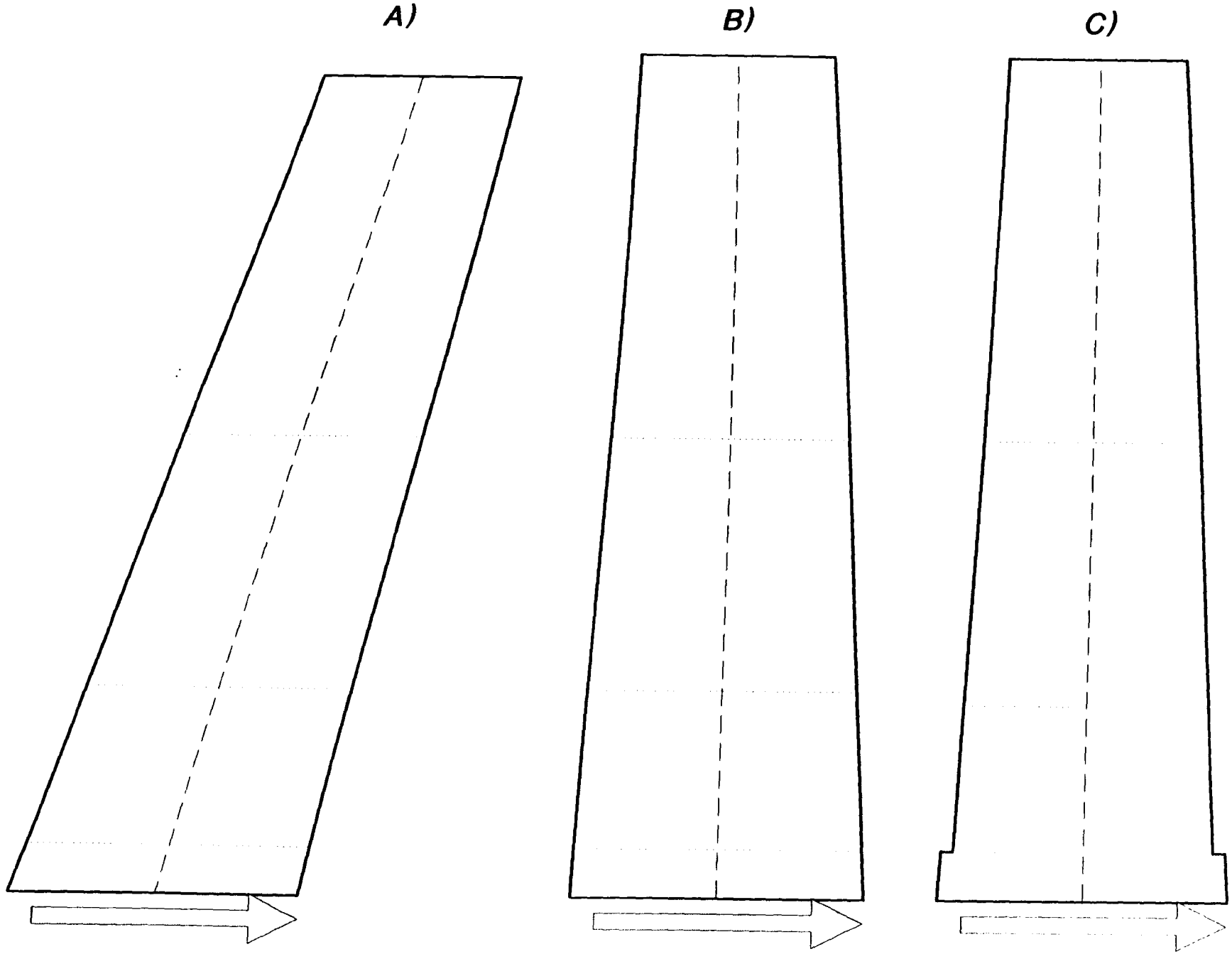

Figure 4.11: New segment and subsegment conceptualisation within *VSAS4*. a) represents the actual segment, b) the *VSAS2* version, and c) the *VSAS4* version

They are delimited along the line running through the element centres, each element is assigned hydrological properties according to which zone the element centre is contained within.

A suction-moisture curve for each soil zone is input (hysteresis is assumed unimportant), from which the Millington-Quirk method (Millington & Quirk (1961)) calculates a table of unsaturated hydraulic conductivities for each soil zone. The value of saturated moisture content (porosity), saturated hydraulic conductivity, and a suction moisture curve is input for each soil zone along with the standard deviations of each value. The actual value of these parameters for each elements is then stochastically derived prior to simulation, drawing the values randomly from a normal distribution of defined mean and standard deviation, to try and account for the heterogeneity in soil physical properties that is known to occur in the field.

The Millington-Quirk method mathematically transforms a known soil suction-moisture curve into an approximated unsaturated hydraulic conductivity curve-moisture curve (see figure 4.12) using the relationship shown in equation 4.7. The relationship between these two curves is based upon the stochastically derived values of saturated moisture content and saturated hydraulic conductivity together with a probability of flow continuity between pores of a certain size (the maximum size is governed by the moisture content).

$$K(\theta)_i = K_{sat} \left(\frac{\theta_i}{\theta_{sat}} \right)^P \frac{\sum_{j=i}^{m} ((2j+1-2i)\psi_j^{-2})}{\sum_{j=1}^{m} ((2j-1)\psi_j^{-2})} \qquad (4.7)$$

$K(\theta)_i$ = Unsaturated hydraulic conductivity at point *i* on the suction moisture curve
K_{sat} = Saturated hydraulic conductivity
θ_i = Moisture content at point *i*
θ_{sat} = Saturated moisture content (porosity)
P = Empirical exponent (see following text)
m = Number of equally spaced points required on the θ axis
i = Counter from 1→m (*i*=1 is highest moisture content ∴ lowest soil suction)
ψ_j = Soil suction at moisture content θ_i

As ψ increases (i.e. soil dries out), *i* increases, decreasing the range of numerator summation and thus reducing the value of the numerator rapidly, relative to the denominator. This in turn reduces the calculated unsaturated hydraulic conductivity value. Physically this represents the observation that as moisture content decreases, the size of pores maintaining continuous contact with each other decreases rapidly. This reduces the possible flow rate and therefore also reduces the unsaturated hydraulic conductivity.

The original value of P in equation 4.2 was 4/3 but subsequent investigations by

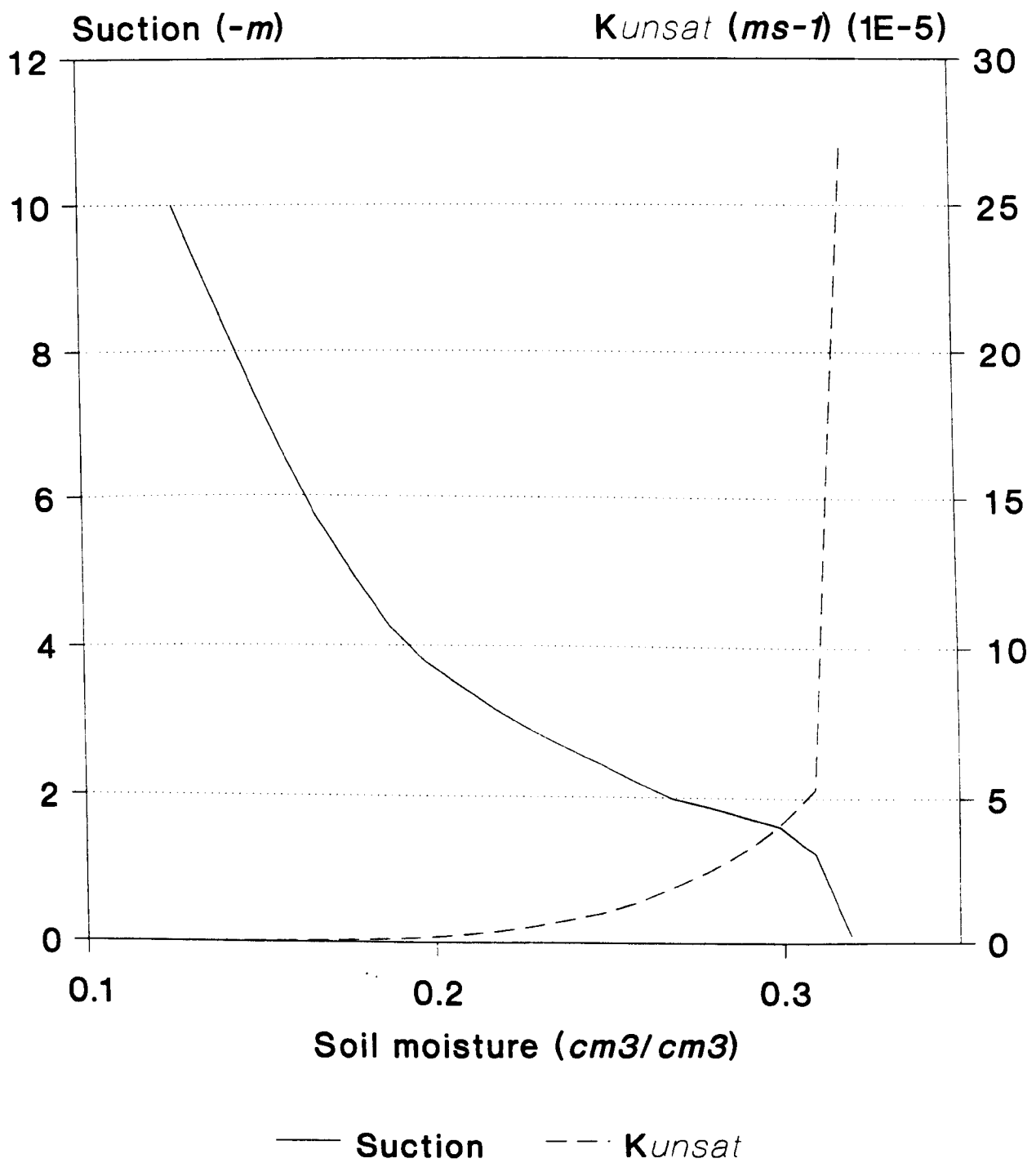

Figure 4.12: Example of a suction moisture curve and unsaturated hydraulic conductivities derived using the Millington-Quirk method

Kunze (1968) and Jackson (1972) have suggested that P=1 is a more realistic value, and this is used in *VSAS4*. A table of values of unsaturated hydraulic conductivities for given soil moisture contents is stored (for each soil zone) and recalled each time step to give the unsaturated hydraulic conductivity for each element centre. Where the moisture content falls between values in the table a linear interpolation is carried out.

4.3.1.7 Computational structure

VSAS4 operates under a system whereby each segment is considered an entirely separate hydrological unit. Rainfall is read in as hourly values prior to the simulation starting (i.e. the complete storm is stored in memory) and the model computes the flows into and out of each segment in turn for the whole storm (see figure 4.3 for a generalised flow diagram of this structure). The hourly rainfall is divided into even increments, the size of the increments being an input value (i.e. setting the internal timestep).

All of the process representations are calculated at this internal timestep except for channel flow which is lagged or every hour. Water passing through the canopy is calculated as a volume (m^3) every timestep and then transferred to a depth (cm) per timestep in order to account for the difference in surface area between the canopy and the segment.

4.3.2 Process representation

The process representations in this section are subdivided into four subsections: rainfall partitioning; soil water flow; overland flow; channel flow.

4.3.2.1 Rainfall partitioning

The rainfall partitioning section of *VSAS4* is largely based upon the Rutter model (Rutter *et al* (1971)) for canopy interception. Figure 4.13 illustrates the structure and water balance components of the Rutter model for a generalised canopy. The major difference is that the scale of computation has been changed from canopy to leaf and stem scale to take advantage of the three dimensional canopy generated as part of the model.

Rainfall partitioning can be divided into four individual parts that are calculated separately within *VSAS4*. These are:

- Direct throughfall (rainfall falling between tree crowns to the soil surface)
- Free throughfall (rainfall draining from a canopy layer and falling directly to the soil surface i.e. not draining to the next layer but falling

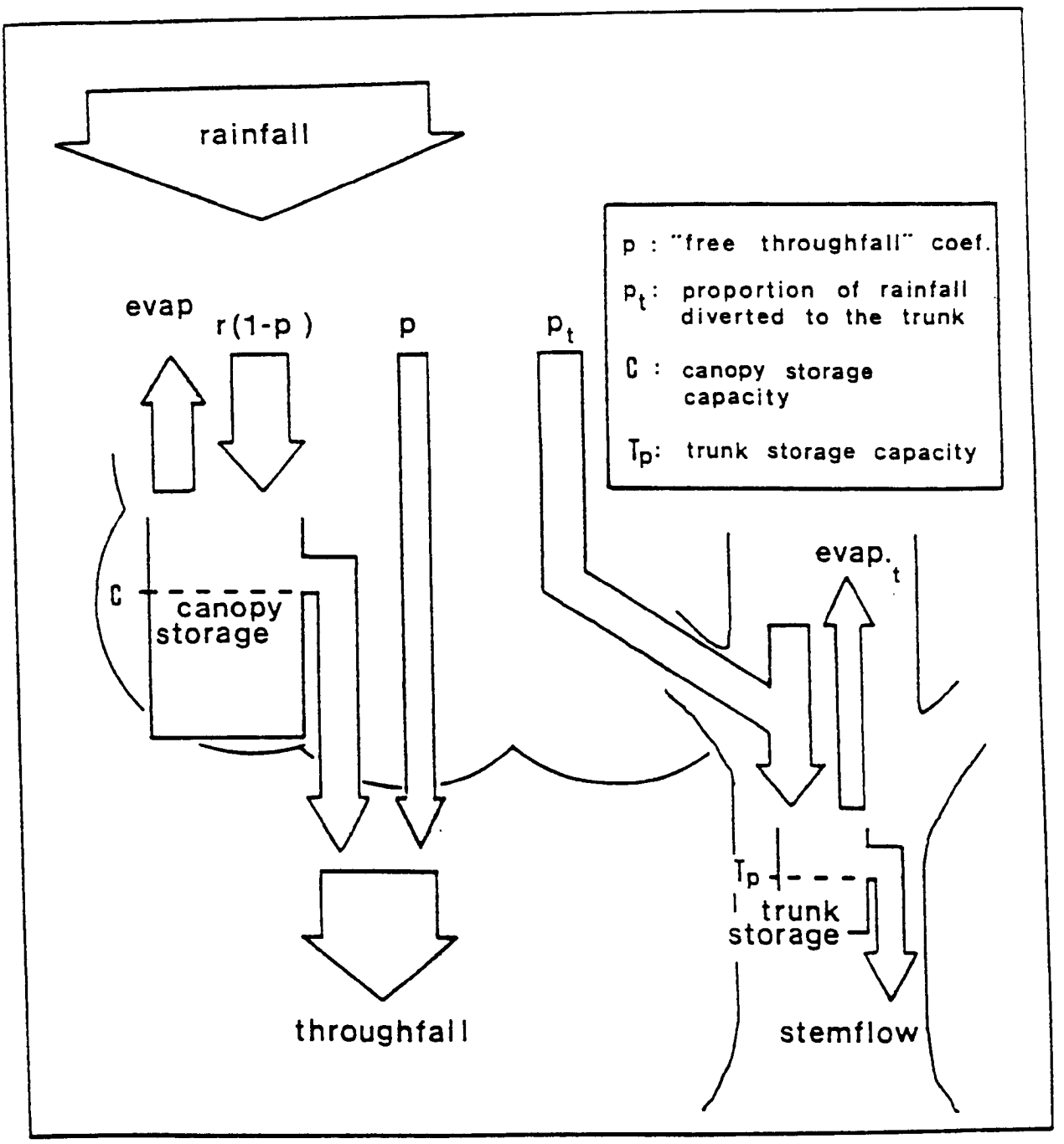

Figure 4.13: Structure and water balance components of the Rutter interception model (Durocher (1991))

through gaps within it†)

- Indirect throughfall (the remainder of rainfall, after direct and free throughfall, that drains sequentially down through the canopy layers until it reaches the soil surface. N.B. The water stored (storage) on each layer is available for evaporation)
- Stemflow

Each of these parts of rainfall partitioning are calculated separately within a timestep and the volumes reaching the soil surface through each of them is totalled as net rainfall below the canopy.

Direct throughfall

To calculate the amount of direct throughfall it is necessary to find the proportion of gap area in each triangle. A Delauney triangle represents the area in between tree crown centres, so that the between gap area is an inherent function of each one (see equation 4.8).

$$Bgap_t = \begin{cases} A_t - \sum_{x=1}^{3} CPA_i & (Bgap_t > 0) \\ 0 & (Bgap_t \leq 0) \end{cases} \qquad (4.8)$$

$Bgap_t$ = Gap area between crowns in a triangle t

Free throughfall

The within crown gap area is given by the probability that a raindrop is intercepted by no leaf layers within a triangle (see equation 4.9). Equation 4.9 is equation 4.4 rewritten with n=0.

$$Wgap = (1-x)\, e^{-[LAI_t\, G(\theta)]} \qquad (4.9)$$

Wgap = Within crown gap area

Equation 4.10 combines equation 4.8 and 4.9 to give the direct throughfall coefficient per triangle as required by the Rutter model.

† The free throughfall occurring through the top canopy layer is effectively direct throughfall but is kept separate because they are calculated in a different manner.

$$f_t = \frac{Bgap_t + (Wgap_t\, CC_t)}{A_t} \quad (4.10)$$

f_t = Free throughfall coefficient per triangle *t*
CC_t = Crown cover excluding overlapping per triangle *t*

This is the proportion area of the triangle that has "holes" allowing rain to fall directly to the surface.

Indirect throughfall and storage

The calculation of indirect throughfall is an inherent part of the mass balance transfer between triangle layers. The equation for the drainage between triangle layers is again taken from the Rutter model and transferred to the triangle scale (equation 4.11). The drainage rate is a function of the depth of water stored in the triangle layer, and allows drainage to occur before the canopy reaches saturation.

$$D_l = aC_l\, e^{(bS_l / C_l)} \quad (4.11)$$

D_l = Drainage from triangle layer *l*
S_l = Storage in triangle layer *l*
C_l = Storage capacity of triangle layer *l*
a,b = Drainage coefficients

Every time water drains from a layer a certain proportion of the volume falls as direct throughfall to the soil surface. The proportion for layer *m* is calculated using equation 4.12 (with reference to equation 4.5).

$$D_l = \sum_{x=m}^{n} P'_x - \sum_{x=m+1}^{n} P'_x \quad (4.12)$$

The change of storage with respect to time for a layer is shown in equation 4.13

$$\frac{\partial S_l}{\partial t} = Q_l - aC_l e^{(bS_l/C_l)} \quad (4.13)$$

Q_l = $W_l - E_l$
W_l = Input water rate (rainfall rate for top layer)
E_l = Evaporation rate (equation 4.19)

There are three possible solutions to equation 4.13, depending on the relative values of: the water input rate minus evaporation (Q_l); the triangle layer storage (S_l); and the layer storage capacity (C_l). Equations 4.14 to 4.17 give the solutions to equation 4.13 using the notation: during a time period (Δt), the storage changes from S_1 to S_2.

Where the storage is less than the storage capacity the solution simply involves the

addition of water and subtraction of evaporation.

$$\text{when: } (S_l < C_l) \qquad S_2 = S_1 + W_l \Delta t - E_l \Delta t \tag{4.14}$$

Where the storage is greater than or equal to storage capacity *and* the water input rate is greater than zero the solution is given by equations 4.15 and 4.17.

$$\text{when: } (S_l \geq C_l \text{ and } Q_l > 0)$$
$$S_2 = C_l - \frac{C_l}{b}\left[(\ln(Q_l) + Y - \ln(Q_l - aC_l e^{(bS_1/C)} + aC_l e^{(Y)}\right] \tag{4.15}$$

where:
$$Y = aC_l(S_1 - C_l) + \frac{Q_l \Delta t\, b}{C_l} \tag{4.16}$$

Where there is no water input but the storage is still greater than the storage capacity the solution is given in equation 4.17.

$$\text{when: } (S_l \geq C_l \text{ and } Q_l \leq 0)$$
$$S_2 = C_l - \frac{C_l}{b}\left[ba\,\Delta t + e^{(-b/C_l\,(S_1 + Q_l \Delta t - C_l)}\right] \tag{4.17}$$

With the new storage calculated, the amount of drainage from a layer is calculated (indirect throughfall if it is the bottom layer) as a simple mass balance equation (equation 4.18).

$$D_l = \begin{cases} S_1 + Q_l \Delta t - S_2 & (D_l > 0) \\ 0 & (D_l \leq 0) \end{cases} \tag{4.18}$$

Evaporation from storage

Evaporation has always been ignored in previous versions of *VSAS*, the rationale being that it is a minor process to consider **during a storm event**. *INTMO* has the capability to estimate potential evaporation using the Penman-Monteith equation which is scaled down to provide evaporation at the leaf scale. To achieve this it is necessary to have measurements of four input variables (net radiation, air temperature, relative humidity, and wind speed) for whatever time step *INTMO* is running at (usually between 1-5 minutes).

The integration of *INTMO* into *VSAS4* means that the capability for evaporation calculation is retained but there are two limiting factors in its usage. The first of these is that it may be difficult to obtain the necessary temporal resolution of meteorological measurements. It may be possible in some locations to have hourly values from an automatic weather station and then divide these into smaller intervals as has been

explained previously for rainfall. The combined measurement and averaging effect error from this method make it highly questionable.

The second limiting factor in the use of the present system of evaporation calculation is that evaporation studies within upland forests (where the majority of afforestation occurs in the UK) indicate that the evaporation rate is frequently greater than the potential evaporation rates calculated using methods such as the Penman-Monteith equation (Calder (1990)). This is because Penman-Monteith assumes that the main energy source driving evaporation is solar radiation whereas in many cases advective energy (normally part of cyclonic storms) may be a larger energy source. This is not the case in all situations but is an important consideration when deciding whether to include the evaporation component of *INTMO* into the *VSAS4* structure.

It is intended to use *VSAS4* as an event based simulator and maintain a simple potential evaporation value. This value may be constant which ignores any temporal variation in evaporation that occurs within a storm period or could be Penman-Monteith values derived from nearby and simply read as input (if these data are available). The full Penman-Monteith version of evaporation can be easily reinstated at a later date if it proves necessary.

Taking the potential evaporation value per timestep described above, this is transformed into actual evaporation in the manner shown in equations 4.19 and 4.20. This assumes that the evaporation is constant throughout the canopy.

$$E_l = E/LAI_t \tag{4.19}$$

where:

$$E = \begin{cases} E_p & (S_l \geq C_l) \\ E_p C_l/S_l & (S_l < C_l) \end{cases} \tag{4.20}$$

E_p = Potential evaporation

Equation 4.19 is only valid when $LAI_t \geq 1$. Where $LAI_t < 1$, the evaporation rate is reduced according to the gap area (equation 4.8).

Within a simulation timestep the amount of evaporation possible from each Delauney triangle layer is calculated and that volume removed from any storage. The drainage from that layer is then calculated in the manner described above (see equation 4.18) and any remaining water is held by the layer as canopy storage until the next timestep.

Stemflow

The computation of stemflow is very similar to the treatment of throughfall, the major difference is that it is computed at the individual tree scale rather than at a Delauney

triangle scale.

In the canopy generation part of *VSAS4* each tree is randomly assigned (from a restricted log-normal distribution) a proportion of its canopy surface area which generates stemflow and the *SAI* is calculated. Each tree has a vertical series of stem layers, the actual number per tree and the proportion area of the triangle in each layer is calculated using a modified Poisson distribution as in equations 4.2 to 4.5. These elements are treated as vertically adjacent, linear stores, the same as with throughfall. The drainage from the each stem layer does not contribute to the next layer or soil surface as in throughfall, but to the trunk layer.

The potential evaporation from the stem layers is related to the potential evaporation (equation 4.19) by an input scaling factor. The scaling factor simply sets the amount of stem potential evaporation as a proportion of the triangle potential evaporation. The actual amount of evaporation is a function of: stem storage capacity; storage; and *SAI*. This is analogous to substituting: *SAI* for *LAI* in equation 4.4; stem storage and storage capacity for leaf storage and storage capacity in equation 4.20.

It is assumed that drainage of water in excess of the stem storage capacity occurs immediately. This means there are only two possible solutions to equation 4.13 (shown in equation 4.21).

$$S_2 = \begin{cases} S_1 + W_s \Delta t - E_s \Delta t & (S_2 < C) \\ C_l & (S_2 \geq C) \end{cases} \qquad (4.21)$$

Some of the drainage will fall directly to the ground in exactly the same manner that direct throughfall occurs from leaf layer drainage in equation 4.11 The drainage from each stem layer to the trunk within a timestep is given by equation 4.18. The drainage from the trunk storage represents the stemflow per time interval.

The stemflow for a stand is calculated separately from throughfall, the area of each crown generating stemflow having already been removed from the Delauney triangles.

4.3.2.2 Soil water flow

It is assumed that all rainfall falling onto an element infiltrates the soil surface (apart from a predesignated amount to account for any impervious surfaces) and is then accounted for by either subsurface soil water flow, or saturated overland flow if the input volume is too great for the element. The rate of subsurface flow is calculated using the Richards generalisation of Darcy's law.

Darcy's law is an empirical relationship derived by Darcy (1856) relating the rate of flow of a liquid through a saturated porous medium to the hydraulic gradient (equation 4.22).

$$Q = -K_{sat} \frac{\partial z}{\partial d} A \tag{4.22}$$

Q	=	Rate of soil water flow (flux)
z	=	Height
d	=	Distance travelled
A	=	Surface area flowed through

Richards (1931) adapted this relationship to account for soil water flow in unsaturated conditions (equation 4.23).

$$q = -K(\theta)\ \Delta h \tag{4.23}$$

q	=	Water velocity (flux density = Q/A)
Δh	=	Hydraulic gradient ($\partial z/\partial d$)

The Richards equation is the basis for all subsurface water flow calculations in *VSAS4*. It is assumed that all soil elements are isotropic and no allowance is made for a capillary fringe. Water compression, air entrapment, and soil matrix deformation are assumed to be negligible.

The Richards equation is combined with the continuity equation (equation 4.24) to give an equation for soil water flow in three dimensions (equation 4.25).

$$\frac{\partial \theta}{\partial t} = \frac{\partial q}{\partial x} + \frac{\partial q}{\partial y} + \frac{\partial q}{\partial z} \tag{4.24}$$

t	=	Time
x,y,z	=	Distance in the x,y, and z dimensions

$$\frac{\partial \theta}{\partial t} = \frac{\partial}{\partial x}\left(K(\theta)_x \left[\frac{\partial \psi}{\partial x} + \frac{\partial z}{\partial x} \right] \right) + \frac{\partial}{\partial y}\left(K(\theta)_y \left[\frac{\partial \psi}{\partial y} + \frac{\partial z}{\partial y} \right] \right) + \frac{\partial}{\partial x}\left(K(\theta)_x \left[\frac{\partial \psi}{\partial x} + 1 \right] \right) \tag{4.25}$$

Equation 4.25 describes only horizontal flow along the x and y axes when in fact these may be sloping. Equation 4.26 accounts for slope by substituting x^* for $x.\cos\alpha$ and y^* for $y.\cos\beta$ (see figure 4.14).

$$\frac{\partial\theta}{\partial t} = \cos^2\alpha \frac{\partial}{\partial x^*}\left(K(\theta)_{x^*}\left[\frac{\partial H}{\partial x^*} + \frac{\partial z}{\partial x^*}\right]\right) + \cos^2 b \frac{\partial}{\partial y^*}\left(K(\theta)_{y^*}\left[\frac{\partial H}{\partial y^*} + \frac{\partial z}{\partial y^*}\right]\right) + \frac{\partial}{\partial z}\left(K(\theta)_{x^*}\left[\frac{\partial H}{\partial z} + 1\right]\right) \quad (4.26)$$

$$H = \psi(\theta) + h$$

Equation 4.26 is the flow equation solved numerically in *VSAS4* using a block centred finite difference scheme. The smooth function representing the change in moisture content over time and space is approximated by linear sections over finite time and space increments. Figure 4.14 shows the flow directions through an element within a timestep. The equation for numerical solution of flow through an element is shown in equation 4.27 (with reference to figure 4.14)

$$\theta_{t+\Delta t} = \theta_t + \frac{\Delta t}{V_s}\left((V_1 - V_4) + (V_2 - V_5) + (V_3 - V_6)\right) \quad (4.27)$$

V_s = Soil element volume
$V_{1\text{-}6}$ = Soil water flow volume in direction shown in figure 4.14

This can be expanded to give the full equation of flow through an unsaturated soil element in three dimensions (equation 4.28) which is solved sequentially (slopewise, lateral, then vertical flows) to represent soil water flow in a three dimensional manner.

The values of K(θ) are obtained from the Millington-Quirk method described in section 4.3.1.6. Areas, volumes of the element and adjoining elements, and surface areas between them are obtained from the soil mantle geometry subroutine (*BLKVOL*).

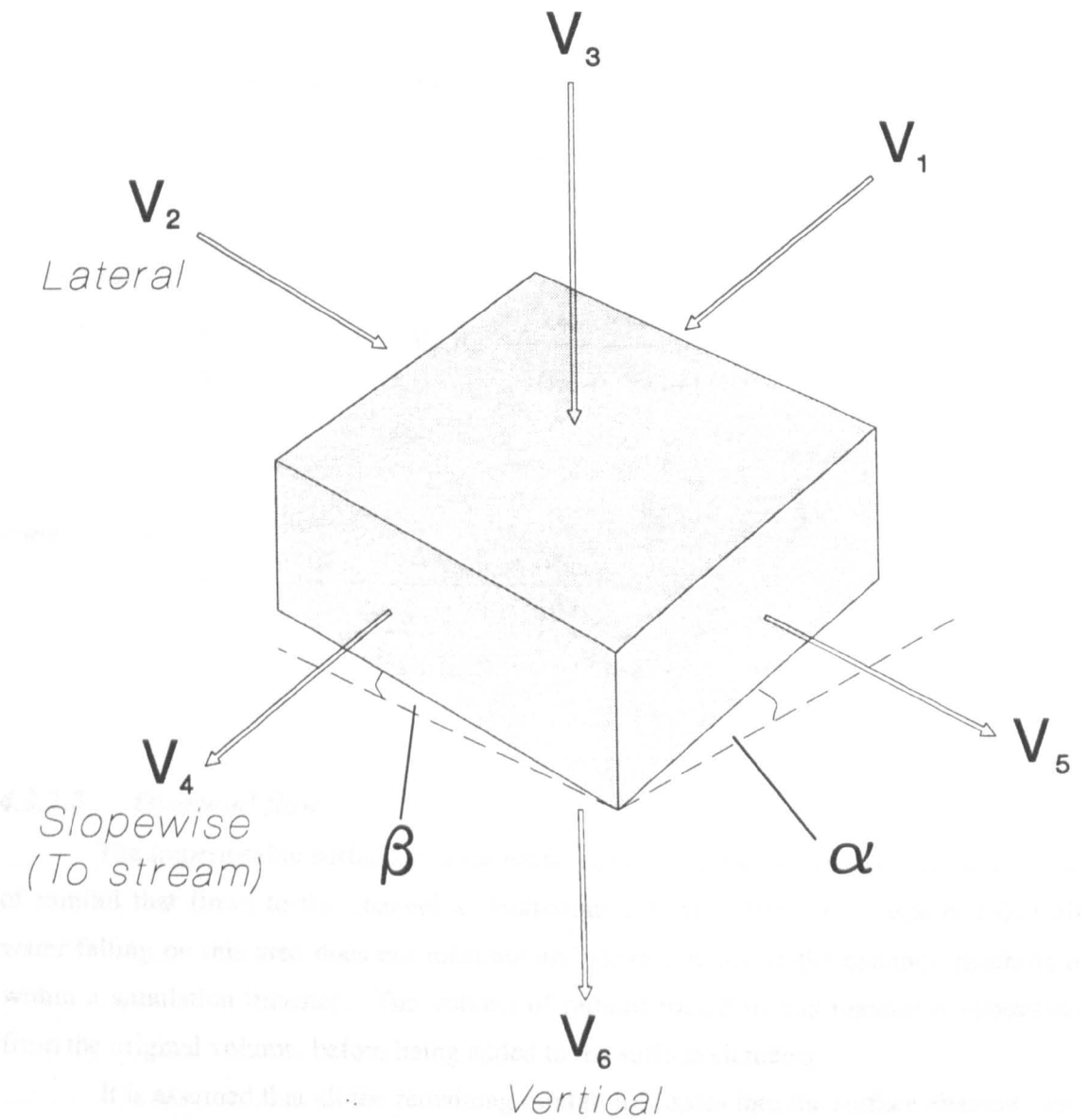

Figure 4.14: Soil water flow directions through an idealised soil element

$$\theta^{t+\Delta t}_{k,n,j} = \theta^{t}_{k,n,j} \quad \frac{\Delta t}{V} \left(\cos\alpha \left[\bar{K}_1 A_1 \frac{(\psi^{t}_{k,n+1,j} - \psi_{k,n,j} + z_{k,n+1,j} - z_{k,n,j})}{x_{k,n+1,j} - x_{k,n,j}} \right] \right.$$

$$- \cos\alpha \left[\bar{K}_4 A_4 \frac{(\psi^{t}_{k,n,j} - \psi_{k,n-1,j} + z_{k,n,j} - z_{k,n-1,j})}{x_{k,n,j} - x_{k,n-1,j}} \right]$$

Lateral

$$\left\{ + \cos\beta \left[\bar{K}_2 A_2 \frac{(\psi^{t}_{k+1,n,j} - \psi_{k,n,j} + z_{k+1,n,j} - z_{k,n,j})}{x_{k+1,n,j} - x_{k,n,j}} \right] \right.$$

$$\left. - \cos\beta \left[\bar{K}_5 A_5 \frac{(\psi^{t}_{k,n,j} - \psi_{k-1,n,j} + z_{k,n,j} - z_{k-1,n,j})}{x_{k,n,j} - x_{k-1,n,j}} \right] \right\} \qquad (4.28)$$

Vertical

$$\left\{ + \left[\bar{K}_3 A_3 \frac{(\psi^{t}_{k,n,j+1} - \psi_{k,n,j})}{z_{k,n,j+1} - z_{k,n,j}} + 1 \right] \right.$$

$$\left. - \left[\bar{K}_6 A_6 \frac{(\psi^{t}_{k,n,j} - \psi_{k,n,j-1})}{z_{k,n,j+1} - z_{k,n,j-1}} + 1 \right] \right) \left. \right\}$$

where:

$$K_1 = \frac{\Delta x_{k,n+1,j} + \Delta x_{k,n,j}}{\left[\frac{\Delta x_{k,n+1,j}}{K(\theta^{t}_{k,n+1,j})} \right] + \left[\frac{\Delta x_{k,n,j}}{K(\theta^{t}_{k,n,j})} \right]} \qquad (4.29)$$

4.3.2.3 Overland flow

The impermeable surface area for each segment is input to calculate the proportion of rainfall that flows to the channel as Hortonian overland flow. It is assumed that all water falling on this area does not infiltrate and flows directly to the channel, reaching it within a simulation timestep. The volume of rainfall routed in this manner is subtracted from the original volume, before being added to the surface elements.

It is assumed that all the remaining rainfall infiltrates into the surface elements and is available for soil matrix flow. If the volume of water entering a surface element (either rainfall or flow from an adjacent element) is too great for the soil storage, the excess water is routed downslope, filling any unsaturated surface elements until the channel is reached. The final amount of this saturated overland flow is added to the direct runoff and subsurface contributions to channel flow.

4.3.2.4 Channel flow

The area of channel within a subsegment is input and any rainfall falling on this is treated in exactly the same manner as Hortonian overland flow.

Channel flows are accumulated for each segment per hour, and are lagged according to the estimated time of travel from each segment to the basin outlet (input value). This involves passing a proportion of a given hours flow to the following hour. The flows from each segment are accumulated to give the final outflow hydrograph.

4.4 Initial testing of VSAS4

Before proceeding with the construction of a model transforming the *VSAS4* input parameters to represent vegetation change, an initial comparison of the *VSAS4* and *VSAS3* performance at rainfall partitioning was performed.

During the coupling of *VSAS3* and *INTMO* it was found that one of the main factors contributing to *VSAS3* attenuation of the recession limb of a storm hydrograph was by continuing to add small amounts of water onto the segment surface long after a storm had finished. This is a result of the way the conceptual tank drains after the above canopy rainfall finished. When this was changed the recession limb of a storm event had considerably less attenuation. It is entirely possible that the attenuation of rainfall input by a forest canopy does affect the recession limb of a hydrograph but the amount of difference discovered when the new rainfall partitioning section was installed suggests that there was an over reliance upon the logarithmic canopy drainage to simulate this process which is normally attributed to soil drainage. The discrepancy between adequate model prediction and the deviation away from the intended method by which the model achieves those results seriously undermines the validity of *VSAS3*.

To test the capability of *VSAS4* in partitioning rainfall and predicting the below canopy rainfall four hypothetical storms were simulated, each representing a different type of storm that might be encountered. Each storm had the same volume of rainfall, only the intensity being varied between them. The four storms can be described as:

- Slowly rising to a high rainfall as in a gradually developing storm
- Initially high rainfall tailing off slowly as when a frontal system storm occurs
- High intensity rainfall with no tail off as in a violent summer storm
- Steady medium intensity rainfall throughout the period as in many winter storms

Subdivision of hour (i.e. internal timestep)	
Number of segments in catchment	
Number of subsegments within each segment	
Length of each subsegment (see figure 4.9)	(m)
Four corner coordinates of each subsegment (x,y)	(m)
Impervious area within subsegment	(m^2)
Channel area within subsegment	(m^2)
Lag time between segment and catchment boundary	$(min.)$
Offset for flow between skewed subsegments (see figure 4.9)	(m)
Number of increments upslope per subsegment (N)	
Elevation of the centre point of each increment per subsegment	(m)
Distance from channel boundary of each increment per subsegment (d_n)	(m)
Soil depth of each increment per subsegment	(m)
Number of elements per increment (number of soil layers)	
Depth of top element per increment	(m)
Proportion of remaining depth for each element per increment	
Proportion of stone content per element	
Position up slope to top of soil zones properties	*(% of total slope length)*
Number of points on the suction moisture curve (*nsmc*)	
Standard deviation of moisture contents on the suction moisture curve	
Moisture content (θ_i, $i = 1 \rightarrow nsmc$)	*(unit %)*
Soil suction (ψ_j, $j = 1 \rightarrow nsmc$)	(m)
Saturated moisture content (θ_{sat})	*(unit %)*
Standard deviation of the saturated moisture content	
Saturated hydraulic conductivity (K_{sat})	(ms^{-1})
Standard deviation of the saturated hydraulic conductivity	
Pattern parameters for Poisson distribution (leaf, and stem clustering) (γ)	
Mean leaf area index (full leaf) of tree species (*LAI*)	

Table 4.2: Input parameters for *VSAS4*

Mean proportion of crown projected area generating stemflow (p_i)	
Standard deviation of stemflow proportion	
Maximum and minimum value of stemflow proportion	
Storage capacity per leaf layer (S_l)	(m)
Storage capacity per stem layer (S_s)	(m)
Trunk storage capacity (S_t)	(m)
Drainage coefficients (a)	
Drainage coefficient (b)	(min^{-1})
Vector of Julian days of change for time varying parameters	
Vector of leaf area index variation	
Vector of stemflow proportion variation	

Table 4.2 (continued): Input parameters for *VSAS4*

All of these storms were run for both winter and summer in a deciduous canopy. The deciduous canopy parameters were those derived by Durocher (1991) for the Leigh woods near Bristol. The below canopy rainfall from *VSAS3* and *VSAS4* was extracted as output from all four storms and is shown in figures 4.15 to 4.17.

Figures 4.14 to 4.16 show that there are four marked differences between the output from the model versions. The first is that *VSAS4* presents a much smoother time series plot than *VSAS3*. Figure 4.17 is an enlargement of the first storm (during summer), to show this in more detail. This is a result of the greater flexibility in ability to respond to a change in rainfall intensity, whether that be a decrease or an increase, in *VSAS4*. This is particularly evident in the summer when the canopy is in full leaf. The attenuation of change in rainfall intensity is what might be expected from a canopy, especially when in full leaf.

The second major difference is that in all storms *VSAS3* takes longer to reach the full rainfall intensity (never reaching it in storm two), but once reached it then matches above canopy rainfall exactly until the storm ends. At the onset of a storm *VSAS3* has to fill a "conceptual tank"; when this tank is full all further rain is routed directly to the surface. In contrast *VSAS4* immediately lets some rainfall reach the surface as direct throughfall, and fills the canopy time step by time step with the remainder. This means that *VSAS4* treats every change in rainfall intensity in the same way while *VSAS3* places considerable emphasis on whether the intensity change occurs at the start or elsewhere of a storm.

The third difference between the model versions output is that *VSAS3* continues to drain water from the canopy for longer after the storm has finished. This is a result of the

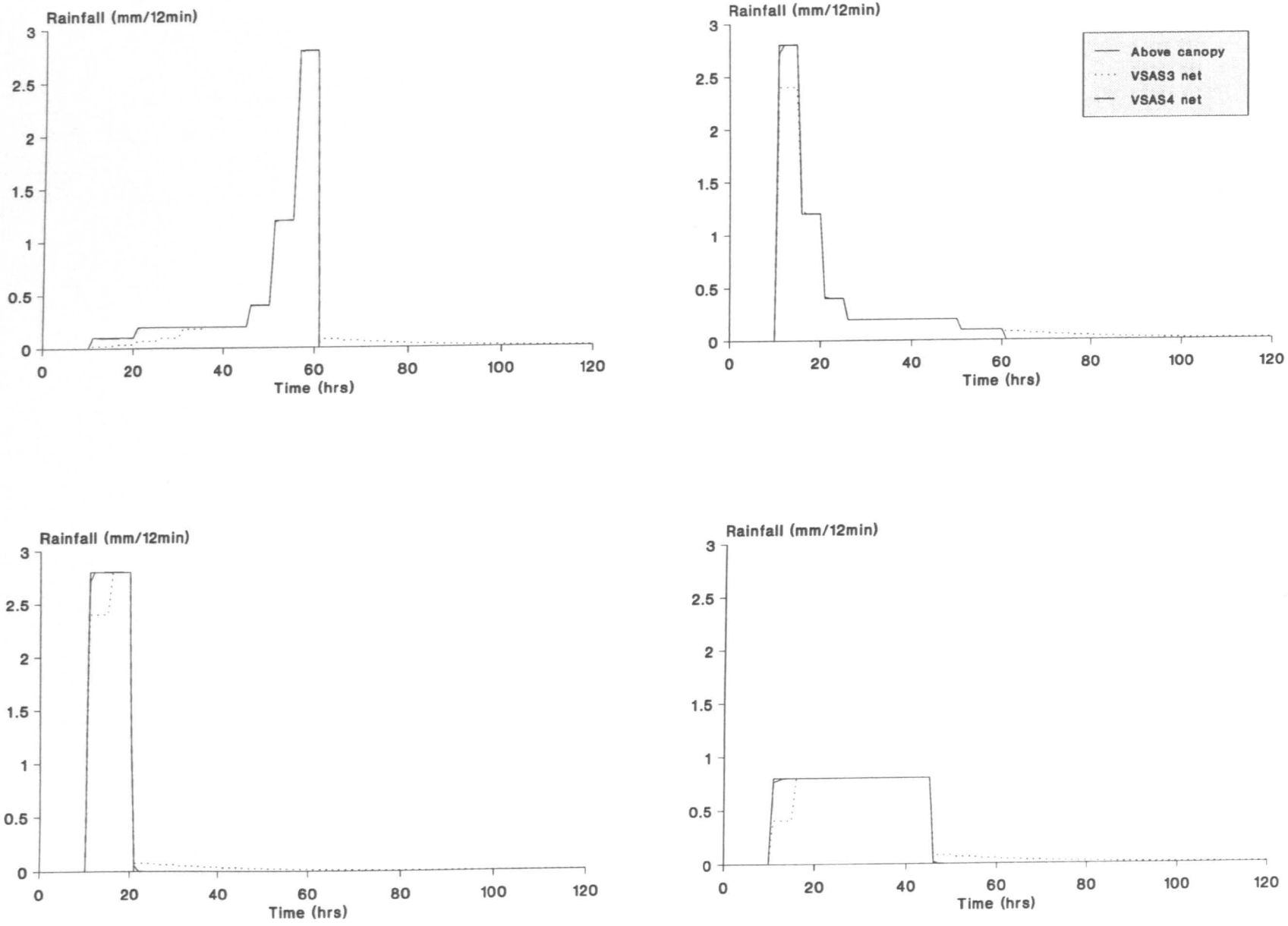

Figure 4.15: Above canopy rainfall and simulated below canopy rainfall for *VSAS3* and *VSAS4* rainfall partitioning routines. 4 storms simulated during winter

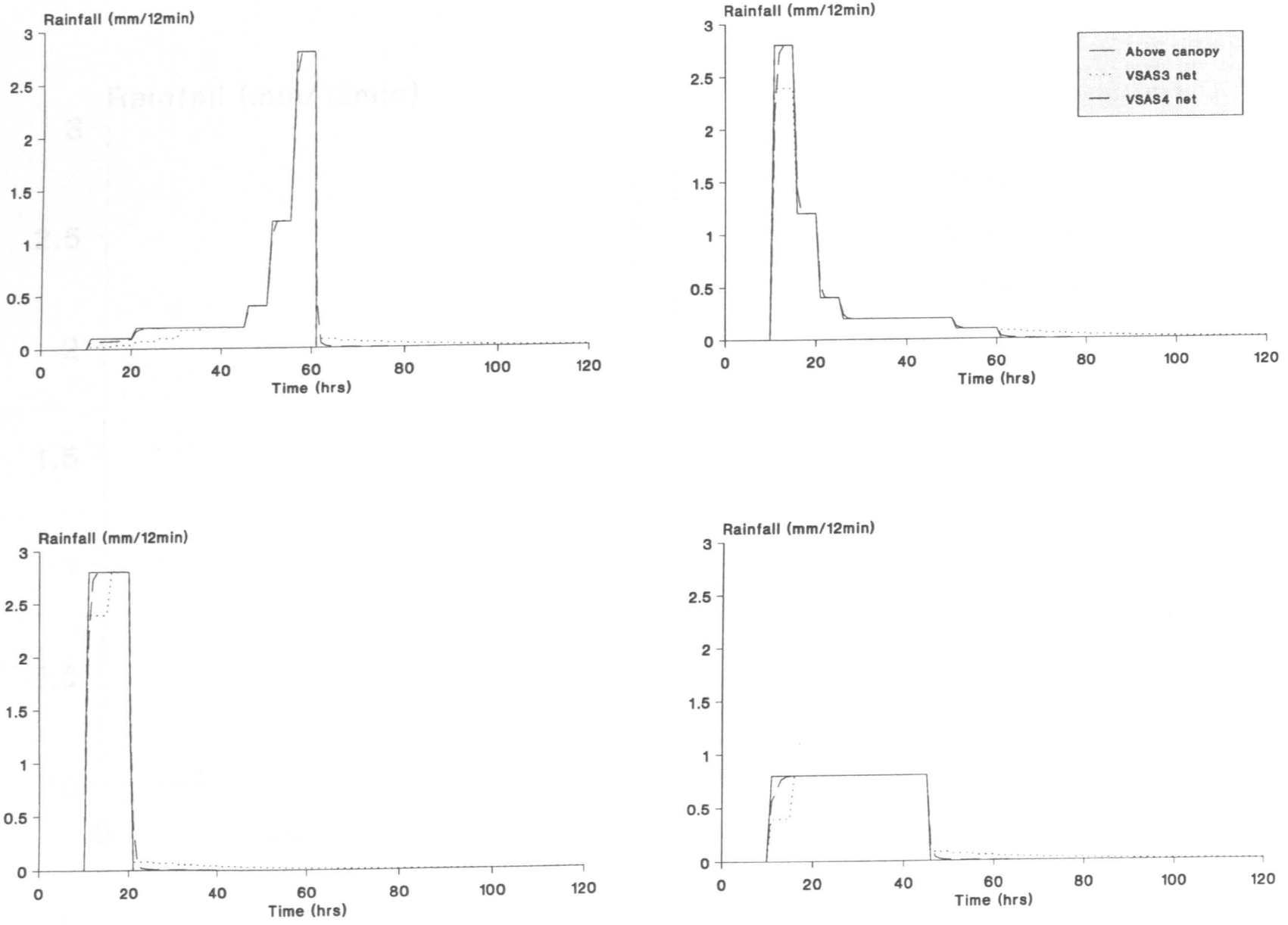

Figure 4.16: Above canopy rainfall and simulated below canopy rainfall for *VSAS3* and *VSAS4* rainfall partitioning routines. 4 storms simulated during summer

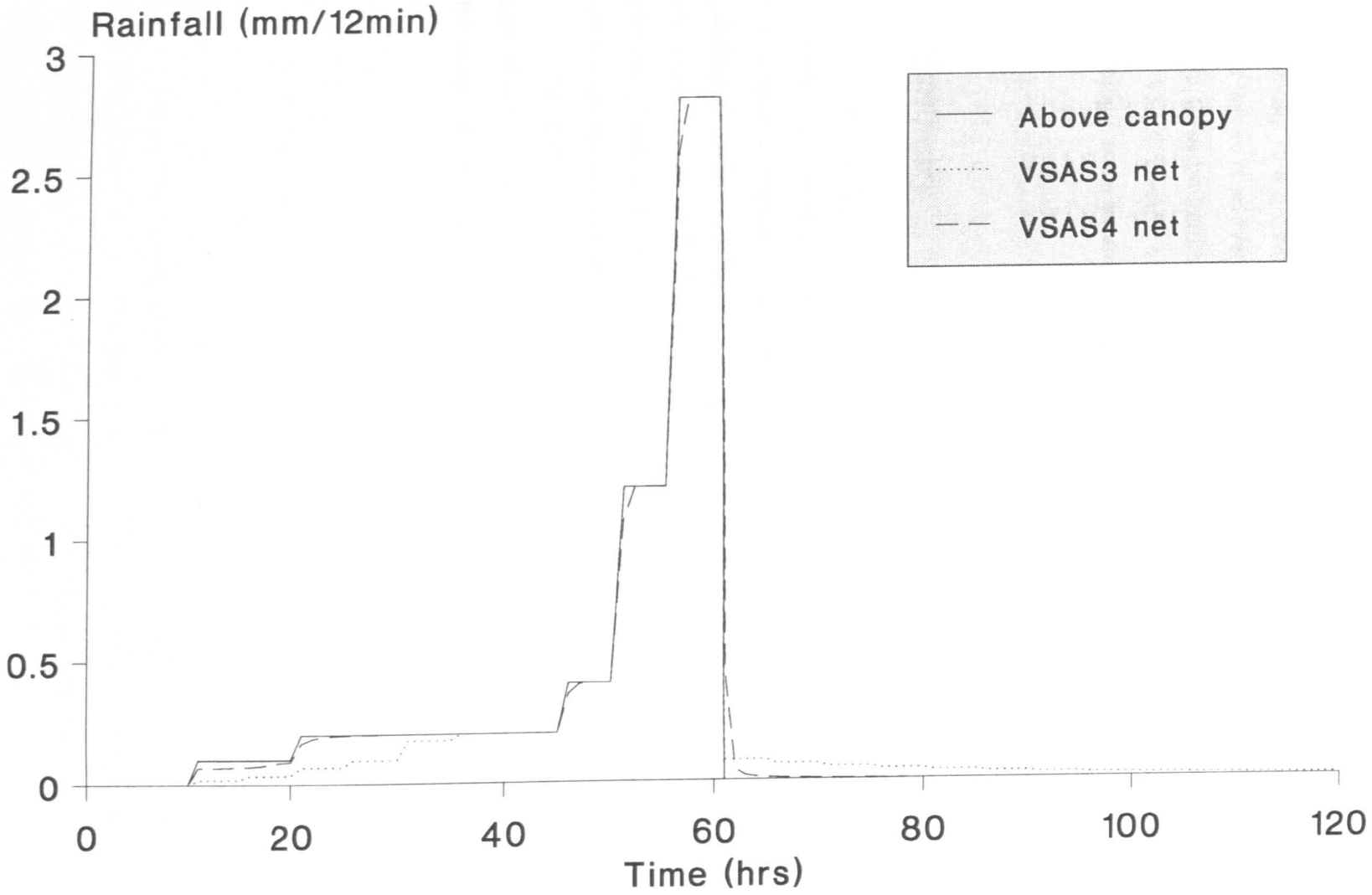

Figure 4.17: Above canopy and simulated below canopy rainfall for *VSAS3* and *VSAS4* rainfall partitioning routines. First summer storm (figure 4.16a) enlarged

logarithmic draining function which attenuates the canopy drainage and consequently the resultant runoff (see above).

The last major difference is that *VSAS4* distinguishes between a summer and winter canopy to a greater degree. This is important for simulation within a deciduous forest but less so in an evergreen coniferous forest.

In these preliminary tests of *VSAS4* the rainfall partitioning is an improvement upon the *VSAS3* version, showing greater flexibility, a more realistic attenuation of rainfall by the canopy, and a greater differentiation between seasons.

4.5 Summary

A new model has been constructed to act as a hydrological storm event simulator in a modelling scheme designed especially to investigate the hydrological effects of long term vegetation change. The new model is an integration of two previously separate hydrological models: a hillslope hydrology model (*VSAS3*) and three dimensional rainfall partitioning model (*INTMO*). The new model (*VSAS4*) is an integration of the rainfall partitioning section into the *VSAS* structure to give a physically based, distributed model with special emphasis placed on soil and canopy hydrology.

The following chapter describes the construction of the model used to transform some of the *VSAS4* input parameters in order to provide a total scheme that is predictive and temporally dynamic.

CHAPTER 5

PARAMETERISATION OF VEGETATION CHANGE WITHIN THE OVERALL MODELLING SCHEME (LUCAS)

Chapter four has described the physically based, distributed model (*VSAS4*) constructed for this study. This represents the first phase of the development of a modelling scheme tailor-made for investigating the hydrological effects of long term vegetation change in a predictive sense. This chapter concerns the second phase of the modelling scheme, that of transforming input parameters through modelling algorithms to represent the gradual change in parameters that occurs during a period of afforestation.

5.1 Introduction

The hydrological model detailed in chapter four has deliberately focussed its physical basis on two process representations: soil water flow and rainfall partitioning. The reasoning behind this decision has been explained in section 4.1 where the major hydrological processes were reviewed with respect to their importance in the field of long term vegetation change. Because this is a first attempt at developing a modelling scheme specifically designed to investigate long term vegetation change, the hydrological model has been simplified to simulate storm flows only.

The two process representations with a physical basis have input parameters capable of transformation over time. This means that they can be transformed in some manner to represent the change in parameters with the growth of a forest. To develop a model that accounts for this transformation the way these governing parameters can change must be well understood. In the case of rainfall partitioning Durocher (1991) found that the four main factors governing rainfall partitioning are:

- Distribution of tree crowns
- Distribution of tree species
- Extent of the understorey layer
- Stemflow variation per tree.

These properties can be modelled by a forest growth model thereby producing a temporally dynamic canopy structure to fit into the *VSAS4* rainfall partitioning section.

The change in soil properties that accompany afforestation are more difficult to quantify. The parameters used within *VSAS4* that might be expected to change as a forest grows above the soil mantle are the saturated hydraulic conductivity, porosity, and the suction moisture relationship. Apart from the deliberately induced hydrological changes from practices such as pre-planting ploughing these parameters will gradually change as a result of tree root development and different bioactivity. There have been numerous studies looking at the impacts of agricultural practices on soil water properties (e.g. Rawls & Brakensiek (1985)) but no work could be found relating these properties to forestry or to some measure of forest growth. This is in part due to the fact that soil water properties are notoriously hard to quantify due to the extreme degree of spatial heterogeneity that can be observed in the field, therefore it is not possible to try and generalise enough to be able to develop transforming algorithms. As a result of the lack of process knowledge on how soil properties change with afforestation this change has been assumed unimportant in this study. It is acknowledged that this may be a shortcoming of the modelling scheme but a study investigating this would form a very large project in itself and it is beyond the scope of this study. Once the modelling scheme has been developed, this may form an area for further investigation.

The remainder of this chapter concerns the transformation of input parameters used by the rainfall partitioning section of *VSAS4* with separate modelling algorithms. The structure of the three dimensional rainfall partitioning section of *VSAS4* is ideal for investigating afforestation as it allows ready adjustment of forest parameters to simulate a canopy growth. There are two possible methods of representing afforestation as part of a modelling scheme utilising *VSAS4*. These are:

- Transforming the input parameters by a simple known algorithm to represent forest growth
- Using a separate set of input parameters in a separate model generating the necessary inputs for *VSAS4* at different stages of forest growth.

These options are shown in figure 5.1 together with measuring the change in input parameters. Measurement has already been discounted in chapter two as it does not allow for predictive assessment of the impacts of long term vegetation change; therefore only the bottom two options shown in figure 5.1 are discussed here.

A simple transformation of the input parameters requires a long term monitoring of a canopy, although it need not be within the catchment under study. This would require the assumption that if a parameter changes with time in a certain manner at one location, the same relationship can be used to transform the same parameter at another location i.e.

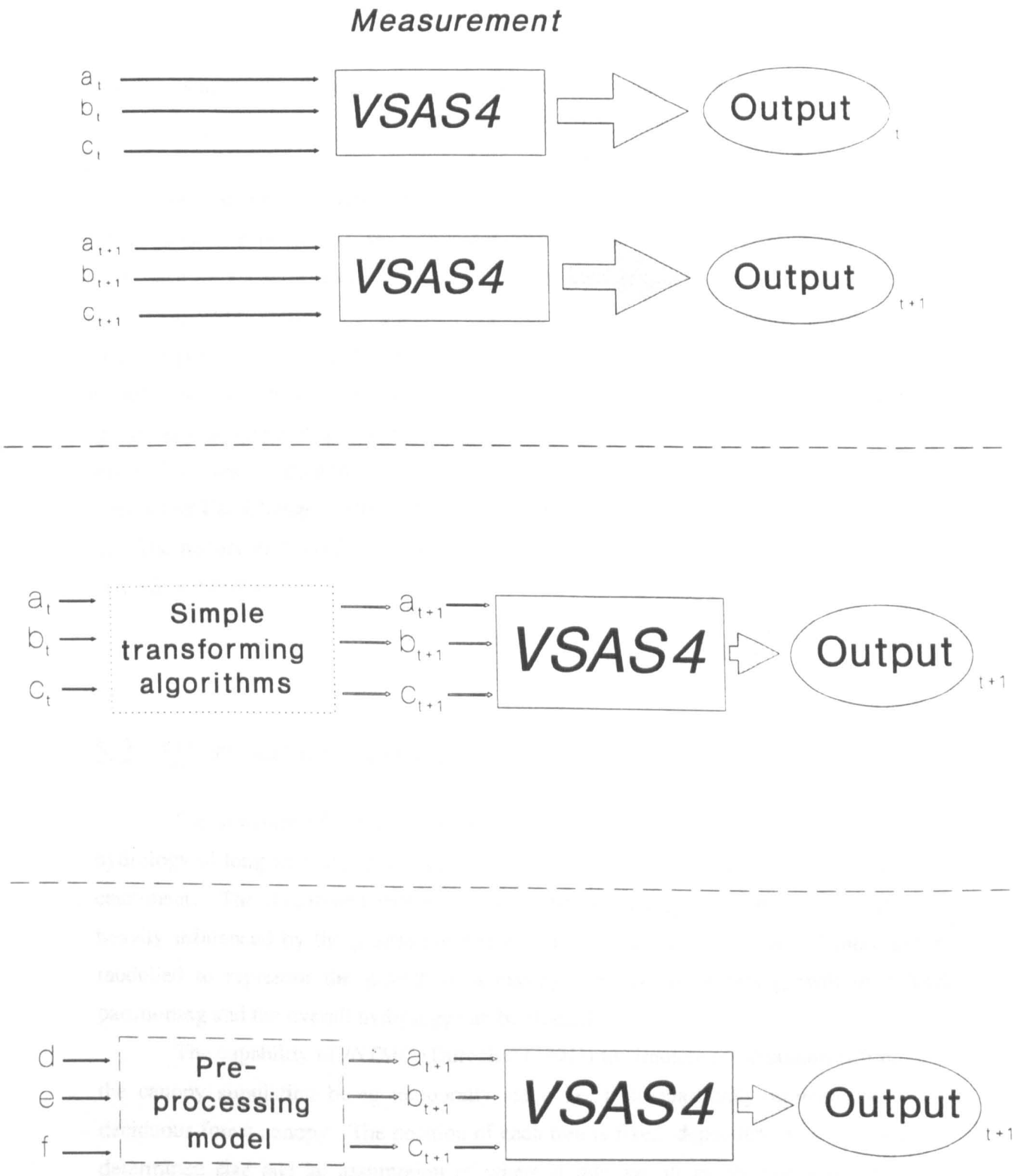

Figure 5.1: Options for transformation of physically based input parameters

transferable in space. This is a reasonable assumption if the controlling conditions (e.g. underlying geology; climate etc.) are the same between locations, and there is no other way of estimating the parameter.

The third option shown figure 5.1 is to have a pre-processor model that uses entirely separate input parameters to derive the required input parameters for *VSAS4*. The pre-processing model should ideally use input variables that are directly measurable and produce output that can be independently validated before being accepted as input parameters for *VSAS4*.

Both of the modelling options shown in figure 5.1 have been pursued for various canopy structural properties, the remainder of this chapter details the form of modelling used. Section 5.2 concerns a forest growth model capable of acting entirely independently of *VSAS4*, while section 5.3 describes the transformation of other input parameters by simple algorithm. Section 5.4 describes the integration of *VSAS4* with the forest growth model described in section 5.2 into the first version of the total modelling scheme specifically designed to investigate the hydrological effects of afforestation in a predictive sense. The overall modelling scheme (*VSAS4* plus the forest growth model) is given the name Land Use Change, Afforestation, Simulator (*LUCAS*) which is used in text from now on. The history and terminology of the different *VSAS* versions and the development of *LUCAS* is shown in figure 5.2.

5.2 Afforestation simulator

The structure of *VSAS4* provides an ideal platform to investigate the affects on hydrology of long term changes in canopy structure such as the growth of a forest within a catchment. The distributed nature of the controlling canopy parameters in *VSAS4* are heavily influenced by the position and size of trees forming the canopy. If these can be modelled to represent the growth of a canopy, the effects of this growth on rainfall partitioning and the overall hydrology can be studied.

The capability of *INTMO* (Durocher (1991)) to simulate afforestation is limited by the canopy simulation being temporally static i.e. it stochastically simulates a *mature* deciduous forest canopy. The position of each tree is fixed, dependent on a stochastically determined size and an assumption of where it may be, given its size and the size of competitors. The model was developed for simulating rainfall partitioning in small deciduous plantations and has proved adequate for this, but has no potential to simulate a change in forest structure with time.

By focussing on designing a model capable of simulating forest growth to provide

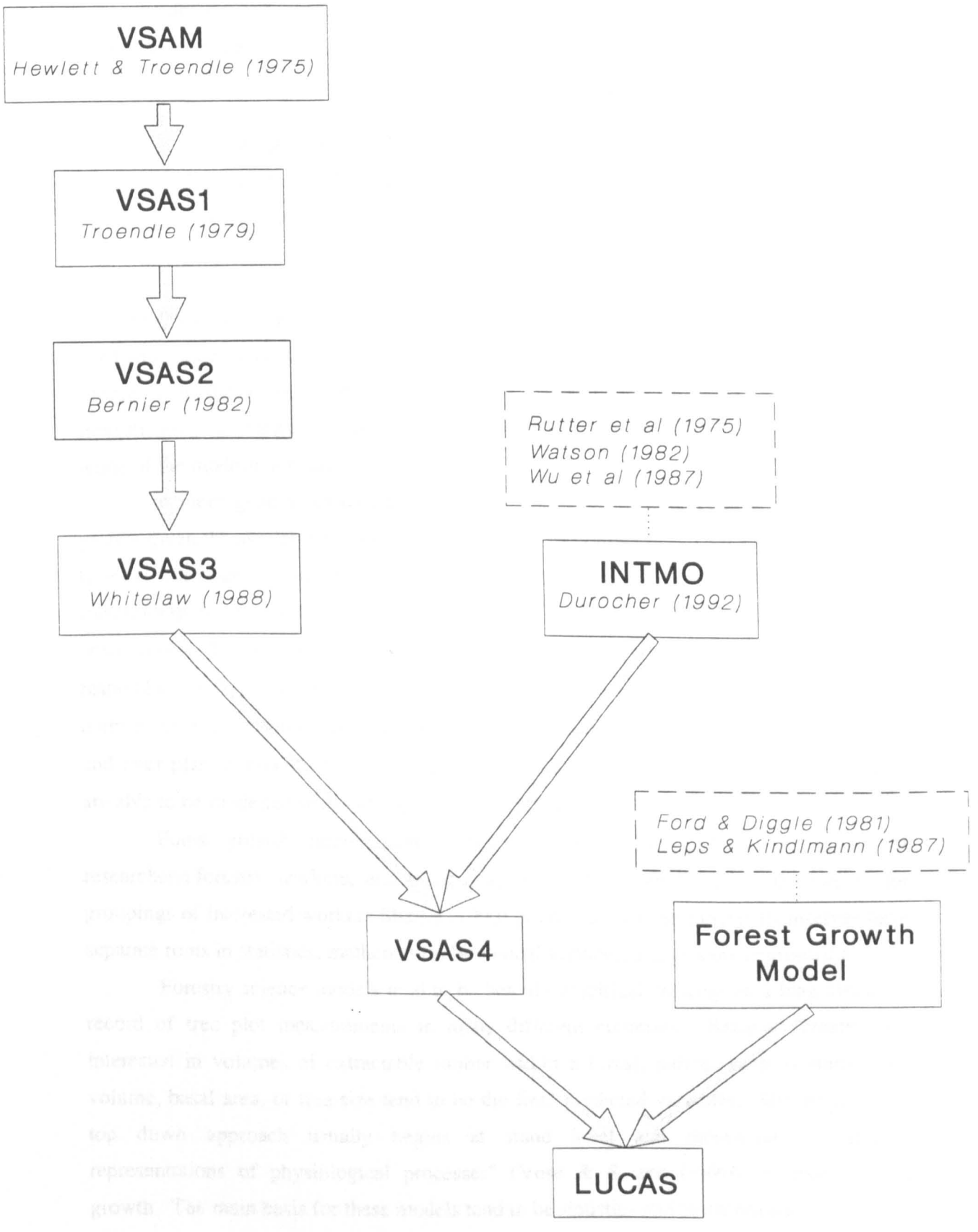

Figure 5.2: History of different *VSAS* versions and subsequent amalgamation into *LUCAS*

input for *VSAS4*, it should be possible to investigate the effect on a catchment of various storms for different stages of a forests growth.

In attempting to model the growth of a tree, numerous interacting processes need to be considered. At the most basic level Mohren & Rabbinge (1990) describe tree growth in the following manner:

> Tree growth is the outcome of a series of physical, biochemical, and physiological processes in which, driven by solar radiation, carbon dioxide from the air is assimilated by the foliage, and the carbohydrates produced by the photosynthetic process are converted into the structural dry matter of the living plant. (p229)

As with the modelling of many natural processes the complex interaction of "physical, biochemical, and physiological processes" is not fully understood, and consequently each attempt to model a trees growth is a necessary simplification of reality. The degree of simplification of reality in simulating these two factors is dependent on the nature and scope of the modelling study.

In more general terms the factors needing to be modelled are a trees potential growth given the available resources, and the effect of competition from surrounding trees. It is a fundamental concept of plant ecology that a plant grown in a plot with no surrounding plants grows at a faster rate than a plant in a similar plot surrounded by competitors. The single plant should grow at the potential growth rate for the available resources. The plants in the other plot have to share the natural resources between themselves and consequently *compete* for sunlight, water, minerals etc. Potential growth and inter plant competition can be quantified from plant measurements and consequently are able to be modelled with varying degrees of success.

Forest growth models have in the main been developed by two groups of researchers: forestry workers, and plant ecologists. Although these are the two major groupings of interested workers Sharpe (1990) points out that the models themselves have separate roots in statistics, mathematics, biological sciences, and process engineering.

Forestry science models tend to be heavily empirical drawing on a long historical record of tree plot measurements in many different countries. Because foresters are interested in volumes of extractable timber within a forest, indices such as stem wood volume, basal area, or tree size tend to be the final predicted variables. The empirical or top down approach usually begins at stand level and incorporates "empirical representations of physiological processes" (Vose & Swank (1990)) to model forest growth. The main basis for these models tend to be statistics and mathematics.

Ecology models tend to be either highly complex attempts at simulating forest development through a very long time period (e.g. forest gap theory, see Shugart (1984)),

or extremely detailed attempts to model plant growth from a physical understanding of the processes driving photosynthesis at the leaf scale. The forest gap models have been mainly developed to predict species diversity in forests. The plant growth (often derived from small plants rather than trees) models tend to predict factors such as plant height. This approach is often termed bottom up, where models begin at the leaf scale and use physiological functions scaled up to stand scale (Vose & Swank (1990)). As might be expected the main basis for these models tends to be biological science and process engineering.

The primary emphasis of this project is on the hydrological effects of long term land use change rather than the development of a detailed forest growth model. A modelling scheme is required that is relatively simple, but still generally applicable. From the description of *VSAS4* in chapter four it can be seen that the parameters needing to be modelled relate to the size and space taken up by an individual tree within a forest canopy. Forest growth models based on forest gap theory do not simulate these parameters and have not been considered in this study. Extremely detailed ecological/biological process models, although possibly simulating the necessary parameters are too complex, and the results too unreliable, to be considered for inclusion. These type of models are useful tools for the understanding of growth processes, but lack the generality of application needed in this study.

Forestry science type models provide a compromise between generality and detail, while not being as focussed on the reality or precision of processes being modelled (Sharpe (1990)). This compromise is considered to be the best for this study, consequently forest growth models considered in the rest of this section tend to be derived from a forestry science background.

A classification of forest growth models is hazardous because, as with many modelling schemes, there is considerable overlap between modelling strategies. Munro (1974) identifies three broad modelling philosophies:

- Distance independent, where the primary unit is stand parameters
- Distance independent, where the primary unit is single tree parameters
- Distance dependent where the primary unit is single tree parameters

Bruce (1990) points out that these three categories correspond to forestry methods of measuring (untagged, remeasured plots; plots with tagged trees; and mapped plots) from which the empirical versions of these models are derived.

The first category are often called whole stand models, these treat a forest as a single unit, governing parameters being factors such as stand density or average size based on average age. Output is usually some form of wood volume per hectare. There are numerous examples of this type of model, ranging from the Forestry Commission yield

tables (Edwards & Christie (1981)) which could be described as empirical or top down, to some quite sophisticated process based stand models e.g. Mohren *et al* (1984). The actual spatial arrangement of trees within the stand is not considered important, a factor such as tree mortality for example can be modelled as a derivative of the self-thinning rule proposed by Yoda *et al* (1963) (also called Yoda's law or the -3/2 power rule) which relates size and density in even aged plant populations. Once the output has been derived it can then be distributed to individual trees either evenly or by assuming the tree population falls into a known distribution. This kind of model is of no use in this project as *VSAS4* requires the precise tree position and size to derive the three dimensional rainfall partitioning parameters.

Individual tree models, as the name suggests, treat a forest as comprised of a series of individual trees competing for space. The distance independent version, although growing each tree independently, treats a factor such as inter plant competition as being uniform throughout the stand (e.g. density dependent). Aikman & Watkinson (1980) developed an empirical model of this sort. Plants were simulated as growing individually according to a defined relationship, while competition was dependent on the overall stand density and the relative size of each tree within the total size of the stand. This category of model is of little use in this study for the same reasons as whole stand models: *VSAS4* requires the actual tree position and size to derive the three dimensional rainfall partitioning parameters.

Distance dependent, individual tree, forest growth models grow each tree as part of a forest stand, each tree competing with each other, on the basis of their absolute position. This is the type of model used to model forest growth as a pre-processor for *VSAS4* as it transforms tree size with respect to absolute tree position. Section 5.2.1 gives background and examples of various types of distance dependent, individual tree, forest growth models before describing the new forest growth model developed as part of this study.

5.2.1 Distance dependent, individual tree, forest growth models

There are two fundamental components for a forest growth model to simulate: potential tree growth; and the effect of neighbouring trees (inter tree competition). For both of these there is a large individual literature but considerably less where they are combined into a distance dependent, individual tree, forest growth model.

To simulate the potential growth of an individual plant the approach can be either deterministic (often called *process modelling* in forestry literature) or empirical. The deterministic approach attempts to model plant growth starting from the known biological processes (see the quotation from Mohren & Rabbinge (1990) at the start of section 5.2) and measurements of the fluxes that drive them. Ludlow *et al* (1990) present an example

of a deterministic, individual tree based, potential growth model. The benefits and drawbacks of the deterministic plant growth modelling approach has many similarities to physically based, distributed, hydrological models described in chapter 2. The benefits are: that once developed the model should be applicable to all situations; and they use physically measurable input parameters. The drawbacks are: that process interaction is probably too complex for the physical equations driving the model; and similarly the scale of representation may be different from the scale the equation was developed for.

A recent study by Briggs & Wickramasinghe (1990) attempted to by-pass the photosynthetic modelling stage by investigating the relationship between potential evapotranspiration during the growing season and tree growth. Briggs & Wickramasinghe (1990) conclude that their model in it s reported form "can explain approximately 60% of variation in annual volume increment and about 50% of the variation in annual basal area increment". Their approach was considered for this study because of it s linkage between hydrology and ecology but was not pursued because the final results seemed not to justify the considerable computational complexity. Their work does present an interesting linkage between hydrology and ecology that deserves further investigation.

The simplest empirical approach to modelling potential plant growth is to measure a size parameter over time and determine relationships between the change in size and other observable variables (Bruce (1990)). This approach can be incorporated in a model structure by a process of curve fitting to empirical data or by assuming that the growth happens in a manner described by a certain predetermined curve. Richards (1959) considers three curves (monomolecular, autocatalytic or logistic, and Gompertz) as possible growth functions. Hunt (1982) contains a fuller and more recent summary of different plant growth curves.

The main emphasis of this study is on modelling the hydrological effects of long term vegetation change; consequently it was decided that detailed deterministic modelling of potential tree growth was not an appropriate part of the study. The computational effort involved in trying to dovetail a heavily theoretical biological modelling approach into a hydrological study is beyond the scope of this project. Consequently it was decided to concentrate on the simpler empirical approach to plant potential growth modelling.

Once the method for simulating potential tree growth has been chosen it is then a question of deciding which method of representing inter-tree competition is to be used. This involves the derivation of an index to quantify the amount of competitive stress on an individual plant. The competitive stress a plant is under is the amount of effect competing for natural resources has upon its growth rate.

Lorimer (1983) groups competition indices into three categories (published examples shown in brackets):

- Relative diameters and distances between subject tree and competitors

(Lorimer (1983))

- Zones of influence among neighbouring trees (Bella (1971))
- Growing space polygons (Moore *et al* (1973)).

Relative diameters and distance indices are distance-weighted size ratios that calculate the competitive effect as the sum of size ratios multiplied by the distance of selected competitors from the study plants. Zone of influence competition indices assume a zone around every plant that is assumed to be related to the crown and root size. Growing space polygons attempt to measure the space available for each plant to grow into as a polygon or polargram defined by the proximity of neighbouring plants (Doyle (1990)).

The computational difference between these three groups is self explanatory, but Lorimer (1983) points out that in previous comparative studies there has been very little difference in predictive ability between the groupings. This suggests that a decision as to which type of competition index to use depends purely on: the input data available; output data required; and any other contributary factor e.g. computational power available or how the model treats plants spatially in other sections.

The forest growth model required within *LUCAS* is needed to act as a pre-processor for *VSAS4* so it is sensible to maintain a continuity of spatial treatment between the two. This means that either a zones of influence or a relative diameter and distance approach can be used as a competition index. The zones of influence approach was chosen because it is conceptually easier to visualise and trees are already represented as circular crowns.

The combination of an empirical potential growth and zones of influence competition index fits the requirements of this study (providing a relatively simple individual tree based, distance dependent growth model to act as a pre-processor for *VSAS4*).

Leps & Kindlmann (1987) developed an empirical, distance dependent, individual plant growth model to simulate the development of spatial patterns within an even aged mono-specific plant population. Potential growth is simulated using the logistic growth curve, and inter plant competition by a form of plant zones of influence. Although the aims of Leps & Kindlmann (1987) were different from this study, their work provides a good starting basis for the development of a pre-processing model for *VSAS4*. The pre-processing model described on in section 5.2.2 draws from the work of Leps & Kindlmann (1987) and Ford & Diggle (1981).

5.2.2 The pre-processing forest growth model for VSAS4

The pre-processing forest growth model for *VSAS4* is a dynamic, mono-specific, either deciduous or coniferous canopy simulator (as opposed to *INTMO* which contains a

static, multi-specific, deciduous canopy simulator). The simplified way that *VSAS4* treats each tree makes it relatively easy to transfer between deciduous and coniferous trees. As can be seen from figure 5.3 the tree cone is inverted for conifers so that the widest part of the crown is at the base rather than the top of the tree, as is the case for deciduous trees. This inversion requires the input of another descriptive parameter, the distance to the base of the crown, and the change of measurement of crown angle (see figure 5.3). This means that the crown projected area can be calculated directly from tree height and crown angle.

Potential growth

The pre-processing model for *VSAS4* uses a logistic growth curve to empirically simulate potential tree growth. The logistic or autocatalytic curve has been used previously by Aikman & Watkinson (1980) and Leps & Kindlmann (1987) as the basis for simulating potential growth in their respective plant growth models. It was also used by Ledig (1969) as a basis for a model simulating the increase in dry matter of pine seedlings. Hunt (1982) presents a table of 44 empirical applications of the logistic curve in plant ecology. Most of these have been in short term studies (within a growth season) but Richards (1959) has indicated that the curve can be used for the complete growth of a plant which is well supported by the modelling studies of Aikman & Watkinson (1980) and Leps & Kindlmann (1987).

The logistic growth curve written as a differential equation is shown in equation 5.1.

$$\frac{dh_t}{dt} = h_t g \left[1 - \frac{h_t}{h_{max}} \right] \qquad (5.1)$$

h_t = Tree height
g = Growth ratio (see text)
h_{max} = Maximum tree height

As can be seen from the example of logistic curve form shown in figure 5.4 the curve is asymptotic towards the maximum tree height. The main controlling parameter on curve shape is the growth ratio which is an intrinsic rate of increase in size. There are limits to the range of g values, when the g is greater than 1 but less than 2.57 the solution to the logistic equation becomes cyclic, and when g is greater than 2.57 the solution exhibits chaotic behaviour (May (1974)). A negative value of g is meaningless in the context of plant growth therefore it is important that g falls between 0 and 1 to maintain a stable solution. It is possible to derive a value for g when the length of time it takes for a tree to reach a certain percentage of the maximum height is known e.g. if it takes 70 years for a tree to reach within 95% of it s maximum height. This is achieved by integrating equation 5.1 in the manner shown in equations 5.2 and 5.3.

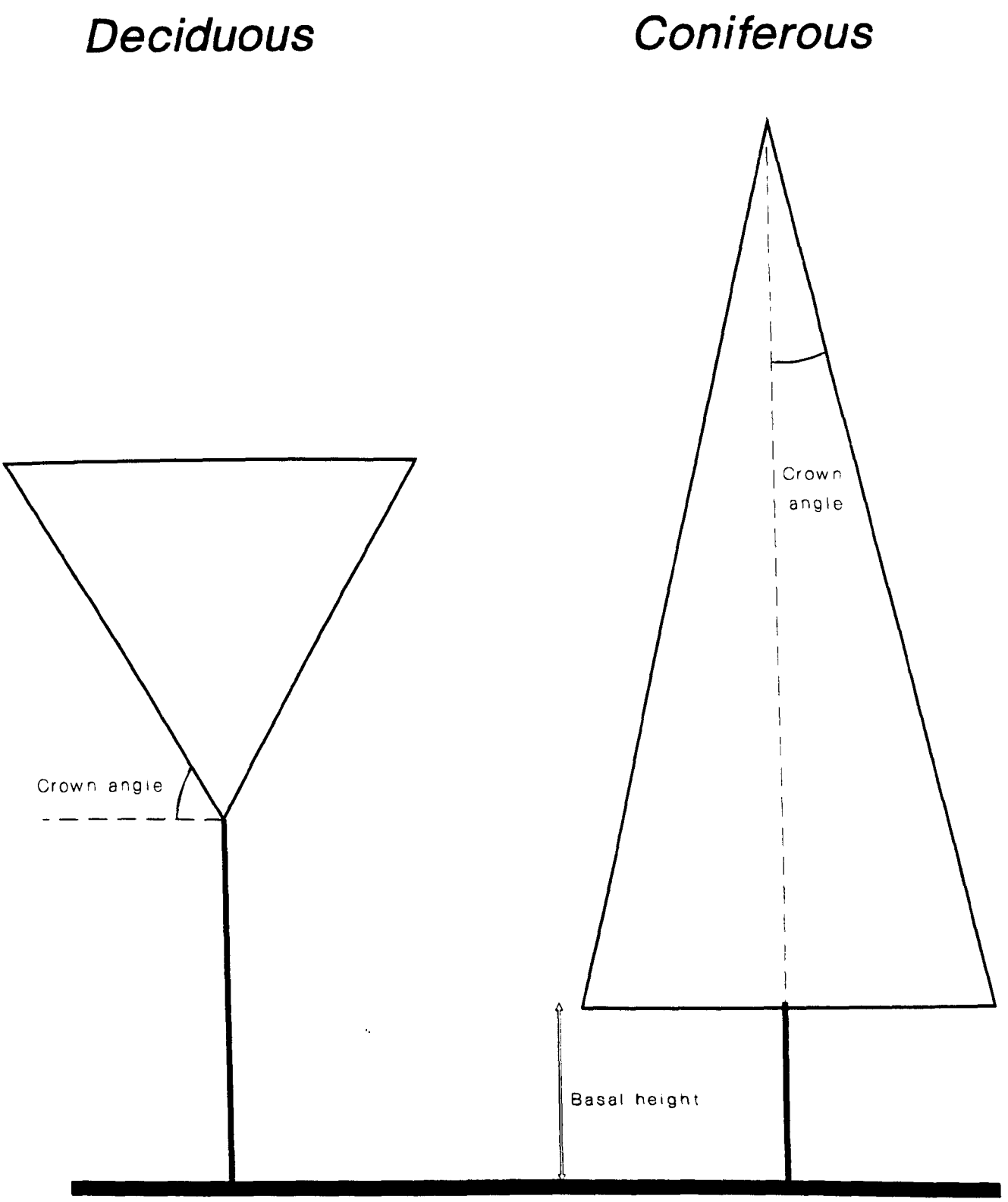

Figure 5.3: Deciduous and coniferous tree discretisation within the forest growth model

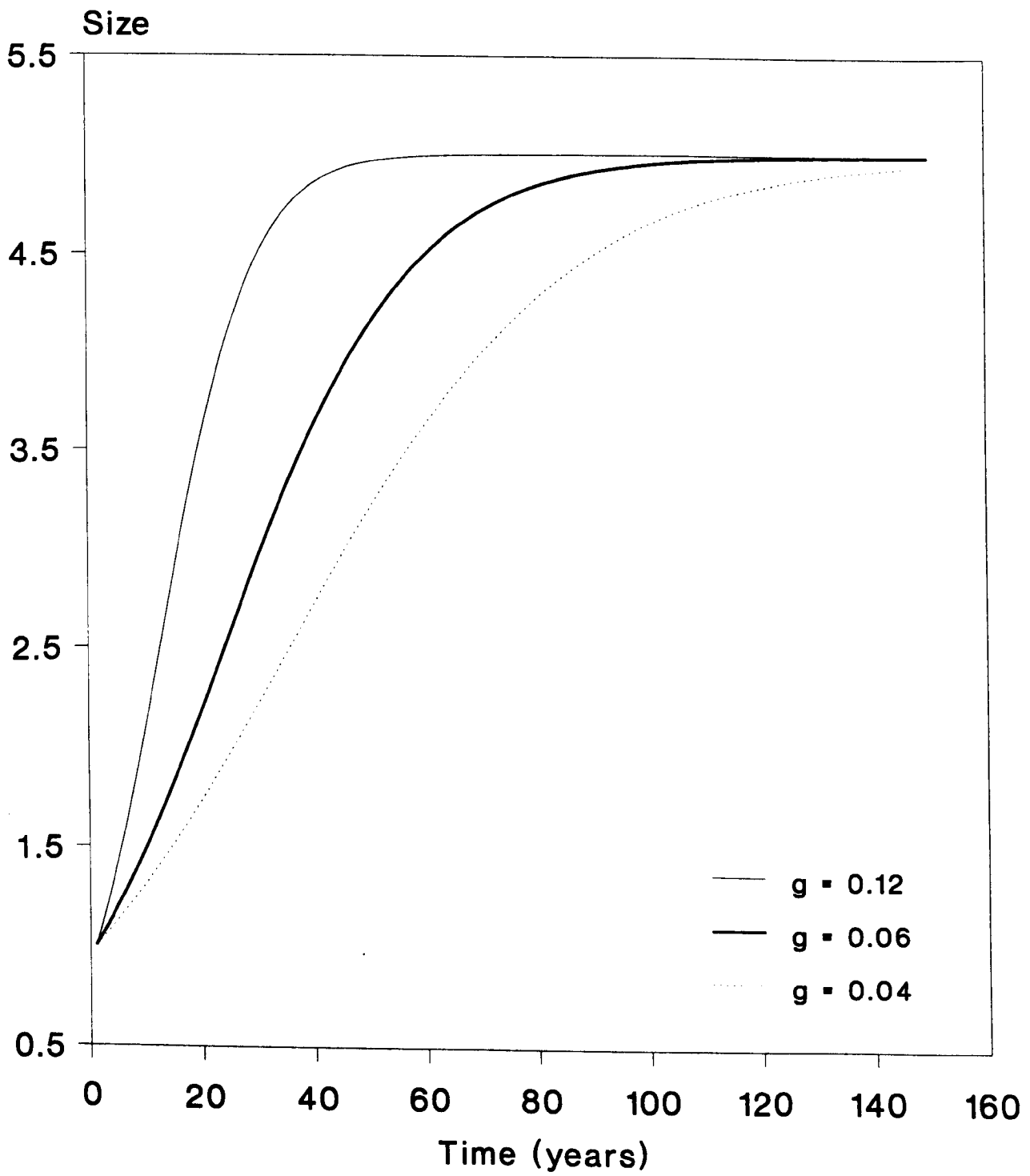

Figure 5.4: Examples of logistic curves for potential tree growth

$$\int \frac{h_{max}}{h_t(h_{max}-h_t)} dh_t = \int g\, dt \qquad (5.2)$$

$$g = \frac{1}{T} \ln\left[\frac{k(h_{max}-h_t)}{(1-k)h_t}\right] \qquad (5.3)$$

k = Proportion of h_{max} required
T = Time taken to reach kh_{max}

Equation 5.1 uses height as the predicted variable, but any plant growth variable can be predicted. *VSAS4* uses a simple linear regression relationship between diameter at breast height (*dbh*) and tree height as verified by numerous studies (e.g. Helvey & Patric (1965), Durocher (1991)), consequently *dbh* is the predicted variable from which tree height is later derived. The equation for numerical solution used by the forest growth model is shown in equation 5.4.

$$dbh_{t+\Delta t} = dbh_t \left[1 + g\left(1 - \frac{dbh_t}{dbh_{max}}\right)\Delta t\right] \qquad (5.4)$$

The value of *g* for each tree is drawn randomly from an assumed normal distribution with input mean and standard deviation. This is achieved by calling on a *NAG* routine from within the *FORTRAN-77* program code, in the case where an assigned *g* value is less than zero or greater than one the value is rejected and another call made to the *NAG* routine. The stochastic nature of assigning *g* is assumed to simulate the difference in tree growth potential that cannot be described by inter tree competition e.g. genetic differences affecting mineral uptake or other growth factors.

Inter-tree competition

Inter tree competition is simulated by a series of zones of influence (ZOI) surrounding each tree. The ZOI of a tree is assumed to represent the zone in which it is assumed to be competing for resources. It is assumed that the major resource being fought for is light i.e. water and minerals are uniformly available to all trees. This assumption has been made in previous modelling studies (e.g. Bella (1971), Ford & Diggle (1981), Gates (1982), Smith (1990)) and although an obvious simplification of reality is not totally unreasonable for temperate environments where soil water is normally readily available to plants. Part of this assumption is that competition is one sided i.e. a large tree affects the growth of a smaller tree but not vice versa.

For a deciduous tree the ZOI is calculated by projecting a cone from the top of the tree to the base and then projecting the upper half of the cone onto the ground, as is shown

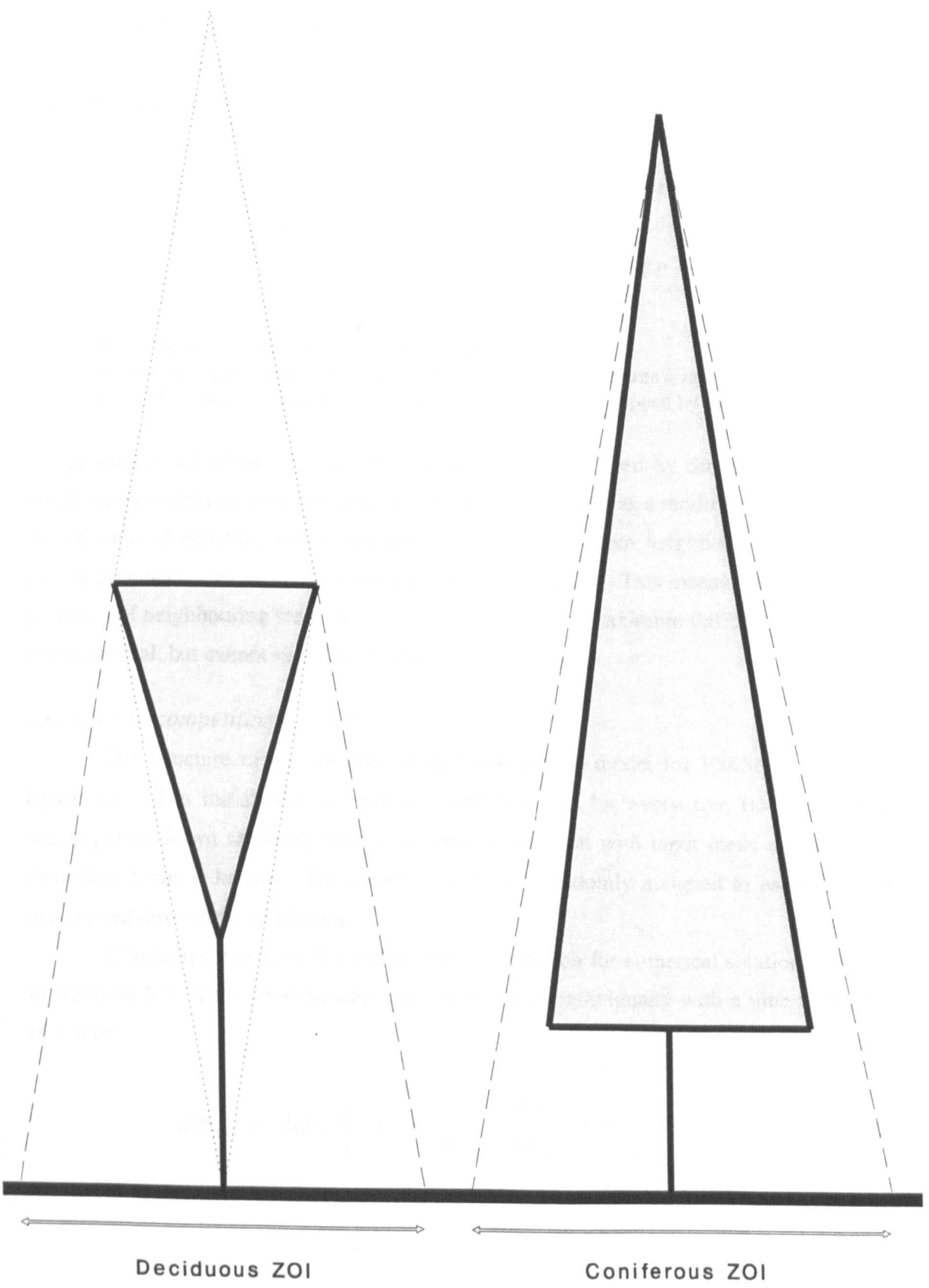

Figure 5.5: Method of calculation of the zones of influence (ZOI) surrounding each tree

in figure 5.5 . For coniferous trees the ZOI is simply assumed to be a set amount of the crown projected area, the actual proportion being input by the user.

For each tree the ZOI is first calculated;then the amount that other trees interfere with the subject tree is calculated as the total amount of overlap of each ZOI and the subject trees crown projected area (see equation 5.5). As mentioned previously competition is assumed one sided so that η is only calculated when the competing neighbour is larger than the subject tree.

$$\eta = 1.05 - \begin{cases} \sum_{j=1}^{n} P_i & \text{if } P_i < 1.0 \\ 1.0 & \text{if } P_i \geq 1.0 \end{cases} \qquad (5.5)$$

η = Amount of interference from neighbouring trees
n = Number of neighbouring trees *j* larger than the subject tree *i*, influencing *i*
P_i = Proportion of subject tree *i* crown projected area overlapped by the ZOI of tree *j*

The proportion of subject tree crown projected area overlapped by the ZOI of its taller neighbour is calculated as the overlap of two circles. η is used as a modifying factor on the growth ratio of equation 5.4, as the amount of influence from neighbours increases the growth ratio decreases in size to a minimum possible amount. This means that the shading influence of neighbouring trees can restrict the growth to a maximum 0.05% of the subject trees potential, but cannot stop it altogether.

Growth and competition combined

The structure of the pre-processing forest growth model for *VSAS4* is shown in figure 5.6. The initial *dbh* is input as either uniform for every tree (as for planted seedlings) or drawn randomly from a uniform distribution with input mean and standard deviation if this is known. The growth rate is then randomly assigned to each tree and maintained throughout its lifetime.

Combining equations 5.4 and 5.5 the full equation for numerical solution is shown in equation 5.6. This is solved step-wise for each tree individually with a time increment of 1 *year*.

$$dbh_{t+1} = dbh_t \left(1 + g \left[1 - \frac{dbh_t}{dbh_{max}} \right] \eta \right) \qquad (5.6)$$

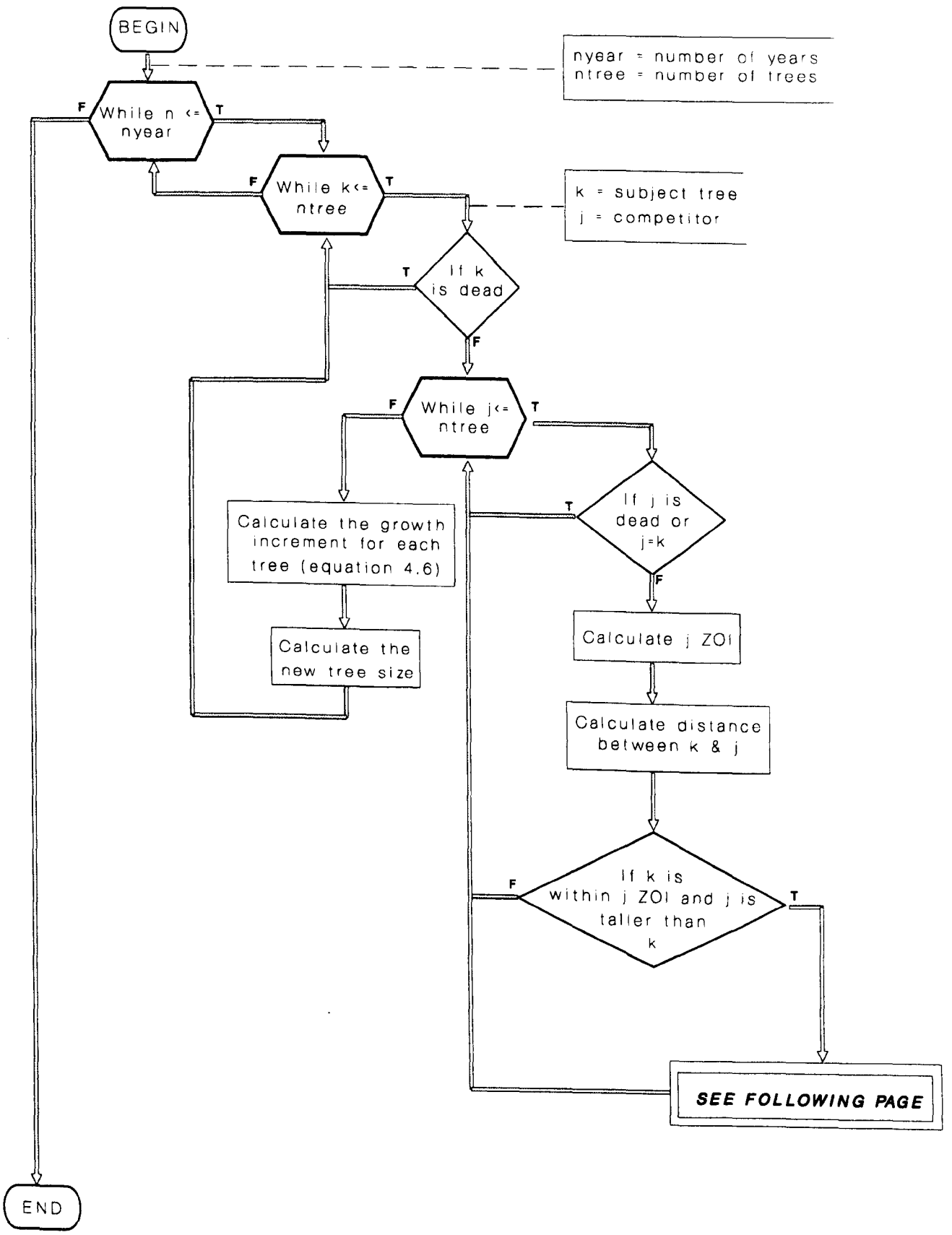

Figure 5.6a: Flow chart of pre-processing forest growth model, part A

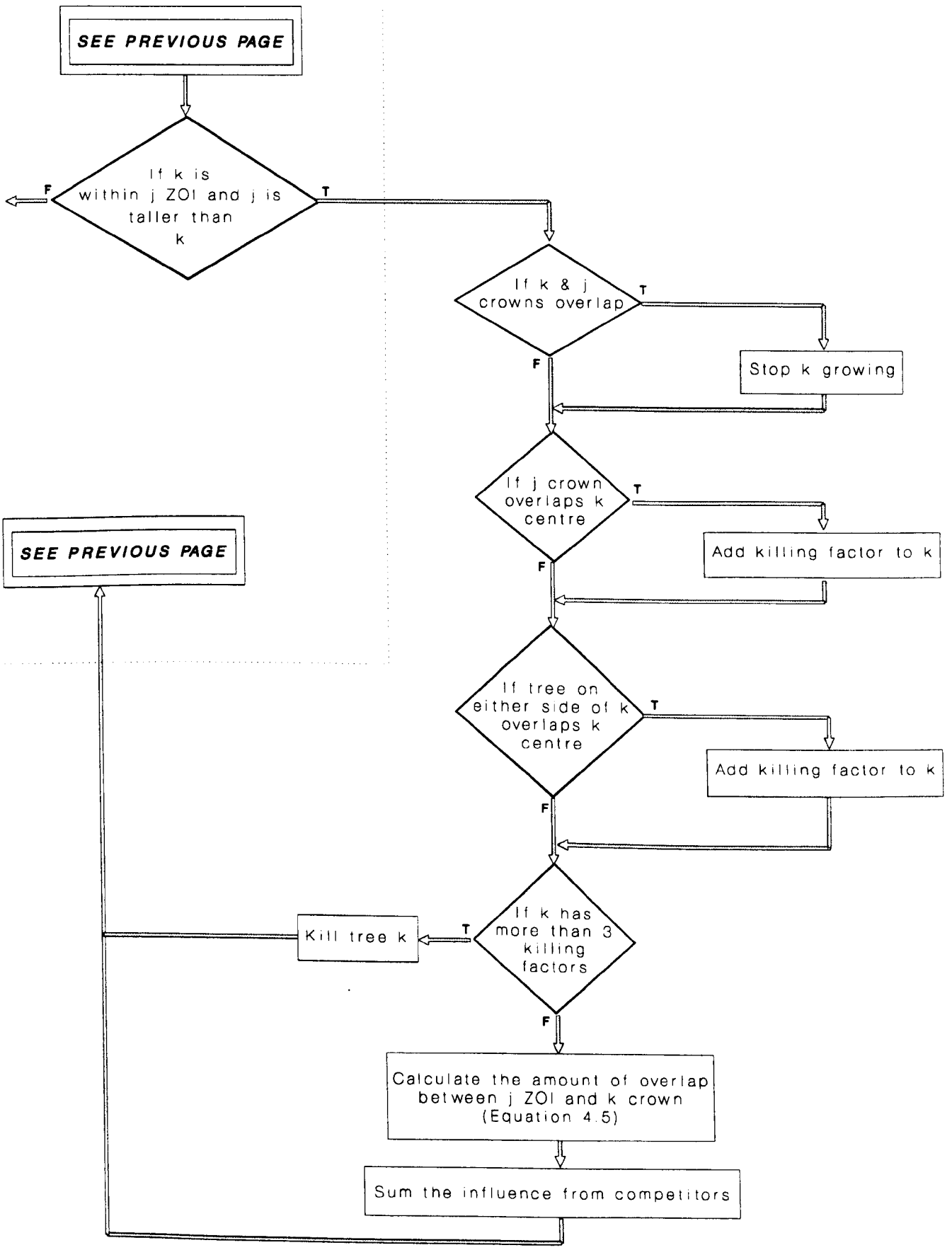

Figure 5.6b: Flow chart of pre-processing forest growth model, part B

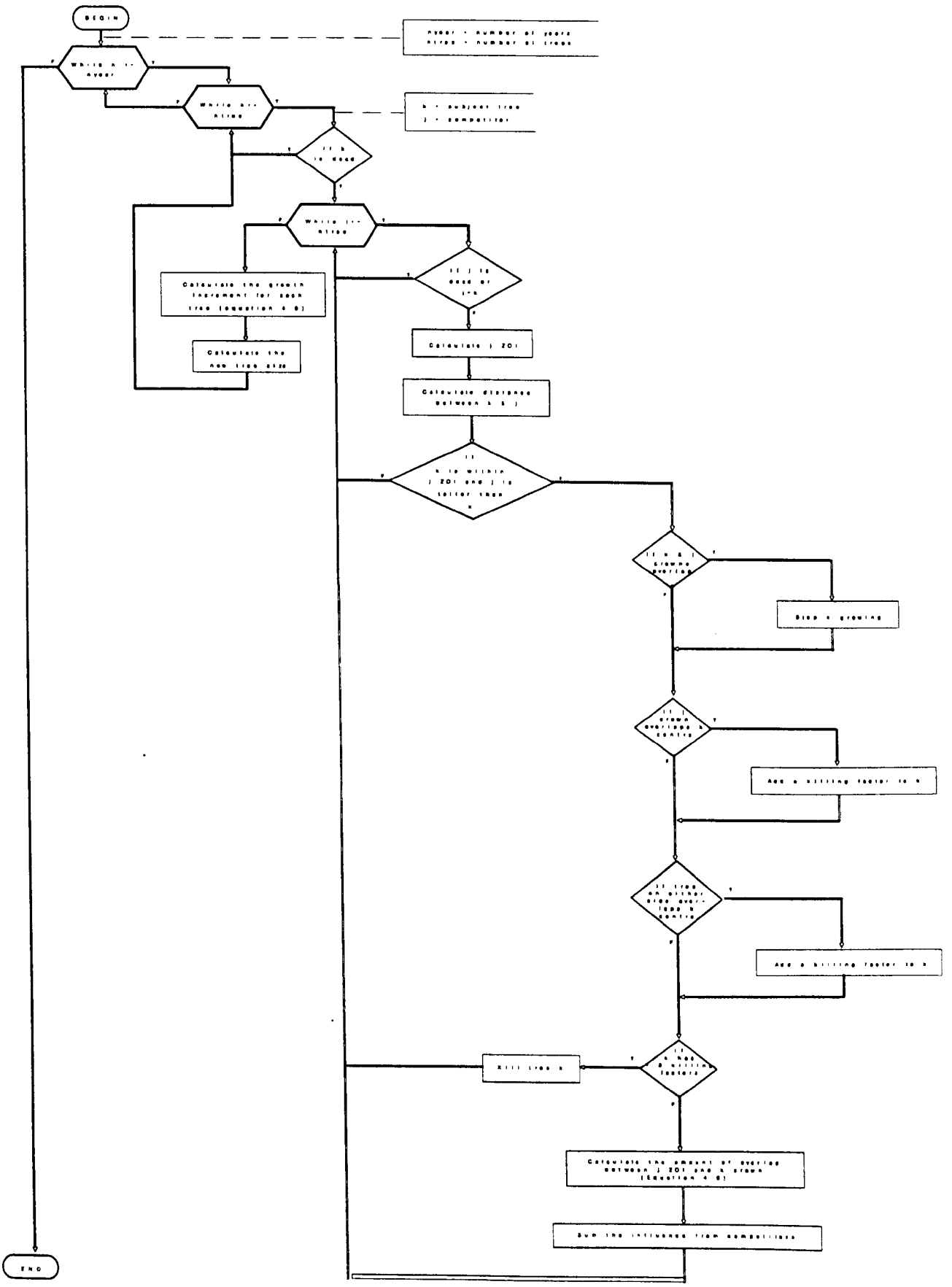

Figure 5.6c: Compressed version of pre-processing forest growth model flowchart showing interlinkage between 5.6a and 5.6b

Condition tested	*Result*
1. If tree crowns overlap	Stop the growth of the smaller tree
2. If the large tree crown totally overlaps the smaller tree crown	Let the tree die after three times
3. If two trees overlap across a tree	Let the tree die after three times

Table 5.1: Set rules on a trees competitive state

For each yearly timestep the model sequentially goes through every tree, calculates the amount its taller neighbours influence the subject tree, and then increases the subject tree *dbh* by an amount defined by equation 5.6.

Within the same subroutine the subject tree is tested against set rules to test if it can survive or carry on growing with the amount of competition from its neighbours. These are devised from sensible rules of competition and have not been used in this form before. The rules are outlined in table 5.1 with respect to figure 5.6. In rules two and three a tree is killed after the rules are contravened three times. This could mean that the same tree has three years of being in contravention or alternatively three competitors could be forcing it to die within the same year. When a tree dies it is removed from the simulation and the space it previously occupied is assumed vacant and available for other trees to grow into (N.B. every tree crown expansion maintains a conical shape).

For the forest growth model presented above there are twelve parameters for coniferous trees and ten parameters for deciduous trees that need to be input by the user. These are outlined in table 5.2.

An attempt has been made to ensure that the forest growth model is in some way physically based so that it can be used in many different circumstances after a series of relatively simple measurements of average forest parameters. The physical basis of the model is achieved in that it has physically measurable input parameters rather than an adherence to strict physical relationships. Of the twelve input parameters for simulation of a coniferous plantation shown in table 5.2 seven are directly measurable, the growth ratio statistics, minimum *dbh*, maximum *dbh*, and the proportion of crown constituting the zone of influence being the exceptions. Estimates of the extreme *dbh* values and mean growth ratio can be obtained from a fairly rudimentary knowledge of tree potential growth and using equations 5.2 and 5.3. The standard deviation of the growth ratio can be estimated by looking at the standard deviation of the *dbh* in any forest in a similar growing environment. This leaves only the size of ZOI as an abstract parameter that needs to be

Coniferous		*Deciduous*	
Length of plot side	(*m*)	Length of plot side	(*m*)
Spacing between trees	(*m*)	Spacing between trees	(*m*)
Period of growth simulation	(*yrs*)	Period of growth simulation	(*yrs*)
Initial *dbh*	(*m*)	Initial *dbh*	(*m*)
Maximum *dbh*	(*m*)	Maximum *dbh*	(*m*)
Mean growth ratio		Mean growth ratio	
Standard deviation of growth ratio		Standard deviation of growth ratio	
Slope of *dbh* v height equation		Slope of *dbh* v height equation	
Intercept of *dbh* v height equation	(*m*)	Intercept of *dbh* v height equation	(*m*)
Crown angle (see figure 5.3)	(*radians*)	Crown angle (see figure 5.3)	(*radians*)
Proportion of height to base of crown			
Proportion of crown area as ZOI			

Table 5.2: Input data required for the forest growth model

derived through calibration. This is a very small number of parameters (1-2 depending on standard deviation of growth ratio) to be calibrated considering the relatively simplistic nature of the model and indicates the general usefulness of the model.

The forest growth model presented here is a combination of parts drawn from several previous plant growth modelling studies and original work. In the form used as part of the overall modelling structure (*LUCAS*) this model is new and original. The composite parts of the model and where they have been used previously is shown in figure 5.7, which gives an idea of the originality.

5.3 Other factors altered by algorithm

The forest growth model described in section 5.2 now gives *LUCAS* a temporally dynamic approach to the investigation of long term land use change. The growth model acts as a pre-processor to *VSAS4*, simulating the growth of a forest to an input age specification which is then able to be discretised into a series of Delauney triangles and tree layers ready for usage by the rainfall partitioning section of *VSAS4* prior to storm event simulations.

The simulated forest growth changes the structure of the forest but some of the rainfall partitioning factors remain static. If some of these parameters that the forest

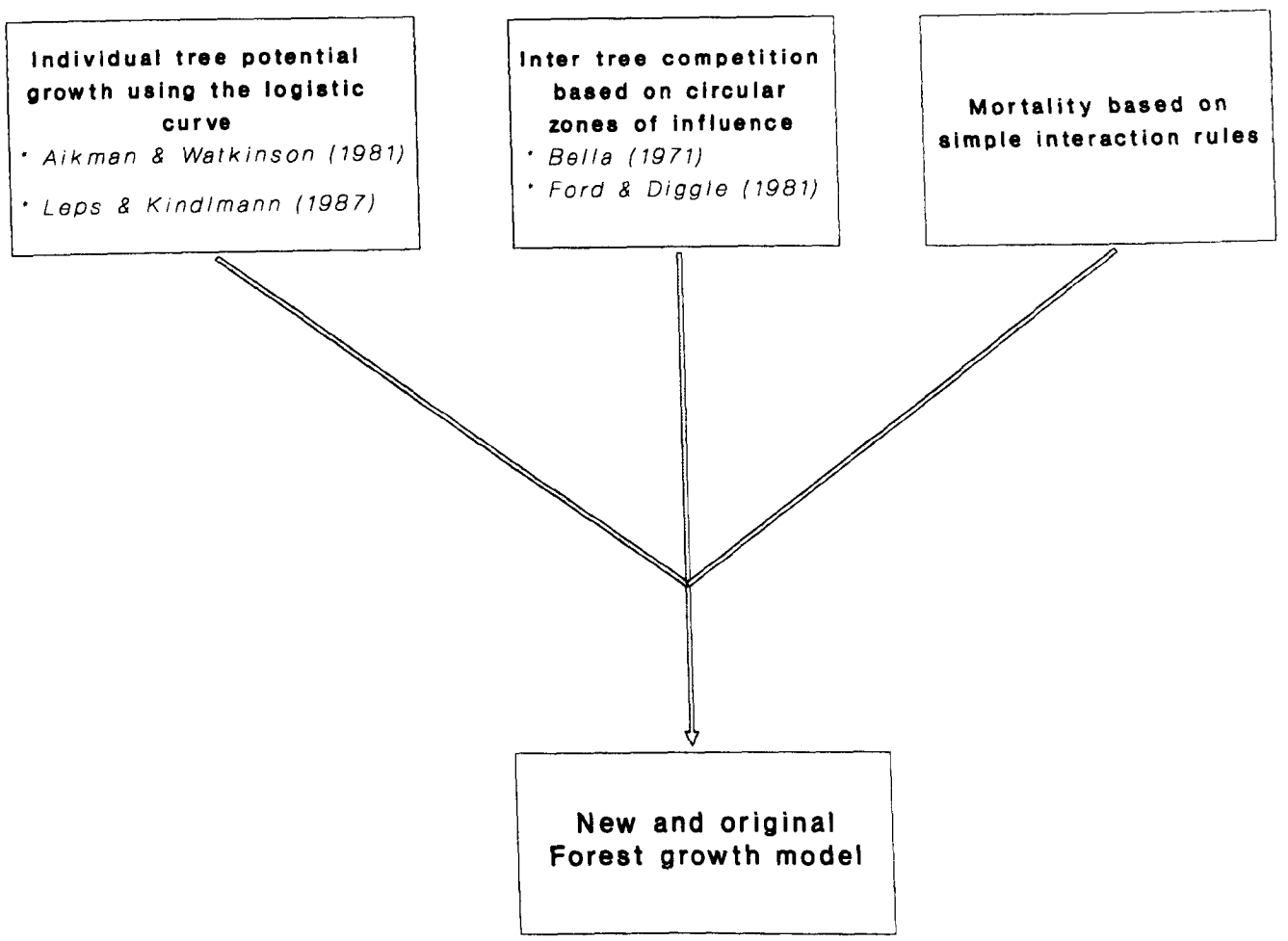

Figure 5.7: Summary of forest growth model components and their genesis

growth model does not alter are known to change in a certain manner with the growth of a canopy then these can be changed separately according to the known relationship. This ties in with section 5.1 where it was stated that the intention was to use both a pre-processing model and the transformation of *VSAS4* input parameters by simple known algorithms (see also figure 5.1).

There are two notable *VSAS4* rainfall partitioning parameters that the pre-processing forest growth model does not change: the proportion of the crown surface area contributing to stemflow and the leaf (and stem) area index. These are both parameters that might be expected to change with the growth of a forest.

5.3.1 Stemflow proportion

Johnson (1991) presents evidence from a collation of field studies in different age coniferous plantations, that the stemflow contribution to below canopy rainfall does change with an increase in canopy age. This is because an individual tree structure changes as it grows, the proportion of leaf area to branch or trunk area alters, although the actual amount is difficult to assess. The data presented by Johnson (1991) suggest that the relationship is not linear, there being a higher percentage of stemflow at a younger age than in the older trees.

In the modelling scheme presented here the mean proportion of crown surface area that contributes to stemflow, and the standard deviation of this mean, are input so that the actual proportion is drawn randomly from a random distribution for each tree. The stochastic allocation occurs at the start of the forest growth simulation and the actual area contributing to stemflow is calculated once the final tree size is known i.e. at the end of the forest growth routine simulation. This means that the **area** of stemflow contribution will be larger for an older tree but the **proportion** of total crown surface area (and therefore the percentage) remains static. It is quite possible that the relationship between stemflow amount and age will not be linear as the growth of each tree is not linear, but a larger tree will definitely produce a greater amount of stemflow than a smaller one.

The fact that the data presented by Johnson (1991) are not all from the same site precludes strong conclusions being drawn (i.e. site factors may be as large the age factors) but it is likely that the proportion of the crown area contributing to stemflow does change as a tree grows. Because the relationship of stemflow proportion to tree age or size is not well understood it was decided to keep the relationship as described above and not include any new transforming algorithm for stemflow.

5.3.2 Leaf and stem area indices

Leaf area index (LAI) is the average number of leaf layers in each triangle. Stem area index (SAI) is the average number of stem layers (excluding the trunk area) in each tree that form a continuous network of intercepting elements capable of transporting water to the trunk. They can be visualised as the average number of times an intercepting surface (leaf or stem) is touched by a plumb-line dropped from the top to bottom of a canopy. These indices are crucial to the rainfall partitioning section of *VSAS4* where they play a large part in controlling the amount of throughfall and stemflow within each triangle by controlling the stochastic assignment of the number of intercepting layers (see equation 4.4).

At present LAI and SAI are input for the individual tree species and then the average value for each triangle (LAI) and actual value for each tree (SAI) is calculated based on the crown surface area (see equation 4.1). This means a large tree will have a larger leaf area than a smaller tree but an identical leaf area index.

The problem with this method is that the average LAI and SAI values that are required as input are difficult to measure, especially in a coniferous forest where the intercepting leaves are in fact needles. Halldin (1985) in an extensive study of leaf and bark area distribution in a pine forest gives a direct relationship between tree size and leaf (needle) area. This relationship is shown in equation 5.7

$$LAI = -0.9045\ dbh + 0.3797\ dbh^2 \qquad r^2 = 0.89 \tag{5.7}$$

LAI_i = Leaf area of tree *i*, calculated from equation 5.7

The *dbh* is required in *cm* and the leaf area (needle surface area) is given in m^2. This relationship has been added into the canopy discretisation part of *VSAS4* so that the leaf area is calculated after the individual tree sizes (*dbh*) have been finalised by the growth model.

The remainder of the canopy discretisation into triangles is performed in exactly the same manner except that instead of the average LAI for the forest plot being input, now the intercepting leaf area is calculated from the known relationship with *dbh*. This is shown in equation 5.8 which can be compared to equation 4.1.

$$LAI_t = \frac{\sum_{i=1}^{3} LAI_i - p_{it}\, LAI_i)}{A_t - \sum_{i=1}^{3} (p_i\, LAI_i)} \tag{5.8}$$

A_t = Area of triangle
p_i = Proportion of tree crown *i* generating stemflow

The SAI is an extremely difficult parameter to measure which led Durocher (1991) to assume that SAI is equal the LAI (this was initially inherited by *VSAS4* from *INTMO*). Halldin (1985) found that the shoot or stem area was approximately one twentieth of the needle area given by equation 5.7. Consequently *VSAS4* has been changed so that the stem area equals the leaf area divided by 20 and SAI is calculated as in equation 5.9.

$$SAI_i = \frac{(LAI_t/20) - p_i (LAI_t/20))}{(p_i (LAI_t/20))} \tag{5.9}$$

This changes the LAI of each Delauney triangle and SAI of each tree from being derived from average input values to them being calculated directly from tree size as predicted by the forest growth model. The advantage is that the average LAI and SAI for a forest are no longer required as model input, as these are particularly difficult to gauge. The disadvantage of this change is that the relationship between *dbh* and LAI/SAI used is for a pine forest in Sweden (Halldin (1985)) and there is a paucity of similar studies for different regions and tree species. This means that the relationship is only used in a coniferous forest simulation (i.e. the original average LAI/SAI value is used for simulations of deciduous growth). The change represents a small improvement to the original canopy discretisation capability of *INTMO* as integrated within *LUCAS*.

5.4 Summary of the total modelling scheme (LUCAS)

The use of a three dimensional rainfall partitioning routine within *VSAS4* has enabled the governing canopy structural properties to be independently modelled, thereby providing a temporally dynamic parameterisation for *VSAS4*. The combination of these two models has been termed Land Use Change, Afforestation, Simulator (*LUCAS*) and this forms the predictive modelling scheme especially designed to investigate the effects of long term vegetation change on stormflow hydrology. The forest growth model described in this chapter is a new distance dependent, individual tree based, forest growth model partly based on previous work by Ford & Diggle (1981) and Leps & Kindlmann (1987) but original in its present form. The different components of the model and their derivation are shown in figure 5.7.

The position of the forest growth model within the overall modelling structure used to investigate long term land use change (*LUCAS*) is exactly the same as for the original multi-specific canopy simulator of *INTMO* (see figure 4.4). It is a semi-

autonomous unit capable of generating a canopy separately and then storing the canopy parameters in an output file ready for multiple simulations by *VSAS4* with the same forest cover.

The combined modelling scheme is shown in figure 5.8. This is an extension of figure 4.4, a comparison of the two diagrams shows that the new mono-specific canopy generation model occupies an analogous position to the original multi-specific canopy simulator of *INTMO*.

It must be emphasised that the forest growth model operates independently from and at a completely separate time scale to *VSAS4*. The forest growth model operates at a forest growth time scale (1-200 *years*) and acts as a pre-processor for *VSAS4* which operates at a storm event time scale (1-200 *hours*).

Chapters three and four together have described the model design involved in *LUCAS*. The following three chapters are concerned with the testing of the *LUCAS* modelling scheme.

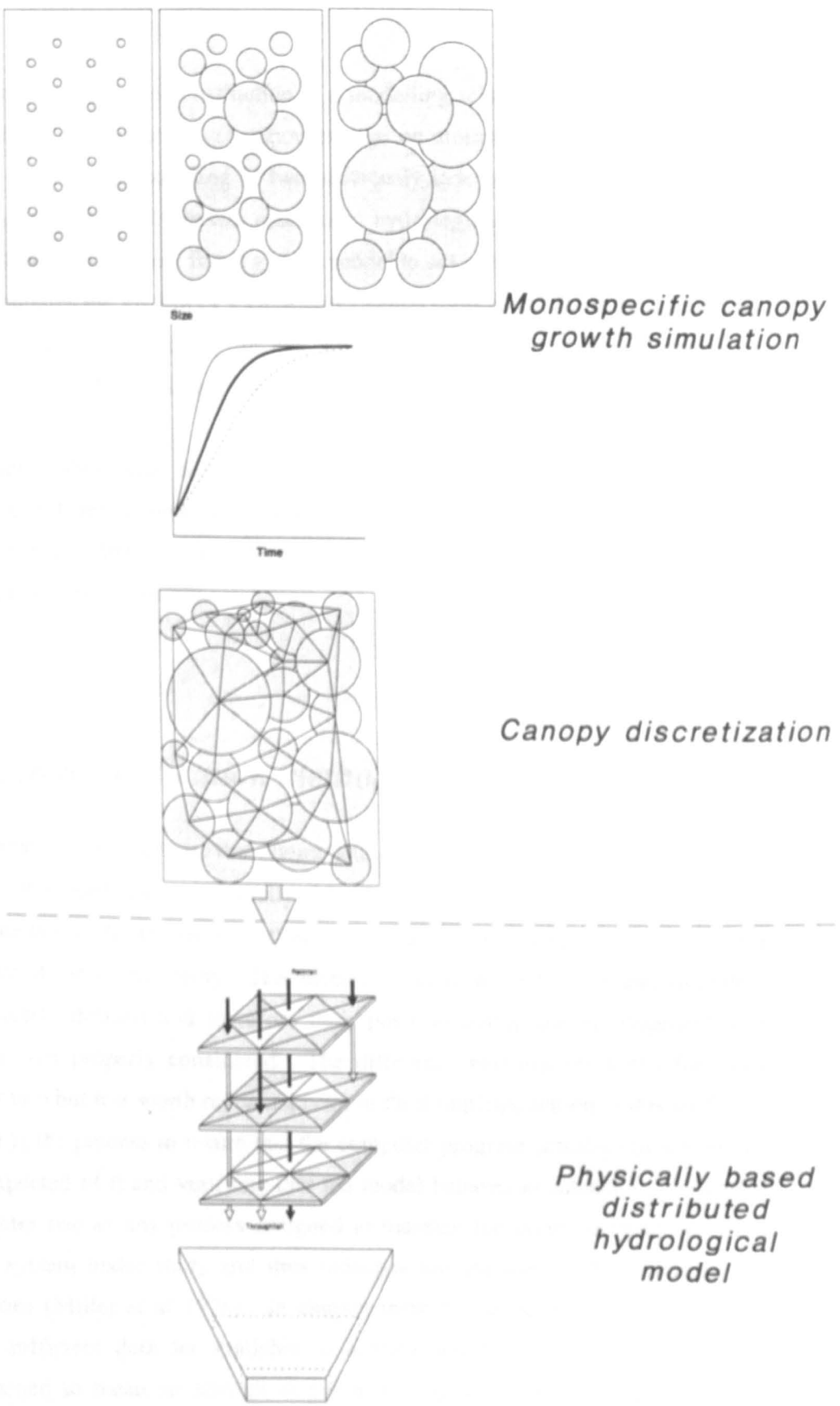

Figure 5.8: Conceptual representation of *LUCAS*

CHAPTER 6

VERIFICATION TESTING OF *LUCAS*

In chapters four and five the construction of a modelling scheme specifically designed to investigate the effects of long term vegetation change on stormflow hydrology has been described. This has involved the coupling of two previously independent models into a new form of mixed conceptual/physically based, distributed hydrological model (*VSAS4*) and the design of a new, individual tree based, forest growth model to act as a pre-processor to *VSAS4*. The pre-processor simulates the growth of a three dimensional canopy and the output from this used as input for the rainfall partitioning section within *VSAS4*. The combined scheme of forest growth model and *VSAS4* has been named *LUCAS* (Land Use Change, Afforestation Simulator).

The remainder of this thesis deals with the testing of *LUCAS* and consequent further additions and changes to different areas within the scheme. This chapter describes simulations using *LUCAS* to test the robustness of the scheme in a range of possible field conditions and to verify the scheme as much as is possible.

6.1 Introduction to verification methods

The development of any scheme that attempts to numerically model physical processes requires some form of model testing. Usually this testing is in the form of a verification exercise to investigate the model for errors, followed by a validation trial to test if the model is an adequate predictor of measured reality. The difference between verification and validation is sometimes not clearly defined and therefore their position within the development of a modelling scheme is not properly considered. The difference between the terms has been explained in chapter two but it is worth repeating prior to their implementation in this study.

Verification is the process to insure that the computer program actually carries out the logical processes expected of it and verifying that the model behaves as intended. *Validation* was defined in chapter two as any process designed to measure the correspondence between the model and the system under study and thus indicates the usefulness of the scheme for predictive applications (Miller *et al* 1976). In chapter three it was acknowledged that there would never be a sufficient data set available to achieve this kind of validation and the definition was loosened to mean an attempt to prove or disprove that the model is a valid representation of the hydrological system.

There is little point in carrying out a validation exercise before verification because any inconsistencies highlighted by verification will require changing before any worthwhile predictions can be made. It is important therefore that an adequate model verification is carried out before any validation attempt is made or the model is used for any predictive purposes.

Model verification involves investigating the model structure to determine whether it adequately simulates the hydrological processes it is supposed to. This takes two forms: an internal check of the mathematics and program code; and an investigation of the model output in a series of well controlled conditions to check the sensibleness of the modelling scheme.The first internal check is often incorporated into the second, in that nonsensical external model output can often be attributed to incorrect mathematics or program code.

The most common form of verification carried out on a modelling scheme is sensitivity analysis. McCuen (1976) defines model sensitivity as the rate of change in one factor with respect to a change in another factor. Sensitivity analysis attempts to measure the overall model sensitivity to changes in individual parameter values. Sensitivity coefficients can be used to quantify the parameter sensitivity, these are usually the partial derivatives of the output variables with respect to the input parameter (McCuen 1976). Alternatively the change in model output can be assessed on a subjective basis and the relative importance of individual parameters assessed.

There are two types of sensitivity analysis, distinguished by the different ways that individual parameter values are derived. The most common method is *factor perturbation* (sometimes called the deterministic method) where individual parameter values are incremented by relatively small amounts while other parameters are kept constant. In the second *stochastic method*, all parameter values are randomly selected from distributions that span their known range of physically measured values. Factor perturbation offers greater control over the parameter variation but complex interactions between parameters may be missed by only varying one parameter at a time. The stochastic method is more likely to detect these interactions between parameters but normally will take longer to perform as more runs are required.

The aims of a sensitivity analysis should be to discover the relative importance of individual input parameters, to give an indication of the degree of accuracy required for their measurement, and to discover the importance and role of different processes and/or parameters in the studied environment. The results from a sensitivity analysis can be used to determine the amount of input data required for an applied study and the degree of accuracy needed in measuring input parameters.

There are three problems associated with a sensitivity analysis of a physically based, distributed hydrological model. The first is to do with the complex nature of these models, this means that a full scale sensitivity analysis which investigates the importance of every parameter is an extremely large and difficult task. The sheer number of input parameters

required to be tested for sensitivity is so large as to make it an almost impossible undertaking. For example in the case of *VSAS4* there are 23 general and specific input parameters that could be investigated for sensitivity which, allowing for approximately 10 runs per parameter, would take approximately 90 days of computing time, let alone the time required to analyse the results (N.B. this is for *VSAS4* not the overall modelling scheme, *LUCAS*).

The second problem is that the complexity of interaction between parameters may not be appreciated or even detected by the factor perturbation method so that either an extremely large stochastic sensitivity analysis is needed or the interaction is ignored.

The third and final problem is that the distributed nature of process representation means that testing the external output as a catchment hydrograph from the total catchment may be misrepresenting the importance of scale representation within the catchment. Either scale representation has to be considered as another parameter to be tested for sensitivity by running the model with many different configurations or it is ignored and assumptions are made as to the representation the modelling scheme offers.

A possible compromise from a full sensitivity analysis is to test the model by running it on a series of hypothetical scenarios varying a limited number of parameters that represent factors that are known to influence certain hydrological processes. The influential factors can be identified as important either by previous studies or can be new elements within the structure which therefore need to be investigated for relative importance. The hypothetical scenarios should represent possible field conditions and likewise the parameter variance has to represent a possible field range. The aims of this kind of analysis are to identify the conditions where each process is important (and therefore to rank the parameters), and to investigate the *robustness* of the model scheme. The term robustness is used to mean that the model responds in a reasonable manner (to a full range of field conditions). The major difference from a sensitivity analysis is that it does not give any indication as to the degree of accuracy required in measuring each input parameter, and that the parameter chosen may not be an individual input parameter but could be a more generalised factor (e.g. forest age can be used as a general input rather than investigating every input parameter in the pre-processing forest growth model for their effect on the output hydrograph). The results from this kind of analysis can be used to highlight scenarios of critical importance for a factor and therefore areas where more detailed research is needed on this factor.

6.1.1 Method and aims

The verification procedure chosen for this study is the reduced form of sensitivity analysis as described in a general manner above. The reason for choosing this type of model verification is threefold:

- A full sensitivity analysis of the modelling scheme is too large an

undertaking for limited results.

- By investigating factors rather than each individual parameter the relative importance of new factors (such as forest age) under different scenarios can be ascertained.
- The results from this kind of analysis give some indication of the importance of different controlling factors in the scheme and therefore the relevance of this modelling scheme for investigating long term land use change.

For the purpose of this study the limited sensitivity analysis undertaken has been called *robustness testing*. This terminology reflects the fact that this is not a full sensitivity analysis and that one of the primary aims is to test the robustness of *LUCAS* as a land use change investigative tool.

The approach taken is similar to that of Anderson (1982) where a modelling scheme was devised and used to identify threshold values of hydraulic conductivity and slope angle that determine different soil moisture flow regimes. While in the case of Anderson (1982) the verification of the modelling scheme was used to back up and extend field studies of topographic convergence affecting soil moisture levels, here the robustness testing is being performed as a possible precursor to field studies and could form the basis for advising areas of investigation within catchments affected (or about to be affected) by land use change.

VSAS4 is an integration of two previously separate modelling schemes therefore any previous sensitivity analysis results can be used as guide-lines for the selection of general factors used in the robustness testing of *LUCAS*. Because *VSAS* forms the structure that *INTMO* has been integrated into, rather than the other way round, the sensitivity analysis performed by Whitelaw (1988) on *VSAS2* is a particularly relevant starting point for any verification of *LUCAS*. The factors or parameters Whitelaw (1988) found to be important can be used as variable factors in the robustness testing, whilst less important parameters can be ignored.

The robustness testing takes the form of varying three general factors in *LUCAS* while keeping all other input parameters static. The choice of factors varied is based on the previous sensitivity work carried out by Whitelaw (1988) on *VSAS3* and considerations of the new elements in *LUCAS*. To keep the system complexity to a minimum these factors are allowed to vary in a series of hillslope planes (segments) rather than over a full catchment where interactions between factors and scale representation of processes may interfere in a manner that is difficult to judge.

Using the factor perturbation method Whitelaw (1988) investigated the sensitivity of *VSAS2* to variations in six input parameters: plan shape; slope angle; saturated hydraulic conductivity; the Campbell *b* constant† ; soil stone content; and the proportion of total soil

† A coefficient in the equation to calculate unsaturated hydraulic conductivity from a suction moisture curve. The

depth within each soil layer. Using a double peaked storm event five outputs were analysed for their changes: stormflow volumes of the peaks (individually); time taken to reach the stormflow peaks (individually); and the time taken to reach basal saturation. The results of this sensitivity analysis are briefly summarised here:

- Plan shape: has a significant effect on the saturated wedge and on the amount of overland flow.
- Slope angle: very important for near stream subsurface outflows.
- Saturated hydraulic conductivity: Very significant on flows but no clear thresholds.
- Campbell *b*: important for its control on the saturated wedge formation.
- Stone content: less critical than others but does affect the subsurface flow.
- Depth proportions: controls the initial response to rainfall through its relative volume compared to rainfall event volume.

The implications of these results are that all the chosen input parameters have an effect on the model outputs but that the general factors of topography (including plan shape and slope angle) and soil hydrology (including saturated hydraulic conductivity, Campbell b; and stone content) are particularly important. The reasoning for this relative importance can be examined on two levels, the first is that *VSAS* deliberately sets out to concentrate computational power on the calculation of subsurface soil water flow and therefore it is not surprising that soil hydrology is a dominant factor. The second very important point is that topography has been identified by numerous field studies to be an important factor governing soil water convergence and hence saturated overland flow (e.g. Anderson & Burt (1978); Anderson & Kneale (1982)). This suggests that *VSAS2* is capable of simulating a hydrological response that is known to occur in the field.

From the results of the sensitivity analysis performed by Whitelaw (1988) and knowledge of important hydrological processes, topography and soil hydrology have been chosen as two of the general factors varied in the robustness testing of *LUCAS*.

The addition of the pre-processing forest growth model simulating the change in canopy input parameters used by *VSAS4* in rainfall partitioning means that the relative importance of this within the *LUCAS* structure needs to be established. The effect of changes in individual input parameters on forest growth is best investigated for the influence on growth outputs rather than on the *VSAS4* output hydrograph where the dominance of other factors

---

Campbell method has since been replaced by the Millington-Quirk method for unsaturated hydraulic conductivity calculation (see section 4.3.1.6).

Factors varied	*Static parameters*
Topography	Segment area
	Number of increments
Soil hydrology	Soil depth
	Soil suction moisture curve
Vegetation	Area of canopy
	Rainfall partitioning parameters
	Storm size*
	Initial moisture conditions*

Table 6.1: Outline of design for robustness testing. *Parameters altered in secondary testing (see accompanying text)

(such as topography and soil hydrology) may mask sensitivity within the forest growth model. Forest age can be isolated to act as a general factor allowed to vary in the robustness testing. Forest age is both a general factor and a direct input parameter within the forest growth model. It is general in that it controls the extent of potential growth for each tree and inter tree competition allowed and thus has influence over every aspect of forest growth, and it is directly input into the forest growth model.

Table 6.1 shows the outline of the design for the robustness testing. The three factors investigated for their relative importance within *LUCAS* are: topography; soil hydrology; and vegetation. The parameters chosen to represent these and their respective values are described in the remainder of section 6.2.1. For each parameter three values were chosen from a range that represents possible field conditions i.e. two values represent fairly extreme values and the middle value of each parameter aims to represent fairly common values. The input parameters (and their values) that remained fixed are given in section 6.2.1.4.

The aims of the robustness testing can be identified as:

- To find the conditions where each of the process representations is important
- To investigate the general robustness of *LUCAS*
- To find the relative importance of the new factor within *LUCAS* (i.e. canopy age).

The initial set of robustness tests involved running *LUCAS* on each of the possible scenarios (a total of 81 runs), the results from these runs are described in section 6.2.3. After

these results were analysed and the pertinent observations made with respect to the three aims of the robustness testing stated above, the second phase of the robustness testing was undertaken. This involved extending the range of initial conditions varied (see asterisked parameters in table 6.1) to test if the observations and conclusions from the preliminary testing held under the new initial conditions. The new initial conditions and results from this secondary set of robustness tests are detailed in section 6.3.

It is important to note that the different scenarios tested in the secondary set of robustness tests are very much derived from the results of the preliminary testing and therefore are detailed in a separate section.

6.2 *Initial robustness testing*

The method used in the first set of robustness testing has been described in the previous section. It involves varying three input factors to find their relative importance within *LUCAS* and the general robustness of this scheme. The parameters chosen to represent the three factors and their respective values are described in section 6.2.1. Section 6.2.2 details the procedure used in the robustness testing, and how the results were analysed. The results from the initial testing is described in section 6.2.3 and summarised in section 6.2.4.

6.2.1 *Initial conditions*

6.2.1.1 Topography

The role of topography in controlling subsurface soil water flow has been discussed earlier with respect to the field studies of Anderson & Burt (1977), Anderson & Kneale (1982) and the modelling study of Anderson (1982). The detection of topography as an important controlling factor in the *VSAS2* structure reinforces these studies and illustrates the relevance of *VSAS* as the choice of base hydrology model in this study.

Within the generalised factor of topography there are three important variables that are input in *VSAS4* for each hillslope plane (segment): plan shape; cross sectional shape; and slope angle. For model applications the input values are derived from topographical information for each segment and so have direct physical relevance. This means that they are not parameters that can be calibrated to fit the data, and therefore the objective of varying them is to identify how different topographic regimes affect the outflow from a segment.

The difference between plan convergence and cross sectional convergence is only in the scale of concentrating subsurface flow i.e. plan convergence occurs down a hillslope (10-

500 *metres*) while cross sectional convergence is within the depth of soil (normally less than 10 *metres*). Because these are essentially the same process there is little point in investigating the variation in both when sensible conclusions can be drawn about cross sectional shape from the results of varying plan shape. Consequently it was decided to alter only two topographic parameters in the robustness testing: plan shape; and slope angle.

The three options chosen for variation in plan shape are shown in figure 6.1. The two extreme options represent convergent and divergent slopes, with the intermediate option being a uniform slope. The area of the segments, and the number of increments upslope (see section 6.2.1.4) are identical in each case.

The slope angles range from 5° to 35° with the intermediate slope being 15° (see figure 6.2). The hillslope hollows used by Burt (1978) and Kneale (1981) in their field studies of soil water conditions had slopes ranging from 6° to 30°.

6.2.1.2 Soil hydrology

The computational importance that *VSAS4* places on the role of subsurface flow means that soil hydrology is always going to be a dominant factor in the model structure. There are several parameters that are part of soil hydrology, most notably saturated hydraulic conductivity, soil stone content, the suction moisture curve, and soil porosity. To keep the number of hypothetical scenarios investigated to a manageable number it was necessary to choose just one parameter to represent soil hydrology.

The parameter chosen to represent soil hydrology is saturated hydraulic conductivity. This was found by Whitelaw (1988) to be the most critical soil parameter in *VSAS2*, confirming work by Freeze (1972) and Anderson (1982) using different modelling schemes for subsurface flow on hillslopes. Saturated hydraulic conductivity is important for unsaturated soil water flow where the unsaturated hydraulic conductivity is related to it by the Millington-Quirk method (equation 4.7), as well as saturated soil water flow.

The three values chosen (1.65×10^{-6}; 1.65×10^{-5}; and 1.65×10^{-4} ms^{-1} or as often expressed: 0.594; 5.94; and 59.4 $cmhr^{-1}$) represent a range that it is likely to be found in the field. In a wide ranging review of soil physical properties for different soil types in the USA Rawls *et al* (1982) describe average saturated hydraulic conductivities for eleven soils ranging from clay to sand. The three values chosen here are close to the average values listed by Rawls *et al* (1982) for clay loam, sandy loam, and sand respectively. In the results section (section 6.2.3) these values are referred to as: low (1.65×10^{-6} ms^{-1}); medium (1.65×10^{-5} ms^{-1}); and high (1.65×10^{-4} ms^{-1}).

6.2.1.3 Vegetation

The influence that vegetation has on storm hydrology is to act as a buffering device, delaying the time taken for any rainfall to reach the surface and continuing the rainfall input to

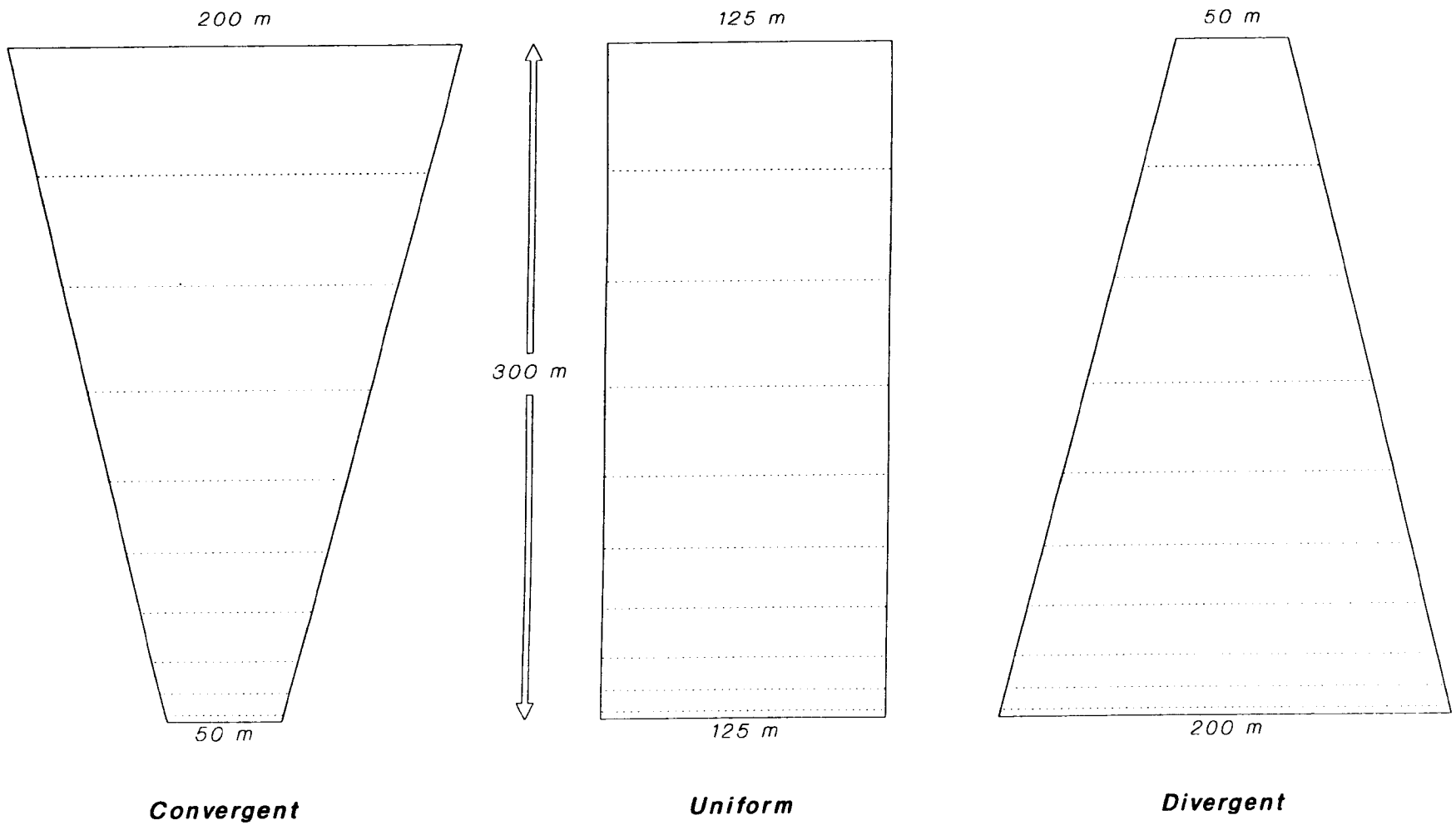

Figure 6.1: Three options for variation in plan shape: convergent; uniform; and divergent

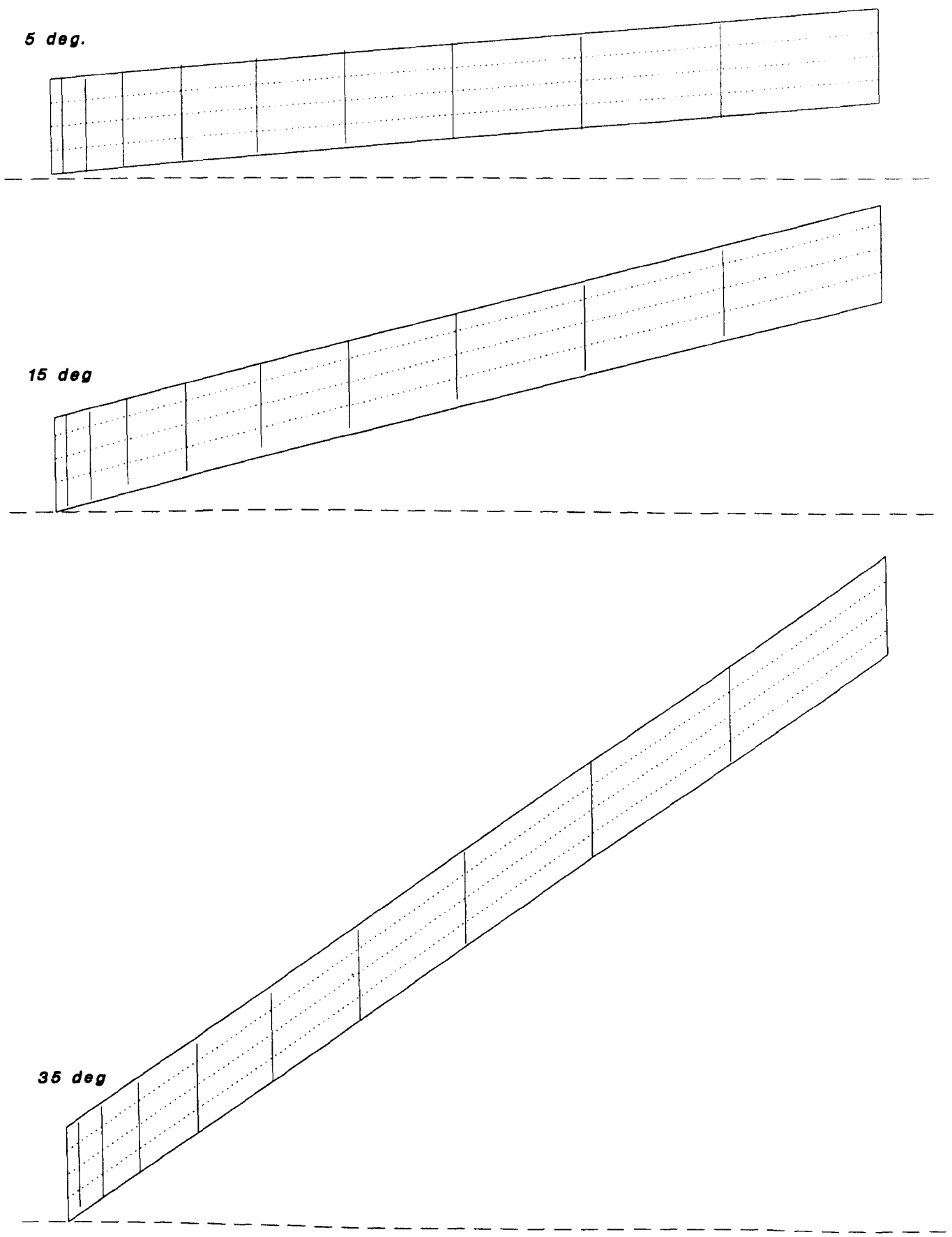

Figure 6.2: Three options for variation in slope angle used in robustness testing. Soil elements also shown

the surface after the above canopy rainfall has finished (by indirect throughfall). Evaporation is also an important canopy process, during a storm event this is mostly through evaporation off the wet leaves rather than transpiration. This has been shown to be a dominant storm process in some forest environments but at present has been largely ignored within *VSAS4* for reasons discussed in section 4.3.2.1.

LUCAS is designed to investigate the role of canopy age on storm events. This is achieved through a new pre-processing element within the scheme and consequently canopy age needs to be investigated for its importance as an input to *VSAS4*, and therefore its importance within *LUCAS*. If the results from the robustness testing indicate that canopy age is an important variable within the modelling scheme then it is worth carrying on with this investigative approach, whereas if it is found to be insignificant then there is little point in developing *LUCAS* any further.

Canopy age is the most logical parameter to use to investigate the role of vegetation in *LUCAS* as it is a general factor as well as being a direct input parameter for the pre-processing forest growth model. The canopy simulated as part of the hypothetical scenarios was deciduous (oak) forest with the rainfall partitioning parameters based on those derived by Durocher (1991) for the Leigh Woods plot site near Bristol. The growth parameters were derived and estimated from the Forestry Commission yield tables (Edwards & Christie (1981)) for oak plantations. The ages of forest chosen for use in the robustness testing were 15, 50, and 200 *years*. These ages correspond to significant periods in the canopy growth, the 15 year old plot is immature, the 50 year plot is in the period of canopy closure, and the 200 year old plot represents a fully mature deciduous canopy.

Figures 6.3 and 6.4 are representations of the simulated canopy growth. Figure 6.3 shows the growth in diameter at breast height (*dbh*) of thirteen selected trees from within the simulated plot. One of the trees is growing to its full potential as can be seen by the classical logistic growth curve shape, others are affected by inter tree competition which appears to flatten their growth curves. There is also some mortality of trees where they have been totally overshadowed by neighbours. Also shown in figure 6.3 is the inverse of unit percentage canopy cover i.e. the percentage of the plot area not covered by canopy, from this it can be seen that canopy closure occurs at around about 40-50 *years*. Figure 6.4 is a representations of the canopy at the respective ages used in the robustness testing (15, 50, and 200 years). This is a plan view showing canopy closure at 50 years and some mortality between 50 and 200 years.

One of the primary aims of the robustness testing is to investigate the importance of canopy age in relation to the three other parameters. This is so that further development can be carried out on the forest growth model if vegetation is found to be an important input factor for *VSAS4*. The canopy growth was simulated at an early stage of the pre-processing model development and consequently the actual growth values may not be totally realistic. They do however aim to give an idea of the **relative** importance of varying canopy age.

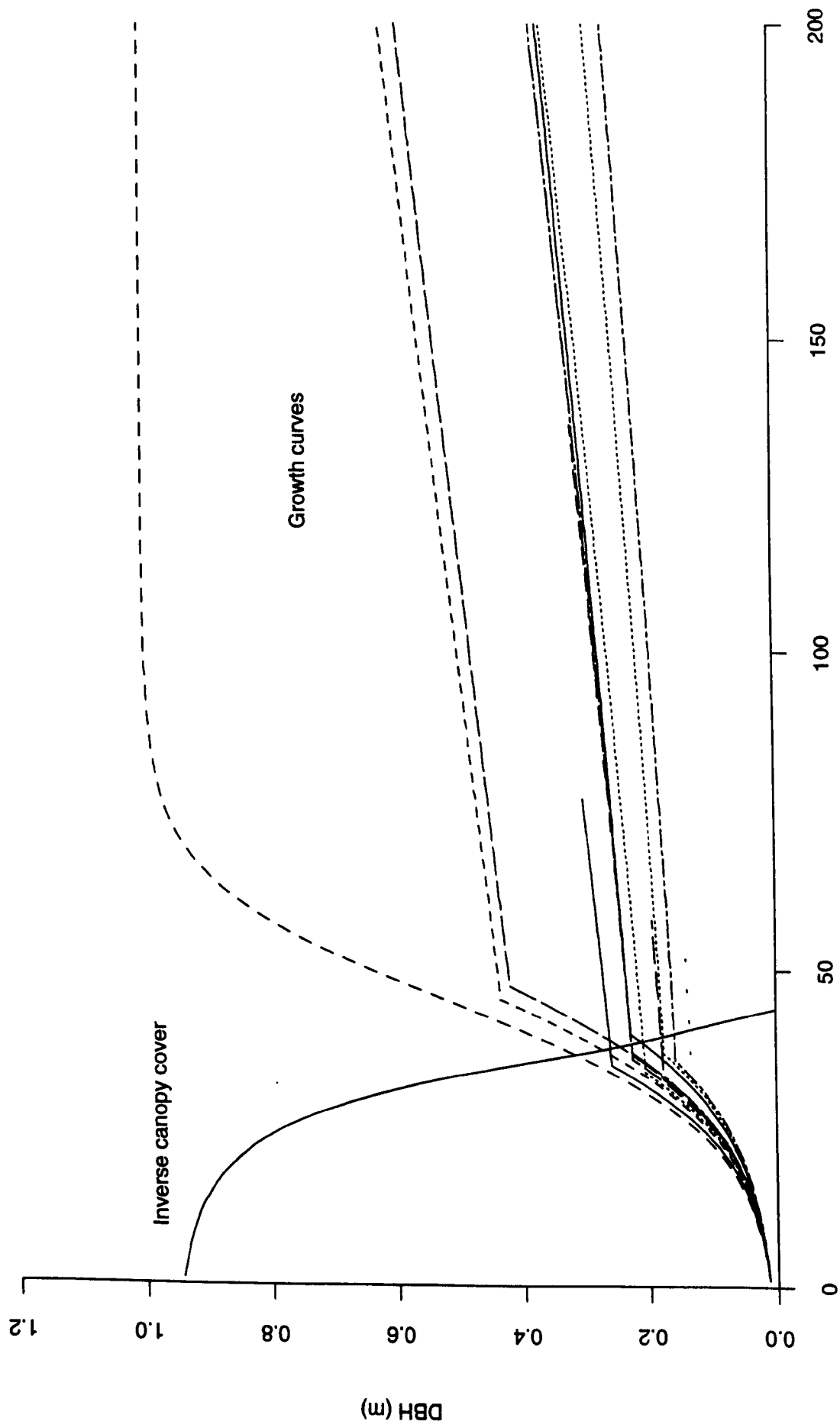

Figure 6.3: Growth curves (dbh) for 13 trees and inverse of canopy cover percentage in simulated plot used in robustness testing

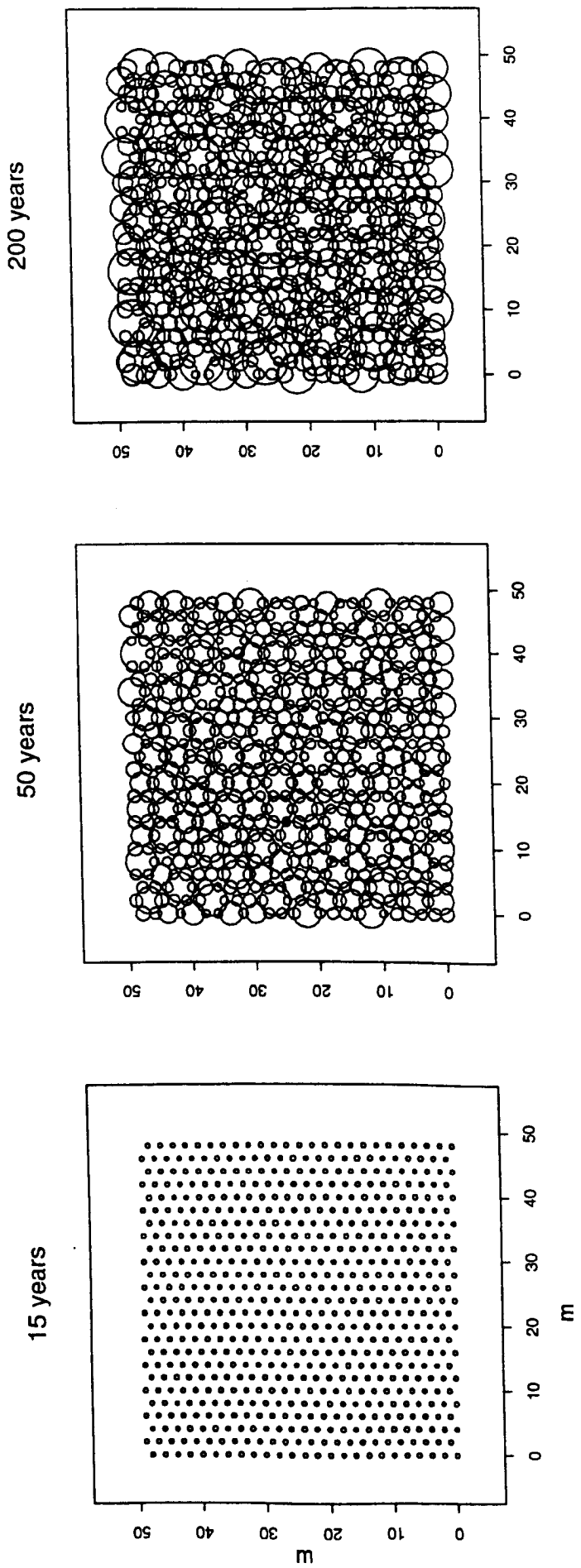

Figure 6.4: Plan view of section of simulated plot used in robustness testing for 3 canopy ages

6.2.1.4 Fixed initial conditions

The previous three sections have dealt with the range of parameter values allowed to vary within the robustness testing. All other input parameters were kept fixed throughout the first part of the robustness tests. The actual values of each of the fixed parameters are detailed below and summarised in table 6.2.

Topography and soil mantle parameters

The individual segments were varied in plan shape (convergence/divergence) and slope angle (see section 6.2.1.1). Although the plan shape was different for different simulations the area of the hypothetical segment was maintained at 37,500m^2 (3.75ha). This was achieved by maintaining the segment length at 300m, this in turn was subdivided into 10 increments upslope for all the robustness tests. This is in line with the finding of Whitelaw (1988) that the number of increments in a segment is not a critical parameter so long as the elements alongside the stream are not too large (in this case the stream-side element has a width of 3m). The segment had no subsegments and therefore the skewness parameters were all set at zero.

The depth of soil throughout the segment length was set at 2 m which was divided equally with depth into four soil elements. The soil type was uniform throughout the segment length and depth, therefore the suction moisture curve was uniform (shown in figure 6.5). The suction moisture curve and porosity values were derived from field analysis of a soil type in a Swiss catchment for use of *VSAS3* by Fawcett (1992). Soil stone content was assumed to be zero.

Forest growth and rainfall partitioning parameters

The area of forest simulated was 10,000m^2 (1ha) for each of the three ages. Trees were initially spaced at 2m in a diamond pattern, the initial *dbh* was 0.012m growing to maximum *dbh* of 1m. The growth ratio was 0.088 with a standard deviation of 0.008. These values give the average age of a tree reaching within 95% of its potential maximum size as approximately 84 years (see equation 5.3). The parameters were derived from the Forestry Commission yield tables (Edwards & Christie (1981)) for oak plantations (apart from the growth ratio and its standard deviation which were estimated).

The rainfall partitioning and individual tree geometry parameters were those derived for oak trees within a mixed deciduous plantation by Durocher (1991).

Miscellaneous parameters

The time step for soil water flow and rainfall partitioning calculations was set at 5 *minutes*. This value was arrived at after initial runs to check for the mathematical stability of this and larger time steps.

The same storm was used for all model runs, and is shown in figure 6.6. The duration

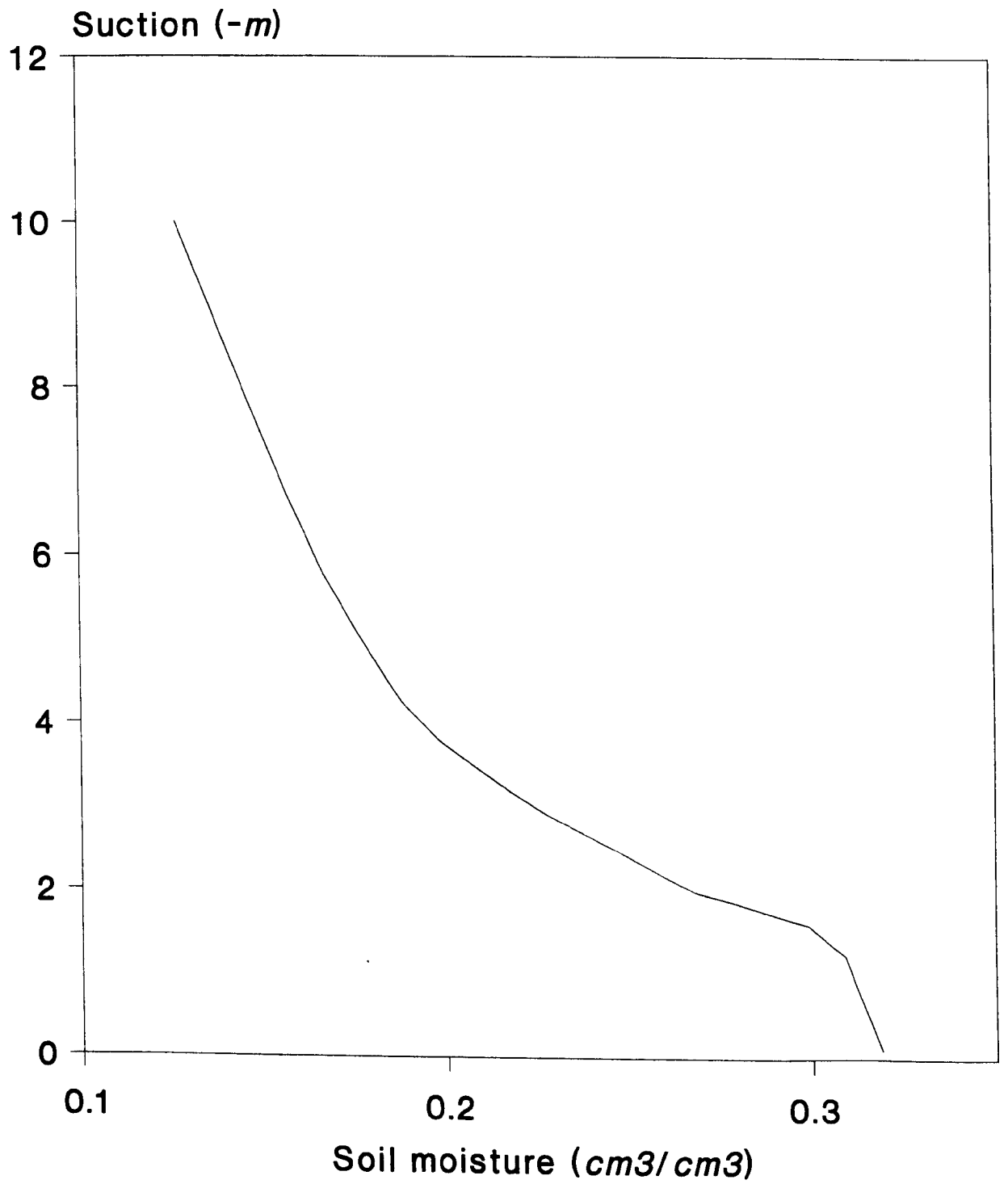

Figure 6.5: Suction moisture curve used in robustness testing

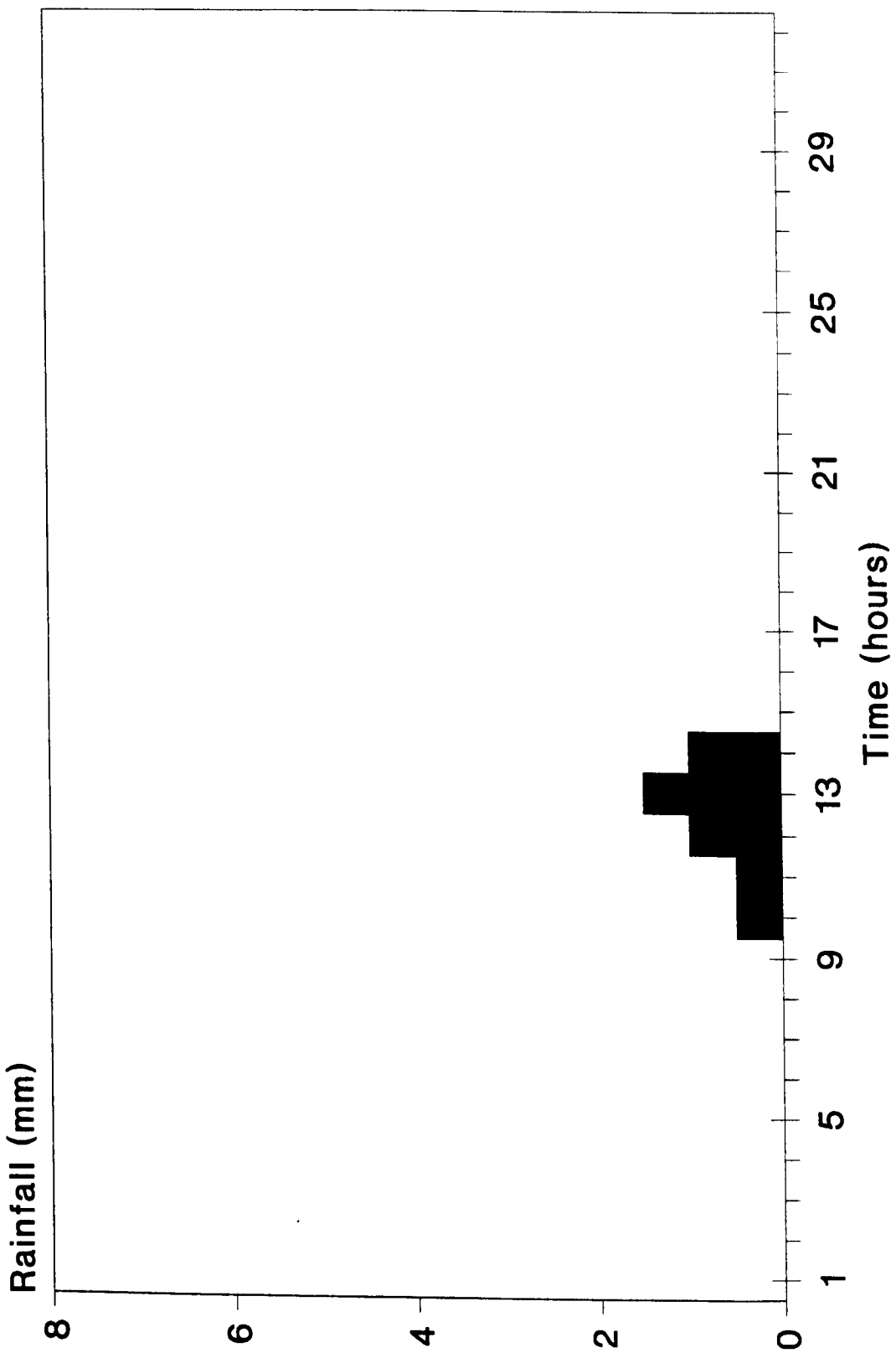

Figure 6.6: Storm rainfall used in initial robustness testing

Rainfall Partitioning		*Tree geometry*	
Leaf storage capacity (*mm*)	0.2	*dbh* v crown radius slope	3.38
Stem storage capacity (*mm*)	0.2	*dbh* v crown radius intercept (*m*)	0.219
Trunk storage capacity (*mm*)	0.4	*dbh* v tree height slope	32.6
a drainage coefficient	3.89	*dbh* v tree height intercept (*m*)	12.04
b drainage coefficient (min^{-1})	3.9×10^{-5}	Crown angle	45°
Stemflow proportion (av.)	0.019	Leaf area index	3.25
Stemflow proportion (s.d.)	0.0174	Number of variations per year†	6
Stemflow proportion (max.)	0.20	Range of variation (unit %)	0.1-1.0
Stemflow proportion (min.)	0.001		

Table 6.2: Fixed forest canopy parameter values used for robustness testing (initial and secondary)

of rainfall within the storm was five hours with nine hours draining before the event and eighteen hours afterwards to simulate the recession limb of a storm hydrograph. The storm was run as if occurring during the summer so that the canopy was in full leaf.

The simulation of evaporation was considered by giving potential evaporation the nominally small value of 0.04 $mmhr^{-1}$. This is the equivalent of saying that the solved value from the Penman-Monteith equation is 1.11×10^{-5} mms^{-1}, though the actual evaporation is still dependent on the storage and storage capacity of each leaf layer (see section 4.3.2.1).

As there was only one segment the lag time for water travelling between the segment and catchment boundary was set to zero.

6.2.2 *Robustness testing procedure*

Once the initial conditions and the three values of each parameter to be varied were determined the modelling scheme was run. The first part of this entailed modelling the growth of the forest canopy to the three ages required. This was done separately and the outputs from each run stored in input files ready for usage by *VSAS4*. *VSAS4* was then run on each of the hypothetical scenarios (81 model runs in all) and the output hydrograph analysed and compared. The output hydrograph was chosen for comparison because it is readily available and of most importance for a storm event simulator. Two other outputs that were collected but not collated were soil moisture and soil suction within the hypothetical hillslope.

The results from the variation in each parameter are shown as the differences in output hydrograph between selected model runs. These are presented as a figure consisting of a series

† Seasonal variation in parameters. The Julian days of variation are 1, 110, 140, 285, 325, and 365.

of three hydrographs, each hydrograph shown has the three parameter value results as separate lines within it. The placing of three hydrographs per figure (referred to in the text as *a* at the top and *c* at the bottom) is purely for space purposes within the thesis and does not reflect a predetermined relationship. **For each parameter the variation in hydrograph is not shown for every scenario as this would require 108 hydrographs, instead the variation is shown for a selected few, the actual number depending on how much variation there is for every separate scenario and whether they are referred to in the text.**

6.2.3 Results

6.2.3.1 Plan shape

The variation in output hydrograph is shown for 9 different scenarios: the three saturated hydraulic conductivities (K_{sat}); and the three slope angles, all with the 50 *year* canopy. The importance of plan shape on the hydrograph form is very much a function of the input K_{sat} and to a lesser extent the slope angle. This can be seen in any of the figures 6.7-6.9 where there is a very large difference with the high value of K_{sat} (a), some difference with the medium K_{sat} (b), and virtually no difference between runs when the low K_{sat} (c) is used.

Under a regime of high K_{sat} convergence of plan shape increases the size of the hydrograph peak, while divergence decreases the size of the peak and to some extent delays the timing of it. Under the medium K_{sat} regime the same applies although there is an exception in figure 6.7b where the uniform and divergent plan shape appear to produce a larger storm peak than the convergent segment. This anomaly to the general trend is in a low slope angle scenario where the effect is a different rising limb to the hydrograph (divergence delaying the rise) although it reaches peak volume at approximately the same time as the other plan shapes. The differences in peak volumes in this case are not large and cannot be considered significant.

The plan shape of the segment has an effect on the amount of baseflow but again this is a function of both the K_{sat} and slope angle value. Under a high K_{sat} convergence of plan shape leads to a higher amount of baseflow than a uniform plan shape which is in turn higher than the divergent baseflow. Where there is very little baseflow (low K_{sat}, low slope angle) there is no noticeable difference between the baseflow volumes with plan shape.

The last result detailed above hints at an explanation for this behaviour within the robustness testing. Plan shape is an important parameter in conditions where soil water flow is a dominant process and therefore a large contributor to the hydrograph but becomes considerably less important where the soil matrix does not drain easily. In the latter conditions it can be assumed the main contribution to storm runoff comes about through saturated overland flow occurring by the soil returning some of the rainfall input. Where soil water flow is an important process topographic convergence concentrates the flow into a smaller and

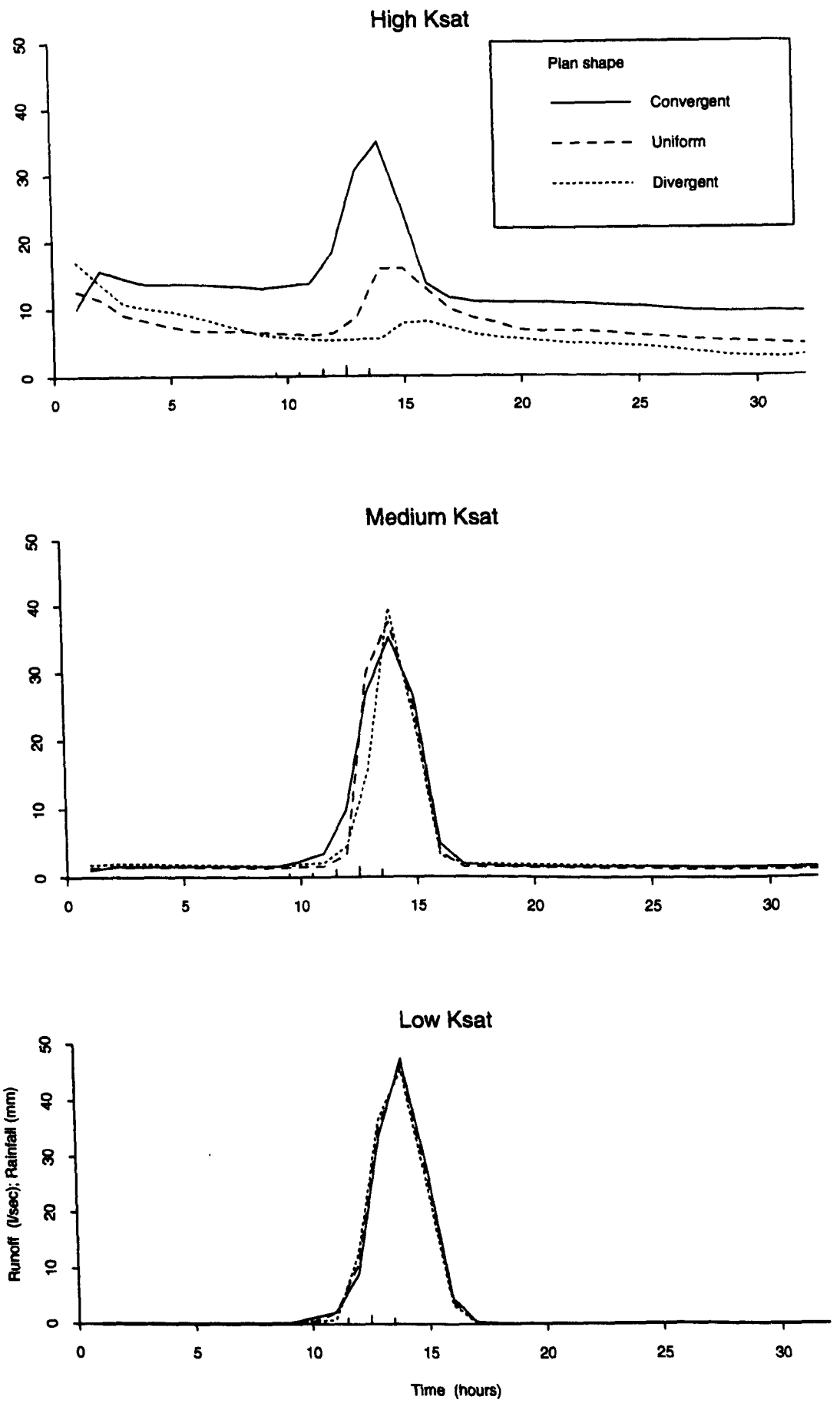

Figure 6.7: Segment runoff response with variation in plan shape and K_{sat} for 5° slope and 50 *year* canopy

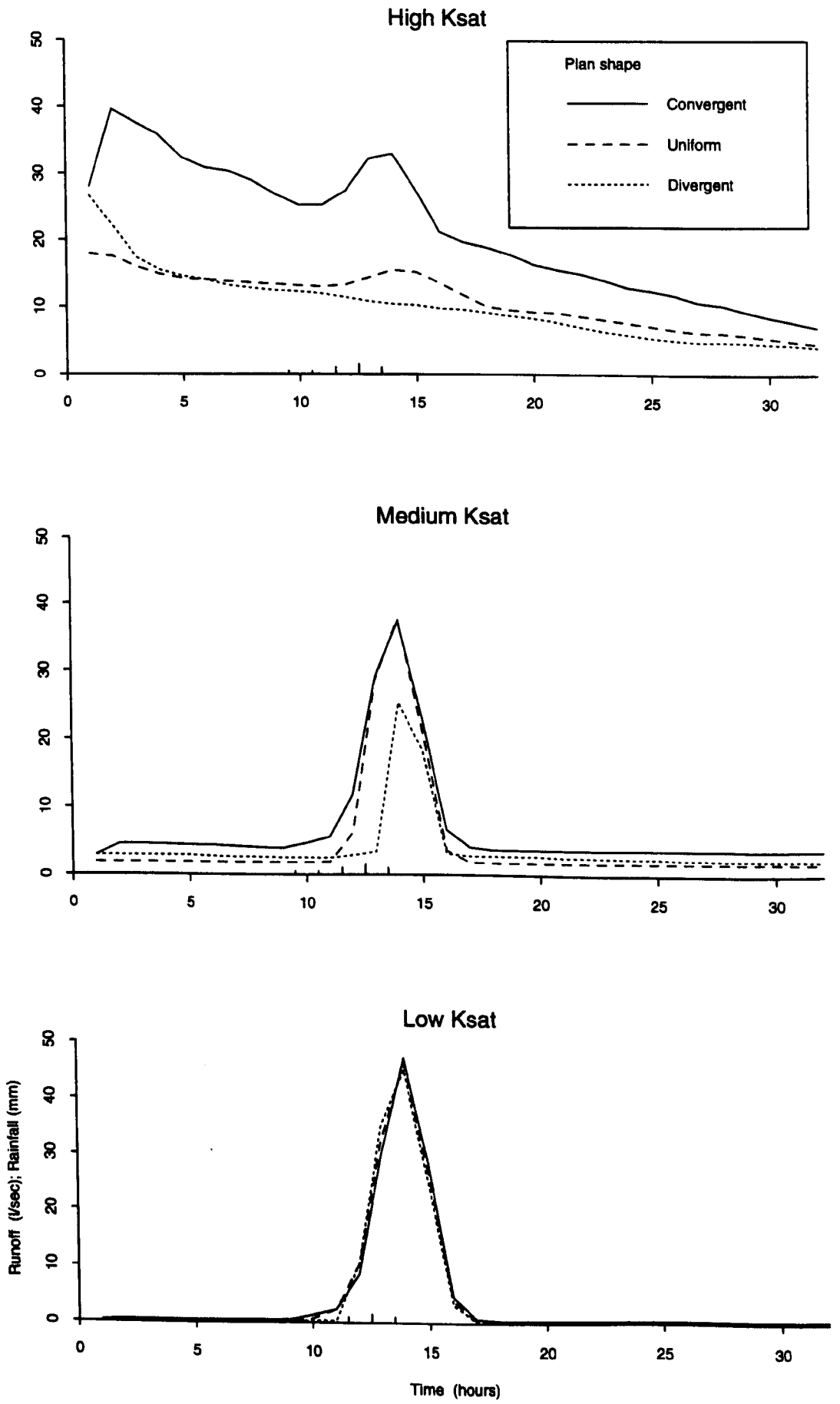

Figure 6.8: Segment runoff response with variation in plan shape and K_{sat} for 15° slope and 50 *year* canopy

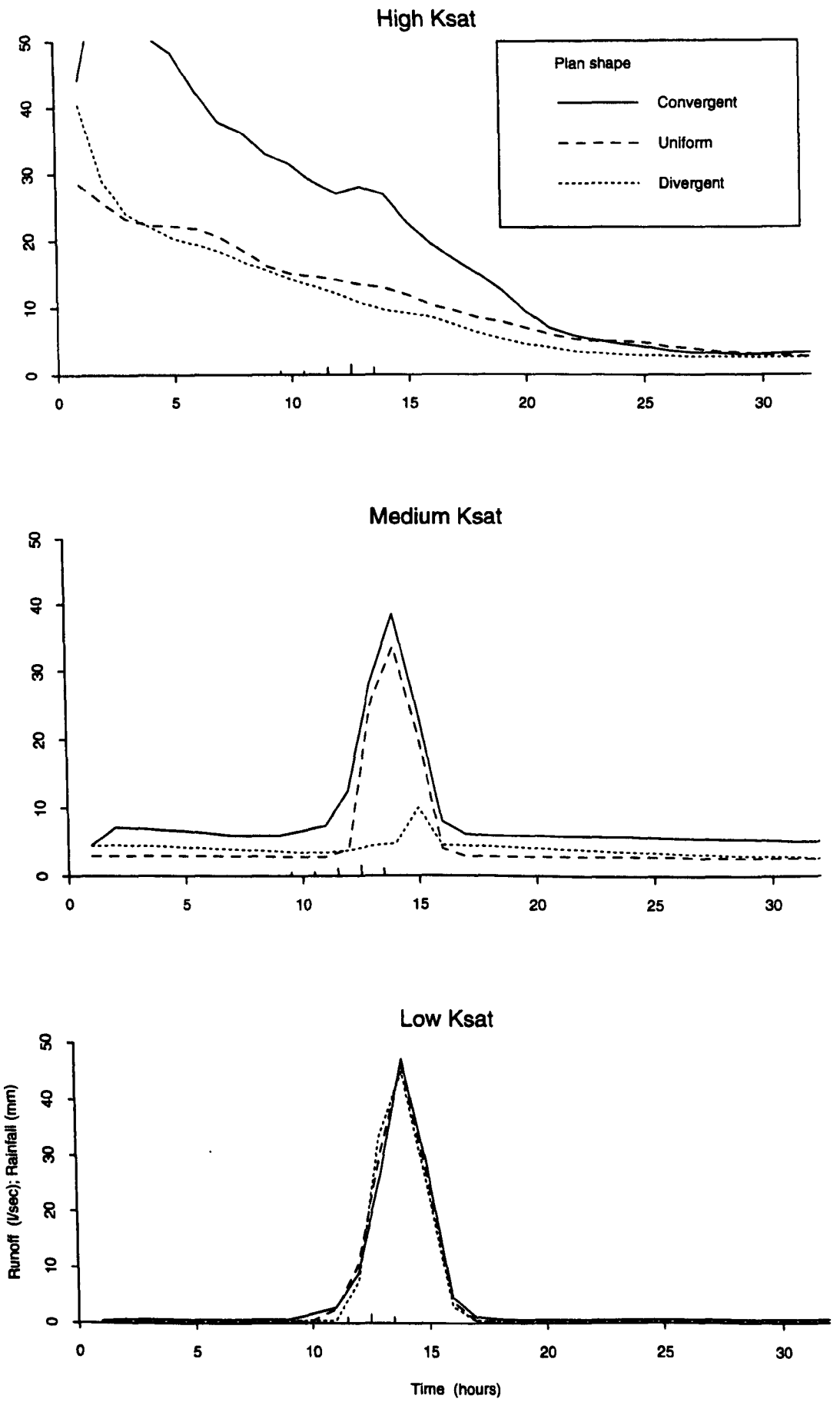

Figure 6.9: Segment runoff response with variation in plan shape and K_{sat} for 35° slope and 50 *year* canopy

smaller volume of soil downslope until the lower elements are saturated and some water is forced to leave the soil as return flow. Any subsequent rainfall falls onto the saturated zones and thus moves quickly to the stream as overland flow. The opposite happens for topographic divergence where there is an increasing volume of soil to absorb the water flowing downslope and therefore it takes a longer period of rainfall before any of the soil water is able to be released as return flow.

The conditions promoting soil matrix flow can be taken to the extreme though, in which case the soil water matrix drains so readily that the addition of storm rainfall is mostly absorbed by the drained soil and therefore there is very little effect on the storm hydrograph (e.g. figure 6.9a). This is when there is a very high K_{sat} and steep slope angle, in which case the difference with plan shape is in the amount of baseflow. As can be seen in figure 6.9a the amount of baseflow equalises after a period of drainage which in these trials is after the storm has passed over the segment. It would be interesting to see the effect of a storm applied once the baseflow levels have equalised, when the soil moisture is at its full gravity drained state. This is explored further in the secondary robustness testing described in section 6.3.

The inter-relationship between K_{sat} and slope angle to produce conditions where topographic convergence becomes an important factor is shown in a comparison between figure 6.7a and 6.9b. The first of these is a high K_{sat} with a low slope angle (5°), but a comparison can be made to 6.9b which creates similar hydrological conditions by having medium K_{sat} but a steeper slope angle (35°). Although there are still large differences between the output hydrographs the effect of a change in plan shape is very similar, divergence virtually eliminating a storm runoff peak and delaying its timing, while convergence greatly increases the peak size as well as the baseflow both before and after the rainfall event. The similarity in output between these two scenarios reinforces that there is a linkage between slope angle, K_{sat}, and plan shape. When K_{sat} and slope angle combine to produce a scenario where soil matrix flow is a dominant process (e.g. figures 6.7a and 6.9b), plan shape has a large effect on the output hydrograph.

The hypothetical scenarios where plan shape appears to be most important to the storm hydrograph are any of the canopy ages† where the slopes are either 5° or 15° and the K_{sat} is high (figures 6.7a and 6.8a). It is also a very important in conditions where there is a medium K_{sat} and the angle is steep (15° or particularly 35°) (figures 6.8b and 6.9b). Conversely the hypothetical scenarios where plan shape appeared to make very little difference are any of those where there is a low K_{sat} under any age canopy and any slope angle (figure 6.7c. 6.8c, and 6.9c). The only discernible difference under these conditions is that the divergent slope reacts to the storm rainfall later but then rises to the storm peak faster than the other two plan shapes. This is more pronounced as the slope steepness increases (figure 6.9c). This

† All other canopy ages were simulated but the results are not shown here because they show the same trends as for the 50 *year* simulations.

difference is not large and may be a factor of the treatment of overland flow by *VSAS4* as much as readily discernible hydrological process.

The importance of plan shape has already been highlighted by field studies such as Anderson & Burt (1977) and Anderson & Kneale (1982), as well as by modelling studies such as Anderson (1982) and Whitelaw (1988). The results of the robustness testing presented here show that *VSAS4* is able to recognise this importance, particularly under scenarios where subsurface soil water flow is a dominant process.

6.2.3.2 Slope angle

The results from the variations in slope angle are presented for 9 different scenarios from those used in the plan shape results in the previous section. These are: every K_{sat}; and every plan shape under the immature 15 *year* canopy.

The strong relationship between slope angle, plan shape and saturated hydraulic conductivity has already been discussed in section 6.2.3.1, and the trends are continued in the figures depicting the effects of a change in slope angle (figures 6.10-6.12). It is only in the scenarios where there is a high or medium K_{sat} that slope angle has any particularly noticeable effect (e.g. see figure 6.12).

The effect of an increasing slope angle in conditions of high K_{sat} is to increase the baseflow and decrease the size of the storm runoff peak. This is well illustrated by figure 6.12a (convergent, high K_{sat}) where a 5° slope has a pronounced storm peak whereas the 35° slope has only a very slight increase in the amount of baseflow to show for the addition of storm rainfall. The explanation for this is similar to the results for a change in plan shape, in conditions where subsurface soil water flow is a dominant process a change in slope angle is an important controlling factor, because it controls the rate of water drainage from the soil water matrix by increasing the hydraulic gradient in Darcys law (see equation 4.22). This soil matrix drainage is giving the initial baseflow. When the storm rainfall is added the soil matrix with the least water in it (i.e. the steepest therefore the most drained) absorbs most of that rainfall rather than routing it as overland flow.

Tables 6.3-6.5 illustrate the difference in water contents immediately prior to the addition of storm rainfall in figure 6.12a, for the three different slope angle conditions. In table 6.5 the steep slope conditions have low water contents in the upper elements because the high K_{sat}, convergence of flow, and steep angle are combining to promote rapid drainage towards the lower elements which remain saturated. Table 6.3 by contrast (flattest slope) has only two surface elements below saturation by the time the storm rainfall is input. The difference in total soil moisture for the segment between 5° and 35° slopes amounts to approximately 5% of the saturated volume i.e. the 35° slope has 5% less soil moisture in the entire segment than the 5° slope.

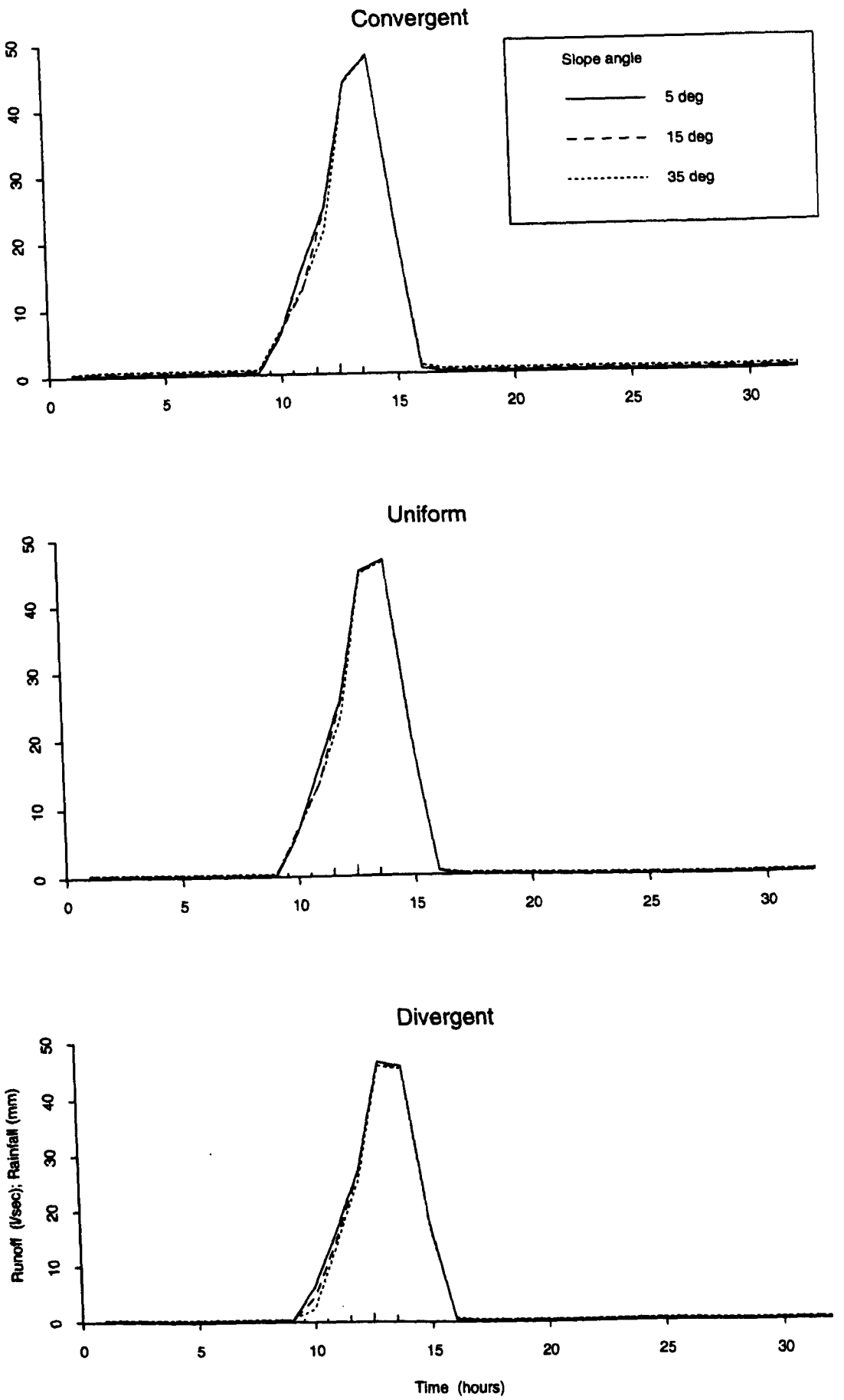

Figure 6.10: Segment runoff response with variation in slope angle and plan shape for low K_{sat} and 15 *year* canopy

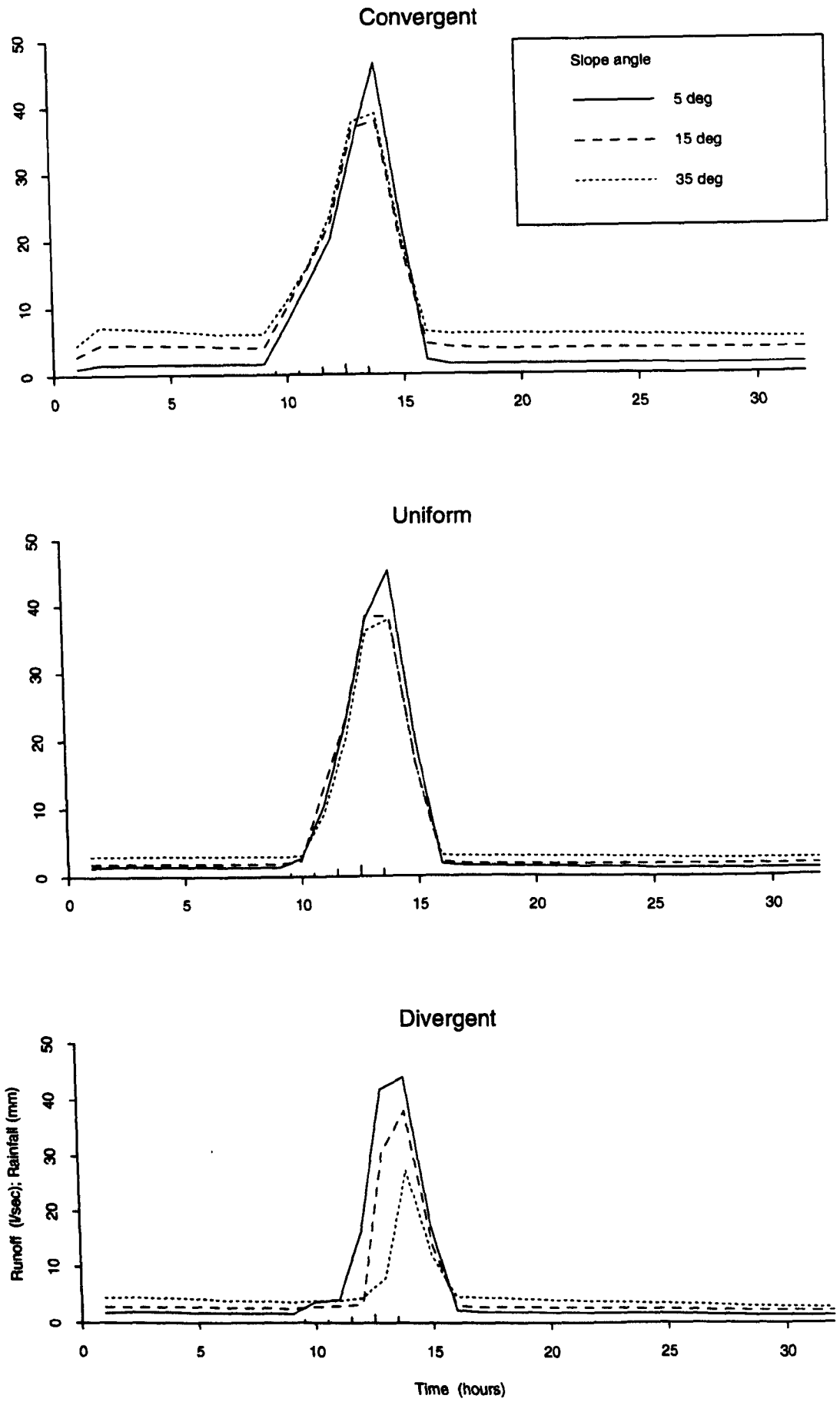

Figure 6.11: Segment runoff response with variation in slope angle and plan shape for medium K_{sat} and 15 *year* canopy

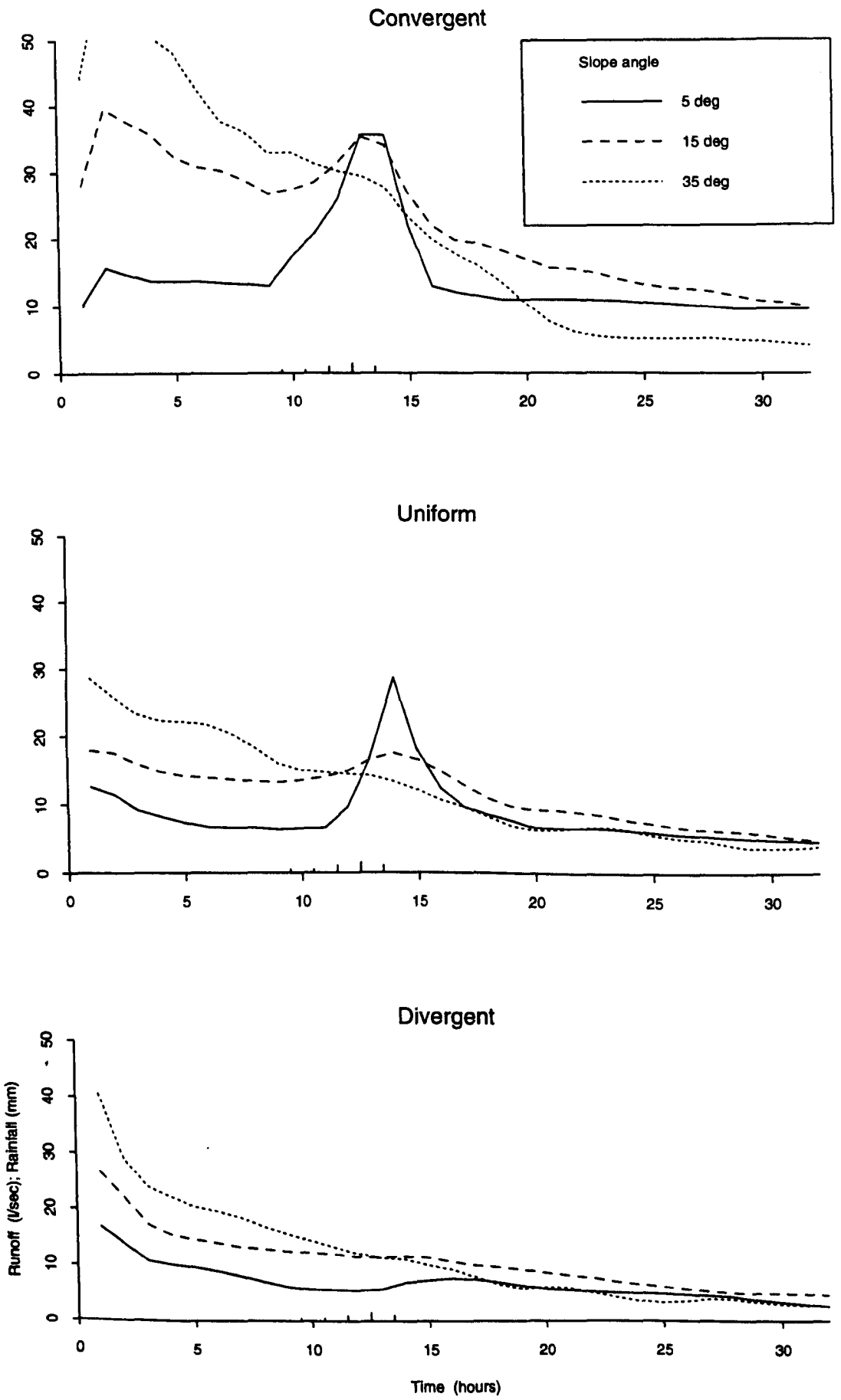

Figure 6.12: Segment runoff response with variation in slope angle and plan shape for high K_{sat} and 15 *year* canopy

1.000	1.000	1.000	1.000	1.000	1.000	1.000	1.000	0.990	0.968
1.000	1.000	1.000	1.000	1.000	1.000	1.000	1.000	1.000	0.977
1.000	1.000	1.000	1.000	1.000	1.000	1.000	1.000	1.000	1.000
1.000	1.000	1.000	1.000	1.000	1.000	1.000	1.000	1.000	1.000

Table 6.3: Unit percentage water contents for the soil elements immediately prior to the addition of storm rainfall on a 5° slope (convergent, high K_{sat}, young canopy)

1.000	1.000	1.000	1.000	1.000	1.000	1.000	0.978	0.970	0.968
1.000	1.000	1.000	1.000	1.000	1.000	1.000	1.000	0.974	0.972
1.000	1.000	1.000	1.000	1.000	1.000	1.000	1.000	0.999	0.973
1.000	1.000	1.000	1.000	1.000	1.000	1.000	1.000	1.000	0.991

Table 6.4: Unit percentage water contents for the soil elements immediately prior to the addition of storm rainfall on a 15° slope (convergent, high K_{sat}, young canopy)

1.000	1.000	1.000	1.000	1.000	0.997	0.976	0.971	0.969	0.968
1.000	1.000	1.000	1.000	1.000	1.000	1.000	0.974	0.972	0.973
1.000	1.000	1.000	1.000	1.000	1.000	1.000	0.996	0.974	0.972
1.000	1.000	1.000	1.000	1.000	1.000	1.000	1.000	0.998	0.978

Table 6.5: Unit percentage water contents for the soil elements immediately prior to the addition of storm rainfall on a 35° slope (convergent, high K_{sat}, young canopy)

On a medium K_{sat} slope the effect of changing slope angle becomes particularly noticeable when the slope is divergent (see figure 6.11c) in which case the hydrograph peak is greatly reduced by a larger slope angle. This can be explained in the same terms as for the above: with the high K_{sat} and steep slope angle the extra drainage occurring prior to the storm means that when the storm rainfall is added more of this is absorbed by the drained soil matrix and therefore the hydrograph peak from overland flow is lower. This is more noticeable in the divergent slope because the absorbed water moving downslope is taken up by the still absorbing soil water matrix downslope. In the convergent downslope soil water matrix there is less volumetric capacity to absorb the extra matrix flow volume.

An extreme condition is reached with high K_{sat} on a divergent slope (e.g. figure 6.12c) where the storm rainfall causes no noticeable effect on the hydrograph peak. The difference here is purely in terms of baseflow, the steeper slope has higher initial baseflow but ends up with lower baseflow, (also apparent in figures 6.12a and 6.12b). This reflects the way the steep slope is almost overdraining the soil and therefore there is not enough matrix soil water left to maintain the baseflow level for as long as in the less steep slopes. The size of storm used here

is too small to cause any storm runoff peak on the divergent slopes; the addition of a larger storm to these conditions is likely to cause more of a peak.

In all of the medium K_{sat} scenarios the level of baseflow, both before and after the storm peak, is higher with the increase in slope angle (e.g. figure 6.11). This suggests that the soil matrix is able to maintain the baseflow at this drainage rate as opposed to the higher rate of the high K_{sat} described above.

There are two sets of critical scenarios for a change in slope angle: the first is where there is high K_{sat} on convergent slopes with any canopy age (e.g. figure 6.12a); the second set are divergent slopes with medium K_{sat} of any age (e.g. figure 6.11c). Conversely the hypothetical scenarios where slope angle has very little effect is when there is low K_{sat} combined with any of the other conditions (i.e. any plan shape and canopy age). Under these conditions there is only a slight difference in the rising limb of the hydrograph which is probably a consequence of the soil being more drained on the steeper slope and therefore able to absorb more of the initial storm rainfall. The differences are not large enough to be truly significant.

As with plan shape, the role of slope angle has been highlighted in both previous field and modelling studies as an important controlling factor within subsurface soil water flow and therefore within hillslope hydrology. The results from the robustness testing of both of the topographic parameters presented here show that topography is an important factor within the model structure and that *VSAS4* is able to recognise their importance through its spatial discretisation.

6.2.3.3 Saturated hydraulic conductivity

The results from runs investigating the importance of saturated hydraulic conductivity are shown for 12 different sets of conditions: uniform plan shape slopes of all three canopy ages and slopes; as well as the three scenarios on a divergent 5° slope. The relationships under scenarios with convergent slopes and the two other divergent slopes can be seen in another form in figures 6.7-6.9.

The importance of K_{sat} in relation to the topographic factors of plan shape and slope angle has been discussed in the previous two sections. The most immediate comment on the role of K_{sat}, as shown by figures 6.13-6.16, is that it has a significant effect in altering the shape of every output hydrograph. This is in contrast to the two topographic parameters which had an effect on only some of the scenarios but not others.

In general terms the role of K_{sat} in altering the storm hydrographs is that the higher the K_{sat} value, more baseflow is produced both prior to and after the storm rainfall, and the lower the hydrograph peak. This is illustrated particularly well by figure 6.13b (uniform 5° slope, with a 50 *year* canopy) here the baseflow for high K_{sat} is approximately $8ls^{-1}$ and the peak volume approximately $18ls^{-1}$. For medium K_{sat} the baseflow drops to around $2ls^{-1}$ while the

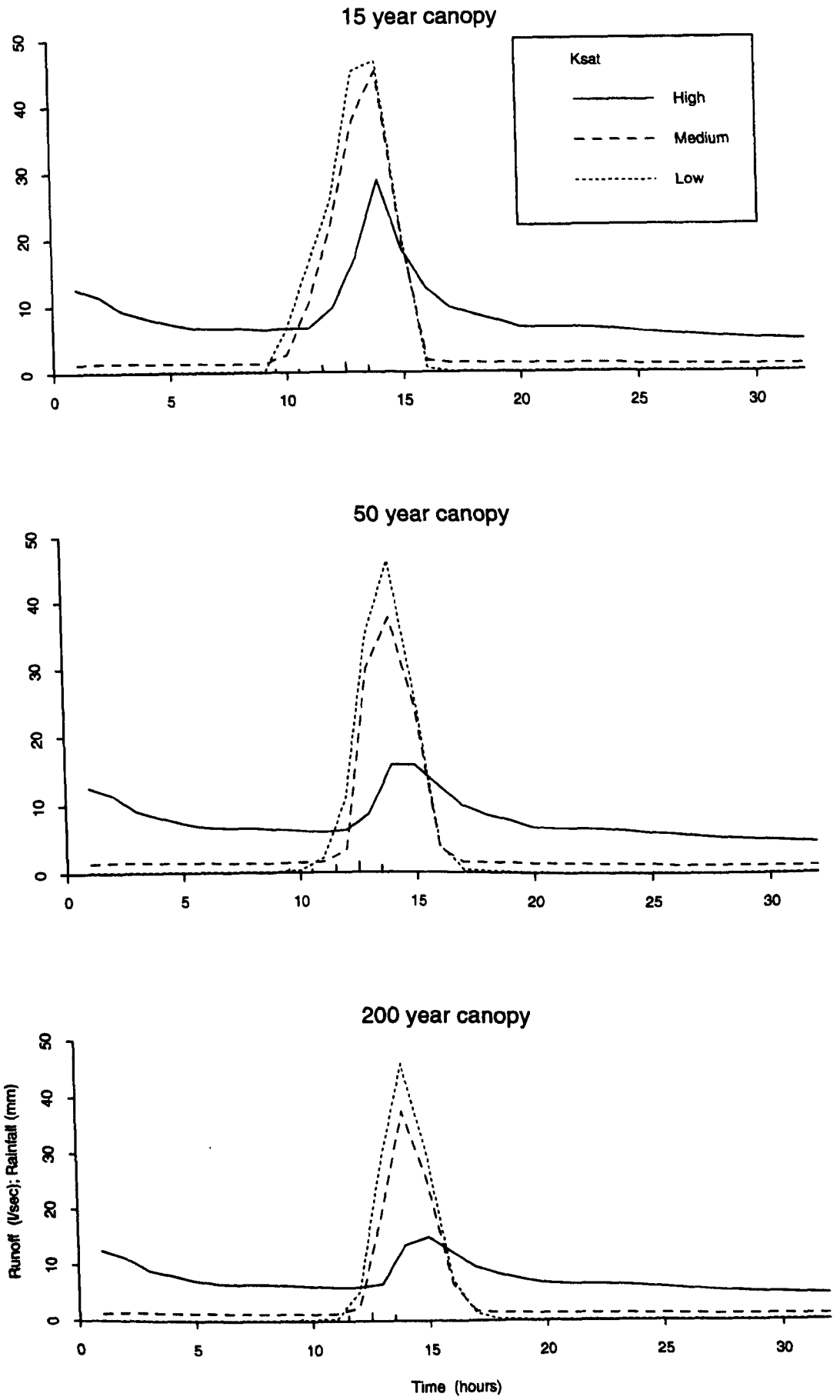

Figure 6.13: Segment runoff response with variation in K_{sat} and canopy age for uniform plan shape and 5° slope

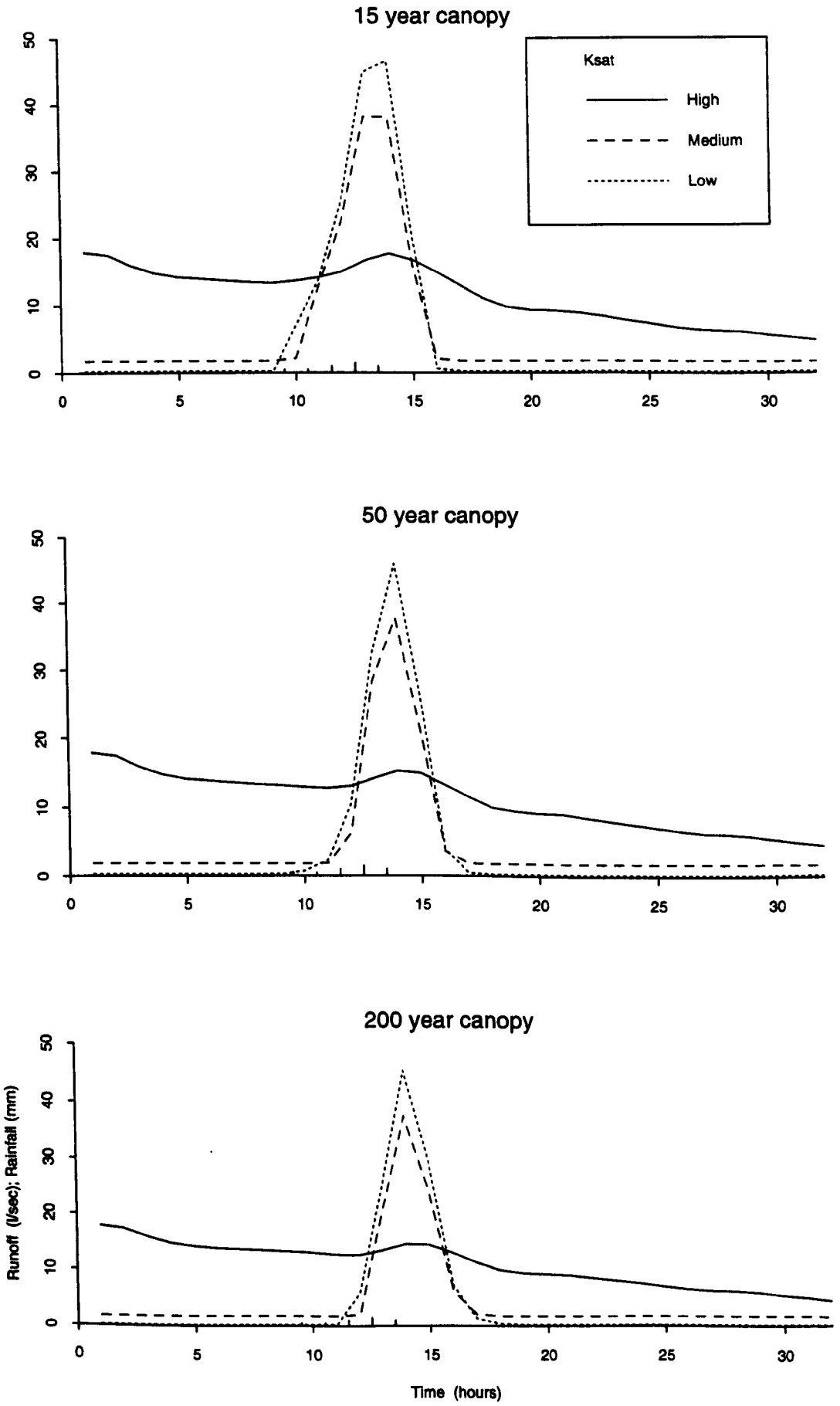

Figure 6.14: Segment runoff response with variation in K_{sat} and canopy age for uniform plan shape and 15° slope

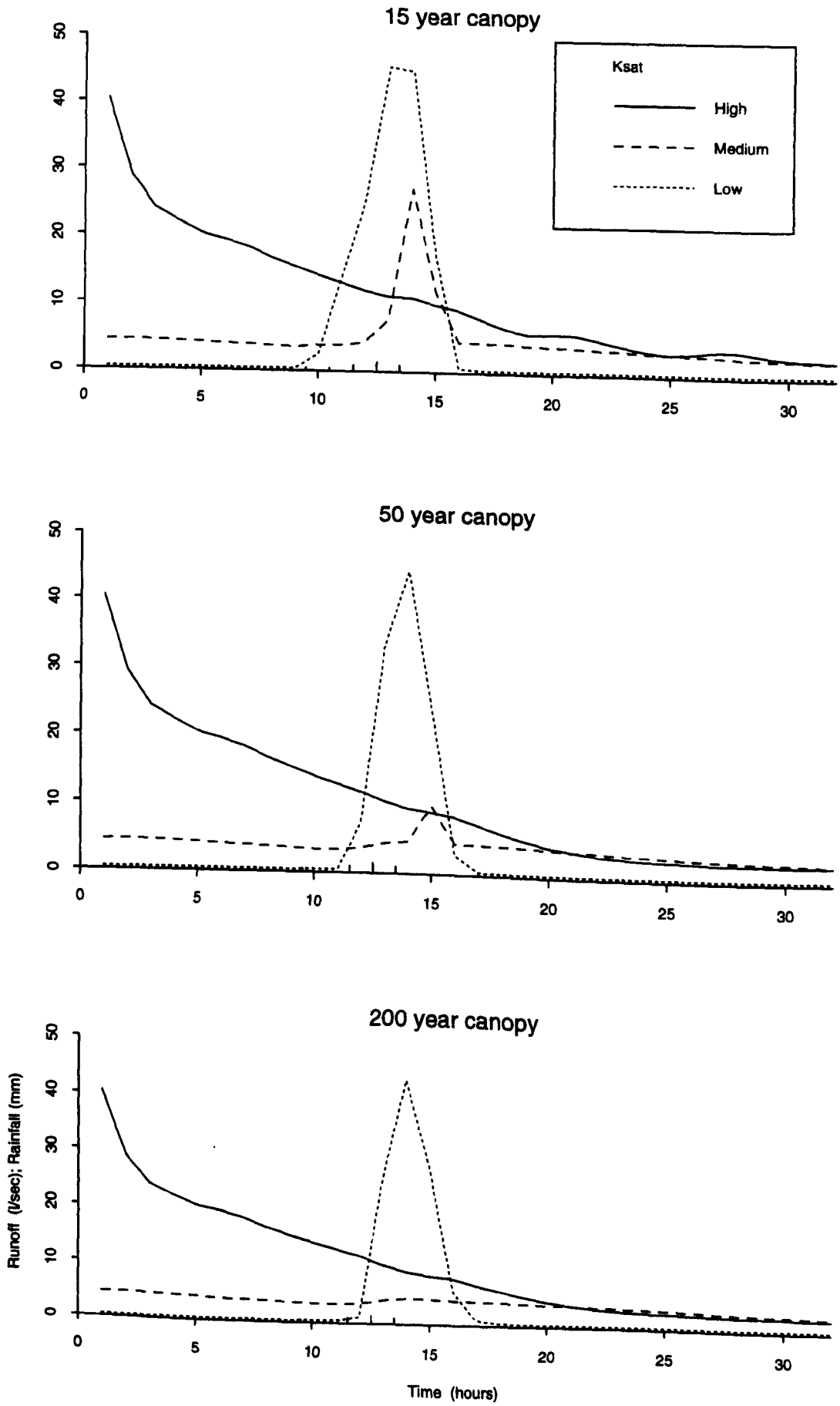

Figure 6.15: Segment runoff response with variation in K_{sat} and canopy age for uniform plan shape and 35° slope

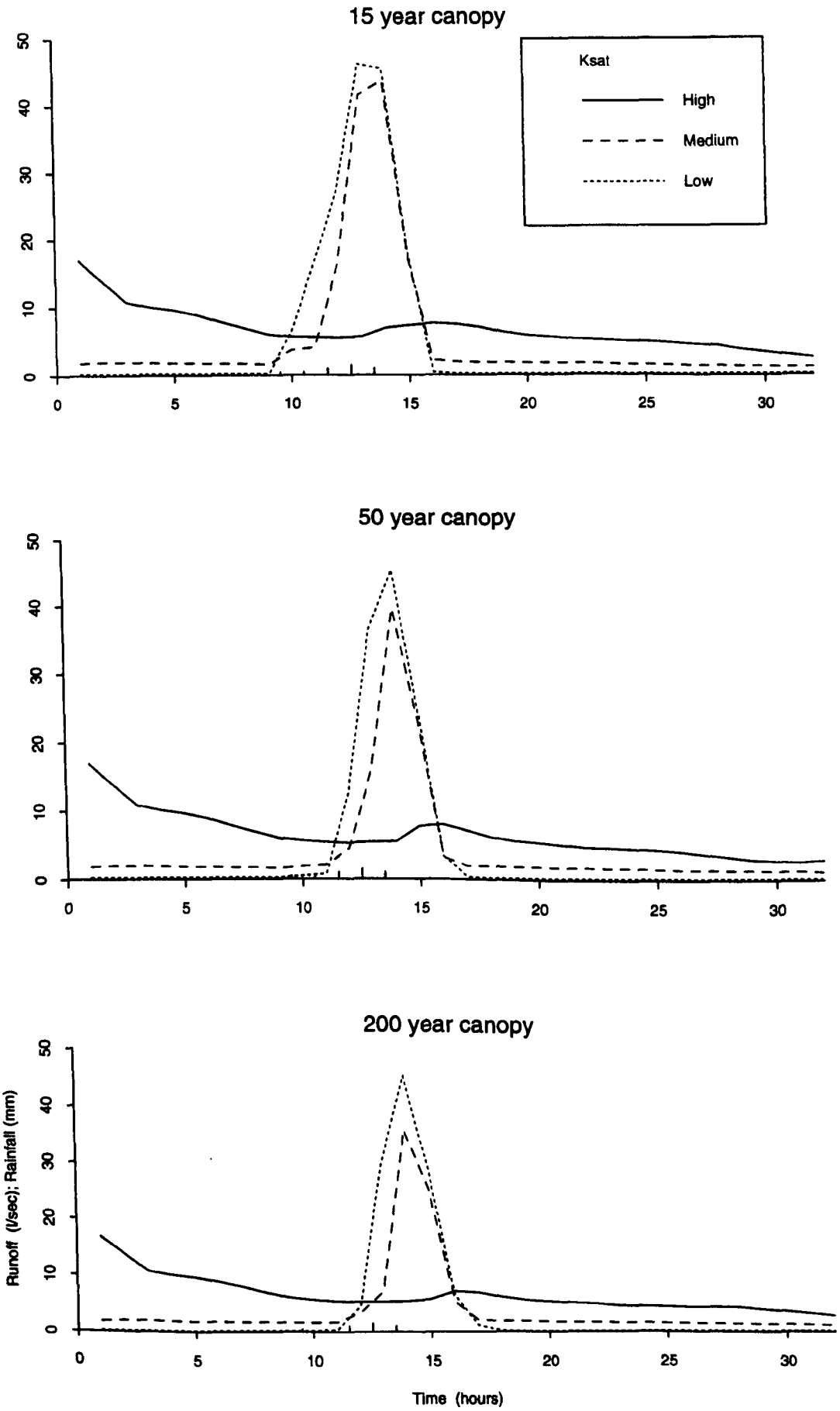

Figure 6.16: Segment runoff response with variation in K_{sat} and canopy age for divergent plan shape and 5° slope

peak volume doubles to approximately $38ls^{-1}$. For the low K_{sat} the baseflow is negligible while the peak volume gets as high as $48ls^{-1}$. The actual timing of peak flow is not greatly different but the receding limb of the storm peak is accentuated by the high K_{sat} scenario.

The role of K_{sat} in controlling the amount of soil water flow has been discussed with respect to the topographic parameters. It is particularly evident in the steep sloped, uniform slope (figure 6.15), and all of the divergent slope scenarios (e.g. figure 6.16), where the storm response ranges from an extreme peak with the low K_{sat} to a series of minor pulses with the high K_{sat}.

The reasoning for the importance of K_{sat} is self evident from the model structure; it is assumed that all subsurface water flow occurs in a Darcian manner and Darcys law relates the rate of water flow to the hydraulic gradient via saturated hydraulic conductivity (see equation 4.22). In the case of unsaturated soil water flow the Millington-Quirk method derives the unsaturated hydraulic conductivity from a known relationship to K_{sat} (see equation 4.7); K_{unsat} then replaces K_{sat} in the Richards generalisation of Darcys law (see equation 4.23). Any rainfall input that cannot be absorbed by the soil matrix and then routed as Darcian flow is treated as overland flow; in this way K_{sat} controls the amount of overland flow as well as the matrix flow. The preeminence of Darcian flow within the model structure means that it is logical that K_{sat} is an extremely important governing parameter. When the slope angle is high the hydraulic gradient between soil elements is high, which combined with a high K_{sat} means the rate of water flow between elements will be high and therefore they will drain quickly resulting in large amounts of storm rainfall being absorbed into the dry soil.

Another point to consider is that in allowing the parameters to vary within reasonable field limits the difference between the highest and lowest saturated hydraulic conductivities is two orders of magnitude whereas the other factors vary by considerably less. This is a reflection of the tremendous variation in saturated hydraulic conductivity between different soil types but does make the results appear extremely dramatic because of the scale difference between the three input values.

A factor not considered in these robustness runs is the role of the soil suction moisture curve, which governs the unsaturated hydraulic conductivity by the Millington-Quirk method. Theoretically this could be significant as the relationship between K_{unsat} and soil moisture is logarithmic and a small difference in the soil suction, to K_{unsat} relationship may transfer through into a large difference in the calculated K_{unsat}. This would mean large differences in the amount of soil matrix flow in non-saturated conditions.

In the robustness testing runs carried out here there are no particular critical scenarios where K_{sat} needs special consideration; it is a critical parameter in all of the modelled scenarios. This has similarities to the conclusion of Whitelaw (1988) in his sensitivity analysis of *VSAS2* that: "the effects of K_{sat} are significant without clear thresholds". Whitelaw recommended that K_{sat} should be measured to within 15% for predictive simulations.

6.2.3.4 Canopy age

One of the stated aims of the robustness testing (see section 6.1.1) was to find the relative importance of canopy age as it is the new factor within *LUCAS*; consequently the results from the runs investigating canopy age are shown for every modelled scenario (figures 6.17-6.25). This does have some repetition from the earlier figures but it is necessary to show clearly the importance of canopy age in every possible permutation.

Described in general terms canopy age modifies the storm hydrograph in three inter-related ways: delaying the rising limb of the storm hydrograph; lessening the peak size; and extending the recession limb. Although the peak size is altered, the actual timing of the peak flows is the same except for on the divergent slopes. It is noticeable from many of the scenario hydrographs that there is a greater difference between the 15 and 50 *year* canopy hydrographs than between the 50 and 200 *year* canopy hydrographs. The 50 *year* canopy is immediately post canopy closure which suggests that this is one of the critical points in affecting storm runoff, once this has occurred the effect of a canopy maturing is not as noticeable.

All of these attributes are evident in figure 6.21c, a uniform plan shape 35° slope, with medium K_{sat}. Between the 15 year and 200 *year* canopy scenarios the start of the rising limb is delayed by 2 *hours* and the ending of the recession limb delayed by 1 *hour*. The peak volumes of storm runoff were 38, 34, and 32ls^{-1} for the 15, 50, and 200 *year* canopies respectively.

An increase in canopy age increases the individual tree sizes which when using the relationship of Halldin (1985) would add to the number of intercepting elements (leaves, stems, branches) within the canopy. Because these simulations are in a deciduous forest this relationship has not been used and the average LAI/SAI values have been used throughout the growth period. This means that the growth of the trees does not affect the number of intercepting layers but does decrease the proportion of inter-tree space within the whole canopy thereby allocating more rainfall to the indirect throughfall process (rather than direct throughfall). This has the effect of delaying the rainfall reaching the soil surface and increasing the amount of water available for interception loss.

The delay in the rising limb of a hydrograph under an mature canopy can be traced to the delay in rainfall reaching the soil as the rainfall moves stepwise through the leaf. Conversely the difference in the receding limb of the hydrograph is a factor of the canopy continuing to drain after the above canopy rainfall has stopped, thereby continuing to add water to the soil after the storm rainfall has stopped. As with delaying the input, the more rainfall partitioned to these intercepting layers the greater the volume of water available to drain in this manner. The difference in peak flow volume with canopy age is through the evaporation loss whilst the water is being delayed by the canopy, therefore providing less below canopy rainfall. Although the input potential evaporation value was fairly small it can become significant when there is water sitting on the intercepting layers (stem and leaf) for a reasonable length of time.

The link between saturated hydraulic conductivity and canopy age is not as strong as

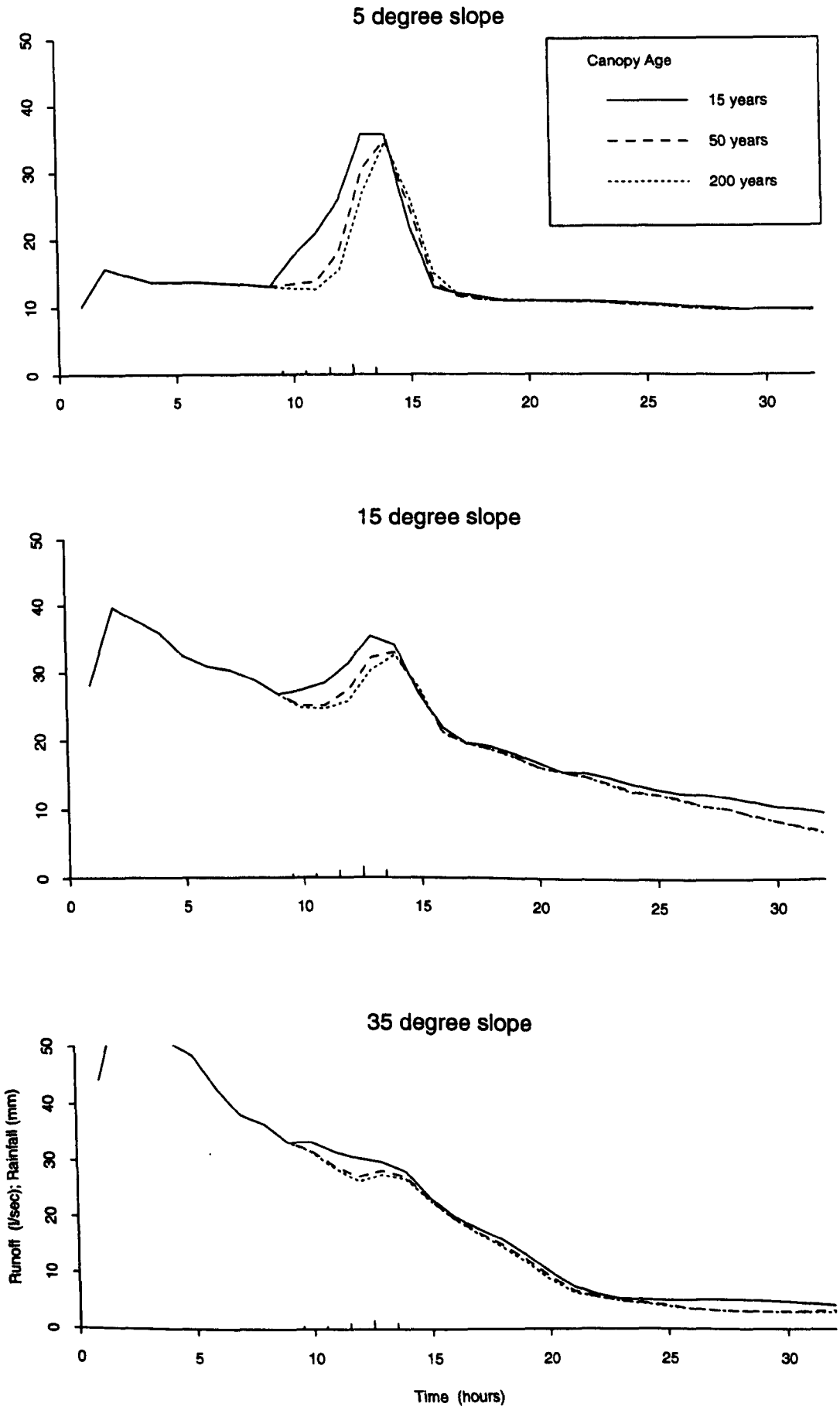

Figure 6.17: Segment runoff response with variation in canopy age and slope angle for high K_{sat} and convergent slope

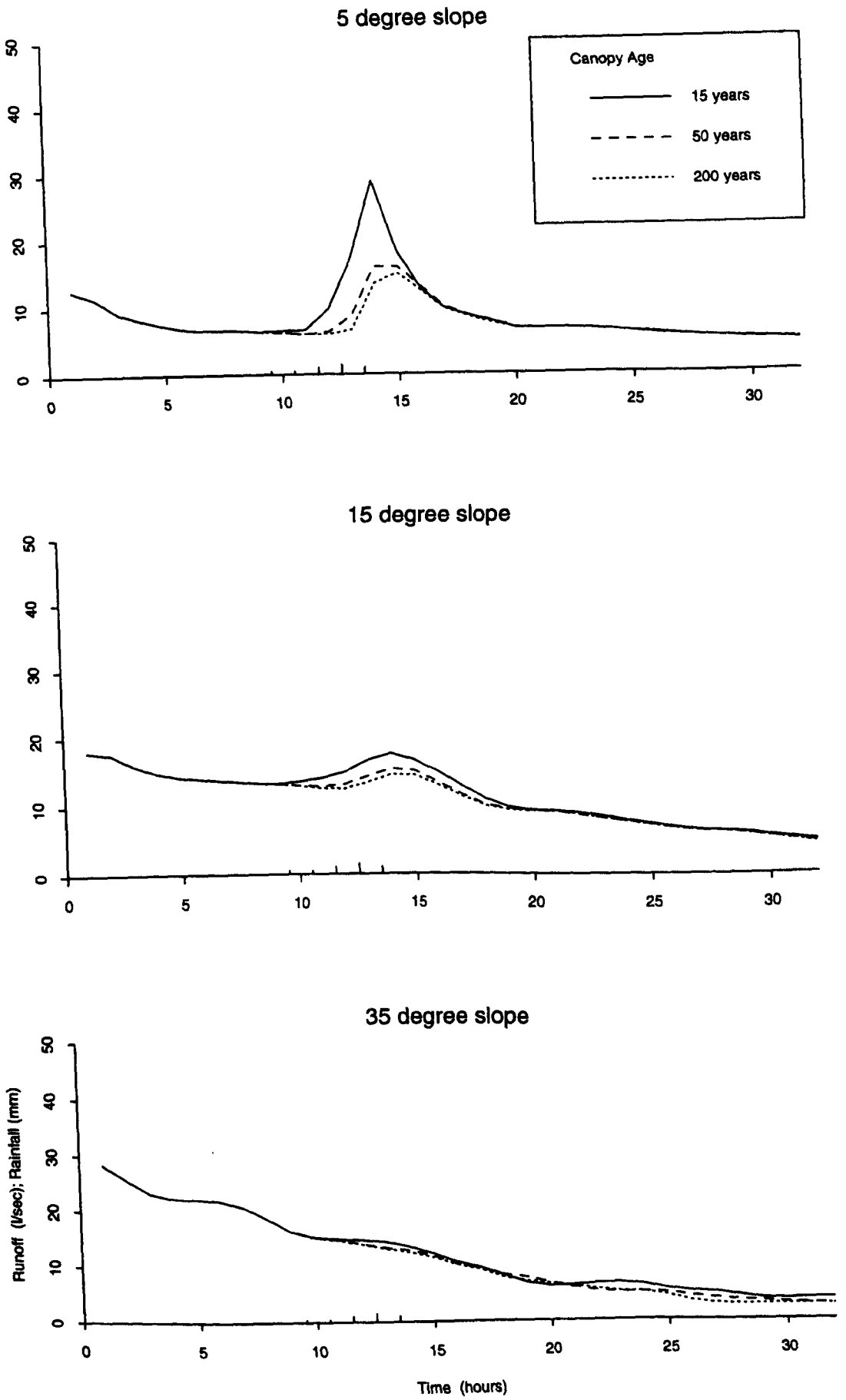

Figure 6.18: Segment runoff response with variation in canopy age and slope angle for high K_{sat} and uniform slope

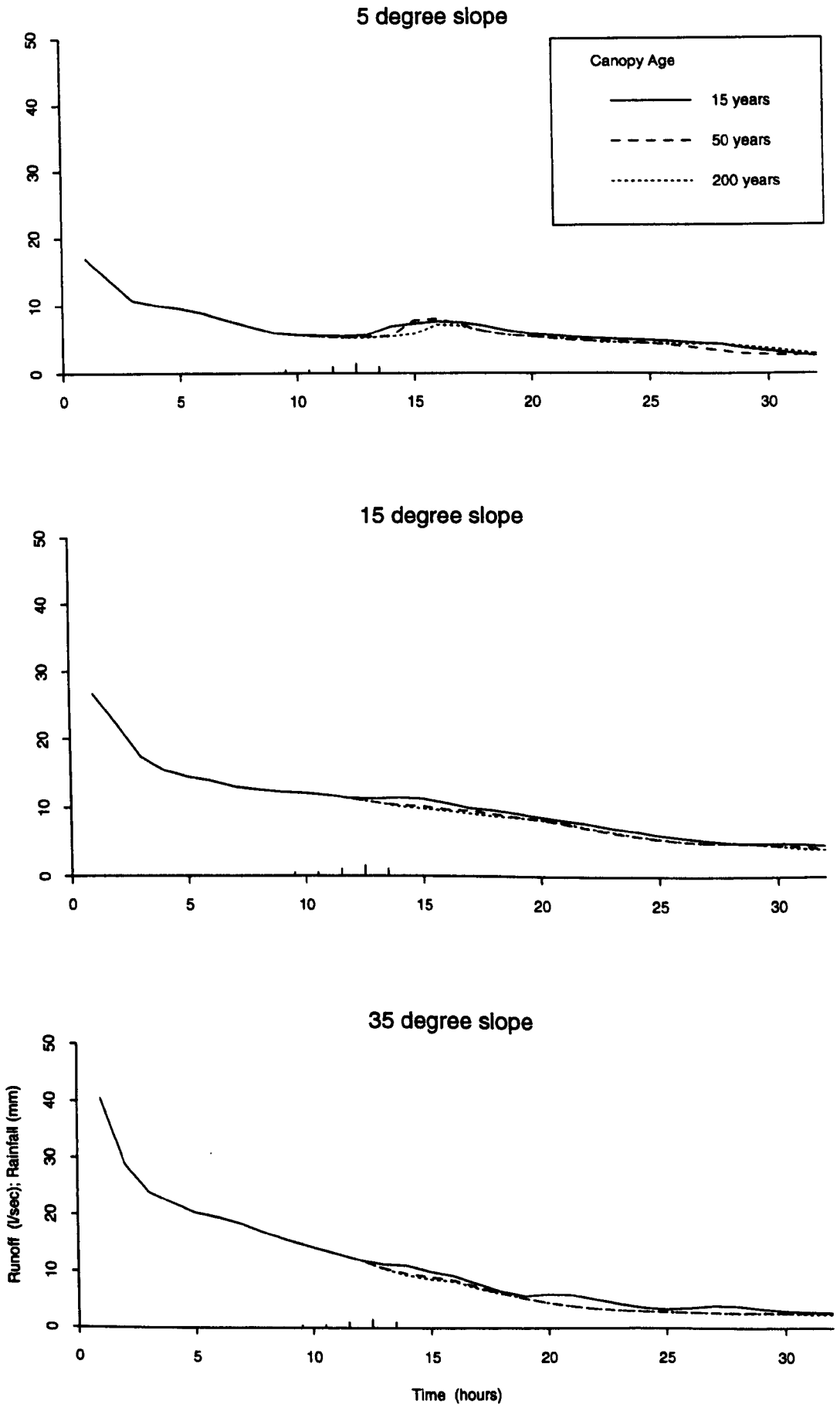

Figure 6.19: Segment runoff response with variation in canopy age and slope angle for high K_{sat} and divergent slope

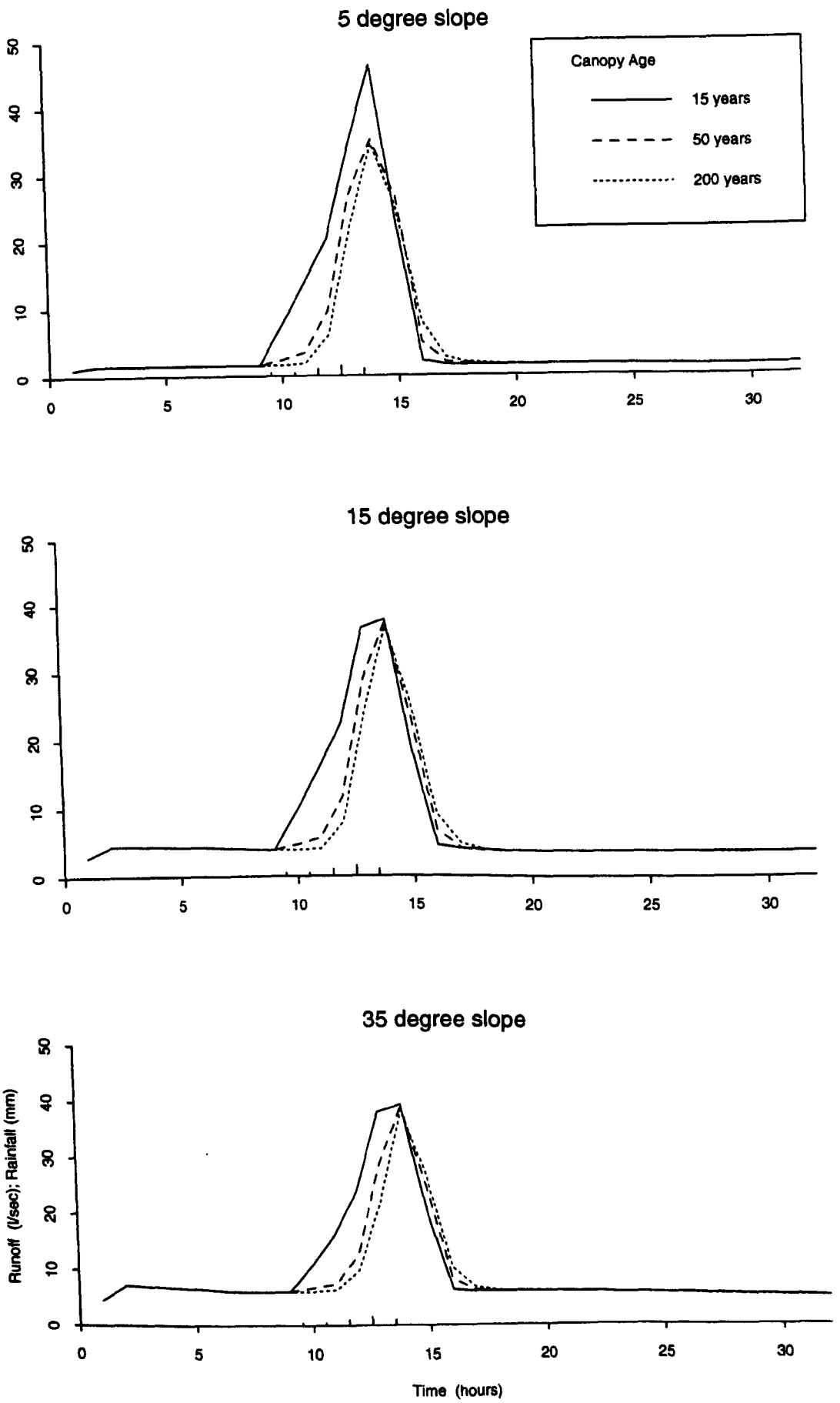

Figure 6.20: Segment runoff response with variation in canopy age and slope angle for medium K_{sat} and convergent slope

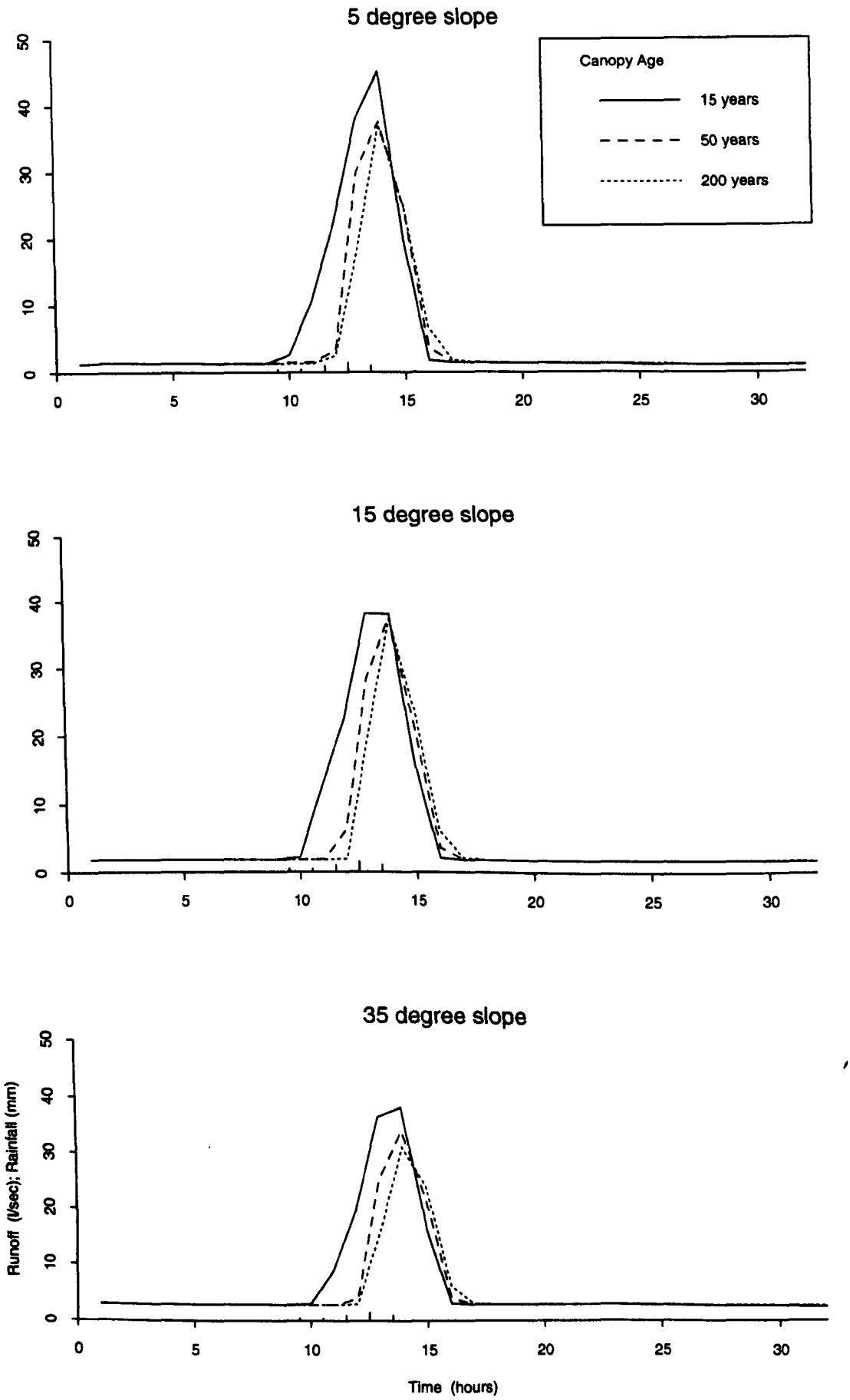

Figure 6.21: Segment runoff response with variation in canopy age and slope angle for medium K_{sat} and uniform slope

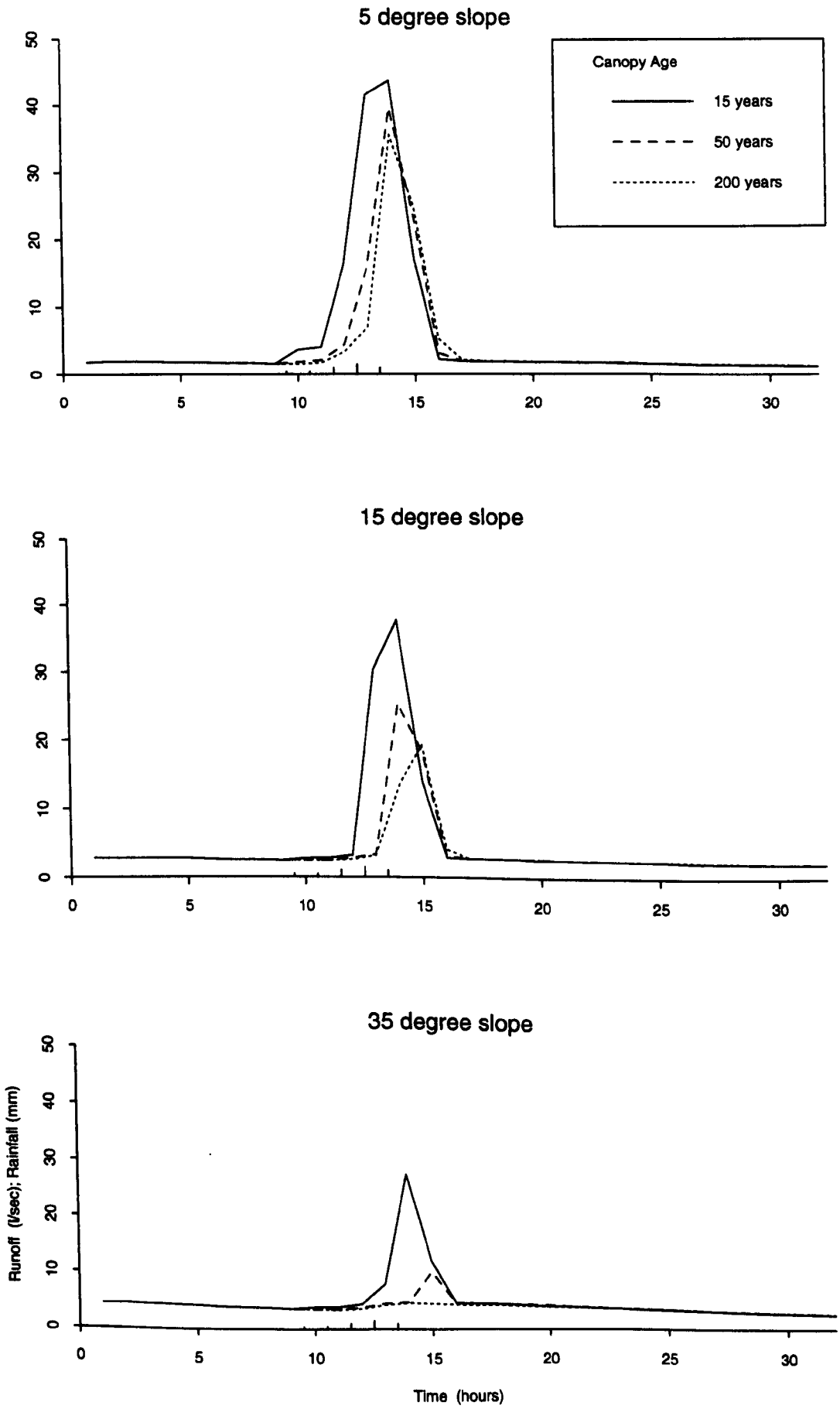

Figure 6.22: Segment runoff response with variation in canopy age and slope angle for medium K_{sat} and divergent slope

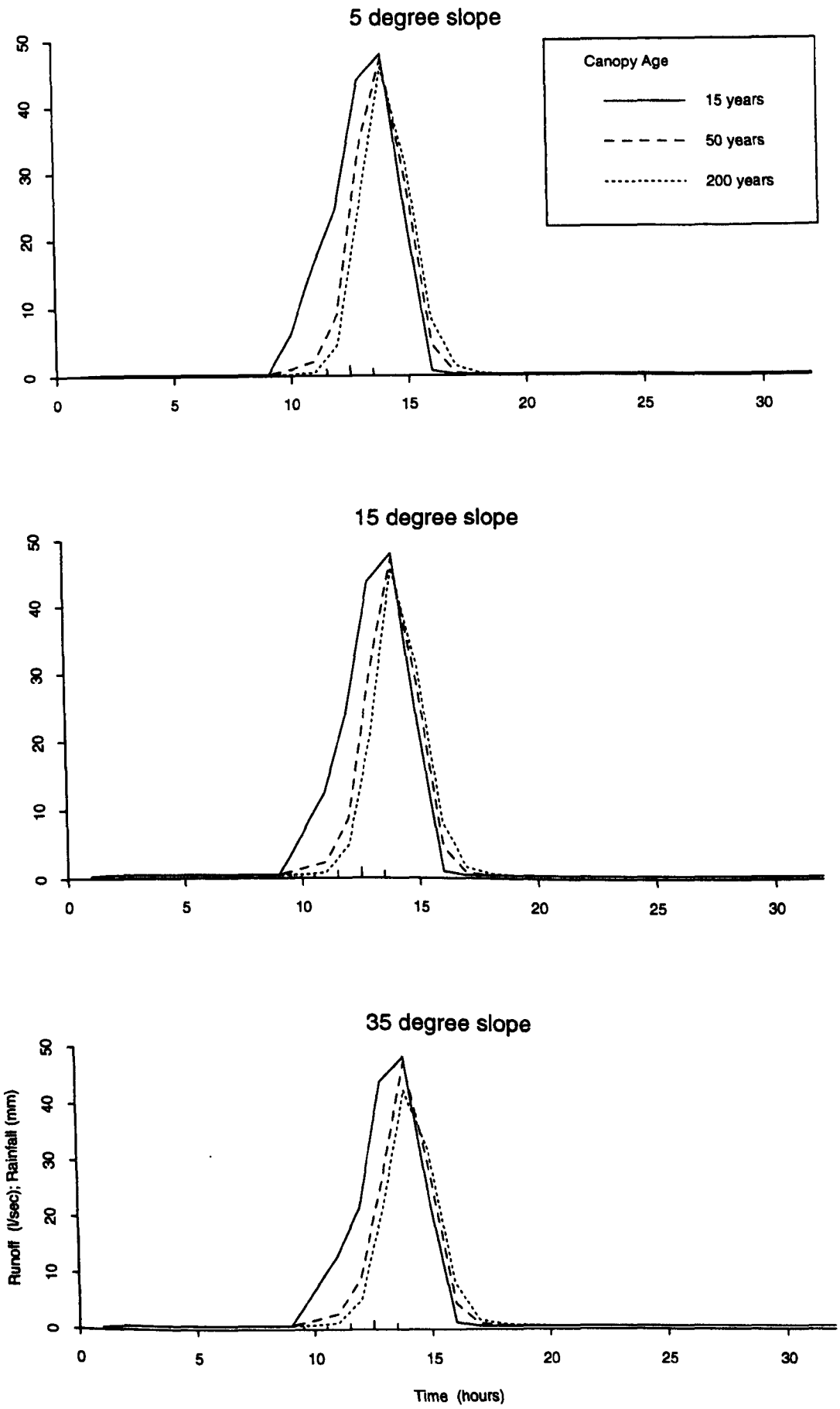

Figure 6.23: Segment runoff response with variation in canopy age and slope angle for low K_{sat} and convergent slope

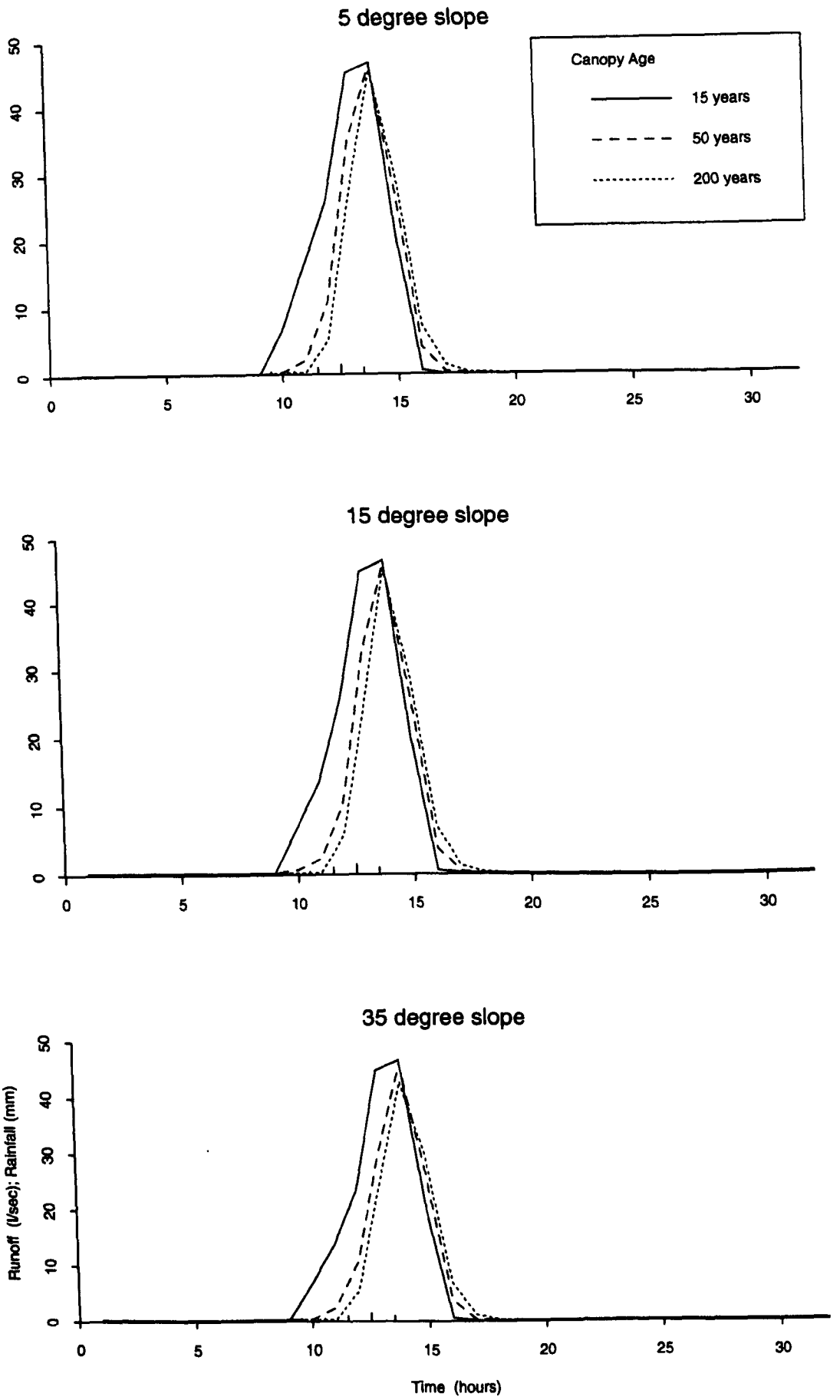

Figure 6.24: Segment runoff response with variation in canopy age and slope angle for low K_{sat} and uniform slope

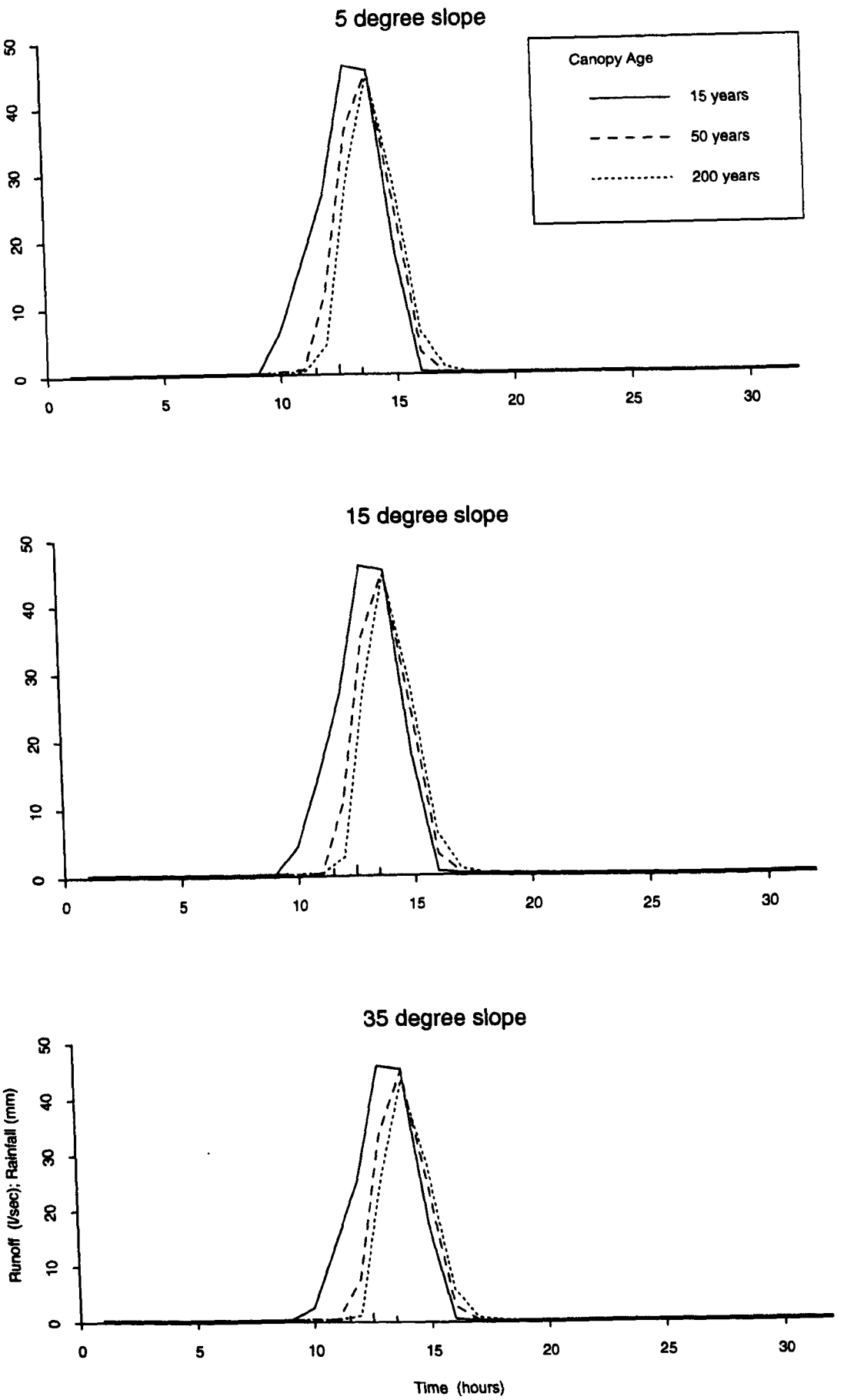

Figure 6.25: Segment runoff response with variation in canopy age and slope angle for low K_{sat} and divergent slope

for the two topography parameters but nevertheless K_{sat} still has a role in shaping the hydrograph responses under the three canopy ages. The differences with K_{sat} are illustrated by comparison of figures 6.19b, 6.22b, and 6.25b (divergent 15° slopes). The hydrographs under high K_{sat} conditions (figure 6.19b) show virtually no change with canopy age as there is virtually no stormflow response to the rainfall, the medium K_{sat} (figure 6.22b) shows a marked difference with canopy age, as does the low K_{sat} (figure 6.25b).

This difference in hydrographs with K_{sat} can still be explained in the same terms as in sections 6.2.3.1 and 6.2.3.2. In soil hydrology conditions where all of the rainfall reaching the surface immediately enters into matrix flow the slow travel time of matrix flow means that the effect of the differing rainfall input will not be as marked on the hydrograph as for the case where a considerable proportion of the rainfall cannot be immediately absorbed and therefore travels to the stream as overland flow†. The former case applies for a high K_{sat} or a steep sloped medium K_{sat} while the latter applies to the low K_{sat} scenarios. It is particularly evident in the divergent plan shape scenario (e.g. figure 6.22c) as there is very little return flow contributing to the overland flow, and the excess overland flow (see footnote) is more able to be absorbed by the greater soil volume downslope. In figure 6.22c the difference in canopy structure is critical enough to make a difference of $22ls^{-1}$ in peak flow volume, there is virtually no storm response of the hillslope segment under the mature canopy.

In the high K_{sat} conditions the canopy age lessens the baseflow after the storm has finished (see figures 6.17-6.19) as there has not been as large a recharge of the soil water by the storm rainfall. This is particularly evident in figure 6.17b (convergent 15° slope) where the soil drainage (hence baseflow), is sustained at a higher rate by the scenario under a 15 *year* canopy.

The only condition where there appears to be an anomaly to the delaying of the recession limb and the different peak volume is in figure 6.19a (divergent 5° slope, fast K_{sat}) where the 50 year old forest generates a slightly higher peak runoff volume than the 15 *year* canopy. It is difficult to explain this anomaly in physical terms; a close analysis of the model output reveals that the 15 *year* canopy scenario has a larger storm peak volume ($203m^3$ between hours 14 and 20 inclusive) than the 50 *year* canopy ($188m^3$) therefore the difference is in timing of the peak not the actual volume. The difference appears to be in the timing of the overland flow pulse. In the case of the 50 *year* canopy the overland flow pulse coincides with an increase in soil matrix flow reaching the segment bottom, whereas the 15 *year* canopy scenario has a more drawn out pulse of overland flow that doesn't coincide quite so well with the soil matrix flow increase. This difference appears to be a function of the high K_{sat} without much force driving rapid matrix flow (i.e. low hydraulic gradient through the 5° slope and topographic divergence) which causes quirks in the routing of matrix and return flow. These differences are not large but are worthy of some consideration because they form an exception

† In this case the water is theoretically absorbed by the soil element but if this addition overfills the element the excess is passed on to the downslope element for the next timestep.

to the general rule.

The hypothetical scenarios where canopy age appears to have the largest effect are shown in figure 6.18a, 6.22b, and 6.22c. Figure 6.18a (high K_{sat}, 5° uniform slope) is particularly noticeable for the change in hydrograph shape, the growth of canopy rounds off the sharp peak evident under the immature 15 *year* canopy. Figures 6.22b and 6.22c are both medium K_{sat}, divergent slopes where the difference of forest age in altering the above and below canopy rainfall inputs is marked on the output hydrograph by a large reduction in peak flow. This reflects the way these slopes have critical subsurface flow regimes that are easily affected by small differences in rainfall input caused by different rainfall partitioning regimes.

It is also noticeable that in the low K_{sat} scenarios canopy age is remarkably consistent in its degree of alteration of the storm hydrograph. When all the low K_{sat} scenarios are viewed together canopy age seems to have a larger effect on the hydrograph than both slope angle and plan shape i.e. the differences within each hydrograph appear larger than those between hydrographs for figures 6.23-6.25.

6.2.4 Summary

The results presented for the initial robustness testing have shown that all of the factors varied do influence the response of the hypothetical hillslope segment to a storm. These results are summarised in table 6.6.

Table 6.6 indicates the scenarios where each parameter appears to have the largest effect; this is important for model validation as it gives some idea of the conditions where the model is likely to be a useful tool for applications and/or how accurately to assess each input parameter in different applications. As an example, from the results presented here it would not be necessary to spend a lot of time subdividing a catchment into many different segments where the saturated hydraulic conductivity is known to be low and there is a mature canopy covering low angle slopes (see figure 6.12c), as plan shape appears to make little difference to the output hydrograph. These conditions are not likely to be found in a temperate environment but if they were, the simplest segmentation possible may give as good a results as a more complex subdivision of the catchment topography, thus simplifying the model application considerably.

It is difficult to quantatively compare the different hydrographs and say which parameter is having the largest effect but some comparison is necessary to establish the relative importance of the new factor, canopy age within *LUCAS*. The predominant theme in all of the results from the robustness testing so far has been the dominant role that hydraulic conductivity (saturated and unsaturated) has played in all of the modelled scenarios. It has been explained

Parameter	*General effect*	*Most important scenarios*	*Comment*
K_{sat}	High = high baseflow and lower peak Low = vice versa	All possibilities	*LUCAS* is most sensitive to this parameter
Plan shape	Med.-high K_{sat} divergence reduces peak size & poss. delays peak	Low-med. angle, high K_{sat} Steep angle, medium K_{sat}	Important where soil matrix flow is dominant
Slope angle	High K_{sat} higher baseflow with steeper angle & reduced peak size	High K_{sat}, convergent slope Med. K_{sat}, divergent slope	Important where soil matrix flow is dominant
Canopy age	Where peak is large, age reduces size and delays the timing at both ends	High K_{sat}, uniform 5° slope Med. K_{sat}, divergent 15° slope Med. K_{sat}, divergent 35° slope	Affects all but consistently where soil matrix flow isn't dominant

Table 6.6: Summary of initial robustness testing results

that this is a function of the model structure but that it is also a reflection of physical reality as understood by various empirical hillslope hydrology studies. In a ranking of the various parameters, saturated hydraulic conductivity has to be number one for its effect on all of the output hydrographs. After that the ranking becomes more difficult and interesting because it appears to differ according to which of the three K_{sat} values are modelled. The ranking shown in table 6.7 is an estimation of the relative importance of each varied parameter under the different K_{sat} conditions.

With a high K_{sat}, slope angle appears to have a greater effect on the output hydrograph than plan shape. For example the difference in each type of line (dotted, dashed, and solid) between figures 6.12a, 6.12b, and 6.12c is greater than the difference within each hydrograph of figures 6.17a, 6.17b, 6.17c. The same thing can be seen by comparing figures 6.7a, 6.8a, and 6.9a in this manner. The difference between slope angle and plan shape is difficult to distinguish but they both have a larger effect on the high K_{sat} hydrographs than canopy age (figures 6.17-6.19).

In the case of the medium K_{sat} the difference between hydrographs with the three parameters is too small and confused to be able to rank at all. For the low K_{sat} scenarios it can plainly be seen that canopy age has a greater effect than plan shape (figures 6.23-6.25). The difference between plan shape and slope angle (e.g. figure 6.15) is harder to distinguish but it appears that plan shape is slightly more important than slope angle.

Rank	*Parameter*		
1	High K_{sat}	Medium K_{sat}	Low K_{sat}
2	Slope angle	Slope angle/plan shape/canopy age	Canopy age
3	Plan shape		Plan shape
4	Canopy age		Slope angle

Table 6.7: Ranking of importance of varied parameters after initial robustness testing

Table 6.7 is interesting for the reversal of ranking between high and low K_{sat} values. The reasoning for this has been discussed earlier, that topography is a critical factor where soil matrix flow is the predominant hillslope hydrology process (e.g. high K_{sat}) while the modification to rainfall that a canopy makes is important for the generation of instant storm peaks through overland flow, which will occur with a low K_{sat}. It is generally accepted that under temperate forest soils tend to have a high saturated hydraulic conductivity and soil matrix flow is an important hydrological process, so it would seem that the conditions where canopy age is more important than topography may be unrealistic. It must be noted that the lowest saturated hydraulic conductivity value used corresponds to a clay loam which it is feasible for forest growth to occur on whereas the highest value corresponds to a sand which is unlikely to be used for forestry. Table 6.6 and the results in section 6.2.3.4 show that canopy age affects the output hydrograph in conditions other than just low K_{sat} scenarios.

The aims of the robustness testing were listed in section 6.1.1 as:

- To find the conditions where each of the process representations is important
- To investigate the general robustness of *LUCAS*
- To find the relative importance of canopy age as a new factor within the scheme.

The first of these aims has been achieved and is summarised in table 6.6. The results from the verification testing have indicated that *LUCAS* has an overall robustness able to cope with the range of conditions modelled. At no time did the model become mathematically unstable giving results that could not be explained with respect to the modelling scheme structure and known hydrological theory. The relative importance of canopy age has been discussed in the previous paragraph with respect to the ranking of variables shown in table 6.7 and the summary shown in table 6.6.

Of the three aims listed above the last two need further testing to be fully achieved as the robustness testing presented so far has been for a fairly narrow range of conditions. Section 6.3 details further robustness testing where some of the fixed initial conditions from this section were allowed to vary.

6.3 Secondary robustness testing

The robustness testing described in section 6.2 was carried out with a series of hypothetical scenarios simulated by varying four parameters, all other input parameters being kept fixed. The results and conclusions from these scenarios need to be tested further to find if they hold under different initial conditions. In particular it is necessary to extend the range of initial conditions to investigate the robustness of the modelling scheme and to find the relative importance of canopy age within *LUCAS* (with respect to the other varied parameters). It is particularly interesting to see if the ranking of variables outlined in table 6.7 holds for different hydrological conditions.

The variation in initial conditions in this section is to extend the range of conditions from those used in the first stage of robustness testing, to see if the same conclusions apply with a different input storm and unsaturated initial soil moisture conditions. The two inputs (storm size and initial moisture conditions) were chosen as they represent more realistic conditions i.e. more than one type of storm on a catchment and soil moisture not being totally saturated initially. The results from the initial robustness testing can be used to design the range of hypothetical scenarios tested in this second set of model simulations, for it may not be necessary to have the full range of saturated hydraulic conductivity values as table 6.7 indicates that the crucial values appear to be the high and low values only.

As stated in section 6.1.1 the aims of this secondary robustness testing are:

- To find if the initial robustness testing conclusions hold for different initial conditions
- To further investigate the modelling scheme robustness.

The new initial conditions and the methods used are outlined in the following section followed by results and some general conclusions on the whole robustness testing exercise in section 6.4.

6.3.1 Initial conditions

The ranking of variables shown in table 6.7 indicate an overall dominance of saturated hydraulic conductivity in affecting the output hydrograph and that the topographical parameters and canopy age switch ranking between high and low saturated conductivity conditions. It was decided that it was only necessary to run the model for the soil hydrology extremes (i.e. high and low K_{sat} values and not for the medium K_{sat}) because this cuts the number of model runs by a third while still being able to achieve the two aims of investigating the initial conclusions, especially the parameter ranking, and the further investigating the modelling schemes general robustness. As in section 6.2 the high and low K_{sat} values were

$1.65 \times 10^{-4} ms^{-1}$ and $1.65 \times 10^{-6} ms^{-1}$ respectively.

A common physically based, distributed modelling procedure when there is no initial soil moisture status information for a catchment is to start the simulation with the soil mantle at its fully saturated state and let the slopes drain for a set time so that the soil moisture content of each slope at the storm outset is in a less than saturated state (e.g. Calver (1988)). This method assumes that the distributed nature of the model discretisation and the physical nature of the governing equations are able to simulate the way the hillslope (or whatever other model unit) drains through soil matrix flow from a fully saturated state. Although this assumption may not be entirely valid it is the only viable method to find the less than saturated soil moisture status when there is no measured information.

This is the method used here to simulate the less than saturated soil segments. To some extent this had already happened in the initial robustness testing where the storm rainfall started after eight hours of draining but this was not enough for the slopes to reach a near static state (theoretically when the matrix pore pressure equals gravity) for high K_{sat} scenarios. Before the final method was decided upon some model simulations were run using the soil moisture status resulting from draining a medium K_{sat}, uniform plan shape 15° slope for 72 hours so that the initial moisture content was the same for all the different scenarios. Although this worked it was always a compromise and each scenario represented implausible initial moisture e.g. too wet for the high K_{sat} and too dry for the low K_{sat} scenarios. Consequently the method that was finally decided upon was to drain each slope individually for a period of 72 *hours* prior to the storm rainfall being applied. This method has the advantage that the initial moisture content reflects as near to physical reality as the model can simulate for a drained hillslope segment but the disadvantage that each initial moisture content is different and thereby gives extra variation to the robustness testing. The initial soil moisture input for the eighteen different scenarios are shown in tables 6.8-6.25 (N.B. the initial moisture content is the same between each canopy age scenario as the slopes are drained without any rainfall input).

The storm used in the initial robustness testing was not extremely large in size and fairly short in duration (5.5*mm* over a six hour period). To further test the general robustness of LUCAS and also to see if the results in table 6.7 hold up in different conditions it was necessary to use a different type of storm, it seems sensible to test it under conditions of a very large storm as *VSAS4* has been designed as an event simulator. The storm chosen (see figure 6.26) was taken from the work of Fawcett (1992) using *VSAS3* on a Swiss catchment. The storm has a total rainfall of 45.5*mm* over a 17 *hour* period, having a return period of around 50 *years*.

In using this very large storm with the same parameters as outlined in section 6.2.1.4 it

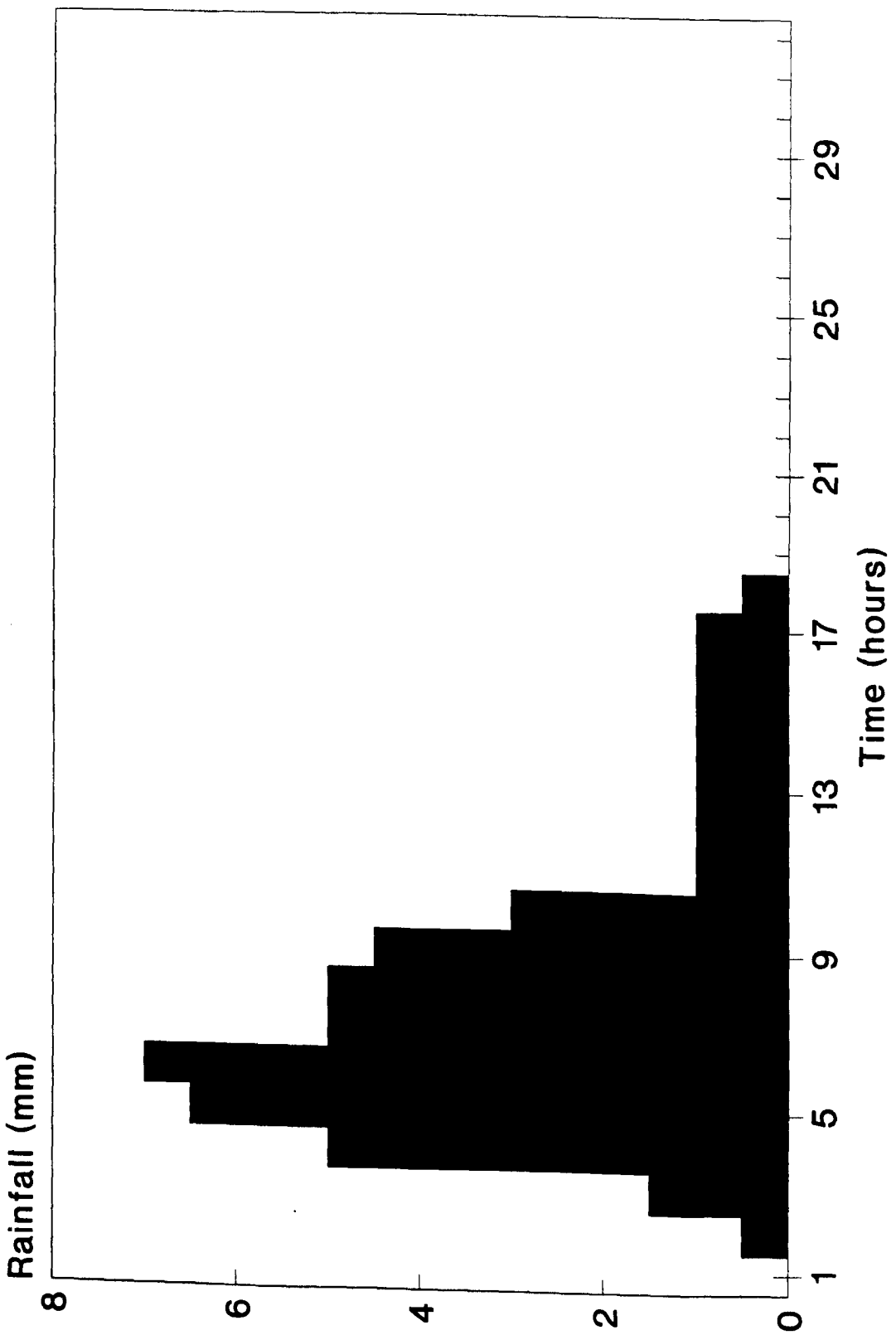

Figure 6.26: Storm rainfall used in secondary robustness testing

1.000	1.00	1.000	1.000	0.994	0.976	0.957	0.948	0.944	0.942
1.000	1.000	1.000	1.000	1.000	1.000	0.982	0.965	0.957	0.961
1.000	1.000	1.000	1.000	1.000	1.000	1.000	0.988	0.969	0.957
1.000	1.000	1.000	1.000	1.000	1.000	1.000	1.000	0.998	0.980

Table 6.8: Unit percentage water contents for the soil elements after 72 hours drainage. High K_{sat}, 5° convergent slope

1.000	1.000	1.000	1.000	1.000	1.000	1.000	1.000	1.000	0.994
1.000	1.000	1.000	1.000	1.000	1.000	1.000	1.000	1.000	1.000
1.000	1.000	1.000	1.000	1.000	1.000	1.000	1.000	1.000	1.000
1.000	1.000	1.000	1.000	1.000	1.000	1.000	1.000	1.000	1.000

Table 6.9: Unit percentage water contents for the soil elements after 72 hours drainage. Low K_{sat}, 5° convergent slope

0.988	0.955	0.953	0.962	0.956	0.951	0.948	0.946	0.944	0.942
1.000	0.992	0.990	0.990	0.982	0.977	0.967	0.960	0.957	0.961
1.000	1.000	1.000	1.000	1.000	1.000	0.993	0.980	0.966	0.957
1.000	1.000	1.000	1.000	1.000	1.000	1.000	1.000	0.995	0.981

Table 6.10: Unit percentage water contents for the soil elements after 72 hours drainage. High K_{sat}, 5° uniform slope

1.000	1.000	0.998	0.999	1.000	1.000	1.000	1.000	1.000	0.994
1.000	1.000	1.000	1.000	1.000	1.000	1.000	1.000	1.000	1.000
1.000	1.000	1.000	1.000	1.000	1.000	1.000	1.000	1.000	1.000
1.000	1.000	1.000	1.000	1.000	1.000	1.000	1.000	1.000	1.000

Table 6.11: Unit percentage water contents for the soil elements after 72 hours drainage. Low K_{sat}, 5° uniform slope

0.949	0.941	0.940	0.944	0.942	0.943	0.943	0.943	0.943	0.942
0.979	0.961	0.961	0.965	0.961	0.960	0.957	0.955	0.958	0.961
1.000	0.991	0.989	0.990	0.985	0.982	0.977	0.972	0.963	0.957
1.000	1.000	1.000	1.000	1.000	1.000	1.000	1.000	0.990	0.981

Table 6.12: Unit percentage water contents for the soil elements after 72 hours drainage. High K_{sat}, 5° divergent slope

1.000	0.998	0.998	0.998	0.999	0.999	0.998	0.999	0.998	0.994
1.000	1.000	1.000	1.000	1.000	1.000	1.000	1.000	1.000	1.000
1.000	1.000	1.000	1.000	1.000	1.000	1.000	1.000	1.000	1.000
1.000	1.000	1.000	1.000	1.000	1.000	1.000	1.000	1.000	1.000

Table 6.13: Unit percentage water contents for the soil elements after 72 hours drainage. Low K_{sat}, 5° divergent slope

0.952	0.952	0.951	0.950	0.949	0.948	0.946	0.945	0.943	0.942
0.971	0.962	0.960	0.958	0.958	0.962	0.963	0.963	0.963	0.963
0.997	0.985	0.981	0.978	0.971	0.963	0.960	0.958	0.956	0.954
1.000	1.000	1.000	1.000	0.999	0.990	0.986	0.982	0.979	0.976

Table 6.14: Unit percentage water contents for the soil elements after 72 hours drainage. High K_{sat}, 15° convergent slope

1.000	1.000	1.000	1.000	1.000	1.000	1.000	1.000	1.000	0.985
1.000	1.000	1.000	1.000	1.000	1.000	1.000	1.000	1.000	1.000
1.000	1.000	1.000	1.000	1.000	1.000	1.000	1.000	1.000	1.000
1.000	1.000	1.000	1.000	1.000	1.000	1.000	1.000	1.000	1.000

Table 6.15: Unit percentage water contents for the soil elements after 72 hours drainage. Low K_{sat}, 15° convergent slope

0.949	0.946	0.945	0.946	0.946	0.945	0.945	0.944	0.943	0.942
0.963	0.961	0.962	0.962	0.962	0.963	0.963	0.963	0.963	0.963
0.965	0.962	0.962	0.962	0.961	0.960	0.958	0.957	0.956	0.954
0.993	0.989	0.988	0.988	0.987	0.985	0.983	0.981	0.979	0.976

Table 6.16: Unit percentage water contents for the soil elements after 72 hours drainage. High K_{sat}, 15° uniform slope

1.000	0.999	0.996	0.998	0.999	1.000	1.000	1.000	0.999	0.985
1.000	1.000	1.000	1.000	1.000	1.000	1.000	1.000	1.000	1.000
1.000	1.000	1.000	1.000	1.000	1.000	1.000	1.000	1.000	1.000
1.000	1.000	1.000	1.000	1.000	1.000	1.000	1.000	1.000	1.000

Table 6.17: Unit percentage water contents for the soil elements after 72 hours drainage. Low K_{sat}, 15° uniform slope

0.945	0.942	0.942	0.943	0.943	0.943	0.943	0.943	0.943	0.942
0.963	0.961	0.961	0.962	0.961	0.962	0.962	0.963	0.963	0.963
0.960	0.958	0.958	0.958	0.958	0.957	0.957	0.956	0.955	0.954
0.987	0.983	0.983	0.983	0.983	0.982	0.981	0.980	0.978	0.976

Table 6.18: Unit percentage water contents for the soil elements after 72 hours drainage. High K_{sat}, 15° divergent slope

1.000	0.995	0.993	0.996	0.996	0.996	0.996	0.996	0.994	0.985
1.000	1.000	1.000	1.000	1.000	1.000	1.000	1.000	1.000	1.000
1.000	1.000	1.000	1.000	1.000	1.000	1.000	1.000	1.000	1.000
1.000	1.000	1.000	1.000	1.000	1.000	1.000	1.000	1.000	1.000

Table 6.19: Unit percentage water contents for the soil elements after 72 hours drainage. Low K_{sat}, 15° divergent slope

0.950	0.948	0.948	0.947	0.947	0.946	0.945	0.944	0.943	0.942
0.956	0.959	0.962	0.964	0.964	0.964	0.964	0.964	0.964	0.964
0.977	0.965	0.962	0.961	0.959	0.958	0.957	0.956	0.955	0.954
1.000	0.994	0.991	0.989	0.986	0.984	0.982	0.979	0.977	0.975

Table 6.20: Unit percentage water contents for the soil elements after 72 hours drainage. High K_{sat}, 35° convergent slope

1.000	1.000	1.000	1.000	1.000	1.000	1.000	1.000	1.000	0.977
1.000	1.000	1.000	1.000	1.000	1.000	1.000	1.000	1.000	1.000
1.000	1.000	1.000	1.000	1.000	1.000	1.000	1.000	1.000	1.000
1.000	1.000	1.000	1.000	1.000	1.000	1.000	1.000	1.000	1.000

Table 6.21: Unit percentage water contents for the soil elements after 72 hours drainage. Low K_{sat}, 35° convergent slope

0.947	0.945	0.944	0.945	0.945	0.944	0.944	0.943	0.943	0.942
0.965	0.964	0.964	0.964	0.964	0.964	0.964	0.964	0.964	0.964
0.960	0.958	0.958	0.958	0.957	0.957	0.956	0.955	0.955	0.954
0.985	0.982	0.982	0.982	0.982	0.981	0.980	0.978	0.977	0.975

Table 6.22: Unit percentage water contents for the soil elements after 72 hours drainage. High K_{sat}, 35° uniform slope

1.000	0.997	0.995	0.998	0.999	1.000	1.000	0.999	0.998	0.977
1.000	1.000	1.000	1.000	1.000	1.000	1.000	1.000	1.000	1.000
1.000	1.000	1.000	1.000	1.000	1.000	1.000	1.000	1.000	1.000
1.000	1.000	1.000	1.000	1.000	1.000	1.000	1.000	1.000	1.000

Table 6.23: Unit percentage water contents for the soil elements after 72 hours drainage. Low K_{sat}, 35° uniform slope

0.944	0.942	0.942	0.943	0.943	0.942	0.943	0.942	0.943	0.942
0.964	0.962	0.963	0.963	0.963	0.963	0.964	0.963	0.964	0.964
0.957	0.956	0.956	0.956	0.956	0.955	0.955	0.955	0.954	0.954
0.981	0.979	0.979	0.979	0.979	0.979	0.978	0.977	0.977	0.975

Table 6.24: Unit percentage water contents for the soil elements after 72 hours drainage. High K_{sat}, 35° divergent slope

1.000	0.992	0.990	0.993	0.995	0.992	0.996	0.992	0.991	0.977
1.000	1.000	1.000	1.000	1.000	1.000	1.000	1.000	1.000	1.000
1.000	1.000	1.000	1.000	1.000	1.000	1.000	1.000	1.000	1.000
1.000	1.000	1.000	1.000	1.000	1.000	1.000	1.000	1.000	1.000

Table 6.25: Unit percentage water contents for the soil elements after 72 hours drainage. Low K_{sat}, 35° divergent slope

was found that the outflows became spurious as a result of mathematical instability within the finite difference scheme. To overcome the instability problems the internal model timestep was reduced to 1 *minute* (from 5 *minutes*), all other input parameters were kept the same as described in section 6.2.1.4 (apart from the initial moisture conditions as mentioned above). The implications of the mathematical instability and a resultant addition to *LUCAS* is described in full in the following chapter.

The four parameters varied in the initial robustness testing (plan shape, slope angle, K_{sat}, and canopy age) were maintained with their initial testing values except for K_{sat} as mentioned earlier.

The results from the second stage of robustness testing are presented in the same manner as in section 6.2, each figure being three hydrographs with three lines per hydrograph representing the different values of the parameter. The following sections describe the results for the four varied input parameters, although only briefly for K_{sat} as this was used as a control parameter for these runs.

6.3.2 Results

The most immediate point noticeable in the second set of robustness testing results is that the size of differences within the individual lines on the hydrographs is not as large as for the initial testing results. This is mostly to do with the scale of presentation, for instance the difference in peak discharge shown within figure 6.36b is $39ls^{-1}$ which is as high as some of the total storm runoff peaks in the first set of robustness tests e.g. figure 6.17c.

6.3.2.1 Plan shape

In section 6.2.3.1 the relationship between plan shape, slope angle, and K_{sat} was highlighted as critical for interpretation of the scenario results. This is also true for these runs on different initial conditions although the inter-relationship seems slightly more complex.

In the high K_{sat} scenarios the main hydrograph difference with plan shape is in the receding limb where the convergent slope has higher runoff for the whole of the recession period although the runoff peak lasts for the same length of time for all three plan shapes. Likewise the uniform slope has higher runoff during this period than the divergent slope. The convergent slope will naturally have a higher amount of return flow contributing to the storm peak as overland flow because of the diminishing volume of soil for the matrix flow water to fill as it moves downslope, conversely the divergent slope will have less return flow in the storm peak total. This is particularly evident in conditions where soil matrix flow is dominant (i.e. high K_{sat} and the steeper slope angles), hence the higher runoff during the recession period for the convergent slope in figures 6.27-6.29. The same process can be observed in the initial robustness testing results (figures 6.7-6.9).

In the high K_{sat}, 5° slope (figure 6.27) the divergent slope maintains a lower baseflow after the stormflow has finished which suggests that the difference in receding limbs described above may also be because of a lower level baseflow in the divergent slope throughout the storm. This is sensible as a flat divergent slope will have less matrix flow draining the resaturated slope than a flat convergent slope.

The 5° slope presents an anomaly to the general trend of high K_{sat} results, especially in the rising limb of the hydrograph where the convergent slope responds to the storm considerably quicker than both the divergent and the uniform slopes. The fact that this occurs only on the 5° slope suggests some process operating that cannot occur with a high K_{sat} on the steeper slopes. A possible explanation is that the 5° slope is the only high K_{sat}, convergent slope able to sustain a saturated wedge at the base of the slope after the 72 *hours* of drainage prior to the storm rainfall. A saturated wedge will often form at the base of a slope as the water draining through the soil matrix from the top of the slope keeps a wedge shaped portion of the lower slope saturated. With the wedge in place the water table is either at the surface or will rise quickly to the surface with the addition of any storm rainfall, consequently the rapid response saturated overland flow from this basal wedge region will consist of either return flow

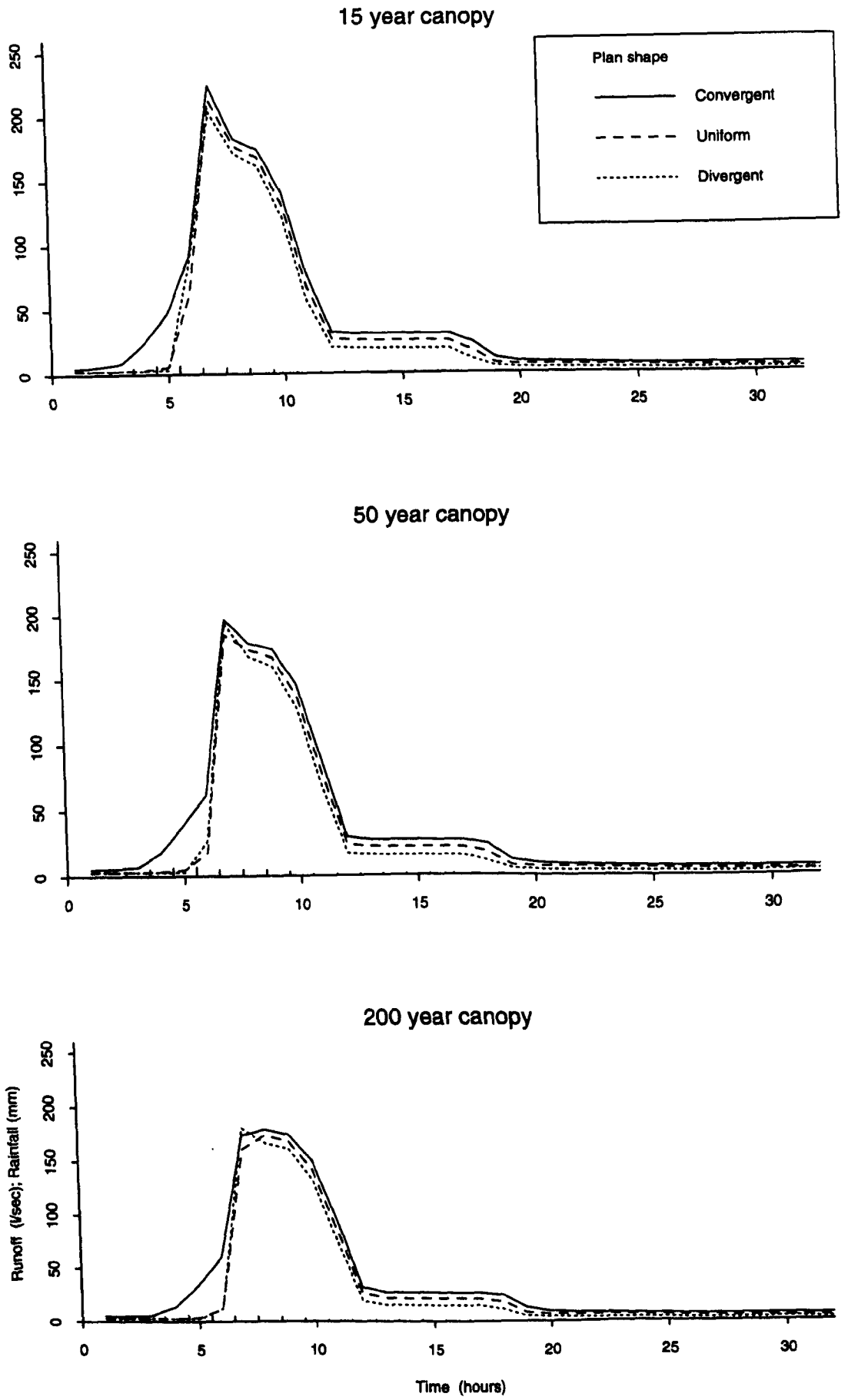

Figure 6.27: Segment runoff response with variation in plan shape and canopy age for high K_{sat} and 5° slope

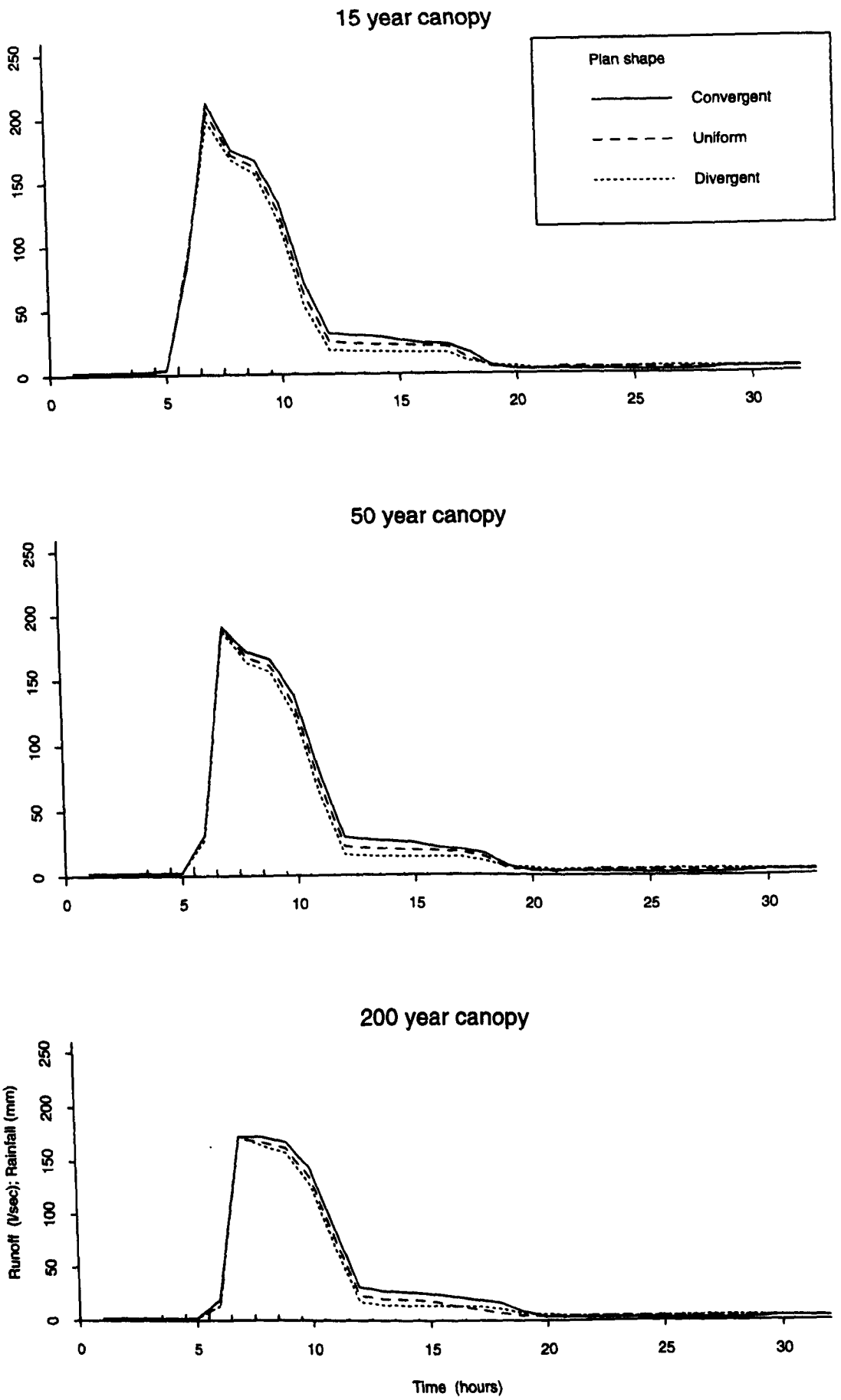

Figure 6.28: Segment runoff response with variation in plan shape and canopy age for high K_{sat} and 15° slope

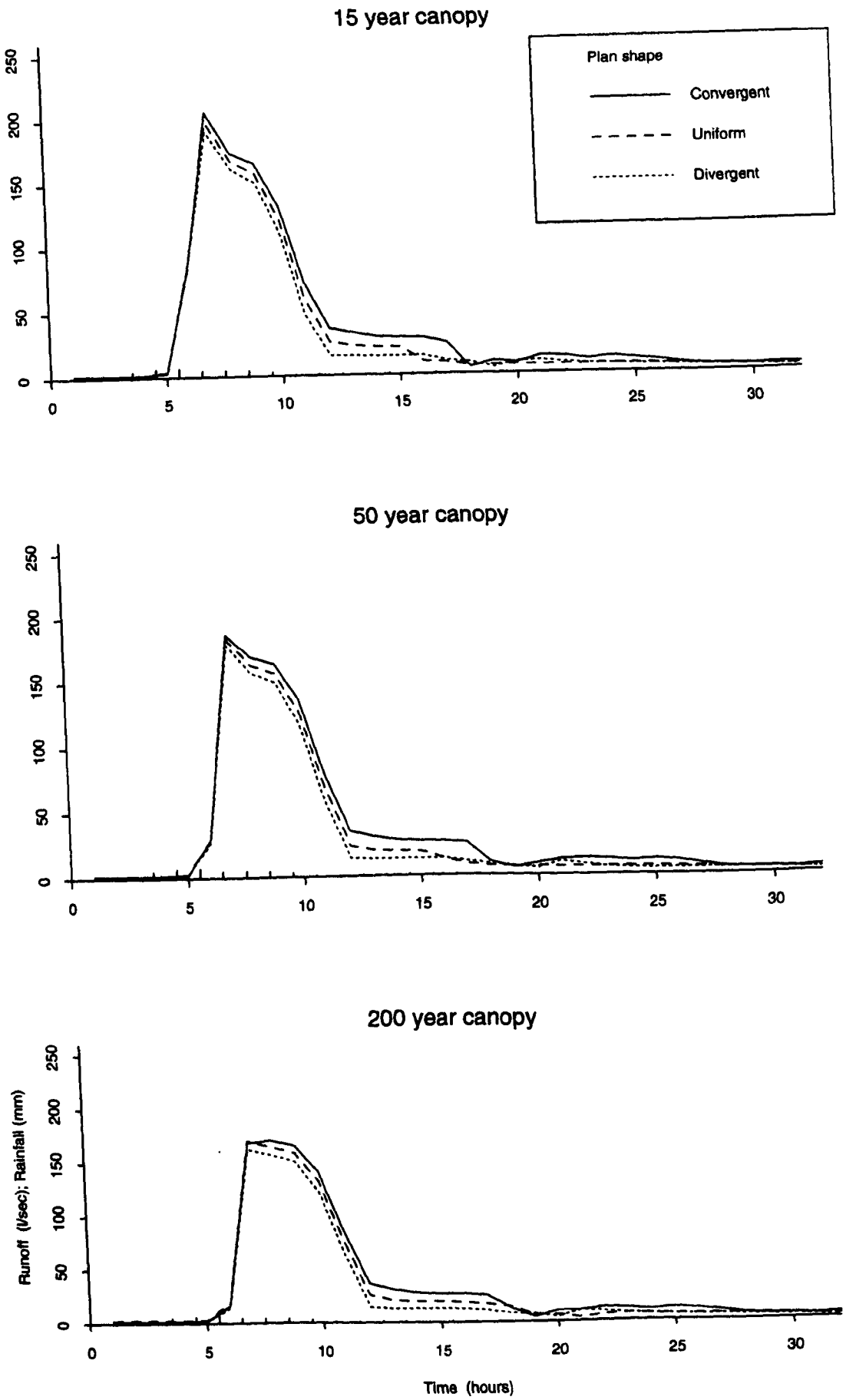

Figure 6.29: Segment runoff response with variation in plan shape and canopy age for high K_{sat} and 35° slope

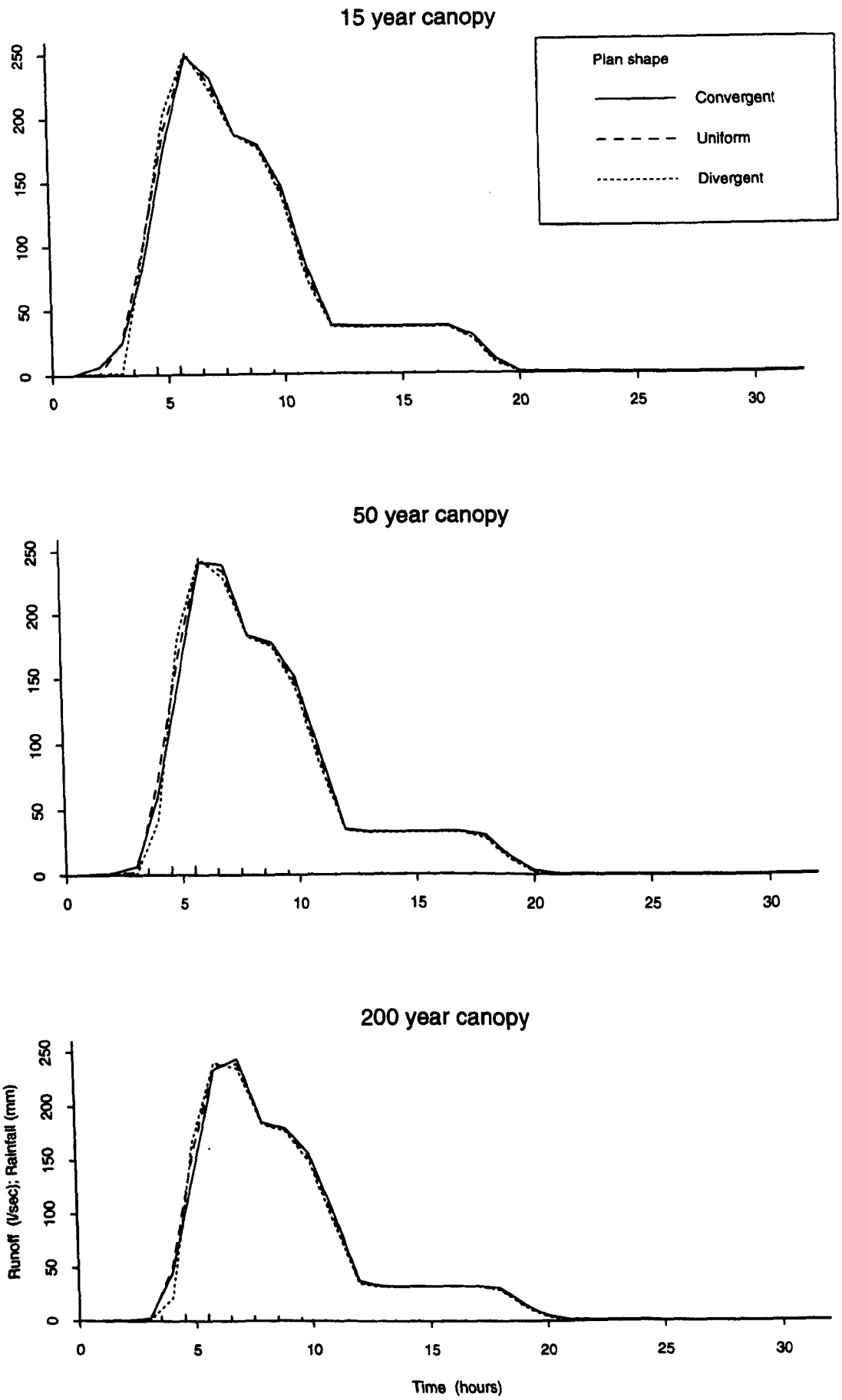

Figure 6.30: Segment runoff response with variation in plan shape and canopy age for low K_{sat} and 5° slope

or rainfall falling onto this saturated area. The presence of a saturated wedge at the base of a slope has been observed (in both field and modelling studies) to be an important prerequisite for rapid response to rainfall.

Tables 6.8, 6.14, and 6.20 show the soil water content after 72 hours drainage for convergent, high K_{sat} slopes and the three different slope angles. It can clearly be seen that the 5° slope has an area of saturation at the base of the slope which could be described as a saturated wedge, this extends up to the fourth element (approximately 50*m* upslope). The steeper slopes have no saturated wedges as the surface soil elements are below saturation for all of the slope length and therefore will absorb the first rainfall until they become saturated themselves. The same kind of difference in the saturated wedge can be seen between the different plan shapes (tables 6.8, 6.10, and 6.12). The 5° convergent slope is the only scenario with a high K_{sat} that has a saturated wedge at the bottom of the slope. This is as a result of the convergence of soil matrix flow from upslope being enough to sustain saturation at the base (as opposed to the other plan shapes where there is not enough soil matrix flow from upslope to replace that draining from the base of the slope) while the slope is not so steep as to overdrain the slope. With this saturated wedge there is a much quicker reaction of the hydrograph to the addition of storm rainfall (see figure 6.27).

In figure 6.29 the hydrograph rises again after the main stormflow has finished (at about 19 *hours*), particularly where the slope is convergent. This is most likely to be from a substantial pulse of soil matrix flow, or return flow from convergent soil matrix flow, which leaves the soil mantle after the main storm peak has passed. The soil matrix flow moves down through the slope as the storm is progressing but only reaches the end of the slope after the storm has finished, it is then sustained for a short period of time before gradually diminishing.

The differences in hydrographs with plan shape for the low K_{sat} scenarios are extremely uniform for different slope angles and consequently are only shown for 5° scenarios (figure 6.30) The main difference is that the divergent slope is slower to respond to the initial rainfall at the start of the storm event but then rises at a steeper rate to the runoff peak. The soil moisture conditions after 72 hours drainage for the three different plan shapes at whatever angle show that the convergent slopes maintain saturation except for the top of slope surface element (see table 6.21) whereas the uniform and divergent slopes dry out considerably (tables 6.23 and 6.25 respectively). This means that the divergent slopes are able to absorb some of the initial storm rainfall and therefore there is the delay in the start of the runoff peak.

In general the plan shape has an effect on the storm hydrograph, particularly on the high K_{sat} scenarios. This is similar to the results from the initial robustness tests although there is less of a difference in the baseflow with plan shape as the main drainage of the saturated slope has occurred previous to the storm rainfall.

6.3.2.2 Slope angle

The results from the variation in slope angle are very similar to those already discussed for plan shape. For the high K_{sat} the difference is mostly in the recession limb of the storm hydrograph, while for the low K_{sat} the differences are very slight and are mostly in the rising limb.

Figure 6.31 illustrates the faster reaction of the convergent 5° slope, compared to the steeper convergent slopes. This has been explained in section 6.3.2.1 with respect to the basal slope saturated wedge that develops after the period of drainage on the 5° slope but not on the others.

In the high K_{sat} scenarios (figure 6.31) the steeper slopes have less runoff in the hydrograph receding limb, particularly at the end of the storm when the convergent and uniform 35° slopes drop quickly. This appears to contradict the results from the plan shape where the conditions promoting soil matrix flow (i.e topographic convergence) had a higher receding limb (see figure 6.27). If the steeper slopes have water moving through the soil matrix at a faster rate this means that there is more water entering the soil matrix and therefore less water available for overland flow. The result of this would be less water in the storm peak and a likely pulse occurring after the main storm peak. In figure 6.31a it can be seen that the steeper convergent slopes have a larger secondary pulse of stormflow after the main storm flow has finished than the two other slopes, this corresponds to a larger contribution of soil matrix flow as described above.

The sudden drop in storm runoff as soon as, or even before, the rainfall stops (18th hour), for the 35° convergent and uniform slopes suggests that the soil matrix is draining at a faster rate than the tail-end rainfall can sustain it. The result of this would be the surface soil elements dropping below saturation and absorbing all the storm rainfall into the matrix with no overland flow.

In the low K_{sat} scenarios the differences in hydrograph with slope angle are very small, mostly with the steeper slopes having a delayed rising limb. This again can be traced back to the initial soil moisture conditions where the steeper slopes dry out more and therefore absorb more of the initial rainfall.

One of the main similarities with the initial robustness testing scenarios is that there is very little difference under the low K_{sat} conditions, reinforcing the importance of topography as an important general factor where soil matrix flow is a dominant process.

6.3.2.3 Saturated hydraulic conductivity

The results from the saturated hydraulic conductivity are shown for all the slope angles and plan shapes although each figure is a different canopy age. As the results for topography have suggested K_{sat} has proved to be the most important input for this secondary part of the robustness tests, as it was for the initial testing, this can be seen from any of figures 6.33-6.35.

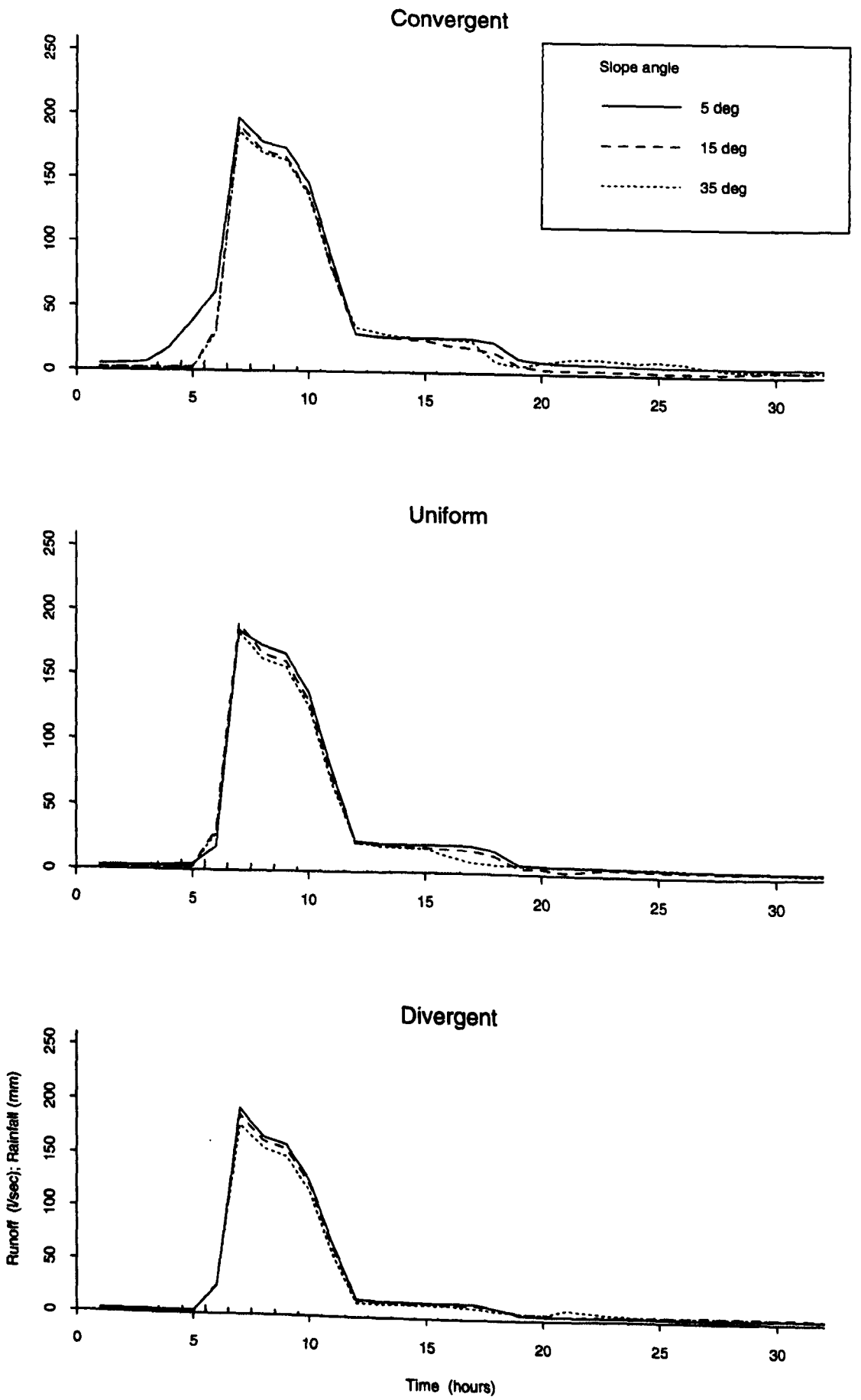

Figure 6.31: Segment runoff response with variation in slope angle and plan shape for high K_{sat} and 50 *year* canopy

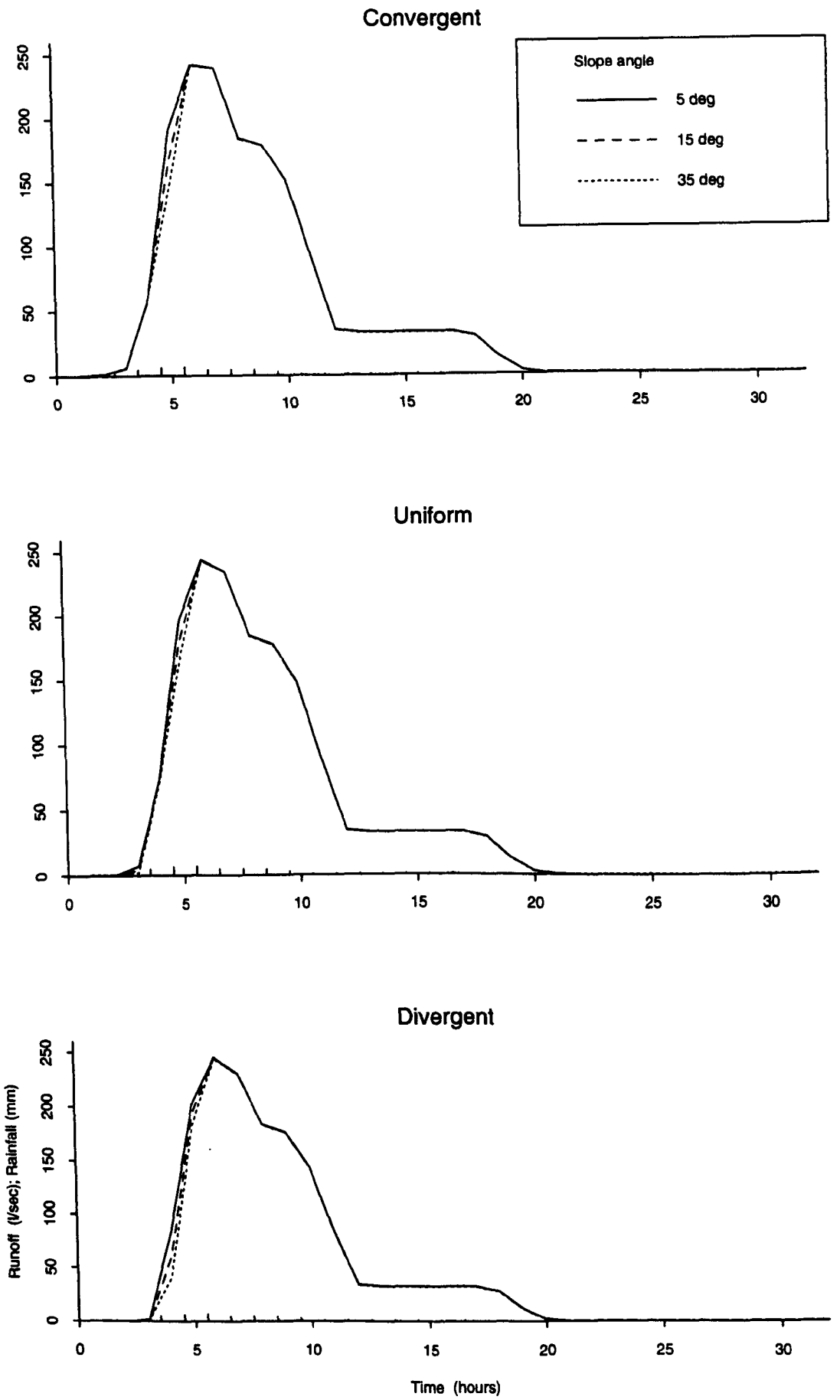

Figure 6.32: Segment runoff response with variation in slope angle and plan shape for low K_{sat} and 50 *year* canopy

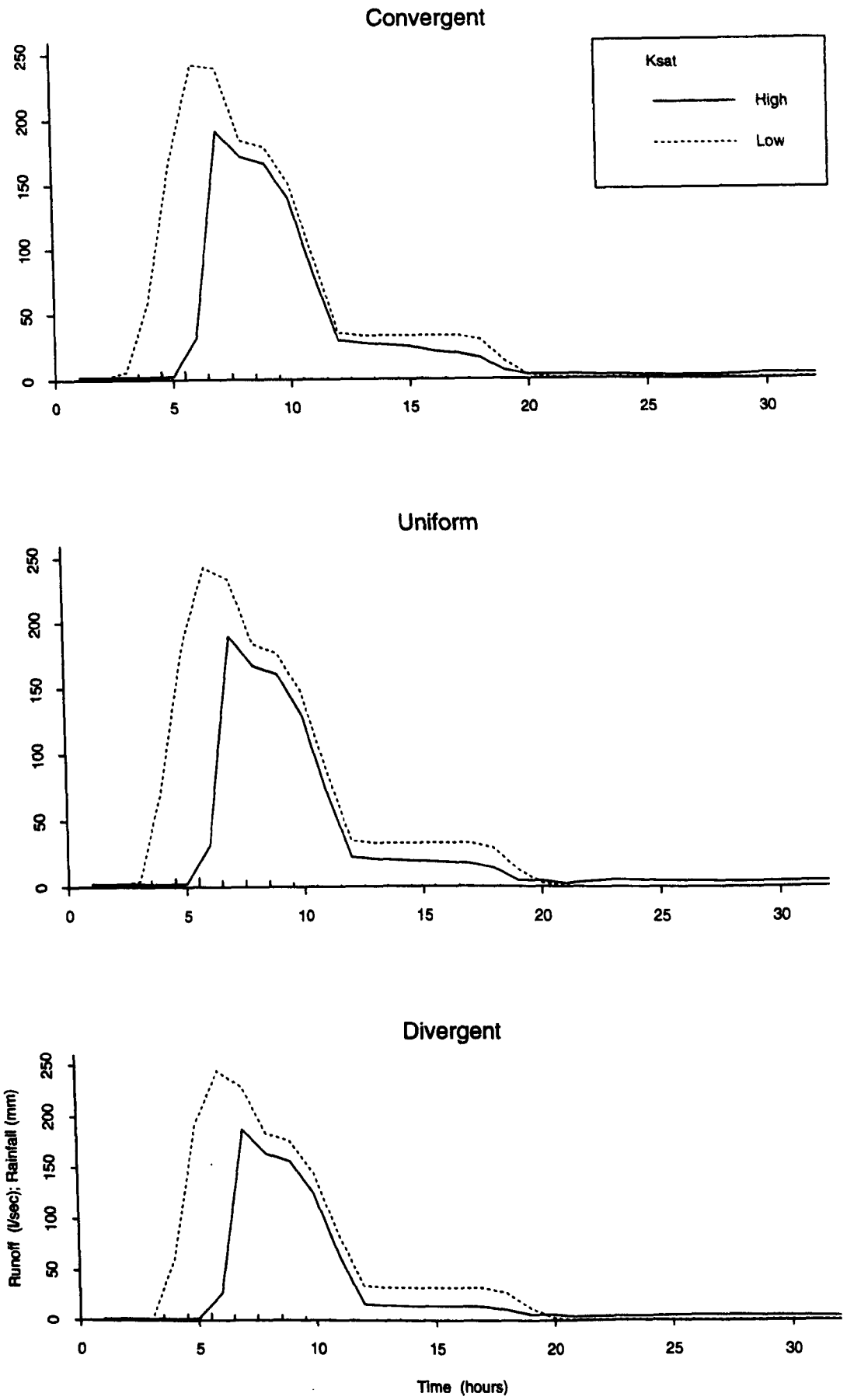

Figure 6.33: Segment runoff response with variation in K_{sat} and plan shape for 15 *year* canopy and 5° slope

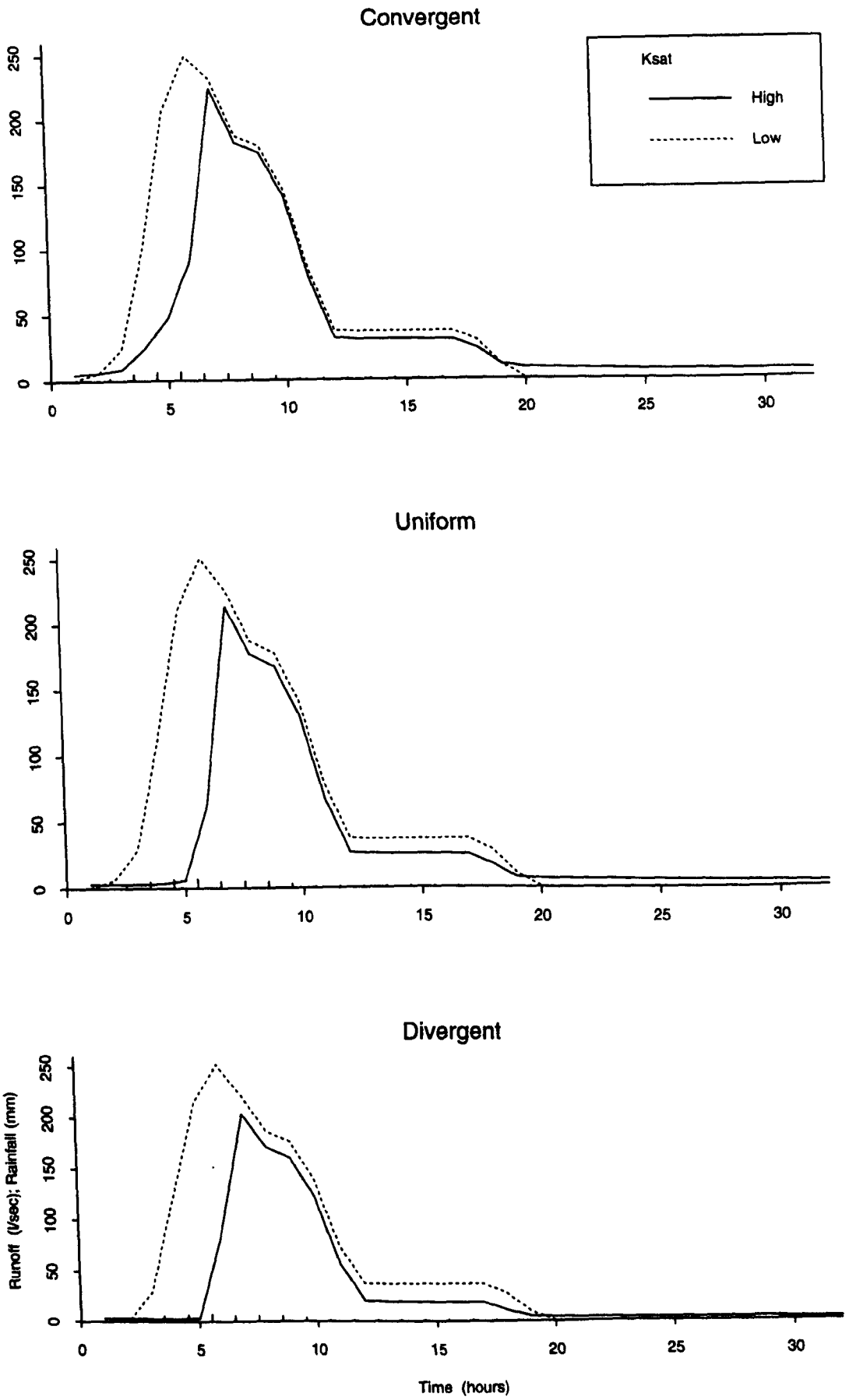

Figure 6.34: Segment runoff response with variation in K_{sat} and plan shape for 50 *year* canopy and 15° slope

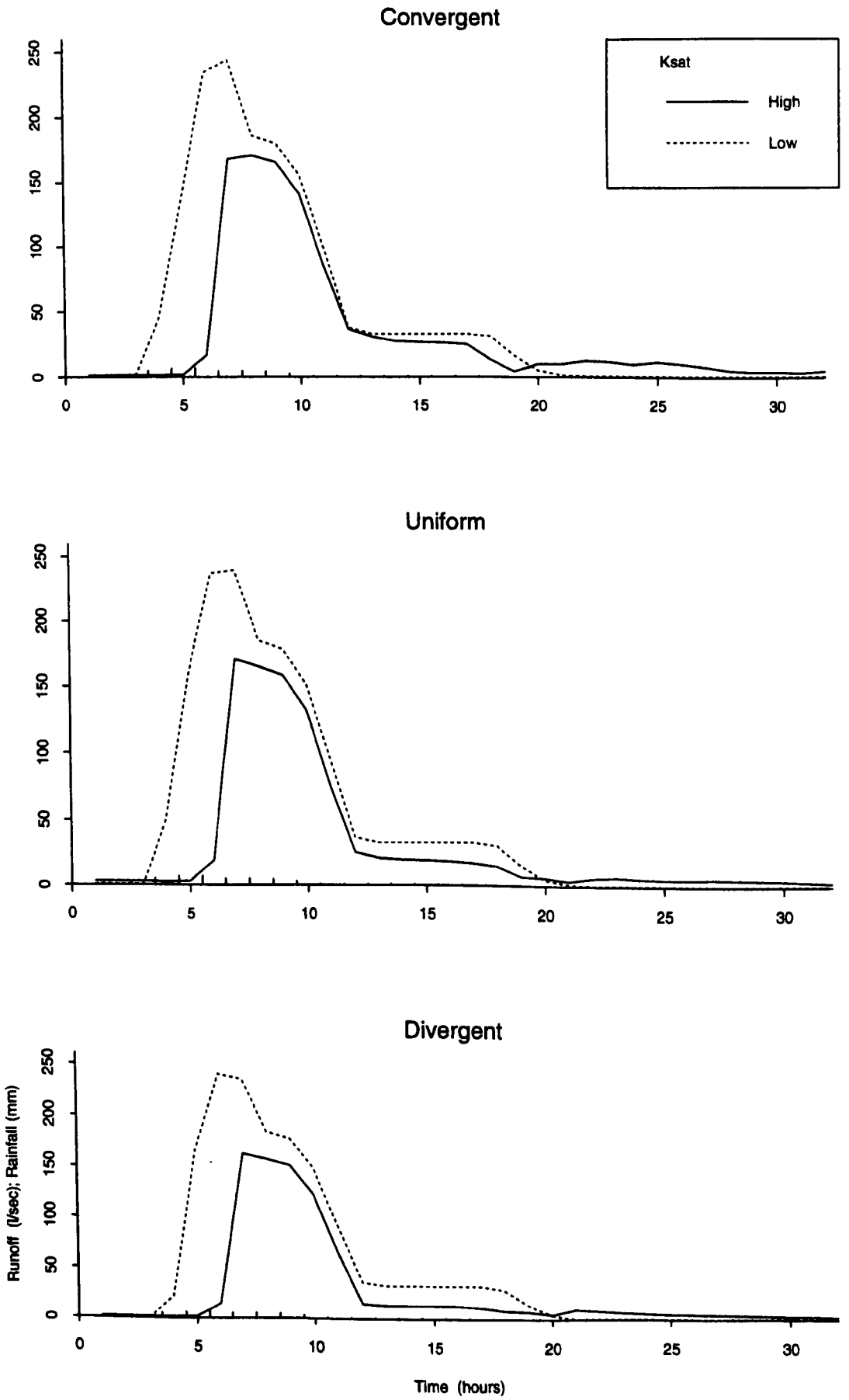

Figure 6.35: Segment runoff response with variation in K_{sat} and plan shape for 200 *year* canopy and 35° slope

All of the hydrographs shown in figures 6.33-6.35 show almost identical trends, a difference in peak flow timing in addition to the difference in peak size and shape on both limbs of the hydrograph as was evident in the first set of robustness tests. The main difference from the initial testing is that here there is a large difference in the peak volume timing (e.g. figure 6.33) that was not so evident in the results presented in section 6.2.3.3.

The delay in rising to the hydrograph peak for the high K_{sat} scenarios is a result of the drained slopes being drier on the surface and therefore being able to absorb the initial rainfall into the soil matrix before any overland flow occurs. The other differences are as a result of the hillslope segment under high K_{sat} conditions absorbing more of the storm rainfall and routing it into soil matrix flow as opposed to the low K_{sat} scenario where more of the rainfall is routed as overland flow. The results of this are a smaller volume of storm runoff but a larger amount of baseflow after the storm has finished, this is particularly evident in figure 6.33b. In the conditions where soil matrix flow is most evident (steep angles, high K_{sat}) a secondary pulse of water can be seen to occur after the main storm peak. This pulse corresponds to the high amount of storm soil matrix flow reaching the downslope segment boundary as explained in section 6.3.2.1 with respect to plan shape.

In general the higher value of K_{sat} causes a delay in the rising limb of the hydrograph, a reduced peak size, a lower receding limb, and more baseflow both preceding and post the storm peak. This confirms the findings of the initial robustness testing that K_{sat} affects all the hydrographs in every respect, especially the storm and baseflow volumes.

6.3.2.4 Canopy age

As in section 6.2.3.4 the results for the change in canopy age are shown for every possible scenario so that it can be assessed relative to the two other factors. In section 6.2.3.4 it was evident that the most consistent changes in the storm hydrograph occurred in the low K_{sat} scenarios. Although there were substantial differences in hydrographs with the other two K_{sat} scenarios they were not as consistently different as for the low K_{sat} conditions. This is not the case for the set of robustness tests presented here (figures 6.36-6.41), the differences in hydrograph are remarkably similar for both K_{sat} scenarios, the only relationship with K_{sat} being in the alteration of the extreme hydrograph peak shape.

In general canopy age has a similar effect under these conditions as in the previous tests i.e. delaying the rising limb, lessening the peak size, and extending the recession limb. The slow reaction of the segment to the initial storm rainfall is as a result of the rainfall being delayed by the canopy structure (plus some interception loss) and as the canopy growth increases the amount of above canopy rainfall allocated to indirect throughfall. This delays the below canopy rainfall further. Similar explanations can be used for the delay in recession limb, this is the rainfall draining from the wet canopy, and there is more area to drain from in the more mature canopy.

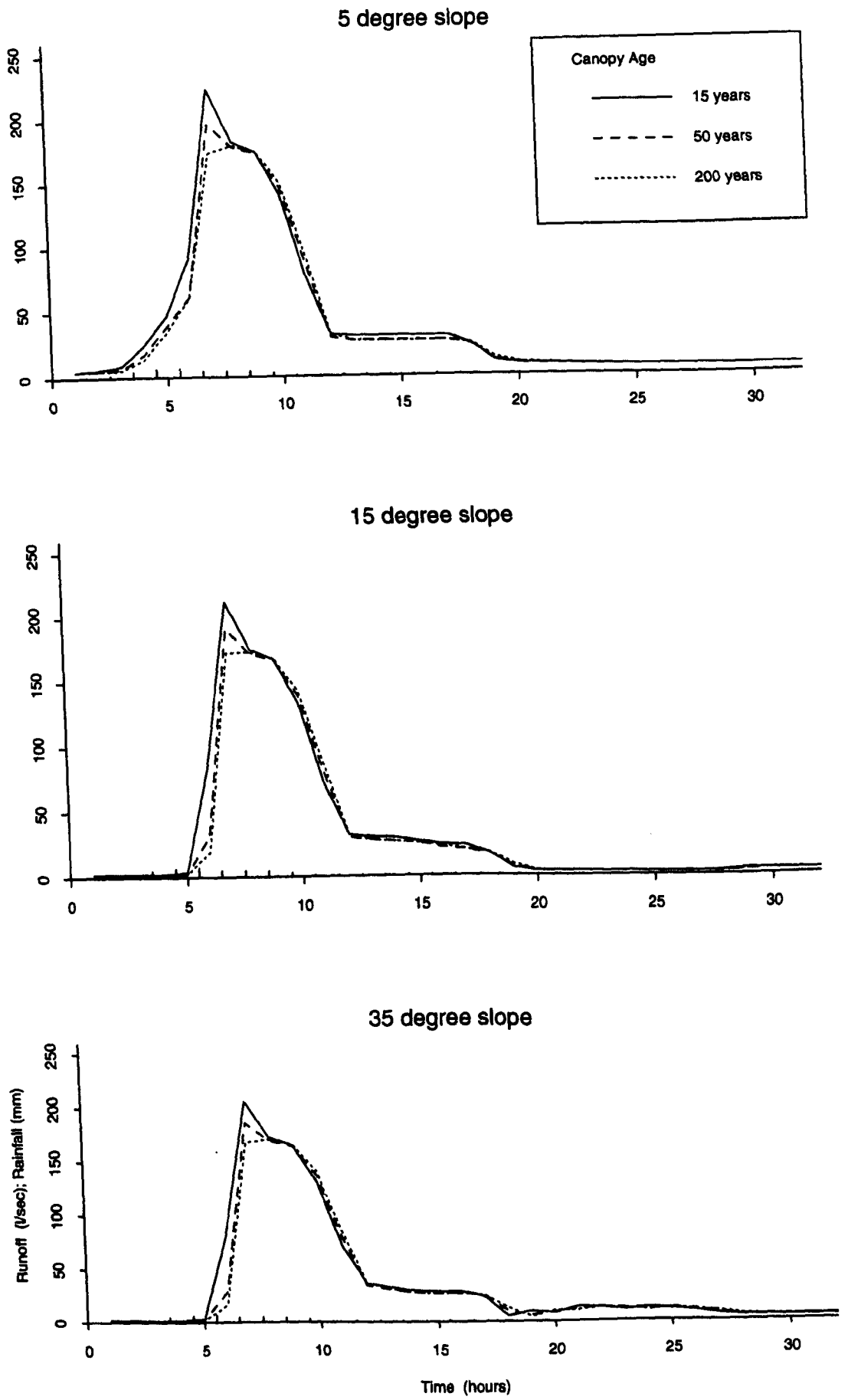

Figure 6.36: Segment runoff response with variation in canopy age and slope angle for high K_{sat} and convergent slope

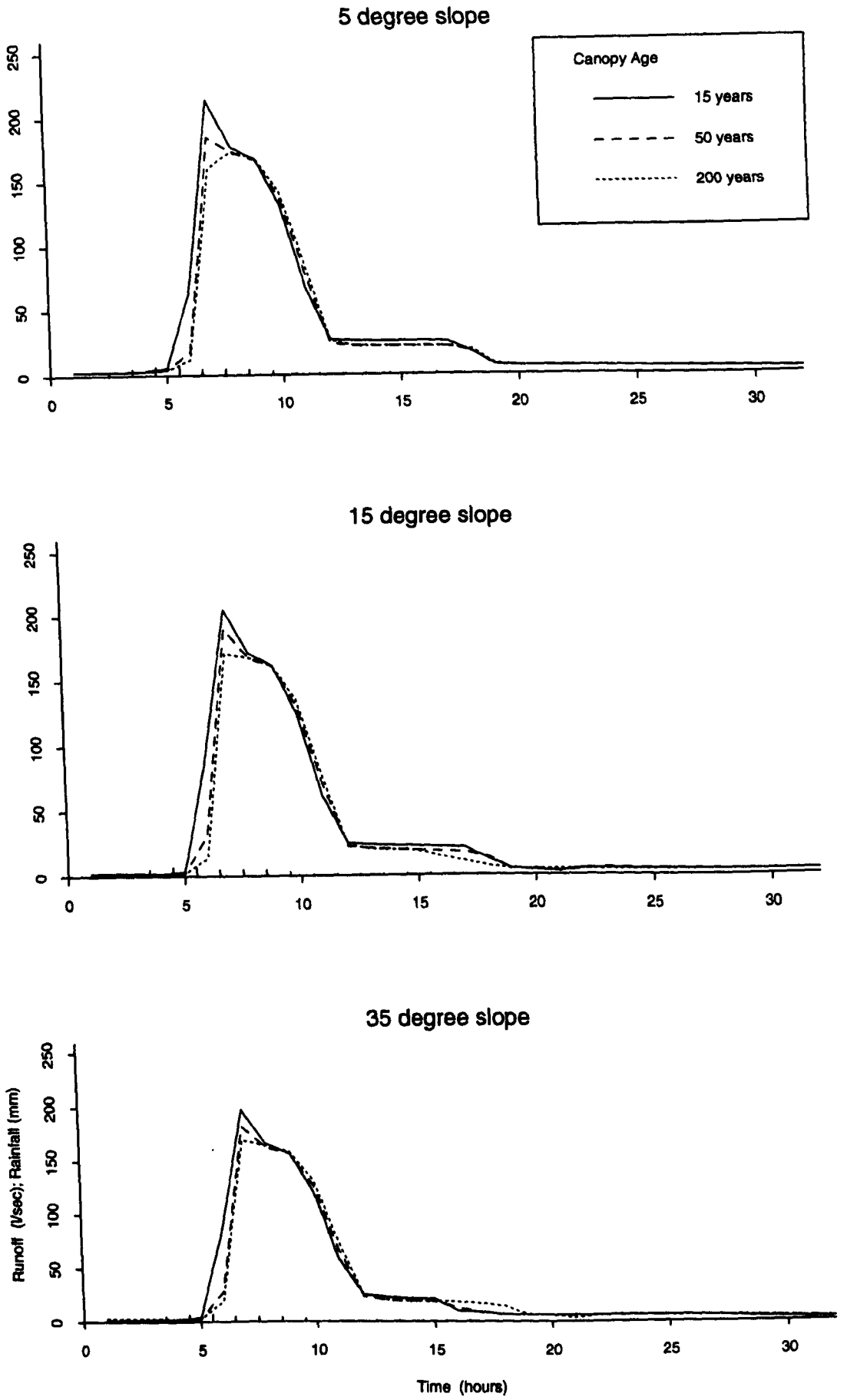

Figure 6.37: Segment runoff response with variation in canopy age and slope angle for high K_{sat} and uniform slope

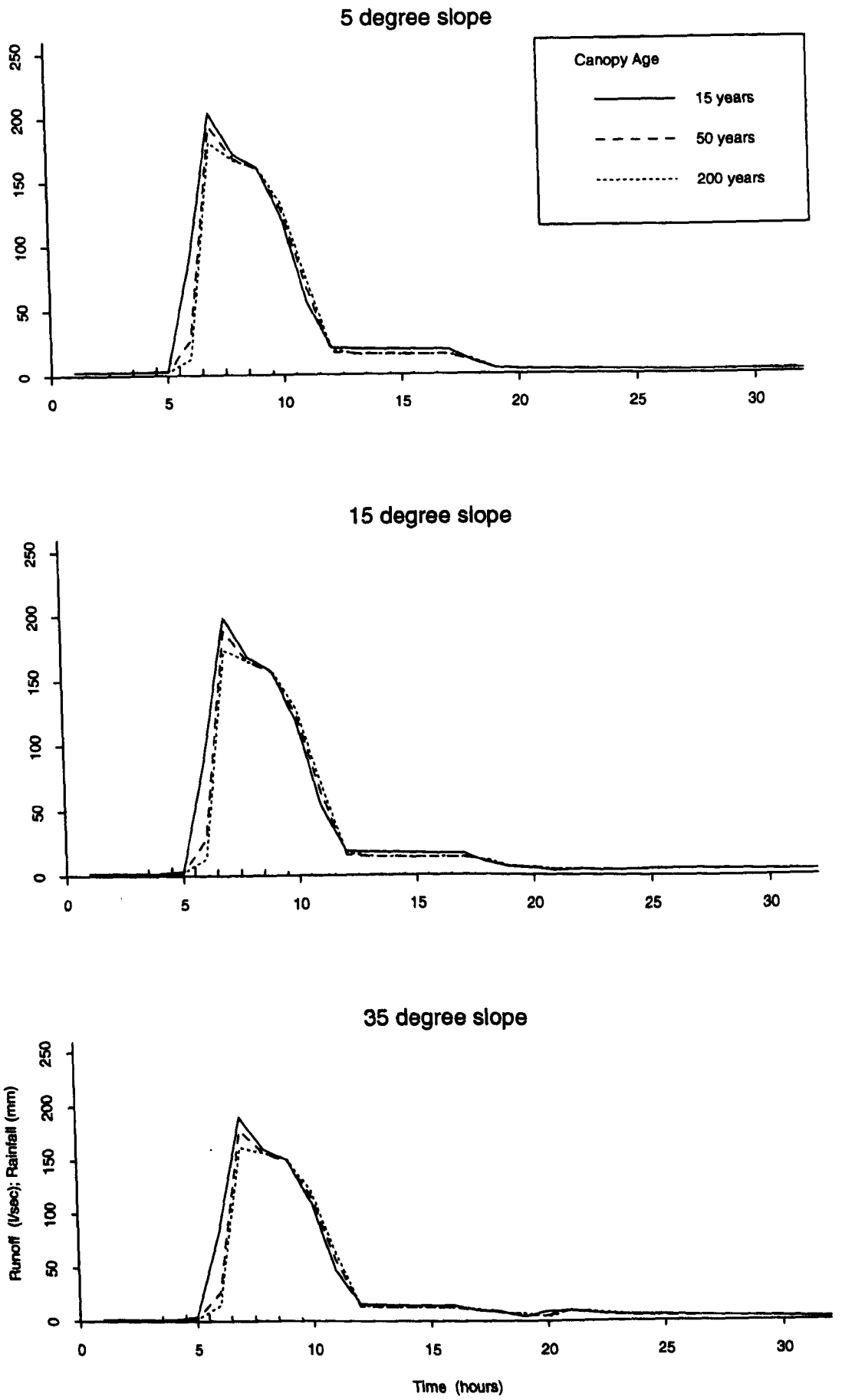

Figure 6.38: Segment runoff response with variation in canopy age and slope angle for high K_{sat} and divergent slope

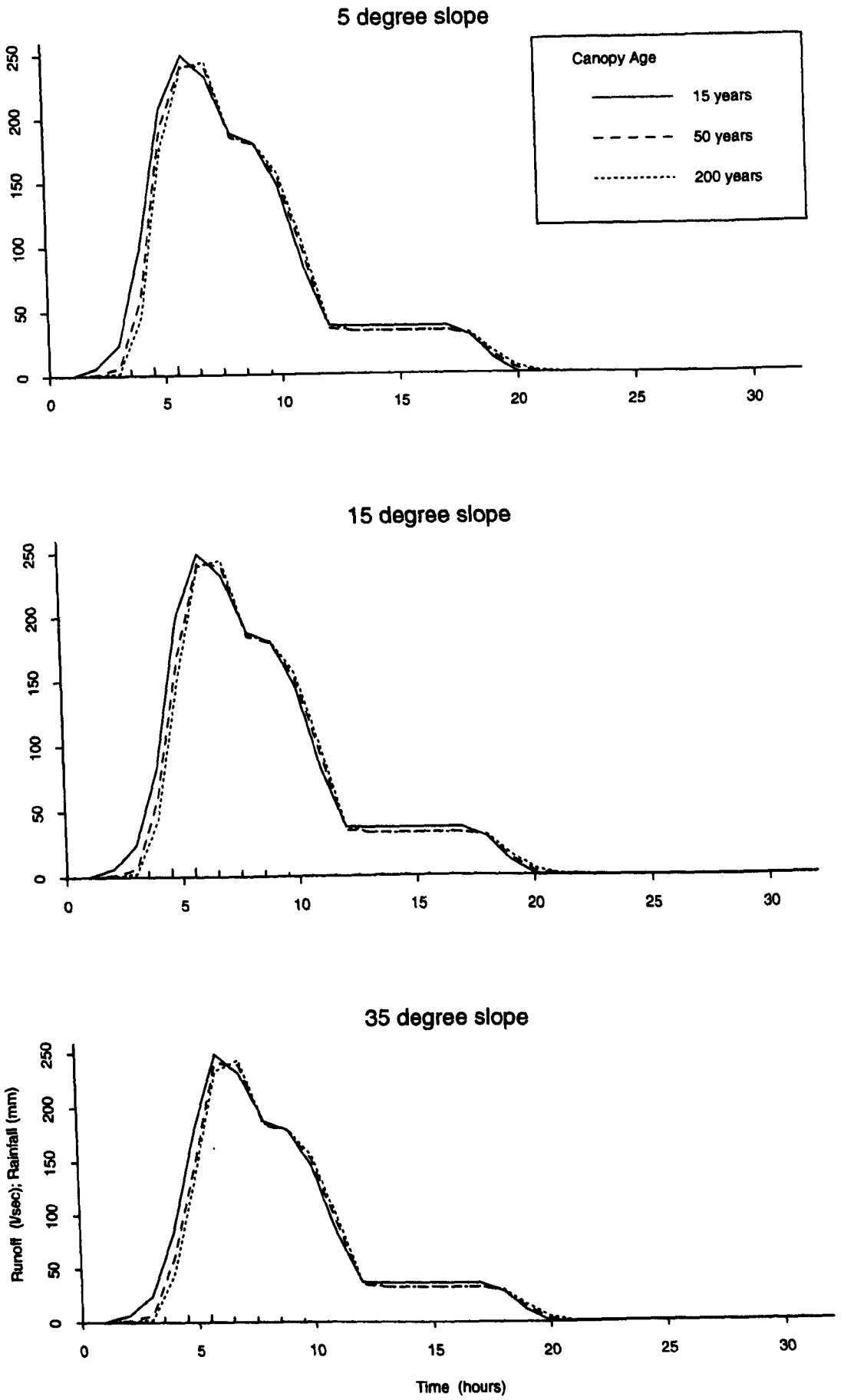

Figure 6.39: Segment runoff response with variation in canopy age and slope angle for low K_{sat} and convergent slope

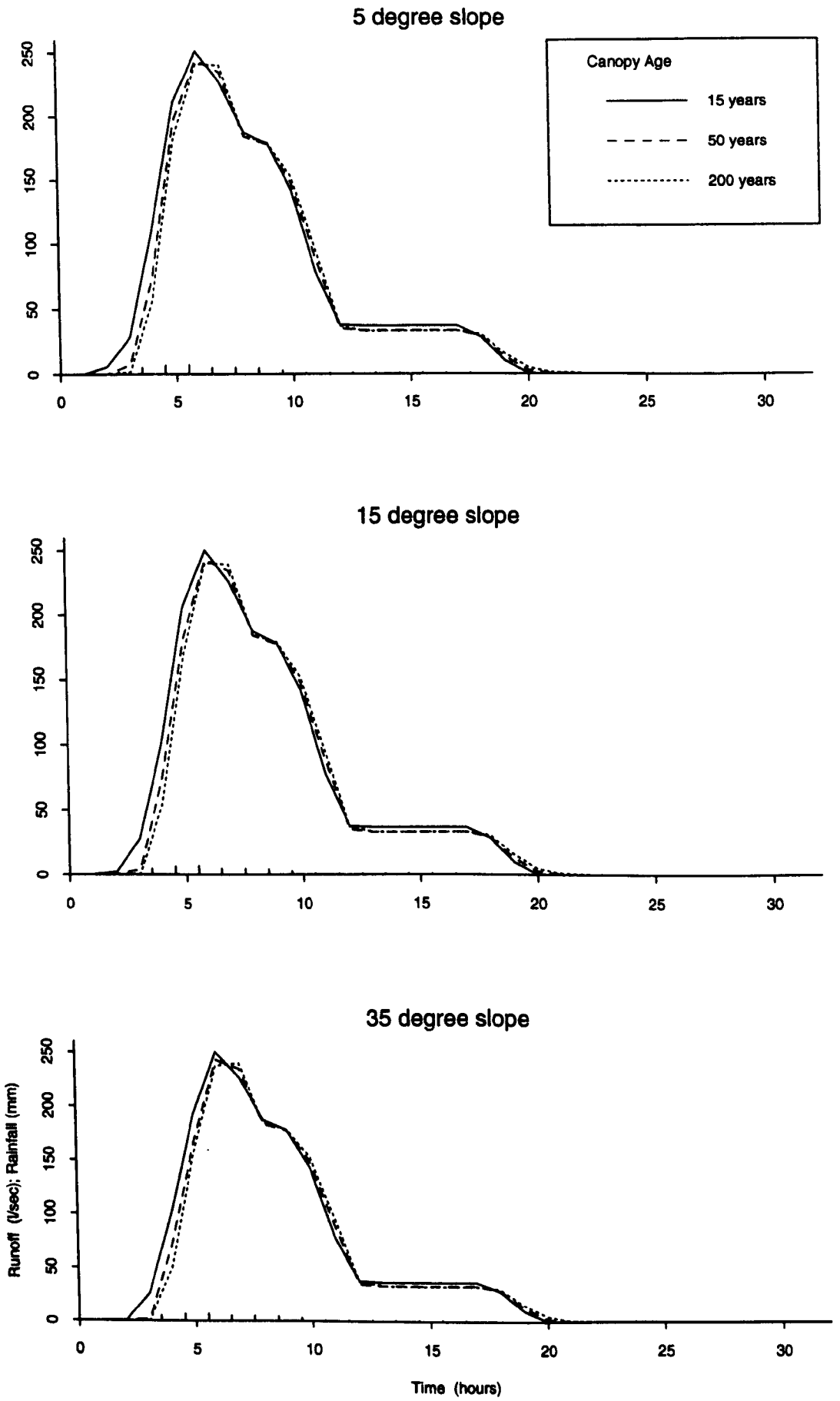

Figure 6.40: Segment runoff response with variation in canopy age and slope angle for low K_{sat} and uniform slope

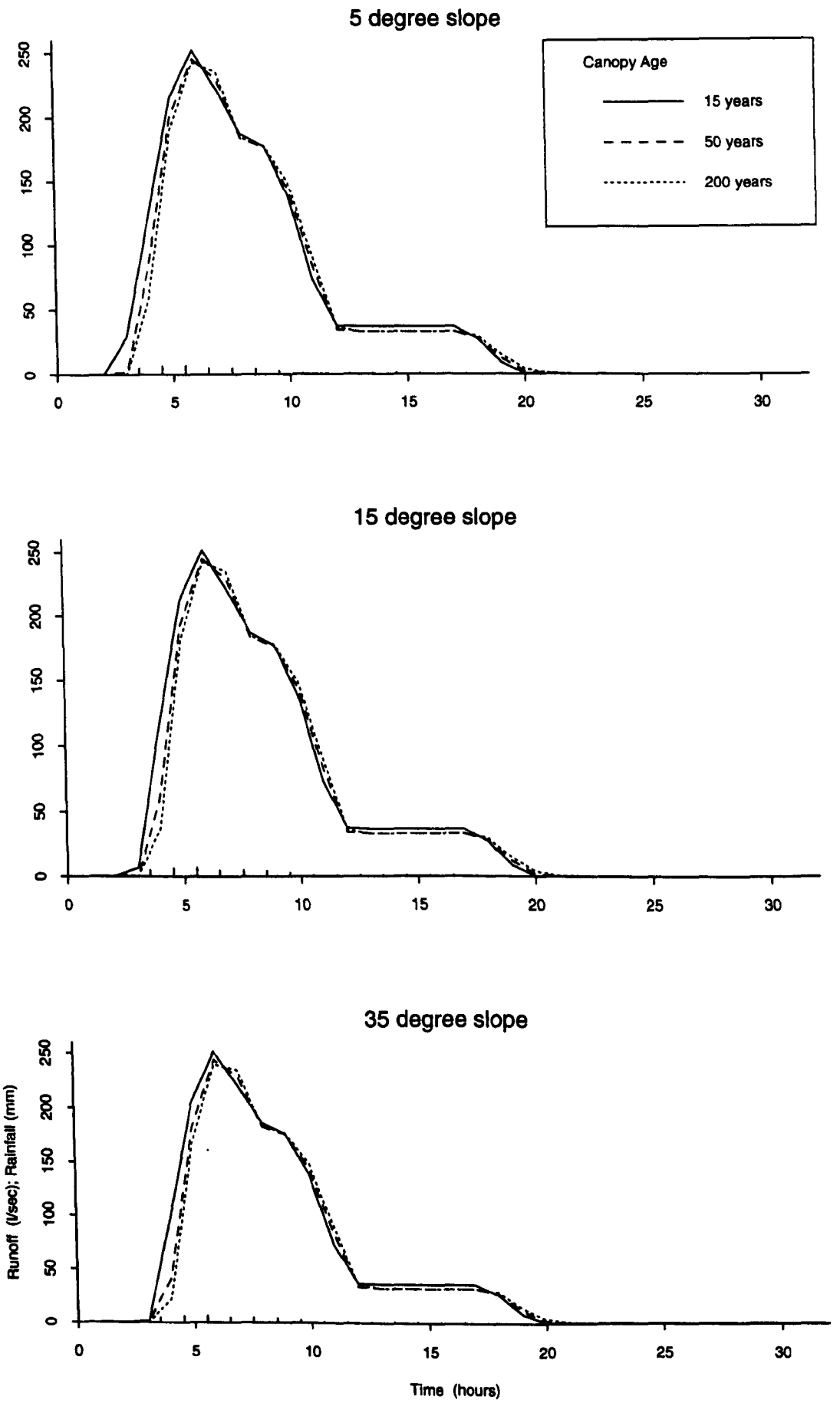

Figure 6.41: Segment runoff response with variation in canopy age and slope angle for low K_{sat} and divergent slope

The change in peak size and shape is one part of the hydrograph that is dependent on the soil hydrological conditions. For the high K_{sat} scenarios (e.g. figure 6.36) the extreme peak of the hydrograph is diminished by the 50 *year* canopy and altogether removed by the 200 *year* canopy. This suggests that the canopy is modifying the rainfall input by a critical amount that is enough to delay the storm peak so that it an extreme peak of rainfall does not occur thereby allowing less water to be routed as overland flow. This is particularly evident in the 5° convergent and uniform slopes (figures 6.36a and 6.37a). A similar trend can be seen in figure 6.18a from the initial robustness testing but the trend was not as general as it is in the secondary robustness tests.

By contrast in the low K_{sat} scenarios (figures 6.39-6.41) the runoff peak is sustained for a longer period as the more mature canopy maintains a high rainfall rate from canopy drainage after the above canopy rainfall rate has diminished. In the low K_{sat} environment this is transferred into the hydrograph quickly thus becoming particularly evident because most of the rainfall reaching the surface will not be absorbed by the soil and moves to the stream rapidly as overland flow.

In the initial set of robustness tests it was observed that there was a greater change in hydrograph between the 15 and 50 *year* canopies than between the 50 and 200 *year* canopies. This is also evident in the results presented here except for in the extreme hydrograph peak diminishment in the high K_{sat} conditions. The possible explanation given in section 6.2.3.4 was that canopy closure is critical to the canopy effect on storm rainfall, therefore the difference between the immature 15 year old forest and the forest simulated as immediately post canopy closure is likely to be critical. The importance of canopy closure has been recognised from field studies as important for many forest hydrological processes (Calder (1990)) and this modelling structure seems to recognise that.

The effect of canopy age on the storm hydrograph has been consistent with most of the different scenarios, it definitely is still an important factor with a larger storm than initially tested and on predrained soil conditions.

6.3.3 Summary

The results presented here have reinforced the first conclusion drawn from the initial set of robustness testing runs, namely that all of the varied factors had some degree of effect on the output hydrographs. This has held for a larger storm occurring on predrained soil conditions, although the hydrograph differences were not always the same as in section 6.2. One of the main reasons for this was that the size of storm meant a storm peak was produced for every scenario as opposed to some of the high K_{sat} scenarios in section 6.2 where the storm has virtually no effect on the hydrograph.

Rank	*Parameter*	
1	High K_{sat}	Low K_{sat}
2	Slope angle/plan shape/canopy age	Canopy age
3		Plan shape
4		Slope angle

Table 6.26: Revised ranking of importance of varied parameters after second set of robustness testing (see table 6.7)

In section 6.2.4 a table of ranking was drawn up for the variables and one of the primary aims of this second set of tests was to see if this ranking still held under different hydrological conditions. Figures 6.33-6.35 have shown that saturated hydraulic conductivity is still the most important parameter and therefore retains its place. Under low K_{sat} conditions it appears that canopy age (figures 6.39-6.41) has a greater effect on the storm hydrograph than plan shape (e.g. figure 6.30) which has a similar if not slightly greater effect than slope angle (e.g. figure 6.32). This confirms the initial conclusions for low K_{sat} although the differences in hydrograph appear smaller because of the storm scale and consequent scale of graphical presentation.

Under the high K_{sat} conditions it is almost impossible to rank the parameters, certainly canopy age has a marked effect (figures 6.36-6.41) as does slope angle, (e.g. figure 6.31), particularly on convergent slopes (figure 6.31a). Plan shape also has a large effect in high K_{sat} scenarios (figures 6.27-6.29), conversely particularly on the 5° slopes (figure 6.27). From this it appears that the relative importance of each parameter cannot be differentiated as was the case for the medium K_{sat} in the initial robustness testing. These results show that table 6.7 needs to be redrawn as shown in table 6.26, for results from scenarios with a large storm on predrained soil slopes.

The modelling scheme has proved to be capable of simulating all of the hypothetical scenario conditions from the second set of robustness testing. The only problem was that the internal timestep (the timestep at which the soil and canopy water movements are calculated) had to be changed to a smaller interval. This was detected early on in the model runs from some spurious hydrographs results, this is discussed further in section 7.2 and a method of checking the model errors has been developed to detect any future periods of mathematical instability.

The model results were interesting in that they presented a large range in hydrographs from the same storm but these were able to be explained with reference to the model structure and known hydrological theory, thereby reinforcing the robustness and relevance of *LUCAS* as a possible predictive tool in a wide range of hydrological conditions.

6.4 Summary of verification exercise

Chapter six has described a series of verification tests on the overall modelling structure (*LUCAS*) that was previously outlined in chapters four and five. The verification took the form of a series of model runs using hypothetical scenarios representing a range of possible field conditions. This was aimed at investigating the general robustness of *LUCAS*. In addition to testing model robustness the hypothetical scenarios were used to identify field conditions where *LUCAS* was particularly sensitive to each of the three general factors varied (topography, soil hydrology, and canopy age), and in particular to find how important the new factor of a temporally dynamic canopy is within *LUCAS*.

The three general factors were defined by four input parameters: plan shape and slope angle for topography; saturated hydraulic conductivity for soil hydrology; and canopy age for vegetation. Each of these parameters were given a range of three values, the two extremes were chosen as close to the range of conditions that could be expected in a humid, temperate environment (conditions that *LUCAS* has been developed for). In the first set of robustness tests (section 6.2) the hillslope segments were assumed to be saturated and a small summer storm was simulated. To further test the results from these initial runs a second set of hypothetical scenarios was simulated (section 6.3) where the soil slopes were drained for 72 hours prior to the application of a considerably larger summer storm.

The robustness testing was successful on several fronts, the first being that the modelling scheme proved itself to be robust enough to cope with the full range of hypothetical conditions imposed upon it. This is an indication that this kind of modelling scheme can be used as a simulator of vegetation change in humid temperate environments. This is not surprising given that both *VSAS* and *INTMO* were developed for this kind of environment, but it does show that *LUCAS* is an adequate modelling scheme for the conditions simulated here.

A second success of the robustness testing has been to identify hypothetical scenarios where *LUCAS* predicts that the value of each varied parameter is critical, this is summarised in table 6.6. This kind of analysis is useful for future modelling, using this or similar modelling schemes, as it identifies scenarios where particular care has to be taken in fixing values to the parameters or conversely where less attention needs to be paid to a particular parameter.

The third successful area from the robustness testing is that canopy age has been shown to be an important factor, and that *LUCAS* is sensitive to changes in the canopy structure. This is important as it is a new element within the modelling scheme and its relative importance needed to be established. If canopy age was found to be unimportant then there would be little point in developing this kind of model structure further especially as the canopy growth routine is the main new element within the overall modelling scheme. Now that its importance has been established it is worth developing the canopy growth routine further,

Parameter	*Initial tests*	*Secondary tests*	*Comment*
K_{sat}	High: high baseflow and lower peak Low: vice versa	Delay of storm peak timing and lower peak volume with high value	*LUCAS* is most sensitive to this parameter
Plan shape	Med.-high K_{sat} divergence reduces peak size & poss. delays peak	Effect of convergence particularly noticeable on high K_{sat} 5° slopes. Main difference in receding limb	Important where soil matrix flow is dominant
Slope angle	High K_{sat} higher baseflow with steeper angle. Reduced peak size for steeper angles	Similar to initial results	Important where soil matrix flow is dominant
Canopy age	Where peak is large, age reduces size and delays the timing at both ends	Affects both high and low K_{sat} to equal degree	Affects all. Consistent effects where soil matrix flow isn't dominant

Table 6.27: Summary of robustness testing results

independently testing to see if it is an adequate forest growth simulator and making any necessary changes to the structure. This testing and further development of the forest growth routine is described in section 7.3.

An important note to make about canopy age in this robustness testing is that it was performed without implementing the relationship between leaf (and stem) area indices and tree size of Halldin (1985). This means that the number of intercepting layers did not change with canopy age (apart from stochastic variations). In simulations using this relationship (i.e. coniferous forest) the effects of canopy age could be expected to be greater as the number of intercepting layers, and therefore the amount of interception loss and indirect throughfall delay, would increase with age. This is likely to have the effect of magnifying the influence of the canopy shown in this chapter.

The following chapter takes the results from the robustness testing and develops *LUCAS* further with respect to some of the individual conclusions drawn.

CHAPTER 7

MODIFICATIONS TO *LUCAS* AND INDEPENDENT VERIFICATION OF THE FOREST GROWTH MODEL

A modelling scheme (*LUCAS*) has been developed as a specific tool to investigate the hydrological effects of afforestation; this has been tested on a series of hypothetical scenarios to verify the robustness of the scheme and its sensitivity to three general factors under a range of different conditions. The previous chapter has described this verification testing; this chapter (seven) deals with some modifications to *LUCAS* that arise from the robustness testing results while the chapter eight details validation testing of *LUCAS*.

7.1 Modifications required

General usage of *LUCAS* and the results from the robustness testing described in chapter six have highlighted several areas within the overall modelling structure that require modification. The encouraging nature of the robustness testing results suggest that *LUCAS* is able to detect some hydrological effects of afforestation which in turn suggests that these modifications are warranted. There are two areas of *LUCAS* that require particular additional modification:

- An error analysis to detect mathematical stability problems
- The verification/validation of the forest growth model as an independent model in its own right

The research design in chapter three highlighted the fact that this project is concerned with the **development** of a modelling scheme to investigate the effects of long term vegetation change on stormflow hydrology. It was stated that the emphasis of the study is on development and assessing the worth of the scheme throughout the whole framework. After the robustness testing of the previous chapter the assessment can be made that *LUCAS* shows considerable promise as a simulator of long term vegetation change, therefore it is worth making further superficial changes to the model that should improve the structure but not radically alter it.

In the second phase of robustness testing (section 6.3) the application of a large

storm onto some of the hillslope segments produced spurious results that were attributed to mathematical instability. The decreasing of the internal timestep within *VSAS4* from five *minutes* to one *minute* solved this problem but highlighted the need for a system to detect the occurrence of instability. To achieve this an error analysis has been incorporated into the *VSAS4* structure, this is detailed in section 7.2.

The forest growth model within *LUCAS* that forms the pre-processing routine for *VSAS4* is an original model combining elements from Ford & Diggle (1981), Leps & Kindlmann (1987), and new work. The model in this original form has not been tested as an independent simulator of forest growth, the emphasis being on getting an early version of *LUCAS* running and tested for its capability of detecting the hydrological effects of afforestation, before testing it fully. Section 7.3 details some testing against a data set and then changes that have been made to the forest growth model in light of this testing. The final part of section 7.3 concerns a sensitivity analysis carried out on the forest growth model as a separate unit i.e. not as part of *LUCAS*.

The changes to *LUCAS* are of a superficial nature and do not invalidate the conclusions drawn about *LUCAS* in the previous chapter. The sensitivity analysis carried out on the forest growth model is complementary to the verification testing in chapter six.

7.2 Error analysis

During the secondary robustness testing (section 6.3) the timestep within *VSAS4* was changed from five to one *minutes* to overcome problems that appeared to be the result of mathematical instability within either the explicit finite difference scheme that solves the soil water flow equations or the explicit scheme within the canopy rainfall partitioning.

An explicit finite difference scheme used to solve partial differential equations (or whatever form the governing equations take) does so by passing a certain amount of water (in this case) between elements within each timestep; the actual amount of water is dependant on the solved partial differential equation. With an explicit scheme the amount of water passed between elements is the maximum possible from the solved partial differential equation as opposed to an implicit scheme where the amount released from one element to another is dependent on a relationship to the amount released during the previous timestep.

The term mathematical instability refers to when the amount of water released from one element is too large a volume for the receiving element to be able to process within the timestep and consequently water may be lost from the system as there is no sink for the extra water. This will not happen in an implicit scheme as the restrictive factor of

being dependent on the previous timestep output prohibits the transfer of large amounts of water between elements. The usual method of overcoming mathematical instability within an explicit scheme is to reduce the computational timestep so that there is less water being passed between elements within the smaller timestep.

VSAS4 has two internal subdivisions of program code that together make up the internal timestep (see figure 7.1). The distinction between these timesteps is important for distinguishing where in the program code the mathematical instability is occurring. The subroutine that deals with subsurface flow between soil elements is entered from the main program by the first subdivision (*KREP*) number of times per hour i.e. if *KREP* equals 5, the subroutine is called 5 times per hour (every 12 *minutes*). Within the subsurface flow subroutine there is a second subdivision (*LREP*) that operates as a loop further subdividing the hourly increment i.e. if *KREP* equals 5 and *LREP* equals 6, the subroutine is entered every 12 *minutes* and then subdivided into 2 *minute* timesteps within the subroutine for subsurface flow and rainfall partitioning calculations.

The reason for the separate subdivisions is that the matrix flow and rainfall partitioning calculations are made within the smaller timestep while the Hortonian overland flow and return overland flow from the surface layers is accumulated and passed downslope within the larger timestep. In the example already used the overland flow (Hortonian plus return) is accumulated from six internal timesteps of matrix flow calculations (i.e. 12 *minutes*) and then passed onto the next downslope element as overland flow ready for absorption by this element. The calculations work upslope so the return overland flow is not considered by the model until the next 12 *minute* timestep. N.B. For the remainder of this section the term timestep is used to mean the combination of *KREP* x *LREP*.

The mathematical instability in the robustness testing was first detected when a large storm was applied to hillslope segments that had been drained for 72 hours as if they were all 15°, uniform plan shape slopes of medium K_{sat} (see section 6.2.1 for actual values). The instability was detected by what appeared to be spurious results from some of the scenarios tested, in particular where there was high K_{sat} (where the slopes were in effect under drained by the predetermined medium range slope drainage) and the canopy was 50 *years* or older. To further investigate the mathematical instability and the effect of changing the *VSAS4* internal timestep one of the scenarios producing unstable results was run for a range of different timesteps and the results analysed. The scenario used as an example was: a 50 *year* canopy; high K_{sat} ($1.6 \times 10^{-5} ms^{-1}$); divergent plan shape; on a 15° slope. The four different timesteps used were: 30 *seconds*; 1; 5; and 15 *minutes*.

Figures 7.2-7.5 show the hydrographs resulting from applying the same storm on the hypothetical scenario described above with the four different timesteps. The hydrographs have been separated into the different process contributions to stormflow as

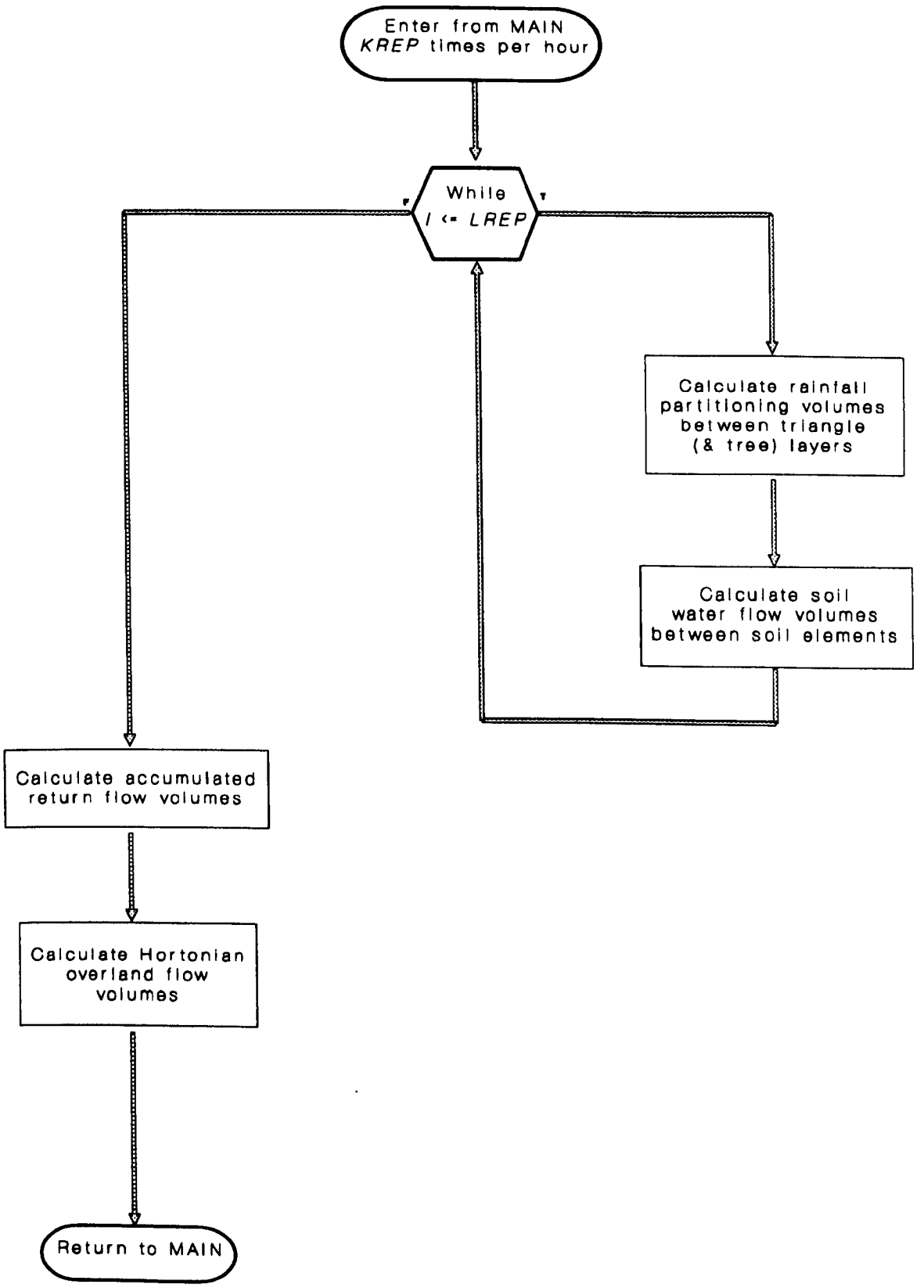

Figure 7.1: Internal timestep subdivisions of *VSAS4*

computed by the model. Matrix flow is the water exiting the hillslope segment from the elements at the base of the slope, overland flow is the water leaving the segment from the surface of the element at the slope base.

The spurious results can be seen in figures 7.2 and 7.3 as twin stormflow peaks when the rainfall has only a single peak and has dwindled off considerably by the time the second runoff peak occurs. There is no obvious physical explanation for this behaviour, especially as the second peak occurs as a change in the amount of overland flow not matrix flow which might have been explainable (i.e. a secondary pulse of soil water has been observed in the field as often occurring in situations where soil matrix flow is an important hydrological process). In figure 7.4 the timestep has been reduced to 1 *minute* causing the second peak to be eliminated which suggests that mathematical instability, either from the passing of overland flow between surface soil elements within the *KREP* timestep, or the transfer of water between canopy layers within each timestep, was the cause of the spurious results.

It is interesting to note that the reduction in timestep between figure 7.2-7.5 has no effect on the amount of matrix flow. In every case this rose to a peak in the sixth hour and gradually declined after the storm had finished. The same cannot be said for overland flow which has the greatest effect on the shape of the storm peak.

Figure 7.6 shows all of the total flows from the different timesteps on the same axes. The difference between the storm responses is extremely large, most noticeably in the timing of the peak flow (a difference of 4 *hours* between the two extremes). This shows that the timestep is an important parameter to consider as it has a large effect on the storm response. In the case shown here the difference with timestep is at least as large as any of the factors varied within the robustness testing in chapter six but it must be emphasised that the example shown here is a special case where mathematical instability is occurring and the differences are not likely to be as large in more stable conditions. This is illustrated by the more stable conditions in figures 7.4 and 7.5 (30 and 60 *second* timesteps) where the difference between hydrograph shapes is not particularly large.

7.2.1 Method

The large difference in output hydrograph shown in figure 7.6 suggests that it is necessary to detect unstable conditions within the model so that corrective measures can be taken before lengthy model simulations are attempted. The method used to detect instability needs to be more objective than analysing output hydrographs for what appear to be spurious results as there may be occasions where the model produces seemingly reasonable results which are in fact partly due to mathematical instability. One method of achieving this is to have an error analysis running concurrently within the model.

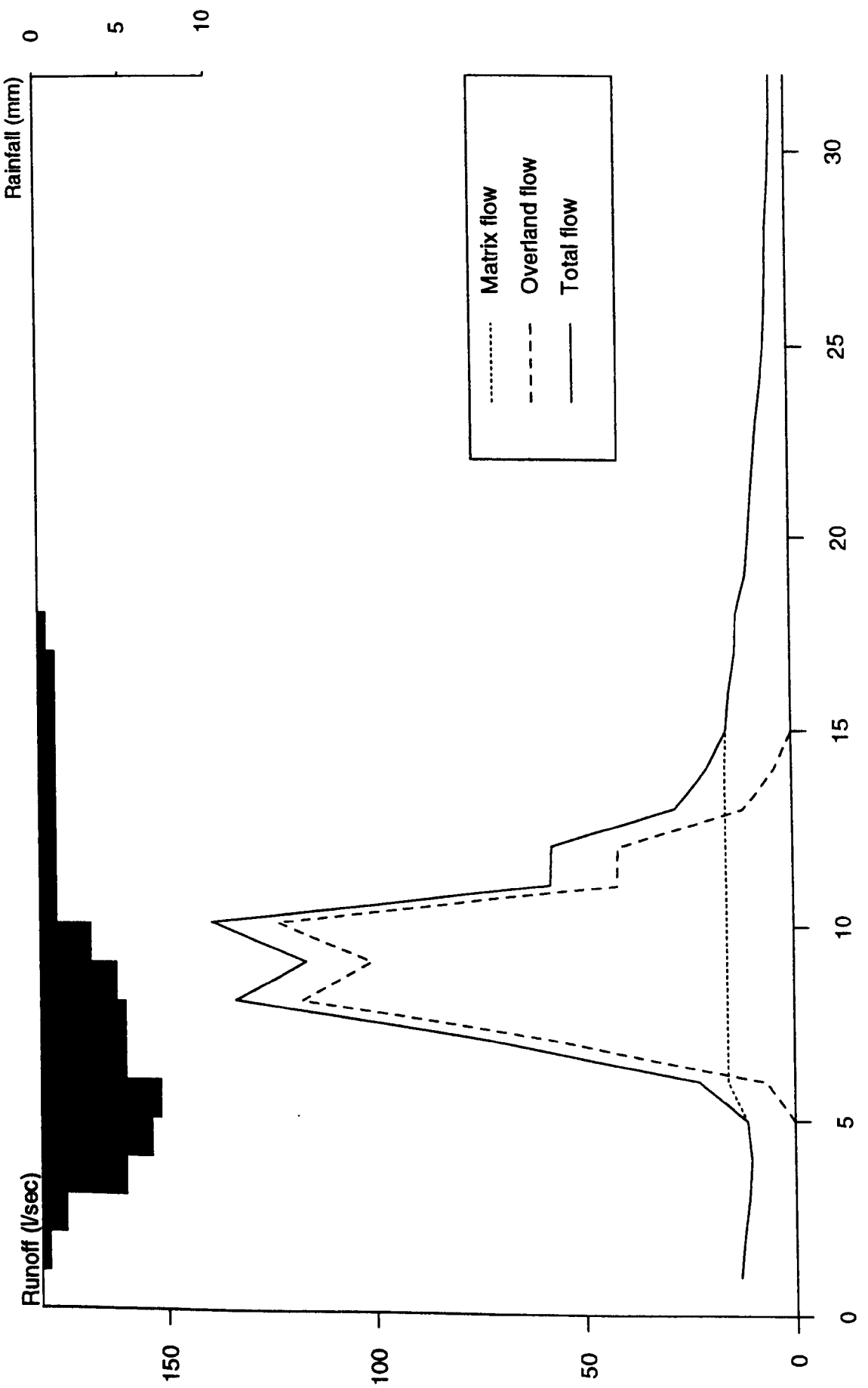

Figure 7.2: Predicted runoff for simulation using 15 *minute* internal timestep

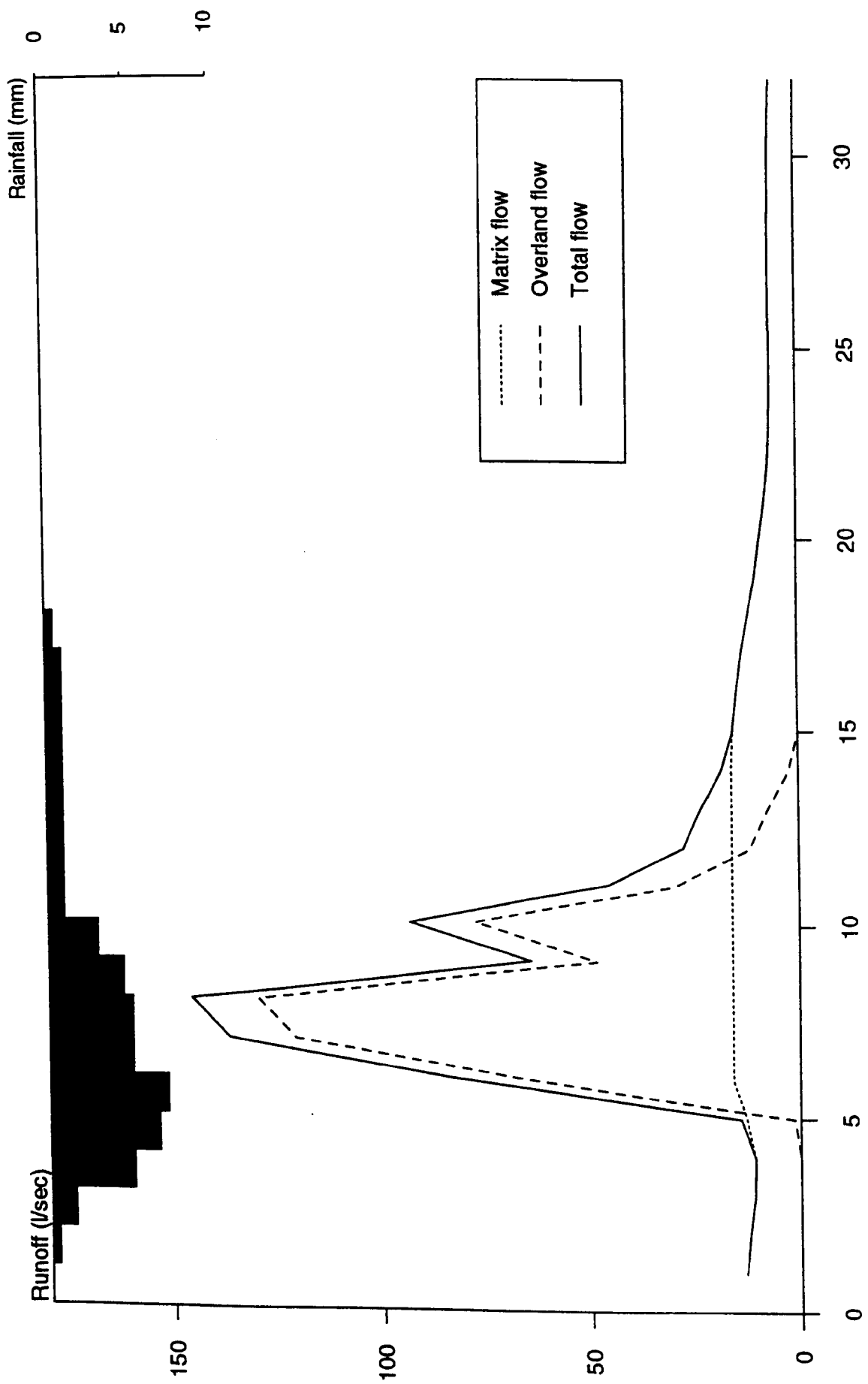

Figure 7.3: Predicted runoff for simulation using 5 *minute* internal timestep

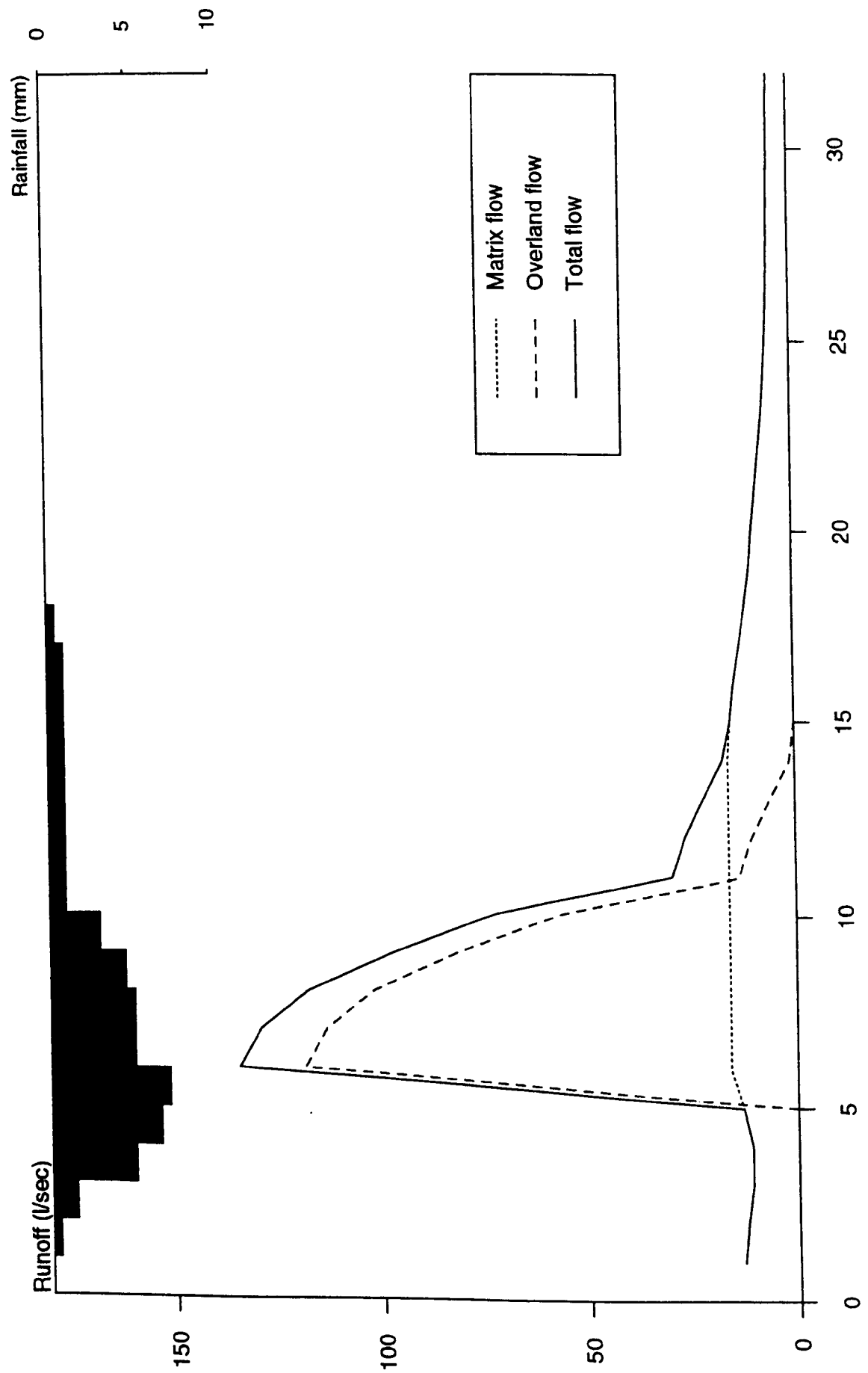

Figure 7.4: Predicted runoff for simulation using 1 *minute* internal timestep

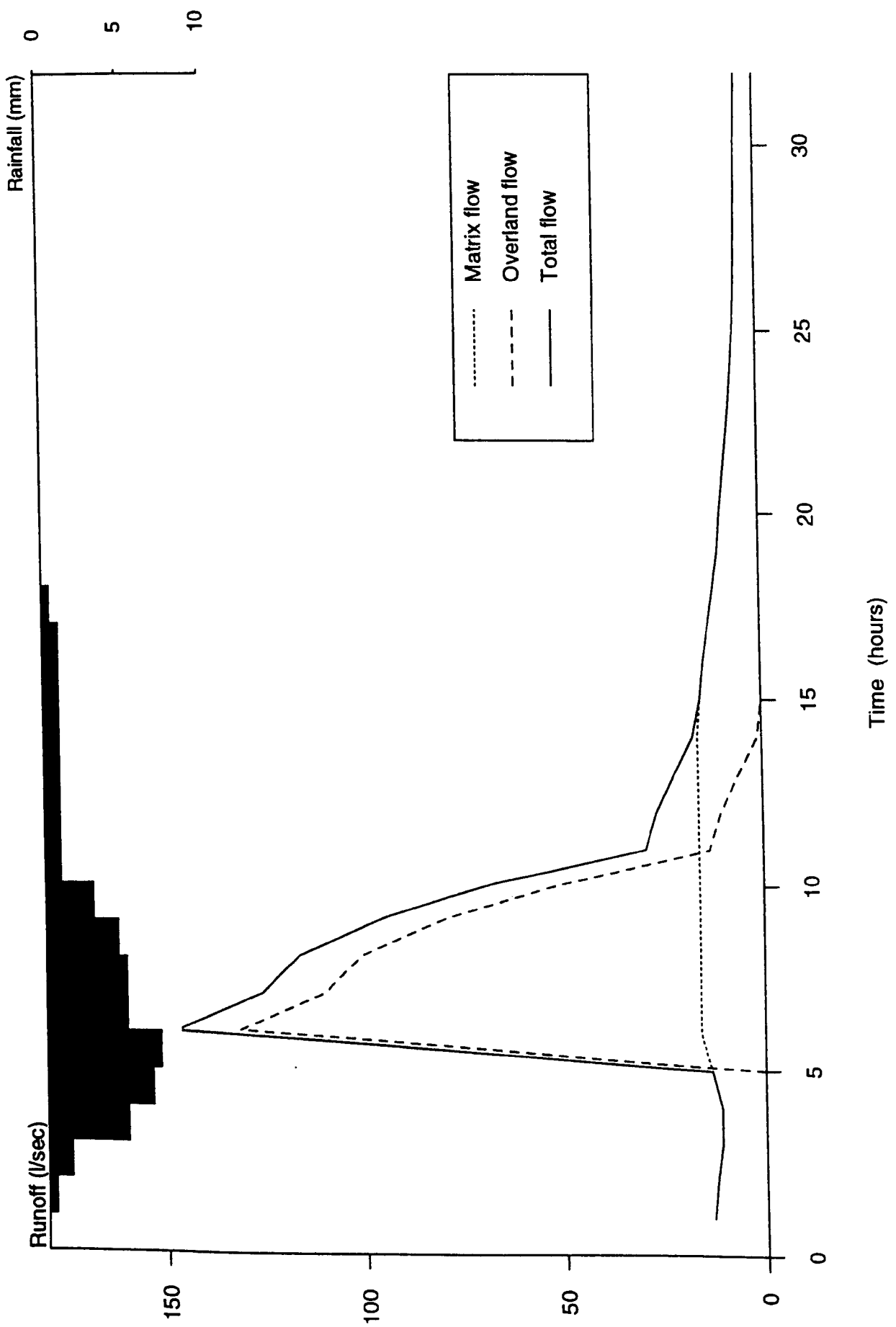

Figure 7.5: Predicted runoff for simulation using 30 *second* internal timestep

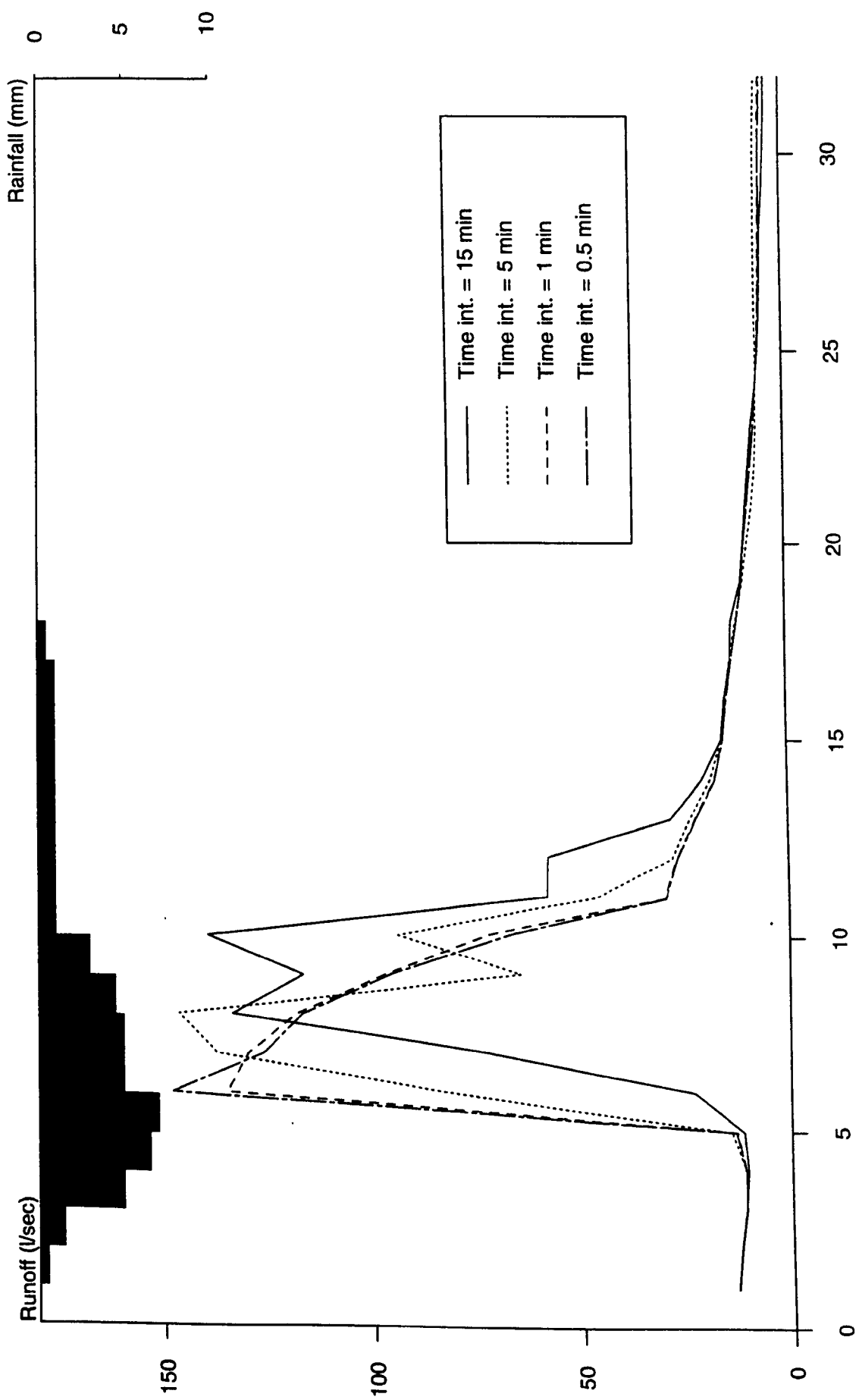

Figure 7.6: Combined simulated total runoff for the different internal timesteps

An error analysis is a simple computational device that sums the amount of input into the model (in this case rainfall) and compares this to the change in various processes (e.g. soil moisture) and the model output. Any discrepancies between the input and output can be attributed to either the accumulation of rounding errors from passing volumes of water between elements within an explicit scheme or mathematical instability where there is a large volume loss over a short time period. An error analysis of this sort has a dual function:

- Detecting periods of mathematical instability
- Analysing which part of the model structure is producing either: the instability; or smaller rounding errors.

The difficulty with this type of analysis within a complex modelling scheme such as *VSAS4* is keeping track of all the water movements within the different process representations, but this in turn makes it even more necessary for detecting errors within the system.

The error analysis that has been formulated within *VSAS4* is shown schematically in figure 7.7. This is a simplification of the *VSAS4* scheme; it illustrates the principles of the error analysis dividing each hillslope segment into two separate storage tanks, one for the canopy and the other for the soil mass. This approach simplifies the model structure and is relatively easy to understand and follow within the program code but a problem arises as to what time scale the errors should be analysed at. If the error analysis is carried out at the smallest timestep or alternatively by summing the inputs and outputs for each individual triangle or tree layer within the canopy, then the number of calculations will make the analysis inaccurate in itself, becoming subject to the same type of rounding errors the analysis is trying to detect. As a compromise each of the error calculations (equations 7.1-7.3; also see figure 7.7) are summed hourly for each individual hillslope segment.

$$E_C = | (V_{CA} - V_{\Delta S} - V_{EV}) - V_{CB} | \quad (7.1)$$

$$E_S = | V_{CB} - V_{\Delta SM} - (V_{SF} + V_{MF} + V_{OF}) | \quad (7.2)$$

$$E_{TOTAL} = | V_{CA} - V_{\Delta S} - V_{EV} - V_{\Delta SM} - (V_{SF} + V_{MF} + V_{OF}) | \quad (7.3)$$

$$= E_C + E_S$$

In equations 7.1-7.3 the errors are summed as absolute values so that there is no

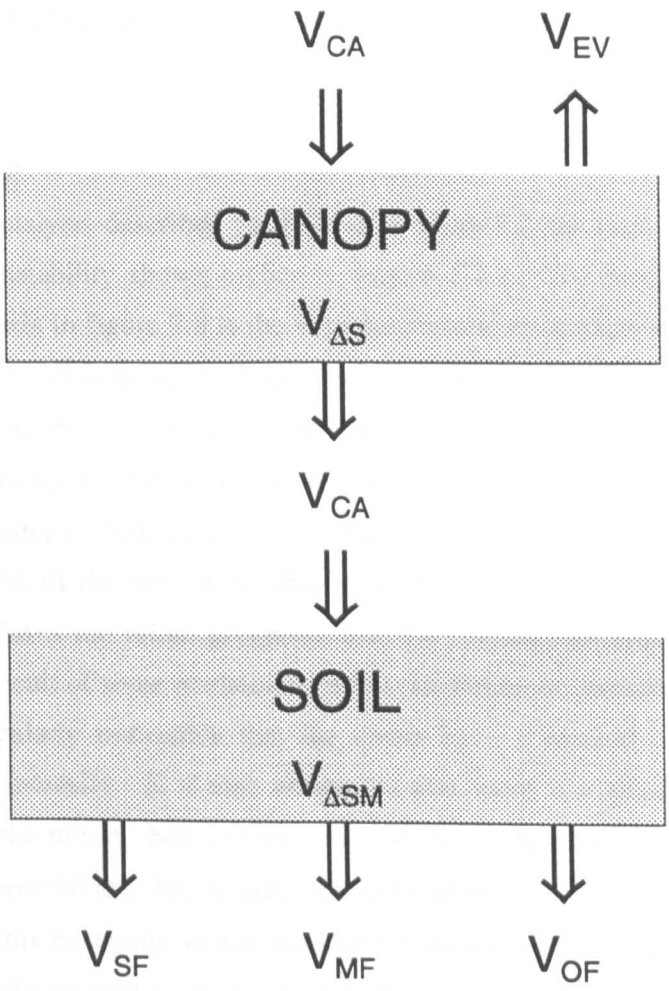

V	= Volume	CB	= Below canopy
E	= Error	CA	= Above canopy
C	= Canopy	EV	= Evaporation
S	= Soil	SF	= Surface flow (Hortonian)
OF	= Overland flow	MF	= Matrix flow
ΔSM	= Change in soil moisture	ΔS	= Change in canopy storage

Figure 7.7: Summary of the new error analysis routine within *VSAS4*

difference between an error loss or an error gain. All losses to the system are given positive values and the change in storage (both soil moisture and canopy) are positive when water is absorbed and negative when water is released from them.

7.2.2 Testing

The error analysis described above and in figure 7.7 has been used to investigate the mathematical instability shown earlier in section 7.2.1. The results are presented in figure 7.8. The *y* axis in figure 7.8 is the cumulative total error expressed as a percentage of the total water in the system. N.B. this is a real percentage so the maximum *y* value shown is 1% not unity. It is clear that there is considerable error involved in the calculations for both the 15 and 5 *minute* timesteps, with considerably less in the 1 *minute* and 30 *second* timesteps. Although the total error for the 15 *minute* timestep at the end of the run is only 0.8% of the total water this is still considerable with respect to the other timesteps and confirms the initial prognosis that the spurious hydrographs in figures 7.2 and 7.3 were as a result of some mathematical miscalculation or instability.

It is particularly noticeable that the errors have a marked increase with every change in rainfall intensity. It is also noticeable that there is a steady increase in error immediately after the rainfall has finished and that this is the same for every timestep. In the smaller timesteps (60 and 30 *seconds*) this error after the rainfall has finished is larger than any of the errors occurring within the storm simulation. The source of this error and the instability should be evident from an analysis of the separate error functions (canopy and soil, equations 7.1 and 7.2 respectively).

Figure 7.9 shows a breakdown of the errors within the storm that used a 15 *minute* timestep (N.B. these are shown as real values not the absolutes so that the type of error can be detected, a negative error means that more rainfall is reaching the surface than should be, and the opposite for a positive error). Figure 7.9 shows that the source of the mathematical instability is within the explicit rainfall partitioning section of *VSAS4*, and not the explicit finite difference scheme for solving the soil matrix flow equations. It should be noted that although the soil error appears to be zero throughout the simulation it does have values it is just that they are very small compared to the canopy error. The double peak of stormflow shown in figures 7.2 and 7.3 is therefore as a result of a variable rainfall input to the soil surface rather than a problem of routing return overland flow down the slope.

The rise in cumulative error after the storm rainfall has finished (evident for all timesteps in figure 7.7) is also within the rainfall partitioning section of *VSAS4*. Some investigations within the model structure have suggested that this is a result of the simplified evaporation function used. The error is not extremely large and has not been

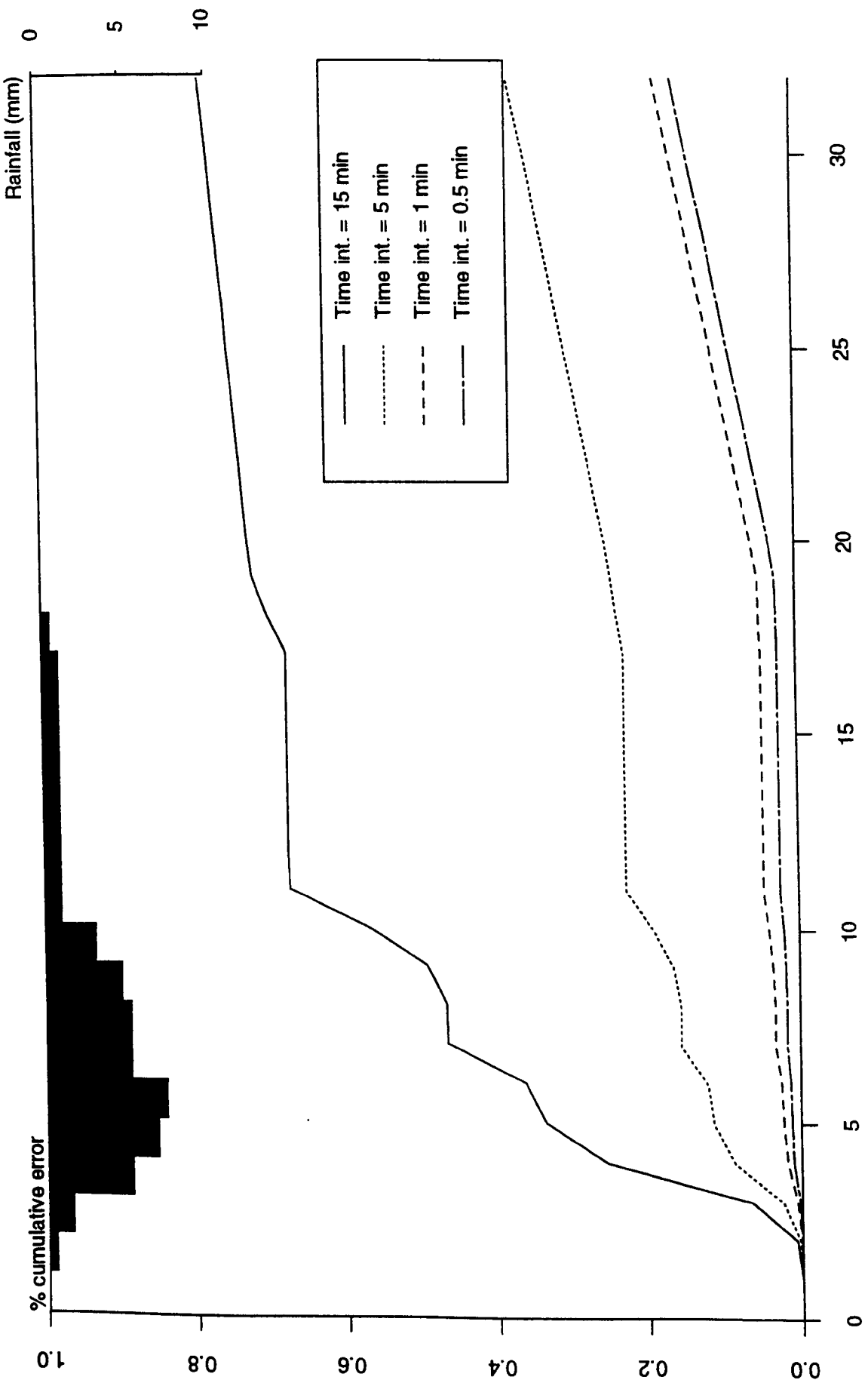

Figure 7.8: Results of error analysis for four internal timesteps (cumulative error)

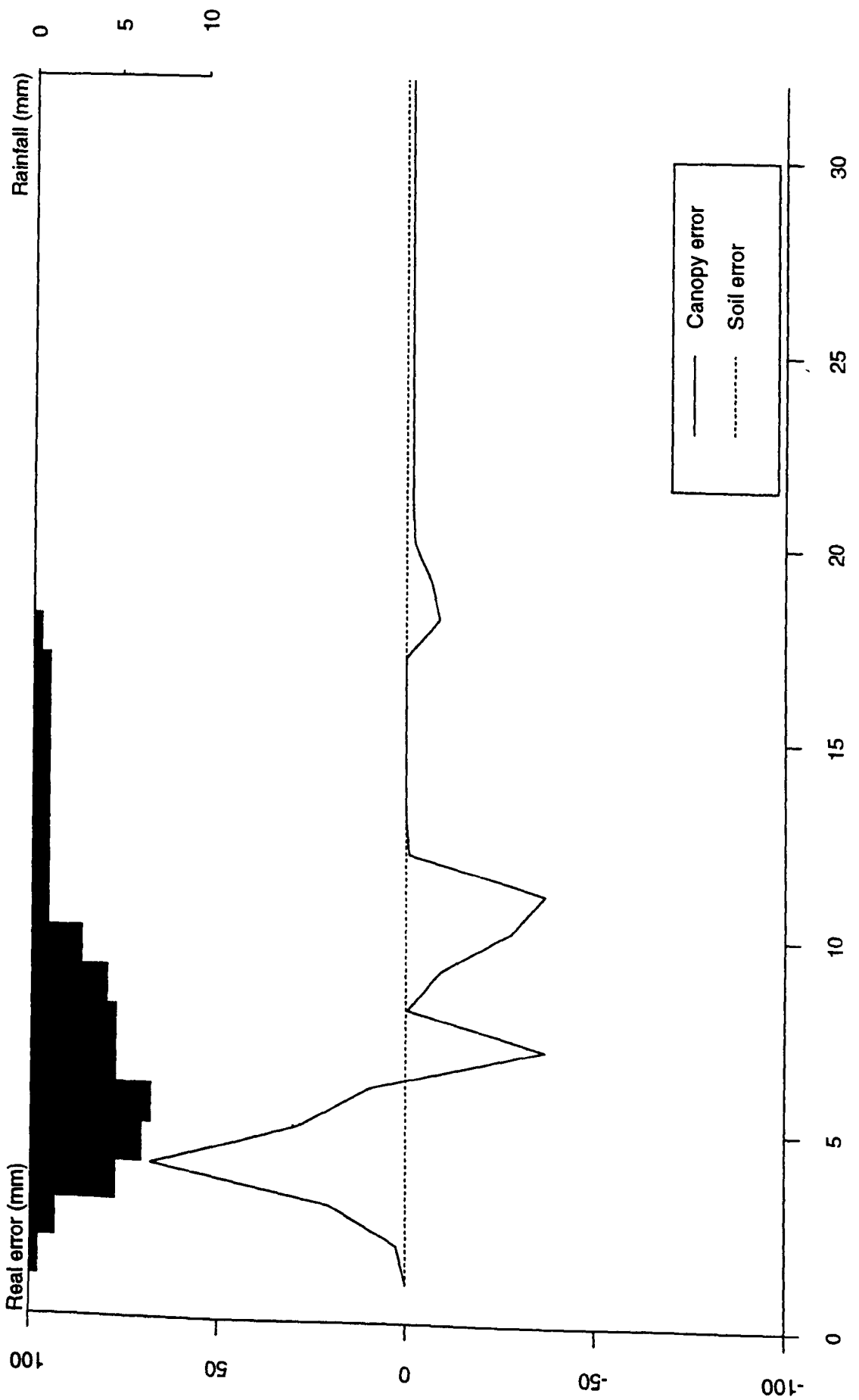

Figure 7.9: Breakdown of errors for 15 *minute* internal timestep (real error)

investigated further.

7.2.3 Summary

The problem of mathematical instability that was detected in chapter six as part of the robustness testing of *LUCAS* has led to the development of an error analysis routine built into the structure of *VSAS4*. The routine sums the amount of inputs and outputs from the model in a separate manner from the model calculations and then finds the error as the difference between the two. Each hillslope segment is split between the canopy and soil storage tanks with a separate error being computed for both of these.

The error analysis results were used to investigate the mathematical instability from one of the hypothetical scenarios used in chapter six. The results of the error analysis showed four important points:

- The error analysis method is able to detect periods of mathematical instability
- The error analysis method is able to detect which part of the model is producing the errors
- The main source of error in mathematical stability was occurring in the rainfall partitioning section of *VSAS4*
- The error occurring after the storm rainfall had finished was also occurring within the rainfall partitioning section.

The first two of these points are the two functions that this kind of analysis aimed to achieve (see section 7.2.2).

7.3 Changes to the forest growth model and independent verification

The forest growth model presented in chapter five combines elements from previous plant growth modelling studies (Ford & Diggle (1981) and Leps & Kindlmann (1987)) with new features developed as part of this study, these together make an original individual tree based, forest growth model. The emphasis of the project so far has been to get an initial version of *LUCAS* up and running and then test that as a possible land use change simulator. It was planned that if the results from this testing were encouraging enough it would then be worthwhile separately testing the forest growth model against some form of data set and if necessary developing it into a verified model in its own right.

The results of the verification testing detailed in chapter six have shown that the *VSAS4* part of *LUCAS* is able to detect the hydrological effects of changes in canopy structure simulated by the pre-processing forest growth model. The encouraging nature of these results means that it is now a feasible exercise to test the forest growth model as an independent simulator of canopy growth. This is described in section 7.3.1, the developments and changes to the forest growth model resulting from this testing are outlined in section 7.3.2. A sensitivity analysis of this final forest growth model structure is described in section 7.3.3.

Within *LUCAS* there are the two distinct modelling units which run at totally different timesteps: the forest growth model which runs at a forest growth timescale (1-200 *years*) and acts as a pre-processor for the second part; *VSAS4* which runs at a storm event time scale (1-200 *hours*). The modular structure of *LUCAS* (see figure 5.8) means that it is possible to test the two models separately as well as in the combined form (as in chapter six). The following section concerns the separate initial testing of the forest growth model as described in section 5.2 and 5.3.

7.3.1 Initial testing against a data set

To test the forest growth model as an independent simulator of forest growth it is necessary to obtain a data set containing the kind of information that the model produces as final output. The main recorder of tree growth measurements in Great Britain is the Forestry Commission who monitor the growth of many tree species in plots at sites throughout the country under different management techniques. The Forestry Commission were approached to see if any of these records could be made available for this project but unfortunately the individual plot records cannot be released to non-Forestry Commission researchers. The only Forestry Commission data generally available are their yield tables (Edwards & Christie (1981)) that have already been used in chapter six for average tree size data. After discussion with a member of the Forestry Commission staff involved in numerical modelling it was decided that these tables give imperfect but adequate information to use in model testing (Dr. A. Ludlow, Forestry Commission Headquarters, Pers. comm.).

The data available from the Forestry Commission yield tables is averaged for all the trees in each plot and then for all the different plot sites around the country. The stochastic nature of parts of the forest growth model used in this study means that a full data set of individual tree growth within a plot would have little relevance for testing (i.e. there is no reason why the initial individual tree growth rates assigned stochastically would correspond to growth rates at those positions) and averaged data would have to be used anyway. The main problem with the yield table data is that they are averaged for sites all over

Great Britain. This means that the model cannot be validated as a forest growth predictor for a specific site but only in a general sense.

The Forestry Commission yield tables give average data for the growth of different tree species that are compiled from monitoring numerous plot sites throughout Great Britain. Table 7.1 is a redrawn sample page taken from the yield tables for unthinned Sitka spruce (*Picea sitchensis*) showing the different information available. Each of the tree species has a different set of data corresponding to each management technique (tree spacing and thinning) and yield class.

Yield class is an arbitrary categorisation applied in forestry management to distinguish between different growth rates of trees under different conditions. The actual yield class is taken from the maximum mean annual volume increment for a plot (see figure 7.10). Maximum mean annual volume increment is the maximum average rate of volume production attained by a tree plot, irrespective of the time at which it is achieved (Edwards & Christie (1981)).

Having decided on the source of data to be used for initial testing it is necessary to decide upon the type of data to be abstracted from this source. This depends upon two factors:

- The sensible choice of general measured data based upon the general aims of the project e.g. tree species, yield class etc.
- The convergence of measured data availability and output from the model.

The most obvious general measured data decision is which tree species to concentrate a model testing exercise upon. Taking into account the fact that the forest growth model has been developed with a general capability for both coniferous and deciduous trees within a mono-specific plantation (see section 5.2), it was decided to concentrate on the growth of coniferous plantations for the two reasons outlined below.

The first is that the most common type of afforestation occurring in Great Britain at present and in the recent past is the planting of conifer plantations in upland and other marginal agricultural areas. The hydrological issues related to this type of land use change are particularly relevant because of its topicality and many of them have been under study by research agencies such as the Institute of Hydrology, Wallingford, U.K. for a number of years.

The second reason for concentrating on coniferous plantations is that deciduous afforestation tends to be multi-specific (e.g. mixed hardwoods such as oak and sweet

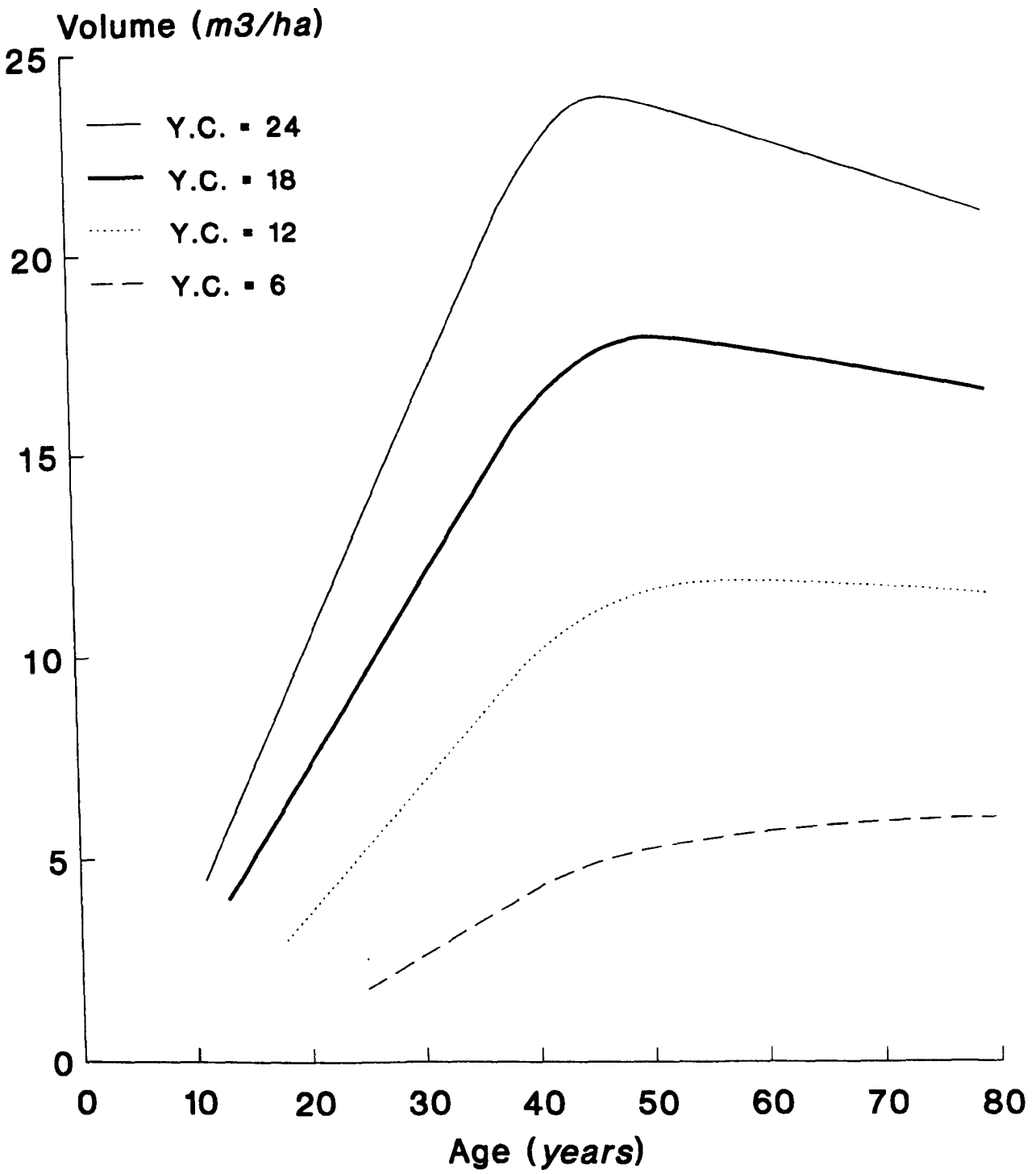

Figure 7.10: Forestry yield classes defined by the maximum mean annual volume increment

Age (*yrs*)	*Height* (*m*)	*Trees per hectare*	*Mean dbh* (*cm*)	*Basal area* (m^3ha^{-1})	*Mean volume* (m^3)	*Volume* (m^3ha^{-1})	*Mortality* (%)	*MAI* (m^3ha^{-1})
19	8.6	1597	14	25	0.05	86	0	4.5
24	11.7	1562	17	37	0.11	174	0	7.2
29	14.8	1395	20	45	0.20	278	2	9.6
34	17.6	1224	23	52	0.32	389	4	11.4
39	20.3	1088	26	57	0.46	496	5	12.7
44	22.5	980	28	61	0.61	593	7	13.5
49	24.5	898	30	64	0.75	677	8	13.8
54	26.2	840	32	66	0.90	752	8	13.9
59	27.6	797	33	69	1.03	818	9	13.9
64	28.8	766	34	71	1.14	876	9	13.7
69	29.8	742	35	73	1.25	928	9	13.4
74	30.7	722	36	75	1.35	973	9	13.1
79	31.5	707	37	76	1.43	1012	9	12.8

Height: Average height of a number of top height trees in a stand

Trees per ha: Number of live trees in the stand (per *hectare*)

Mean dbh: Mean diameter of tree trunks measured at 1.3*m* above the ground

Basal area: Sum of the overbark cross sectional area of the stems of all live trees (measured at 1.3*m* above the ground)

Mean volume: Average volume of all live trees

Volume: Overbark volume of all live trees

Mortality: Volume of dead trees expressed as a percentage of the cumulative volume production

MAI: Mean annual volume increment (cumulative volume production to date divided by age)

Table 7.1: Yield table for Sitka spruce (2.4*m* spacing, yield class 16). From Edwards & Christie (1981)

chestnut) and the forest growth model developed as part of *LUCAS* is for mono-specific plantations. With recent government policy advocating the development of community forests in rural areas surrounding urban centres in Great Britain it is likely that deciduous afforestation will be an increasingly topical subject but at present *LUCAS* does not have the capability to simulate anything other than mono-specific afforestation.

The decision to concentrate on coniferous trees was made after consultation with

Institute of Hydrology staff as to the best option. The most common type of coniferous plantation within Great Britain is Sitka spruce (*Picea sitchensis*) and consequently this is the tree species used for all further testing.

The yield class of Sitka spruce used is dependent on the growth conditions for the intended simulation. Because the testing exercise is for no particular site in Great Britain it was decided to concentrate on a medium class, consequently yield class 16 was chosen from a range between 6 and 24.

The yield tables provide data for all different types of plantation management i.e. different thinning techniques (including no thinning at all) and different spacing between trees. It would be possible to incorporate thinning techniques into the forest growth program structure by removing a certain number of trees arbitrarily at set time intervals at the same time as trees are killed for reasons of overcrowding (see figure 5.6). This would require further programming code to be added which was judged to be unnecessary at this stage of development of *LUCAS*. Consequently the yield table data used is for unthinned Sitka spruce plantations of the same spacing (3*m*).

The second choice on the type of data to be extracted from the Forestry Commission yield tables concerns what is available within the tables and how that matches the data output from the forest growth model. There is no set model output apart from the structural parameters required by the rainfall partitioning section of *VSAS4*; consequently the output can be changed to fit the available yield table data. Of the columns shown in table 7.1 the data that fit into the model outputs best are the average tree growth and the number of trees per hectare (plot density) which implicitly give the tree mortality (N.B. this is different from the listed *per cent mortality* in table 7.1 which is the volume of dead trees, expressed as a percentage of cumulative volume production, Edwards & Christie (1981)). These two measures were used as yardsticks to test the predictive ability of the forest growth model that is part of *LUCAS*.

Table 7.2 shows the actual data values used in this initial testing of the forest growth model. Using these input values the model was run for a 1 *hectare* plot and then the two values of output data stored per years tree growth i.e. number of trees per *hectare* and average *dbh*.

For each plot there was a 10*m* area around the edge where the trees were grown but their size values and mortality were not included in the results to allow for edge effects. Edge effects are a well known phenomena in the numerical modelling and field investigation of any environmental process, they are where the sudden change in conditions developing from a difference in spatial distribution of the studied phenomena may have large effects on the modelled or measured output. In the forest growth model the

Tree spacing	2.4 *m*
Initial *dbh*	0.05 *m*
Maximum *dbh*	0.60 *m*
Growth period	80 *yrs*
Mean growth ratio*	0.09
Standard deviation of growth ratio	0.022
Crown angle	11°
Proportion of tree height to base of crown	10 %
Proportion of tree crown as zone of influence (ZOI)	150 %

Table 7.2: Input data used in initial testing runs of the forest growth model. * Reaches within 99% of maximum potential size at 78 years (see equation 5.3).

trees growing at the edge of the plot have less competition from neighbouring trees than those in the middle of the forest stand. This is obviously something that occurs in physical reality but where the model acts as a pre-processor for *VSAS4* the simulated forest plot is assumed to be a representative example of the forest covering **all of the hillslope segment**. The edge effects will be greater on the smaller simulated plot than for a larger hillslope segment and therefore should be eliminated or at least minim ised. In some studies the emphasis may be on modelling the impacts of edge effects but here the case is one of trying to diminish edge effects as they are a product of the model structure and do not equate to the physical reality.

The exclusion of trees simulated on the edge of the forest plot means that the simulated area is less than 1 *hectare* which requires a calculation in the model structure to estimate the number of trees per hectare from the actual number of trees per 0.64 *hectares*. The *dbh* is averaged for all trees in the plot not counting those within the exclusion zone.

The results of these initial model simulations are shown in figures 7.11 for average tree growth and figure 7.12 for the plot density. The most striking feature of both of these figures is how far from the yield table results the model predictions are.

In figure 7.11 the predicted average diameter at breast height is considerably lower than the yield class results at all stages. The predicted growth rate is never as steep as the yield table results although the actual form of growth curve is similar. The small blips in the predicted average *dbh* (especially at later stages of simulation) is due to the small number of trees remaining in the plot. The small total of trees means that the death of one large tree can affect the average *dbh* considerably.

The forest growth model appears to have similar difficulties predicting forest plot density although in this case the predicted mortality is too high (i.e. too many trees die). In the yield table the decline in tree numbers is quite gradual ending with 707 trees per

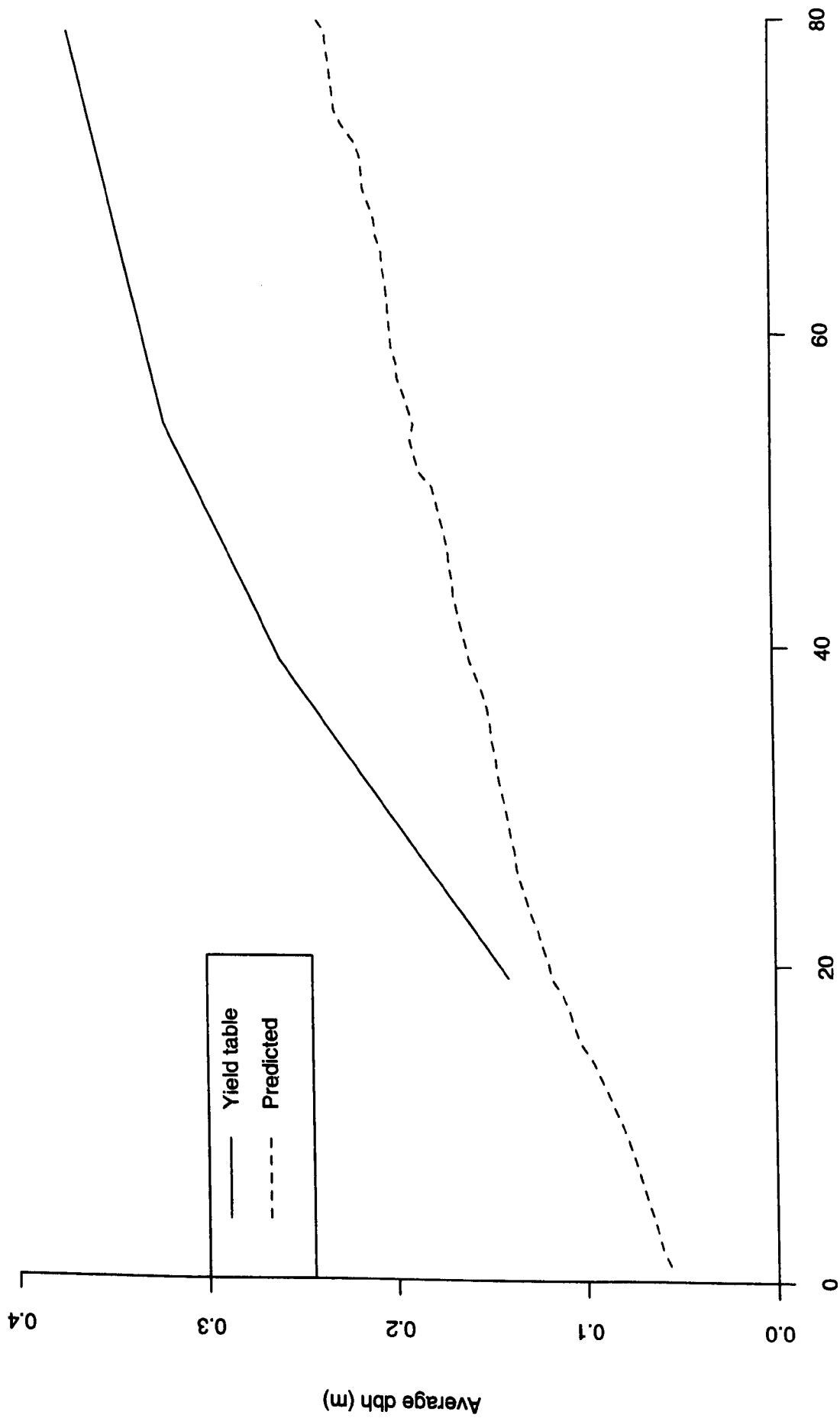

Figure 7.11: Observed versus predicted average dbh results for initial model simulations

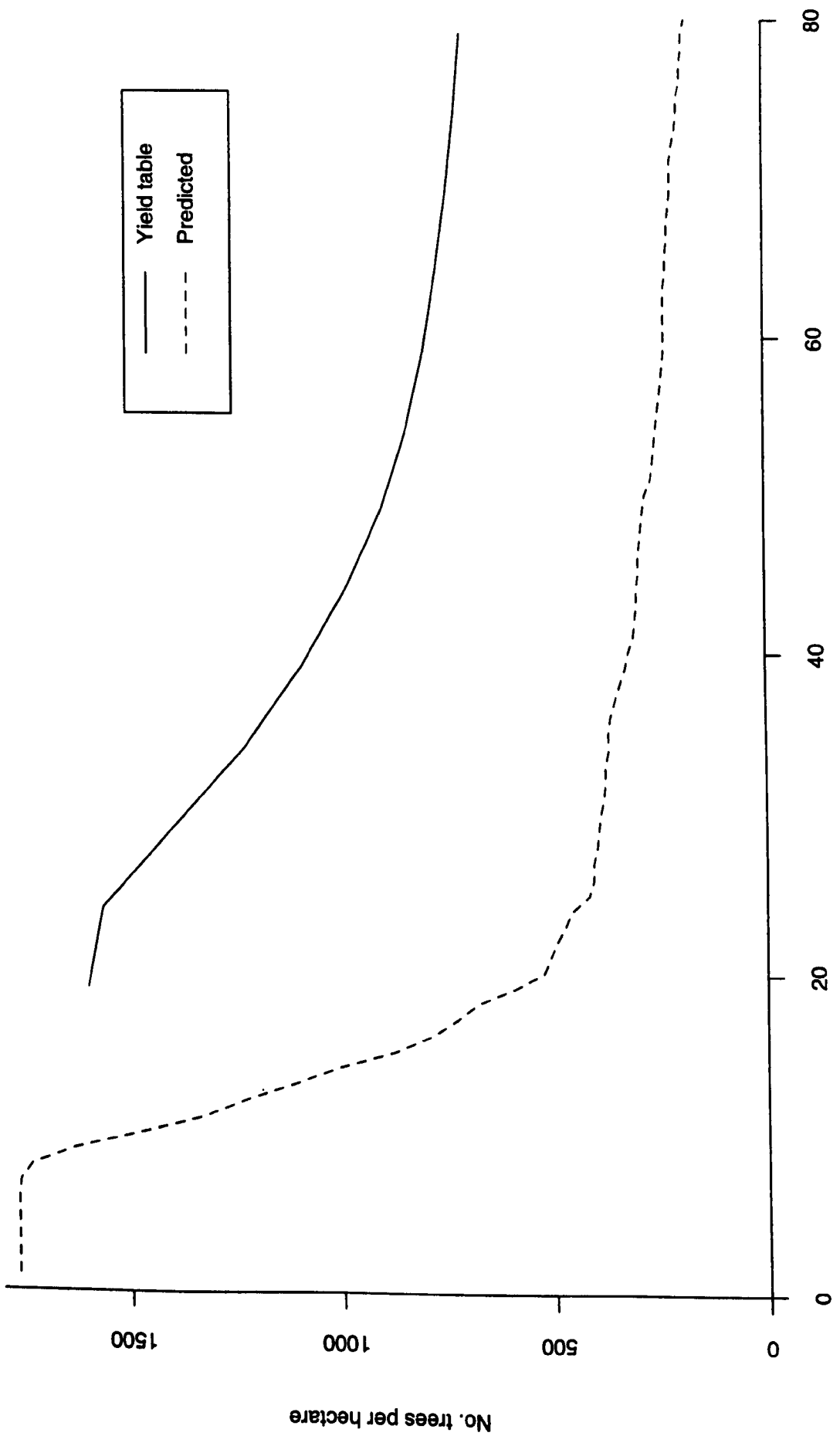

Figure 7.12: Observed versus predicted plot density results for initial model simulations

hectare, whereas the simulation has an extremely rapid decline culminating with 200 trees per *hectare*. The simulated decline in tree numbers starts occurring as soon as the trees start interfering with one another, in the presented case this is about 15 *years* after the simulation begins. At this stage there is an enormous drop in the number of trees which gradually flattens off reaching very close to the minimum number of tree per *hectare* within 40 *years*.

The initial testing results presented here have involved no calibration of model parameters which may or may not have improved the general performance. There is little point in calibrating the model before a sensitivity analysis takes place as there is no way of knowing which parameters are likely to affect the different outputs and in what manner. Before this sensitivity analysis was undertaken several changes were made to the model structure to try and improve the predictive ability. The changes to the forest growth model structure and retesting are detailed in the following section (7.3.2) with the sensitivity analysis being described in section 7.3.3. The validation testing of the forest growth model resulting from the sensitivity analysis is contained within the validation testing of the overall *LUCAS* scheme (chapter eight).

7.3.2 Changes to the forest growth model structure

The results of initial testing of the current forest growth model against a limited data set have suggested that this is not a particularly accurate simulator of a forest growth. It is important to recall that there was no calibration attempted in this initial testing but it is obvious despite this that there are improvements that could be made to the model structure.

Figure 7.13 (a repeat of figure 5.7) indicates that there are three areas that make up the forest growth model structure: potential growth on a logistic curve; inter tree competition based on circular zones of influence; and plot mortality using simple interaction rules (N.B. these are interlinked more than this conceptual diagram suggests, see figure 5.6 for a full flow diagram of the model structure). As is indicated in figure 7.13 the potential growth curve and inter tree competition methods have been used previously in various forms of plant growth models whereas the tree mortality rules have not been used by other modelling studies.

A combination of the lack of previous usage of the mortality rules and the difficulty that the model had predicting plot mortality (see figure 7.12) suggests that this is a potential area to change the model structure to try and improve its predictive ability. Changing this section of the model has the added advantage that it is not going to drastically alter the integral model structure as a change in the driving equations might. This means that the forest growth model will still be an individual tree based, forest growth model and the majority of work carried out so far using it will still be valid.

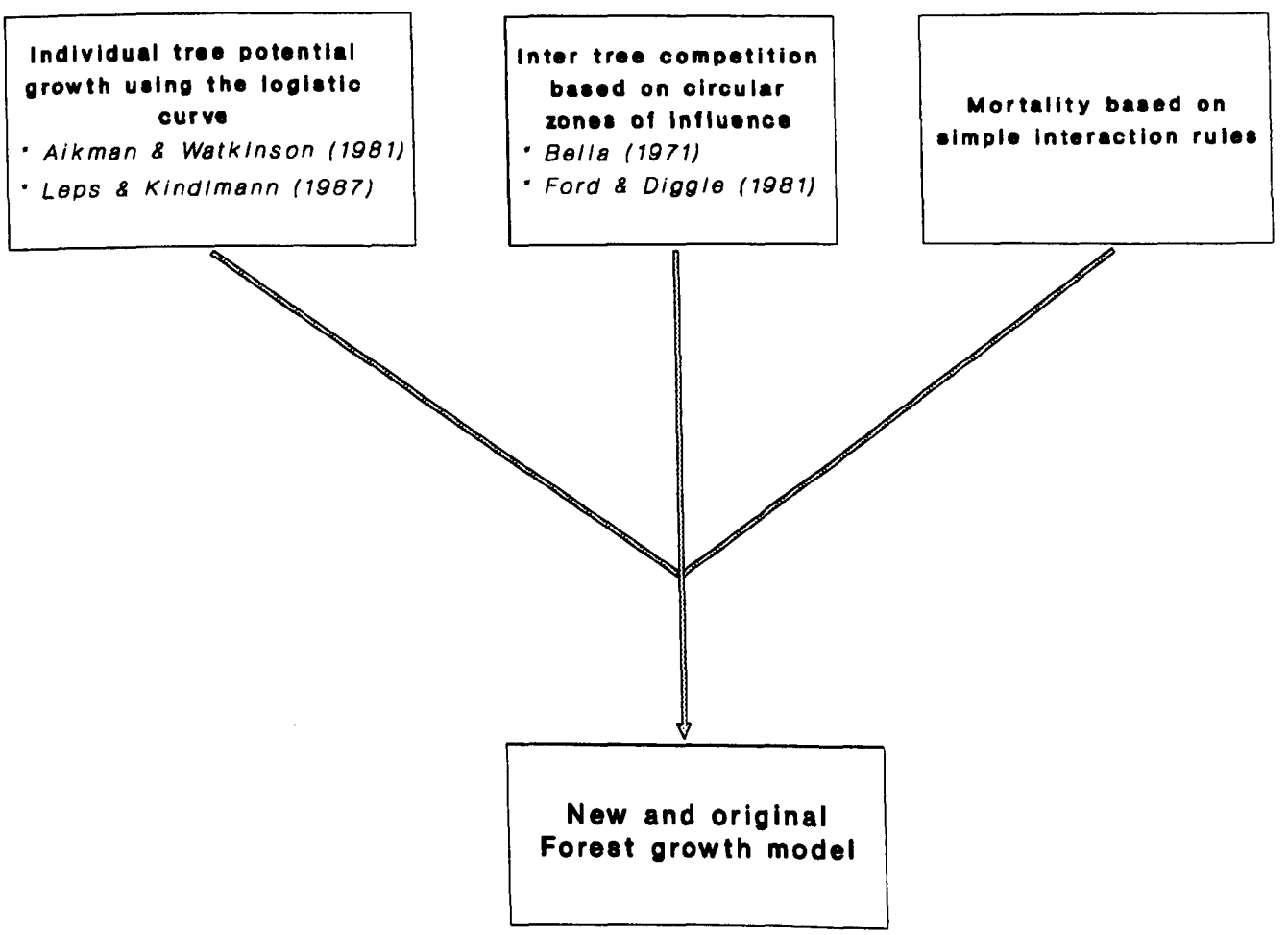

Figure 7.13: Components of current forest growth model

Having decided to alter the mortality section the decision then has to made as to what type of change can be made to the interaction rules governing plot mortality. There are two choices:

- Making new interaction rules, perhaps slackening the mortality criteria so that mortality is decreased
- Basing the mortality on other criteria altogether, such as known mortality rates.

The designing of new interaction rules to govern mortality presents no guarantied improvements over the current version of the forest growth model but has the distinct advantage that it would retain much the same structure as is already present. It would be possible to have different interaction rules for different tree species or sites but this would be difficult to validate using the yield table data alone.

Although a change in mortality criteria altogether means a change in model structure, if a criteria can be found that uses known values of mortality it may well improve the overall predictive ability. One possibility for a different mortality criteria is to use the plot density data (number of trees per *hectare*) from the Forestry Commission yield tables (see table 7.1) that has been utilised in the previous section. This would mean that a certain number of trees would be killed every year based on the plot density figure extracted from the yield tables for the species and conditions present. In adopting this the forest growth model would then be unable to be used in conditions outside the yield table range (e.g. outside Great Britain) but similar data may be available for these situations.

The second of the two options listed above was undertaken and the model structure has been changed so that the mortality criteria is now based on the yield table plot density data. It was decided to develop this form as it presented a relatively simple change to the model structure and hopefully it should improve the models predictive ability.

Once the decision had been made to kill a certain number of trees per year it then has to be decided which trees are to die and which will be allowed to continue living for another year. The selection criteria for this can be either random or based upon the ranking of all the trees according to some measured variable that has relevance to the likelihood of a tree dying.

A random choice of trees would make the model almost fully stochastic and therefore there would be little need for calculating the effect of inter tree competition. It has the advantage of making the mortality selection totally objective but the disadvantage of making the model totally non-process driven i.e. it is totally dependent on statistical relationships and loses any deterministic relationships between the trees. At present the forest growth model contains some stochastic elements (e.g. the assignment of growth ratio to each tree) but is broadly deterministic (e.g. the intertwining of tree growth with

calculated inter tree competition) which fits in with the deterministic status of *VSAS4.*

Using a mortality selection criteria based upon the ranking of some variable would maintain the deterministic status of the forest growth model. The two most obvious ranking selection criteria of this sort are tree size or the amount of competition each tree encounters from its neighbours (η in equation 5.6). Of these two η is the most obvious choice of ranking criteria as it assumed that this corresponds to the amount of stress an individual tree suffers from inter tree competition, and logically the more stress a tree is under the more likely it is to die. This reinforces the role of competition as an important process within the forest growth model structure whereas a ranking based on tree size places more emphasis on the stochastic assignment of growth ratio.

The decision was made to concentrate the ranking of trees ready for culling on the amount of stress each tree is under from the competition for light with neighbours (η in equation 5.6) at the end of each yearly timestep. At the same time some of the simple interaction rules need to be retained to stop the growth of trees in positions where they clearly could not survive.

7.3.3 New model structure

The flow diagram that describes the new growth routine for the forest growth model is shown in figure 7.14. This represents the model structure that is used for all future model testing.

The basic structure of the forest growth model is the same as before, as can be seen from a comparison with figure 5.6, except for some rearrangements of code. There are now two stages within the model where a tree can be killed: within the initial sweep through every tree and its competitors (see the second part of figure 7.14); and after the sorting of trees into ascending degree of competitive status (see the left hand side of the first part of figure 7.14).

As can be seen from the second part of figure 7.14 it has been necessary to maintain some of the original interaction laws so that trees cannot grow in locations that are not feasible e.g. a tree cannot grow directly underneath another tree crown. The change in interaction laws from the original version is twofold: the growth of the smaller tree is no longer stopped if the tree crowns overlap; and a competitor has to completely overlap another tree crown before the smaller tree is killed (previously it just had to overlap the centre of the tree crown). This means that the plot mortality may be higher than the input plot densities at timesteps (*years*) where these rules cull more trees than the input values. The new interaction laws effectively slacken the mortality criteria so that the main culling should occur from the new mortality routine.

The plot density information extracted from the Forestry Commission yield tables

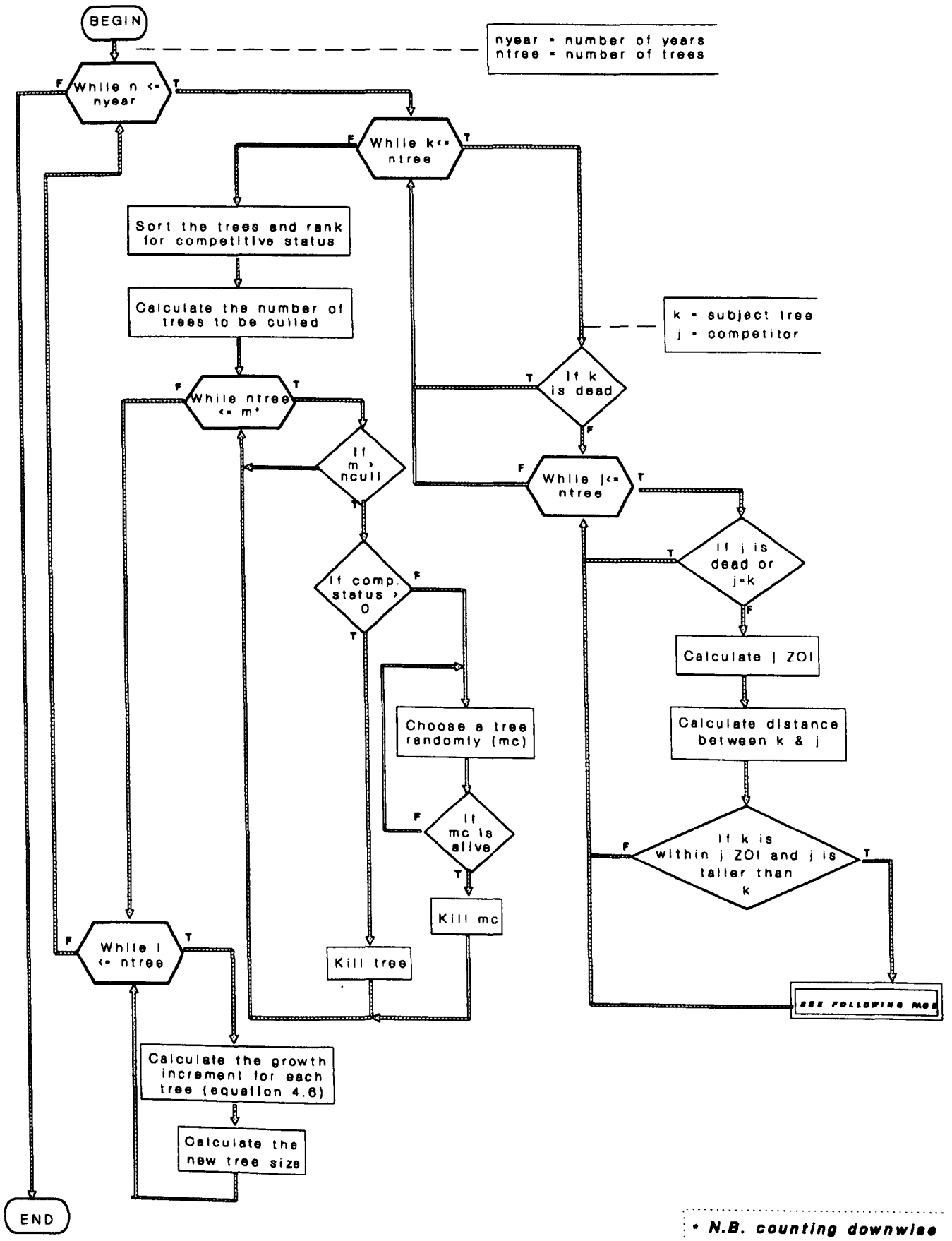

Figure 7.14a: Flow diagram of revised forest growth model (continued overleaf)

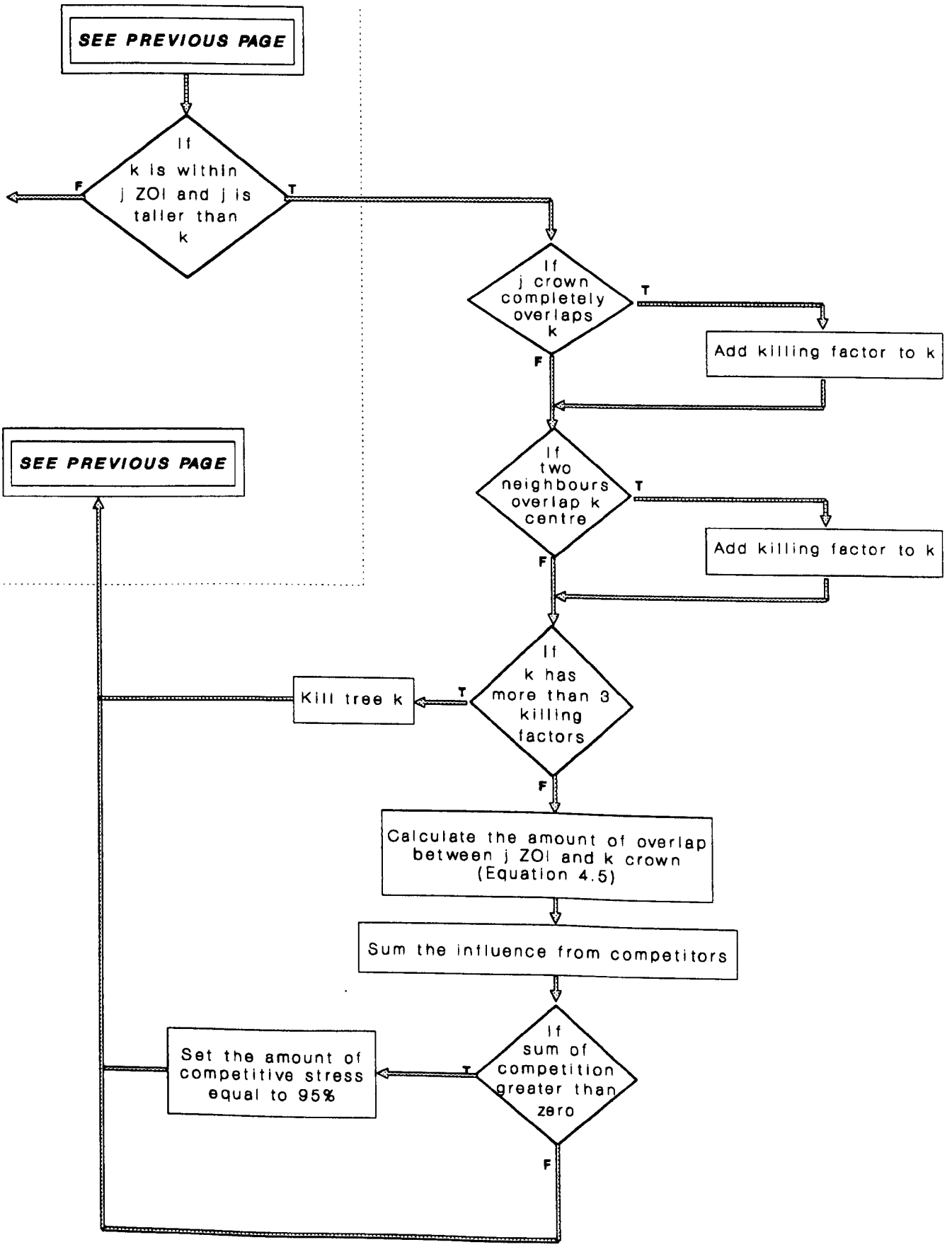

Figure 7.14b: Flow diagram of revised forest growth model (continued)

is read into the model as preliminary input and the number of trees that are needed to be culled in a single year calculated by extrapolation between the entered values and consideration of the area of forest simulated. The tree sorting is performed by a series of *NAG* routines called into the *FORTRAN-77* code; these rank the data according to the η values of each tree while retaining the original tree number for cross reference. Culling occurs for those trees of highest η until the simulated plot density equals the input density.

On the occasions where the input density data requires that some trees are culled but not enough trees suffer competitive stress (e.g. at the start of the simulation before the trees start to interact $\eta = 0$ for many trees) trees are selected randomly from all of the plot. This means that comparatively healthy trees may be killed at this stage; these are in effect random deaths that can be attributed to factors other than competition for light e.g. predation. The number of these random killings are likely to be small so that it can still be stated that the primary process causing mortality within this model is the competition for light.

The input parameters now required for a coniferous plantation plot simulation are listed in table 7.3. A comparison with table 5.2 reveals the three differences are the plot density inputs required for the new mortality routine. The different components of the new forest growth model are illustrated by figure 7.15, a revision of figure 7.13.

7.3.4 Initial testing of changed model structure

As a simple test of the new model structure a simulation was performed using exactly the same input criteria as were used in section 7.3.2 (see table 7.2 for the actual input values) where the old model version was tested against Forestry Commission yield table data. The results from this new simulation are presented in figures 7.16 and 7.17 where the new simulation is compared to the old simulation as well as the yield table data.

There is a marked improvement in the mortality prediction (figure 7.17) although it is still higher mortality (i.e. more tree killed) and occurring earlier in the simulation than the yield table data. The actual form of the mortality curve is very close to the yield table data, only the mortality is too high throughout.

The average *dbh* prediction (figure 7.16) for the new version of the forest growth model is similar to the original simulation prediction. This reflects the fact that the changes have been mainly concerned with mortality rather than growth.

As in the original model version testing (section 7.3.2) no calibration of the model has been attempted. It is possible that the model performance could be considerably improved by some form of calibration but it is pointless to undertake this without having

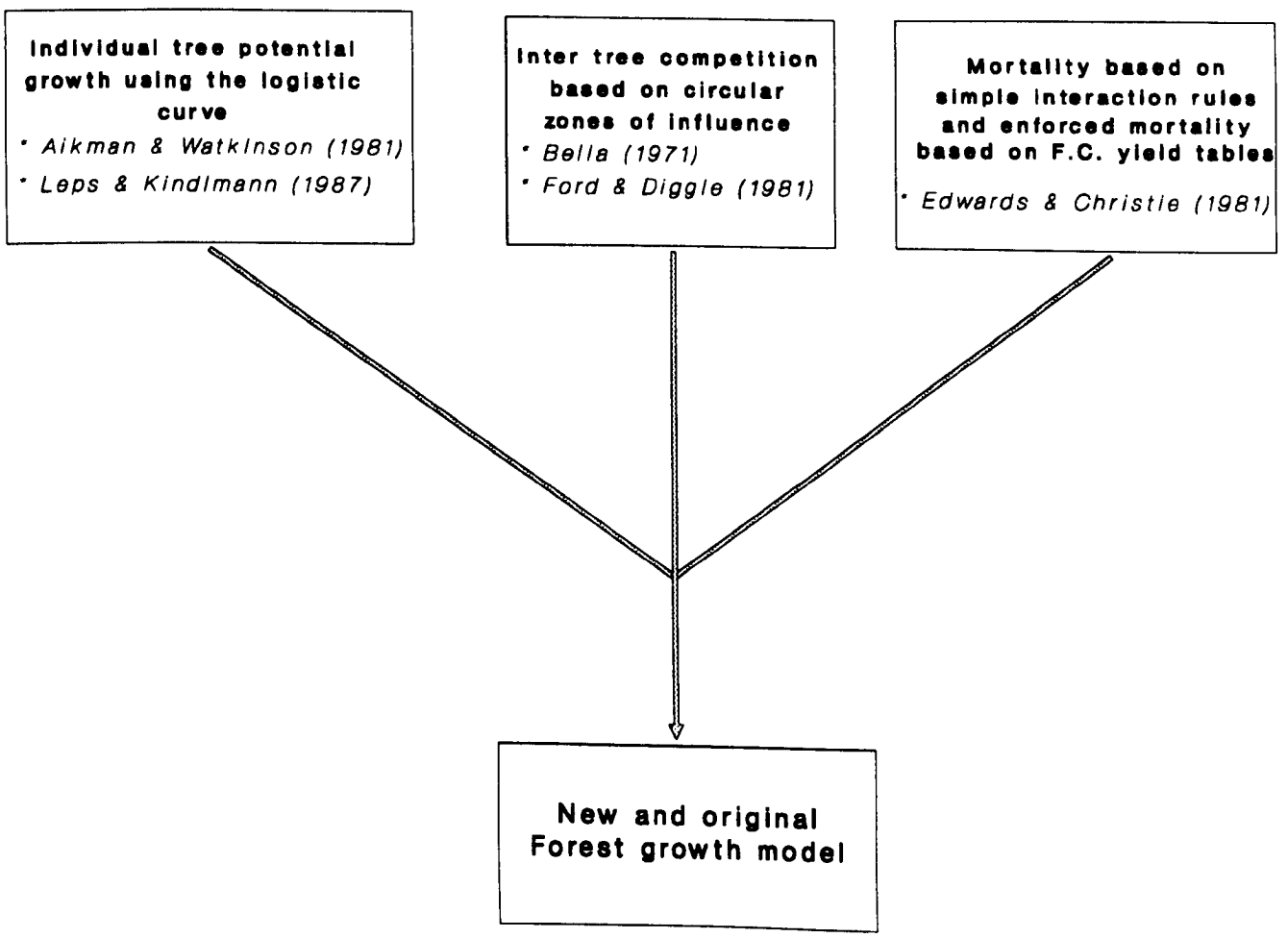

Figure 7.15: Components of revised forest growth model (figure 7.13 redrawn)

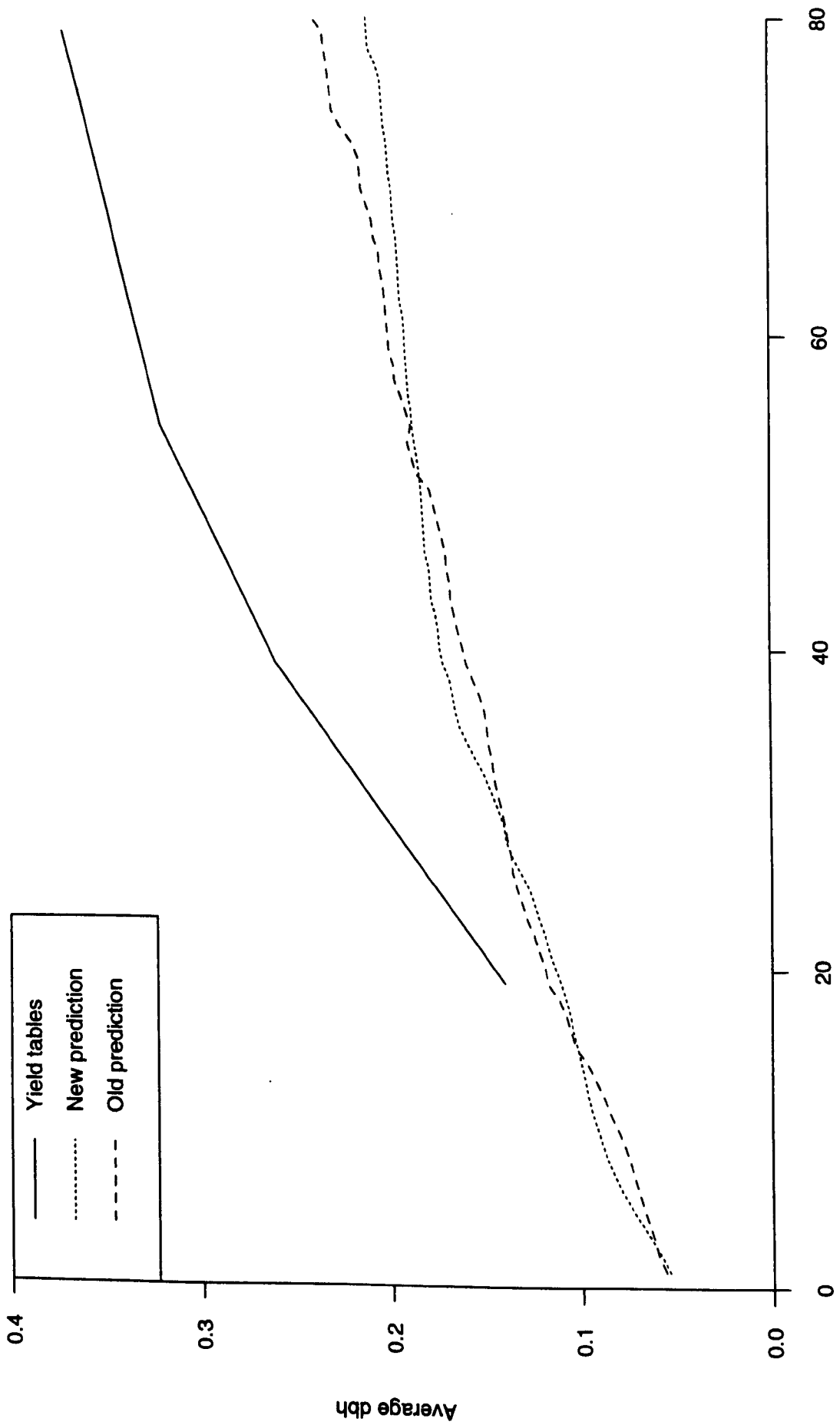

Figure 7.16: Comparison of new forest growth version prediction (average dbh), old version, and observed values (from yield tables)

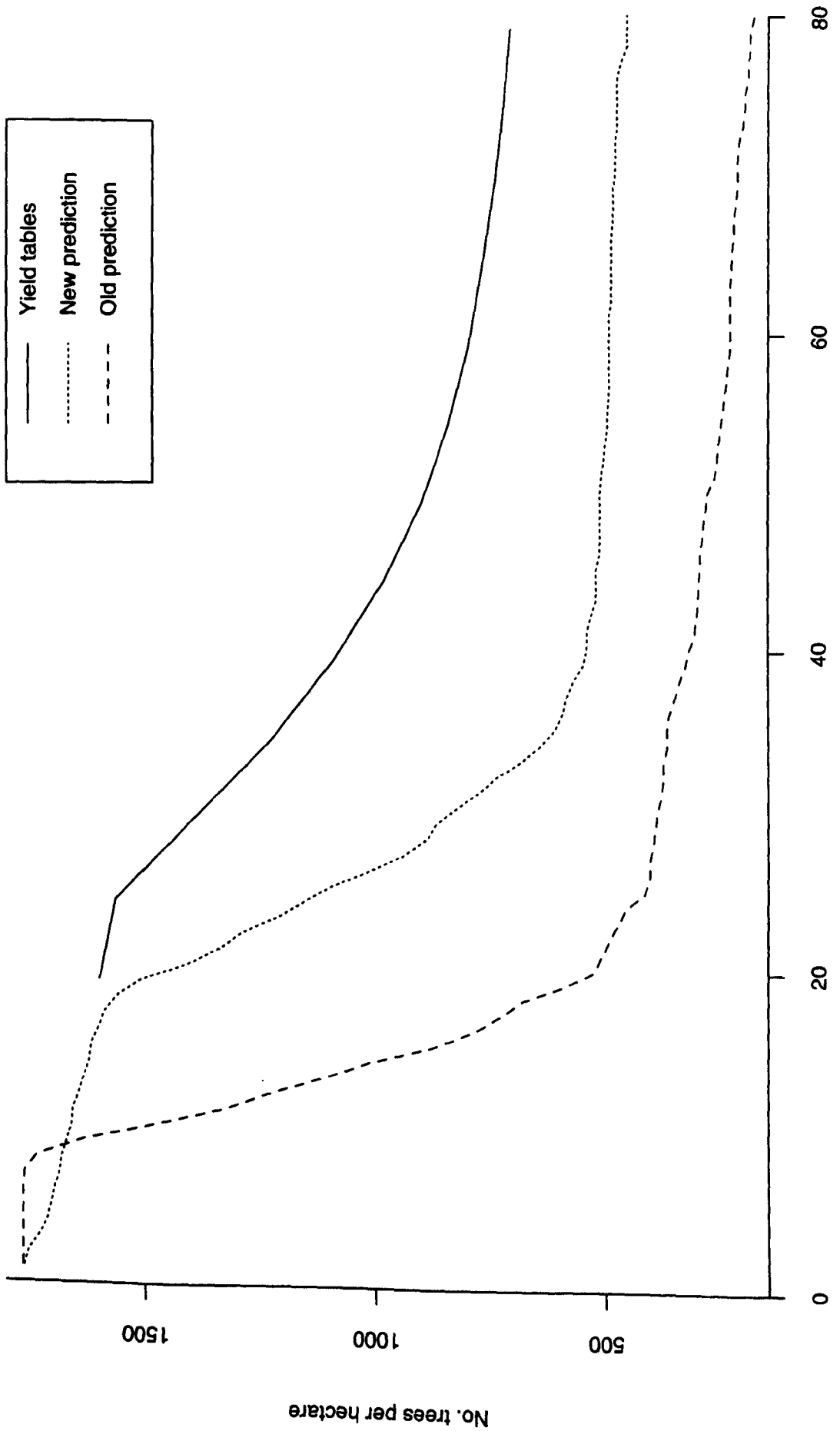

Figure 7.17: Comparison of new forest growth version prediction (plot density), old version, and observed values (from yield tables)

Length of side of plot to be simulated	(*m*)
Spacing between trees	(*m*)
Period of growth simulation	(*years*)
Initial *dbh*	(*m*)
Maximum *dbh*	(*m*)
Mean growth ratio (g in equations 5.1-5.6)	
Standard deviation of growth ratio	
Slope of *dbh* v height relationship	
Intercept of *dbh* v height relationship	(*m*)
Crown angle (see figure 5.3)	(*radians*)
Proportion of tree height to base of crown	
Proportion of crown area as ZOI	
Number of plot density measurements	
Year number of plot density measurements	(*years*)
Plot density for the corresponding age	(*treesha*$^{-1}$)

Table 7.3: Input parameters required for the new version of the forest growth model (for coniferous plot simulations)

performed a sensitivity analysis that gives an idea of the influence of different input parameters on model output. A sensitivity analysis of the model structure outlined in this section is described in section 7.3.5.

7.3.5 Sensitivity analysis

In section 6.1 the various types of verification testing for modelling schemes in general were discussed and the role of sensitivity analysis described with respect to *LUCAS*. The aims of a sensitivity analysis were listed as:

- To discover the relative importance of individual input parameters
- To give an indication of the degree of accuracy required for measurement of these parameters
- To discover the importance and role of different processes and/or parameters in the studied environment.

These three aims all hold as important for the proposed sensitivity analysis of the forest growth model. The final aim, to find the importance of different processes (e.g. inter tree competition and assigned growth ratios) and/or parameters within the model is not so

important for **processes** because the model is not claiming to be a physically based forest growth model. But in many respects this aim is the most important for discovering the role of **parameters** in controlling model output. With this kind of information the model can then be calibrated ready for usage in a validation exercise.

The aims of the sensitivity analysis described in the remainder of section 7.3.5 are the three listed above. With these as the aims there are three different types of final results that can be expected: a ranking of parameters for the first aim; a quantitative assessment from the second; and a qualitative assessment from the final aim.

7.3.5.1 Method

The sensitivity analysis was performed using the factor perturbation method† and the two types of output used in the previous testing of the model (i.e. plot density and average *dbh* of the tree trunks in the simulated plot) analysed for sensitivity. The use of plot density as output for analysis is complicated by the fact that it is now a model input for mortality (see section 7.3.3) but as this is not the only criteria for trees to be killed (some simple tree interaction rules also control mortality) it is justified.

The plot density and average growth curves for the variation in each parameter are analysed separately; these results are contained in section 7.3.4.3. In order to compare the sensitivity of the model to different parameters it is necessary to have an independent measure of sensitivity. McCuen (1976) suggests that in the use of a factor perturbation sensitivity analysis method the sensitivity can be judged by the relationship in equation 7.4.

$$S = \frac{\Delta F_o}{\Delta F_i} \tag{7.4}$$

S = Sensitivity factor
F_o = Model output
F_i = Input parameter

A difficulty arises in using equation 7.4 to compare the sensitivity of the model to separate parameters because the units of the input parameters may not, and in the forest growth model are not, the same. Consequently the denominator of equation 7.4 would vary and the S values would not be comparable for the separate input parameters. To overcome this problem equation 7.4 has been rewritten so that the percentage change in model input and output are used instead of absolute values. This is expressed in equations 7.5 and 7.6.

† See section 6.1 for a discussion on the relative merits of factor perturbation and stochastic sensitivity analysis methods.

$$S = \frac{\%\Delta F_o}{\%\Delta F_i} \tag{7.5}$$

where:

$$\%\Delta F = \frac{F_{max} - F_{min}}{F_{min}} \tag{7.6}$$

The S value in equation 7.5 is then able to be used in a comparison in sensitivity of the model to the different parameters.

Of the fifteen input parameters for a coniferous forest simulation shown in table 7.3 there are several that could be varied to find their effects on model outputs. Of particular interest for the sensitivity analysis are the input parameters that are unable to be easily measured or obtained from relevant literature sources because they can be manipulated during a calibration, as their real value is unlikely to be known. The first five parameters in the following list fit this category; the remaining three should be easily obtained from measurements or literature sources.

- Mean growth ratio
- Standard deviation of the mean growth ratio
- Crown angle
- The proportion of tree crown as the ZOI
- Proportion of tree height to the base of the tree crown
- Minimum *dbh*
- Maximum *dbh*
- Tree spacing.

It is not necessary to carry out a sensitivity analysis using all of these input parameters as several of them have overlapping roles. In particular the initial *dbh*, maximum *dbh*, and average growth ratio overlap as they all define the shape of the potential growth curve that each tree is grown along before the effect of inter tree competition. Of these three, the average growth ratio was chosen as the parameter to vary the shape of the potential growth curve in the sensitivity analysis.

Whereas the mean growth ratio affects the shape of the potential growth curve the standard deviation of this affects the distribution of the growth ratio allocated to individual trees. A high standard deviation means a large spread in potential growth curves and vice versa for a small input standard deviation. Because of the large difference in role between these two statistics they were both included in the sensitivity analysis.

Two input parameters that were considered for variation but not included were the slope and intercept of the tree height versus *dbh* relationship. It was decided that this was

not necessary for two reasons: the crown angle relates the height to the crown area so that an increase in crown angle effectively is the same as an increase in tree height; and it cuts the number of parameters varied down to a manageable size (six).

The six input parameters used as input parameters to be varied in the sensitivity analysis are: mean growth rate; standard deviation; crown angle; ZOI; height to base of crown; and tree spacing. These parameters can be roughly split into two categories: those that influence the assigned potential growth curves (mean growth rate and standard deviation); and those that influence the amount of competition (crown angle, ZOI, height to base of crown, and tree spacing). The values for all the input parameters during the runs when another parameter was being varied are given in table 7.4.

During the sensitivity analysis the random number generator within the forest growth model was switched to a repeatable mode. This means that the same growth ratio was assigned to trees between simulations i.e. each tree had a random growth ratio drawn from a normal distribution within a simulation and these values were retained between simulations. This means that the stochastic element of the growth model is operating but is not affecting the comparison between simulations which is the fundamental basis of a sensitivity analysis.

7.3.5.2 Results

Mean growth ratio

Within the forest growth model structure the mean growth ratio determines the shape of the potential growth curve (the curve that an individual trees growth would follow without any inter tree competition) each tree is assigned at the start of the simulation (see section 5.2). The higher the value of growth ratio the steeper the logistic growth curve and therefore potentially it takes less time for a tree to reach its maximum size (this may be altered by the effects of inter tree competition).

For the sensitivity analysis the average growth ratio was varied nine times between 0.05 and 0.175. The nine values varied are the equivalent of a tree potentially reaching within 99% of its maximum size at the following times: 139 (0.05); 116 (0.06); 100; 87; 78; 70; 56; 47; and 40 *years*. This range covers the span of growth for a normal coniferous tree in Great Britain.

The standard deviation of the mean growth ratio was not kept at 0.022 for all the simulation as suggested by table 7.4 but at 25% of the mean value (i.e. 0.022 when the mean is 0.09, 0.044 when the mean is 0.175 etc.). This is so the normal distribution that the growth ratio for each tree is drawn from remains of similar shape between simulations.

Figure 7.18 shows the effect that altering the mean growth ratio has on the average

Length of plot side	100*m*
Tree spacing*	3.0*m*
Initial *dbh*	0.05*m*
Maximum *dbh*	0.60*m*
Growth period	100 *yrs*
Mean growth ratio*	0.09
Standard deviation of growth ratio*	0.022
Slope of height v *dbh* relationship	81.40
Intercept of height v *dbh* relationship	0.00
Crown angle*	11°
Proportion of tree height to base of crown*	5%
Proportion of tree crown as zone of influence (ZOI)*	1.5
Number of plot density measurements	13

Year	1	22	27	32	37	42	47	52	57	62	67	72	77
Density	1139	1066	1031	956	875	800	737	689	653	626	605	588	573

Table 7.4: Input data used in forest growth model sensitivity analysis * parameters varied

dbh of the simulated plots. As might be expected the higher growth ratio values give larger average tree sizes. There is a difference in shape of the average growth curve with growth ratio: the very low value simulations have an almost straight line growth whereas the higher values have a sharp initial growth period that flattens off at an increasingly early time. This change in slope gives some indication of when the effects of inter tree competition start to heavily influence the individual trees growth.

The mean growth ratio patterns described above occur throughout the simulated period except for a brief period where the 0.125 line has a higher growth than the 0.15 case. In this cases the difference in average size is not very large and the death of some larger trees in the higher growth ratio plot may cause the smaller growth ratio simulation to have a slightly higher average *dbh* value for several years.

The difference in average *dbh* between the highest and lowest average growth ratio at the end of the simulation (time equal to 100 *years*) is 0.13*m* which represents a 46% increase with a 250% increase in the mean growth ratio value.

The effect on mortality (figure 7.19) of changing the mean growth ratio is similar to the average growth: a high average growth ratio value means a high mortality (i.e. more trees die therefore less trees per *hectare*). In fact the final number of trees per hectare is not a lot different between the highest and lowest values (28 trees ≈ 10% of smallest value), the major difference is in the timing of the mortality which is reflected in the shape

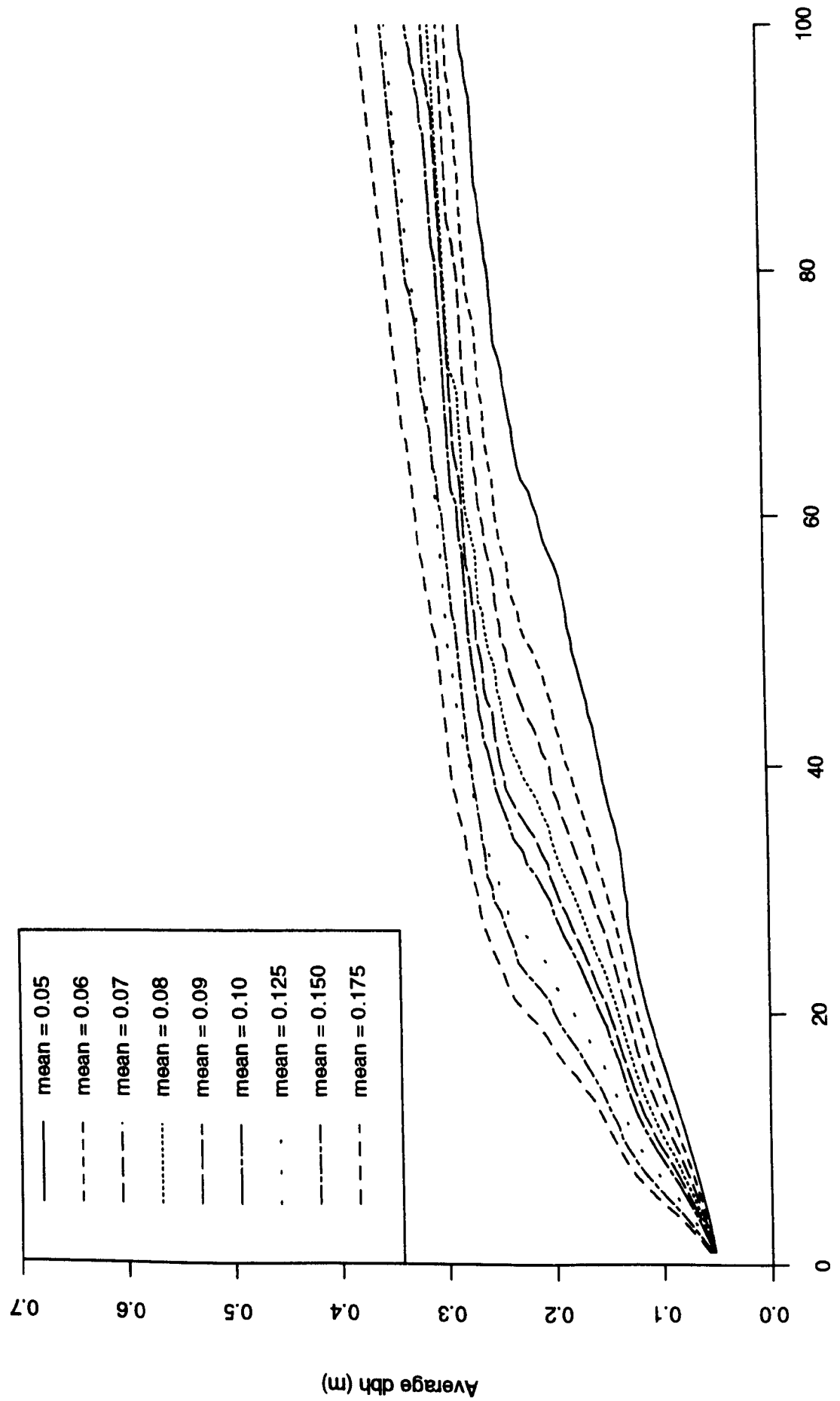

Figure 7.18: Sensitivity of average dbh to changes in mean growth ratio

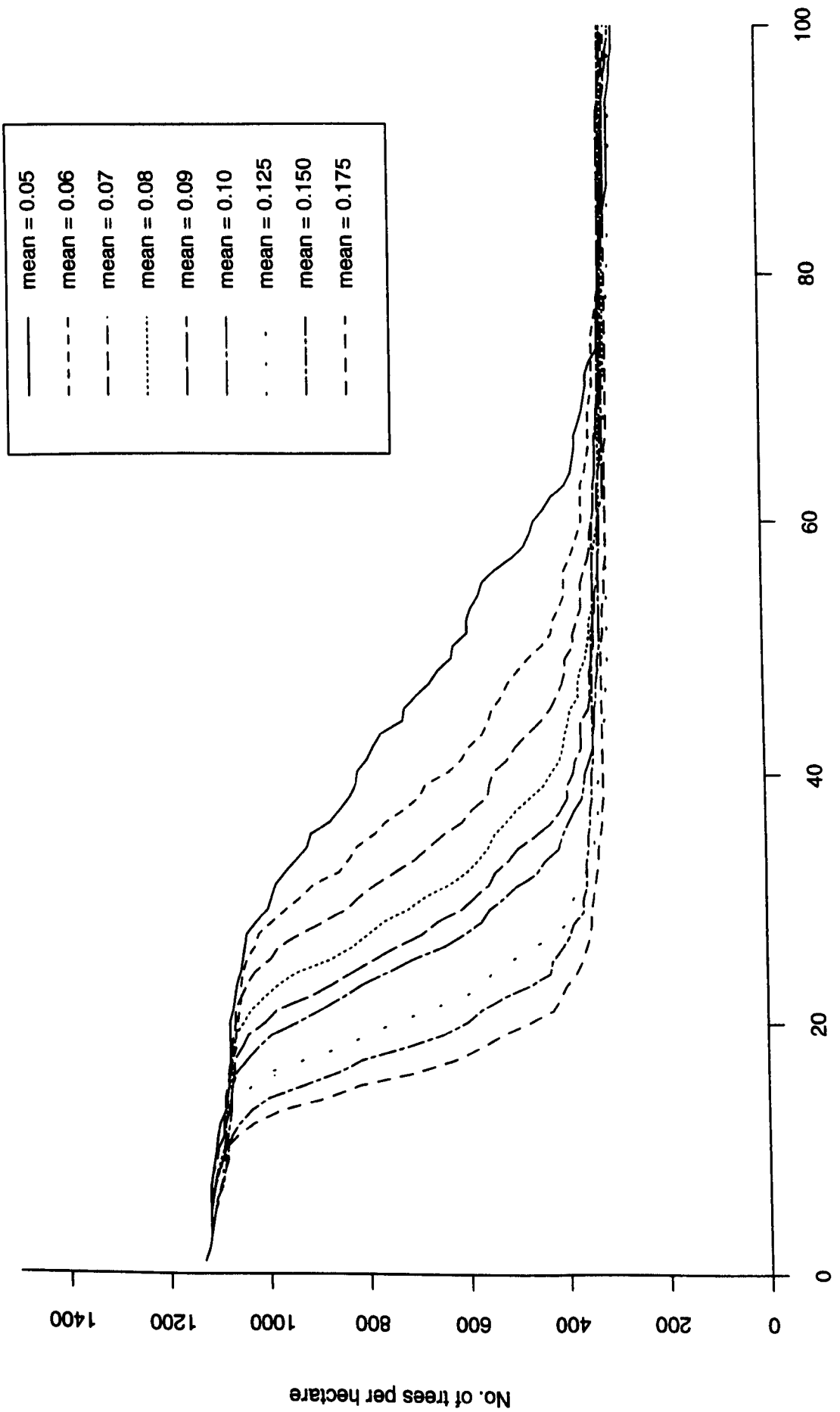

Figure 7.19: Sensitivity of plot density to changes in mean growth ratio

of the mortality curve.

For a the highest mean growth ratio (0.175) there is a very steep drop in the number of trees per *hectare* occurring at around 10-15 *years* into the simulation that has flattened off to very close to the minimum by the thirtieth year. This is reminiscent of the mortality curve produced by the original forest growth model in figure 7.12. In the lowest mean growth ratio (0.05) the mortality curve is much more gradual throughout, the steepest gradient occurs between 30 and 70 *years* and it never approaches the mortality rate of the 0.175 value curve. The remainder of the mortality curves are spread at fairly even intervals between these two extremes.

The greater mortality and mortality rate of the higher mean growth ratio value simulations is a result of greater competitive interaction between trees as they reach a larger size at an earlier stage. This means that they have mortality occurring from the interaction rules to a large extent whereas the lower value simulations derive their mortality more from the input density values.

An increase in the mean growth ratio generally causes a higher growth rate but at the expense of greater mortality. Any use of growth ratio in a calibration exercise would have to take the combined effect into account.

Standard deviation of the mean growth ratio

Whereas the mean growth ratio controls the shape of the potential growth curve the standard deviation of the mean growth ratio controls the shape of the distribution curve that the growth ratio for each individual tree is randomly drawn from. In short a larger standard deviation will give a larger range of individual growth ratios, the actual size is dependent on the size of the mean value. A large range in assigned growth ratio values within a simulated plot means there is likely to be a large range in tree sizes at the end of a simulation and vice versa for a small standard deviation.

The standard deviation was varied from a minimum of zero to a maximum equal to the mean growth ratio value (0.09) in ten increments of 0.01 each.

A standard deviation of zero means that all the trees would be assigned an initial growth ratio of 0.09 and any increase widens the range of values assigned. N.B. the model structure makes it impossible for a growth rate of less than zero or greater than one to be assigned (see section 5.2.2). By assigning every tree the same growth ratio the trees all grow at the same rate, this means they are all always exactly the same height and therefore the competition between trees is never calculated (competition is one sided and is only computed when one tree is larger than another, see figure 7.14). This means the growth curve for a standard deviation of zero is in fact the unaltered logistic curve and the mortality curve is that derived from the input plot densities. After this was detected by the sensitivity analysis the model structure was changed so that a standard deviation of zero is never allowed. The results for a standard deviation of zero are included in the figures of

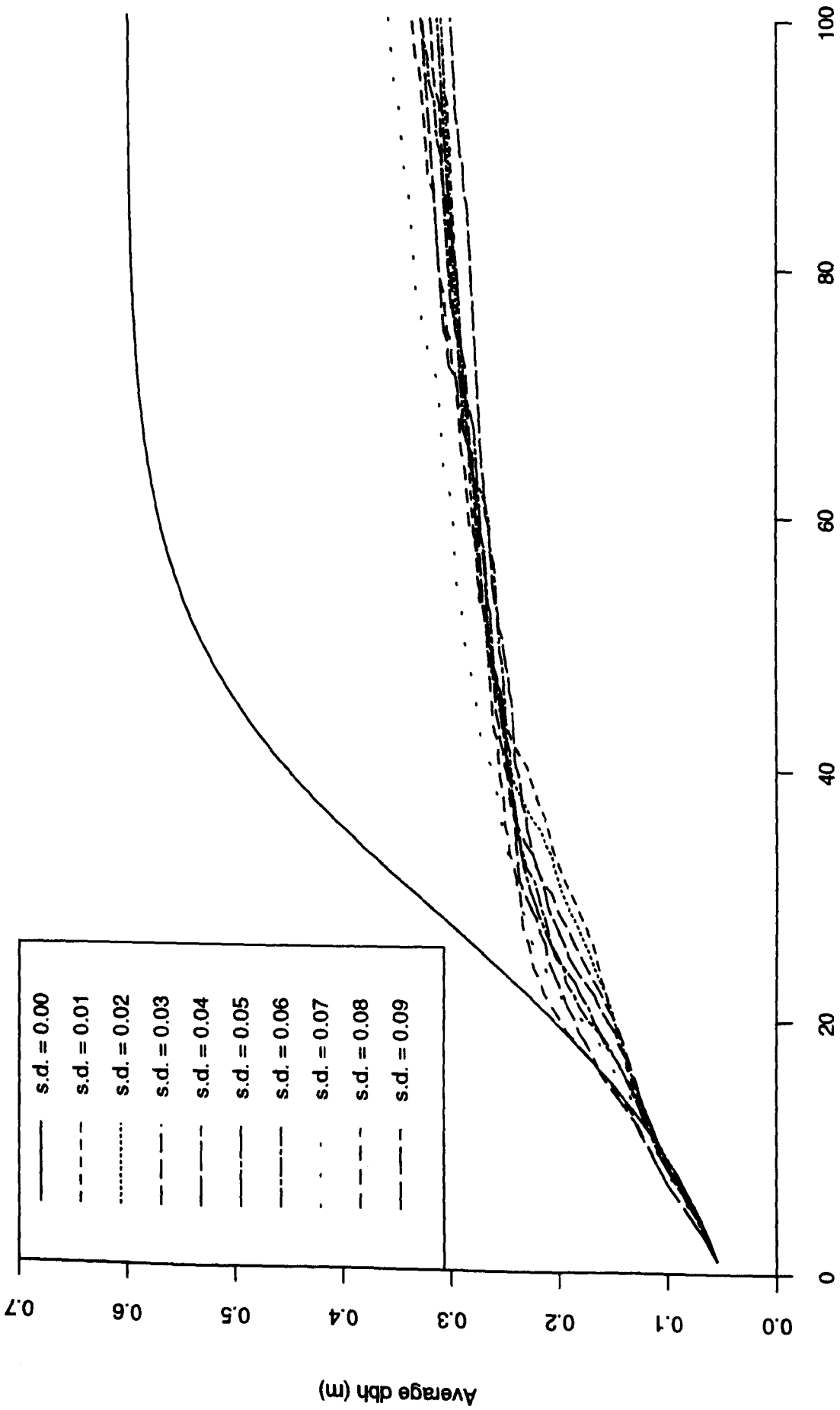

Figure 7.20: Sensitivity of average dbh to changes in standard deviation of the mean growth ratio

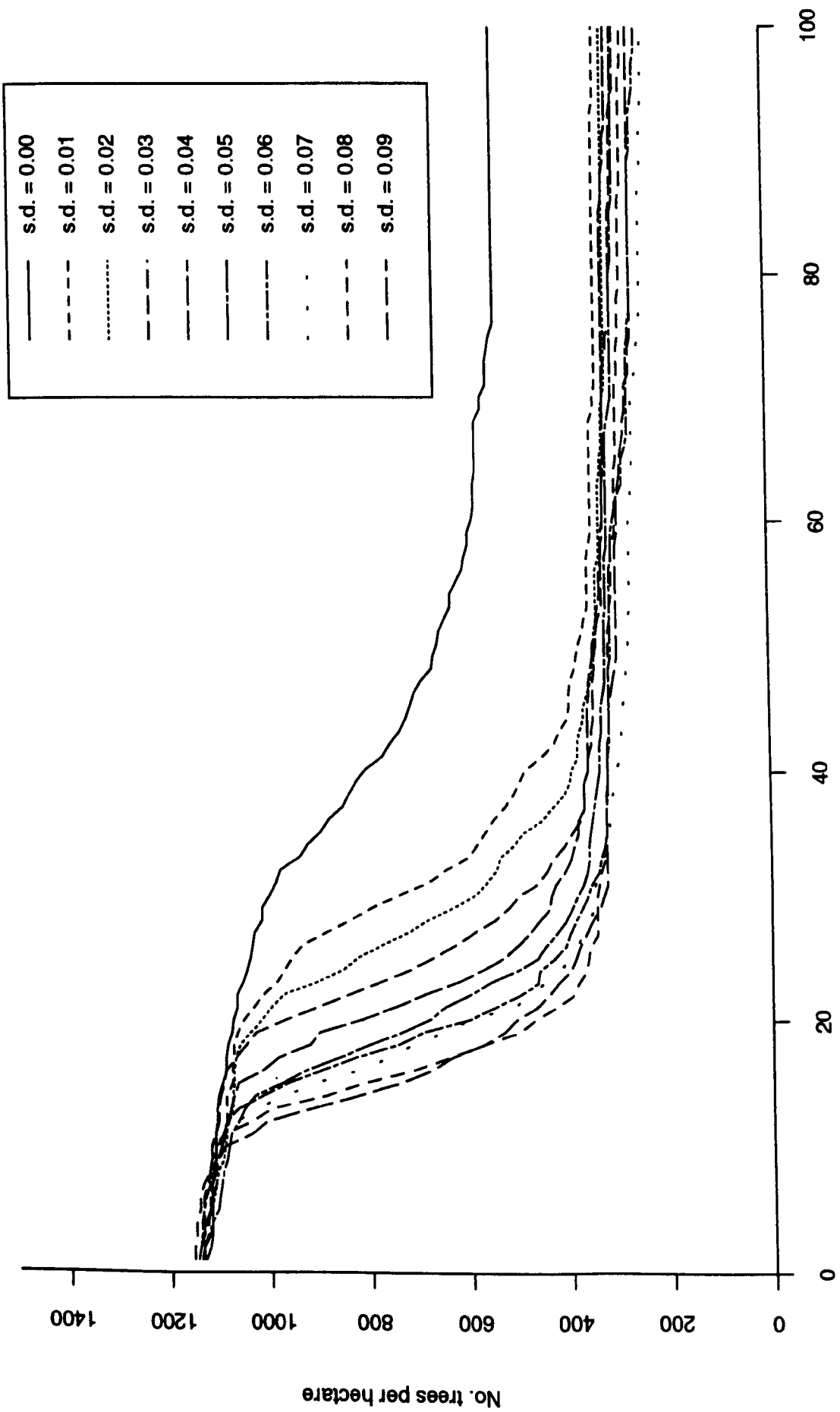

Figure 7.21: Sensitivity of plot density to changes in standard deviation of the mean growth ratio

average growth (figure 7.20) and plot density (figure 7.21) but are an exceptional case and not discussed in the following text.

The complicated effect that varying the standard deviation has on the average growth curve can be seen in figure 7.20. The main difference between standard deviation values occurs in the first 40 *years*, after this the average growth curves converge so that difference between the highest and lowest final *dbh* is only 19% of the lower value. During the first 40 *years* the average growth curves spread out to a pattern of the highest standard deviation having the least growth and vice versa. As competition effects start to dominate the growth the curves come together again and it is very difficult to separate one from another. The highest and lowest final *dbh* values are for standard deviations of 0.07 and 0.04 respectively. The fact that these are not the highest and lowest parameter values suggests that there is some complex interactions with inter tree competition occurring that make it difficult to predict the effect on average growth of changing the standard deviation values.

The effect on plot density of varying standard deviation is more clear-cut (figure 7.21). A smaller value gives a more gradual mortality and in general higher final plot density values and vice versa for a large standard deviation. The difference in mortality rates is greatest between 15 to 50 *years* with the highest final plot density value (0.01) representing a 41% change from the smaller value (0.07).

Where there is a large range in growth ratio values (high standard deviation) there will be a large range in tree sizes after an initial period of tree growth unaffected by inter tree competition. When the competition begins to effect growth the larger trees have an innate advantage in shading (this is reflected in the model structure by the one sided nature of competition) and therefore the mortality rates are likely to be high as the smaller trees die off under the competitive stress. This means for a large standard deviation value the main source of mortality is from the interaction laws rather than the input plot densities, hence the steeper mortality curves.

When the range in growth ratio values is small (small standard deviation) the tree sizes are likely to be quite uniform at the time of inter tree competition effects starting to be felt. This means that all the trees will be affected to a similar degree by competition and single trees are less likely to totally overshadow others, therefore the mortality is likely to occur more from the input plot densities than the tree interaction rules. A comparison between the standard deviation equals zero (mortality entirely as a result of the input plot density values) and 0.01 indicates that there is still considerable mortality occurring from the interaction rules in the 0.01 case although it is a lot less than for the larger standard deviation values.

The effects of changing the standard deviation on the mean growth ratio is definite for plot density (large value, high mortality) but difficult to predict for average growth.

The actual range of average growth curves is not large and a manipulation of standard deviation is likely to have an effect on the mortality rate but not necessarily final plot density.

Crown angle

The crown angle is the angle which, combined with the tree height, defines the width of the half conical shape that is assumed to represent a coniferous tree (see figure 5.3). It is important to the model structure because the size of the tree crown defines the size of the zone of influence surrounding each tree which has a large bearing on the amount of competitive stress one tree can apply to another. Although it is the sort of parameter that would be relatively easy to measure an average value for, it is not generally available from literature sources as not many studies require it. Consequently it is possible to vary it in a range during any calibration as a measured value may not be readily available.

The crown angle was varied ten times between 2° and 20° with an interval of 2°. N.B. the crown angle is actually entered into the model in *radians* but the sensitivity analysis uses *degrees* as these are more commonly understood.

The effect of varying the crown angle on the average *dbh* values (figure 7.22) is extremely large. The lower the crown angle the larger the average *dbh* values at all times except for when the crown angle exceeds 16°. The final *dbh* value has a 106% increase in size between the highest (2°) and lowest (16°) crown angle simulations.

The large difference in average growth curves is most marked between the 2° and 8° crown angles. The average growth curve for the 2° simulation is very close to the potential logistic growth curve (as in figure 7.20 where the standard deviation of the mean growth ratio equals zero) which suggests that there is hardly any competition influencing tree growth. Once the angle has exceeded 8° there is not a great deal of difference in average growth curves and the three largest crown angle simulations (16°, 18° and 20°) end up with reversed final average *dbh* values. This is a result of there being less trees still surviving at the latter stages of the higher crown angle simulation and these being the larger trees.

The plot density curves (figure 7.23) for the change in crown angle are as equally well spread as the average growth curves described above. The difference in plot density is visible throughout the whole simulation, with a higher crown angle producing a higher mortality rate as soon as competition effects start to affect tree growth (approximately 15 *years* for the 20° simulation). The difference between the highest (2°) and lowest (20°) final plot density figures is a 422% increase from the lowest.

The three lowest crown angle simulations have similar plot density results, each follows very close to the input plot density values as there is little competitive interaction between trees. This is because the crown radii of the trees are so small that each ZOI (1.5

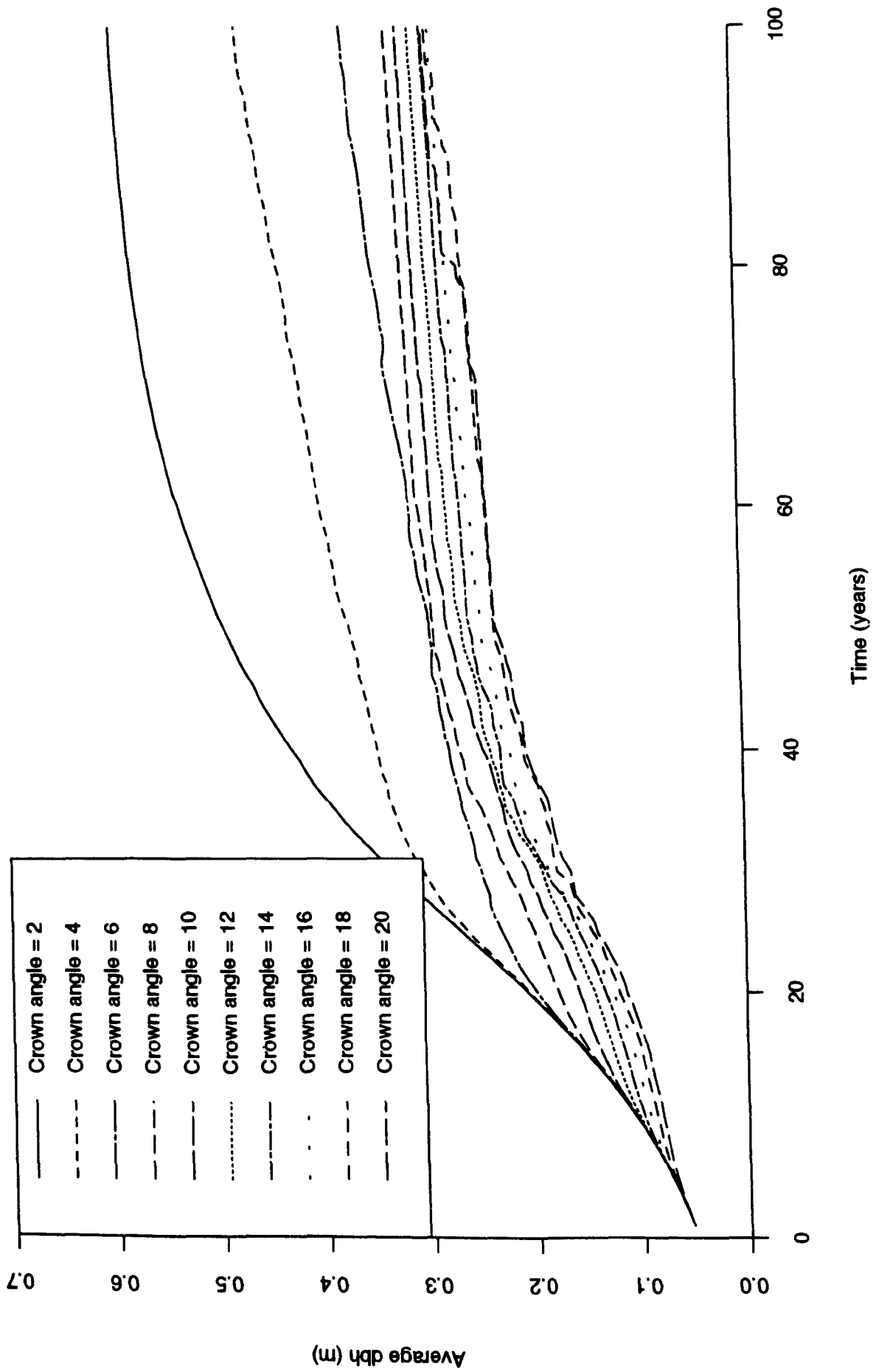

Figure 7.22: Sensitivity of average dbh to changes in crown angle

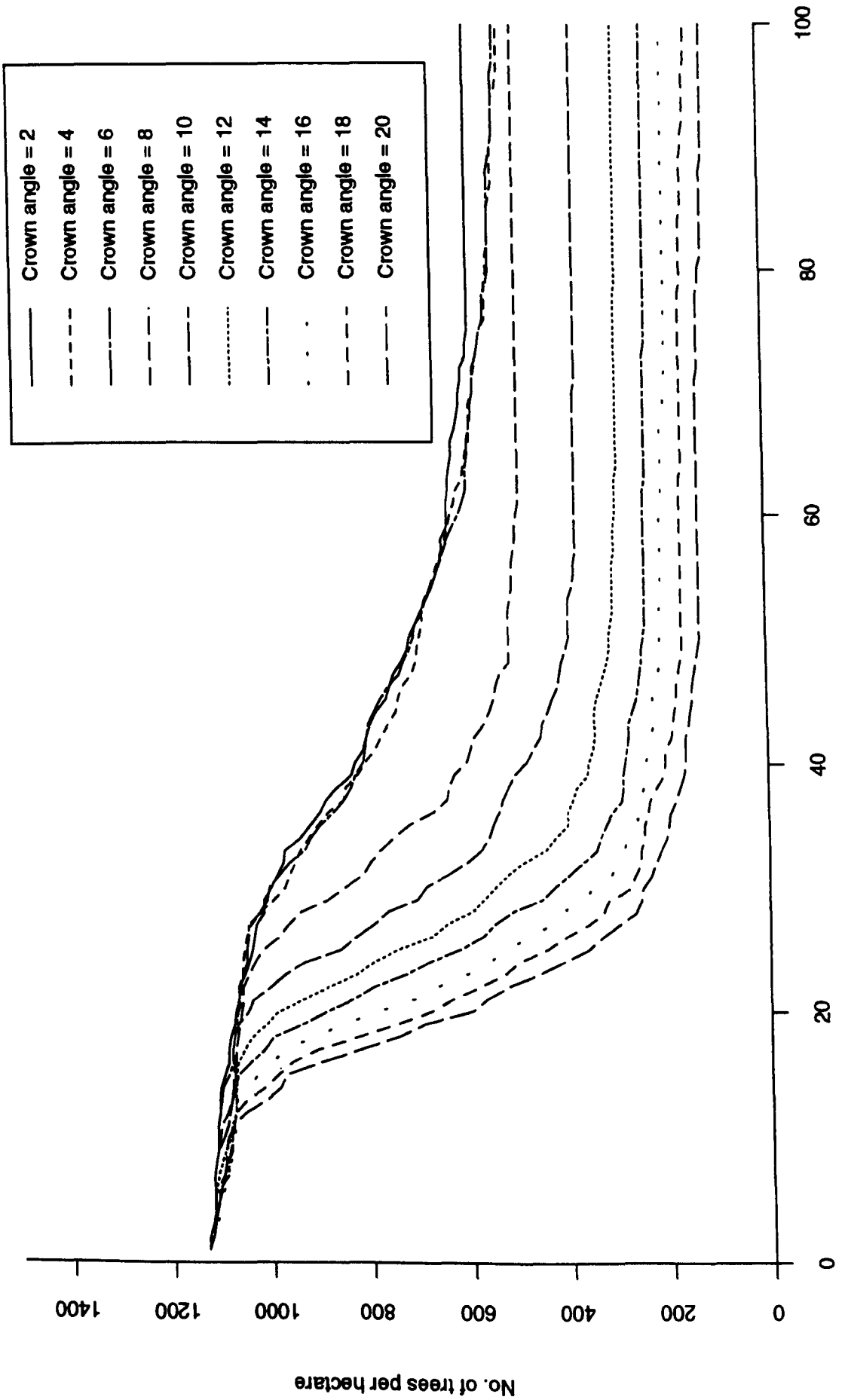

Figure 7.23: Sensitivity of plot density to changes in crown angle

times the crown radius) does not intersect the other.

In general the crown angle has a very large effect on both average *dbh* and plot density. A low crown angle produces very high average *dbh* figures and high plot density. The effect is particularly noticeable on average *dbh* when the values fall below 8° and on plot density when the values are greater than 8°.

Zone of influence

The ZOI is the circular area surrounding a tree that is assumed to represent the zone in which each tree competes for resources. For coniferous trees this is calculated as a certain proportion of the crown radius, the actual value being an input parameter. Because the ZOI is dependent on the crown radius of a tree and this in turn is dependent on the crown angle, a variation in ZOI does have a similar influence as a change in crown angle. The ZOI is included in the sensitivity analysis despite this repetition because it is an input parameter that cannot be adequately measured and therefore represents a possible parameter to vary in a calibration of the forest growth model. It is important in this case to establish the extent of change produced by small variation in the proportion of crown radius making the ZOI.

The ZOI has been allowed to vary eleven times in a range from 1.0 to 2.0 with an increment of 0.1. A value of 1.0 means the ZOI of a tree is exactly equal to the crown radius, a value of 2.0 means the ZOI is twice the size of the tree crown radius. The values have not been taken below 1.0 because this would mean having a zone of influence less than the crown radius of a tree which is conceptually difficult to imagine. It is also impossible within the model structure as a tree could be physically overlapping causing mortality without actually interfering with the growth of the smaller tree.

The average *dbh* results from varying the ZOI proportion can be seen in figure 7.24. There is a very even spread of growth curves with the larger ZOI values producing lower growth rates for almost all of the simulation. The highest average *dbh* value at the end of the simulations (1.0) is 118% greater than the lowest value (2.0). Although this does not appear as great a range as for the crown angle variations (figure 7.22) the ZOI results from a 100% change in initial parameter as opposed to a 900% change in crown angle value.

The effect of changing the proportion of crown radius representing ZOI on the plot density (figure 7.25) is different from the other mortality curves presented so far. The mortality stays similar for all ZOI for approximately 25 *years* before they start to diverge ending with the highest value (2.0) being 104% of the lowest value (1.0). The real difference between the curves occurs in the second stage of mortality when the higher ZOI values seem to carry on killing trees while the lower values tail off.

A notable point about figure 7.25 is that it differs markedly from figure 7.23 (plot densities for changes in crown angle), in that a large ZOI produces high densities whereas

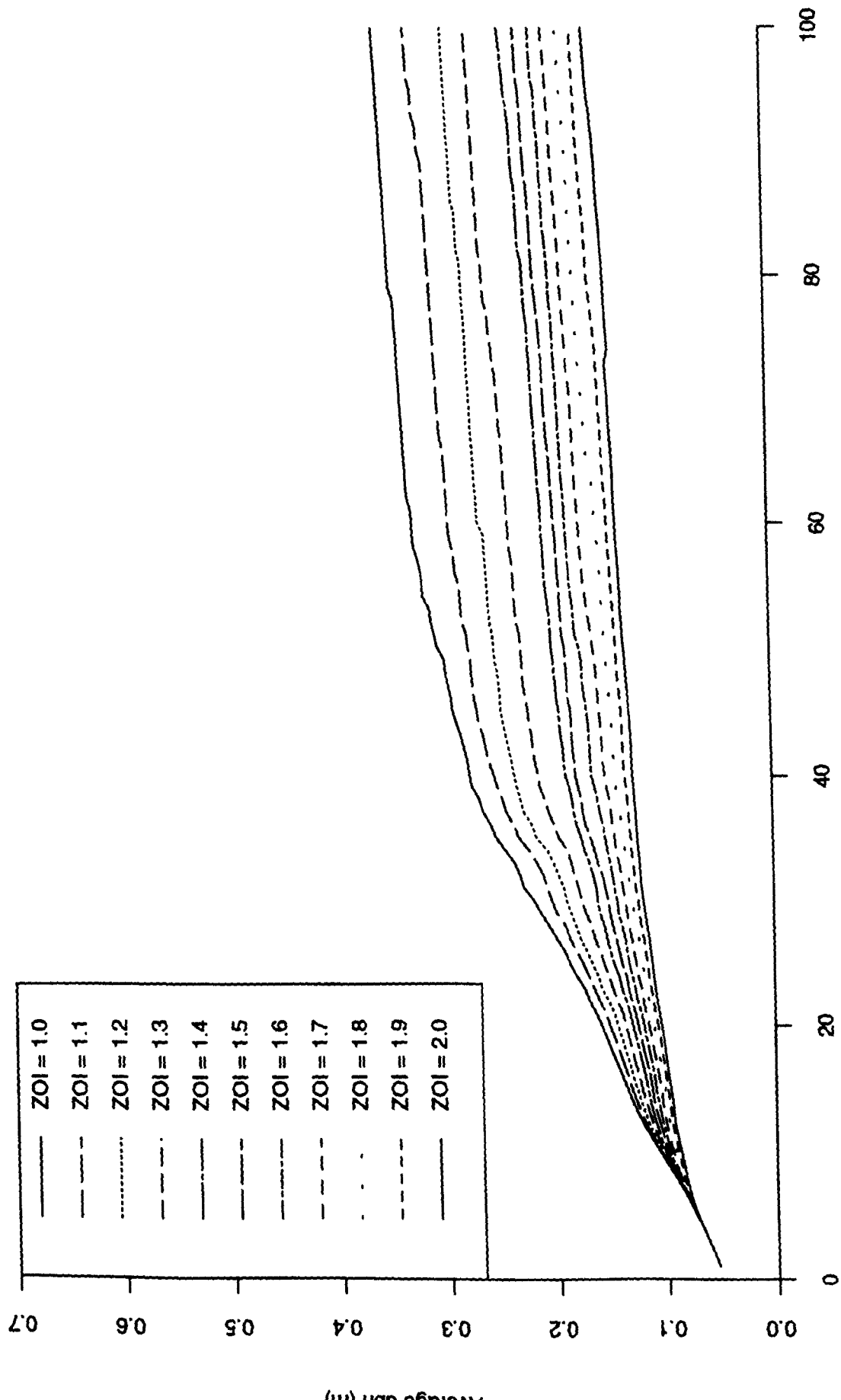

Figure 7.24: Sensitivity of average dbh to changes in zone of influence

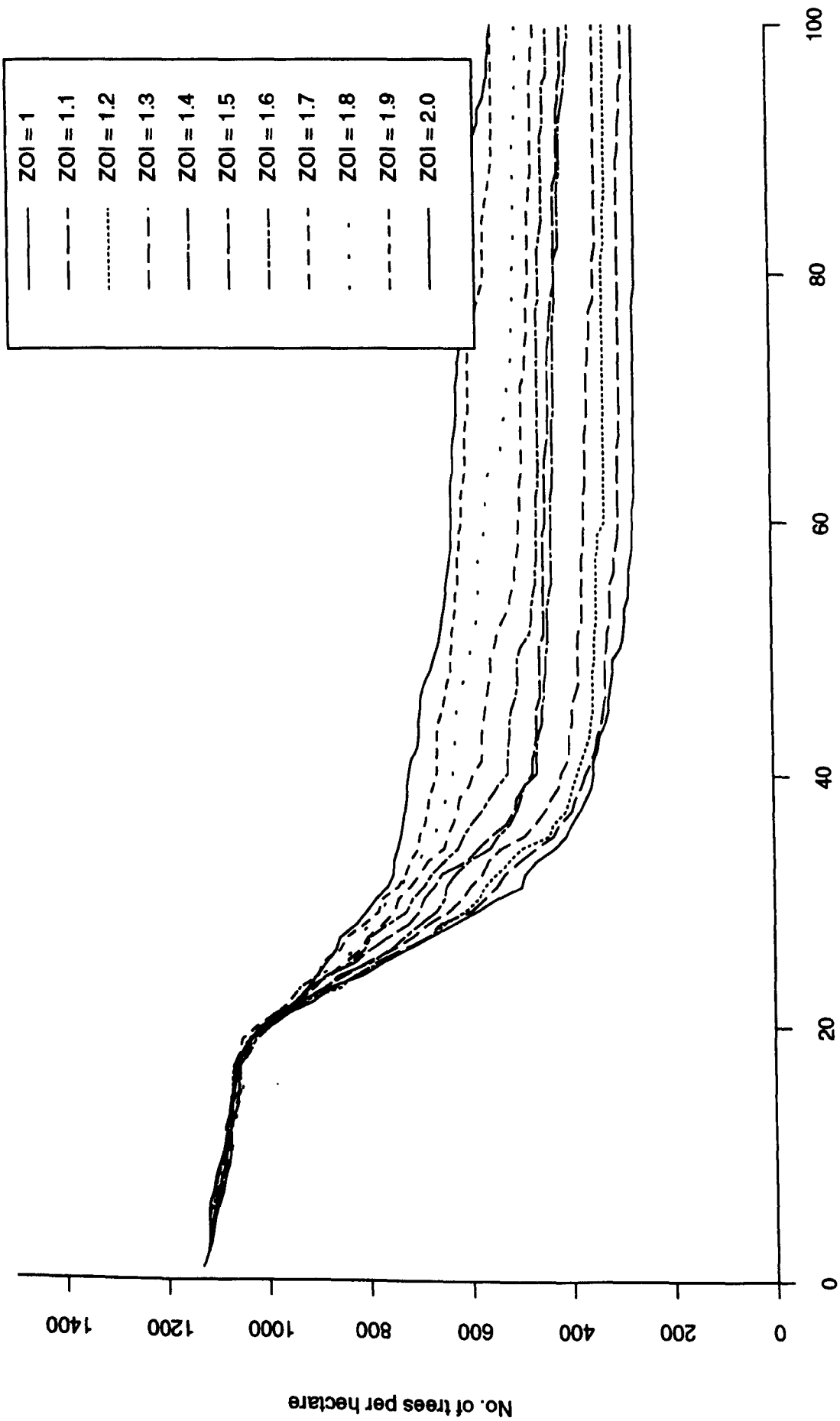

Figure 7.25: Sensitivity of plot density to changes in zone of influence

a large crown angle produces low plot density. This is initially surprising and justifies the inclusion of both of these factors in the sensitivity analysis when on the surface they should have a very similar effect (because a large crown angle automatically increases the size of ZOI). The reason for this difference is that crown angle directly affects the set mortality rules while the ZOI only affects the growth rate of individual trees. A large ZOI proportion slows down the growth of trees and therefore they interact less and consequently less die. In contrast to this a large crown angle also slows down the tree growth but each tree is larger and it is easier for one tree to completely grow over another and consequently cause the second trees death.

With a small ZOI the trees grow faster (as can be seen in figure 7.24) and therefore the interaction is greater and more are killed by the interaction rules. The spread of plot density curves is fairly uniform after the first 25 *years* although there is some mixing up of the mid values (1.4, 1.5, and 1.6) towards the end of the simulation.

In general changing the proportion of crown radius constituting the ZOI has a very clean effect on both average size and plot density i.e. the effect appears straight forward. A large ZOI proportion value gives low average *dbh* values and high final plot density.

Height to base of tree crown

The height to the base of the tree crown is the distance from the ground to the first branches that make up part of the tree crown (see figure 5.3). This is input as a proportion of the tree height so that it increases as the forest grows. The main purpose of this input parameter is so the conical shape that defines a coniferous tree shape does not extend all the way to the ground and therefore the crown radius can be computed at a height above the ground. The higher the proportion of tree height to the base of the tree crown the less the width of the tree crown and therefore the competitive status of a tree is downgraded. This parameter is similar to the crown angle in that it is possible to measure it but it is not a figure readily available in the literature as it is not often required.

The proportion of tree height to the base of the crown was initially varied as a percentage from 0.5 to 18% in eleven increments. After the simulations finished it was found that this produced only two curves: one for 8% and less; and the other for 10% and greater. Consequently the results presented are shown for only those values so that it is clear which curve corresponds to which set of values. One of the likely reasons for the lack of variation is that the basal height proportion only affects the competition status of a tree indirectly through the crown radius. The lack of direct relationship means that neither average growth or plot density are particularly sensitive to changes in the basal height proportion.

The actual difference between the two curves shown in the average *dbh* output (figures 7.26) and the plot density (figure 7.27) is very little. The final value of *dbh* is only 4% greater than the lowest value and the highest final plot density only 9% greater than the

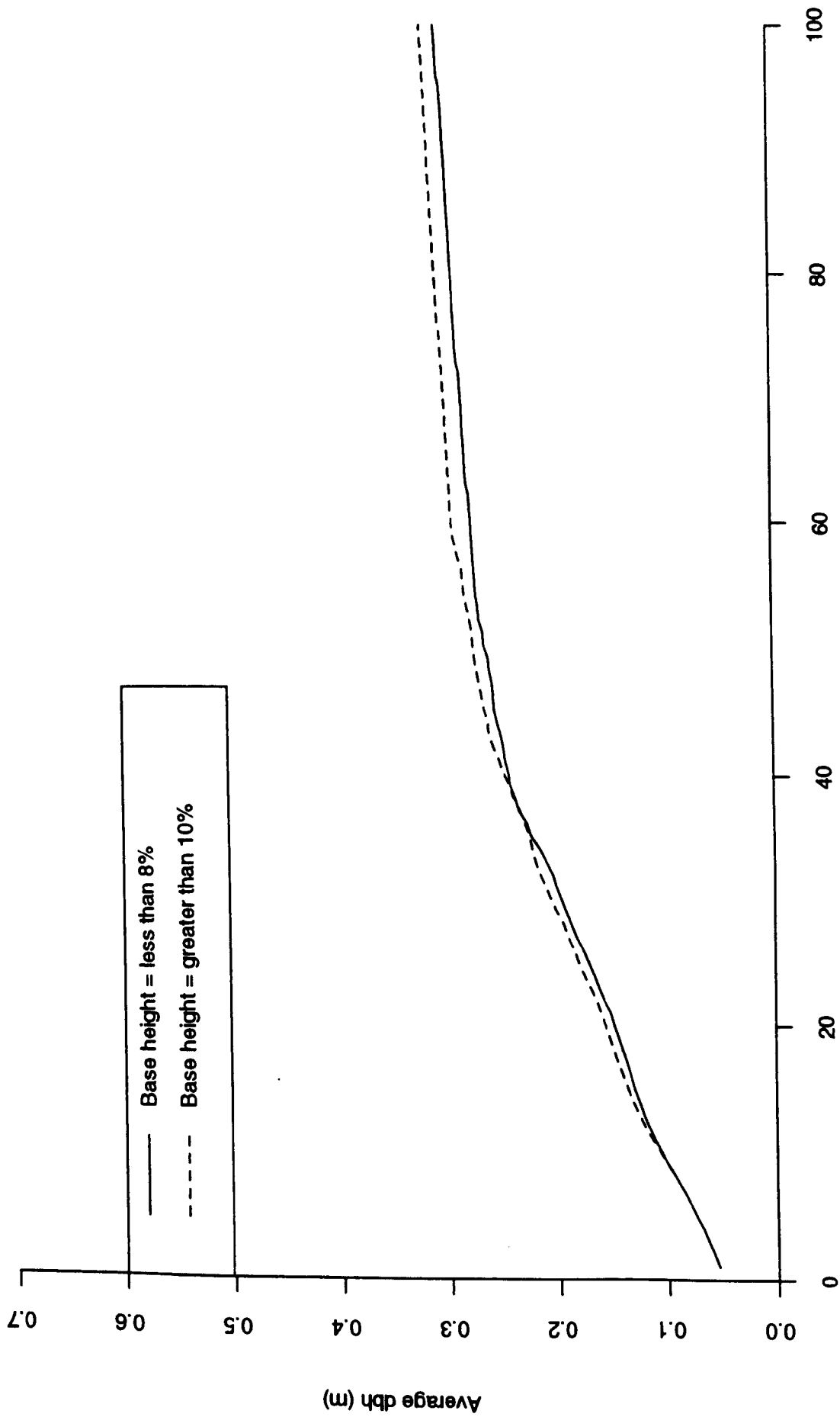

Figure 7.26: Sensitivity of average dbh to changes in height to base of tree crown

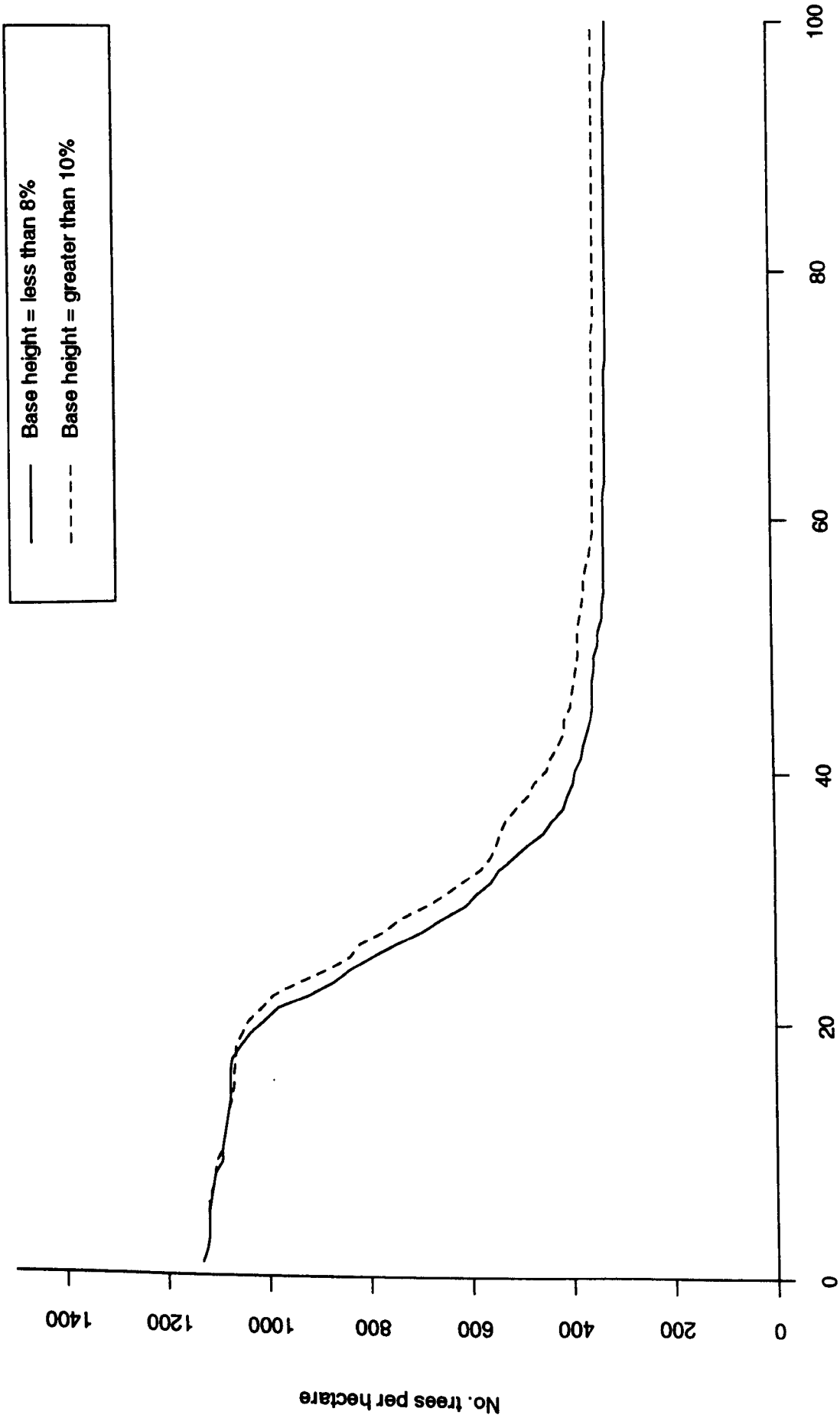

Figure 7.27: Sensitivity of plot density to changes in height to base of tree crown

lowest. The larger basal height figure maintains a higher average *dbh* value for almost the entire simulation.

In the plot density simulations the two curves follow each other very closely throughout the simulation with the 10% and higher simulations having a slightly higher final plot density value.

The higher basal height maintains a higher plot density and growth rate as the crown radius is smaller and therefore the amount of competitive interaction reduced. The results from the variation in basal height proportion indicate that the forest growth model is not very sensitive to this parameter.

Tree spacing

The inter tree spacing is important for defining the amount of competitive interaction between individual trees at the early stages of forest growth. A small tree spacing means that the ZOI of each tree start to intersect with each other at an earlier time and therefore the individual tree and plot average growth rate will slow down at an earlier stage than for a large tree spacing.

Tree spacing cannot really be used as an adjusted parameter for a model calibration as it is a definite parameter that is normally known from the forest management record. It is tested here for model sensitivity to discover its relative importance rather than as a potential parameter to be adjusted for calibration.

The tree spacing values chosen vary from 0.9*m* to 3.0*m*, the actual interval between each variation is not identical as only those tree spacing values with relevant entries in the Forestry Commission yield tables could be used (so that the plot density data could be entered for tree mortality). The results presented include those for plot density although these have little comparative value because the actual number of trees per *hectare* is so different with the different tree spacing values.

The range of growth curves for different tree spacing values is not large (see figure 7.28), and the actual average *dbh* values at the end of the simulation only vary by 0.05 *m* (8% of the smaller value). The most notable point in the growth curve is the cross-over that occurs at around 35 *years* where the curves that originally were displaying slow growth increase markedly and the higher growth rate curves start to slow down growth. For the first 30 *years* the 0.9 *m* spaced trees have the lowest average *dbh* value and the 2.6 *m* spacing the second to highest average *dbh*, but by the end of the simulation the 0.9 *m* spaced trees have the highest *dbh* and the 2.6 *m* plot the lowest.

The explanation for this changeover behaviour can be found by looking at the plot density results in figure 7.29. All of the mortality curves converge to a point at around 35 *years* where the number of trees per hectare is very similar (the scale in figure 7.29 is deceptive the actual difference is 88 trees per *hectare*, a 30% increase between the lowest and highest value). This means that for the first 30 *years* the trees are growing at different

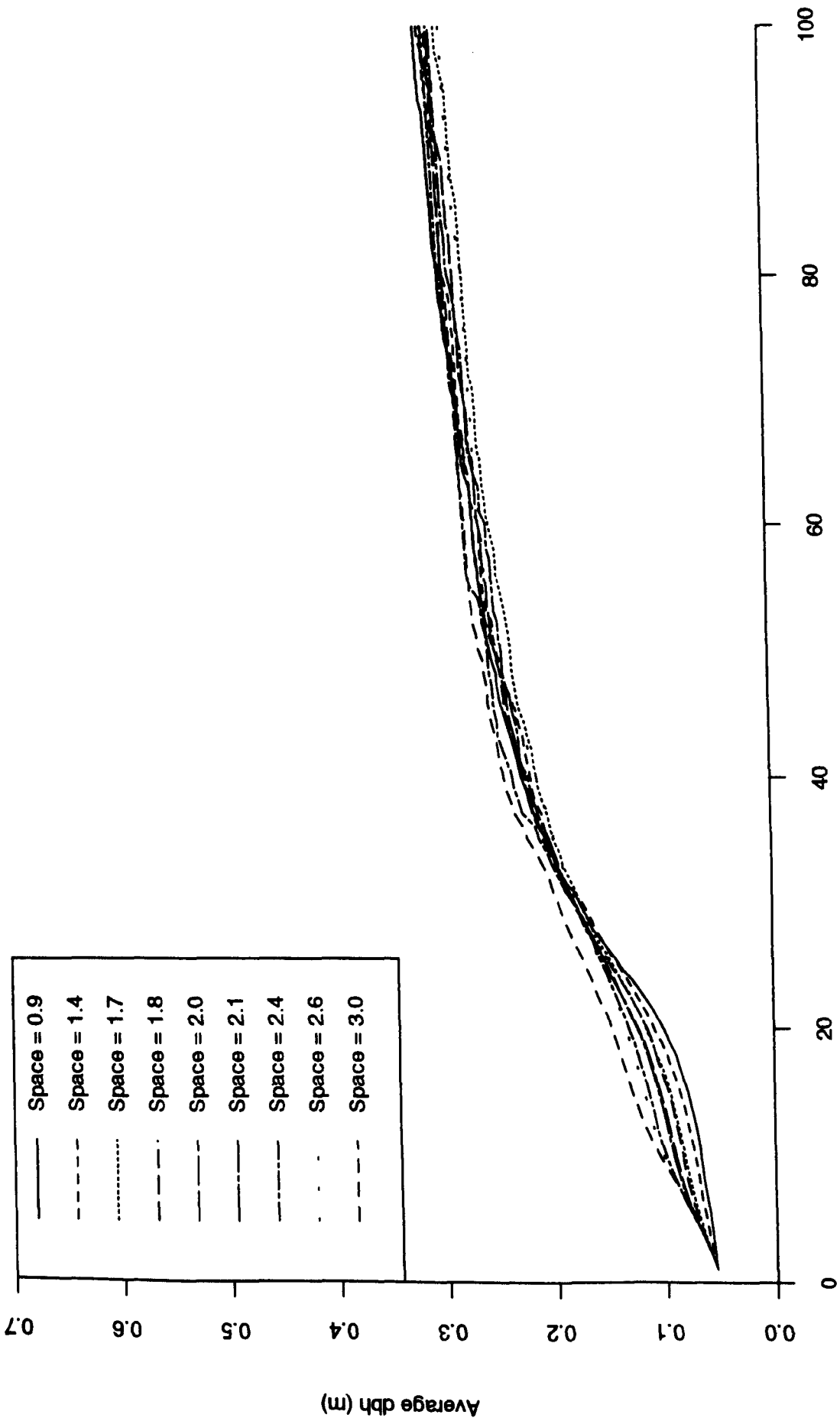

Figure 7.28: Sensitivity of average dbh to changes in tree spacing

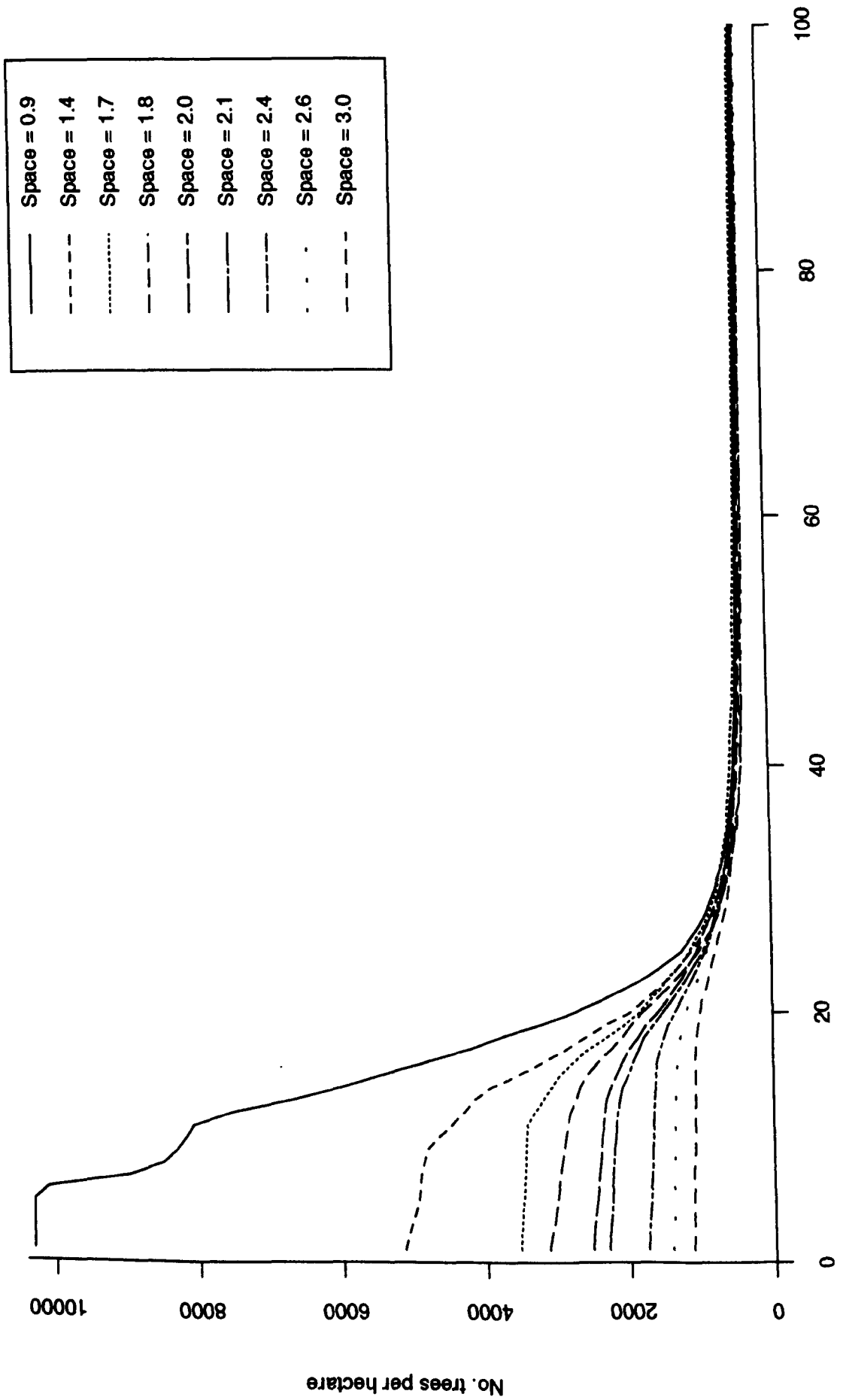

Figure 7.29: Sensitivity of plot density to changes in tree spacing

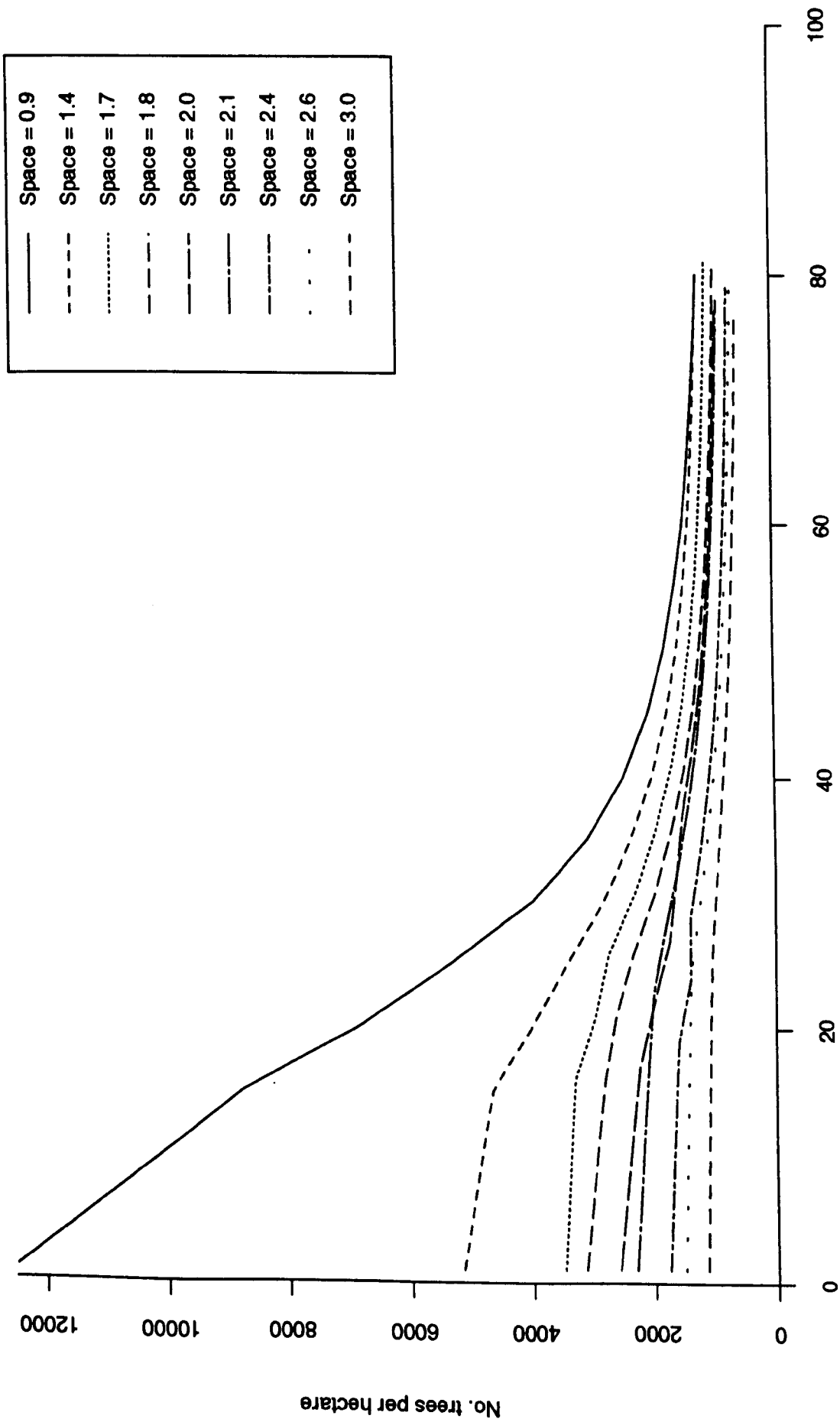

Figure 7.30: Yield table plot density curves for different tree spacings (from Edwards & Christie (1981))

levels of inter tree competition with the highest competitive influence for the 0.9 *m* spacing, hence the lower growth rate. By the time the plot densities have converged they are all on equal footing except that the smaller spacing plots have more spaces to grow into whereas the larger spacing values are still competing against the same neighbours. Consequently the 0.9*m* spacing plot grows faster into the spaces and ends up with a slightly higher average *dbh* value.

The fact that all the tree spacing simulations converge the plot density values (figure 7.29) at around 30 *years* is a surprising result. Figure 7.30 shows the plot density curves derived from the Forestry Commission yield tables and used as input in the model. Although these do converge (final difference of 638 trees per *hectare*) it is nowhere near the extent shown by the simulations in figure 7.30. This suggests that the model is still always predicting a higher mortality rate than the yield table data for the parameter inputs used. The results from variation in other parameters have shown that these can be manipulated to give lower mortality (particularly the size of the ZOI) which should make the plot density for different tree spacing values match closer to the yield table data.

Overall the variation in tree spacing has surprisingly little effect on the model output, particularly the average *dbh* values. It is surprising because the model bases its competition index on the allocation of space to intercept light which suggests that tree spacing would be an important influence. This is certainly why tree spacing is important for the first 40 *years* of tree growth but after that the trees have grown enough in all simulations so that they have an equal interception of ZOI and the plot density is fairly uniform, consequently growth is fairly similar between tree spacing values.

Comparison between parameters

The comparative results using the S values computed from equation 7.5 are shown in figure 7.31 for average *dbh* and figure 7.32 for plot density. The tree spacing is not included in this comparison because the model output is so different as a result of the inter-relationship between input and output. The S values on the *y* axis are dimensionless measures of the model sensitivity to each of the five input parameters varied. These S values use the model outputs (F_0 in equation 7.5) resulting from the maximum and minimum input parameter values, which in some cases may not give the highest or lowest output value e.g. figure 7.21 where a standard deviation of 0.07 gives a lower plot density than a standard deviation of 0.09.

Both of figures 7.31 and 7.32 show that the model sensitivity to different parameters is dynamic i.e. dependent on the period of simulation. This is an extremely important result because in using the forest growth model as a pre-processor for *VSAS4* the simulation period will be variable i.e. the forest growth model is being used to simulate all age forests not just a mature forest. For both average *dbh* and plot density the model is extremely sensitive to changes in the mean growth ratio during the first 40 *years* but less so

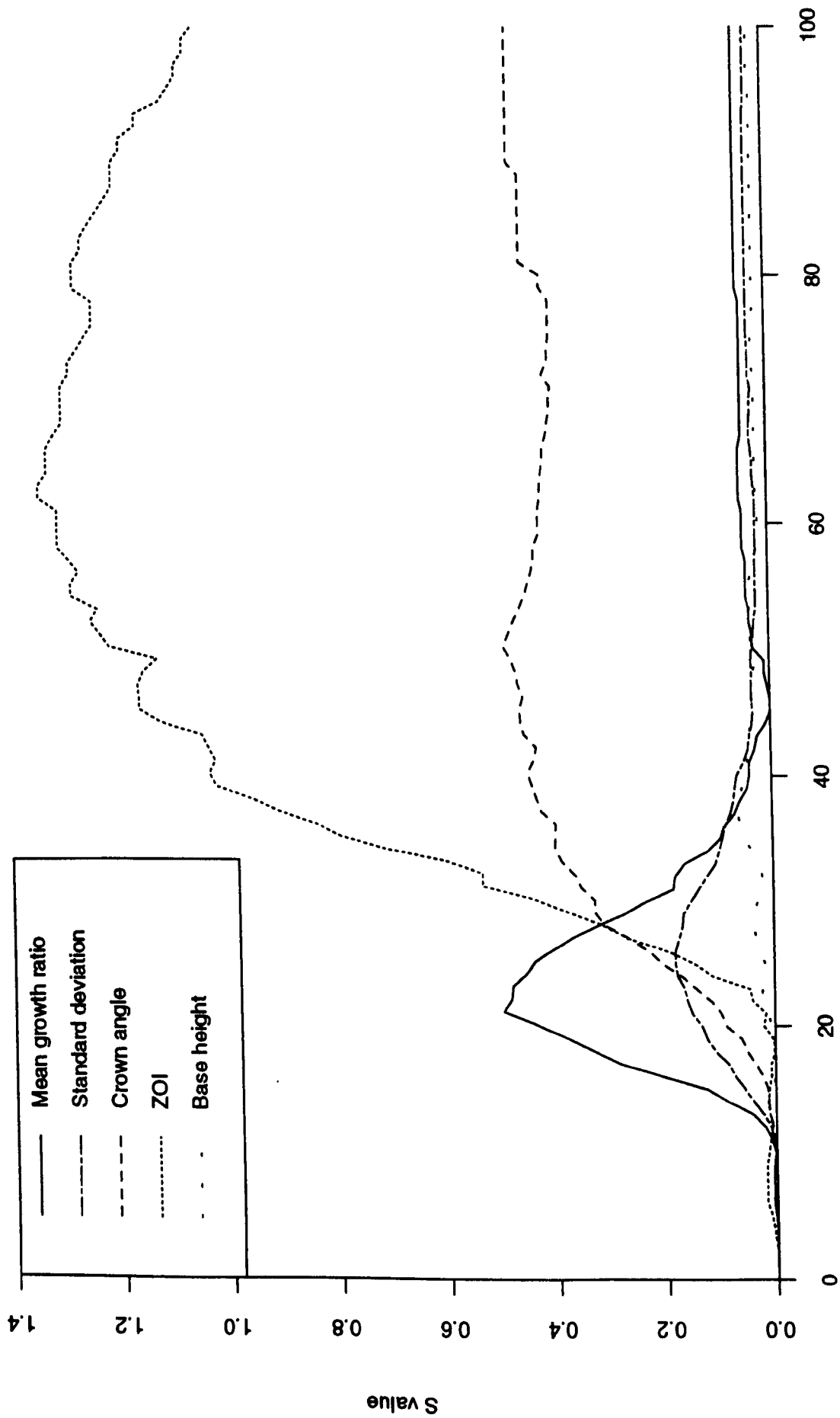

Figure 7.31: Sensitivity values (S in equation 7.5) with time for average dbh

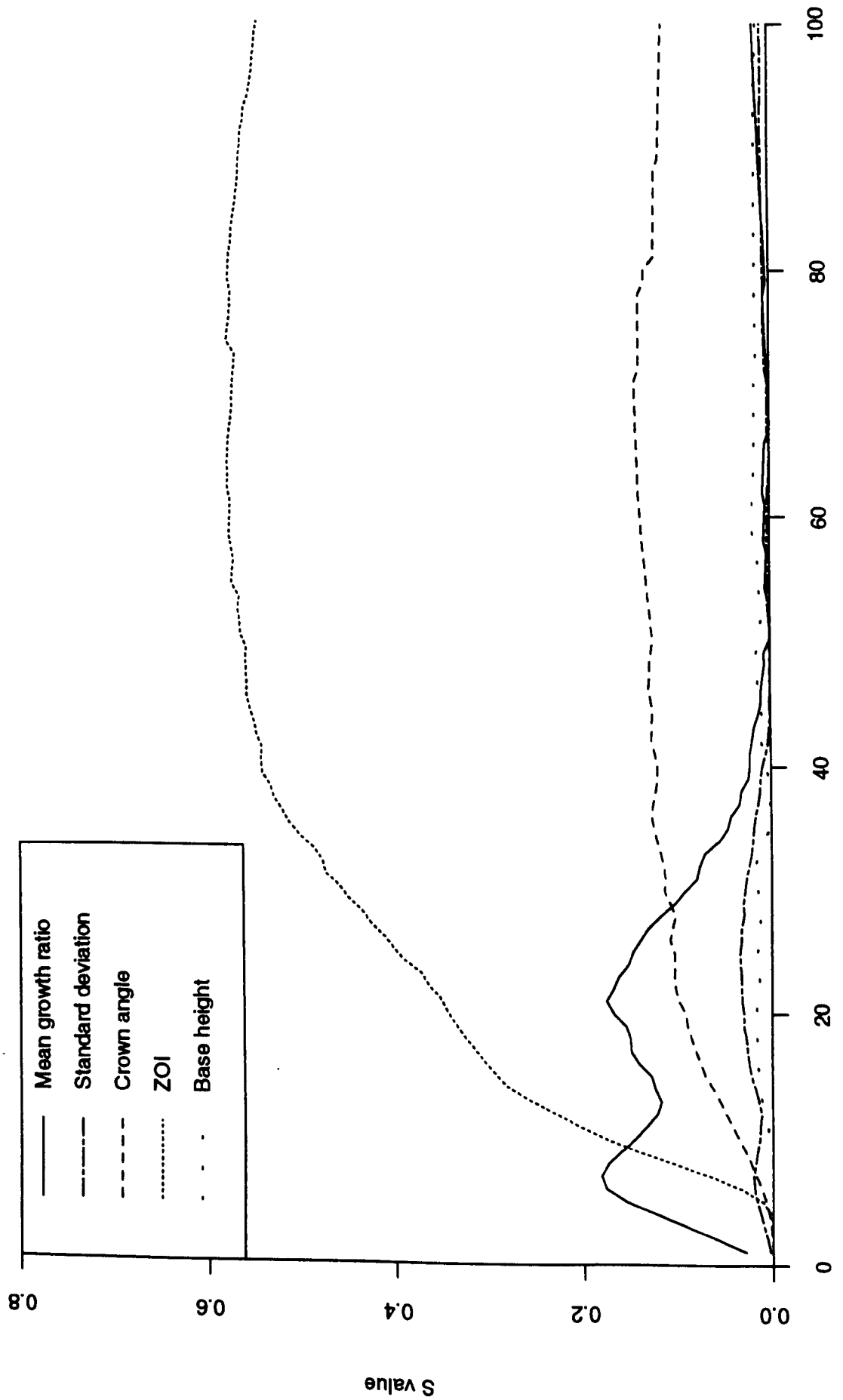

Figure 7.32: Sensitivity values (*S* in equation 7.5) with time for plot density

later than this. By way of contrast the model is extremely sensitive to changes in ZOI and to a lesser extent crown angle, particularly in the latter stages of a 100 *year* simulation.

In almost all of the model simulations presented in this section, after 40 *years* the output plot density has reached close to its minimum value for the simulation. This is also the watershed mark for the model sensitivity in figures 7.31 and 7.32, therefore it seems that after the plot density has reached close to its minimum the most important factors are the proportion of crown angle as ZOI and crown angle. Before this time mean and standard deviation of the growth ratio are as, if not more important than the ZOI.

As might be expected from the results presented earlier in this section the model is never particularly sensitive to the proportion of tree height to the base of the tree crown.

7.3.5.3 Summary

Six input parameters for the forest growth model within *LUCAS* were allowed to vary individually whilst others were kept static in the controlled conditions of a sensitivity analysis. Two sets of model output, average size and plot density, were analysed to assess the effects of variation of the parameters. A summary of these results is given in table 7.5.

At the start of section 7.3.5 it was stated that there were three types of final results that could be expected from the aims of a sensitivity analysis of this kind: a ranking of parameters; a quantitative assessment of parameters; and also a qualitative assessment of the parameters.

A ranking of the parameters has to be split between the two outputs considered and also based on some objective criteria such as the S value of equation 7.5. It is difficult to use this criteria in that it is temporally dynamic as demonstrated in figures 7.31 and 7.32 and therefore the time of ranking is critical. To overcome this two sets of ranking are used, one for after 25 *years* and another for after 100 *years* of simulation.

The ranking of parameters based on the S values after both of these time periods is shown in table 7.6 but is slightly different from the S values used in figures 7.31 and 7.32. The S value used here is still from equations 7.5 and 7.6 but the F_{max} and F_{min} values are the actual maximum and minimum output values (as opposed to the outputs from the maximum and minimum inputs used in the earlier examples). This means that the rankings may seem slightly different from how they appear in figures 7.31 and 7.32.

Parameter	*S values after after 25 years*	*S value after 100 years*	*Affect on average growth curves*	*Affect on plot density curves*	*General comments*
Mean growth ratio	0.74 (density) 0.42 (av. dbh)	0.05 0.14	High value = high final dbh Reasonably even spread of curves	High value = high early mortality Large effect on mortality rate but similar final densities	Higher average tree growth is at expense of plot mortality density
Standard dev. of growth ratio	0.23 0.05	0.07 0.25	Difficult to predict. Initial effect evens out by 40 *years*	High value = high early mortality Medium initial affect but evened out by 50 *years*	Complicated interactions
Crown angle	0.20 0.10	0.47 0.15	Large angle = low growth rate. Very large effect particularly 2 - 8°	Large angle = high mortality Very large effect	8° critical threshold, below this very little effect. Higher average tree growth not at expense of mortality
Zone of influence	0.17 0.67	1.04 1.18	Large ZOI = low growth rate Very large effect	Large ZOI = low final density Very large effect on latter stages	The cleanest effect of all. Higher average tree growth is at expense of mortality
Height to base of tree crown	0.001 0.001	0.002 0.001	Little change	Little change	Only difference is between 8 - 10%
Tree spacing	0.25 0.10	0.57 0.01	Little overall effect except in the first 40 *years*	Difficult to compare. A convergence of final density occurs	Unable to vary as input plot densities are fixed from this

Table 7.5: Summary of the forest growth model sensitivity analysis results

Ranking	*Average dbh*	*Plot density*
1	ZOI	Mean growth ratio
2	Mean growth ratio	Tree spacing
3	Crown angle	Standard deviation of mean g.r.
4	Tree spacing	Crown angle
5	Standard deviation of mean g.r.	ZOI
6	Height to base of tree crown	Height to base of tree crown

Table 7.6: Ranking of variables for their effect on forest growth model output after 25 *years* of simulation. The ranking is based on the S (sensitivity) value as described in equation 7.5

Ranking	*Average dbh*	*Plot density*
1	ZOI	ZOI
2	Standard deviation of mean g.r.	Tree spacing
3	Crown angle	Crown angle
4	Mean growth ratio	Standard deviation of mean g.r.
5	Tree spacing	Mean growth ratio
6	Height to base of tree crown	Height to base of tree crown

Table 7.7: Ranking of variables for their effect on forest growth model output after 100 *years* of simulation. The ranking is based on the S (sensitivity) value as described in equation 7.5

The ranking of variables in tables 7.6 and 7.7 shows:

- The importance of the zone of influence on the model in all cases except for plot density after 25 *years*
- The relative unimportance of the height to base of tree crown
- The temporally dynamic nature of the model sensitivity to the parameters but especially with respect to the mean growth ratio
- The difference in sensitivity for the separate model outputs

It is extremely difficult to give an actual figure for the degree accuracy required in the measurement of the input parameter (the quantitative assessment). All that can be done is to combine the results in tables 7.6 and 7.7 to see which of the parameters need to be measured with particular accuracy. Some of the parameters are abstract and therefore

cannot be properly measured (growth ratio statistics and size of ZOI) and therefore their actual values are likely to be derived from a calibration of the model. Of the remaining parameters it is obvious that crown angle needs particular care in measurement and height to base of tree crown needs very little attention.

The third of the final results, a qualitative assessment of the role of processes and/or parameters within the model, is provided by the final three columns in table 7.5. This information is of particular use for a calibration of the forest growth model as it gives some idea of which parameters can be altered to get a particular type of output result.

In section 7.3.5.1 the point was made that the first two parameters in table 7.4 could be grouped together under the process category of plant growth and the remainder of parameters under a competition category. In very general terms it could be said that altering the plant growth parameters causes high mortality during the early active growth phase of a forest whilst the competition parameters tend to influence the latter stage mortality. Apart from this there is very little that can be deduced as to the separate role of the two major processes occurring in the model. This reflects the complex interactions between processes occurring within the forest growth model which in turn is a reflection of the complex interactions occurring within natural forest systems.

The sensitivity analysis has been a success in that it has given considerable insight into the influence of various parameters on the selected model outputs which will be of considerable help during the validation testing of *LUCAS* which is described in the following chapter. It also shows that by adjusting some of input parameters there is considerable scope for improvement on the initial testing results that appeared so poor in section 7.3.1 and section 7.3.4.

The major points established from the sensitivity analysis can be summarised as:

- Each of the six input parameters varied influence the model outputs to different degrees and in different manners
- A change in the crown angle and the zone of influence provide the cleanest effect on model output
- A great range of output is available from varying six of the input parameters
- The model sensitivity is temporally dynamic (responds with different sensitivity at different time periods)
- A ranking of parameters based on sensitivity is not really possible because of the temporally dynamic nature

7.4 Summary

Chapter seven has involved the further development of various facets within the *LUCAS* modelling scheme stemming from the encouraging robustness testing results in chapter five and general model usage. The modification and testing has been in three parts.

The first part involved the integration of an error analysis into the *VSAS4* structure to detect periods of mathematical instability and pin-point the regions in the model where this or any rounding errors may be occurring. The error analysis runs concurrently with *VSAS4* accumulating any differences between inputs and outputs from two conceptual tanks that represent the canopy and hillslope segments storage. Although this is simplistic in form it was successful in pin-pointing the source of some mathematical instability first detected during the robustness testing in chapter six. This was described in section 7.2.

The second and final part of development within *LUCAS* concerned the tree growth model that acts as a pre-processor to *VSAS4*. This model acts at a totally different timescale from *VSAS4* and needed to be verified as a forest growth model in its own right. To achieve this the model had some initial testing against a data set which was not particularly successful. Following this the structure was modified to improve its predictive ability, and the model tested again. Finally a sensitivity analysis of the forest growth model was undertaken which showed the effect that variation in six different input parameters had on two different model outputs. The sensitivity analysis was successful in highlighting the influence of model parameters and also indicating the range of output that can be obtained by calibration.

The *LUCAS* modelling scheme has now been fully constructed and verification testing carried out on its various components. All that remains is for the scheme to be validated as a simulator of the effects of long term vegetation change on stormflow hydrology. Chapter eight concerns the validation of *LUCAS*.

CHAPTER 8

VALIDATION TESTING OF LUCAS

The previous two chapters have detailed the verification of the *LUCAS* scheme as an investigative tool for the hydrological effects of long term vegetation change. This involved robustness testing of the total scheme in chapter six and following some superficial changes, the independent verification of the forest growth model in chapter seven. The research design for this thesis outlined in figures 3.1 and 3.2 shows that all that is left to achieve is validation of modelling scheme using any available empirical data and hypothetical scenarios.

The validation is described in this chapter. The first section of the chapter gives background to model validation further to the general discussion in chapter two. The second section details the various choices of validation data available and then describes the catchment finally selected. The third section gives the initial input data values before the actual results being presented and discussed in section 8.4. The validation exercise is summarised and *LUCAS* assessed as a predictor of long term land use change in section 8.5.

8.1 Introduction

In chapter two the role of verification and validation in numerical modelling was discussed; the definitions of these terms were given as follows. Verification is the process to insure that the computer program actually carries out the logical processes expected of it and verifying that the model behaves as intended. Validation is any process designed to measure the correspondence between the model and the system under study and thus indicates the usefulness of the scheme for predictive applications (Miller *et al* 1976). The definition for validation was changed in chapter three to become: ensuring that the model is a valid representation of the hydrological system as it was noted that there would never be an adequate data set to validate a physically based, distributed model in the original sense. The new looser definition allows for different methods of validation to be used apart from straight predicted versus observed hydrographs.

After the verification testing of *LUCAS* and the independent sensitivity analysis (a form of verification) of the forest growth model it is now necessary to undertake some form of validation testing. The actual form of validation depends on the data set available

and the model structure. The *LUCAS* modelling scheme is complicated by the presence of two separate models with different outputs running at unmatched time scales. This makes it impossible to validate the overall scheme from a single data set. The previous chapter (seven) has described some initial testing of the forest growth model which gives some idea of the data necessary for validating this section of *LUCAS*. The storm event runoff simulator (*VSAS4*) could be validated by many different sorts of data but the most logical would involve rainfall-runoff data. Of these two data sets the rainfall-runoff data is the most important because *LUCAS* has been specifically designed as a detector of the effects of afforestation on storm event runoff. This means that forest growth data can be used to validate the forest growth model but following this **rainfall-runoff data can be used to validate all of *LUCAS*** (in as much as rainfall-runoff data can ever validate a distributed model).

At this point a differentiation must be made between application and validation of a hydrological model. An application involves using the model to simulate some real or proposed conditions often after some form of calibration. A validation purely assesses the correspondence between the model and the system under study and tests the applicability of a model, rather than actually applies it. The use of calibration in application and in some cases validation (e.g. Calver (1988)) means that these phrases are often interlinked, but validation must be performed prior to a full calibration where calibration is required for application purposes.

In the strictest sense calibration prior to validation nullifies the validation of physically based, distributed models; Stephenson & Freeze (1974) point out that a validation requires perfect *a priori* knowledge of the boundary conditions and that where calibration is used "the resulting flexibility almost ensures that a satisfactory validation will be obtained". This extremely rigid view (as discussed in chapter two) is difficult to adhere to when there is not a perfect data set available but has to be acknowledged as a limitation to the validation. The validation testing presented here involves some calibration of the forest growth model within the validation of *LUCAS* but is not a full calibration of the overall modelling scheme.

In the critique of physically based, distributed models contained in chapter two model validation was listed as one the major problems. Two criticisms of validation were highlighted. Firstly that rainfall-runoff data are not adequate to fully validate a modelling scheme that aims to predict the distribution of many hydrological processes within a catchment. Secondly that often the validation involves calibration of the internal boundary conditions (see above). Even though *VSAS4* has been designed as a focussed version of a physically based, distributed hydrological model to try and overcome these kind of difficulties, they are still apparent here.

By investigating the effects of long term vegetation change on stormflow

hydrology a further temporal complication is added, thus further diluting the ability to fully validate the scheme. This means that the problems of model validation can be examined on two inter-related levels:

- Lack of empirical data
- Lack of the data over a long time period.

The first of these problems means that simplifications have to be made to the validation procedure resulting in the most commonly available data (rainfall-runoff) being used in validation, and calibration occurring within the internal boundary conditions. The lack of empirical data is partly because the measurement methods available at present are not capable of sensibly measuring the parameters at the necessary scale and partly due to a lack of data for these models as they have only been in general use for 10-15 years. There is no ready made answer to the lack of data for validation; it is a limitation that has to be acknowledged and the best made of what is available. Consequently it is desirable to find a validation location that has as much data available as possible, or to measure the necessary parameters before the validation is attempted.

The second problem, lack of data for a study involving a long time frame, means that it is not feasible to measure the data within this study. It compounds the difficulty of inadequate data but if the data required are restricted to rainfall-runoff there are two alternative data sets that could be obtained for a validation of *LUCAS* as a simulator of the hydrological impacts of long term vegetation change:

- A catchment that has been planted and well monitored for the entire period or at least a decent length of afforestation
- A series of catchments each at different stages of afforestation.

In a validation using the first data set selected events could be extracted from the records and the ability of the model to predict the runoff at these time periods examined. In the second data set the ability to predict runoff from each catchment individually would be examined and inferences drawn from similarities or differences between the catchment results.

The first data set has the serious problem attached to it that it requires hydrological data covering a long time period, but the lack of this length of field data was one of the original grounds given in chapter one for the development of a modelling system such as *LUCAS*. A validation attempt of *LUCAS* presents a circular modelling problem where the model is developed to make up for of a lack of field data and then cannot be fully validated because of the very same lack of field data. This does not mean that a model cannot be developed on a single series of data and then applied elsewhere but as discussed in chapter two the existence of hydrological records covering the full period of afforestation on a

catchment are very unlikely. The general trend in hydrological modelling;to explore issues beyond the range of available field data has been discussed in chapter two where it was decided that this is a necessary part of modelling development and should not be seen as a restrictive factor in modelling studies. Consequently an attempt can be made to use this type of data set even when the records appear rather short.

The series of afforested catchments in the second option listed above need not be closely related except perhaps in size. Each catchment would present a snapshot of the hydrological effects of the stage of afforestation at their respective age. This type of data set overcomes the circular validation problem by effectively providing a long term record through the series of snapshots but there are two inter-related problems associated with this approach. The first is that it would be very difficult to establish how much of the difference between model predictions is a result of afforestation or the difference in catchment characteristics i.e. the between site variation may be greater than the temporal variation. The second problem is that the errors in any measurement of empirical data will be magnified by more than one measurement site and equipment. These two problems combined provide an almost definite case where the results may well end up saying "more about the quality of data used, rather than confirming the model mechanisms themselves" (Anderson & Burt (1985)).

It is clear that neither of these data sets provides a perfect tool for validation therefore it is necessary to look for a data set that is the best available. The various options are explored further in section 8.2.

8.1.1 Method and aims

There are various methods available that can be used in validation of hydrological models. Pilgrim (1975) and Klemeš (1986) describe some operational procedures that can be used for validation on various types of models, the choice of procedure being dependent on the degree of model, and problem, sophistication. Unfortunately for this study these tests are all designed for black box or conceptual models and do not apply for a physically based model used in purely research terms. It is possible to devise a numerical test for closeness of fit of data but this achieves little more than a subjective analysis of predicted versus observed hydrographs would. This is in line with the view of Pilgrim (1975) that "validation requires subjective judgements".

The validation of *LUCAS* presented here is by a qualitative comparison of predicted and measured hydrographs for various storm events with no numerical analysis attempted. This method allows scope for interpretation of the results within a knowledge of the methods used to mathematically represent hydrological processes within the *LUCAS* structure.

The aims of the validation testing of *LUCAS* are straightforward, they can be listed as:

- To test the predictive ability of *LUCAS* against a data set
- To explore the possibilities for predicting beyond the data set range

The second of these aims moves slightly outside the original definition of validation given at the start of this section but is within the redefined terminology. It is necessary because of the validation problems discussed earlier, by restricting the study to solely the first aim very little could be deduced as to the ability of the model as the data set is likely to be inadequate. By extending the aims to look at conditions outside the data set range an idea of the models worth as a predictor of the hydrological effects of long term vegetation change can be built up and the model can be used to highlight areas of long term vegetation change investigation that require further research.

This chapter is divided into four further sections. The first of these (section 8.2) concerns the choice of data available from monitored catchments within Great Britain to use in validation and goes on to describe the catchment selected and the choice of storm data. Section 8.3 deals with the model set-up for both the pre-processing forest growth and the hydrological simulation model (*VSAS4*) that together form *LUCAS*. The set-up for the forest growth model includes the calibration involved in determining the final input parameter values. Section 8.4 details the results of the validation simulations. These are split into two separate subsections: the straight storm simulations that fulfil the first aim of the validation (see above); and the simulations using hypothetical scenarios (the second aim). Finally section 8.5 summarises validation exercise carried out in the chapter.

8.2 Data available for validation

The problems with selecting a data set for a validation exercise have already been discussed in section 8.1. This section is concerned with the selection of the necessary data set for the best possible validation, the criteria being suitability to the model and providing the fullest records for the validation.

The two major collectors of rainfall-runoff records in Great Britain are the National Rivers Authority and the Institute of Hydrology. The Institute of Hydrology collects most of its records as part of research catchment studies; these are of particular use to a study of this sort as there are often extra data available such as soil water status and evaporation which can be of use for setting up a simulation using a modelling scheme such as *LUCAS*.

8.2.1 Catchment data

The Institute of Hydrology were approached and readily agreed to make available necessary data from their relevant land use change research catchments. There are three catchments of particular interest for this study:

- The Plynlimon experiment. A paired catchment study in mid Wales (upper reaches of the Severn and Wye rivers), each of the two catchments are subdivided into smaller subcatchments with data held for all of these
- The Balquhidder experiment. A paired catchment study (Kirkton and Monachyle) in highland Scotland
- The Coalburn catchment. A small research catchment on the Northumberland-Cumbria border.

The Plynlimon experiment was set up by the Institute of Hydrology in 1967 to investigate various hydrological implications of forestry. Despite it not being a strictly controlled paired catchment study (i.e. one of the two catchments already had the land use change on it at the beginning of the experiment) Plynlimon has gained world wide recognition for the pioneering work achieved in the field of land use change and in particular forest hydrological processes. The experiment is still running although with less intensive research occurring than during the 1970s. Of the two catchments the Wye (10.5 km^2) is predominantly unforested and consists of four subcatchments (Nant Iago, Gwy, Cyff, and Gerig) while the Severn (8.7 km^2) is approximately 68% afforested and consists of 3 subcatchments (Hore, Hafren and Tanllwyth). The subcatchments were started to be monitored at later stages in the experiment than the main Severn and Wye river flows.

Various areas of the Plynlimon experiment have been used for model validation exercises in the past e.g. Bathurst (1986a) using the *SHE* model on the Wye and both Rogers (1985) and Calver (1988) using *IHDM4* on the Tanllwyth. The Wye and Severn are both too large to be used viably by *LUCAS* but the various subcatchments do present feasible alternatives.

The Balquhidder experiment in the southern Highlands of Scotland (60 *km* north of Glasgow) was set up by the Institute of Hydrology in 1981 and is still actively running. The main objective of the study is:

> To replicate and extend the Plynlimon study in mid-Wales, on the effects of upland afforestation on water resources into Highland Scotland where the indigenous vegetation, typically coarse grasses and heather, is aerodynamically rougher than the sort cropped grass found in Wales and where the distribution and type of precipitation is

different. (Johnson (1991), p2)

Both afforestation and deforestation are under investigation at Balquhidder, the Monachyle (7.7 km^2) being mostly moorland with 14% recently afforested, and the Kirkton (6.85 km^2) being mainly mature forest with 50% recently deforested. The only modelling studies carried out at Balquhidder so far have involved calibrating *TOPMODEL* (a distributed semi-physically based model) and *HYRROM* (a lumped conceptual model) for the catchments (Johnson (1991)).

The Coalburn research catchment is a study of afforestation on the Northumbrian moors 40 *km* northeast of Carlisle. The catchment is small (1.5 km^2) and has been monitored by the Institute of Hydrology since 1967, although there is some doubt on the accuracy of recent runoff recordings due to a faulty gauge structure. The catchment was ploughed ready for planting in 1972 and then planted during 1973, the trees have grown very slowly and have not reached the full canopy closure stage during 1991 (M. Robinson, Institute of Hydrology, pers. comm.). The main study carried out by the Institute of Hydrology so far has been to investigate the effects of the pre-planting ploughing on the hydrological regime of the Coal burn (Robinson 1986). The catchment has never been used in a modelling study.

In order to decide which of the catchments are feasible to use in a validation of *LUCAS* it is necessary to consider all of the catchment attributes in combination with the model attributes. The correspondence of model and catchment attributes of particular interest is the capability of *LUCAS* in representing different processes and whether these processes occur or are measured separately within the catchment. Because the validation will involve observed versus predicted hydrographs the main attributes considered are for the *VSAS4* part of *LUCAS* e.g. catchment size as used by previous *VSAS* versions. The combination of model and catchment attributes is shown in table 8.1. Within the Plynlimon experiment the Tanllwyth subcatchment of the Severn has been singled out because it has been used in similar modelling exercises by Rogers (1985) and Calver (1988).

Of the two Balquhidder catchments the Kirkton seems the most useful as it has had a mature canopy and has recently been clearfelled whereas the Monachyle has only recently been planted and therefore the effects of afforestation are probably not well established enough on the Monachyle for hydrological effects to be detectable. This in itself does not preclude the Monachyle but there seems little point in using the entire *LUCAS* scheme when the effects of trees is likely to be very small and camouflaged by other effects such as pre-planting ploughing. Both the Monachyle and the Kirkton are considerably larger than any catchments that the *VSAS* scheme has been used for previously, this is the major reason why neither of the Balquhidder catchments has been used in the validation exercise here.

	LUCAS scheme		*Data Available*			
Process	***Current capabilities***	***Previous VSAS testing***	***Kirkton***	***Monachyle***	***Coalburn***	***Tanllwyth***
Rainfall-Runoff prediction	Good	Troendle (1979) Bernier (1982) Whitelaw (1988) Fawcett (1992)	1981 → Good records	1981 → Good records	1967 →; Good early records; some doubt on recent runoff*	1975 → Good records
Soil water dynamics	Good	Whitelaw (1988)	2 measurement sites	2 measurement sites	None	None
Afforestation	Unknown	None	Mature canopy on 46% of catchment	Planting started 1986	Planted 1973	Mature canopy; planted 1948-50
Deforestation	Unknown	None	Clearfelling began 1986	N/A	N/A	None
Catchment size	Small catchments	0.24-1.9 km^2	6.85 km^2	7.7 km^2	1.5 km^2	0.92 km^2
Altitude range	Only important for snowmelt contribution		242-852 *m*	292-906 *m*	270-330 *m*	380-680 *m*
Snowmelt contribution	Not incorporated	Modified *VSAS2* version used by Prevost *et al* (1990)	High	High	Moderate	Low/moderate

Table 8.1: Summary of information on model attributes and Institute of Hydrology research catchments. * See accompanying text

Both the Coalburn and the Tanllwyth are small enough to be used by *VSAS4* and they both present different stages of afforestation in a catchment. They therefore appear to present ideal catchments for the validation and consequently it was decided that both of these catchment would be used in a validation of *LUCAS*. Unfortunately on gathering data from these catchments it was found that the most recent storm data available from the Coal burn was during 1977 which was only 5 *years* after the planting of trees (M. Robinson Institute of Hydrology, pers. comm.). This therefore is a similar situation to the Monachyle where there seems little point in using the data when the effects of afforestation are as likely to be disguised by ploughing etc.. Consequently it was decided to concentrate the validation attempt of *LUCAS* on the Tanllwyth data.

The following section involves a description of the Tanllwyth catchment, which is derived from Newson (1976), Kirby *et al* (1991), and visits to the catchment.

8.2.2 The Tanllwyth catchment

The Tanllwyth catchment is a small ($0.92km^2$) headwater tributary to the Severn river in Mid Wales, the location and shape of the catchment is shown in figure 8.1. The catchment is hydrologically monitored by the Institute of Hydrology as a subcatchment within the Plynlimon experiment described in section 8.2.1; the land is owned by the Forestry Commission, constituting part of the Hafren forest.

The Tanllwyth is approximately $3km$ in length with an height range of $215m$. The stream channel profile shown in figure 8.2 indicates a fairly flat bottom reach rising steeply to the upper slopes where there is a slight flattening off (N.B. this is a stream profile not a hypsometric curve). The slopes are fairly gentle with 70% of the slopes being less than 10° with none greater than 20° (these are all well within the range of slopes used in the robustness testing in chapter five). 80% of the slopes have a southeast aspect; the remainder are predominantly northeast facing.

The soils are mostly peaty podzols on the interfluves and inflectional slopes and peaty gleys on lower slopes and valley bottoms. The textures range from silty clay to stony and the depths vary between $1\text{-}2m$. The catchment is underlain by Ordovician and Silurian shales and mudstones that are largely impermeable.

The natural vegetation of the Severn catchment consists of *Festuca/Nardus* grassland mainly used for extensive grazing. The are also areas of heath communities (mainly *Eriophorum*) and mire communities (mostly *Juncus* and *Eriophorum*) in the boggy areas along valley bottoms and on some broad interfluves. In the Tanllwyth this vegetation has been replaced by the planting of the coniferous Hafren forest. The majority of the Tanllwyth is now covered by Sitka spruce (*Picea sitchensis*) planted between 1948 and 1950. A map within the report by Newson (1976) indicates that the extreme upper reaches

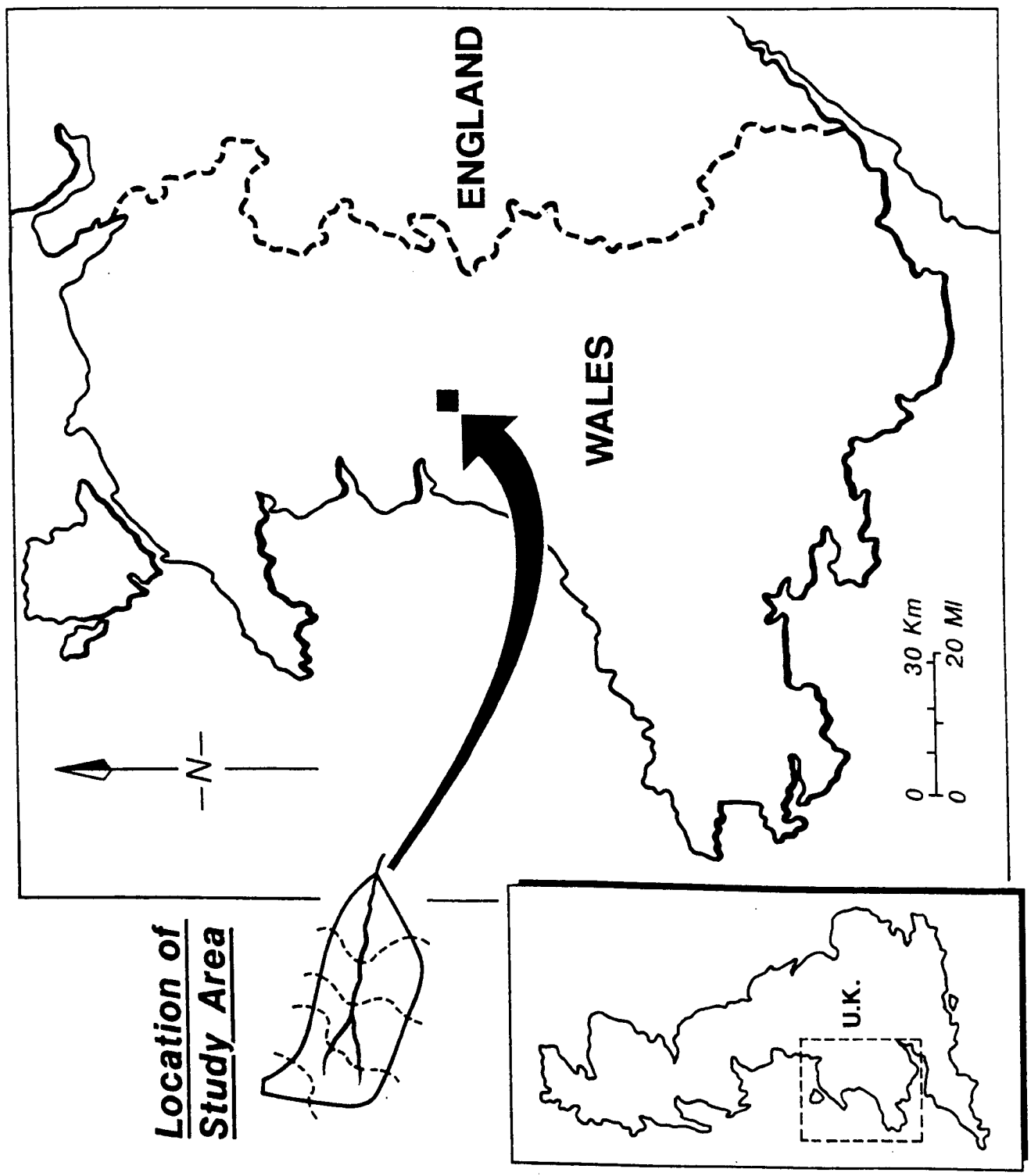

Figure 8.1: Location of study catchment (Tanllwyth) in the United Kingdom

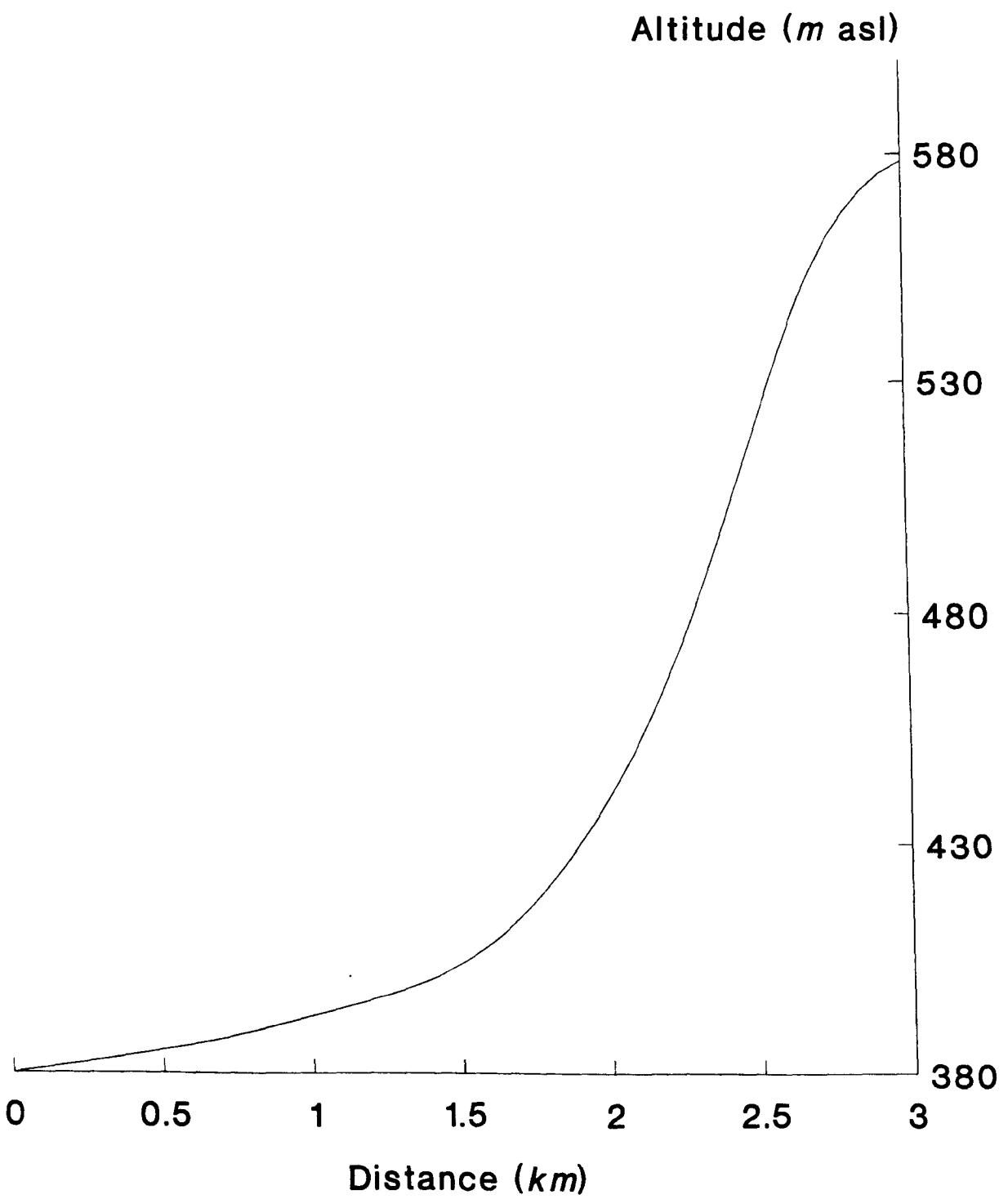

Figure 8.2: Stream profile for the Tanllwyth catchment

of it were planted between 1963 and 1964 with the hardier Lodgepole pine (*Pinus contorta*), although a site inspection could find no indication of this. Prior to planting the areas were drained by tractor ploughing in a manner similar to the Coalburn treatment described by Robinson (1986).

The Forestry Commission do not keep detailed records of management within the Hafren forest (J. Hudson, Institute of Hydrology, pers. comm.) so the forest management record has been assumed from a site inspection and discussions with Institute of Hydrology staff posted at Plynlimon. In the lower reaches of the Tanllwyth the trees were planted at a spacing of 1.4 *m* and there was some thinning (cutting of every third row) after 20 *years* of growth. The thinning was only carried out on a very small area in the lower reaches of the catchment, it was stopped when it became uneconomic after a severe slump in pulp and paper prices during the early 1970s. A small sample of tree sizes and the number of trees surviving indicates that these trees belong to yield class 12 in the forestry commission yield table data (see Edwards & Christie (1981)); this is expanded further in section 8.3.2. In the upper reaches of the Tanllwyth the initial tree spacing was reduced to 0.9*m* and there was no thinning. These trees also belong within yield class 12. Within the forest the ditching carried out prior to planting is barely visible after over 22 *years* of growth.

The mean annual rainfall for the Tanllwyth (1976-1985) is 2540*mm* with a monthly maximum in November (328*mm*) and minimum in April (106*mm*). The mean flow of the Tanllwyth for the period 1975-1987 was 0.058*cumecs* (m^3s^{-1}). From a variety of sources Calver (1988) deduces that the main hydrological processes operating within the Tanllwyth are: throughfall; pipe flow; overland flow; and channel flow in natural channels or drainage ditches.

The predominance of pipe flow is a problem for simulations using *VSAS4* as all soil water flow is assumed to be capillary flow. The implementation of macropore flow (of which soil pipe flow is an extreme example) into physically based, distributed models is one of the primary recommendations of the summary of process representations of Fawcett (1992). At the same time Fawcett (1992) acknowledged that the theory on macropore flow is not advanced enough to adequately represent it in a physically based manner. For now *VSAS4* ignores the role of soil pipes in subsurface hydrology but the acknowledgement is made that this may be serious disadvantage when using the Tanllwyth data.

The Tanllwyth has a flume that provides hourly streamflow data for the catchment. Very close to the flume site there is an automatic weather station which provides the main meteorological data. The rainfall that is measured here is averaged for the whole of the Tanllwyth using earlier studies of rainfall distribution within the Severn catchment, before being entered into the Institute of Hydrology data bank. Also available from this site are potential evaporation estimates at hourly intervals, calculated using the Penman-Monteith equation.

The availability of hourly potential evaporation estimates from a weather station site within the watershed area is an example of the kind of extra data available from research catchments (see section 8.2.1) that other catchments do not have. The version of *VSAS4* used in the robustness testing (chapter six) had potential evaporation as a fixed amount per timestep, thereby providing a simple estimate of potential loss through evaporation. With a temporally variable potential evaporation estimates available this can be simply read in as an input file and used as a replacement for the original single figure. This has the advantage of obtaining a potential evaporation estimate without undergoing the calculations of the Penman-Monteith equation in full. As described in section 4.3.2.1 the potential evaporation estimate is transferred to the leaf and stem scale and the actual evaporation volume computed with respect to available water (storage and/or rainfall) at that scale. This will be better than the original single value of potential evaporation, in that it will account for temporal variation and provide a rough guide to evaporation but there are still two problems associated with this estimate. In chapter four the observations of Calder (1990) that advection often produces more energy than radiative energy sources (assumed to be the main energy in the Penman-Monteith equation) in upland forests still apply. This suggests that the Penman-Monteith equation is not necessarily an accurate estimate of potential evaporation in these circumstances. The second problem is that the meteorological measurements used in the Penman-Monteith calculations are from a site in the valley at the bottom of the catchment, this means they cannot be considered representative of the whole forest in the catchment. This problem cannot be overcome without detailed measurements at numerous sites within the catchment which is well beyond the scope of this study. Both of these problems are insurmountable within this modelling study but the accuracy of the potential evaporation estimation has to be borne in mind when analysing the results.

The Tanllwyth data are not perfect as provides only one or two snapshots (runoff records are 18 *years* in length) of an afforestation occurring within a catchment but it presents the best available alternative. In section 8.1.2 it was stated that the main part of the validation involves testing simulated model predictions against observed storm hydrographs. As there is no other data source available to test the model at different stages of afforestation hypothetical simulations are then run to imitate the effects of more or less forest growth occurring.

The use of a single catchment for the validation means that the first of the options given at the start of this section (using data from throughout the length of the hydrological record) has to be used in validation testing. The length of hydrological record at Tanllwyth is less than the period of afforestation so it is necessary to select storms from as much of the record as is possible. The storms were selected from the historical record as a series of similar storms (in peak rainfall size) from different periods within the afforestation period.

These sets of data were obtained by searching through the daily rainfall records for the Tanllwyth to find the necessary storms and then extracting the rainfall, runoff, and evaporation data for the hourly timestep ready for direct usage in *VSAS4*. The three events chosen for initial detailed investigation are summer storms with an estimated stormflow return period of 1-2 *years*. The reasoning for the choice of summer storms is that then snowmelt contribution is not a contributory factor to the runoff. N.B. The storms were selected from daily rainfall records and therefore may not appear as similar in size and shape when the hourly rainfall and flow records are obtained and plotted.

After the simulations of these relatively simple (i.e. single or double peak) hydrographs two further storms were selected to test the ability of *LUCAS* in more extreme conditions. These storms were very large complex events (20 and 50 *year* return period stormflows) occurring in February (with no measured snowfall) and September.

8.3 LUCAS initial conditions

In order to move away from the approach that combines validation with calibration (e.g. Calver (1988)) as much input data as was possible was derived from several sources. These included field visits to the catchment, previous studies in the catchment, and other derived sources. The use of independently derived input data in the model ensures that it is run **without attempting to fit the output to the observed**, and therefore an objective assessment can be made on model performance. There are two exceptions to this: some of the forest growth parameters had to be obtained through calibration; and the initial soil moisture conditions were obtained through draining the catchment until the flows were close to the baseflows prior to each storm. The forest growth parameters were obtained through calibration because there was no other method of finding their values, and there was no initial soil moisture data that could be used.

The use of drained initial moisture conditions is not unreasonable for a scheme such as *LUCAS* as it is intended as a predictive tool. This means it can be used to investigate the likely effects of a forests growth on a given storm and the prior baseflow can be calibrated using data prior to afforestation. The assumption then has to be made that the baseflow would be the same following afforestation. This may not be an entirely valid assumption as the forest canopy transpiration may drain a catchment to a greater extent than an unforested catchment but without a linked transpiration-root uptake routine this could not be tested.

8.3.1 Topography and soil mantle geometry

The first task in the topographical representation used in *LUCAS* is to subdivide the catchment into a series of hillslope planes or segments as described in section 4.3.1.5. To achieve the appropriate scale of segmentation it was necessary to consult the previous applications of the *VSAS* model and to a lesser extent consider the scale used in previous modelling studies of the Tanllwyth that have used similar discretised modelling schemes.

Table 8.2 sets out the previous applications of *VSAS* in more detail than is shown in table 8.1. In previous physically based, distributed modelling studies using the Tanllwyth (i.e. Rogers (1985); Calver (1988); both using the *IHDM4*) the catchment was subdivided into three large planes, one triangular shaped at the catchment head and two more rectangular planes running down the valley sides. Apart from the Les Alloux segmentation of Fawcett (1992), where the problems of discretisation and scale were being investigated, all the previous applications of *VSAS4* have used a higher number of hillslope segments than three (see table 8.2) despite the catchments being smaller than the Tanllwyth. To maintain the strict guide-lines on topography set out in section 4.3.1.5 for the discretisation of the Tanllwyth it is necessary to have more than three segments.

The segmentation of the Tanllwyth used for the validation testing is shown in figures 8.3 and 8.4. The use of twelve segments (four of which are further divided into three subsegments each) gives a greater emphasis to the hillslope scale than the previous *IHDM4* applications on the Tanllwyth (Rogers (1985) and Calver (1988)). This is also useful for the difference in forest management within the catchment, as separate forest inputs can be used for the different segments and therefore the greater the number of segments the greater that discretisation can be. The segmentation was carried out using a 1:5000 topographical map of the upper Severn catchment specially prepared for the Institute of Hydrology. This extremely detailed map is an example of the additional data available from a research catchment, as the largest scale topographical map normally available in the United Kingdom is 1:10000.

The segments and subsegments were divided into ten increments upslope except where the distance from stream to watershed boundary was particularly small (segments 3,4,8, and 12 in figure 8.4) in which case the number of increments was set at six.

The soil mantle was assumed to be $2m$ deep throughout the catchment (Newson (1976)) and this was subdivided into three element depths. The soils map in Newson (1976) was used to gain an estimate of the different soil types within the Tanllwyth. It was decided to use two soil types, the majority of the catchment being a peaty gley (soil type 1) but some of the upper reaches being a peaty podzol (soil type 2). Figure 8.5 shows the soils discretisation used in the validation runs. The physical properties of these soils are detailed in section 8.3.3.

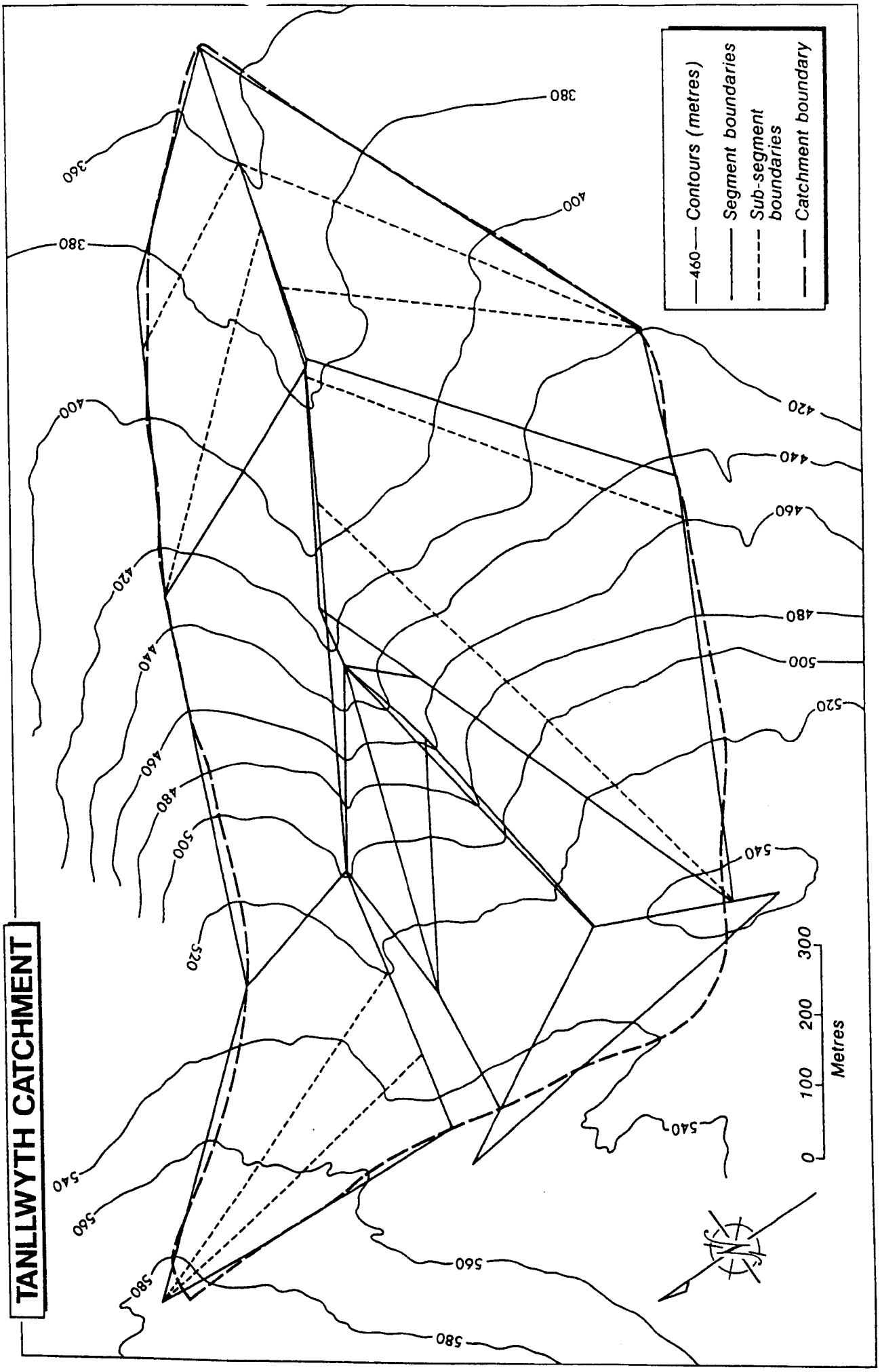

Figure 8.3: The Tanllwyth catchment with segments and subsegments

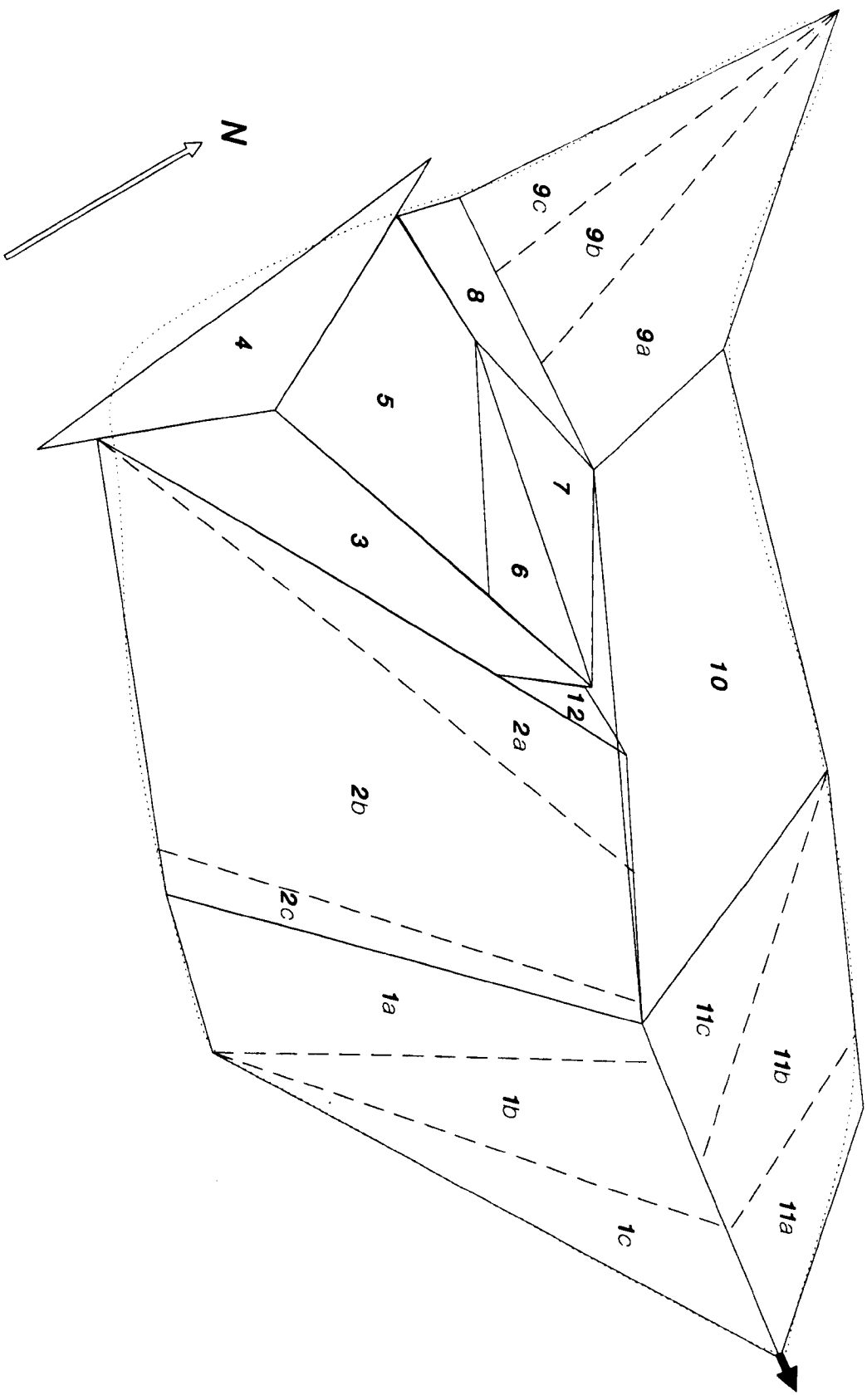

Figure 8.4: Segment numbers for Tanllwyth segmentation

Catchment	*Size (km^2)*	*No. of segments*	*Model version*	*Reference*
Fernow, West Virginia, U.S.A.	0.38	19	*VSAS1*	Troendle (1979), (1985)
Whitehall, Georgia, U.S.A.	0.24	23	*VSAS2*	Bernier (1982), (1985)
" " "		19-23	*VSAS3*	Whitelaw (1988)
Bicknoller, Somerset, U.K.	0.50	15	*VSAS3*	Whitelaw (1988)
Lac Laflamme, Quebec, Canada	0.68	9	*VSAS2*	Prevost *et al* (1990)
Les Alloux, Switzerland	0.035	1	*VSAS3*	Fawcett (1992)
La Corbassier, Switzerland	1.88	29	*VSAS3*	Fawcett (1992)

Table 8.2: Previous segmentations using the *VSAS* scheme

8.3.2 Forest growth

Three methods were used to obtain the forest growth input parameters: field measurement; knowledge of tree growth in the area; and subsequent model calibration using the results from the sensitivity analysis in section 7.3.5. The actual values of input parameters for the forest growth model are presented at the end of this section in table 8.5.

A field visit to the Hafren forest, of which the Tanllwyth is a part, was used to derive important forest data for the growth model. It was found that there have been two major types of forest management within the catchment. The first of these was in the lower reaches of the catchment and involved tree planted with an initial spacing of $1.4m$ and some thinning occurring in a very small area at the base of the catchment. The second management type on the remainder of the catchment involved a planting inter-tree spacing of $0.9m$ with no thinning at any stage. For each management type a location within the Tanllwyth catchment was chosen and a small sample of trees analysed to find which Forestry Commission yield class they belonged to. This involved sampling trees along several planting lines and recording: the *dbh* (diameter at breast height) of each live tree; and the number of live trees in each sample. The results from these two samples are shown in table 8.3 along with data from two yield classes for the same management record. Table 8.3 indicates why it was decided that the Tanllwyth forest appears to be within yield class 12.

The forest growth model simulates the growth of a mono-specific forest within a representative area of each hillslope segment and then assumes that the forest is uniform within the segment. This means that a different forest can be simulated on the separate segments of the Tanllwyth to represent the two different management records found within

Figure 8.5: Discretisation of soil types for *VSAS4* on the Tanllwyth

	0.9 metre spaced			*1.4 metre spaced*		
Statistic	***Measured***	***Yield class 11***	***Yield class 12***	***Measured***	***Yield class 11***	***Yield class 12***
Sample size	32	-	-	42	-	-
Mean *dbh* (*m*)	0.165	0.11	0.15	0.175	0.15	0.18
% live trees	35	47	25	50	59	47

Table 8.3: Results from samples of trees measured within the Tanllwyth catchment. The yield class data is from Edwards & Christie (1981) for forest with the same management record i.e. same spacing and age with no thinning.

the catchment. Consequently the forest simulations within the catchment were subdivided in the manner shown in figure 8.6 with the 0.9*m* spacing forest being in the upper reaches of the catchment. In the lower reaches where the forest was 1.4*m* spaced the thinning has been ignored because evidence for it was only found in a very small region at the base of the catchment.

The second part of the field measurement was to establish the *dbh* to tree height relationship for the forest, a selection of twenty trees were measured to establish this relationship that forms a fundamental part of the forest growth model. The trees were selected from sites all over the Hafren Forest as the trees within the Tanllwyth are of fairly uniform height and do not present the full range of tree sizes necessary for the model to predict size throughout the forest growth. The tree heights, where higher than arm reach, were measured using an Abney level and tape measure laid out along the slope. Tree *dbh* was measured as a trunk circumference at 1.3*m* above the ground and converted to diameter at a later stage. The measured values are presented as a scatter plot in figure 8.7 with the least squares regression relationship line and equation also shown. The good relationship obtained between *dbh* and height (87.3% of the variance in tree height is accounted for by the regression line) from a sample of twenty trees is common for trees in any environment. This confirms the ease at which this relationship can be obtained, ready for usage within the forest growth model.

If the regression equation shown in figure 8.7 were used in the forest growth model the smallest tree possible would be 1.2*m* high which is close to reality as the *dbh* of a tree is measured at 1.3*m* above ground level and therefore any tree less than 1.3*m* in height would have no *dbh*. A height of between 1.2*m* is larger than the normal size of seedlings planted by the Forestry Commission (normally approximately 0.5*m*) but has been used as a

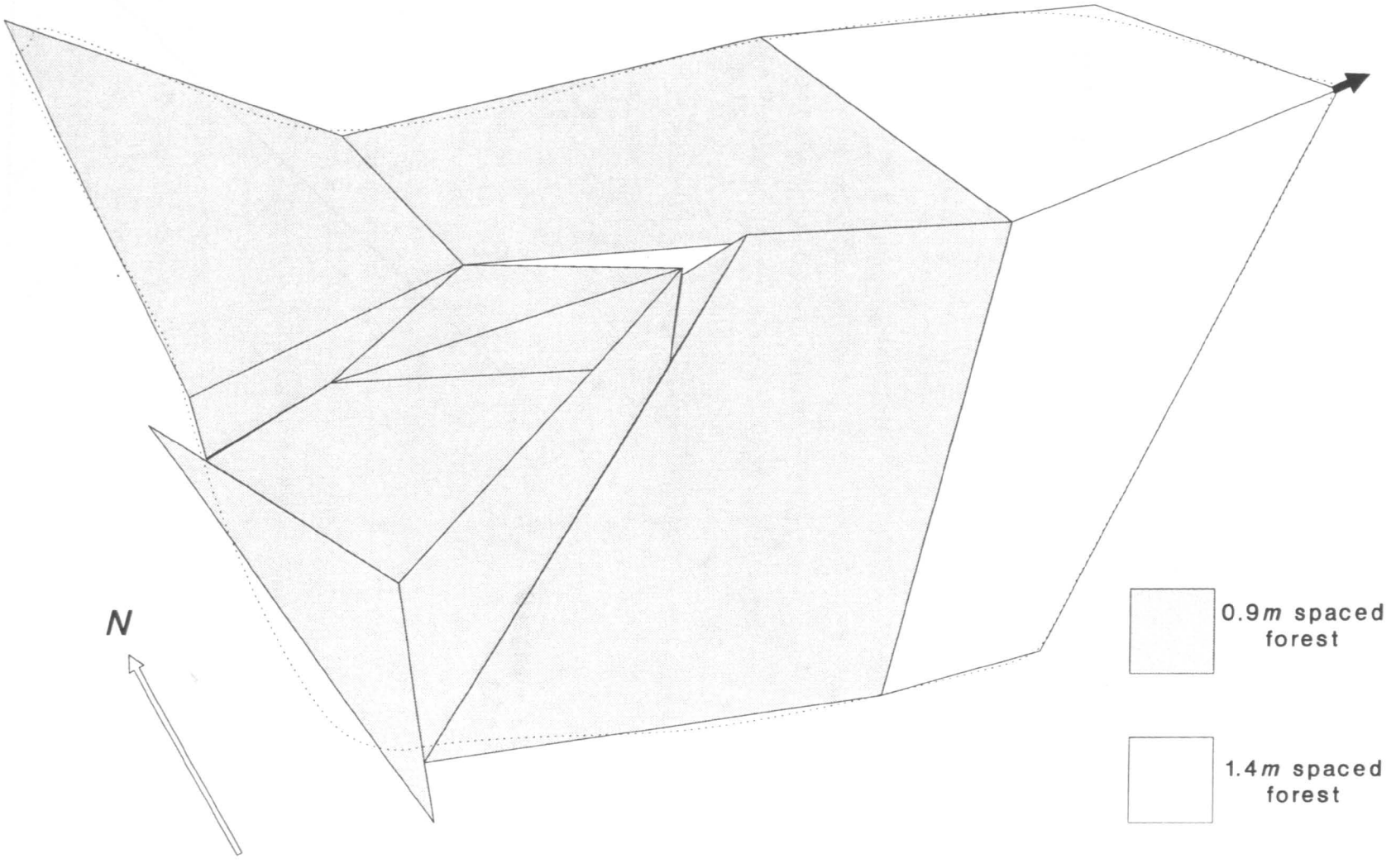

Figure 8.6: Discretisation of forest types (inter tree spacing) for *LUCAS* on the Tanllwyth

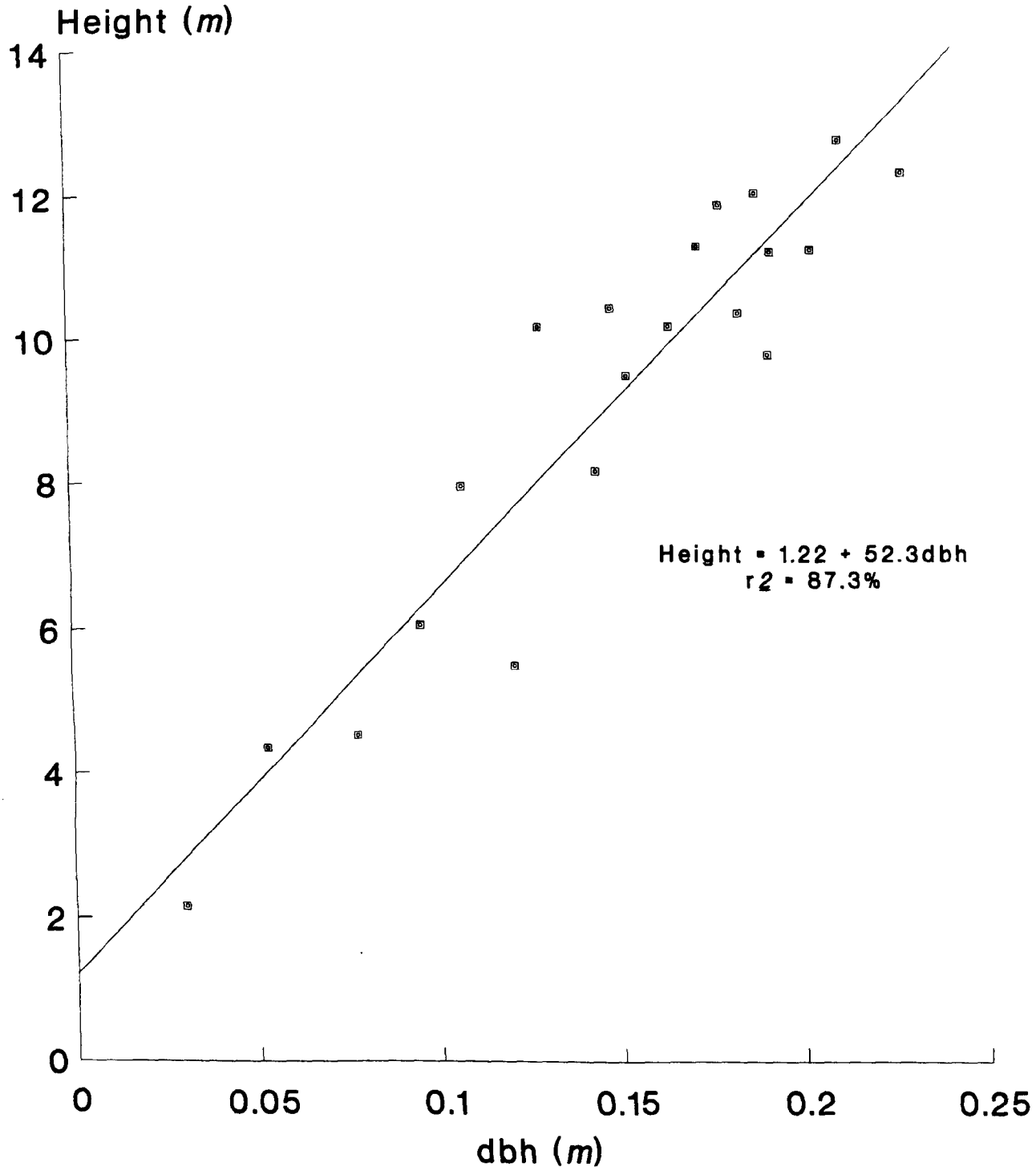

Figure 8.7: Scatter graph of measured relationship between tree diameter at breast height (dbh) and total height

	0.9m spacing		*1.4m spacing*	
Run	***Crown angle***	***ZOI***	***Crown angle***	***ZOI***
A	6°	1.35	7°	1.40
B	6°	1.27	6°	1.44
C	6°	1.30	6°	1.35
D			6°	1.42

Table 8.4: Input data used in calibration runs for forest growth model shown in figures 8.8-8.11

starting point for the tree growth here because *dbh* is used as the growth statistic not total height. The fact that the growth starts at a slightly larger value than reality is acknowledged as a model limitation but little can be done to overcome it and the effects are likely to be confused by the advent of inter-tree competition.

The mean growth ratio (g) was derived from assuming that the growth of the trees allowed them potentially to grow to close to their full size within 70-75 *years*. This is a fair to conservative estimate of a trees potential growth in Great Britain; it has been kept conservative to allow for the fairly severe conditions of upland Mid-Wales. N.B. the potential full size is not the actual size reached in a forest plantation prior to logging; in the example used here the potential full height is approximately 38m, while the maximum height reached in simulation is closer to 18m. The standard deviation of the growth ratio was assumed to equal 25% of the mean value.

The remainder of the model inputs were derived by calibrating the model against the yield table measurement for the relevant tree spacing simulations. The calibration simulations were started once the mortality data had been extracted from the Forestry Commission yield tables for the relevant yield classes discussed earlier. Initial values of the input parameters were estimated and then simulations run until the results converged to close to yield table average *dbh* and plot density curves (as were used in section 7.3), this process is shown in figures 8.8-8.11 with the varied values shown in table 8.4. The two parameters varied to gain a convergence of results were: the proportion of the crown as the zone of influence (ZOI); and the crown angle. There are two reasons why these were used: the sensitivity analysis in section 7.3.5 indicated that the model was particularly sensitive to these parameters (see table 7.5); and there were no applicable measurements to set them from. The input values derived from this calibration are shown in table 8.5.

As can be seen from figures 8.8-8.11 a fairly good correlation was obtained

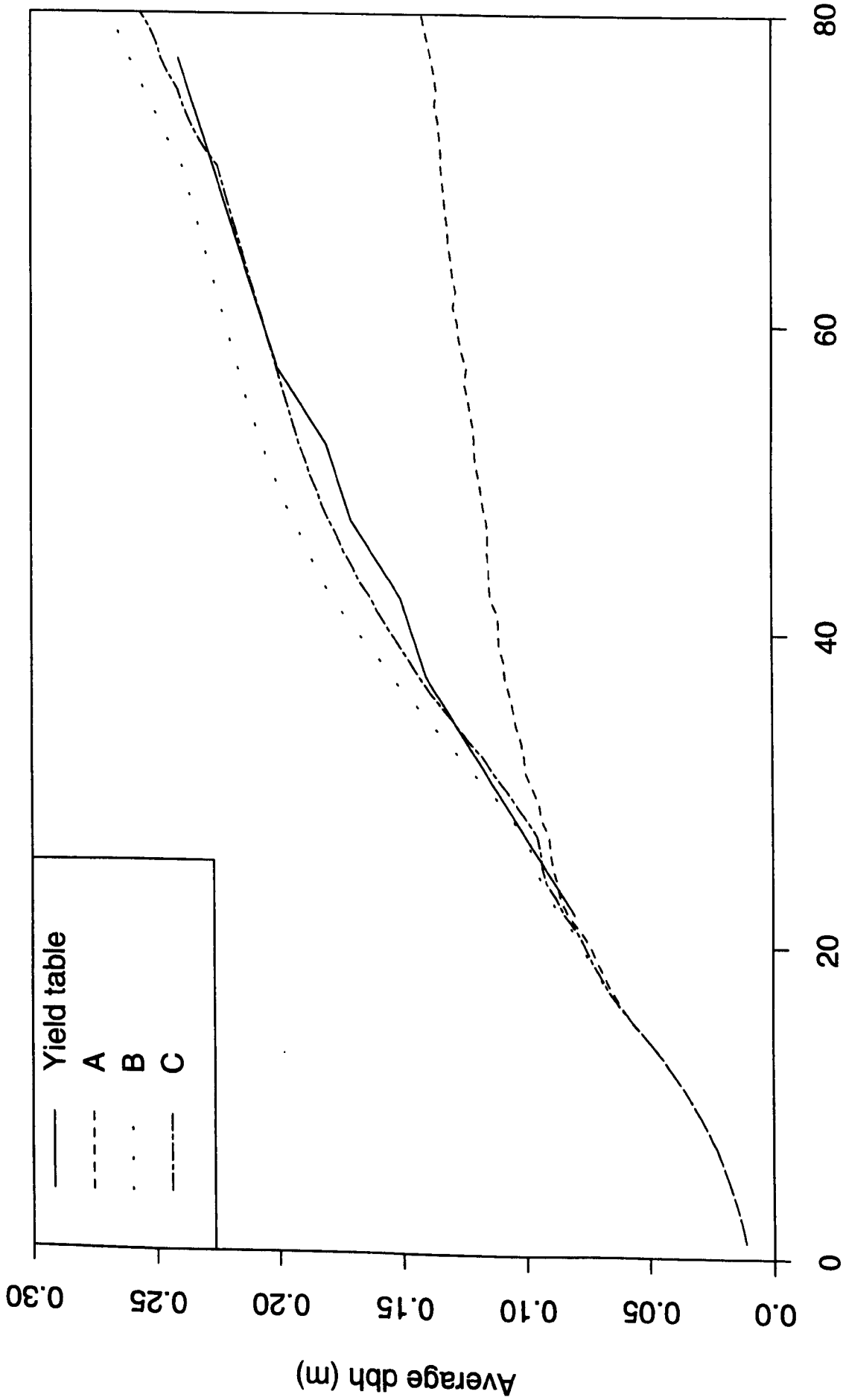

Figure 8.8: Average growth (dbh) curves for calibrated parameters (0.9*m* spaced forest plot; yield class 12). See table 8.4 for input values of calibration curves

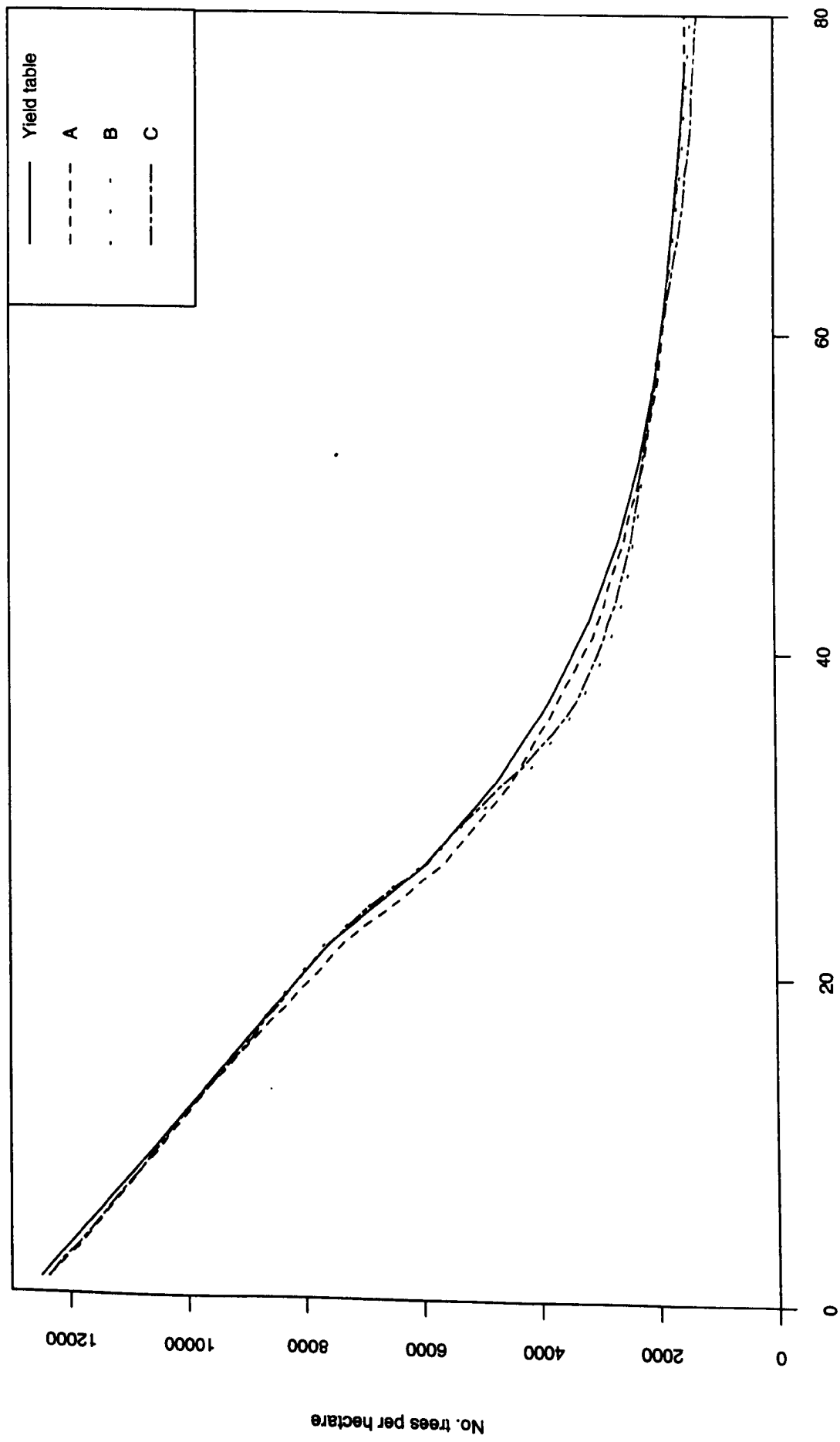

Figure 8.9: Plot density curves for calibrated parameters (0.9*m* spaced forest plot; yield class 12). See table 8.4 for input values of calibration curves

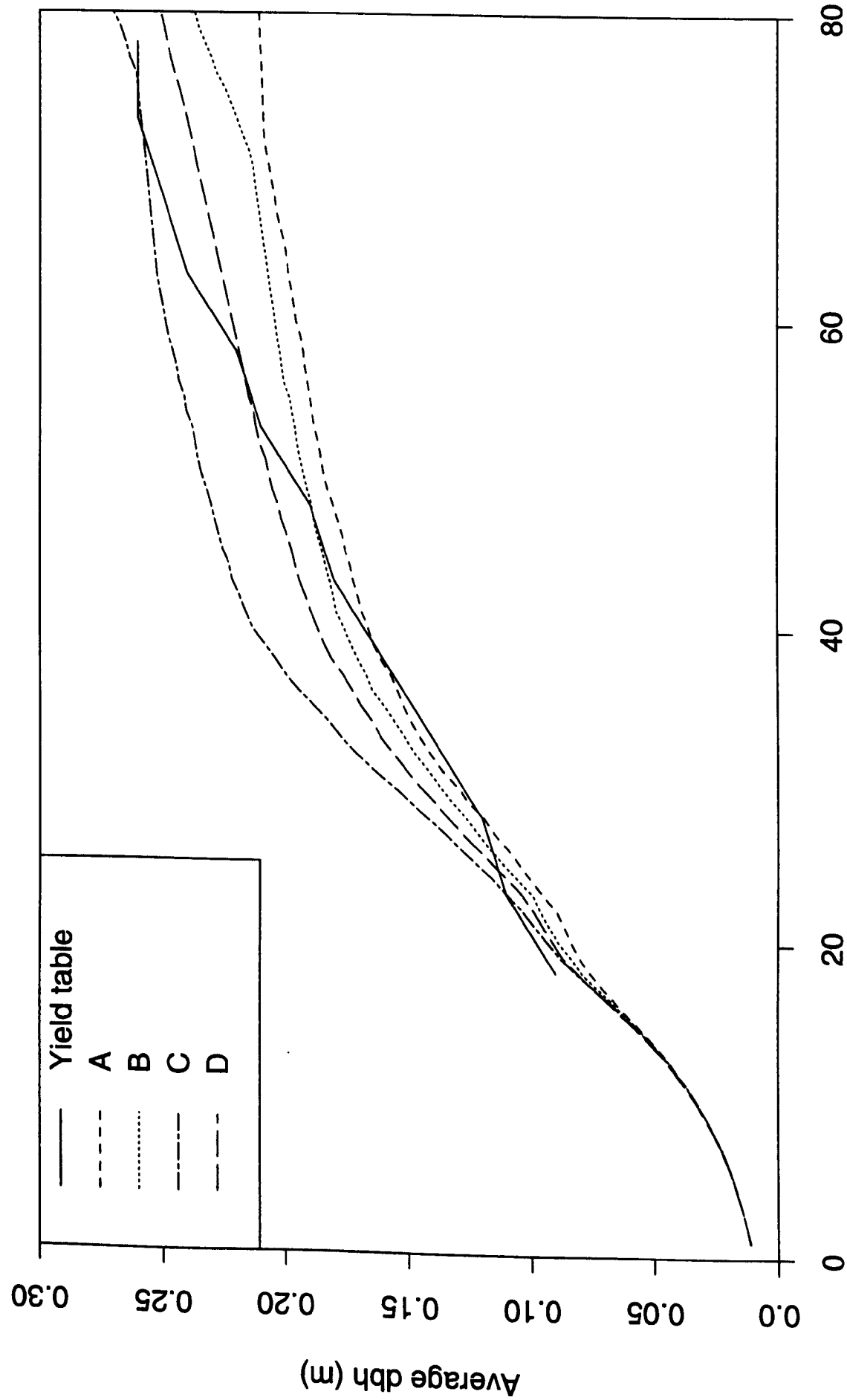

Figure 8.10: Average growth (dbh) curves for calibrated parameters (1.4*m* spaced forest plot; yield class 12). See table 8.4 for input values of calibration curves.

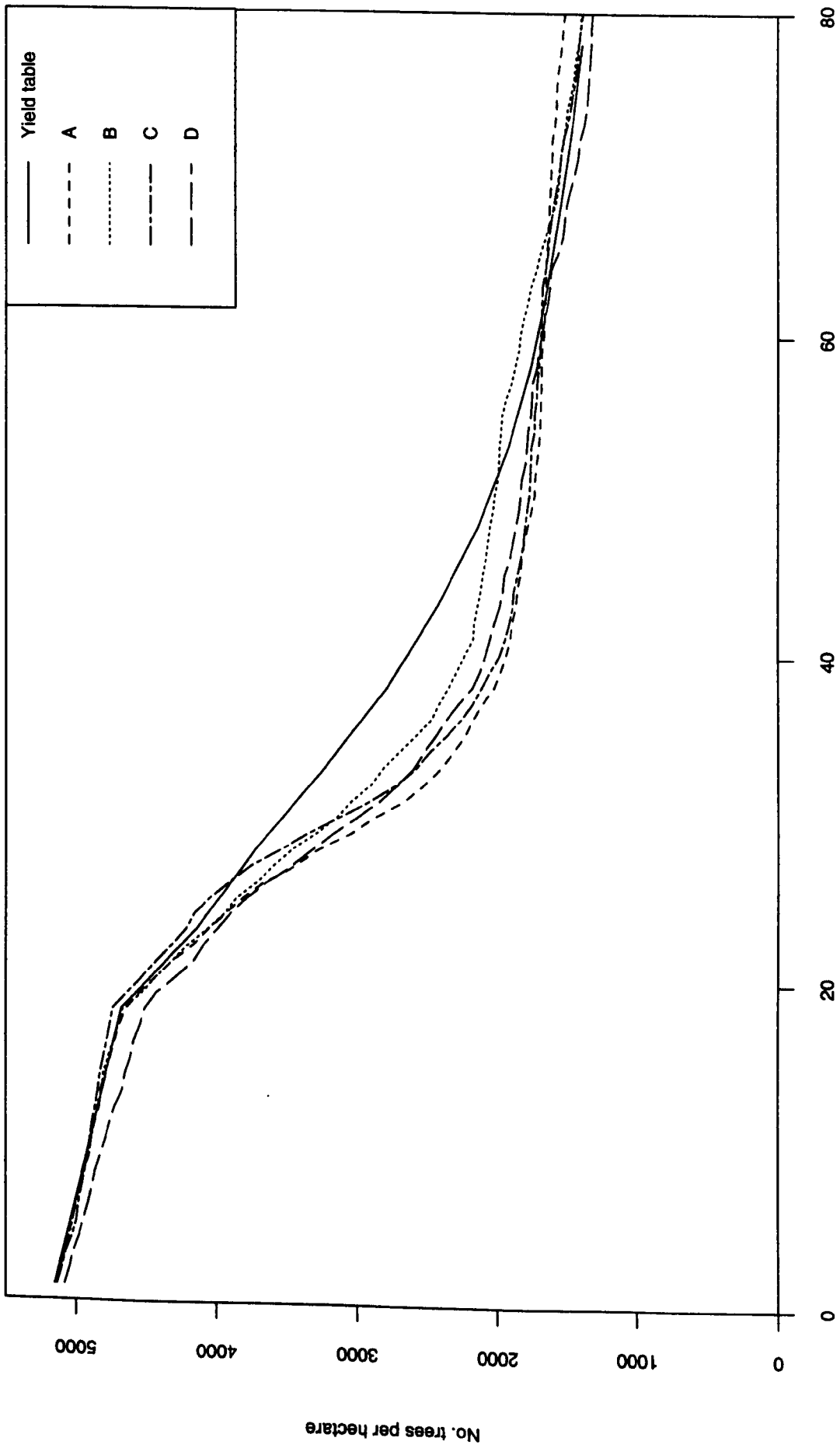

Figure 8.11: Plot density curves for calibrated parameters (1.4*m* spaced forest plot; yield class 12). See table 8.4 for input values of calibration curves

Length of plot side	110 *m*
Initial *dbh*	0.01 *m*
Maximum *dbh*	0.70 *m*
Growth period	80 *years*
Mean growth ratio	0.126
Standard deviation of growth ratio	0.032
Slope of height v *dbh* relationship	52.3
Intercept of height v *dbh* relationship	1.22
Crown angle	6°
Proportion of tree height to base of crown	5%
Proportion of tree crown as zone of influence (ZOI)	1.30 (1.42)
Number of plot density measurements	13 (14)

0.9*m* spacing

Year	1	22	27	32	37	42	47	52	57	62	67	72	77
Density	12488	7652	5922	4736	3820	3133	2637	2278	2022	1838	1697	1579	1483

1.4*m* spacing

Year	1	18	23	28	33	38	43	48	53	58	63	68	73	78
Density	5148	4675	4144	3717	3224	2772	2419	2131	1913	1752	1632	1537	1453	1386

Table 8.5: Final input data used in forest growth model (yield class 12). Values in brackets are for 1.4*m* spacing simulation.

between predicted and observed size and plot density. This confirms the applicability of the forest growth model as a canopy growth predictor as the conditions simulated here are considerably different for those used during the sensitivity analysis in section 7.3.5. The amount of calibration required was not large but does indicate that at present it would be difficult to use this part of *LUCAS* without some kind of measured forest growth data to calibrate the model against.

For the 0.9*m* spaced forest (figures 8.8 and 8.9) both the average *dbh* and the plot density were well predicted by the final combination of parameters (C). The predictions were not quite so good for the 1.4*m* spaced forest where the final parameter combination (D) was not so able to predict the average *dbh* curve in figure 8.10 (over-predicting between 25 and 55 *years* and then under-predicting after this) and also over-predicting the mortality between 25 and 60 *years* in the plot density curve (figure 8.11).

The results shown in figures 8.8-8.11 are a validation of the forest growth model as a predictor of forest growth. Because the validation involved a degree of calibration it

cannot be seen as a totally independent validation, but the fact that the forest growth model is not fully physically based means there is no other way of obtaining the necessary input parameters. The results shown in figures 8.8-8.11 do show that the model is able to reproduce with considerable accuracy the average growth statistics of a forest canopy under two separate management records and therefore is a reasonable model to act as a pre-processor within the *LUCAS* scheme.

8.3.3 VSAS4

The input parameters required for the hydrology section of *LUCAS* (i.e. *VSAS4*) were derived from previous studies in the Tanllwyth and other studies in similar surroundings. The parameter values chosen are listed at the end of this section in table 8.6.

8.3.3.1 Soil properties

The discretisation of the soils in the Tanllwyth (as used by *VSAS4*) is shown in figure 8.5, the two soils being a peaty gley (type 1) and a peaty podzol (type 2) in the upper reaches. In a calibration of the *IHDM4* model on the Tanllwyth, Calver (1988) found that the optimised porosity value (i.e. maximum volumetric proportion of water the soil can hold) of the soil was 0.3 which was compared to the value of 0.5 obtained by Bathurst (1986a) using the *SHE* on the contiguous Wye headwaters. The value of 0.3 is very low for any soil containing a fair degree of peat in its structure (Rawls *et al* (1982) list a porosity of 0.385 for a clay soil and 0.432 for a silty clay loam). The porosity values chosen for this study are 0.33 for the peaty gley (soil type 1) and 0.425 for the peaty podzol. The higher value for the second soil type reflects the fact that there is a greater amount of peat within its structure. The suction moisture curves for these soils were derived from the porosity values using a standard shape and are shown in figure 8.12.

Calver (1988) derived a saturated hydraulic conductivity (K_{sat}) for the Tanllwyth of $100 cmhr^{-1}$ in the calibration of *IHDM4* whereas Rogers (1985) used a value of $0.09 cmhr^{-1}$ in simulations of the Tanllwyth. The extreme sensitivity of *VSAS4* to K_{sat} has been shown in chapter six, so it is important to try get a good idea of the actual value for validation. The derived value of Calver (1988) seems very high (it corresponds roughly to the highest K_{sat} used in chapter six) for the type of soils within the catchment but the value used by Rogers seems correspondingly low (lower than the lowest value used in chapter six). As a measure of comparison Rawls *et al* (1982) give an average saturated hydraulic conductivity of $1.32 cmhr^{-1}$ for a loam which might be expected to be close to peaty gleys or podzols. The difference between the K_{sat} values of Calver (1988) and others can partly be explained by the fact that it is a derived value following model calibration. This means that the parameters optimised become effective parameters within the *IHDM4* scheme and

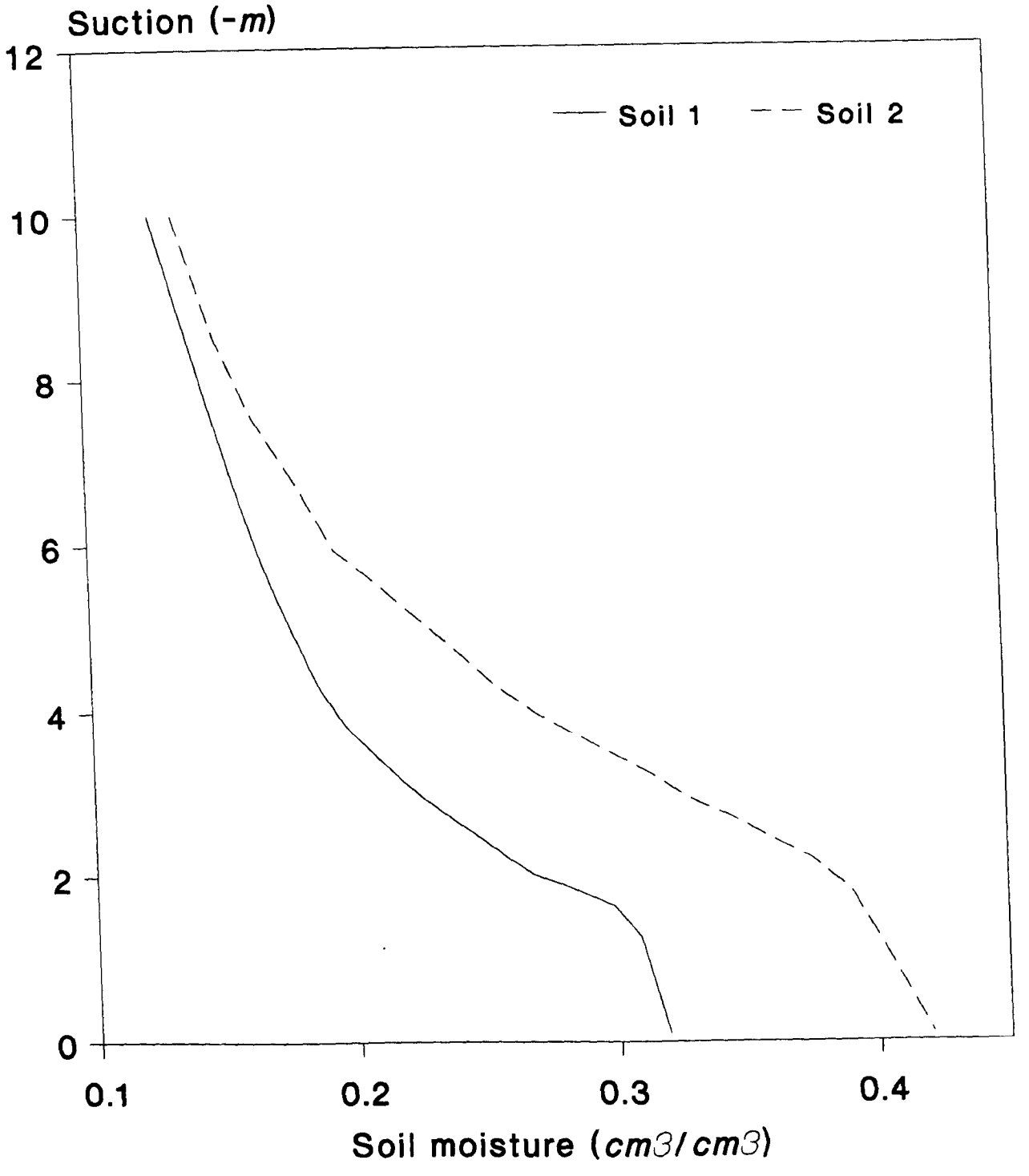

Figure 8.12: Suction moisture curves used by *VSAS4* for the two Tanllwyth soil types

have no real value outside the particular model simulation runs. This highlights the difficulties in using models to derive parameter values for specific sites (e.g. Morris (1980) to describe land use change) as it probably says more about the model than the site or land use change.

VSAS4 represents soil matrix flow as the only form of soil water flow occurring in the Tanllwyth i.e. macropore and pipe flow has not been represented. The assumption is made that one average K_{sat} value (allowed to vary around this mean value) will cover all of the catchment although this is a patently inaccurate assumption as it does not take into account differential flow rates with soil depth or the influence of macropore flow. But there is no empirical evidence as to how saturated hydraulic conductivity does vary within the catchment and little theoretical work into how macropore flow can be incorporated into a physically based model structure so the assumption has been forced upon the study. This means that whatever K_{sat} value is chosen becomes an effective parameter because it is known to be only an average rather than actual measured value. The question is whether to keep the value at a strictly physically realistic value (such as $1.32 cmhr^{-1}$) or use the parameter to represent more soil water flow than just matrix flow?

A compromise between these two options was decided upon and a value of 8.6 $cmhr^{-1}$ was chosen. This value is equivalent to a loamy sand on the Rawls *et al* (1982) scale, the intention being that it allows some larger pore flow than the lower values do. The standard deviation of K_{sat} was set at 25% of the actual value.

8.3.3.2 Rainfall partitioning

The input parameters controlling rainfall partitioning section of *VSAS4* (see table 8.6) were derived from studies of interception in Sitka spruce where these could be found or correlated from the work of Durocher (1991).

The leaf and stem pattern parameters (γ in equation 4.3) which govern the degree of leaf clustering within each Delauney triangle was set at 0.35 (to give a normal distribution) as there was no evidence to the contrary. The value of the mean proportion of tree crown generating stemflow can be derived from the slope of a linear regression between stemflow and rainfall. For Sitka spruce Law (1958) observed that 7% of the above canopy rainfall was accounted for by stemflow although this seems quite high when compared to the average value of 3% reported by Lee (1980) for spruce trees. The chosen average stemflow proportion value (0.04 or 4%) represents a compromise between these values that is closer to the average value of Lee (1980). The standard deviation about the mean was kept high (75% of the mean value) as numerous studies (including Durocher (1991)) have found the variation in stemflow between trees to be extremely high.

The storage capacity for leaf layers, stem layers, and trunk was derived from the

Number of elements per increment (number of layers)	3
Depth of top element per increment	0.5*m*
Proportion of remaining depth for each element	50%
Porosity (saturated moisture content) (soil 1)	0.33
Porosity (soil 2)	0.42
Standard deviation of porosity	0.0
Saturated hydraulic conductivity (K_{sat}) (both soils)	2.4x10^{-5} *ms*$^{-1}$
Standard deviation of K_{sat}	6.0x10^{-6}
Leaf pattern parameter	0.35
Stem pattern parameter	0.35
Mean proportion of crown generating stemflow	0.04
Standard deviation of stemflow proportion	0.03
Maximum value of stemflow proportion	0.20
Minimum value of stemflow proportion	0.001
Storage capacity per leaf layer	0.04*mm*
Storage capacity per stem layer	0.04*mm*
Trunk storage capacity	0.02*mm*
Drainage coefficient a	3.7
Drainage coefficient b	3.9x10^{-5}
Internal time step	2 *min*
Impervious area per segment	0.0%

Table 8.6: Tanllwyth input parameters for *VSAS4*

fact that Leyton *et al* (1967) report a total canopy storage capacity for Norway spruce of 1.5*mm* with a leaf area index of 15. By dividing the storage by the leaf area index a measure of the total storage per layer is derived (0.1*mm*) which is then subdivided between leaf, stem and trunk. The greater proportion is shared between leaf and stem layers as these represent more likely storage surfaces without direct drainage. The drainage coefficients were kept the same as derived by Durocher (1991) as no values could be found for Sitka spruce at the correct temporal and spatial scale.

8.3.3.3 Other parameters

The internal timestep (for the calculation of soil water flow and rainfall partitioning within the canopy) was set to 2 *minutes*.

The impervious area within each segment (area contributing Hortonian overland flow directly to the stream) was kept at zero because there was no evidence to the contrary.

Initially it was hoped that this parameter could be used to simulate pipeflow in the catchment but there are two physical reasons why this is not possible. Firstly there is no measurements of how much area is drained by pipes and secondly, it would require the pipes to be a continuous network draining directly to the stream to work within a timestep as the parameter is intended (i.e. without calibration).

The lag in time for the channel flow between each segment and the catchment boundary was derived by measuring the distance from a topographical map and dividing by the average stream velocity. The average stream velocity was derived from knowledge of the average flows in the Tanllwyth (1975-1987) and the dimensions of the stage recorder.

8.4 Results

The forest growth model that acts as a pre-processor for *VSAS4* within *LUCAS* has been shown to be an adequate predictor of average forest growth statistics although it does require some calibration. The observed versus predicted results for this part of *LUCAS* are presented in figures 8.8-8.11. The results for the hydrological model (*VSAS4*) simulations are presented in the remainder of this section.

The results of the validation testing presented in this section are split between the two aims listed in section 8.1.3. The first section concerns the simulation of the actual data to reproduce the measured storm hydrographs. The second section concerns the examination of *LUCAS* as a simulator of the hydrological effects of long term vegetation change using hypothetical scenarios. This involves using essentially the same data set but altering the canopy structure to see how sensitive the modelled catchment is to these changes. The simulated hypothetical scenarios are used to further investigate the initial conclusions drawn from the empirical validation. They are also used to highlight areas of further development within the model, and to investigate the possibilities for predicting beyond the data set range.

8.4.1 Hydrograph reproduction

The first three summer storms simulated occurred in July 1976, July 1982, and July 1989, consequently the forest growth model simulated the growth of a 28, 34 and 41 *year* canopy respectively (assuming all planting carried out in 1948). The second set of storms (larger and more complex) both occurred in February 1988 and September 1988 so a forest growth period of 40 *years* was used.

July 1976

The storm in July 1976 (figure 8.13) produces an observed triple peak hydrograph caused by four significant rainfall events on a dry catchment (it has the lowest pre-storm baseflow of all events). The model predicts the form of response to a reasonable extent (except for predicting a quadruple rather than triple response) but in all peaks the timing of maximum flow is too early. The shape of the rising and falling limbs of the hydrograph is reasonably close to the observed values although the volume of baseflow following the storm is considerably under-predicted. The model does predict the second storm peak being larger than the first (despite a less intense rainfall) but inaccurately shows the third peak as the largest and shows up a fourth small peak that was not in the observed values.

The volume of streamflow for the entire simulation (including baseflow prior to and after the stormflow peaks) was under predicted by 27%.

July 1982

The July 1982 storm produces an observed single peak hydrograph after two significant, but barely separated, rainfall events (figure 8.14). The response predicted by *VSAS4* corresponds well with the observed hydrograph in timing and shape although the peak volume is slightly over-predicted. The model also predicts a more defined initial peak that is not evident in the observed values. The falling limb of the predicted hydrograph is steeper than that observed but the volume of baseflow after the event is well predicted.

The volume of streamflow for the entire simulation (including baseflow prior to and after the stormflow peaks) was over-predicted by 11%.

July 1989

The storm in July 1989 produces an observed single peak hydrograph from two significant and several minor rainfall events (figure 8.15). *VSAS4* predicts a greater response to all of the rainfall events than that observed but the timing of the main event is fairly well predicted. The main problem with the simulation is the prediction of smaller peaks either side of the main peak that were not in the observed data set. The baseflow following the storm events is well predicted.

The volume of streamflow predicted for the entire simulation (including baseflow prior to and after the stormflow peaks) was over-predicted by 15%.

February 1988

In the more complex storm event occurring in February 1988 (see figure 8.16) the model provides a reasonable prediction except for the recession limbs of the multiple peaks within the main storm peak. This is especially marked in the recession limb and baseflow at the end of the storm event. The actual size and timing of storm peaks is quite well

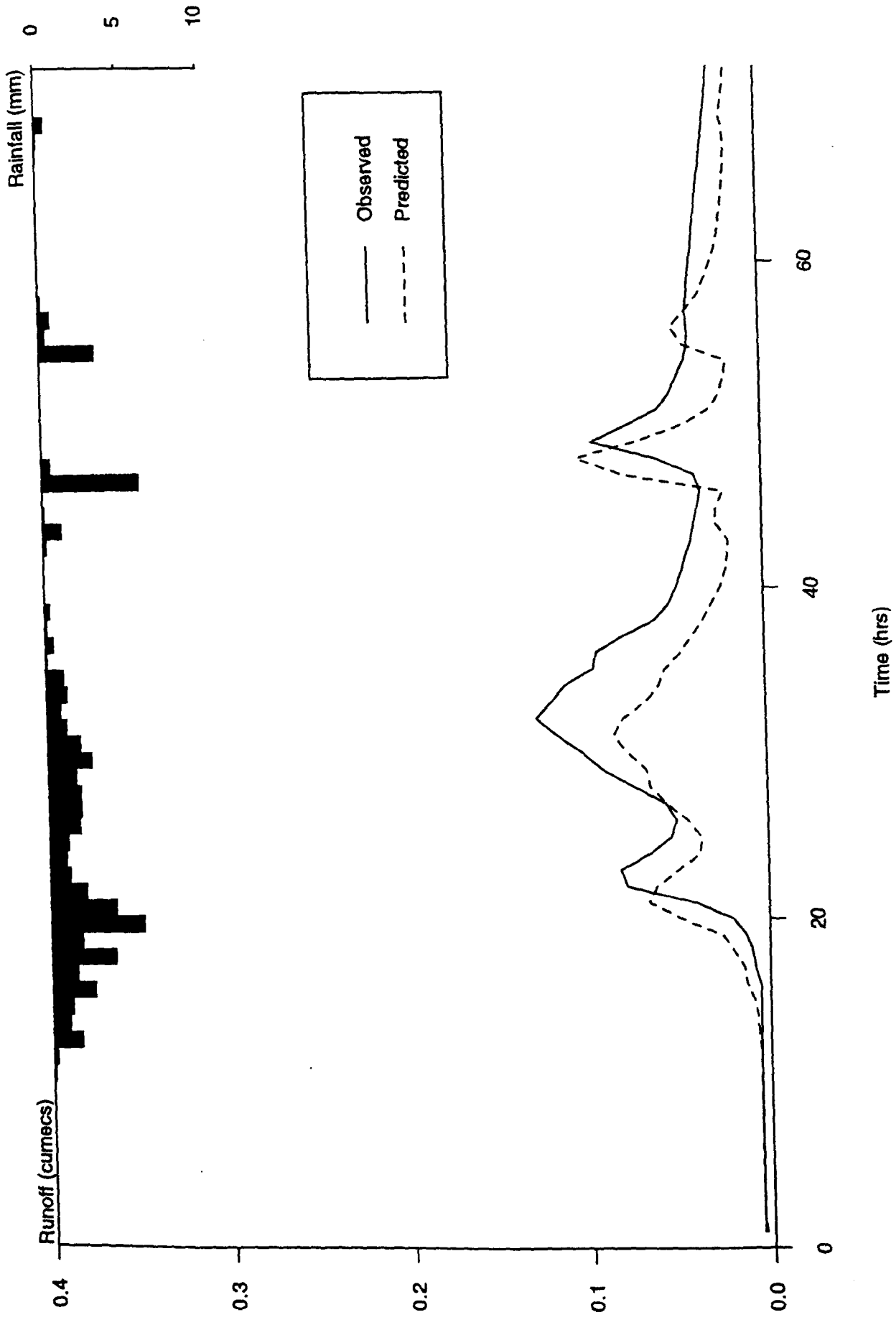

Figure 8.13: Observed versus predicted hydrograph for July 1976 storm event

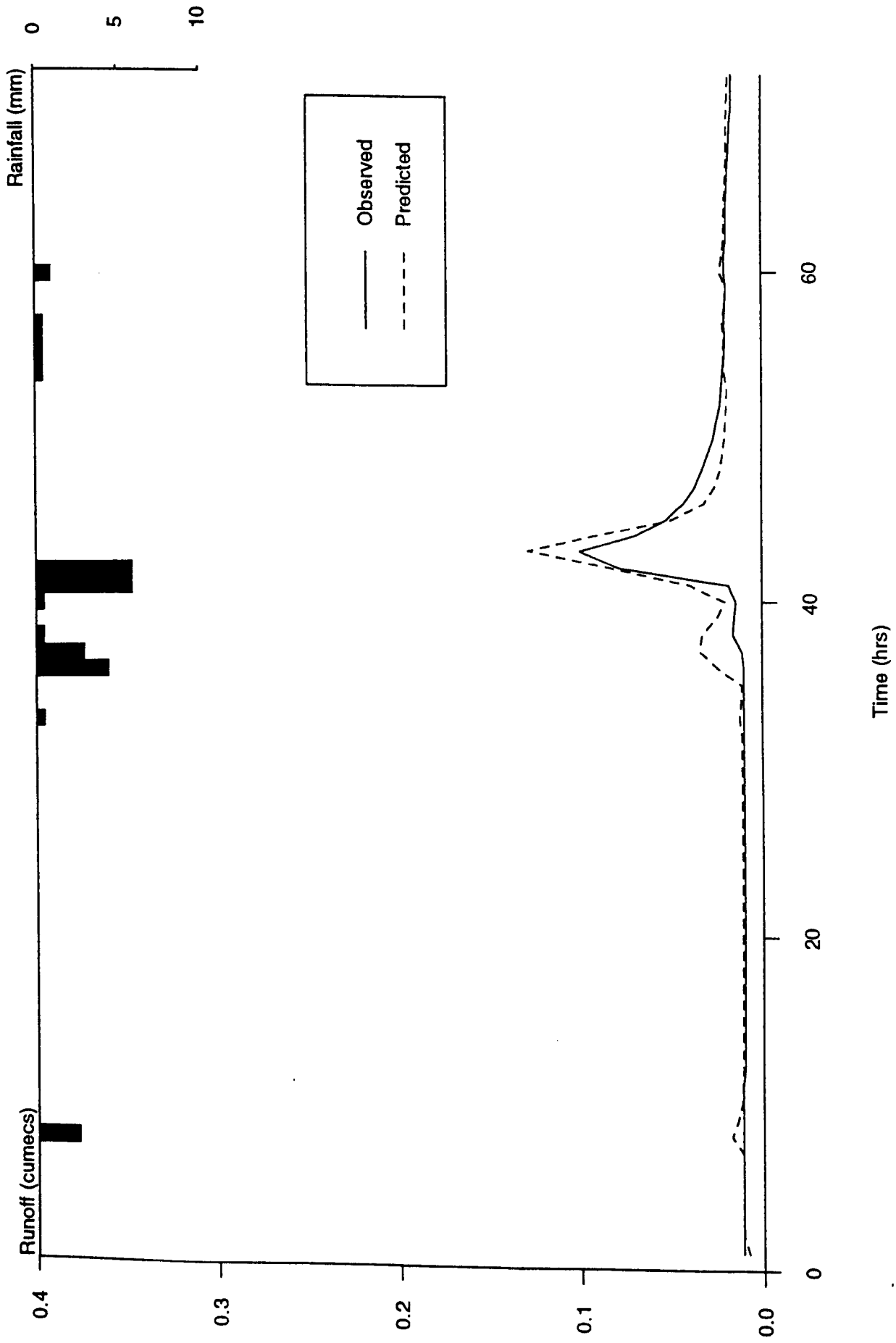

Figure 8.14: Observed versus predicted hydrograph for July 1982 storm event

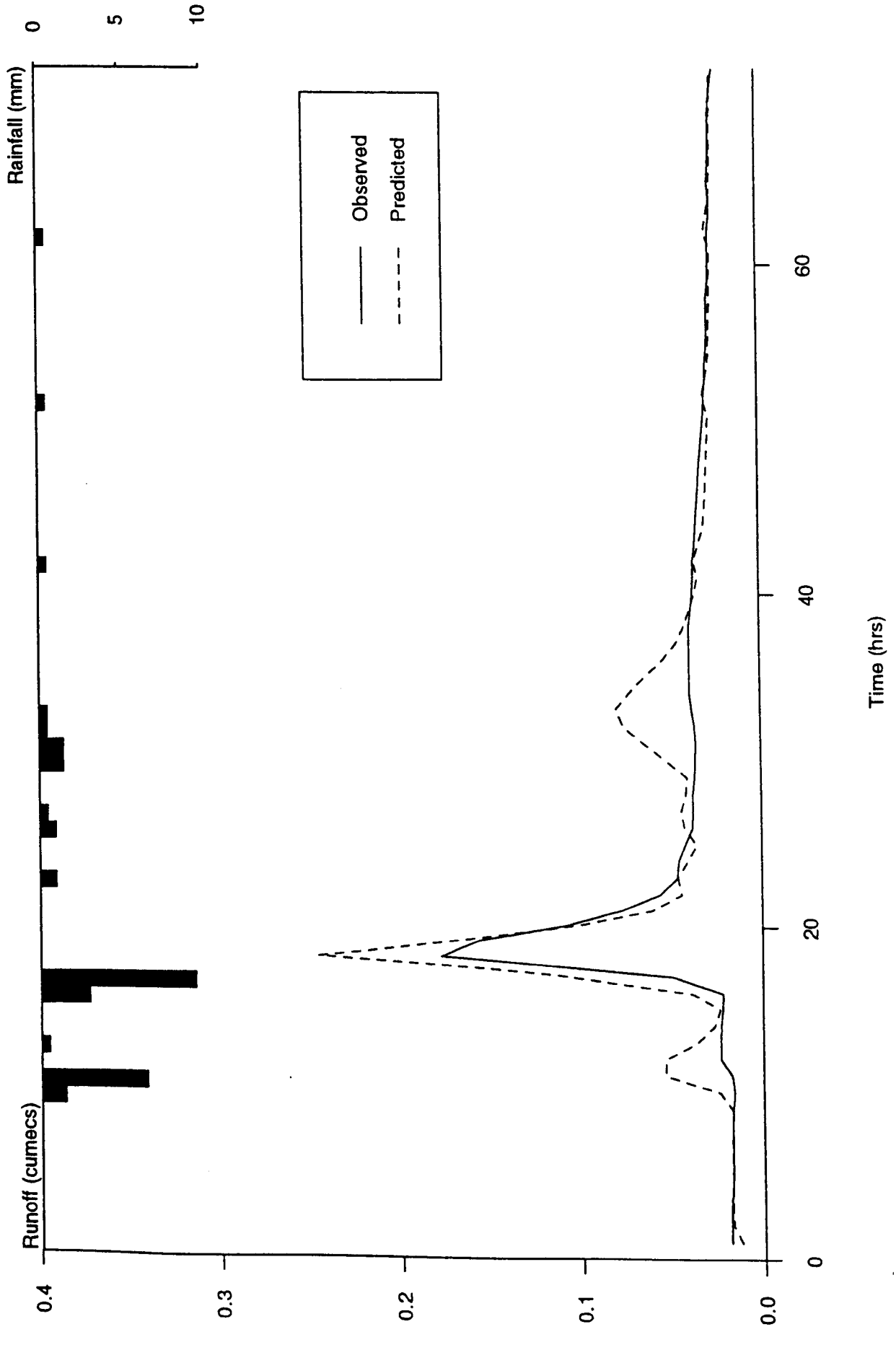

Figure 8.15: Observed versus predicted hydrograph for July 1989 storm event

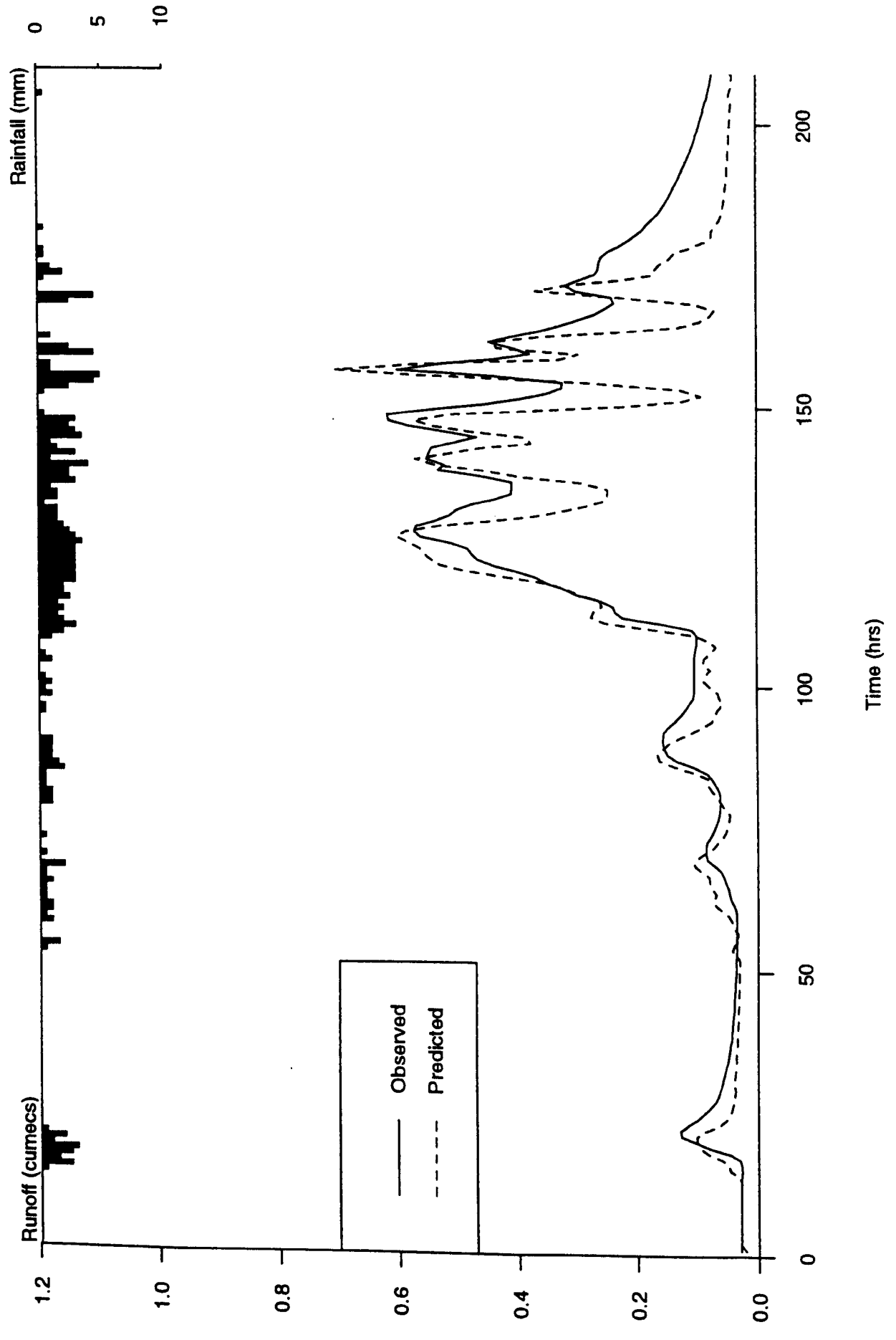

Figure 8.16: Observed versus predicted hydrograph for February 1988 large storm event

predicted but the model seems to be predicting much less soil water flow than in the observed hydrographs, hence the poor correspondence of recession limbs.

The volume of streamflow for the entire simulation (including baseflow prior to and after the stormflow peaks) was under-predicted by 17%.

September 1988

The results for the large storm event in September 1988 (see figure 8.17) provide the worst simulation of these model runs. The model predictions are wrong in size of the peak flows and it also has difficulty with the timing, especially at the latter stages of the storm. The recession limb and baseflow after each peak is considerably different from the observed values.

The volume of streamflow for the entire simulation (including baseflow prior to and after the stormflow peaks) was under-predicted by 33%, reflecting the poor model prediction.

Discussion

The storm hydrographs simulated here show that *VSAS4* is reasonable at reproducing the main features of the hydrographs although it has more difficulty when simulating complex events such as in the September 1988 examples.

In order to investigate the validity of the *LUCAS* scheme it is necessary to look at the three hydrographs that represent similar storms over a 13 *year* period (i.e. 1976, 1982, 1989). If the model is over-predicting the effects of a forest then it might be expected that the 1989 event would be under-predicted, in comparison to the 1976 event, and vice versa for an under-prediction. A comparison of figures 8.13 and 8.15 shows that the predicted response from the 1989 storm is over-predicted whereas the 1976 event is under-predicted, suggesting that *LUCAS* is under-predicting the effects of a forest. This suggestion is by no means conclusive as only three storms have been compared and the length of record is not particularly long. The investigation of the Tanllwyth using hypothetical scenarios should reveal more detail on these predictions and the validity of *LUCAS* as a simulator of the hydrological effects of long term vegetation change.

The main error in the *VSAS4* predictions has been in the receding limb of the hydrograph and subsequent baseflow. This probably reflects the fact that the only soil water flow considered is in the soil matrix although the K_{sat} value chosen was deliberately set high to allow for some large pore matrix flow. The lack of any soil water flow other than matrix flow is a severe restriction to the modelling effort, and although the K_{sat} value can be adjusted to allow for more rapid flow than could be reasonably expected in the matrix, this denigrates the physical basis of the study.

If the estimate of K_{sat} is reasonable for all soil water flow and the rainfall partitioning routine is accurately predicting interception loss then the storm response for a

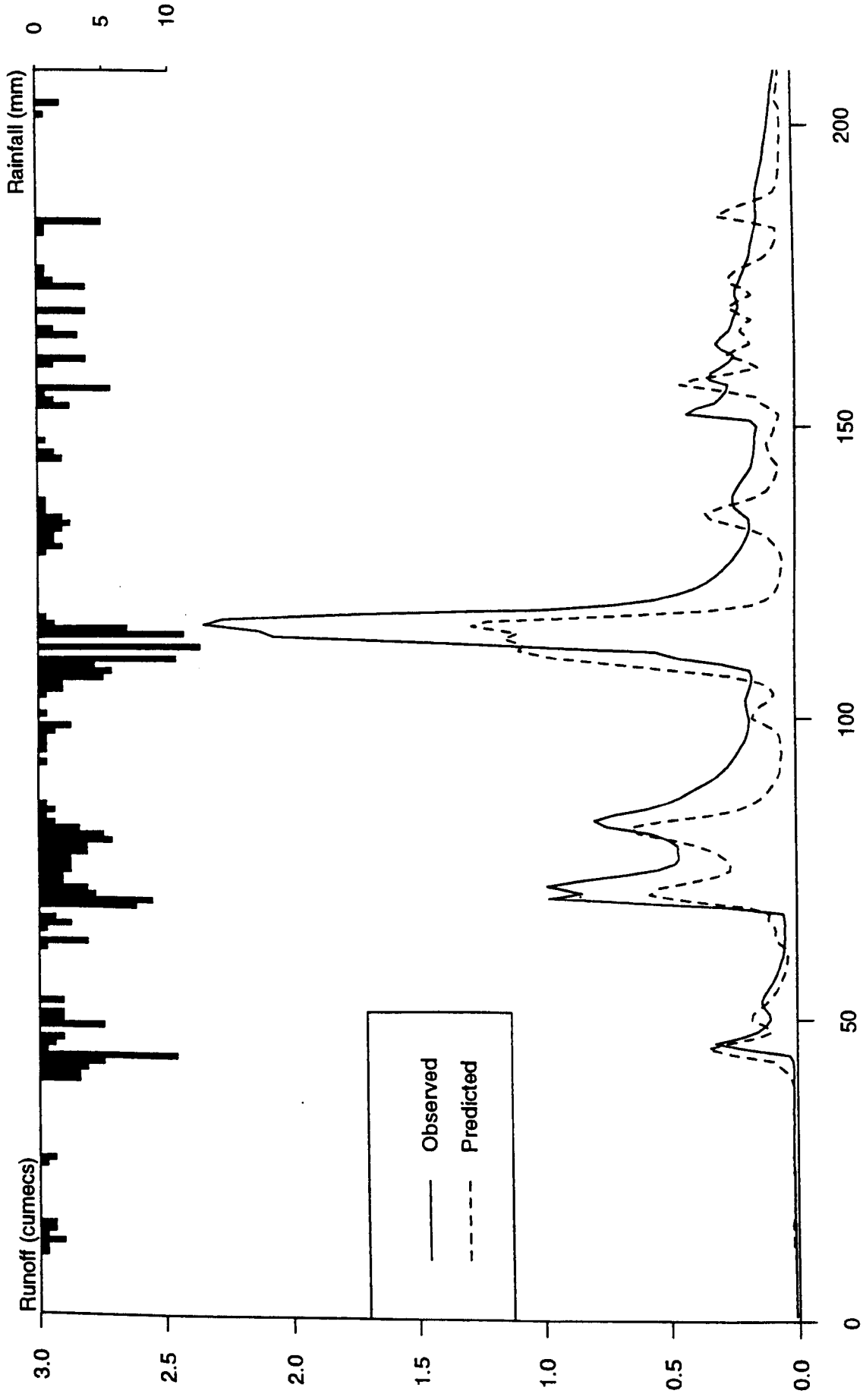

Figure 8.17: Observed versus predicted hydrograph for September 1988 large storm event

non-forested catchment could be expected to be larger than for the afforested catchment. Figure 8.18 shows the storm response during the 1976 event assuming the catchment was totally non-forested. This prediction has a considerably flashier response than the forested catchment and the baseflow after the peak is under-predicted suggesting that K_{sat} estimate is too low in this case. There are two conclusions that could be drawn from this and no way of distinguishing the correct option. The first conclusion is that the forest canopy is having a very large effect on catchment response. The second conclusion requires the assumption that K_{sat} does not change with forest growth (as *LUCAS* assumes) in which case it is possible that the input K_{sat} value is too low and that the rainfall partitioning routine may be overestimating the interception loss to produce the reasonably good estimates shown in figure 8.13-8.18.

As there is no way of knowing what the observed rainfall partitioning totals were during the simulated storms all that can be done is look at the total figures and see if these appear reasonable (see table 8.7). Zinke (1967) reports that the amount of interception loss in conifers is commonly between 20-40% (10-20% for hardwoods) and Johnson (1991) reports values of between 28-49% for sites in upland Britain (25% for Plynlimon). Johnson (1991) also reports stemflow proportions of between 2 and 39% for sites in upland Britain (18% for Plynlimon). The values shown in table 8.7 span the range of the other reported results and cannot be considered unreasonable. The difficulty with comparing these results is that the reported values are predominantly average yearly values (but not all) whereas the *VSAS4* results are on a storm basis. N.B. the variation in throughfall percentages shown in table 8.7 is a result of the different canopy ages plus (or minus) the different meteorological conditions occurring at the time which effects the potential evaporation. It is noticeable that there was less interception loss during the February 1988 event which might be expected for a winter storm event.

Given that the simulated rainfall partitioning appears to be within reasonable limits then the model is predicting that the addition of a forest is having a severe affect on the storm events for the Tanllwyth.

The *VSAS4* rainfall partitioning routine has not been tested previously in a coniferous forest (*INTMO* has been tested extensively on a deciduous hardwood plantation) and although the simulated values appear reasonable a more detailed testing in this type of canopy provides an avenue for future research.

The timing of the predicted hydrograph peaks corresponds fairly well to the observed values except in the 1976 and parts of the September 1988 events. The use of hourly rainfall input in *VSAS4* (then subdivided evenly into 2 *minute* timesteps for rainfall partitioning) means that the response may not be simulated in the best possible manner. The model is structured in this manner because hourly rainfall totals are the most common form available although in the case of the Tanllwyth half hourly totals were available. It

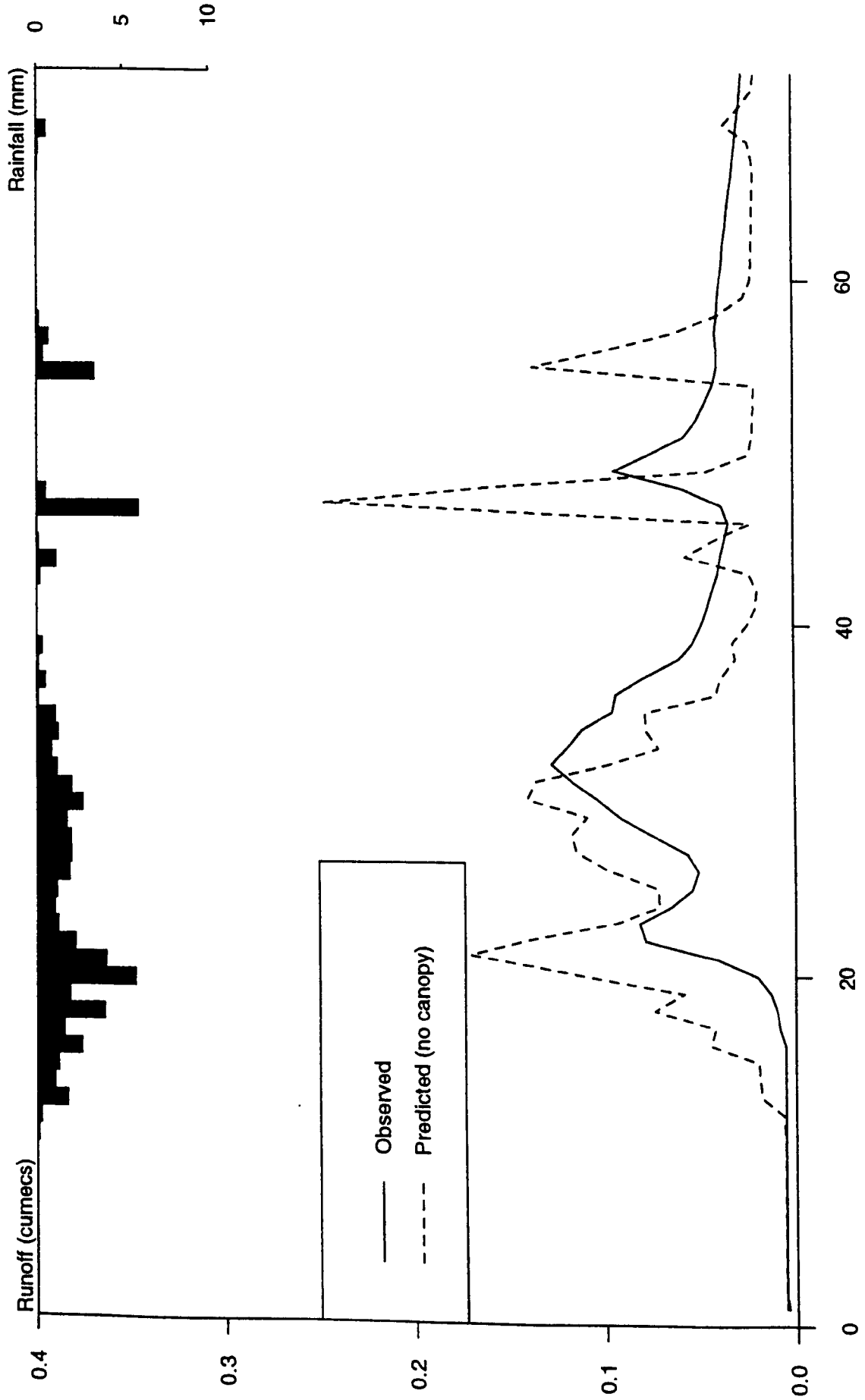

Figure 8.18: Observed versus predicted (without canopy cover) hydrograph for July 1976 storm event

Storm	*Throughfall*	*Stemflow*	*Interception loss*
July 1976	64%	6%	30%
July 1982	51%	7%	42%
July 1989	54%	8%	38%
Feb. 1988	74%	8%	18%
Sep. 1988	70%	8%	22%

Table 8.7: Rainfall partitioning percentages of above canopy rainfall (total for storm)

was decided not to change the model structure to accommodate this extra data because of the fairly large rearrangement of program code this would have required for one data set.

8.4.2 Hypothetical scenarios

The results presented in the previous section have indicated that *VSAS4* has some capability at predicting stormflows on an afforested catchment when the storm event involves a single or double hydrograph peak but the capability declines as the storm events become larger and more complex. This does very little to assess the worth of the model as a predictor of the hydrological effects of long term vegetation change. In order to achieve this the modelling scheme must be run on a series of hypothetical scenarios to see how the predictions change given a different set of conditions. This section of the results is split into two subsections based upon the part of the *LUCAS* capability being assessed. These are:

- Investigate the effect of different canopy ages
- Investigate the effect of canopy in different regions of the catchment

The hypothetical scenarios all use the same input parameters as specified in section 8.3 except for the forest age and canopy distribution when these are deliberately altered.

8.4.2.1 Canopy age

In order to look at the effect that canopy age has on the simulated hydrographs all five storms were simulated using no canopy cover, their normal canopy cover (i.e 28, 34, 41, 40, and 40 *years*) and an 80 year old forest to represent a fully mature forest stand. The results of these simulations are presented in figures 8.19-8.23.

There are two important points to note from figures 8.19-8.23. The first point is

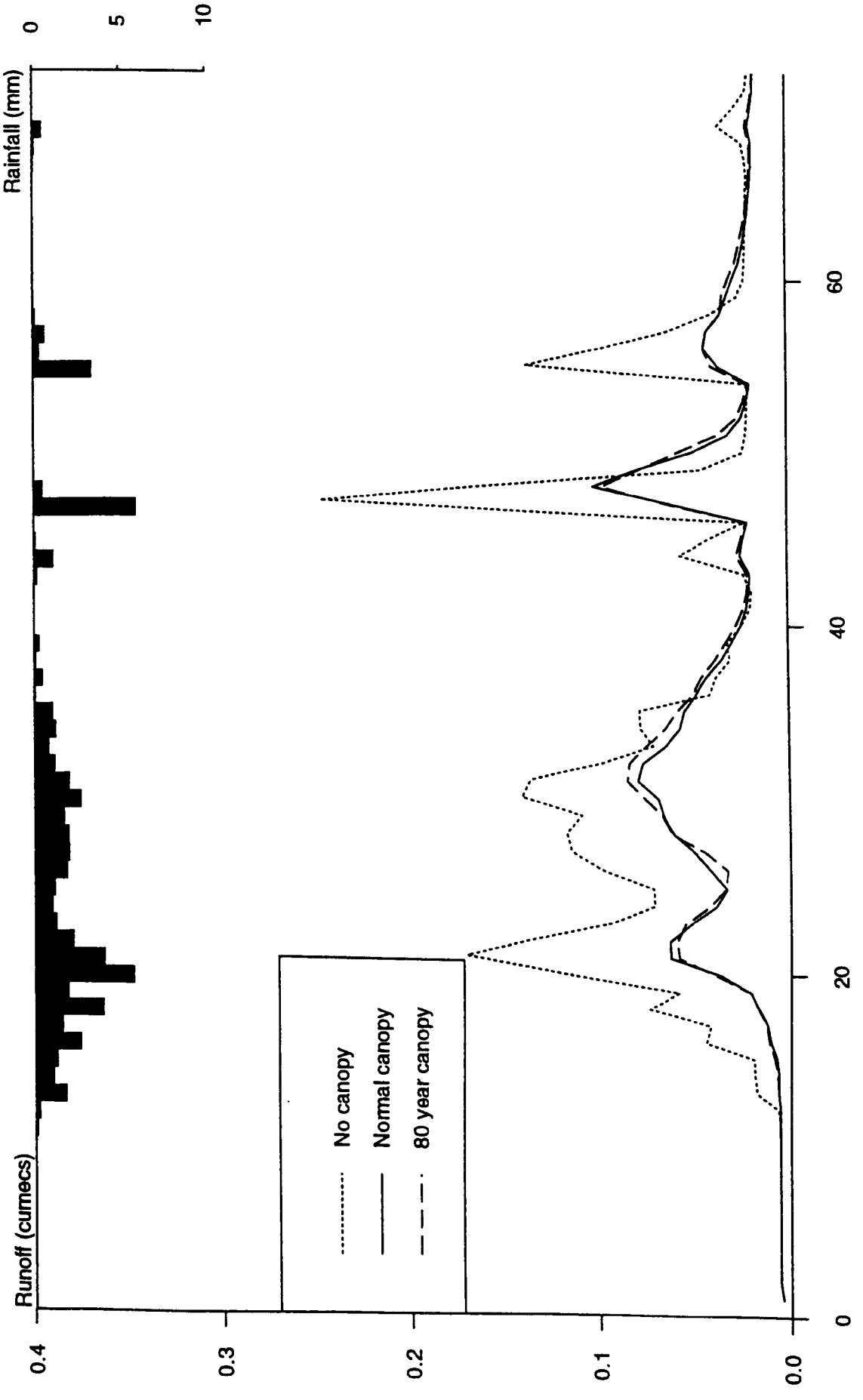

Figure 8.19 Predicted hydrographs for July 1976 storm event with three different simulated canopy ages spanning the life of a forest

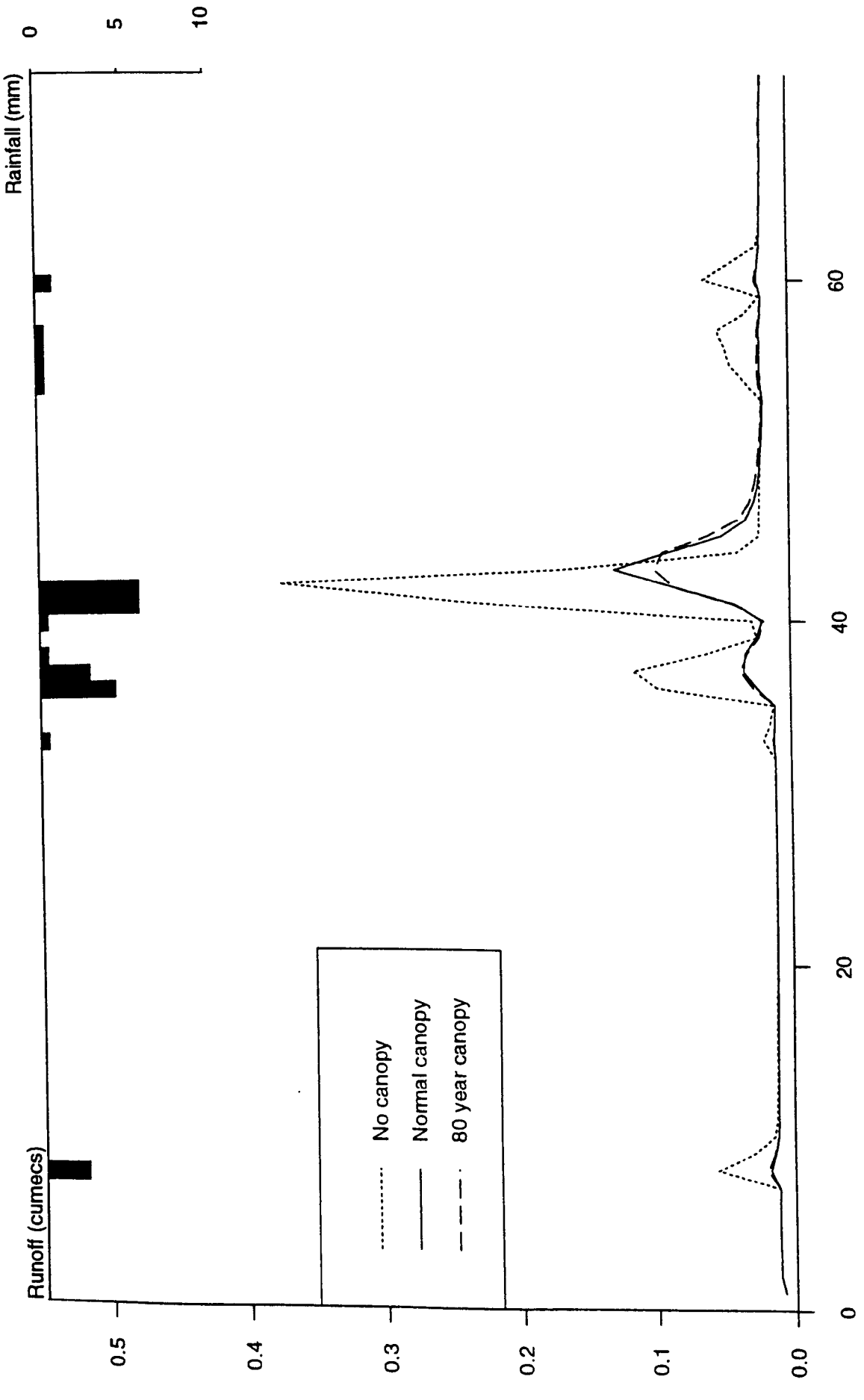

Figure 8.20: Predicted hydrographs for July 1982 storm event with three different simulated canopy ages spanning the life of a forest

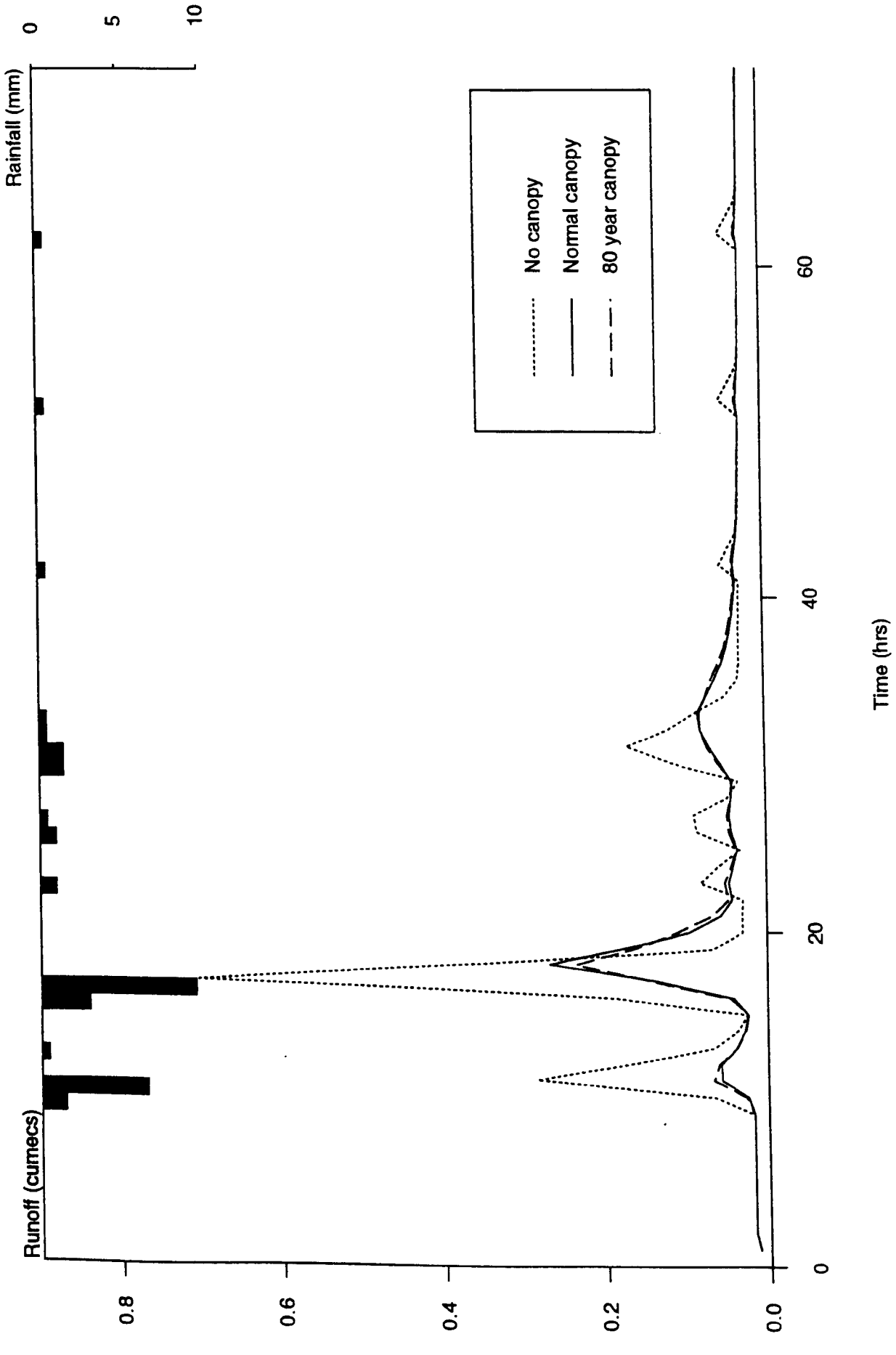

Figure 8.21: Predicted hydrographs for July 1989 storm event with three different simulated canopy ages spanning the life of a forest

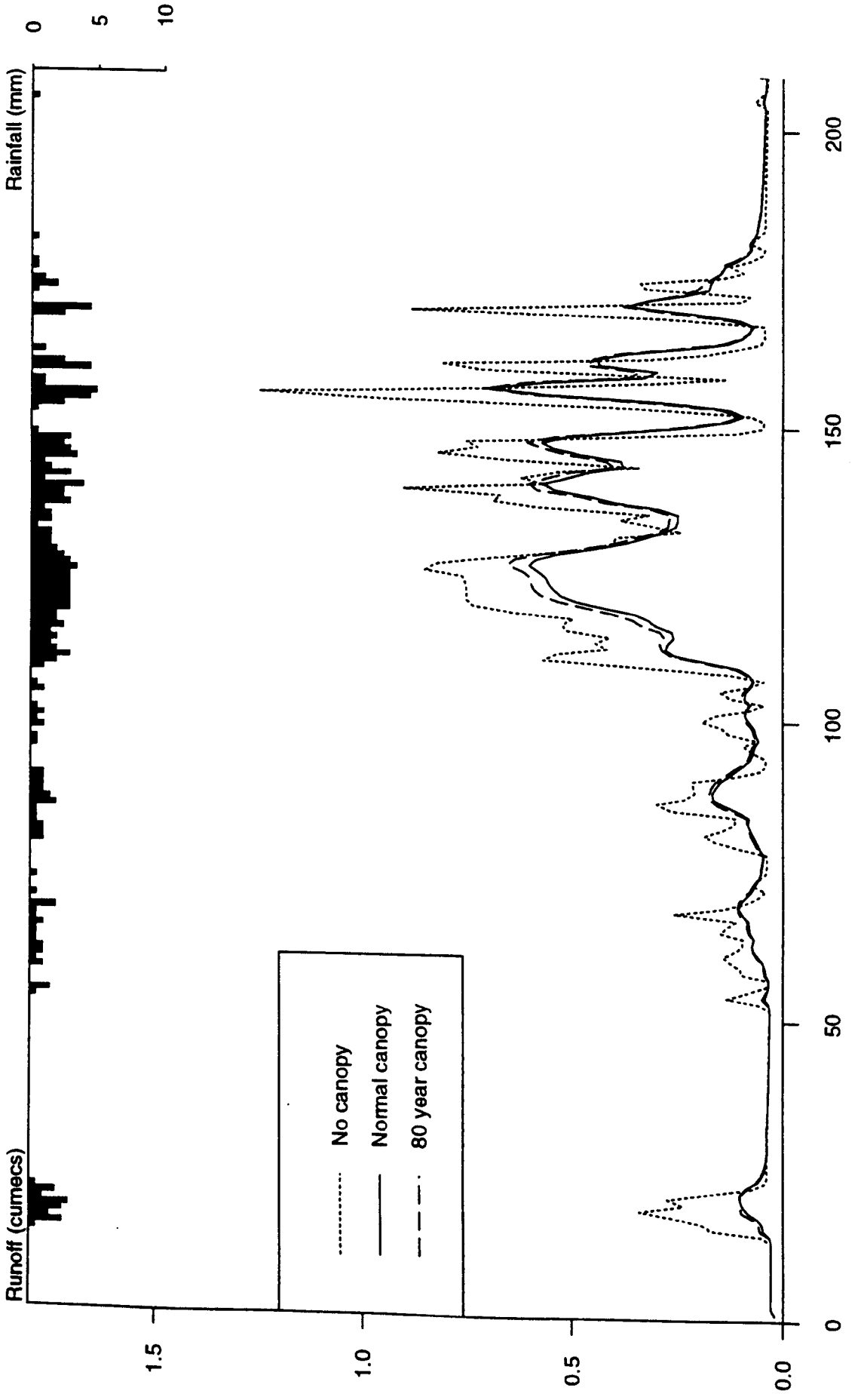

Figure 8.22: Predicted hydrographs for February 1988 large storm event with three different simulated canopy ages spanning the life of a forest

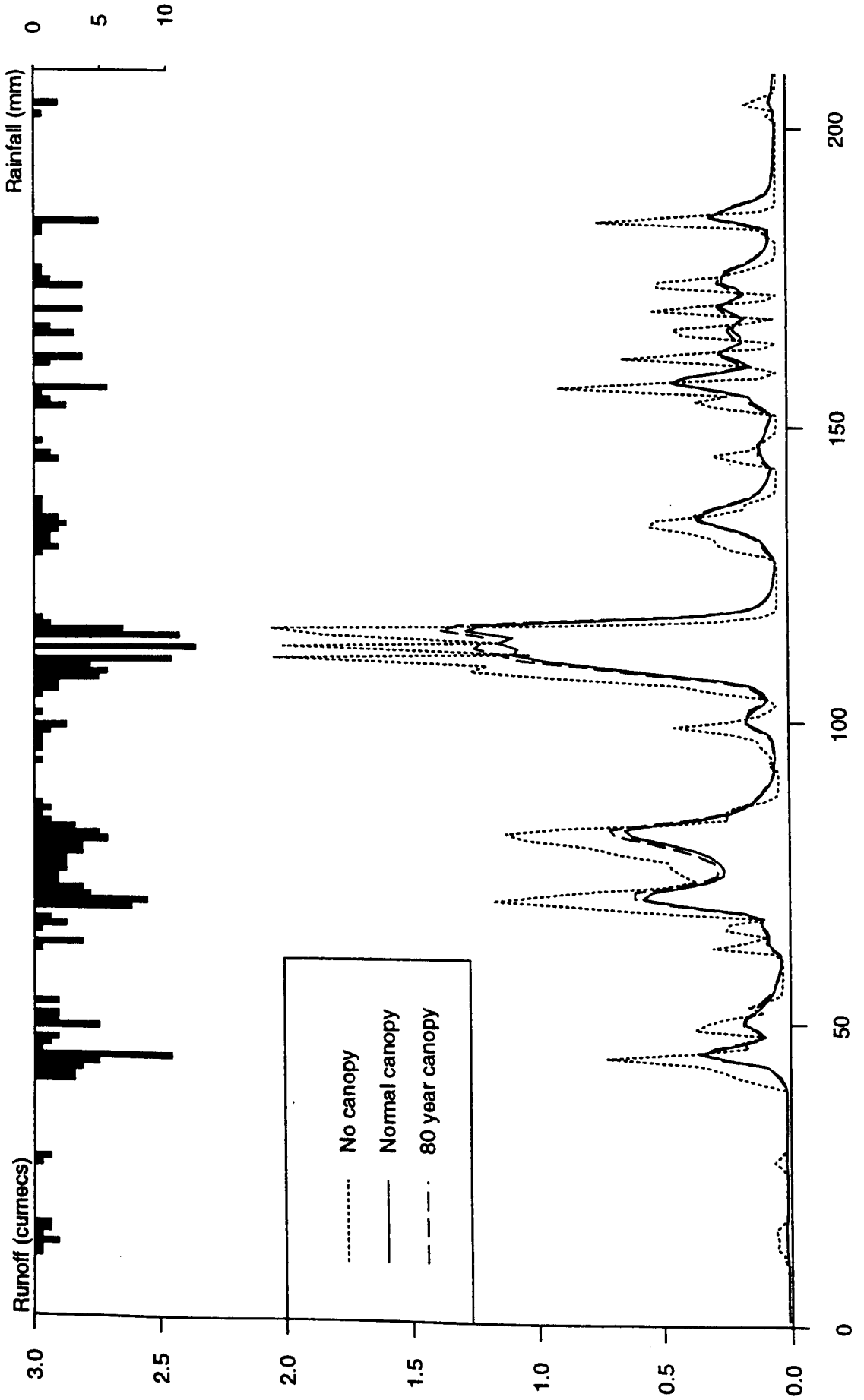

Figure 8.23: Predicted hydrographs for September 1988 large storm event with three different simulated canopy ages spanning the life of a forest

that the older forest canopy simulations are providing most of the drawn out recession limbs of the storm peaks i.e. the indirect throughfall is probably contributing to the recession limb to a greater extent than soil water flow. This can be seen particularly well in the 1982 storm (figure 8.20) where the simulation without canopy cover has an extremely abrupt recession limb whereas the two afforested simulations have relatively drawn out recession limbs (slightly greater for the older canopy). This suggests that the recession limb is being caused by indirect throughfall reaching the soil surface and then being routed as saturated overland flow. There is no way of ascertaining the degree of soil water flow contributing to the observed hydrographs but it has been commonly observed that catchments have attenuated recession limbs through the soil and groundwater contributions (e.g. Hursh (1944)). If this is the case for the Tanllwyth then the recession limbs of the hydrographs predicted in figures 8.13-8.17 although appearing correct may have been caused by the incorrect hydrological process. This result is important because it emphasises the usefulness of hypothetical scenarios in validation, especially when the ideas of Konikow & Bredehoeft (1992), that models cannot be validated only invalidated, are used. The recession limbs of the hydrographs shown in figures 8.13-8.18 could be used to say the model is a valid reproducer of soil water flow but further investigation using hypothetical scenarios suggests that this is not the case and brings the original conclusion into doubt.

The second, and most striking point to be gleaned from figures 8.19-8.23, is that in all cases there is a large difference in storm peak volumes between no canopy and normal canopy but very little distinction between the normal and 80 year old forest cover. This is particularly noticeable in figure 8.19 where the difference between the normal canopy and the 80 year old version is 52 *years*. This shows that the 52 *years* of canopy growth has very little effect on the storm hydrograph. These results suggest that the canopy is having its most major influence on storm hydrographs prior to 28 *years* of growth.

In order to test this further and to see if *LUCAS* is able to distinguish any canopy age threshold the forest growth model was model was run to simulate 10, 20, and 34 *year* canopies and the three summer storms simulated using these parameters. The three summer storms were used because it is easier to distinguish features than in the more complex 1988 events. The results of these simulations are shown in figures 8.24-8.26.

The hydrographs in figures 8.24-8.26 show remarkably similar results, the simulations with no and 10 *year* canopy are almost identical while the 20 *year* canopy is approximately half way between the extremes. Given that in figures 8.19-8.23 the normal and 80 year old forest were very similar, the 34 year old forest can be said to represent a mature canopy. This means the major modification in storm hydrographs is taking place between the tenth and thirtieth *year* of a forests growth.

By looking at various forest growth model outputs an attempt can be made to see

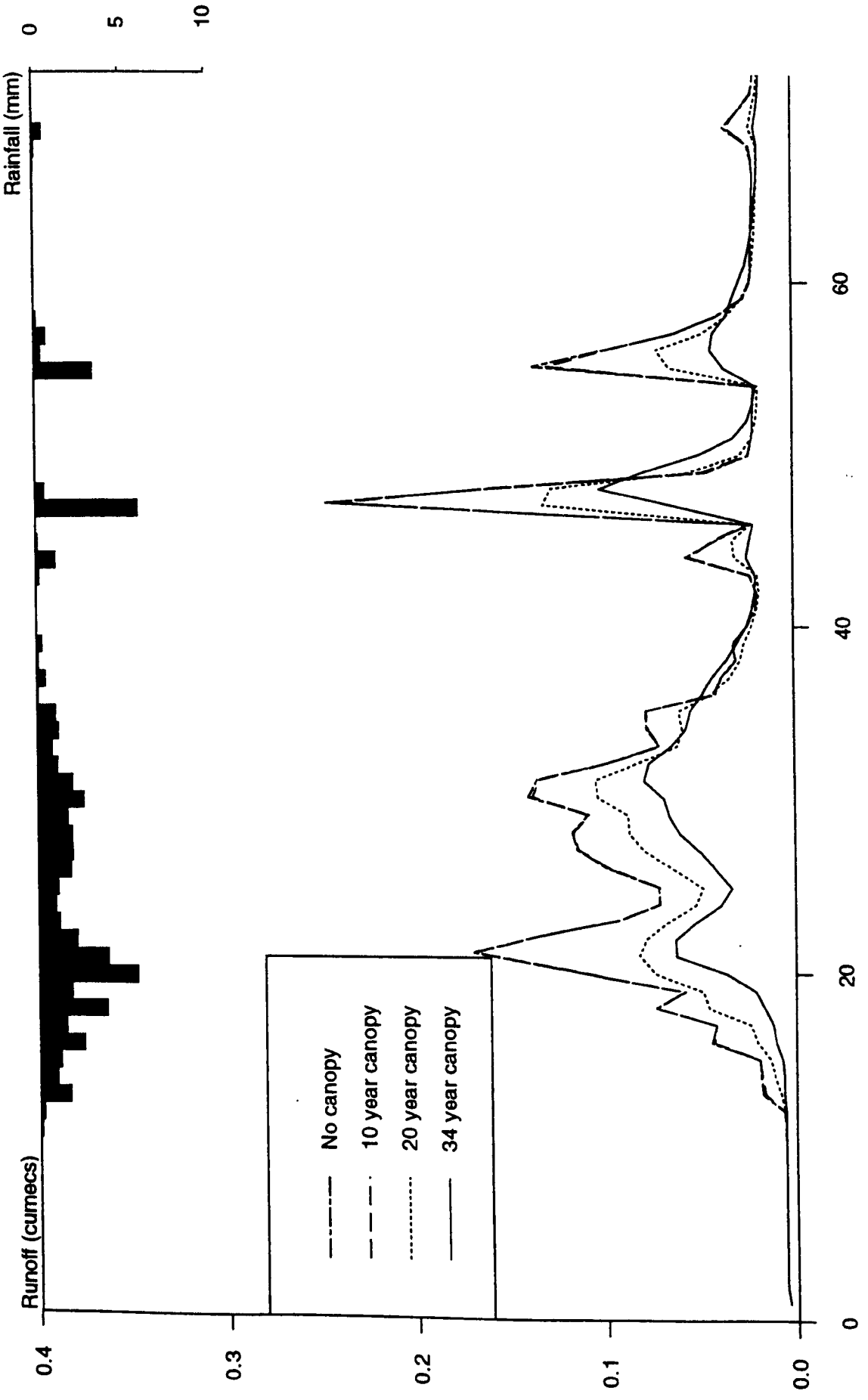

Figure 8.24: Predicted hydrographs for July 1976 storm event with three different simulated canopy ages spanning the first 34 *years* of a forest

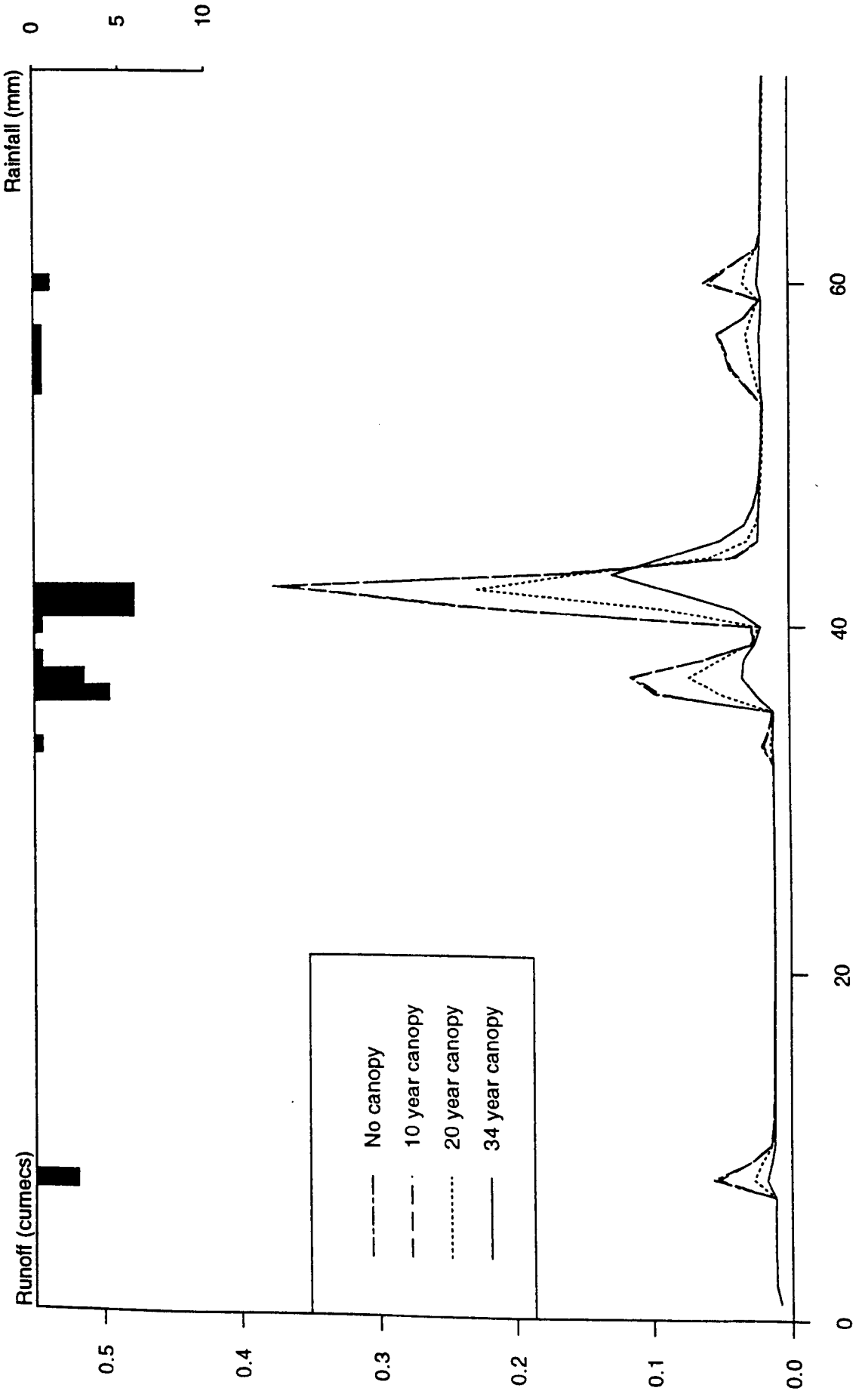

Figure 8.25: Predicted hydrographs for July 1982 storm event with three different simulated canopy ages spanning the first 34 *years* of a forest

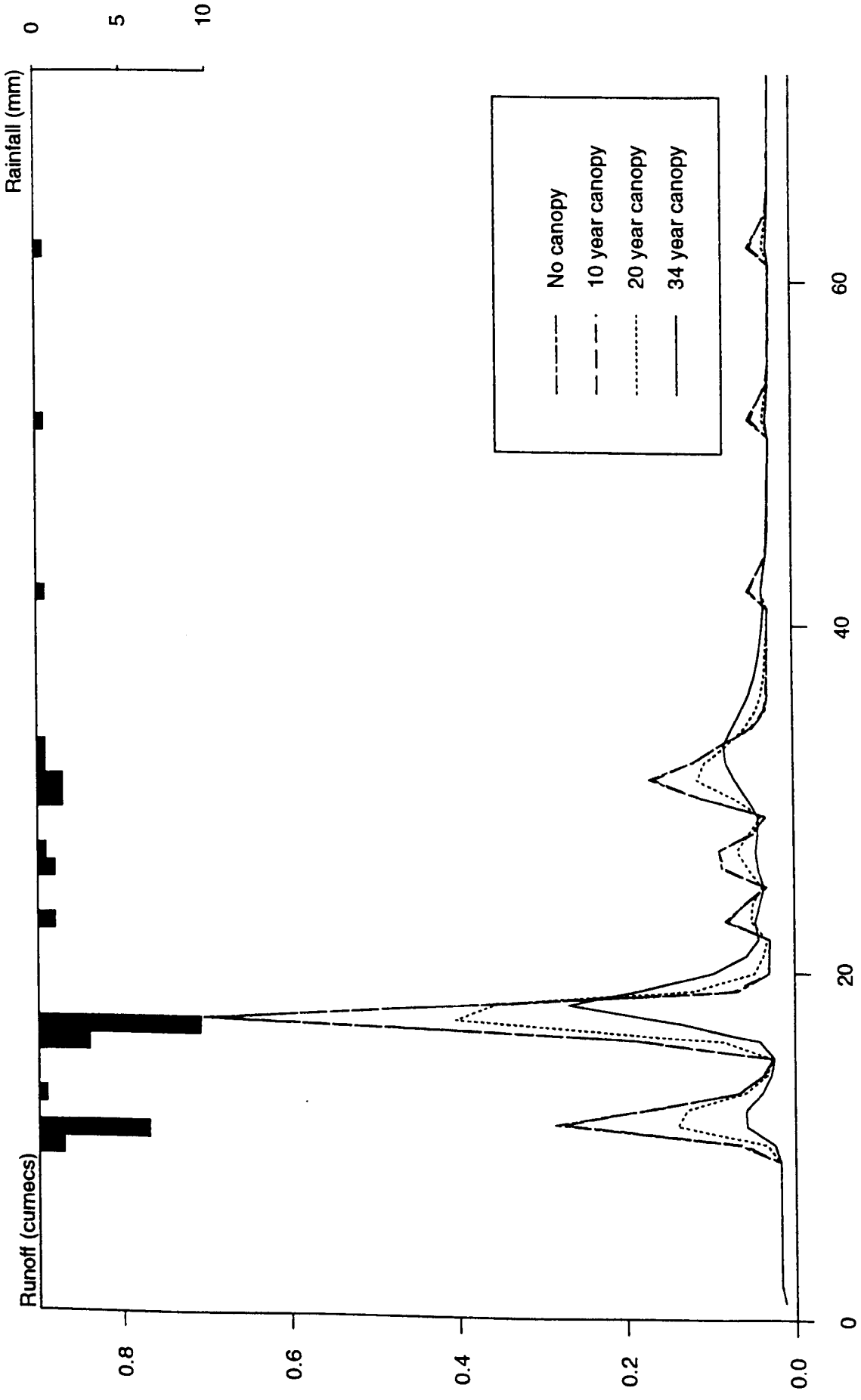

Figure 8.26: Predicted hydrographs for July 1989 storm event with three different simulated canopy ages spanning the first 34 *years* of a forest

which part of the model is having such a critical effect on the storm hydrographs simulated by *LUCAS*. In chapter six it was pointed out that, very broadly speaking, the forest growth model performs two functions: growing the trees in the horizontal dimension towards each other thereby decreasing the volume of direct throughfall; and growing the trees in the vertical dimension thereby increasing the number of rainfall intercepting layers in each tree, and hence increasing the amount of indirect throughfall. To measure these two functions the percentage canopy cover over the plot and the average number of intercepting layers per tree were output from the forest growth simulations. The canopy cover is an estimation calculated by totalling the crown area of each tree in the plot and dividing by the total plot area. This does not account for overlap between trees hence it being only an estimate. The average number of intercepting layers per tree is analogous to the average leaf area index (LAI) for the simulated forest

The results of these are plotted in figure 8.27. The first most important point to note from figure 8.27 is that the number of intercepting layers per tree is being overestimated. This parameter is derived from the relationship of Halldin (1985) linking tree diameter at breast height and the number of intercepting layers. The simulation shown here has a LAI of approximately 25 by the time the canopy reaches the age of 30 *years* and rising to nearly 41 in the 80 year old canopy. These values are very high (Leyton *et al* (1967) report a LAI of 15 for a mature Norway spruce plantation; Ford (1982) report a LAI of 7.5 for a mature Sitka spruce plantation) and reflects an obvious inaccuracy within the model. This inaccuracy can be traced to two factors: the relationship derived by Halldin (1985) is for a different tree species (Scots pine); and the relationship was for trees growing separately from each other (i.e no competition). The transfer of this relationship to a Sitka spruce plantation has obvious limitations but there is no analogous relationship for this species. The results shown in figure 8.27 suggest that this relationship needs to be measured for the different tree species.

The second point to note from figure 8.27 is that the factor that changes most between 10 and 30 *years* of growth is the percentage canopy cover. The percentage canopy cover increases from 20% after 10 *years* to 80% after 20 *years* of growth and canopy closure is being predicted to occur in the 23rd *year* of forest growth. The LAI continues to increase at a similar rate throughout the simulation. When this result is tied in with figures 8.24-8.26 it suggests that canopy closure is having the greatest effect on the storm hydrographs and that the increase in intercepting layers is less important.

As a canopy closes the proportion of above canopy rainfall reaching the soil surface as direct throughfall decreases and a certain proportion of the rainfall becomes indirect throughfall. As the number of intercepting layers increases the time taken for the indirect throughfall to reach the surface increases thereby delaying the impact of the storm rainfall. This result is suggesting that the amount of direct throughfall is more important

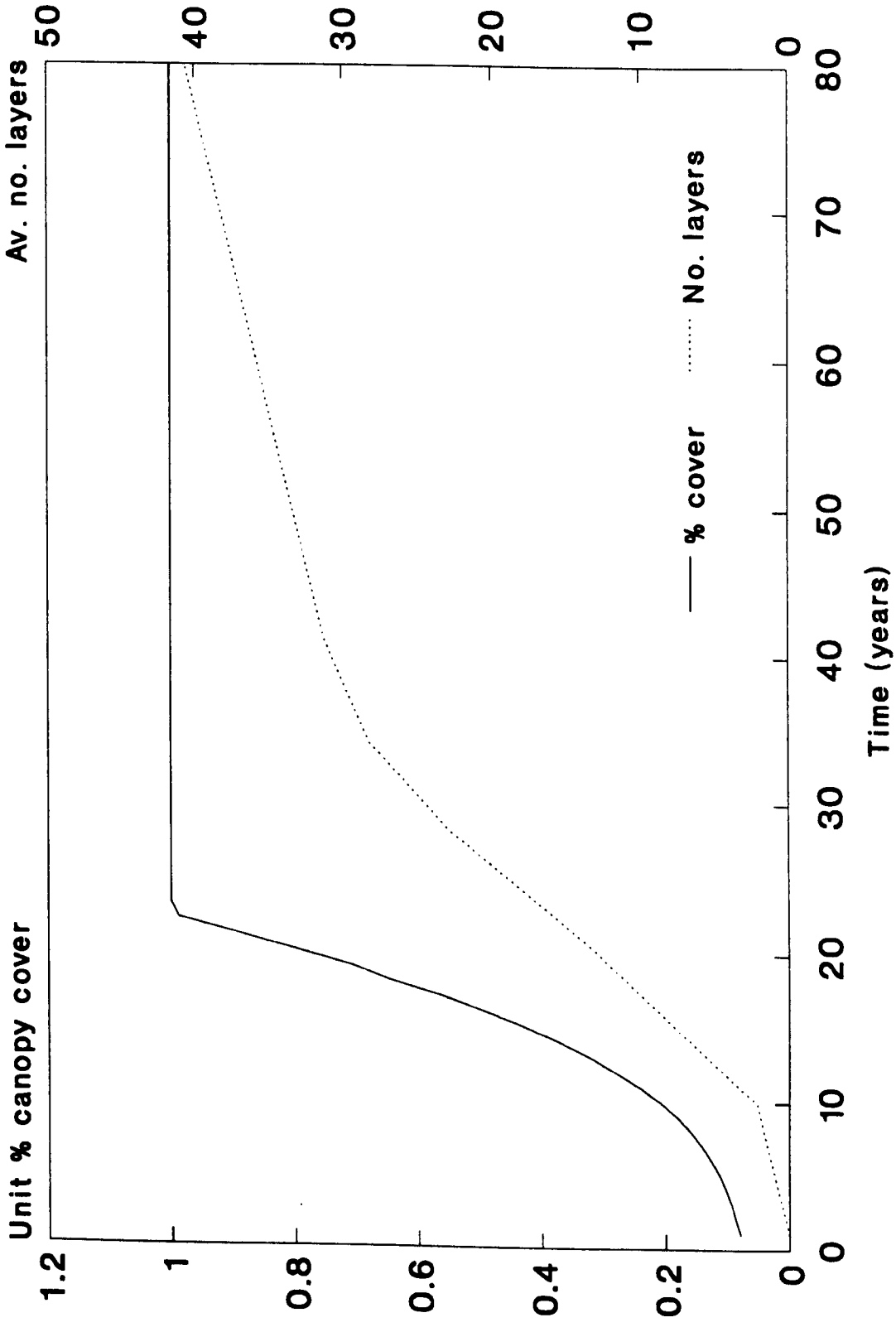

Figure 8.27: Predicted percentage canopy cover (shown as a unit %) and average leaf are index (LAI) for the simulated growth of a 0.9*m* spaced forest (yield class 12)

than the number of intercepting layers for the indirect throughfall. This result is slightly surprising as the greater the number of intercepting layers the greater the amount of potential interception loss and therefore the less rainfall could be expected to reach the soil surface. It ties in with the robustness testing results of chapter six where the average number of intercepting layers was kept constant and yet the canopy age made a large difference to the resultant hydrographs. These simulations extend the results from chapter six by simulating both factors and showing the amount of canopy cover is more important than LAI.

VSAS4 may be exaggerating the importance of canopy closure but Calder (1990) does emphasise its importance within forest hydrology and meteorology. In the simulations shown in figures 8.19-8.23 it was noted that there did not seem to be enough soil water flow which suggests that almost all of the hydrograph peak is caused by water routed as saturated overland flow. This is reinforced by the way the forest canopy seems to produce a longer recession limb with greater canopy age, suggesting that this is caused by the indirect throughfall volume (delayed by the intercepting layers) also being routed as overland flow. In a situation where the hydrograph peak is being produced mainly by overland flow it is sensible that the degree of canopy cover is critical because the direct throughfall is available for immediate routing, whereas indirect throughfall is delayed to a certain extent no matter how many layers there are.

There is no record kept of when canopy closure did occur in the Tanllwyth so the exact timing of this result cannot be validated. The important feature of this result is that the *LUCAS* modelling scheme predicts that the amount of canopy cover is the most important governing factor in altering a storm hydrograph through rainfall partitioning and that canopy closure is a critical feature to ascertain in the forest growth simulation. This confirms the usefulness of using hypothetical scenarios to explore the possibilities for predicting beyond the data set range and highlights the usage of a modelling scheme such as *LUCAS* to point towards areas for further investigation.

The simulations carried out using the Tanllwyth data with different canopy ages has helped in the validation of *LUCAS*. The results of these simulations have confirmed several features of the hydrograph reproduction simulations and also highlighted new results. The salient points can be summarised as:

- The attenuated recession limbs of the simulated hydrographs appear to be caused by indirect throughfall being routed as overland flow
- The largest distinction in hydrograph with canopy age can be seen between the ages of 10 and 34 *years*
- This last result can be attributed to canopy closure occurring during this period
- The average number of intercepting layers per tree is being over-

predicted

- Despite this inaccuracy the percentage of canopy cover has more influence on the storm hydrographs than the average number of intercepting layers.

These results are an important part of the validation procedure for *LUCAS*.

8.4.2.2 Canopy distribution

In order to further test *LUCAS* as a predictor beyond the data set range *VSAS4* was runs using different canopy configurations. This is to see if the model predicts differences in hydrological response if the canopy cover is restricted to various parts of the catchment reflecting possible forestry practises. This tests the ability of *VSAS4* as a distributed hydrological model within the *LUCAS* framework. There is an endless number of hypothetical scenarios that could be tested here to investigate the different forestry practises and little would be achieved by pursuing them all. Consequently only one possibility was pursued, figure 8.29 shows the canopy distributions chosen to represent different forestry managements. The example shown is as if the forest was restricted to purely the headwaters of the Tanllwyth (or alternatively the sides were logged), the reverse of this situation was also simulated (i.e. the headwaters logged or the sides afforested). These different model configurations were used to simulate the July 1976 storm. The results are shown in figure 8.29 for no canopy, the two configurations, and a full canopy. Figure 8.30 is the same simulation detailing the difference between the headwaters and the sides being logged.

Figures 8.29 and 8.30 show that *VSAS4* is able to distinguish a difference in hydrograph response with the change in canopy distribution. This is especially marked during the first hydrograph peak where the lack of forest on the catchment sides matches the response for having no canopy at all whereas the lack of forest on the headwaters is closer to, but not the same as, the full canopy option.

The difference between the different regions being without canopy cover is that the when the sides are deforested the storm hydrograph has larger peaks and responds in a quicker manner than when the headwaters are deforested. This is probably a function of two factors, firstly the area of catchment represented as sides is larger than the headwaters and therefore the volume of overland flow from the direct rainfall will be greater. The second factor is that the headwaters are further from the catchment outlet and therefore any delaying factors on overland flow that the canopy produces through indirect throughfall will be magnified by the extra distance required to be travelled in the stream.

This last point is interesting because it suggests a sensitivity of the modelling scheme to distance travelled by the flood waters even though it uses a simple lagging

Figure 8.28: Discretisation of forest used to simulate the growth of trees purely in the Tanllwyth headwaters. N.B. The reverse of this was also simulated

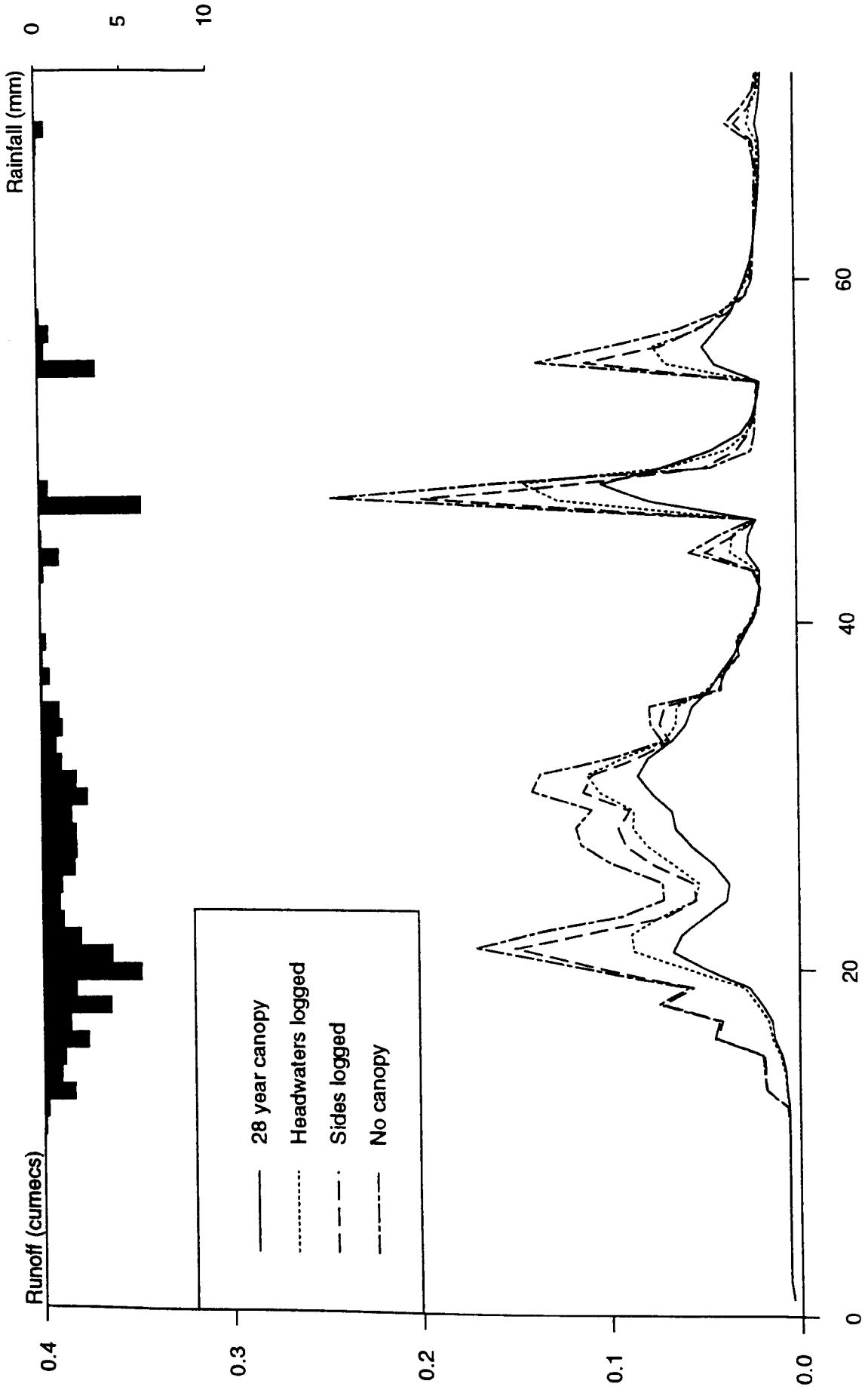

Figure 8.29: Predicted hydrographs for various hypothetical discretisations of forest within the Tanllwyth catchment

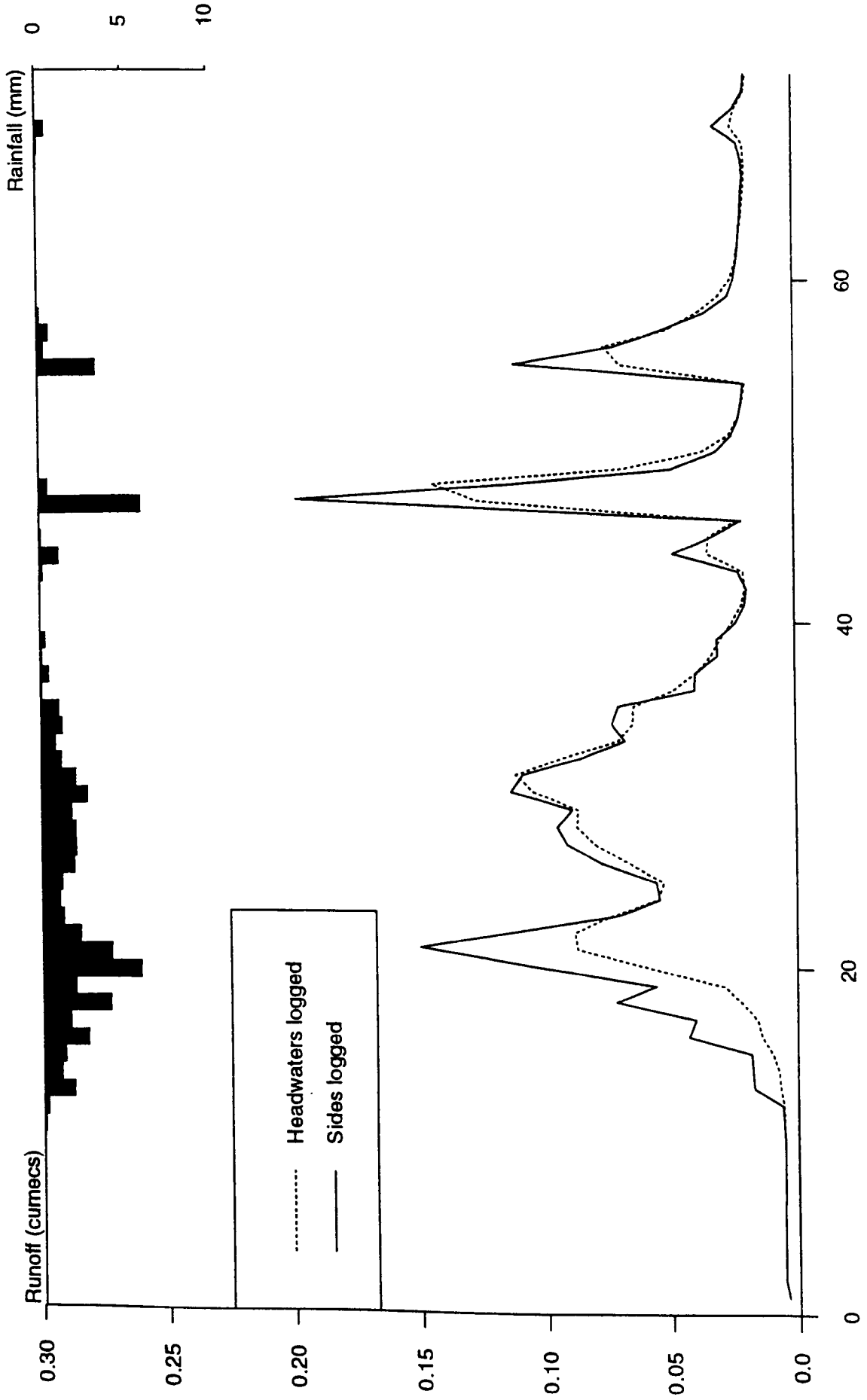

Figure 8.30: Predicted hydrographs for the confinement of forest to the headwaters and valley sides (separate simulations) of the Tanllwyth

function to simulate channel flow. This provides a limited form of validation for the channel flow lagging function.

The results of using *LUCAS* to simulate these two hypothetical, but entirely possible, scenarios indicates that the scheme does have some use as a simulator of different forestry practises when these are varied within a catchment. This is only possible because of the distributed nature of the process representation within *VSAS4* and *LUCAS*. There is no way of knowing whether the predictions are correct but they do fit into hydrological reasoning. The results presented here suggest that *LUCAS* does have capabilities for predicting beyond an observed data set using its distributed process representation.

8.5 Summary of validation exercise

The validation exercise undertaken in this chapter does not allow a conclusion to be drawn that *LUCAS* is a valid modelling scheme for all conditions. This is due largely to the fact that the issue under investigation is long term vegetation change and there are very few long term hydrological records of this sort available. The modelling scheme was developed in order to be predictive and therefore could be used without reference to long term hydrological records. This has meant that the validation attempted used the best data set available for limited testing against observed hydrographs and then went on to simulate various hypothetical scenarios. These were used to further investigate the initial conclusions drawn from within the data set, to highlight areas of further development within the model, and to investigate the possibilities for predicting beyond the data set range.

The pre-processing forest growth model has been shown to produce a good estimate of an average forest growth for Sitka spruce forest covering the Tanllwyth, so that the main validation testing has involved simulations using the hydrological model section (*VSAS4*) within *LUCAS*.

The first set of observed versus predicted hydrographs for five storm events of various sizes and degrees of complexity showed that *LUCAS* could be used to produce reasonable estimates of storm runoff for a range of different canopy ages but there were difficulties in reproducing the multiple peaked hydrographs. The fact that the model did not drastically under or over estimate the totals at either end of the forest growth period indicates that the scheme has some validity as a predictor of the hydrological effects of long term vegetation change.

The rainfall partitioning totals for each storm appeared within reasonable limits for an upland coniferous plantation and the model did simulate less interception loss for the

winter storm event. It was pointed out that a separate validation of the *VSAS4* rainfall partitioning routine under a coniferous forest has not been attempted and this provides an avenue for future research using detailed plot study results.

The results from this hydrograph reproduction section indicate that the model appeared to be a valid modelling scheme but further investigation using the hypothetical scenarios altered this conclusion. By simulating the storms using a range of canopy ages on the catchment it was found that the attenuated recession limb of the hydrograph was being reproduced by the addition of indirect throughfall to the soil surface, (and probable transferrance to the stream as saturated overland flow) when it is likely that the observed recession limb is caused by soil and groundwater flow. This highlighted the use of a single effective parameter value of saturated hydraulic conductivity to represent all soil water flow and the assumption that macropore and pipe flow is negligible. This simplification means that the modelling scheme cannot be considered valid for hydrograph reproduction because a different hydrological process was causing the predicted effect rather than what might be expected to be observed in the field.

The hypothetical scenarios with the same storm occurring on different canopies showed that *LUCAS* was predicting a very large difference between no canopy cover and the actual age canopy cover. Further investigation of this showed that the critical age for this simulation was between 10 and 30 *years* which it was illustrated is when canopy closure occurs. The results suggest that canopy closure has a greater influence on storm hydrograph than the vertical growth of the forest (and consequent increase in intercepting layers). This surprising result can be attributed partly to the predominance of overland flow in the hydrograph peak (due to Darcian soil matrix flow being the only soil water flow mechanism simulated) and subsequent reliance of the peak on precipitation falling between tree crowns (direct throughfall). Despite this simplification it is still an interesting result and highlights the importance of getting a good estimation of canopy closure time from the forest growth model.

Finally the model was used to investigate the effect of different canopy distributions within the catchment upon one storm hydrograph. These results indicate that the model is sensitive to changes in canopy distribution and as such has considerable potential to predict beyond the data set range in both age and canopy distribution.

As mentioned earlier in this section the results detailed in this chapter do not allow a conclusive statement to be drawn as to whether *LUCAS* is a valid predictor of the hydrological effects of long term vegetation change. The results have indicated several areas that require further development and/or testing within the scheme (e.g. soil water flow to allow for different mechanisms, relationship between LAI and tree size). The main constraints to the accurate prediction of the effects long term vegetation change on storm hydrographs are within the process representations, suggesting that with some further

development of these a greater predictive ability could be obtained. The approach of parameterising the effects of long term vegetation change by using a pre-processing forest growth model has been shown to be workable and to have considerable potential for further development.

As with any physically based, distributed modelling scheme there is considerable doubt that it could ever be used in a directly deterministic application. The scheme will never be fully validated and so strictly speaking can never be used in this manner although it is feasible that it could be if a probabilistic approach is implemented. The testing of the model has highlighted several areas that require further development before it could be used in any applicational sense; these are discussed further in the final chapter.

CHAPTER 9

SUMMARY AND FUTURE RESEARCH DIRECTIONS

At the end of chapter three the objectives of this study were listed as:

- The design and construction a physically based, distributed hydrological model with the primary aim of investigating the effects on hydrology of long term vegetation change
- The modelling of the input parameters for this model so that the overall scheme is predictive
- An attempt at verification and validation of the overall scheme
- An assessment of the modelling schemes capabilities as a predictive model investigating the hydrological effects of long term vegetation change.

These objectives have all been carried out in the preceding chapters therefore all that remains is a summary of the main research findings (section 9.1) and a discussion on future research directions based on the findings from the research (section 9.2).

9.1 Summary of research findings

In chapter one the need was established for individual studies to investigate the hydrological effects of vegetation change at a site, as despite numerous empirical monitoring studies no direct relationship can be drawn between degree or type of change and the alteration to the hydrological regime. A review of the different methods available to investigate the hydrological effects of long term vegetation change came to the conclusion that physically based distributed modelling offers the only viable option as it has a predictive ability through its input parameters being transferable over space and time. The scope of this study was stated as developing a new physically based, distributed modelling framework for investigating the effects of long term vegetation change on stormflows in humid temperate environments

In chapter two a critique of physically based, distributed modelling revealed that there are considerable problems involved with applying the current generation of these

models to practical problems, stemming from the fact that they can never be fully verified or validated, and as used in applications are not truly physically based or distributed. Despite this it was pointed out that they still have uses, especially to investigate complex problems such as long term vegetation change. It was suggested that because the current generation of physically based, distributed models do not perform as their title suggests there is no need stick to their rigid structure and a modelling scheme could be developed for a specific topic that concentrates its physical basis on hydrological processes that are known to be important for a particular region or issue of study. It was also suggested that the input parameters for those processes that have a representation based on physical equations could be taken and transformed by modelling algorithms in order to parameterise the hydrological effects of long term vegetation change. These ideas form the basis of the approach taken in this thesis to develop a new predictive method for investigating long term vegetation change on stormflow hydrology.

In chapter three the strategy was set out for developing the modelling scheme that forms this new predictive method for investigating the hydrological effects long term vegetation change. The point was made that model development that focussed the model towards direct application was no longer possible as the scheme could never be fully verified or validated. Consequently the model development focussed on gaining an assessment of the schemes worth as a predictor of the hydrological effects of long term vegetation change, to explore implications of making certain assumptions about the nature of the real world system, and to point the way for further investigation. It was decided that the lack of full verification and validation did not rule out usage of the model to some applied problems but this would need to be in a probabilistic rather than deterministic framework.

Chapter four detailed the design and construction of *VSAS4* which is the new mixed conceptual/physically based distributed model constructed as part of this study. The model is a storm event simulator that is an amalgamation of two previously used models and concentrates its physical basis on the computation of soil water flow and rainfall partitioning. This was a deliberate strategy to focus the construction as a base model for the investigation of the hydrological effects long term vegetation change.

In chapter five modelling algorithms were detailed that provide the parameterisation of vegetation change for *VSAS4*. The main part of this is a forest growth model that acts a separate pre-processor for *VSAS4*, simulating the growth of the canopy structural parameters that influence rainfall partitioning. The individual tree, distant dependent, mono-specific, forest growth model was constructed as part of this study combining elements from previous work in this field. The combination of this pre-processing forest growth model and *VSAS4* was termed *LUCAS* (Land Use Change, Afforestation, Simulator) and was used as the modelling scheme for the remainder of the

study.

The remaining three chapters were concerned with testing and some additional superficial changes to *LUCAS*. Chapter six involved verification testing. Even though this is a specifically focussed modelling scheme a detailed sensitivity analysis was not a realistic undertaking due to the number of input parameters. Consequently the verification testing involved a reduced form of sensitivity analysis that was termed robustness testing. This terminology reflects the fact that one of the primary aims of the testing was to investigate the robustness of the model under a range of possible conditions using a variation in general factors (topography, soil hydrology, and vegetation). The testing was undertaken in two stages, the first was designed to find model sensitivity to the general factors, and the second to test the initial conclusions against a wider range of initial conditions.

The results from the robustness testing showed that the modelling scheme is robust enough to be able to cope with the full range of hypothetical conditions imposed upon it and therefore indicated that it can be used as a simulator of the hydrological effects of long term vegetation change. The testing also was able to identify conditions where a change in each varied factor is critical. This was particularly important for canopy age because it represented a new part within the original *VSAS* structure that had not had any form of verification testing previously. It was found that canopy age affected all simulated conditions by reducing the stormflow peak and attenuating the peak at both ends, and it was especially noticeable where soil water flow was not a dominant process. A ranking of the importance of the varied parameters showed that saturated hydraulic conductivity was consistently the greatest influence of the storm hydrographs and in low K_{sat} conditions canopy age ranked above plan shape and slope angle.

The results from the robustness testing were encouraging enough to make some changes to *LUCAS* in order that it could be used in validation testing. These changes were superficial in nature so that the limited verification of the scheme could be carried through to the validation. Chapter seven detailed these alterations and an independent verification of the forest growth model. The first change involved the addition of an error analysis designed to indicate periods of mathematical instability within *VSAS4* and highlight which section of the model was providing the instability. The second part of chapter seven involved the tree growth model which was tested against an independent data set and then changed slightly to improve the performance. The new version of the tree growth model was then verified independently from *VSAS4* to establish it as a predictor of forest growth in its own right. This involved a sensitivity analysis using the factor perturbation method on six important input parameters. This sensitivity analysis established that the change in crown angle and size of zone of influence had the largest effect on model outputs but that all parameters varied did influence the average forest growth. The sensitivity analysis

highlighted the way that the different outputs influence the average growth outputs which is useful when calibration of the parameters is required. An interesting extra point established from the sensitivity analysis was that the model responded with different sensitivity to model parameters at different times within the simulation.

The final chapter in the model testing part of the thesis (chapter eight) involved an attempt at validation for *LUCAS*. Physically based models can never be fully validated due to lack of data to validate them against and any scheme looking at long term vegetation change has even more difficulties obtaining an appropriate data set (i.e. the same data is required but over a long monitoring period). To overcome this the definition of validation was loosened to mean a test to find whether the model is a valid representation of the hydrological system. Consequently validation included tests against a limited catchment data set and then hypothetical scenarios were simulated using basically the same catchment initial conditions. The hypothetical scenarios were used to investigate further the tentative conclusions drawn from testing against the data set and then to explore the possibilities for predicting outside the data set range.

The results from the pre-processing forest growth model provided good estimates of forest growth after only limited calibration. The remainder of the validation showed several interesting points but as expected could not be used to say the scheme was a valid predictor of the hydrological system. It was clear that *VSAS4* is an invalid predictor of the soil water flow and consequent saturated overland flow volumes and this was highlighted as an area for future investigation. A slightly surprising result was produced in that the *VSAS4* storm hydrograph is more sensitive to the percentage canopy cover in a simulated plot than the average number of intercepting layers for a tree. The use of hypothetical scenarios to investigate possible different forestry management practises illustrated that *LUCAS* was able to make predictions beyond the data set range that appeared reasonable (there was no way of validating them independently).

In summary the approach taken in this study (developing a physically based, distributed model and then parameterising long term vegetation change through a pre-processing forest growth model) has been developed and shown to have considerable capability. It has not been possible to fully validate the scheme but the attempts at this have not completely invalidated the scheme, suggesting that there is considerable potential for further development using this type of approach.

9.2 Future research directions

The discussion of future research directions is split between the options for *LUCAS* (section 9.2.1) and a more general discussion on modelling of long term vegetation change (section 9.2.1).

9.2.1 *LUCAS future directions*

In chapter eight the validation testing of *LUCAS* has highlighted four areas within the modelling scheme where further investigation is warranted. These four areas are:

- Separately validating the rainfall partitioning section of *VSAS4*, with parameters derived from the forest growth model for a coniferous plantation
- Improving the soil water flow estimation so that flows other than Darcian matrix flow can be included.
- Obtaining a better estimate of the relationship between leaf area index and tree size
- Testing the forest growth models ability to predict the exact date of canopy closure.

These four areas for further investigation have all been identified after validation testing of *LUCAS*. This confirms the view of Konikow & Bredehoeft (1992) stated in chapter three that models can be used to point the way for further investigation and should not be seen purely as tools for applied tasks.

The first option given would mean obtaining a detailed rainfall partitioning data set for a coniferous plantation similar to that measured by Durocher (1991) (for a deciduous plantation) and validating the rainfall partitioning totals for a variety of time scales. This has not been attempted in this study because it was felt the work of Durocher (1991) and previous validations of the Rutter model provided enough basis to proceed with *VSAS4*.

The second option, improving the soil water flow estimation so that factors such as macropore and soil pipe flow can be included, is one that is a problem for all physically based, distributed hydrological models. Watts (1989) developed a two domain model that accounted for matrix and macropore flow using a threshold exceedence mechanism. The main problem Watts (1989) found with this approach is that it creates an artificial split in classification between micropores and macropores when in fact they represent a continuum of pore sizes. This type of approach could be included into the *VSAS4* structure where it is understood that non-matrix flow forms a large part of the hydrograph, representing a significant improvement in soil water flow representation. It would also lessen the need

for effective parameter values such as the saturated hydraulic conductivity value used in chapter eight.

The gathering of further data on the relationship of leaf area index and tree size is one that is required by *LUCAS* if it is to be used in any applications but as the hypothetical scenarios in section 8.4.2 have illustrated the scheme is not always particularly sensitive to this relationship. This means a study does not have to be extremely detailed to provide the necessary data.

The investigation of the importance of canopy closure, and consequently the ability of the forest growth model to predict this accurately is perhaps the most interesting avenue for future research because its importance has been highlighted as a direct result of the validation testing and was not something that was immediately obvious prior these simulations. This involves further testing of the forest growth model as a forest growth predictor.

Apart from the areas of *LUCAS* highlighted in the validation testing for further investigation there are three areas of the modelling scheme that have been largely ignored in development so far. These are:

- The addition of a soil water root extraction function tied to transpiration so that the scheme can be extended to include low flows
- The change in soil hydrology with time
- Making *LUCAS* fully distributed.

The first two of these options have been discussed in chapters four and five respectively. They form significant studies in their own right and were ignored here for this reason. Further study into them and an incorporation into *LUCAS* would represent a significant improvement in capability and process representation.

One of the key areas of discrepancy within *LUCAS* as a physically based, distributed model is that the canopy is an entirely separate unit from the hillslope, it can be of any size and acts as a form of rainfall modulator above, but not connected to the hillslope. This means that the rainfall partitioning, although three dimensional, is not spatially distributed within the segment i.e. the canopy can be different between hillslope segments but not within segments. Consequently land use changes occurring within the hillslope scale cannot be simulated except by changing the catchment segmentation to fit the land use requirements rather than the topographic requirements. This is clearly not feasible as catchment segmentation is designed to simulate the topography; the rules dealing with the number and size of segments all reflect this. Consequently the planting of trees only to certain elevation within a catchment (a common forestry policy) cannot be simulated by the model.

At the time of redevelopment following the successful robustness testing (see

chapter seven) an attempt was made to make *LUCAS* fully distributed. This involved the growth of a forest over however much of each segment is required, and the below canopy rainfall being summed for each surface element (increment) of the segment. This version of the scheme was programmed but subsequent initial testing of the program showed that the large arrays necessary meant that it used too much memory for the Mainframe used (*MIPS* 2000). On very small segments (approximately 100*m* in length) using a tree spacing of 3*m* the forest growth simulation of 40 *years* took approximately 14 days to complete. This meant that it was impractical to use in the validation exercise using the Tanllwyth where the segments are mostly larger than this and the tree spacing is smaller (consequently the number of trees per segment would be greater).

A conceptual representation of the fully spatially distributed version of *LUCAS* is shown in figure 9.1 and the flow diagrams showing the changes to the growth model and *VSAS4* are shown in figure 9.2-9.4. This version of *LUCAS* provides an avenue for future development within the scheme as it allows the model to operate in a fully distributed manner but it will require either rewriting in a less repetitive manner or further computing hardware improvements before it can become properly operational. The changes made are superficial, mostly being to do with the scale of model operation, so the fully distributed version of *LUCAS* would not necessarily require complete retesting.

The avenues for future research detailed in this section have concentrated on either areas highlighted by *LUCAS* or areas within *LUCAS* that could be improved. The final part of the thesis considers modelling long term vegetation change in more general terms.

9.2.2 Future of modelling long term vegetation change

In chapter one it was pointed out that any study investigating long term vegetation change would need to have a predictive ability, as site specific measurement is beyond the scope (in time and expense) of most researchers. Consequently the use of physically based, distributed hydrological models as base units and the modelling of their inputs to parameterise the degree of change was advocated. This approach has been developed in this thesis using a specially designed modelling scheme, given the name *LUCAS*. The approach has been successful in showing an ability to predict the effects of long term vegetation in a temporally dynamic manner but it is difficult to ascertain exactly how accurate these predictions are as there is no applicable data set to test the model predictions against.

The success of the scheme described above indicates that this type of approach is a reasonable investigative method. The use of a modelling scheme to investigate a complicated issue such as long term vegetation change where there are no empirical data base to back up the predictions is becoming more common as computing hardware allows

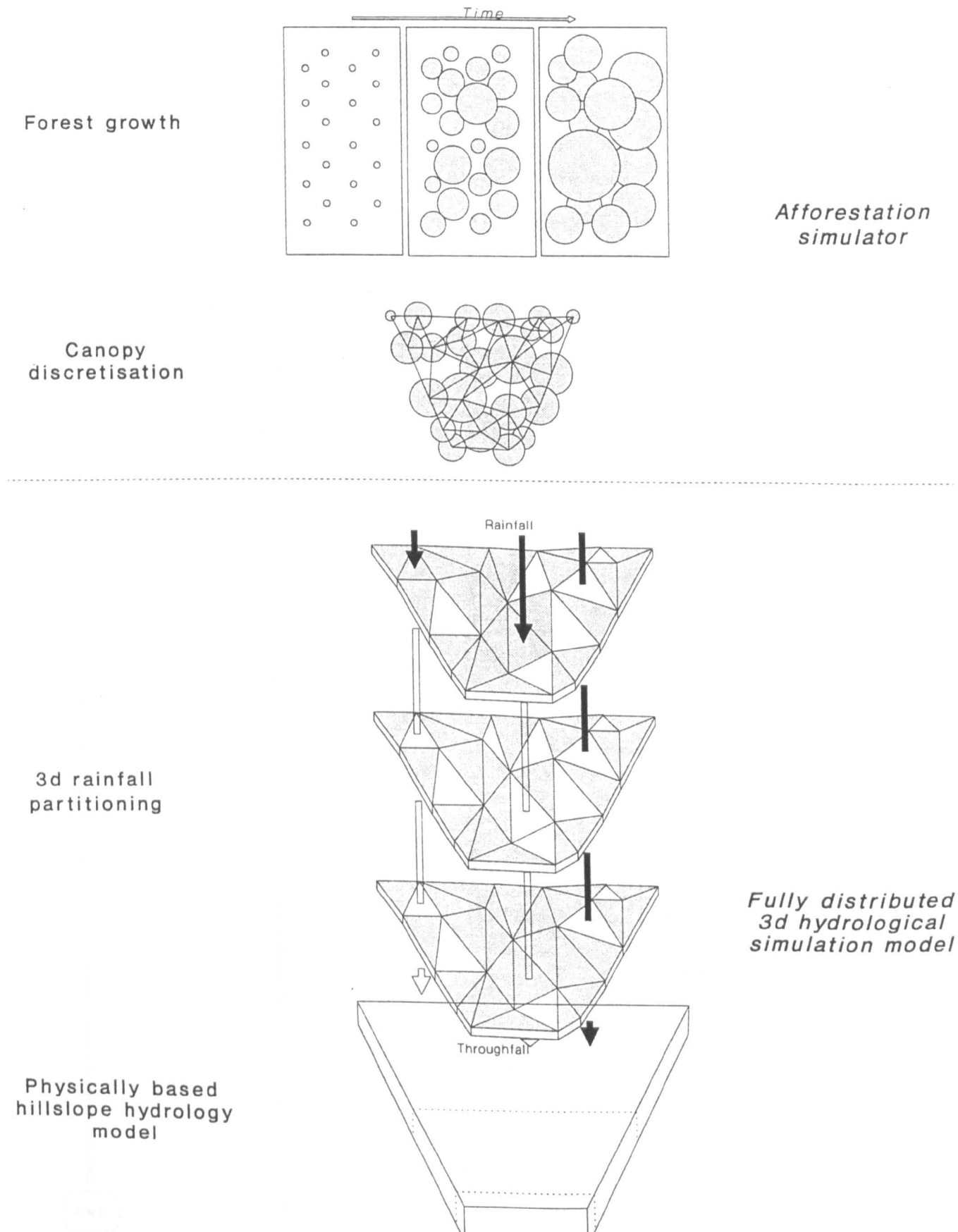

Figure 9.1: Conceptual representation of the fully distributed version of *LUCAS*

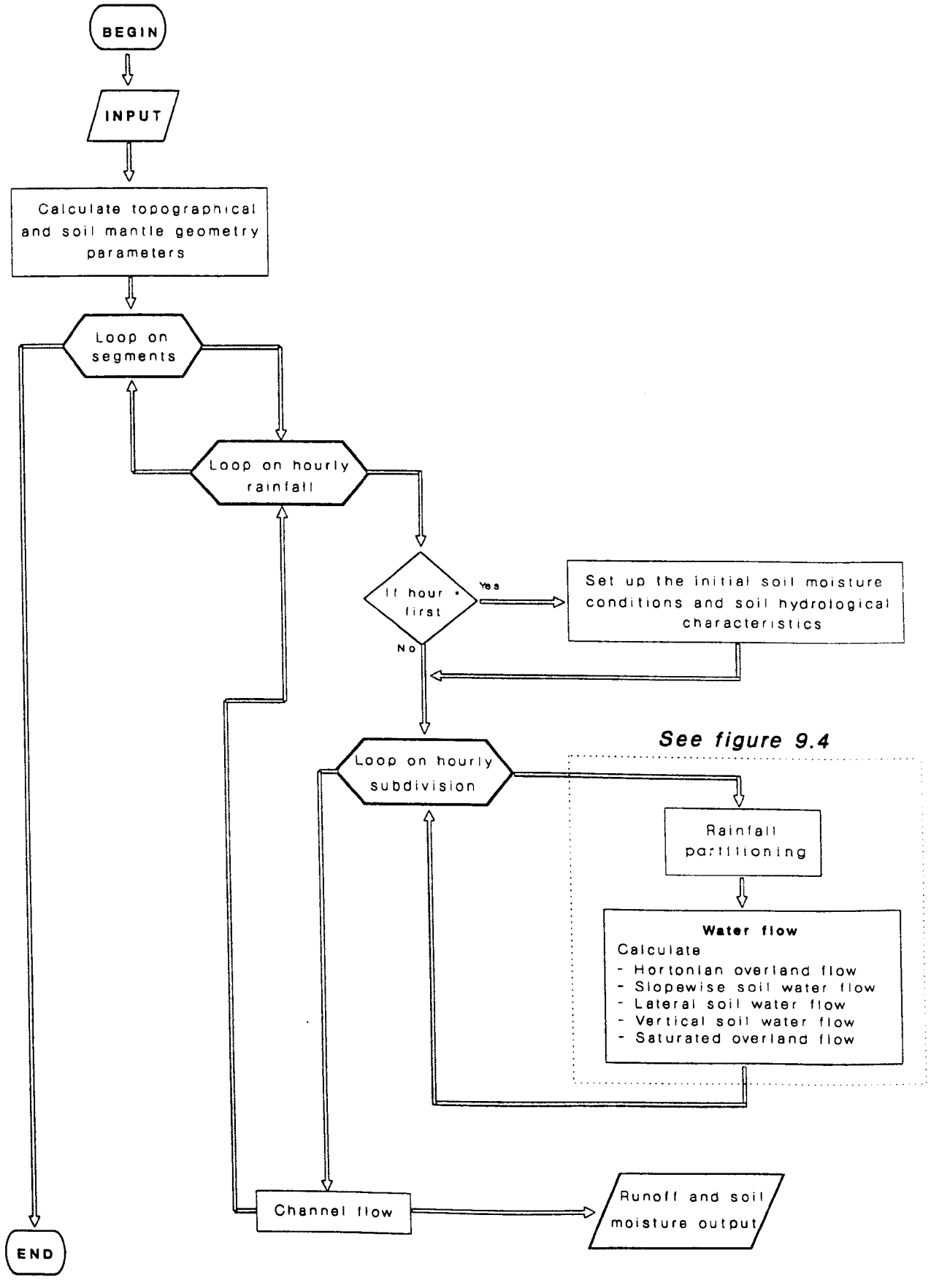

Figure 9.2: Flow diagram showing the structure of the fully distributed version of *LUCAS*

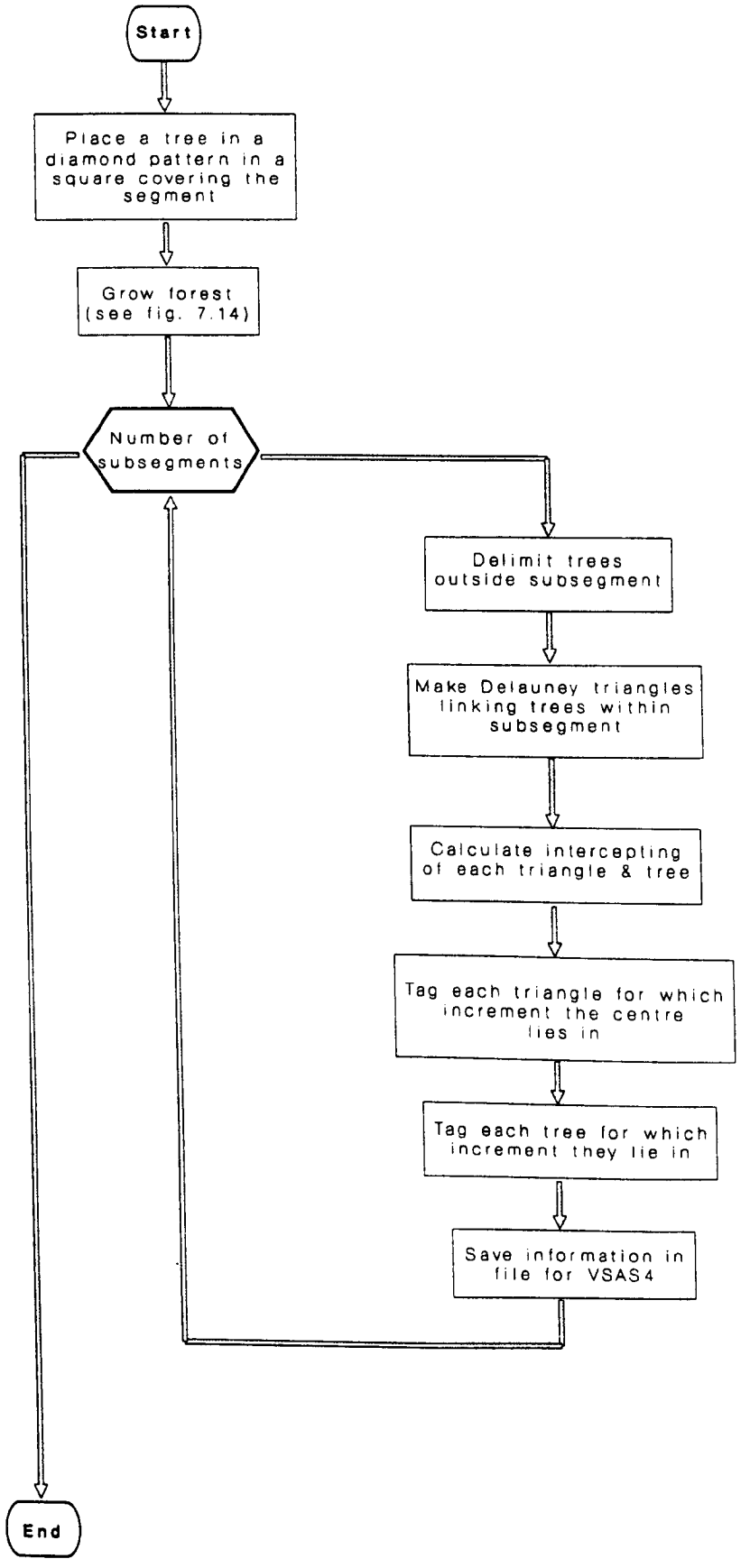

Figure 9.3: Flow diagram of the forest growth routine within the fully distributed version of *LUCAS*

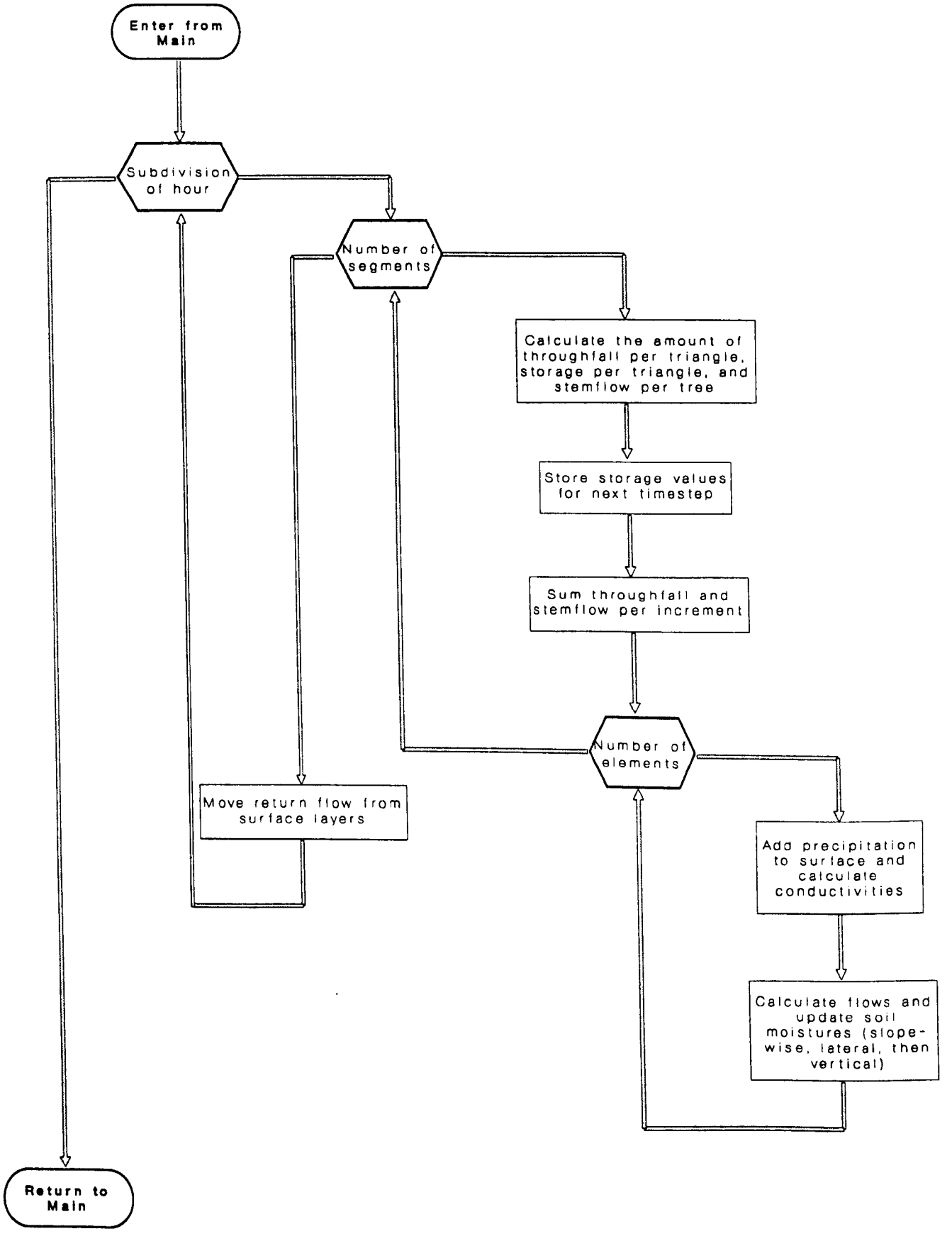

Figure 9.4: Flow diagram of the *DRAIN* (surface and subsurface hydrology) subroutine within the fully distributed version of *LUCAS*

modelling techniques to develop rapidly. In this study the problem of inadequate verification and limited validation was overcome by restricting the model to development and highlighting areas for further investigation. If these kind of schemes are going to be used in applications then a more rigid framework has to be arrived at that, that allows for the lack of verification and validation. The most logical way for this framework to develop is in a probabilistic manner so that a full range of predictions are presented as possible rather than the single option provided by a deterministic framework. This provides a large area for future development in the field of modelling long term vegetation change.

The approach used here has been successful in exploring implications of making certain assumptions about long term vegetation change and consequently pointing out avenues for future research. This provides probably the most effective usage of any scheme modelling long term vegetation change as it can highlight the areas of process representation that need further empirical study or theoretical development. A different modelling approach to the same problem may well reveal different process representations that require further investigation; the aim must be to gain several modelling opinions on where further development is required and then focus on providing this development so that both hydrological knowledge and consequently the modelling capability is increased.

BIBLIOGRAPHY

Abbott M.B., Bathurst J.C., Cunge J.A., O'Connell P.E., and Rasmussen J. (1986a): An introduction to the European Hydrological System - Système Hydrologique Européen, "SHE", 1. History and philosophy of a physically-based distributed modelling system. *Journal of Hydrology* **87**:45-59

Abbott M.B., Bathurst J.C., Cunge J.A., O'Connell P.E., and Rasmussen J. (1986b): An introduction to the European Hydrological System - Système Hydrologique Européen, "SHE", 2. Structure of a physically based, distributed modelling system. *Journal of Hydrology* **87**:61-67

Aikman D.P and Watkinson A.R. (1980): A model for growth and self-thinning in even-aged monocultures of plants. *Annals of Botany* **45**:419-427

Anderson M.G. (1982): Modelling hillslope soil water status during drainage. *Transactions of the Institute of British Geographers N.S.* **7**:337-353

Anderson M.G. and Burt T.P. (1978): The role of topography in controlling throughflow generation. *Earth Surface Processes* **3**:331-344

Anderson M.G. and Kneale P.E. (1982): The influence of low-angled topography on hillslope soil-water convergence and stream discharge. *Journal of Hydrology* **57**:65-80

Anderson M.G. and Burt T.P. (1985): Modelling strategies. In: Anderson M.G. & Burt T.P. (eds) *Hydrological Forecasting*, John Wiley & Sons Ltd. pp 1-13

Anderson M.G. and Rogers C.C.M. (1987): Catchment scale distributed hydrological models: a discussion of research directions. *Progress in Physical Geography* **11**:28-51

Bathurst J.C. (1986a): Physically-based distributed modelling of an upland catchment using the Système Hydrologique Européen. *Journal of Hydrology* **87**:79-102

Bathurst J.C. (1986b): Sensitivity analysis of the Système Hydrologique Européen. *Journal of Hydrology* **87**:103-123

Bathurst J.C. and O'Connell P.E. (1992): Future of distributed modelling: the Système Hydrologique Européen (SHE). *Hydrological Processes* **6**:265-277

Bella I.E. (1971): A new competition model for individual trees. *Forest Science* **17**:364-372

Bernier P.Y. (1982): *VSAS2: A revised source area simulator for small forested areas.* Unpublished PhD. thesis. University of Georgia, Athens, Georgia, USA

Bernier P.Y. (1985): Variable source areas and storm-flow generation: an update of the concept and simulation effort. *Journal of Hydrology* **79**:195-213

Betson R.P., Hawkins R.H., Schneider V.R. and Wallace J.R. (1985): Evaluation of hydrologic models used to quantify major land-use change effects. Report by the task committee on quantifying land-use change effects of the watershed management and surface-water committees of the irrigation and drainage division. *Proceedings of the American Society of Civil Engineers, Journal of Irrigation and Drainage Engineering* **111**:1-17

Beven K. (1989): Changing ideas in hydrology - the case of physically-based models. *Journal of Hydrology* **105**:157-172

Bosch J.M. and Hewlett J.D. (1982): A review of catchment experiments to determine the effect of vegetation changes on water yield and evapotranspiration. *Journal of Hydrology* **55**:3-23

Briggs D.J. and Wickramsinghe A. (1990): Modelling forest growth - environment relationships: theory and applications. *Applied Geography* **10**:187-204

Bruce D. (1990): Development of empirical forest growth models. In: Dixon, Meldahl, Ruark, and Warren (eds) *Process modeling of forest growth responses to environmental stress.* Timber Press, Oregon. pp 191-199

Burt T.P. (1978): *Runoff processes in small upland catchments with special reference to the role of hillslope hollows.* Unpublished PhD. thesis, University of Bristol

Calder I.R. (1990): *Evaporation in the uplands.* John Wiley & Sons. 148p

Calder I.R. and Wright I.R. (1986): Gamma ray attenuation studies of interception from Sitka spruce: some evidence for an additional transport mechanism. *Water Resources Research* **22**:409-417

Calver A. (1988): Calibration, sensitivity, and validation of a physically-based rainfall-runoff model. *Journal of Hydrology* **103**:103-115

Darcy H. (1856): *Les Fontaines Publique de la Ville de Dijon.* Dalmont, Paris

Doyle T.W. (1990): An evaluation of competition models for investigating tree and stand growth processes. In: Dixon, Meldahl, Ruark, and Warren (eds) *Process modeling of forest growth responses to environmental stress.* Timber Press, Oregon. pp 271-277

Dunn S., Savage D., and Mackay R. (1992): Hydrological simulation of the Rede catchment using the Système Hydrologique Européen (SHE). In: Whitby M.C. (ed) *Land use change: the causes and consequences.* ITE symposium no. 27

Durocher M.G. (1991): *Spatial variability of rainfall interception by forest.* Unpublished PhD. thesis. University of Bristol, Bristol, UK

Edwards P.N. and Christie J.M. (1981): *Yield models for forest management.* Forestry Commission booklet 48

Fawcett K.R. (1992): *Hydrological physically based distributed models: Parameterization and process representation.* Unpublished PhD. thesis, University of Bristol, UK

Fleming G. (1979): *Deterministic models in hydrology.* FAO irrigation and drainage paper 32

Ford E.D. (1982): High productivity in a Polestage Sitka spruce stand and its relation to canopy structure and development. *Forestry* **55**:1-17

Ford E.D. and Diggle P.J. (1981): Competition for light in a plant monoculture modelled as a spatial stochastic process. *Annals of Botany* **48**:481-500

Freeze R.A. (1972): The role of subsurface flow in the generation of surface runoff. Baseflow contributions to channel flow. *Water Resources Research* **8**:609-23

Freeze R.A. and Harlan R.L. (1969): Blueprint for a physically-based digitally-simulated hydrological response model. *Journal of Hydrology* **9**:237-258

Gash J.H.C. (1979): An analytical model of rainfall interception by forest. *Quarterly Journal of the Royal Meteorological Society* **105**:43-55

Gates D.J. (1982): Competition and skewness in plantations. *Journal of Theoretical Biology* **94**:909-922

Halldin S. (1985): Leaf and bark area distribution in a pine forest. In: Hutchinson B.A. and Hicks B.B. (eds) *Forest-Atmosphere interaction* D. Ridel Publishing pp 39-58

Helvey J.D. and Patric J.H. (1965): Canopy and litter interception of rainfall by hardwoods of eastern United States. *Water Resources Research* **1**:193-206

Hewlett J.D. and Hibbert A.R. (1963): Moisture and energy conditions within a sloping soil mass during drainage. *Journal of Geophysical Research* **68**:1081-89

Hewlett J.D. and Hibbert A.R. (1967): Factors affecting the response of small watersheds to precipitation in humid areas. In: Soper W.E. and Lull H.W. (eds) *Forest Hydrology* Pergamon, Oxford. pp 275-290.

Hewlett J.D. and Nutter W.L. (1970): The varying source area of stream flow from upland basins. *Interdisciplinary aspects of watershed management, Proceedings of Symposium*, Bozeman, Montana, American Society of Civil Engineers, pp 65-83.

Hewlett J.D. and Troendle C.A. (1975): Non-point and diffused water sources: a variable source area problem. In: *Watershed Management, Proceedings of Symposium*, American Society of Civil Engineers, Irrigation and Drainage division. Logan, Utah, pp 21-46.

Hillman G.R. and Verschuren J.P. (1988): Simulation of the effects of forest cover, and its removal, on subsurface water. *Water Resources Research* **24**:305-314

Hoogland J.C., Belmans C., and Feddes R.A. (1981): Root water uptake depending on soil water pressure head and maximum extraction rate. *Acta Horticulturae* **119**:123-136

Horton R.E. (1933): The role of infiltration in the hydrologic cycle *Transactions of the American Geophysical Union* **14**:446-460

Howes S. (1985): *A mathematical hydrological model for the ungauged catchment.* Unpublished PhD. thesis, University of Bristol, England. 404p

Hunt R. (1982): *Plant growth curves.* Edward Arnold (publishers) Ltd., London. 248p

Hursh C.R. (1944): Report of the subcommittee on subsurface flow. *Transactions of the American Geophysical Union* **25**:743-746

Ingwersen J.B. (1985): Fog drip, water yield, and timber harvesting in the Bull run municipal watershed, Oregon. *Water Resources Bulletin* **21**:469-473

Jackson R.D. (1972): On the calculation of hydraulic conductivity. *Soil Science Society of America Proceedings* **36**:380-382

Johnson R.C. (1991): *Effects of upland afforestation on water resources. The Balquhidder experiment 1981-1991.* Institute of Hydrology report no. 116

Kirby C., Newson M.D., and Gilman K. (eds) (1991): *Plynlimon research: The first two decades.* Institute of Hydrology report no. 109

Klemeš V. (1986): Operational testing of hydrological simulation models. *Hydrological Sciences Journal* **31**:13-24

Konikow L.F. and Bredehoeft J.D. (1992): Ground-water models cannot be validated. *Advances in Water Resources* **15**:75-83

Kneale P.E. (1981): *Soil water processes in low permeability soils with reference to hillslope hydrology and slope stability.* Unpublished PhD. thesis, University of Bristol.

Kunze R.J., Vehara G., and Graham K. (1968): Factors important to the calculation of hydraulic conductivity. *Soil Science Society of America Proceedings* **32**:760-765

Law F. (1956): The effects of afforestation upon the water yield of water catchment areas. *Journal of British Waterworks Association* **38**:489-94

Law F. (1958): Measurement of rainfall, interception and evaporation losses in a plantation of Sitka spruce trees. *International Association of Scientific Hydrology Publication 44* pp 397-411

Ledig F.T. (1969): A growth model for tree seedlings based on the rate of photosynthesis and the distribution of photosynthate. *Photosynthetica* **3**:263-275

Lee R. (1980): *Forest Hydrology.* Columbia University Press, New York. 349p

Leps J. and Kindlmann P. (1987): Models of the development of spatial development of spatial pattern of an even-aged plant population over time. *Ecological Modelling* **39**:45-57

Leyton L., Reynolds E.R.C., and Thompson F.B. (1967): Rainfall interception in forest and moorland. In: Soper W.E. and Lull H.W. (eds) *Forest Hydrology* Pergamon, Oxford. pp 163-168

Lorimer C.G. (1983): Tests of age independent competition indices for individual trees in natural hardwood stands. *Forest Ecology and Management* **6**:343-360

Ludlow A.R., Randle T.J., and Grace J.C. (1990): Developing a process-based growth-model for Sitka spruce. In: Dixon, Meldahl, Ruark, and Warren (eds) *Process modeling of forest growth responses to environmental stress.* Timber Press, Oregon. pp 249-262

May R.M. (1974): Biological populations with non-overlapping generations: stable points, stable cycles, and chaos. *Science* **186**:645-647

McCuen R.H. (1976): The anatomy of the modelling process. In: Brebbia C.A. (ed) *Mathematical models for environmental problems.* Pentech Press, London. pp 401-412

McIlroy I.C. and Angus D.E. (1964): Grass, water and soil evaporation at Aspendale. *Agricultural Meteorology* **1**:201-224

McKim H.L., Cassell E.A., and LaPotin P.J. (in press): Water resource modelling using remote sensing and object-oriented simulation. *Hydrological Processes*

Miller D.R., Butler G., and Bramall L. (1976): Validation of ecological system models. *Journal of Environmental Management* **4**:383-401

Millington R.J. and Quirk J.P. (1961): Permeability of porous solids. *Transactions of the Faraday Society* **57**:1200-1207

Mohren G.M.J., Van Gerwen C.P., and Spitters C.J.T. (1984): Simulation of primary production in even aged stands of Douglas Fir. *Forest Ecology and Management* **9**:27-49

Mohren G.M.J. and Rabbinge R. (1990): Growth influencing factors in dynamic models of forest growth. In: Dixon, Meldahl, Ruark, and Warren (eds) *Process modeling of forest growth responses to environmental stress.* Timber Press, Oregon. pp 229-240

Moore J.A., Budelsky C.A., and Schlesinger R.C. (1973): A new index representing individual tree competitive status. *Canadian Journal of Forestry Research* **3**:495-500

Morris E.M. (1980): Forecasting flood flows in grassy and forested basins using a deterministic distributed mathematical model. *Hydrological Forecasting, Proceedings of the Oxford Symposium.* IAHS publication 129, pp 247-255

Munro D.D. (1974): Forest growth models - a prognosis. In: Fries J. (ed) *Growth models for tree and stand simulation* IUFRO working party S4.0-4 Proceedings of meetings in 1973 Institutionen för skogsproduktion, Research notes Nr 30. Skogshögskolan, Royal College of Forestry. pp 7-21

Newson M.D. (1976): *The physiography, deposits and vegetation of the Plynlimon catchments (a synthesis of published work and initial findings).* Institute of Hydrology report no. 30

Penman H.L. (1963): Vegetation and hydrology. *Technical Communication* **53**. Commonwealth Bureau of Soils, Harpenden, England

Pilgrim D.H. (1975): Model evaluation, testing and parameter estimation in hydrology. In: Chapman T.G. and Dunin F.X. (eds) *Prediction in catchment hydrology.* Australian Academy of Science pp 305-333

Popper K. (1959): *The logic of scientific discovery.* Harper & Row, New York

Prevost M., Barry R., Stein J., and Plamonden A.P. (1990): Snowmelt runoff modelling in a Balsam fir forest with a variable source area simulator (VSAS2). *Water Resources Research* **26**:1067-1077

Rawls W.J., Brakensiek D.L., and Saxton K.E. (1982): Estimation of soil water properties. *Transactions of the American Society of Agricultural Engineers* **25**:1316-1320

Rawls W.J. and Brakensiek D.L. (1985): Agricultural management effects on soil water retention. In: DeCoursey D.G. (ed) *Proceedings of the Natural Resources Modeling Symposium, Pingree Park, Co, October 16-21 1983.* United States Department of Agriculture Agricultural Research Service ARS-30, pp 115-117

Richards F.J. (1959): A flexible growth function for empirical use. *Journal of Experimental Botany* **10**:290-300

Richards L.A. (1931): Capillary conduction of liquids through porous mediums. *Physics* **1**:318-333

Robinson M. (1986): Changes in catchment runoff following drainage and afforestation. *Journal of Hydrology* **86**:71-84

Rogers C.C.M. (1985): *Further development of distributed hydrologic models with reference to the Institute of Hydrology Distributed Model.* Unpublished PhD. thesis, University of Bristol, England. 462p.

Ross B.B., Contractor D.N., and Shanholtz V.O. (1979): A finite element model of overland and channel flow for assessing the hydrologic impact of land-use change. *Journal of Hydrology* **41**:11-30

Rutter A.J., Kershaw K.A., Robins P.C., and Morton A.J. (1971): A predictive model of rainfall interception in forests. I. Derivation of the model from observations in a plantation of Corsican pine. *Agricultural Meteorology* **9**:367-384

Sargent R.G. (1982): Verification and validation of simulation models. In: Cellier F.E. (ed) *Progress in modelling and simulation.* Academic Press, pp 159-169

Sharpe P.J.H. (1990): Forest modeling approaches: compromises between generality and precision. In: Dixon, Meldahl, Ruark, and Warren (eds) *Process modeling of forest growth responses to environmental stress.* Timber Press, Oregon. pp 180-190

Shugart H.H. (1984): *A theory of forest dynamics* Springer-Verlag, New York 278p

Smith W.R. (1990): The static geometric modeling of three-dimensional crown competition. In: Dixon, Meldahl, Ruark, and Warren (eds) *Process modeling of forest growth responses to environmental stress.* Timber Press, Oregon. pp 294-302

Son I. (1990): *Modelling the effects of land-use change in a small catchment.* Unpublished PhD. thesis, University of Southampton, U.K.

Stephenson G.R. and Freeze R.A. (1974): Mathematical simulation of subsurface flow contributions to snowmelt runoff, Reynolds Creek Watershed, Idaho. *Water Resources Research* **10**:284-298

Stewart J.B. (1977): Evaporation from the wet canopy of a pine forest. *Water Resources Research* **13**:915-921

Tiktak A. and Bouten W. (1992): Modelling soil water dynamics in a forested ecosystem. III: Model description and evaluation of discretization. *Hydrological Processes* **6**:455-465

Troendle C.A. (1979): *A variable source area model for stormflow prediction on first order forested watersheds.* Unpublished PhD. thesis, University of Georgia.

Troendle C.A. (1985): Variable source area models. In: Anderson M.G. and Burt T.P. (eds) *Hydrological Forecasting*, John Wiley & Sons Ltd. pp 347-403

Vose J.M. and Swank W.T. (1990): A conceptual model of forest growth emphasising stand leaf area. In: Dixon, Meldahl, Ruark, and Warren (eds) *Process modeling of forest growth responses to environmental stress.* Timber Press, Oregon. pp 278-2872

Ward R.C. & Robinson M. (1990): *Principles of Hydrology Third edition*, McGraw-Hill Book Company, London. 365p

Watson D.F. (1982): ACORD: Automatic contouring of raw data. *Computer Geoscience* **8**:97-101

Watts G.P. (1989): *Modelling the subsurface hydrology of semi-arid agricultural terraces.* Unpublished PhD. thesis, University of Bristol, UK.

Whitelaw A.S. (1988): *Hydrological modelling using variable source areas.* Unpublished PhD. thesis, University of Bristol, Bristol, UK. 382p

Wu H., Malafant K.M., Penridge L.K., Sharpe P.J.H., and Walker J. (1987): Simulation of two dimensional point patterns: Applications of lattice framework approach. *Ecological Modelling* **38**:299-308

Yoda K., Kira T., Ogawa H., and Hozumi K. (1963): Self-thinning in overcrowded pure stands under cultivated and natural conditions (Intraspecific competition among higher plants XI). *Journal of the Institute of Polytechnics, Osaka City University, Series D* **14**:107-129

Zinke P.J. (1967): Forest interception studies in the United States. In: Soper W.E. and Lull H.W. (eds) *Forest Hydrology*. Pergamon, Oxford, pp 137-161

APPENDIX A

LUCAS PROGRAM CODE

LIST OF VARIABLES

a1 . . . . . Impermeable area in segment (m^2)
a2 . . . . . Channel area (m^2)
adepth . . . . . .Depth of top soil layer (*m*)
aidex . . . . . .Leaf area index of a tree
aleng . . . . . .Length of plot side for forest simulation (*m*)
asdrop . . . . . .Elevation drop between subsegment elements (*m*)
asr1 . . . . . Saturated moisture content (porosity)
assIln . . . . . Slopeline length between subsegment elements (*m*)
asslp . . . . . .Slope between subsegment element centres (unit %)
astcon . . . . . .Saturated hydraulic conductivity (ms^{-1})
avdrop . . . . . .Elevation drop along slopewise length of element (*m*)
avele . . . . . .Elevation of element centre (*m*)
avlen . . . . . .Plan length of increment (*m*)
avslln . . . . . Slopeline length of element (*m*)
avslp . . . . . .Slope of element (unit %)
avvol . . . . . .Volume of element (m^3)
avwid . . . . . Width of element at mid increment point (*m*)
ax . . . . . Moisture contents on suction-moisture curve
bdepth . . . . . .Proportion of soil mantle in remaining layers (i.e. not top layer; see *adepth*)
bdr . . . . . .Drainage coefficient (a in table 4.2)
bhght . . . . . Proportion of tree height below crown (see figure 5.3)
cdr . . . . . .Drainage coefficient (b in table 4.2)
covin(jt,i) . . . . Amount of tree i contained within a triangle jt (m^2)
cponly . . . . . .Logical variable whether only a canopy is required i.e. no *VSAS4*
croang . . . . . .Crown angle (*radians*)
bstcap . . . . . .Branch storage capacity (*mm*)
cocor(n,1) . . . . .x coordinate of subsegment/segment corner n (numbered 1 - 4 clockwise from bottom left)
cocor(n,2) . . . . .y coordinate of subsegment/segment corner n
dbhlog . . . . . .Logical variable whether the initial dbh is randomly assigned (T) or a fixed value
dbhmax . . . . . Maximum dbh value (*m*)
dbhval . . . . . .Value of initial dbh, if dbhlog = .false. (*m*)
depmax . . . . . Depth of soil mantle under each increment (*m*)
dist . . . . . .Distance between computational point and next element centre
dstij . . . . . Distance between tree i and competitor tree j (*m*)
elev . . . . . Elevation of element at top of increment (*m*)
evap . . . . . .Potential evaporation per hour ($cmhr^{-1}$)
extra . . . . . .Return flow from elements (m^3)
fa . . . . . .Free throughfall proportion per triangle layer
fdr . . . . . Drainage between triangle layers (*mm*) (suffix *old* means drainage from previous timestep)
fstcap . . . . . Leaf storage capacity (*mm*)
fsto . . . . . .Storage per triangle layer (*mm*)
flow . . . . . Outflows from each streamside element (m^3)

grad . . . . . Gradient between elements for soil matrix flow
grmean . . . . . Mean growth rate
grsd . . . . . Standard deviation of mean growth rate
hicept . . . . . Intercept of relationship between dbh and tree height
hlen . . . . . Orthogonal distance between projected length of the streamfront and the upper of subsegment (see figure 4.9) (*m*)
hslope . . . . . Slope of relationship between dbh and tree height
irout . . . . . Lag for flow between segment and catchment boundary (*minutes*)
isdead(i) . . . . . Killing factor for tree i (when it reaches 3 the tree dies)
itetr(jt,i) . . . . . Tree number at vertex i in triangle jt
ittlo . . . . . Length of forests growth (*years*)
ix . . . . . Counter for which direction soil matrix flow is being computed. 1=vertical, 2=slopewise then lateral flow
jno . . . . . Number of elements per increment (i.e. number of layers)
kno . . . . . Number of subsegments per segment (maximum 5)
krep . . . . . Outer timestep subdivision (see figure 7.1)
lrep . . . . . Inner timestep subdivision (see figure 7.1)
mno . . . . . Number of segments
newcpy . . . . . Logical variable whether a new canopy is required or use old output file
nfola(jt) . . . . . Number of leaf layers per triangle jt
nlimk . . . . . Number of increments per segment/subsegment
nost . . . . . Number of soil types
nsmc . . . . . Number of points on suction moisture curve
nstla(i) . . . . . Number of stem layers per tree i
ntint . . . . . Number of time intervals of used in plot density inputs
ntr . . . . . Number of triangles
ntree . . . . . Number of trees
nyear . . . . . Times of plot density inputs (*years*)
ntrel . . . . . Plot density inputs (from Forestry Commission yield tables)
oflow . . . . . Saturated overland flow (m^3)
pat(1) . . . . . Pattern parameter to control Poisson distribution for leaf clustering (see figure 4.6)
pat(2) . . . . . Pattern parameter to control Poisson distribution for stem clustering
pnet . . . . . Net below canopy rainfall (*cm* per timestep)
pnt(i,1) . . . . . x coordinate of tree i (*m*)
pnt(i,2) . . . . . y coordinate of tree i (*m*)
pnt(i,3) . . . . . DBH of tree i (*m*)
pnt(i,4) . . . . . Crown radius of tree i (*m*)
pnt(i,5) . . . . . Height of tree i (*m*)
pnt(i,6) . . . . . Proportion of crown surface area generating stemflow
pnt(i,7) . . . . . Growth rate of tree i
pnt(i,8) . . . . . Zone of influence (ZOI) of tree i
pnt(i,9) . . . . . Unit % amount that tree i's growth is affected by competitors
pos . . . . . Proportion of segment length in each soil type
precip . . . . . Above canopy rainfall ($cmhr^{-1}$)
ptot . . . . . Total *pnet* for each hour ($cmhr^{-1}$)
roffst . . . . . Offset for flow between skewed subsegments (see figure 4.9) (*m*)
sai . . . . . Stem area index of tree
sarea . . . . . Surface area for flow to pass through between elements (m^2)
sdx . . . . . Standard deviation of moisture contents on suction moisture curve
sdsr . . . . . Standard deviation of saturated moisture content
sdsat . . . . . Standard deviation of saturated hydraulic conductivity
sflow . . . . . Soil matrix flow from streamside elements (m^3)
sgarea . . . . . Area of each subsegment (m^2)
smcvol . . . . . Soil moisture content of each element (m^3)
square . . . . . Logical variable whether the pattern between trees is square (T) or diamond
space . . . . . Inter tree spacing (*m*)

stdr . . . . . Stem layer drainage (*mm*) (suffix *old* means drainage from previous timestep)
ssto . . . . . Stem layer storage (*mm*)
stonec . . . . . Stone content (%)
stm . . . . . Mean stemflow proportion value
stmin . . . . . Minimum stemflow proportion
stmax . . . . . Maximum stemflow proportion
stsd . . . . . Standard deviation of *stm*
tbfree . . . . . Total direct throughfall (m^3)
tost . . . . . Total stemflow (m^3)
totsa . . . . . Total surface area of canopy (summed from triangles) (m^2)
tothro . . . . . Total indirect throughfall (m^3)
totar . . . . . Total catchment area (summed from *sgarea*) (m^2)
trscap . . . . . Trunk storage capacity (*mm*)
trees . . . . . Logical variable whether segment has a canopy cover
triano(jt,1) . . . . x coordinate of triangle jt centrepoint (*m*)
triano(jt,2) . . . . y coordinate of triangle jt centrepoint (*m*)
triano(jt,3) . . . . Triangle jt surface area (m^2)
triano(jt,4) . . . . Between crowns gap surface area in triangle jt (m^2)
triano(jt,5) . . . . Total crown cover within triangle jt (m^2)
triano(jt,6) . . . . Internal angle 1 of triangle jt (*radians*)
triano(jt,7) . . . . Internal angle 2 of triangle jt (*radians*)
triano(jt,8) . . . . Internal angle 3 of triangle jt (*radians*)
ttfree . . . . . Throughfall falling directly onto trunk (m^3)
twfree . . . . . Total free throughfall (m^3)
uscon . . . . . Unsaturated hydraulic conductivity for soil matrix flow between elements
xa . . . . . Distance from stream to top of increment (*m*)
xlai . . . . . Leaf area index of triangle
xi . . . . . Distance from stream to increment centre (*m*)
y . . . . . Suctions on suction moisture curve (*m*)
yi . . . . . Elevation of increment centre point (*m*)

```
::::::
```

```
      rewind 21
      rewind 23
C
      pi = (atan(1.0)) * 4
      totar = 0.
c
      read(8,50)MNO,NAME
      write(23,*)'MNO,        NAME'
      write(23,51)MNO,NAME
 50   FORMAT(/,I3,A40)
 51   FORMAT(I3,5x,A40)
      read(8,60)NOTE
      write(23,*)
      write(23,*)'NOTE'
      write(23,61)NOTE
 60   format(/,a40)
 61   format(a40)
      read(3,102)IDAY,IMONTH,IYEAR
 102  FORMAT(2I2,I4)
      read(8,91)KREP,LREP,nouta,ntmp,nost
      write(23,*)
      write(23,*)'KREP, LREP,  NOUTA, NTMP,  NOST'
      write(23,92)KREP,LREP,nouta,ntmp,nost
 91   format(/,5(i3,3x))
 92   format(5(i3,4x))
 c
      do 800  jkk=1,nost
       call smc
       satcs(jkk)=satcon
       srs(jkk)=sr1
       do 801 i=1,20
        smxs(jkk,i)=smx(i)
        smys(jkk,i)=smy(i)
        smzs(jkk,i)=smz(i)
        smgs(jkk,i)=smg(i)
        smgzs(jkk,i)=smgz(i)
 801    continue
 800   continue
 c
       call read1
       call outa1(totsa)
       IEND=IHR-1
 c
 c""""Start of segment specific simulation. READ2 contains data for each segment.
 c
  100 call read2
       IF(KNO.GE.99) GOTO 340
       IMIN=0
       IHOUR=0
       IT=0
       IXM=0
 C
       qq = 0.
 c
 c     Calculate the segment geometry and print it.
       totar2 = 0.0
       call BLKVOL
       if (nouta.eq.0) call outa2
```

```
      k = k+1
c
c  If the segment is forested there is the option of either generating a NEW random canopy
c  or calling on a file containing canopy data for the segment from an old run.
c
c     read forest growth parameters
 35   call read3
c
      kmmax = 0
      call CANOPY
c
      if (cponly .and. isgno .lt. mno) then
       isgno = isgno + 1
       goto 100
      endif
c
      if (cponly) goto 999
c
c     Set up time steps between VSAS and INTMO (inter.f)
      tstep = 3600/(krep*lrep)
c
c ================================================================
c
c     Start of hourly simulation. IT represents hours, and DRAIN is called every KREP times
c     per hour, with LREP repetitions within each call. The loop onto 161 allows for an
c     increased timestep to be used from the start of simulation until an 8. is found in the
c     data set, at which time the steps revert to 15 & 5 mins or whatever the LREP & KREP
c     values are set to below.
c ================================================================
c
 160    IT=IT+1
        IF(IT.GT.IEND) GOTO 100
        IF(PRECIP(IT).LT.8.)GOTO 161
        LREP=3
        KREP=4
c      PR is the precipitation (mm) per tstep for INTER
c      pef is the potential evaporation (mm) per tstep for INTER
 161    PR=(PRECIP(IT)*10.)/(krep*lrep)
        pef = evap(it)/(krep*lrep)
c
c     INTER is called to calculate the effective precip and surflo calcs the surface runoff.
c     PNR is effective precipitation minus the amount taken as surface runoff (ie so that it's
c      not added to the subsurface as well in drain)
c
c  Julian day from VSAS date:
       nday = julian(iday,imonth,iyear)
c  Initial time:
       tint = ((nday-1)*86400) + (nhr*3600) + (nmin*60)
c  Set current time equal to initial time:
       if (it .eq. 1) then
        time = tint
        call TVARY
       endif
c
c
c     The loop below calls INIT on the first pass for each segment and DRAIN on every
c     pass. The K passed to drain is not K as in subsegments, but K from KREP
c
```

```
      ptot(it)=0.
      oflow(it,1)=0.0
      oflow(it,2)=0.0
      oflow(it,3)=0.0
c
      write(6,*)'it=',it
      DO 305 K=1,KREP
       if(it.eq.1.and.k.eq.1) call init
       call DRAIN(K)
       IX=IXM+1
305   CONTINUE
C
      CSS=0.
      IF (PTOT(IT).GT.0.)call SURFLO(A1,A2,PTOT,CSS,IT)
c
c     The next bit (down to 310) adds together the direct runoff (from SURFLO above) and
c     the flow to the stream emerging DRAIN. FLOW(K,J) is outflow from each depth (j) of
c     each subsegment (k).
c
      q=css
c
      write(17,609)it
      write(17,610)(k,k=1,kno)
      do 311 k=1,kno
       eflow(k) = 0.
       DO 310 J=1,JNO
        eflow(k)=eflow(k) + flow(k,j)
        q=q+flow(k,j)
         write(17,611)j,(sflow(lm,1,j,2),lm=1,kno)
310    continue
       fredb(k) = eflow(k) - oflow(it,k)
311   continue
      write(17,612)(fredb(k),k=1,kno)
      write(17,608)(oflow(it,k),k=1,kno)
      write(17,*)'                ==========='
c
      write(16,309)it,precip(it),ptot(it),fredb(1),oflow(it,1),eflow(1)
309   format(i3,5(6x,f8.3))
608   format('Total Saturated Overland Flow (mm) = ',7x,5f10.4)
609   format(/,'AFTER',i3,'  HOURS')
610   format(3x,'J; K',4x,5(i3,4x))
611   format(3x,i2,4x,5(f10.6,2x))
612   format(/,'Total Soil Water Flow (mm per subsegment) = ',
     &          5f10.4)
c
C *** Accumulate all flows in m3/hr
c
      qq=qq+q
c
c     OUTA3 print an hourly results summary, OUTB1 is called to accumulate results to be
c     printed at the end of the simulation.
c
      if(ntmp.eq.0) call outa3(totsa)
      call outb1(it,q)
      do 503 k=1,kno
       ecum(it,k) = eflow(k)
       do 504 n=1,nlimk(k)
        do 505 j= 1,jno
```

```
      do 506 ix = 1,2
       sflow(k,n,j,ix) = 0.
506    continue
505   continue
504   continue
503  continue
C
     if (it.ge.(iend-1))qqq(isgno)=qq
c
     goto 160
C *** New array to sum total runoff volumes for each segment
C
 340 if(ntmp .eq. 0) call outb2(it,mno,jno)
C
     do 600 nnn=1,mno
600   qqqq=qqqq+qqq(nnn)
C
     if (ntmp .ne. 0) goto 999
     WRITE(7,500)
     WRITE(7,501)(NNN,QQQ(NNN),NNN=1,MNO)
     WRITE(7,502)QQQQ
500   FORMAT(1X,'OUTFLOW VOLUMES PER SEGMENT (M3)')
501   FORMAT(5X,I2,3X,16(F15.3))
502   FORMAT(1X,'TOTAL OUTFLOW FOR SIM. PERIOD (M3)',F15.3)
C
 999  continue
      STOP
      END
```

```
::::::
```

```
      cdist = xwidth(k,1)
      ses = (adist + bdist + cdist)/2
      aresg = sqrt(ses*(ses-adist)*(ses-bdist)*(ses-cdist))
     else
      adist = sqrt(((cocor(k,1,1)-cocor(k,2,1))**2) + (cocor(k,1,2)-cocor(k,2,2))**2)
      bdist = xwidth(k,2)
      cdist = sqrt(((cocor(k,3,1)-cocor(k,1,1))**2) + (cocor(k,3,2)-cocor(k,1,2))**2)
      ses = (adist + bdist + cdist)/2
      aretr1 = sqrt(ses*(ses-adist)*(ses-bdist)*(ses-cdist))
      adist = sqrt(((cocor(k,1,1)-cocor(k,3,1))**2) + (cocor(k,1,2)-cocor(k,3,2))**2)
      bdist = sqrt(((cocor(k,3,1)-cocor(k,4,1))**2) + (cocor(k,3,2)-cocor(k,4,2))**2)
      cdist = xwidth(k,1)
      ses = (adist + bdist + cdist)/2
      aretr2 = sqrt(ses*(ses-adist)*(ses-bdist)*(ses-cdist))
      aresg = aretr1 + aretr2
     endif
     widest = amax1(xwidth(k,1),xwidth(k,2))
     thinn = amin1(xwidth(k,1),xwidth(k,2))
     sqarea = thinn * xa(k,nlimk(k))
     trarea = ((widest-thinn)/2) * xa(k,nlimk(k))
     sgarea = sqarea + trarea
77    if ((abs(sgarea - aresg)) .lt. 0.05) goto 75
     factor = aresg/sgarea
     xwidth(k,2) = xwidth(k,2)*factor
     xwidth(k,3)= xwidth(k,3)*factor
     widest = amax1(xwidth(k,3),xwidth(k,2))
     thinn = amin1(xwidth(k,3),xwidth(k,2))
     sqarea = thinn * (xa(k,nlimk(k))-xa(k,1))
     trarea = ((widest-thinn)/2) * (xa(k,nlimk(k))-xa(k,1))
     are1in = ((xwidth(k,1)+xwidth(k,3))/2) * xa(k,1)
     sgarea = sqarea + trarea + are1in
     goto 77
 75  totar2 = totar2 + aresg
 76  continue
c-----SECTION 1c-----
c
c    This section calculates the angular shifts for the non central flow lines (eg k=1 & k=3
c    for kno = 3 ). hlen is input as the horizontal distance from the stream to the watershed
c    running at 90 deg from the stream.
c
     do 30 k = 1,kno
      if(hlen(k).gt.xa(k,ni))then
       write(6,33)
       write(6,34)k,hlen(k),k,ni,xi(k,ni),k,ni,xa(k,ni)
       stop
      endif
      alpha(k) = asin(hlen(k)/xa(k,ni))
 30   continue
 33   format('ERROR IN BLKVOL..LINE 49',/,
     & 'hlen cannot be larger than xa(k,ni)',2x,'(cf xi(k,ni)')
 34   format('hlen(',i2,')=',f7.2,'  xi(',i2,',',i2,')=',f7.2,
     & ' xa(',i2,',',i2,')=',f7.2)
c
     ksum = 0
     do 32 k = 1,kno
      ksum = ksum + k
 32  if(k.eq.kno) ik = ksum / kno
c
```

```
      do 35 k = 1,kno
       diff(k) = abs(alpha(k)-alpha(ik))
   35 shift(k) = cos(diff(k))
c
c
c-----SECTION 2------
c
c   This section calculates the elevation of each element centre [avele], and elevation of
c   the top edge of each element [elev]. N.B. elev is only an approximation as the exact
c   topography is not known.
c
      do 42 k=1,kno
       ni = nlimk(k)
       do 41 n=1,ni
        avdep(k,n,1) = adepth
        avele(k,n,1) = yi(k,n) - avdep(k,n,1) / 2.
        rdep = depmax(k,n) - avdep(k,n,1)
        sumdep = avdep(k,n,1)
        avlen(k,n) = xa(k,n) - xa(k,n-1)
        do 40 j=2,jno
         jx = j-1
         avdep(k,n,j) = bdepth(jx) * rdep
         sumdep = sumdep + avdep(k,n,j)
         avele(k,n,j) = yi(k,n) - (sumdep - avdep(k,n,j)/2.)
   40    continue
   41    continue
   42   continue
c
      do 45 k = 1,kno
       ni = nlimk(k)
       do 44 j = 1,jno
        do 43 n = 1,ni-1
         tdist = xi(k,n+1) - xi(k,n)
         propn = (avlen(k,n)/2.)/tdist
         elev(k,n,j)=avele(k,n,j)+(propn*(avele(k,n+1,j)-avele(k,n,j)))
    43   continue
        elev(k,0,j)=avele(k,1,j)-(elev(k,1,j)-avele(k,1,j))
        elev(k,ni,j)=avele(k,n,j)+(avele(k,ni,j)-elev(k,ni-1,j))
    44  continue
    45 continue
c
c
c-----SECTION 3-----
c
c   This section calculates the rest of the soil element geometry like the volume [avvol], the
c   width [avwid], the slope line length [avslln] (remember avslln is only estimated as it is
c   based from avele, see section 2), the drop in elevation over an element [avdrop] etc.
c   The distances and slopes for between subsegments i.e. for lateral flow are denoted by
c   "as" prefix.
c
      do 50 k=1,kno
       km = k-1
       ni = nlimk(k)
       do 49 n=1,ni
        widest = amax1(xwidth(k,3),xwidth(k,2))
        thinn = amin1(xwidth(k,3),xwidth(k,2))
        if (xwidth(k,3) .gt. xwidth(k,2)) then
         if(n .eq. 1) then
```

```
      avwid(k,n) = (xwidth(k,1)+xwidth(k,3))/2
      temp = xa(k,ni) - xa(k,1)
     else
      avwid(k,n)=widest-((((xi(k,n)-xa(k,1))/temp))*(widest-thinn))
     endif
    else
     if(n .eq. 1) then
      avwid(k,n) = (xwidth(k,1)+xwidth(k,3))/2
      temp = xa(k,ni) - xa(k,1)
     else
      avwid(k,n)=thinn+((((xi(k,n)-xa(k,1))/temp))*(widest-thinn))
     endif
    endif
    if(k.gt.1) aslen(km,n) = (avwid(k,n)/2.)+(avwid(km,n)/2.)
    sumar(k,n) = avlen(k,n) * avwid(k,n)
    do 48 j=1,jno
     avdrop(k,n,j) = elev(k,n,j) - elev(k,n-1,j)
     avslln(k,n,j) = sqrt((avdrop(k,n,j)**2) + (avlen(k,n)**2))
     avvol(k,n,j) = avdep(k,n,j)*avwid(k,n)*avlen(k,n)*(1-stonec(j))
     avslp(k,n,j) = avdrop(k,n,j) / avlen(k,n)
     smln(k) = smln(k) + avlen(k,n)
     if(k.eq.1) goto 48
     asdrop(km,n,j) = avele(k,n,j) - avele(km,n,j)
     asslp(km,n,j)  = asdrop(km,n,1) / aslen(km,n)
     asslln(km,n,j) = sqrt(asdrop(km,n,j)**2 + aslen(km,n)**2)
 48  continue
 49  continue
 50 continue
C
C
C************SECTION 4
C
C    Now that most of the averaging proceedures have been removed, and the remainder
c    transferred to section 3 above, this section remains simply to calculate the total area.
C
     sgarea = 0.
     do 70 k=1,kno
      ni=nlimk(k)
      do 60 n=1,ni
 60    area(k)=area(k)+sumar(k,n)
 70   sgarea=sgarea+area(k)
     totar = totar + sgarea
     return
     end
```

subroutine CANOPY

```
c
c   This is a replacement of the CANOPY subroutine in VSAS4, it is bits of
c   INTMO and new (15/1/91) bits written by Tim.  There are five parts:
c     1) Setting out the trees in a grid pattern (square or hexagonal) within a square area.
c     2) Generating a random DBH (and therefore crown radius and tree height) and
c       proportion generting stemflow.
c     3) Calls the GROWTH subroutine to model the tree growth with time.
c     4) Calls the TESSEL subroutine that makes the Delauney triangles linking each tree.
c     5) Evaluates the intercepting surface elements of each triangle
c
c
      include 'BLOCK/speci.canopy'
      include 'BLOCK/speci.lcpy'
      include 'BLOCK/speci.init'
      include 'BLOCK/spec.com2'
      include 'BLOCK/spec.geom'
      include 'BLOCK/spec.index'
      include 'BLOCK/speci.tess'
      parameter(limit=5000)
      character*15 filen, ff*2
      logical take,valid,lgsai,newcpy,trees,skewlg,cponly,dbhlog,square
      real xx(3),yy(3),d123(3,3)
      double precision G05DEF,stm,stsd,grmean,grsd,G05DAF,G05DDF
      double precision abc,bcd
      integer intrq(5000)
c
c     Read canopy structure input file if the current simulation is based on a structure
c     generated from a previous simulation
      jnnk = 10 + isgno
      if (space .eq. 1.4) jnnk = 11
      if (space .eq. 0.9) jnnk = 12
      write(ff,562)jnnk
  562 format(i2)
      filen = 'CANOPY/struc.'//ff
      if (newcpy) goto 1001
       open(100,file=filen,status='old')
       rewind 100
       read(100,79) ntree
       read(100,79)ntr
   79  format(28x,i5)
       read(100,*)(take(i),i=1,ntree)
       do 993 i=1,ntree
        if(take(i)) then
         read(100,676)(pnt(i,j),j=1,6),covin(i),tpa(i)
        endif
  993   continue
       do 990 jt=1,ntr
        read(100,68)(triano(jt,i),i=3,5),(itetr(jt,i),i=1,3),
     &          (triano(jt,i),i=6,8)
  990   continue
      read(100,*) totsa,totpa,tocca,tobgap
      close(100)
c
```

```
1001  read(11,30) fstcap, bstcap, trscap, bdr, cdr
      bdr = bdr/fstcap
      cdr = cdr*fstcap
c
      read(11,35) stm, stsd, stmin, stmax
      read(11,36) lgsai
c
      if (lgsai) then
       read(11,37) saiput
       read(11,38) hicept, hslope, bhght
      else
       read(11,46) hicept,hslope, bhght
      endif
c
      read(11,39) aidex, croang,zoi,ntint
      read(11,41) (nyear(n),n=1,ntint)
      read(11,42) (ntrel(n),n=1,ntint)
c
 30   format(///,3(f4.2,6x),f4.2,3x,f9.7)
 35   format(/,4(f6.4,6x))
 36   format(/,l1)
 37   format(/,f4.2)
 38   format(/,2(f6.2,10x),f4.2)
 39   format(/,3(f6.4,7x),i2)
 41   format(/,14(i3,2x))
 42   format(/,i5,x,13(i4,x))
 46   format(///,2(f6.2,10x),f4.2)
c
      areatr = (aleng**2)/10000
      do 350 jw = 1, ntint
       ntrel(jw) = anint(ntrel(jw)*areatr)
 350  continue
c     return to MAIN if computation of new canopy is not required
      if (.not. newcpy .or. .not. trees) goto 999
      nrow = (int(aleng/space))+1
      ntree=nrow**2
      if (ntree .gt. limit) then
       write(*,*)"ARRAY SIZE TOO SMALL FOR PONT IN CANOPY.F"
       write(*,*)"exiting program....."
       stop
      endif
      itt = 1
c
c     if sqaure lattice continue, if diamond skip next section
      if (.not. square) goto 64
c ==========================================================================
c     Put a tree at every point in a square grid pattern of xleng size.  pnt(i,1)=x coordinate;
c     pnt(i,2)=y coordinate
c ==========================================================================
      i=1
      do 63 l=1,nrow
c
       do 50 knn=1,nrow
        if(l .eq. 1) then
         pnt(i,1)=0.0
         if(kn .eq. 1)then
          pnt(i,2)=0.0
         else
```

```
       pnt(i,2)=pnt(i-1,2)+space
      endif
     else
     if(kn .eq. 1)then
      pnt(i,1)=pnt(i-nrow,1)+space
      pnt(i,2)=pnt(i-nrow,2)
     else
      pnt(i,1)=pnt(i-1,1)
      pnt(i,2)=pnt(i-1,2)+space
     endif
    endif
    i=i+1
 50  continue
 63  continue
c
 64  if (square) goto 74
c
c=====================================================================
c    Put a tree at every point in a diamond lattice pattern within a square of xleng size. (if
c    not square lattice) pnt(i,1)=x coordinate; pnt(i,2)=y coordinate
c=====================================================================
    i=1
    do 73 l=1,nrow
c
     do 40 kn=1,nrow
      if(l .eq. 1) then
       pnt(i,1)=0.0
       if(kn .eq. 1)then
        pnt(i,2)=0.0
       else
        pnt(i,2)=pnt(i-1,2)+space
       endif
      else
      x=l/2.0
      xtemp=mod(x,1)
      if(kn .eq. 1)then
       if(xtemp .eq. 0.0) then
        pnt(i,1)=pnt(i-nrow,1)+space
        pnt(i,2)=pnt(i-nrow,2)+(0.5*space)
       else
        pnt(i,1)=pnt(i-nrow,1)+space
        pnt(i,2)=pnt(i-(2*nrow),2)
       endif
      else
       pnt(i,1)=pnt(i-1,1)
       pnt(i,2)=pnt(i-1,2)+space
      endif
     endif
     i=i+1
 40  continue
 73  continue
c
c=====================================================================
c  Generate the random DBH (pnt[j,3]), crown radius (pnt[j,4]), tree height (pnt[j,5]), and
c  random proportion of crown radius generating stemflow (pnt[j,7])
c=====================================================================
c    set random number generator to a repeatable state
c74  call G05CBF(0)
```

```
c    set random number generator to a non-repeatable state
 74   call G05CCF(0)
      abc=0.01
      bcd=0.4
       do 23 j=1,ntree
        intrq(j) = 0
        isdead(j) = 0
        take(j) = .true.
        if (dbhlog) then
         pnt(j,3)=real(G05DAF(abc,bcd))
        else
         pnt(j,3)=dbhval
        endif
        pnt(j,5) = (pnt(j,3) * hslope) + hicept
        calcht = pnt(j,5) * bhght
        pnt(j,4)= (pnt(j,5)-calcht) * tan(croang)
        pnt(j,6)=real(G05DEF(stm,stsd))
        pnt(j,6)=log(pnt(j,6))
        if (pnt(j,6) .lt. stmin) pnt(j,6)=stmin
        if (pnt(j,6) .gt. stmax) pnt(j,6)=stmax
 c    Generate the random growth rate of each tree (pnt[i,8])
       jl = 0
  778   pnt(j,7)=G05DDF(grmean,grsd)
       if (jl .gt. 10) then
        write(*,*)'!!!!!!!!!!!!!!!!!!!!!!!!!!!!!!!!!!!!!!!!!!!!!!!!!!!!!!!!!!!'
        write(*,*)'   Growth rate out of range 0 - 1'
        write(*,*)'       reset grmean and grsd    '
        write(*,*)'!!!!!!!!!!!!!!!!!!!!!!!!!!!!!!!!!!!!!!!!!!!!!!!!!!!!!!!!!!!'
        write(*,*)' EXITING PROGRAM.....'
        stop
       endif
       if (pnt(j,7) .le. 0.0 .or. pnt(j,7) .ge. 1.0) then
        jl = jl + 1
        goto 778
       endif
  23   continue
 c=====================================================================
 c  Set up loop for calling GROWTH subroutine: computing amount of growth per time
 c  interval
 c=====================================================================
      do 84 itt=1,ittlo
       call GROWTH(bhght)
  84   continue
 c=====================================================================
 c    Make the delauney triangles linking each tree to it's 2 nearest neighbours
 c=====================================================================
 c
      call TESSEL
 c
 c     Initialize tree crown cover inside the simulated area
       do 95 i=1,ntree
         covin(i) = 0
   95  continue
       totpa = 0.
       tocca = 0.
       totsa = 0.
       tobgap = 0.
  c
```

```
c.....Loop on Delaunay triangle (jt=1,ntr) .....
c
      nvtr = 0
      do 200 jt=1,ntr
       itetr(jt,1) = itetr(jt,1)-3
       itetr(jt,2) = itetr(jt,2)-3
       itetr(jt,3) = itetr(jt,3)-3
       valid(jt) = .true.
       ii = 0
       temp1 = aleng
       temp2 = aleng
c ------------------------------------------------------------------------------------------------------------
c  loop on trees forming the triangle to verify if the triangle is connected with initial dummy
c  point
c ------------------------------------------------------------------------------------------------------------
       do 110 i=1,3
        if (itetr(jt,i).lt.1) valid(jt) = .false.
        if (itetr(jt,i).gt.ntr) valid(jt)=.false.
 110   continue
c
c      if triangle not acceptable, goto next triangle
       if (.not. valid(jt)) goto 200
c ============================================================================
c      Evaluate intercepting surface elements of the triangle
c ============================================================================
c      Calculate the distance between the 3 neighbours and the coordinates for the centre of
c      each triangle
c
       tot1 = 0.
       tot2 = 0.
       do 125 i=1,3
        intrq(itetr(jt,i)) = intrq(itetr(jt,i)) + 1
        xx(i) = pnt(itetr(jt,i),1)
        yy(i) = pnt(itetr(jt,i),2)
        tot1 = tot1 + pnt(itetr(jt,i),1)
        tot2 = tot2 + pnt(itetr(jt,i),2)
  125   continue
       d123(1,2) = ((xx(1)-xx(2))**2 + (yy(1)-yy(2))**2) **0.5
       d123(1,3) = ((xx(1)-xx(3))**2 + (yy(1)-yy(3))**2) **0.5
       d123(2,3) = ((xx(2)-xx(3))**2 + (yy(2)-yy(3))**2) **0.5
       triano(jt,1) = tot1/3.
       triano(jt,2) = tot2/3.
c
c      Calculate the 3 angles of the triangle
       temp = d123(1,2)**2 + d123(1,3)**2 - d123(2,3)**2
       triano(jt,6) = acos(temp / (2 * d123(1,2) * d123(1,3)))
       temp = d123(1,2)**2 + d123(2,3)**2 - d123(1,3)**2
       triano(jt,7) = acos(temp / (2 * d123(1,2) * d123(2,3)))
       temp = d123(1,3)**2 + d123(2,3)**2 - d123(1,2)**2
       triano(jt,8) = acos(temp / (2 * d123(1,3) * d123(2,3)))
c
c      Calculate surface area of the triangle & total surface of the simulated area
       triano(jt,3) = 0.5 * d123(1,2) * d123(1,3) * sin(triano(jt,6))
       totsa = totsa + triano(jt,3)
c
c      Calculate crown cover area of each tree & total crown cover of the triangle
       temp1 = 0.5 * pnt(itetr(jt,1),4)**2 * triano(jt,6)
       temp2 = 0.5 * pnt(itetr(jt,2),4)**2 * triano(jt,7)
```

```
      temp3 = 0.5 * pnt(itetr(jt,3),4)**2 * triano(jt,8)
      triano(jt,5) = temp1 + temp2 + temp3
      if (triano(jt,5) .gt. triano(jt,3)) triano(jt,5) = triano(jt,3)
c
      covin(itetr(jt,1)) = covin(itetr(jt,1)) + temp1
      covin(itetr(jt,2)) = covin(itetr(jt,2)) + temp2
      covin(itetr(jt,3)) = covin(itetr(jt,3)) + temp3
c
c     Calculate trunk basal area of each tree and each triangle and trunk basal area of the
c     whole simulated area
      temp1 = 0.5 * (pnt(itetr(jt,1),3)/2)**2 * triano(jt,6)
      temp2 = 0.5 * (pnt(itetr(jt,2),3)/2)**2 * triano(jt,7)
      temp3 = 0.5 * (pnt(itetr(jt,3),3)/2)**2 * triano(jt,8)
      tpa(itetr(jt,1)) = tpa(itetr(jt,1)) + temp1
      tpa(itetr(jt,2)) = tpa(itetr(jt,2)) + temp2
      tpa(itetr(jt,3)) = tpa(itetr(jt,3)) + temp3
      temp = temp1 + temp2 + temp3
      totpa = totpa + temp
c
c     Between tree gap surface area (of the triangle) and total gap area (whole simulated
c     area)
      triano(jt,4) = triano(jt,3) - triano(jt,5)
      tobgap = tobgap + triano(jt,4)
      nvtr = nvtr + 1
c
c     goto next triangle
  200 continue
c
c     Total crown cover area (whole simulated area)
      tocca = totsa - tobgap
c     Count the number of valid trees, and disallow trees not included in any valid triangles
      numb = 0
      do 994 i = 1,ntree
       if(intrq(i) .lt. 1.) take(i) = .false.
       if (take(i)) numb = numb + 1
  994 continue
c ==========================================================================
c     save canopy structure information
c==========================================================================
        open(18,file=filen,status='unknown')
        write(18,995) ntree
        write(18,996) nvtr
  995   format('   Number of valid trees = ',i5)
  996   format('Number of valid triangles = ',i5)
       write(18,*)(take(i),i=1,ntree)
       do 991 i=1,ntree
        if (take(i)) then
         write(18,676)(pnt(i,j),j=1,6),covin(i),tpa(i)
        endif
  991  continue
  676  format(2(f8.4,x),4(f7.4,x),f8.4,x,f7.4,x)
       do 992 jt=1,ntr
        if(valid(jt)) then
        write(18,68)(triano(jt,i),i=3,5),(itetr(jt,i),i=1,3), (triano(jt,i),i=6,8)
        endif
  992  continue
   68  format(3(f8.3,x),3(i5,x),3(f6.4,x))
   67  format(3(f8.3,x),3(i5),3(f6.4,x))
```

```
      write(18,*) totsa,totpa,tocca,tobgap
      close (18)
999   return
      end
```

function con2(tpbv)

```
c
      include 'BLOCK/spec.phys'
      include 'BLOCK/spec.index'
      include 'BLOCK/spec.smc'
c
c     Check given moisture values are not outside calculated limits
c
      if(tpbv.ge.sr1)then
        con2=satcon
       else
        if(tpbv.lt.smx(1))con2=smz(1)
       endif
c
c     Linear interpolation of conductivity values for moisture contents between
c     smx(20) and sr1
c
      smgz(20)=(satcon-smz(20))/(sr1-smx(20))
      if(tpbv.gt.smx(20).and.tpbv.lt.sr1) con2=smz(20)+smgz(20)*(tpbv-smx(20))
c
c     Calculate unsaturated conductivities from given moisture contents
c
      do 1 j=1,19
      if(tpbv.ge.smx(j).and.tpbv.lt.smx(j+1))con2=smz(j) + smgz(j)*(tpbv-smx(j))
1     continue
      con2=con2*360000.
      return
      end
```

SUBROUTINE DEPTHI

```
c
      include 'BLOCK/spec.geom'
      include 'BLOCK/spec.phys'
      include 'BLOCK/spec.index'
      include 'BLOCK/spec.clock'
      include 'BLOCK/spec.com2'
c
      dimension fswp(10,10,20)
      dimension cnt(10,10,20)
      dimension ccdepth(10,10,20)
c
      do 700 k=1,kno
       nn=nlimk(k)
       do 699 n=1,nn
        ccdepth(k,n,1)=avdep(k,n,1)/2.0
```

```
      do 698 j=2,jno
       ccdepth(k,n,j)=ccdepth(k,n,j - 1) + 0.5 * (avdep(k,n,j-1) + avdep(k,n,j))
 698   continue
 699  continue
 700  continue
 c
     do 8000 k=1,kno
      nn=nlimk(k)
      do 7999 n=1,nn
       do 810 j=1,jno
        cnt(k,n,j)=0.0
        fswp(k,n,j)=0.0
 810     if(poten(k,n,j).ge.-5.00)cnt(k,n,j)=1.0
        jjn=jno+1
        cnt(k,n,jjn)=0.0
        fswp(k,n,jjn)=0.0
 c   Soil water pressures calculated in centimetres
        if(cnt(k,n,1).eq.1.0) fswp(k,n,1) = ccdepth(k,n,1) * 100.
        cntsum=0.0
        do 830 j=1,jno
 830     cntsum=cntsum+cnt(k,n,j)
        if(cntsum.eq.0.0)goto 843
        do 831 j=2,jno
         if(cnt(k,n,j).eq.0.0)goto 831
 c    Soil water Pressures calculated in centimetres
          fswp(k,n,j)=0.5*100.*(avdep(k,n,j - 1) + avdep(k,n,j)) + fswp(k,n,j-1)
        if(fswp(k,n,j-1).eq.0.0) fswp(k,n,j) = fswp(k,n,j) - 0.5 * avdep(k,n,j) * 100.
 831      continue
 c
 c
         j1=1
 832      continue
         do 833 j=j1,jno
          jog=j
          if(cnt(k,n,j).eq.1.0)goto 834
 833      continue
         goto 846
 834     continue
        jg=jog+1
        do 836 j=jg,jjn
        if(cnt(k,n,j).eq.0.0)jbt=j-1
        if(cnt(k,n,j).eq.0.0)goto 835
 836    continue
 835   continue
       do 838 j=jog,jbt
 838    poten(k,n,j)=fswp(k,n,j)
 877    j1=jbt+1
       if(j1.lt.jno)goto 832
 843   continue
 846   continue
 7999  continue
 8000  continue
       end
```

```
:::::::
```

```
c    add net precip to surface and calculates conductivities and matric potentials.
c
       tpbv = smcvol(k,ns,js)/avvol(k,ns,js)
       if(js.eq.1) smcvol(k,ns,js) = smcvol(k,ns,js) + (pnr * sumar(k,ns)/100)
       tpbv = (tpbv+smcvol(k,ns,js)/avvol(k,ns,js))/2.
       tpbv = amin1(poros(k,ns,js),tpbv)
c
c    SECTION ADDED TO SET PARAMETERS USED BY EACH SOIL TYPE
c
       do 778 jkk=1,nost
        if(dummy(k,ns,js).eq.jkk)then
         sr1=srs(jkk)
         satcon=satcs(jkk)
         do 804 i=1,20
          smx(i) = smxs(jkk,i)
          smy(i) = smys(jkk,i)
          smz(i) = smzs(jkk,i)
          smgz(i) = smgzs(jkk,i)
          smg(i) = smgs(jkk,i)
 804       continue
        endif
 778    continue
       poten(k,ns,js) = xmatr2(tpbv)
       conduc(k,ns,js) =  con2(tpbv)
  78    continue
c   ------------------------------------------------------------------
c
   45   if (avvol(k,ns,js).le.0.)     goto 90
       if (tpbv.lt.0.01)            goto 90
       if (nx.ne.0)                 goto 50
c
c-----section 3-----flow from streamside elements into stream
c
       eldrop = avele(k,ns,js) - elev(k,0,js)
       grad = (poten(k,ns,js) + eldrop*100.)/dist(k,ns,js,ix)
       uscon = conduc(k,ns,js)
       goto 65
c
c-----section 4-----calcs parameters for flow between elements
c
   50   eldrop = avele(k,ns,js)-avele(k,nx,jx)
       potdif = poten(k,ns,js) - poten(k,nx,jx)
       grad = (potdif + (eldrop * 100.)) / dist(k,ns,js,ix)
       if (ix.eq.1) then
        top = (avdep(k,ns,js)+avdep(k,nx,jx))*100.
        bots = (avdep(k,ns,js)*100.)/conduc(k,ns,js)
        botx = (avdep(k,nx,jx)*100.)/conduc(k,nx,jx)
        uscon = top / (bots+botx)
       else
        top = dist(k,ns,js,ix)
        propn = (avlen(k,ns)/2)/(xi(k,ns)-xi(k,nx))
        bots = (propn*dist(k,ns,js,ix))/conduc(k,ns,js)
        botx = ((1-propn)*dist(k,nx,jx,ix))/conduc(k,nx,jx)
        uscon = top / (bots+botx)
       endif
c
c-----section 5-----calculates flows and updates moisture contents
c
```

```
 65     xflo(k,ns,js) =  grad * sarea(k,ns,js,ix) * uscon * fac
        if(ix.eq.2) xflo(k,ns,js) = xflo(k,ns,js) * shift(k)
        if (nx.eq.0) goto 85
        if (ix.eq.2) goto 80
        extra = smcvol(k,nx,jx) + xflo(k,ns,js) - smcmax(k,nx,jx)
        if(extra.le.0.) goto 80
c
        xflo(k,ns,js)  = xflo(k,ns,js) - extra
c
   80   smcvol(k,nx,jx)  = smcvol(k,nx,jx)  + xflo(k,ns,js)
   85   smcvol(k,ns,js)  = smcvol(k,ns,js)  - xflo(k,ns,js)
        sflow(k,ns,js,ix) = sflow(k,ns,js,ix) + xflo(k,ns,js)
c
c    Make sure the conductivity of the adjacent element in the next subsegment has been
c    calculated before entering LATFLO2
c
        if (k .lt. kno)  then
         tpbv = smcvol(k+1,ns,js)/avvol(k+1,ns,js)
         tpbv = (tpbv + smcvol(k+1,ns,js)/avvol(k+1,ns,js))/2.
         tpbv = amin1(poros(k+1,ns,js),tpbv)
         poten(k+1,ns,js) = xmatr2(tpbv)
         conduc(k+1,ns,js) = con2(tpbv)
        endif
   90   continue
   91   continue
       if (ix.eq.1) then
        ix = 2
        goto 95
       else
        if(k .lt. kno) call latflo2(k)
        ix=1
       endif
c
c     xflo has now been declared as an array in order to allow the outflows to be
c     accumulated after the call to latflo has been made.
c
       if(l.ne.1.or.kk.ne.1) goto 117
       do 115 j = 1,jno
        flow(k,j) = 0.
  115  continue
  117  continue
c
       do 120 j = 1,jno
        flow(k,j) = flow(k,j) + (xflo(k,1,j)/3.6)
  120  continue
       goto 30
   95  continue
c
c-----section 6-----slopewise flows from surface layers
c
       do 110 k = 1,kno
        ni = nlimk(k)
        do 109 n = 1,ni
         extra = amax1(0.,smcvol(k,n,1)-smcmax(k,n,1))
         if (n.eq.1) then
          flow(k,1) = flow(k,1) + extra
          oflow(it,k) = oflow(it,k) + extra
         endif
```

```
      smcvol(k,n,1) = smcvol(k,n,1)     - extra
      if (n.gt.1) smcvol(k,n-1,1)=smcvol(k,n-1,1)+extra
      do 108 j = 1,jno
       pres(k,n,j) = amax1(0.,pres(k,n,j))
       pbv(k,n,j)  = smcvol(k,n,j) / avvol(k,n,j)
 108   continue
 109  continue
 110  continue
 100 continue
     return
     end
```

FUNCTION FACTOR (n)

```
c
c    Function to calculate the factorial N! of which N > 0
c
     integer n,i
c
     factor = 1
     if (n .gt. 0) then
      do 10 i=1,n
       factor = factor * i
 10    continue
     end if
     end
```

subroutine GROWTH(bhght)

```
c
c    This subroutine (called from CANOPY) calculates the amount of growth of each tree
c    per time step (normally one year) from the logistic growth equation with a competition
c    factor based on "zone of influence": ZOI.
c*************************************************************************
c
     include 'BLOCK/speci.canopy'
     include 'BLOCK/speci.lcpy'
     double precision grmean, grsd,xtemp(5000),M01DAF,M01ZAF,M01CAF
     logical dbhlog,valid,take,lgsai,newcpy,trees,skewlg,cponly,square,within(5000)
     integer norig(5000),list(5000),G05DYF
c
     amoun = 0.0
     nnn = 1
     avdbh = 0.0
     ntrha = 0
     iigk = 0
     write (*,*)'itt =',itt
c ========================================================================
c  Run through every tree point
c ========================================================================
      do 40 i=1,ntree
       within(i) = .true.
       if (.not. take(i)) goto 40
```

```
      pnt(i,9) = 0.0
c   Calculate the ZOI of i tree
      pnt(i,8) = zoi * pnt(i,4)
c ---------------------------------------------------------------------------------------------------
c   Run through every competitor tree
c ---------------------------------------------------------------------------------------------------
      do 39 j=1,ntree
       if (.not. take(j) .or. j .eq. i) goto 39
c   Calculate the ZOI of surrounding tree
      pnt(j,8) = zoi * pnt(j,4)
c   Calculate distance between i and competitor
       xij = pnt(i,1) - pnt(j,1)
       yij = pnt(i,2) - pnt(j,2)
       dstij = sqrt(xij**2 + yij**2)
       temp1=dstij-pnt(i,4)
       temp2=pnt(j,4)+pnt(i,4)
       temp3=dstij + pnt(i,4)
c    if tree i falls within the competitors ZOI and the competitor is taller than "i" then
c    proceed
       if (temp1.lt.pnt(j,8).and.pnt(j,5).gt.pnt(i,5)) then
c   if the competitor completely overlaps i, add a killing factor
        if (pnt(j,4) .ge. temp3) isdead(i) = isdead(i) + 1
c  if  two competitor trees completely overlap a tree add a killing factor
        if (j .eq. (i+1) .and. i .gt. 1) then
         xxa = pnt(i-1,1)-pnt(j,1)
         yya = pnt(i-1,2)-pnt(j,2)
         diffy = sqrt(xxa**2+yya**2)
         radda = pnt(i-1,4)+pnt(j,4)
         if(diffy .lt. radda .and. pnt(i,5) .lt. pnt(i-1,5)) then
          isdead(i) = isdead(i) + 1
         endif
        endif
c    After 3 killing factors the tree dies.
        if(isdead(i) .ge. 3) then
         take(i) = .false.
         pnt(i,3)=5.
         goto 40
        endif
c    if the competitor tree (j) completely overlaps i set i's "amount affected" to 95% i.e. very
c    little growth
        if (pnt(j,8) .gt. temp3) then
         pron = 1.0
         goto 97
        endif
c    calculate the amount of influence j has on the growth of i tree
        rj = pnt(j,8)
        ri = pnt(i,4)
        Angj = acos((rj**2 + dstij**2 - ri**2) / (2 * rj * dstij))
        Angi = acos((ri**2 + dstij**2 - rj**2) / (2 * ri * dstij))
        Areaj = 0.5 * rj**2 * (2*Angj - sin(2*Angj))
        Areai = 0.5 * ri**2 * (2*Angi - sin(2*Angi))
        Areat = Areaj + Areai
        pron = Areat/(ri**2 * pi)
c    Sum the amount of influence of all other trees
 97     pnt(i,9) = pnt(i,9) + pron
        if(pnt(i,9) .gt. 1.0) pnt(i,9) = 1.0
        xtemp(nnn) = dble(pnt(i,3))
       endif
```

```
 39   continue
      pnt(i,9) = 1.05 - pnt(i,9)
      if(pnt(i,9) .gt. 1.0) pnt(i,9) = 1.0
      norig(nnn) = i
      nnn = nnn + 1
 40   continue
      nnn = nnn - 1
c ------------------------------------------------------------------------------------------------------------
c     Sort through the tree and rank them for the amount of competition ready for culling
c ------------------------------------------------------------------------------------------------------------
      call M01DAF(xtemp,1,nnn,'a',list,ifail)
      if(ifail .gt. 0) write(*,*)'DAF: Ifail = ',ifail
      call M01ZAF(list,1,nnn,ifail)
      if(ifail .gt. 0) write(*,*)'ZAF: Ifail = ',ifail
      call M01CAF(xtemp,1,nnn,'a',ifail)
      if(ifail .gt. 0) write(*,*)'CAF: Ifail = ',ifail
c     sort out how many trees need to be culled for this year
      do 34 jw =1, ntint
       if (itt .ge. nyear(jw) .and. itt .lt. nyear(jw+1)) then
        fract = real((itt-nyear(jw)))/real((nyear(jw+1)-nyear(jw)))
        nctot = ntrel(jw)-(anint(fract*(ntrel(jw)-ntrel(jw+1))))
        goto 35
       endif
   34  continue
   35  ncull = nnn - nctot
       if (ncull .le. 0) goto 89
c      start culling trees that are not required
       do 33 ij = nnn,1,-1
        if (ij .gt. nctot) then
         if (xtemp(ij) .gt. 0.0) then
          take(norig(list(ij))) = .false.
          pnt(norig(list(ij)),3) = 5.
         else
          nlow = 1
  997     nun = G05DYF(nlow,ij)
          if (.not. take(nun).or. xtemp(nun) .gt. 0.0) goto 997
          take(norig(list(nun))) = .false.
          pnt(norig(list(nun)),3) = 5.
         endif
        endif
   33   continue
c ------------------------------------------------------------------------
c     calculate the growth amount of the remaining live trees
c ------------------------------------------------------------------------
   89   do 36 i=1, ntree
         if (.not. take (i)) within(i) = .false.
         if (.not. take(i)) goto 36
         temp7 = 1 - (pnt(i,3)/dbhmax)
         temp8 = temp7 * pnt(i,7) * pnt(i,9)
         pnt(i,3) = pnt(i,3) * (1+temp8)
         pnt(i,5)= (pnt(i,3) * hslope) + hicept
         calcht = pnt(i,5) * bhght
         pnt(i,4)=(pnt(i,5)-calcht) * tan(croang)
         amoun = amoun + (pnt(i,4)**2 * pi)
         if (pnt(i,1).lt.0 .or. pnt(i,1).gt.15.0) within(i)=.false.
         if (pnt(i,2).lt.0 .or. pnt(i,2).gt.15.0) within(i)=.false.
         if (within(i)) then
          ntrha = ntrha + 1
```

```
      avdbh = avdbh + pnt(i,3)
     endif
     if (itt .eq. ittlo) then
      if(.not.within(i)) take(i) = .false.
      if(take(i)) then
       jonny = 1
       write(2,45)i,jonny,pnt(i,1),pnt(i,2),pnt(i,5),pnt(i,4),pnt(i,8),pnt(i,3)
       iigk = iigk + 1
       take(iigk) = .true.
       do 564 jjh = 1,8
        pnt(iigk,jjh) = pnt(i,jjh)
564     continue
      else
       jonny = 0
      endif
     endif
 36  continue
     avdbh = avdbh/ntrha
c    ntrha = ntrha * 4
     write(21,*)itt,ntrha,avdbh
     write(1,46)pnt(1,3),pnt(2,3),pnt(3,3),pnt(4,3),pnt(5,3),pnt(6,3),pnt(7,3),pnt(8,3),pnt(9,3),
    &  pnt(10,3),pnt(11,3),pnt(12,3), amoun
 46  format(13f6.3)
 45  format(2(i5,x),6(x,f9.4))
     if (itt .eq. ittlo) ntree = iigk
     return
     end
```

subroutine init

```
C
     include 'BLOCK/spec.geom'
     include 'BLOCK/spec.phys'
     include 'BLOCK/spec.index'
     include 'BLOCK/spec.com2'
     include 'BLOCK/spec.water'
c
     dimension tpos(10)
C
C**** This is a revised version of the INIT subroutine designed to allow the use of three
c    dimensional procedures in DRAIN Moisture contents and soil properties are still
c    allocated in the same manner, with an outside loop for k (kno-1) being the number of
c    internal grid networks. The geometric properties are derived from the new version of
c    BLKVOL.
C
     do 210 k=1,kno
      nii = nlimk(k)
      do 209 n=1,nii
C
C    This section allocates soil moisture properties to the geometric elements from
c    BLKVOL. The three proportional distances represented by POS 1-3 are converted to
c    real distances and used to choose which of the soil property set should be given to
c    that element. It should be noted that the distances are not the same for each
c    subsegment
c
```

```
      do 778 jkk=1,nost
       tpos(jkk) = xa(k,nlimk(k))*pos(jkk)
  778  continue
c
      do 777 jkk = 1,nost
       if(xi(k,n).gt.tpos(jkk)) goto 777
       do 250 j=1,jno
        dummy(k,n,j)=jkk
        cmax(k,n,j)=cmaxs(jkk,k,j)
        poros(k,n,j)=poross(jkk,k,j)
        if (j .eq. jno) goto 209
  250   continue
  777   continue
  209   continue
  210 continue
C
C     The next section calcultes areas and distances for inter element flows. The
c     recalculation is required here to allow for possible future uses of RECOM
C
      do 300 k=1,kno
       smerv(0,k) = 0.
       nii = nlimk(k)
       do 299 n=1,nii
        do 280 j = 1,jno
         if(j.ne.jno) then
          dist(k,n,j,1)=(avdep(k,n,j)+avdep(k,n,j+1))*50.
         endif
         if(n.eq.1)then
          elbetw = avele(k,n,j) - elev(k,0,j)
          dist(k,n,j,2) = 100*(sqrt(xi(k,n)**2 + elbetw**2))
         else
          hdist = xi(k,n) - xi(k,n-1)
          elbetw = avele(k,n,j) - avele(k,n-1,j)
          dist(k,n,j,2) = 100*(sqrt(hdist**2 + elbetw**2))
         endif
         if(k.lt.kno) dist(k,n,j,3)=(assiln(k,n,j)+assiln(k+1,n,j))*50.
  C
         if(j.ne.jno) sarea(k,n,j,1) = avlen(k,n) * avwid(k,n) * (1-stonec(j) + stonec(j+1))/2.
         sarea(k,n,j,2) = avvol(k,n,j)/avsiln(k,n,j) * avlen(k,n)/avsiln(k,n,j)
         sarea(k,n,j,3)=avvol(k,n,j)/avwid(k,n)
         smcmax(k,n,j)=poros(k,n,j)*avvol(k,n,j)
  C
         pbv(k,n,j) = pbv(k,n,j) * poros(k,n,j)
         pbv(k,n,j) = amin1(poros(k,n,j),pbv(k,n,j))
         smcvol(k,n,j) = pbv(k,n,j) * avvol(k,n,j)
         smerv(0,k) = smerv(0,k) + smcvol(k,n,j)
    280  continue
    299  continue
    300 continue
  C
        return
        end
```

subroutine INTER(hhk)

```
c
c    Subroutine INTER (and the 2 routines that it calls) contains the algorithms for
c    calculating the interception. It has 2 main functions:
c    1) Calculate the transfer of water between `foliage' or `stem' layers (this transfer is
c       governed by the tree structure estimated in CANOPY and TVARY)
c    2) Calculate the water balance components (free throughfall, throughfall, stemflow,
c       storage, evaporation) at
c       i) the tree scale (stemflow) or Delaunay triangle scale (throughfall and free
c          throughfall)
c         ii) the hillslope scale (simulated surface area)
c    The water balance components at the layer scale are computed in routines THFALL
c    and STEM (throughfall and stemflow are computed separately)
c
c*****************************************************************************************************
c
c    DATA SPECIFICATIONS
c
      parameter(nsize=5000,nnum=10000)
      logical valid,take,trees,skewlg,lgsai,newcpy,cponly,dbhlog,square
      double precision grmean,grsd
c
c
      include 'BLOCK/spec.index'
      include 'BLOCK/speci.canopy'
      include 'BLOCK/speci.tvary'
      include 'BLOCK/speci.init'
      include 'BLOCK/speci.main'
      include 'BLOCK/speci.lcpy'
      include 'BLOCK/spec.water'
      include 'BLOCK/speci.cptio'
      include 'BLOCK/spec.error'
      include 'BLOCK/spec.geom'
c
      dimension thro(nnum), fstold(nnum,51), fsto(nnum,51),wfree(nnum),bfree(nnum),
     &          fth(nnum,51), fdrold(nnum,0:51),fev(nnum), fdr(nnum,0:51)
c
      dimension sstold(nsize,51), ssto(nsize,51), stout(nsize,51),sdrold(nsize,0:51),
     &          stdr(nsize,0:51), sev(nsize),stcpa(nsize), sttpa(nsize), trfree(nsize),tost,
     &          twfree,tothro,tbfree,ttfree
c
c
c          FIRST CASE: THROUGHFALL AND FREE THROUGHFALL
c
      if (ntree .gt. nsize) then
       write(*,*)"  Array size of most tree variables is too small"
       write(*,*)"     program stopping....."
       stop
      endif
      tost = 0.
      ttfree = 0.
      tbfree = 0.
      tothro = 0.
      twfree = 0.
```

```
      tfevol = 0.
c     Loop on Delaunay triangles
      do 10 jt=1,ntr
c     if (.not. valid(jt)) goto 10
      if (nfola(jt) .eq. 0) goto 10
c
      if (xlai(jt) .gt. 1) then
        ev = pef / xlai(jt)
      else
        ev = pef
      endif
c
c     Calculate wat. bal. components for individual layers
      thro(jt) = 0.
      fevol = 0.
      fstov = 0.
c.....Loop on number of throughfall layers.....
      do 20 i=1,nfola(jt)
c
c     Set storage (mm) and drainage (mm/s) at the beginning of the time step equal to those
c     at the end of the previous time step fstold(jt,i) = fsto(jt,i) fdrold(jt,i) = fdr(jt,i)
      if (hhk .eq. 1) then
        fdrold(jt,0) = 0.0
        fstold(jt,i) = 0.0
        fdrold(jt,i) = 0.0
        fdr(jt,i) = 0.0
        fsto(jt,i) = 0.0
      endif
c
c     actual layer = top layer ?
      if (i .eq. 1) then
c.....
c       Calculate free throughfall (within and between crowns)
c.....
c       Volume (cu. meter):
        wfree(jt) = pr/1000 * wgap(jt)
        twfree = twfree + wfree(jt)
c       convert from cubic meter to mm (at the triangle scale)
        wfree(jt) = (wfree(jt) / triano(jt,3)) * 1000
        bfree(jt) = pr/1000 * triano(jt,4)
        tbfree = tbfree + bfree(jt)
c       convert from cubic meter to mm
        bfree(jt) = (bfree(jt) / triano(jt,3)) * 1000
c
c       Set drainage from above layer to the rainfall rate (mm/tstep)
        fdrold(jt,i-1) = pr
c
      else
c
c       Calculate gap proportion area underneath the above layer
        apr = fa(jt,i-1) - fa(jt,i)
c       Volume of water draining to the soil
        fth(jt,i-1) = fdrold(jt,i-1)/1000 * apr
        thro(jt) = thro(jt) + fth(jt,i-1)
c       remove free throughfall from drainage to next layer (convert drainage
c       to volume first)
        fred = (fdrold(jt,i-1)/1000)*triano(jt,3)
        fred1 = fred - fth(jt,i-1)
```

```
      fdrold(jt,i-1) = (fred1/triano(jt,3))*1000
c     free throughfall in mm/tstep
      fth(jt,i-1) = (fth(jt,i-1)/triano(jt,3))*1000
     endif
c     Move to next layer if storage and drainage = 0
     if((fdrold(jt,i-1) .eq. 0) .and. (fstold(jt,i) .eq. 0)) goto 20
c     Calculate storage, drainage & evapo. of the layer
     call THFALL (jt,i,fdrold,fdr,fstold,fsto,ev,evd,fstcap,bdr,cdr,it)
c
c     accumulated volume of water evaporated so far (cu. meter):
     fevol = fevol + (evd/1000) * fa(jt,i)
c     water volume stored on the complete foliage:
     fstov = fstov + (fsto(jt,i)/1000) *fa(jt,i)
     if (jt .eq. 11 .and. i .eq. 1) then
     endif
c
 20  continue
c.... End of loop on `foliage' layers .....................
c
c     water balance of the current throughfall elements (triangle):
c
c     (1) Evaporation:
c
c     Accumulated evapo. vol. for the whole simulated area
     tfevol = tfevol + fevol
c     convert evapo. from a volume to a depth (mm)
     fev(jt) = (fevol / triano(jt,3)) * 1000
c
c     (2) Throughfall:
c
c     throughfall volume (cu. meter):
     fth(jt,nfola(jt)) = (fdr(jt,nfola(jt))/1000)
     &          * fa(jt,nfola(jt))
     thro(jt) = thro(jt) + fth(jt,nfola(jt))
c     add the volume draining from the bottom layer
c     accumulated through. vol. for the whole simulated area
     tothro = tothro + thro(jt)
c     convert thro from a volume to a depth (mm)
     thro(jt) = (thro(jt) / triano(jt,3)) * 1000
c
c     (3) Storage:
c
c     accumulated storage vol. for the whole simulated area
     tfstov = tfstov + fstov
c     Convert storage from a volume to a depth
     tfsto(jt) = (fstov / triano(jt,3)) * 1000
c     go to next triangle
  10 continue
c
c*****************************************************************
c              SECOND CASE: STEMFLOW
c*****************************************************************
c
      tsstov = 0
      tsevol = 0
c     Loop on number of trees
      cnt = 0
      do 30 i=1,ntree
```

```
      if (.not. take(i)) goto 30
c
      cnt = cnt + 1
      if (sai(i) .ge. 1) then
       ev = pef / sai(i)
      else
       ev = pef*sai(i)
      endif
      trin = 0
      sevol = 0
      sstov = 0
c
c..... Loop on the number of stemflow layers .....
       do 40 j=1,nstla(i)
c
c     Set storage (mm) and drainage (mm/s) at the beginning of the time step equal to those
c     at the end of the previous time step sstold(i,j) = ssto(i,j)
      sdrold(i,j) = stdr(i,j)
       if (hhk .eq. 1) then
        sdrold(i,0) = 0.0
        sstold(i,j) = 0.0
        sdrold(i,j) = 0.0
        stdr(i,j) = 0.0
        ssto(i,j) = 0.0
       endif
c
c     Layer = top layer ?
      if (j .eq. 1) then
        sdrold(i,j-1) = pr
c       volume of water falling directly on trunk (cu. meter)
        trin = pr/1000 * stgap(i)
        ttfree = ttfree + trin
        trfree(i) = (trin / covin(i)) * 1000
        sstcap = bstcap
      end if
c
c     Layer = intermediate layer ?
      if ((j .gt. 1) .and. (j .lt. nstla(i))) then
c       Calculate surface area of the above layer draining directly to the trunk layer (m2)
        apr = sa(i,j-1) - sa(i,j)
c       Volume of water draining to the trunk (accumulated so far)
        stout(i,j-1) = sdrold(i,j-1)/1000 * apr
        trin = trin + stout(i,j-1)
        stout(i,j-1) = (stout(i,j-1) / covin(i)) * 1000
        sstcap = bstcap
      end if
c
c     Layer = Trunk layer (last layer) ?
      if (j .eq. nstla(i)) then
        trin = trin + sdrold(i,j-1)/1000 * sa(i,j-1)
c       Convert trunk water input from a volume to a rate (mm/s)
        sdrold(i,j-1) = (trin/stcov(i)) * 1000
        sstcap = trscap
      end if
c
      if ((sdrold(i,j-1) .le. 0) .and. (sstold(i,j) .le. 0)) goto 40
c     calculate layer storage, drainage and evaporation
      call STEM (i,j,sdrold,stdr,sstold,ssto,ev,evd,sstcap)
```

```
c
c    Accumulated volume of water evaporated so far:
     sevol = sevol + (evd/1000) * sa(i,j)
c    Volume of water stored on the stem layers:
     sstov = sstov + (ssto(i,j)/1000) * sa(i,j)
c
c.... go to next layer .....
  40 continue
c
c    Water balance of the current stemflow elements (tree scale)
c
c    (1) Evaporation:
c    Total volume of water evaporated (whole simulated area)
     tsevol = tsevol + sevol
c    Convert evapo. from a volume to a depth (mm)
     sev(i) = (sevol / stcov(i)) * 1000
c
c    (2) Stemflow:
c    stemflow volume (drainage from the trunk layer)
     stvol = (stdr(i,nstla(i))/1000) * stcov(i)
c    accumulated stemflow vol. for each increment
     tost = tost + stvol
c    Stemflow per crown projected area (mm)
     stcpa(i) = (stvol / covin(i)) * 1000
c    Stemflow per trunk projected area (depth)
     sttpa(i) = (stvol / tpa(i)) * 1000
c
c    (3) Storage:
c    accumulated storage vol. for the whole simulated area
     tsstov = tsstov + sstov
c
c.... go to next tree .....
  30 continue
c
c.....
c    Accumulated water balance components values from the start of the simulation)
c.....
c
c    components in depth of water (mm):
     hfev = (tfevol / totsa) * 1000
     chfev = chfev + tfevol
     hsev = (tsevol / totsa) * 1000
     chsev = chsev + tsevol
     chbfre = chbfre + hbfree
     chwfre = chwfre + hwfree
     chtrfr = chtrfr + htrfre
     chthro = chthro + hthro
     chstpa = chstpa + hstpa
     hfsto = (tfstov / totsa) * 1000
     hssto = (tsstov / totsa) * 1000
     hstore = tfstov + tsstov
     cchsto = cchsto + (hstore - hstold)
     cpre = cpre + ((pr/1000)*totsa)
c
c    Water balance error
     fpre = cpre
     ffev = chfev
     fsev = chsev
```

```
      fbfre = chbfre
      fwfre = chwfre
      fstem = fstem + hstem
      ftrfr = chtrfr
c     fthro = hthro
c
 33   time = time + tstep
c  accumulate the throughfall + stemflow for timestep
      pnet = 0.
      pnet = tost + ttfree + tbfree + tothro + twfree
      c    put pnet in cm  ready for drain
      pnet = (pnet/totsa)*100
 601  format(6(f9.6))
c   accumulate the rainfall for usage in SURFLO
      ptot(it) = ptot(it) + pnet
      tost = (tost/totsa)*100
      ttfree = (ttfree/totsa)*100
      tbfree = (tbfree/totsa)*100
      tothro = (tothro/totsa)*100
      twfree = (twfree/totsa)*100
c
      hstold = hstore
 999  return
      end
```

Function julian(day,m,year)

```
c
      integer day,year,sum,m,month(12)
      logical leapyr
      data month(1),(month(i),i=3,12)/2*31,30,31,30,2*31,30,31,30,31/
      if (leapyr(year)) then
       month(2) = 29
      else
       month(2) = 28
      endif
      sum = day
      do 100 i=1,m-1
        sum = sum + month(i)
  100 continue
      julian = sum
      end
```

subroutine latflo2(k)

```
c
c    This is a service subroutine for drain to calculate the lateral flows between the grids
c    within segments.  It is called after the stream directed slopewise flows have been done
c    in drain (ie when ix = 2)
c
     include 'BLOCK/spec.geom'
     include 'BLOCK/spec.phys'
     include 'BLOCK/spec.index'
     include 'BLOCK/spec.com2'
c
     fac= 0.01 /(float(krep*lrep))
     ni = min0 (nlimk(k),nlimk(k+1))
     do 10 j = 1,jno
      do 20 n = 1,ni
       recpt = xi(k,n) - roffst(k)
       if(recpt.le.0.) goto 20
       if(recpt.gt.xa(k,ni)) goto 20
       do 30 n2=1,ni
        xpt1 = xi(k+1,n2)
        xpt2 = xi(k+1,n2+1)
        if(xpt1.le.recpt.and.xpt2.gt.recpt) nkeypt = n2
   30  continue
       test1 = smcvol(k,n,j)/avvol(k,n,j)
       test2 = smcvol(k+1,nkeypt,j)/avvol(k+1,nkeypt,j)
       test3 = smcvol(k+1,nkeypt+1,j)/avvol(k+1,nkeypt+1,j)
       if(test1.le.0.10.or.test2.le.0.10.or.test3.le.0.10) goto 20
       rlen2 = xi(k+1,nkeypt+1) - recpt
       rlen1 = recpt - xi(k+1,nkeypt)
       if(rlen1.lt.0..or.rlen2.lt.0.)goto 20
       weigh1 = rlen2/(rlen1+rlen2)
       weigh2 = rlen1/(rlen1+rlen2)
       fdist = (assiln(k,n,j) + ((assiln(k+1,nkeypt,j) * weigh1) + (assiln(k+1,nkeypt+1,j) *
     &         weigh2)))/2.
       eldrop = avele(k,n,j)-((avele(k+1,nkeypt,j) * weigh1) + (avele(k+1,nkeypt+1,j)*weigh2))
       potdif = poten(k,n,j)-((poten(k+1,nkeypt,j) * weigh1) + (poten(k+1,nkeypt+1,j)*weigh2))
       if (eldrop.le.0.) potdif = abs(potdif)
       grad = (potdif + (eldrop * 100.)) /(fdist*100.)
       top = (assiln(k,n,j)+assiln(k+1,nkeypt,j))*100.
       bots = (assiln(k,n,j)*100.)/conduc(k,n,j)
       botx = (assiln(k+1,nkeypt,j)*100.)/conduc(k+1,nkeypt,j)
       uscon1 = top / (bots+botx)
       top = (assiln(k,n,j)+assiln(k+1,nkeypt+1,j))*100.
       botx = (assiln(k+1,nkeypt+1,j)*100.)/conduc(k+1,nkeypt+1,j)
       uscon2 = top / (bots+botx)
       uscon = (uscon1*weigh1) + (uscon2*weigh2)
       farea1 = sarea(k+1,nkeypt,j,3) * weigh2
       farea2 = sarea(k+1,nkeypt+1,j,3) * weigh1
       farea = farea1 + farea2
       xfloA = grad * farea * uscon * fac
       xflo1 = xfloA * weigh1
       xflo2 = xfloA * weigh2
       smcvol(k+1,nkeypt,j) = smcvol(k+1,nkeypt,j) + xflo1
       smcvol(k+1,nkeypt+1,j) =smcvol(k+1,nkeypt+1,j) + xflo2
```

```
      smcvol(k,n,j) = smcvol(k,n,j) - (xflo1+xflo2)
   20 continue
   10 continue
      return
      end
```

Logical function leapyr(year)

```
c
      integer year
      logical y4,y100,y400
      y4 = mod(year,4) .eq. 0
      y100 = mod(year,100) .eq. 0
      y400 = mod(year,400) .eq. 0
      leapyr = (y4 .and. .not. y100) .or. y400
      end
```

subroutine outa

```
C
      include 'BLOCK/spec.geom'
      include 'BLOCK/spec.phys'
      include 'BLOCK/spec.index'
      include 'BLOCK/spec.water'
      include 'BLOCK/spec.clock'
      include 'BLOCK/spec.smc'
      include 'BLOCK/spec.char'
      include 'BLOCK/spec.error'

C
      dimension pmc(5,16,5),satvol(5),sv75pc(5),ptotk(5),peror(5),error(5), delpbv(5,16,5),
c           precv(5), pruc(500)
      character*40 name,note,form*23,form1*23
C
      ENTRY OUTA1(ittlo)
C
      WRITE (7, 100)
      WRITE (7, 110)
      WRITE (7, 120)NAME
      WRITE (7, 110)
      WRITE (7, 130)MNO
      WRITE (7, 110)
      WRITE (7, 140)IDAY,IMONTH,IYEAR
      WRITE (7, 110)
      WRITE (7, 150) NOTE
      write(7,110)
      WRITE (7, 110)
      WRITE (7, 100)
      write(17,151)
      write(17,152)
      write(17,153)
  100 FORMAT(79('*'))
  110 FORMAT('*',77(' '),'*')
```

```
120  FORMAT('*',10(' '),A40,27(' '),'*')
130  FORMAT('*',10(' '),'TOTAL NUMBER OF SEGMENTS;',I4
   *     ,38(' '),'*')
140  FORMAT('*',10(' '),'DATE OF EVENT (DAY/MONTH/YEAR);'
   *      ,I3,'/',I2,'/',I4,25(' '),'*')
150  FORMAT('*',20(' '),A40,17(' '),'*')
151  format('       ------------------------------------------')
152  format('        SOIL WATER FLOW WITH DEPTH FOR EACH SEGMENT')
153  format('       ------------------------------------------',/)
155  format(11x,'Rainfall',8x,'Net',22x,'Saturated',7x,'Total')
156  format(' Hour',4x,'above canopy',4x,'rainfall',6x,'Soilflow',3x,
   &     'overland flow',5x,'flow')
157  format(75('-'))
     RETURN
C
C
      entry outa2
     do 112 k=1,kno
C
     ni = nlimk(k)
     WRITE (7, 200)ISGNO
     write (7, 205)k
     WRITE (7, 210)
     WRITE (7, 220)(n,n=1,ni)
     WRITE (7, 230)(J,(avele(k,n,j),N=1,10),J=1,JNO)
     WRITE (7, 240)
     WRITE (7, 220)(n,n=1,ni)
     WRITE (7, 230)(J,(avslp(k,n,j),N=1,10),J=1,JNO)
     WRITE (7, 250)
     WRITE (7, 220)(n,n=1,ni)
     WRITE (7, 230)(J,(avdep(k,n,j),N=1,10),J=1,JNO)
     WRITE (7, 260)
     WRITE (7, 220)(n,n=1,ni)
     WRITE(7,230)' 1',(avslln(k,n,1),N=1,ni)
     WRITE(7,270)
     WRITE(7,220)(n,n=1,ni)
     J=1
     WRITE (7, 230) J,(avwid(k,n),N=1,ni)
     if(k.eq.kno) goto 112
     write(7,275)k,k+1
     write(7,220)(n,n=1,ni)
     write(7,230)(j,(asslp(k,n,j),n=1,ni),j=1,jno)
   112 continue
   210  FORMAT(///' ELEVATION OF EACH SOIL ELEMENT (metres)')
   220  format('J; N ',i4,10i7)
   230  format(' ',i2,x,10f7.2)
   240  FORMAT(/' SLOPE OF EACH SOIL ELEMENT ')
   250  FORMAT(/' DEPTH OF EACH SOIL ELEMENT (metres) ')
   260  FORMAT(/' SLOPEWISE LENGTH OF EACH INCREMENT (metres) ')
   270  FORMAT(/' WIDTH OF EACH INCREMENT (metres) ')
   200  format(/1x,'HYDROGRAPH SIMULATION FOR SEGMENT No ',I3)
   205  format(1x,'                    COMPONENT No ',i3)
    275 format(/1x,'SLOPES BETWEEN COMPONENT',i3,'  AND',i3)
        RETURN
```

```
      entry outa3(totsa)
C
C
      ix=ixm+1
C
      do 10 k=1,kno
       satvol(k)=0.
       sv75pc(k)=0.
       do 20 j=1,jno
        ni=nlimk(k)
        do 20 n=1,ni
         delpbv(k,n,j) = smcvol(k,n,j) / avvol(k,n,j)
         pmc(k,n,j)=delpbv(k,n,j)/poros(k,n,j)
         if(pmc(k,n,j).ge.0.750) sv75pc(k) = sv75pc(k) + avvol(k,n,j) * poros(k,n,j)
   20    if(pmc(k,n,j).ge.0.998) satvol(k) = satvol(k) + avvol(k,n,j) * poros(k,n,j)
   10  continue
 C
       do 28 k=1,kno
        satvol(k)=0.
        sv75pc(k)=0.
        precv(k) = 0.
        pruc(k) = 0.
        smerv(it,k) = 0.
        everv(k) = chsev + chfev
        ptotk(k) = ((cpre - cchsto - everv(k))/totsa)*1000
    28 continue
       cpre = 0.
       cchsto = 0.
       pwfre = 0.
       chsev = 0.
       chfev = 0.
       fthro = 0.
       kstem = 0.
       do 30 k=1,kno
        ni=nlimk(k)
        soils(k) = 0.
        do 35 n=1,ni
         precv(k) = precv(k) + (ptotk(k)*avwid(k,n)*avlen(k,n))/1000
         pruc(k) = pruc(k) + ((ptot(it)*10)*avwid(k,n)*avlen(k,n))/1000
         fthro= fthro + ((chthro*avwid(k,n)*avlen(k,n))/1000)
         pstem = pstem + ((fstem*avwid(k,n)*avlen(k,n))/1000)
         pwfre = pwfre + ((fwfre*avwid(k,n)*avlen(k,n))/1000)
         pbfre = pbfre + ((fbfre*avwid(k,n)*avlen(k,n))/1000)
         ptrfr = prtrfr + ((ftrfr*avwid(k,n)*avlen(k,n))/1000)
         do 34 j=1,jno
          smerv(it,k) = smerv(it,k) + smcvol(k,n,j)
          if (n .eq. 1) then
           soils(k) =  soils(k) + sflow(k,n,j,2)
          endif
          do 52 ix = 1,2
           sflow(k,n,j,ix) = sflow(k,n,j,ix)/((avwid(k,n)*avlen(k,n))/1000)
    52     continue
    34    continue
    35   continue
         overs(k) = oflow(it,k)
         chsmv(k) = smerv(it,k) - smerv(it-1,k)
         error(k) = precv(k) - chsmv(k) - (soils(k) + overs(k) + css)
         canerr = precv(k) - pruc(k)
```

```
      allwat = precv(k) + smerv(it-1,k)
      peror(k) = peror(k) + abs((error(k)/ allwat * 100))
30    continue
789   format(i2,8(f9.3))
      chthro = 0.
      fstem = 0.
      pstem = 0.
      fwfre = 0.
      chwfre = 0.
      chbfre = 0.
      chtrfr = 0.
      fbfre = 0.
      ftrfr = 0.
      pbfre = 0.
      ptrfr = 0.
      write(7,500)
      write(7,505)it,q
C
      form = '(2x,i2,4x,10f6.3)'
      write(form(11:12),'(i2)')nlimk(1)
      form1 = '(8x,10(i3,3x))'
      write(form1(5:6),'(i2)')nlimk(1)
      write(7,*)
      write(7,*)'UNIT % MOISTURE CONTENTS '
      write(7,form1)(n,n=1,nlimk(1))
      write(7,form)((j,(pmc(k,n,j),n=1,nlimk(1)),j=1,jno),k=1,kno)
      write(7,*)
       call depthi
  500 format(/1x,79('=')/)
  505 format(1x,i4,' ##  ','Q = ',f9.5)
C
C
      return
      end
```

;;;

```
      ITIME=0.
      START=9999.
      STRFLO=0.
      STORM=0.
  110 continue
      IF(precip(INDEX).EQ.0.)GOTO 120
      IF(START.NE.9999.)GOTO 120
      START=AMIN1(STRFLO,CMSK)
      IITIME=INDEX
  120 STRFLO=CMSK
      GOTO 300
C
C
      ENTRY OUTB2(IT,MNO,jno)
C
      IIDAY=0.
      ITIME=0
      write(7,*)
      write(7,*)
      write(7,*)'                          SEGMENT'
      WRITE(7,601)
      WRITE(7,606)
  300 continue
      DO 385 INDEX=1,IT-1
       IJ=IMIN+(INDEX*60)
       IMM=MOD(IJ,60)
       IHH=IJ/60
       ITIME=(IHOUR+IHH)*100+IMM
       ITIME=ITIME-(2400*IIDAY)
       IF(ITIME.GE.2400)IDAY=IDAY+1
       IF(ITIME.GE.2400)IIDAY=IIDAY+1
       IENTRY=3
       if (mno .eq. 1) then
        write(7,602)index,precip(index),(ecum(index,k),k=1,mno), tflow(index)
       elseif (mno .eq. 2) then
        write(7,603)index,precip(index),(ecum(index,k),k=1,mno), tflow(index)
       elseif (mno .eq. 3) then
        write(7,604)index,precip(index),(ecum(index,k),k=1,mno), tflow(index)
       elseif (mno .eq. 4) then
        write(7,605)index,precip(index),(ecum(index,k),k=1,mno), tflow(index)
       endif
  c    tflow(index) = (tflow(index)/totar)*1000
       precip(index)=precip(index)*10
       ptot(index)=ptot(index)*10
       write(12,607) index,tflow(index),precip(index),ptot(index)
  385 CONTINUE
  400 CONTINUE
C
  601 format('  INDEX  RAIN',2x,
     & '-------- SUBSURFACE OUTFLOWS --------- TOTAL')
  602 format(3x,i3,2x,f6.2,f8.4,32x,f8.4)
  603 format(3x,i3,2x,f6.2,2f8.4,24x,f8.4)
  604 format(3x,i3,2x,f6.2,3f8.4,16x,f8.4)
  605 format(3x,i3,2x,f6.2,6f8.4)
  606 format(10x,'(cm)',15x,'litres / sec',14x,'(ROUTED)'/)
  607 format(3x,i3,4x,f9.3,3x,f9.3,3x,f9.3)
      RETURN
      END
```

```
:::::::
```

```
      endif
      pd(j,1) = k
      if(pd(j,2) .lt. 0.0001) pd(j,2)=0
      if(pd(j,2) .gt. 1.0) pd(j,2) = 1.0
c
c     cumulative probability:
      cump = cump + pd(j,2)
c
      if ((k .gt. xmocc) .and. (pd(j,2) .lt. 0.02)) goto 20
 10   continue
c
c     Merge probabilities of variates larger than k
 20   pd(j,2) = (1-cump) + pd(j,2)
      if(pd(j,2) .lt. 0.0001) pd(j,2)=0
      pd(j,1) = k
      npd = j
c
      return
      end
```

subroutine read

```
C
      logical  trees,skewlg,newcpy,cponly,dbhlog,valid,lgsai,square,take
      double precision grmean,grsd
      character*12 form
c
      include 'BLOCK/spec.geom'
      include 'BLOCK/spec.phys'
      include 'BLOCK/spec.index'
      include 'BLOCK/spec.water'
      include 'BLOCK/spec.clock'
      include 'BLOCK/spec.com2'
      include 'BLOCK/spec.smc'
      include 'BLOCK/speci.canopy'
      include 'BLOCK/speci.main'
      include 'BLOCK/speci.lcpy'
c
      entry read1
c
      IHR = 0
 10   IHR=IHR+1
      III=IHR+7
      read(3,110)(PRECIP(II),II=IHR,III)
      read(19,112)(evap(ii),ii=ihr,iii)
 110  FORMAT(8(F5.3,x))
 112  FORMAT(8(F8.6,x))
      IF(PRECIP(IHR).GE.9.) RETURN
C The 9.card marks the end of the precipitation deck
      IHR=III
      GOTO 10
C
      entry read2
c
      read(8,120)ISGNO,KNO,JNO,IROUT,TREES
```

```
      write(23,*)
      write(23,*)'ISGNO, KNO,  JNO,  IROUT, TREES'
      write(23,121)ISGNO,KNO,JNO,IROUT,TREES
  120 FORMAT(//,3(I2,2X),I3,2X,L1)
  121 FORMAT(2x,3(I2,4X),I3,6X,L1)
      IF(KNO.GE.99)RETURN
      read(8,130)(stonec(j),j=1,jno)
      write(23,*)
      write(23,*)'(stonec(j),j=1,jno)'
      write(23,131)(stonec(j),j=1,jno)
  130 format(/,10f7.3)
  131 format(10f7.3)
      read(8,135)(nlimk(k),k=1,kno)
      write(23,*)
      write(23,*)'(nlimk(k),k=1,kno)'
      write(23,136)(nlimk(k),k=1,kno)
  135 format(/,5(i3,2x))
  136 format(5i3)
      form = '(6x,10f6.3)'
      write(form(5:6),'(i2)')nlimk(1)
      read(4,form)(((pbv(k,n,j),n=1,nlimk(1)),j=1,jno),k=1,kno)
      write(23,*)
      write(23,*)'(((pbv(k,n,j),n=1,nlimk(1)),j=1,jno),k=1,kno)'
      write(23,form)(((pbv(k,n,j),n=1,nlimk(1)),j=1,jno),k=1,kno)
      do 139 k=1,kno
       nn = nlimk(k)
       read(8,140)(yi(k,n),n=1,nn)
       write(23,*)
       write(23,*)'(yi(k,n),n=1,nn)'
       write(23,141)(yi(k,n),n=1,nn)
       read(8,140)(depmax(k,n),n=1,nn)
       write(23,*)
       write(23,*)'(depmax(k,n),n=1,nn)'
       write(23,141)(depmax(k,n),n=1,nn)
       read(8,140)( xi(k,n),n=1,nn)
       write(23,*)
       write(23,*)'( xi(k,n),n=1,nn)'
       write(23,141)( xi(k,n),n=1,nn)
       read(8,147)cocor(k,1,1),cocor(k,1,2),cocor(k,2,1),cocor(k,2,2)
       write(23,*)
       write(23,*)'cocor(k,1,1),cocor(k,1,2),cocor(k,2,1),cocor(k,2,2)'
       write(23,148)cocor(k,1,1),cocor(k,1,2),cocor(k,2,1),cocor(k,2,2)
       read(8,147)cocor(k,3,1),cocor(k,3,2),cocor(k,4,1),cocor(k,4,2)
       write(23,*)
       write(23,*)'cocor(k,3,1),cocor(k,3,2),cocor(k,4,1),cocor(k,4,2)'
       write(23,148)cocor(k,3,1),cocor(k,3,2),cocor(k,4,1),cocor(k,4,2)
  139 continue
  140 format(/,10f7.3)
  141 format(10f7.3)
  147 format(/,4(f7.2,4x))
  148 format(4(f7.2,4x))
      JJ=JNO-1
      read(8,150)ADEPTH,(BDEPTH(J),J=1,JJ)
      write(23,*)
      write(23,*)'ADEPTH,(BDEPTH(J),J=1,JJ)'
      write(23,151)ADEPTH,(BDEPTH(J),J=1,JJ)
  150 FORMAT(/,10F6.3)
  151 FORMAT(10F6.3)
```

```
      read(8,170) a1,a2,(roffst(k),k=1,kno-1)
      write(23,*)
      write(23,*)' a1,a2,(roffst(k),k=1,kno-1)'
      write(23,171) a1,a2,(roffst(k),k=1,kno-1)
  170 format(/,f5.1,f10.1,4f7.2)
  171 format(f5.1,f10.1,4f7.2)
      read(8,180)(pos(k),k=1,nost),(hlen(k),k=1,kno)
      write(23,*)
      write(23,*)'(pos(k),k=1,nost),(hlen(k),k=1,kno)'
      write(23,181)(pos(k),k=1,nost),(hlen(k),k=1,kno)
  180 format(/,11(f7.2,x))
  181 format(11(f7.2,x))
c
      do 778 jkk=1,nost
       do 300 k=1,kno
        do 111 j=1,jno
         cmaxs(jkk,k,j)=satcs(jkk)*360000.
         poross(jkk,k,j)=srs(jkk)
  111    continue
  300   continue
  778  continue
C
      RETURN
c
      entry read3
C
      if (isgno .eq. 1) then
       read(14,73)newcpy
      else
       read(14,68)newcpy
      endif
      read(14,74)cponly,skewlg
c
c     length of square side; space between trees;DBH distribution random?;square pattern?
c     (or diamond)
      read(14,67) aleng,space,dbhlog,square
      if (.not. dbhlog) then
c      value of uniform DBH
       read(14,70)dbhval
c      period of forest growth (years); time interval (years),pattern parameters for leaf
c      distribution
       read(14,72)perod,tmint,pat(1),pat(2)
      else
       read(14,71)perod,tmint,pat(1),pat(2)
      endif
c     mean growth rate; s.d. growth rate; dbhmaximum
      read(14,77)grmean,grsd,dbhmax,ittlo
      if (grsd .le. 0.00) then
       write(*,*)'Standard deviation cannot be equal to zero or less'
       write(*,*)'grsd =',grsd
       write(*,*)'Exiting program .....'
       stop
      endif
   67 format(/,2(3x,f6.2),2(6x,l1))
   68 format(///,3x,l1,f9.7,2x,f9.7)
   70 format(/,6x,f8.5)
   71 format(///,2(i4,4x),2(f5.1,4x))
   72 format(/,2(i4,4x),2(f5.1,4x))
```

```
 73   format(//////,3x,I1,f9.7,2x,f9.7)
 74   format(/,3x,I1,5x,I1)
 77   format(/,3x,f6.4,5x,f7.5,4x,f4.2,4x,i4)
c
      RETURN
      END
```

::

subroutine smc

::

```
c
      include 'BLOCK/spec.phys'
      include 'BLOCK/spec.index'
      include 'BLOCK/spec.smc'
c
      DIMENSION G(50),Y(50),XD(50),GZ(50),Z(50),xnew(51),ynew(51),ax(50)
      DOUBLE PRECISION G05DDF,DLOG10,AX,ASR1,ASTCON,BSTCON,SDSR,SDX,
     &      SDSAT
C
        read(10,*)nsmc,sdx
        read(10,*)(ax(i),i=1,nsmc)
        read(10,*)(y(i),i=1,nsmc)
        read(10,*)asr1,sdsr
        read(10,*)astcon,sdsat
C
C     ---------------------------------------
c     PARAMETER VARIABILITY
c     ---------------------------------------
c       Soil water content at saturation
        sr1=g05ddf(asr1,sdsr)
c
c       Soil moisture content at given tensions
c
        call smcurv(sr1,sdx,nsmc,ax,y,xnew,ynew)
        do 127 i=1,20
        xd(i)=xnew(i)
 127      y(i)=ynew(i)
c
c       Saturated conductivity
        bstcon=dlog10(astcon)
        satcon=g05ddf(bstcon,sdsat)
        satcon=10**satcon
c
c     ---------------------------------------------------------------------------------
c     CALCULATION OF UNSATURATED HYDRAULIC CONDUCTIVITY
c     ---------------------------------------------------------------------------------
c     Millington & Quirk method used to calculate unsaturated hydraulic conductivity
      NQJ=20
c
      DO 845 I=1,NQJ
      IIJ=NQJ-I+1
      XII=XD(IIJ)
      TOPS=0.
      BOTS=0.
      M=NQJ
      DO 846 J=1,M
```

```
      JF=M-J+1
      YJJ=Y(JF)
  846 BOTS=((2*J-1)*YJJ**(-2))+BOTS
      II=I
      DO 847 J=II,M
      JF=M-J+1
      YJJ=Y(JF)
  847 TOPS=((2*J+1-2*I)*YJJ**(-2))+TOPS
      JT=NQJ-I+1
      Z(JT)=SATCON*(XII/SR1)*TOPS/BOTS
      smz(jt)=z(jt)
  845 continue
c
c     Calculation of the gradients of the suction-moisture curve and the K-moisture curve for
c     each layer.
c
      DO 260 i=1,20
      smx(i)=real(xd(i))
      smy(i)=real(y(i))
  260   continue
      DO 261 I=1,19
      G(I)=(Y(I+1)-Y(I))/(XD(I+1)-XD(I))
      smg(i)=real(g(i))
      GZ(I)=(Z(I+1)-Z(I))/(XD(I+1)-XD(I))
  261 smgz(i)=real(gz(i))

c     ------------------------------------------------------------------------------------------
c     WRITE OUT START CONDITIONS AND GENERATED K-MOISTURE TABLE
c     ------------------------------------------------------------------------------------------
c
      WRITE(9,636)
  636 FORMAT ('    GENERATED SOIL SUCTION MOISTURE CURVE',/,/,
     &      'Moisture(cm3/cm3) Suction (m)    K-unsat (m)')
      DO 633 I=1,20
  633 WRITE(9,*)XD(I),Y(I),Z(I)
  632 FORMAT(3F12.8)
      return
      end
C
c     ------------------------------------------------------------------------
      SUBROUTINE SMCURV(SR,SDX,NQ,AX,Y,XNEW,YNEW)
c     ------------------------------------------------------------------------
C
C Generates a stochastic suction moisture curve to be fed into smc.f
c     DOUBLE PRECISION G05DDF, AX
      DIMENSION AX(20),X(20),XNEW(20),YNEW(20),G(20),Y(20)
C
C Determine the stochastic values of moisture
C
      X(1)=G05DDF(AX(1),SDX)
      IF(X(1).LT.0.)X(1)=0.001
C
      DO 100 I=2,NQ
      X(I)=G05DDF(AX(I),SDX)
  100 IF(X(I).LE.X(I-1))X(I)=X(I-1)+0.001
      IF(X(NQ).GE.SR)SR=X(NQ)+0.001
C
C Calculate gradients of this new suction-moisture curve
```

```
c
      NNQ=NQ-1
      DO 200 I=1,NNQ
200   G(I)=(Y(I+1)-Y(I))/(X(I+1)-X(I))
C
C Calculate max and min moisture values, and determine the size of equal intervals.
C
      XMAX=RMAX(X,NQ)
      XMIN=RMIN(X,NQ)
      XINT=(XMAX-XMIN)/19.
C
C Determine the new values of moisture-equal intervals
C
      XNEW(1)=XMIN
      DO 300 I=2,20
300   XNEW(I)=XNEW(I-1)+XINT
C
C Determine the associated new values of suction
C
      YNEW(1)=Y(1)
      DO 350 I=2,19
        DO 400 J=1,NNQ
          IF(XNEW(I).GE.X(J).AND.XNEW(I).LT.X(J+1))
     &    YNEW(I)=Y(J)+G(J)*(XNEW(I)-X(J))
400     CONTINUE
350   CONTINUE
      YNEW(20)=Y(NQ)
      RETURN
      END
C
C-------------------------------------------------------------------------
C
      FUNCTION RMAX (X,NQ)
      DIMENSION X(NQ)
C
      RMAX=X(1)
      DO 10 I=2,NQ
10      IF(X(I).GT.RMAX)RMAX=X(I)
C
      RETURN
      END
C-------------------------------------------------------------------------
C
      FUNCTION RMIN(X,NQ)
      DIMENSION X(NQ)
C
      RMIN=X(1)
      DO 10 I=2,NQ
10      IF(X(I).LT.RMIN)RMIN=X(I)
C
      RETURN
      END
```

subroutine STEM (i,j,sdrold,stdr,sstold,ssto,ev,evd,sstcap)

```
c
c    Subroutine STEM calculates the storage, drainage & evaporation of individual layer
c    generating stemflow.  The water input to the layer and the evaporation rate have
c    been previously calculated in routine INTER.
c
     parameter(nsize=5000)
     dimension sdrold(nsize,0:51), stdr(nsize,0:51), sstold(nsize,51), ssto(nsize,51)
      include 'BLOCK/speci.main'
c
c    CALCULATE STORAGE, DRAINAGE & EVAPORATION BY THE APPROPRIATE
c                          METHOD
c
c    Convert ev from a rate to a depth (mm)
     evd = ev
c
c.....First case: When SSTOLD >= SSTCAP.....
     if (sstold(i,j) .ge. sstcap) then
c
c      Calculate net supply of water after evaporation (mm)
       qs = sdrold(i,j-1) - evd
c      Temporary storage:
       ssto(i,j) = sstold(i,j) + qs
c
c      Calculate new storage and drainage
       if (ssto(i,j) .ge. sstcap) then
c        (Assume that drainage of water in excess is immediate)
         stdr(i,j) = ssto(i,j) - sstcap
         ssto(i,j) = sstcap
       end if
       if ((ssto(i,j) .lt. sstcap) .and. (ssto(i,j) .ge. 0)) then
         stdr(i,j) = 0
         ssto(i,j) = ssto(i,j)
       end if
       if (ssto(i,j) .lt. 0) then
c        Adjust evaporation loss (mm)
         evd = evd + ssto(i,j)
         stdr(i,j) = 0
         ssto(i,j) = 0
       end if
     end if
c
c.....Second case: When SSTO < SSTCAP.....
     if (sstold(i,j) .lt. sstcap) then
c
c      Add the supply of water to the layer (no evapo.) (mm)
       ssto(i,j) = sstold(i,j) + sdrold(i,j-1)
c      Evaporation is reduced by the factor S1
       s1 = ssto(i,j) / sstcap
       if (s1 .gt. 1) s1=1.
c      Calculate evaporation loss and temporary storage (mm)
       evd = evd * s1
       ssto(i,j) = ssto(i,j) - evd
c
```

```
c     Calculate new storage and drainage (mm)
      if (ssto(i,j) .ge. sstcap) then
       stdr(i,j) = ssto(i,j) - sstcap
       ssto(i,j) = sstcap
      end if
      if ((ssto(i,j) .lt. sstcap) .and. (ssto(i,j) .gt. 0)) then
       stdr(i,j) = 0
       ssto(i,j) = ssto(i,j)
      end if
      if (ssto(i,j) .lt. 0) then
c       Adjust loss by evaporation
       evd = evd + ssto(i,j)
       stdr(i,j) = 0
       ssto(i,j) = 0
      end if
     end if
c
     return
     end
```

SUBROUTINE SURFLO(A1,A2,PTOT,CSS,IT)

```
C
     dimension  ptot(500)
c
C    A1=channel  A2=imp. surface area
C
     CI=A1*PTOT(IT)/100.
     OF=PTOT(IT)*A2/100.
     CSS=CI+OF
C
     RETURN
     END
```

subroutine TERPO (yrel,time,ytab,ttab,nct,vary)

```
c
c    This is a service subroutine having the function of updating the one-dimensional time-
c    varying vegetation parameters by interpolating (linearly) between tabulated data
c    values according to the current time.  It is called from subroutine TVARY (therefore
c    once).
c
     dimension ytab(20), ttab(20)
     logical vary
     ncterp = nct
     oldyr = yrel
     icurr = time/86400 + 1
c
c.... Search the time-values table to find which 2 rows of the tabulated data will be used in
c    the interpolation (time-values which lie either side of the current time)
c
c    N.B. iterp has a value > 1 if the current time has exceeded a new value of ttab (table of
```

```
c     times) or 0 if it has not.
c
 10   iterp = (icurr - ttab(ncterp)) / (ttab(ncterp+1) - ttab(ncterp))
      if (iterp .ge. 1) then
       ncterp = ncterp + 1
       goto 10
      endif
c
c.... Calculate new relative value .....................
      diffa = ytab(ncterp+1) - ytab(ncterp)
      diffb = ttab(ncterp+1) - ttab(ncterp)
      diffc = icurr - ttab(ncterp)
      yrel = ytab(ncterp) + diffc * diffa / diffb
c
      diff = abs(yrel - oldyr)
      if (diff .gt. 0.001) vary = .true.
c
      nct = ncterp
c
      return
      end
```

```
c ::::::::::::::::::::::::::::::::::::::::::::::::::::::::::::::::::::::::::::::::::::::::::::::::::::::::::::::::::::::::::::::::::::::
```

subroutine THFALL (jt,i,fdrold,fdr,fstold,fsto,ev,evd,fstcap,
& bdr,cdr,it)

```
c ::::::::::::::::::::::::::::::::::::::::::::::::::::::::::::::::::::::::::::::::::::::::::::::::::::::::::::::::::::::::::::::::::::::
c
c     Once the water input to a "foliage" layer has been determined in INTER, the new
c     storage amount, drainage rate and loss by evaporation of the layer are calculated in
c     THFALL.  N.B. The modelling of those components are based on Rutter's model with
c     storage capacity changed for storage capacity per unit leaf area.
c
c
      include 'BLOCK/speci.main'
      dimension fdrold(10000,0:51), fstold(10000,51), fsto(10000,51),fdr(10000,0:51)
c
c     Calculate the net rate of supply of water to the layer after evaporation (mm/tstep)
      qf = fdrold(jt,i-1) - ev
c     Convert ev from a rate to an amount (mm)
      evd = ev
c
c     CALCULATE NEW STORAGE AND DRAINAGE BY THE APPROPRIATE METHOD
c
c.....First case: When FSTOLD >= FSTCAP and QF > 0.....................
      if ((fstold(jt,i) .ge. fstcap) .and. (qf .gt. 0)) then
c
c       Calculate new canopy storage (mm)
        ct1 = fstold(jt,i)
        temp = bdr * (ct1 + qf)
        fsto(jt,i) = 1/bdr * (log(qf) + temp - log(cdr*exp(temp) - cdr*exp(bdr*ct1) + qf))
c
c       Calculate layer drainage (mm)
        fdr(jt,i) = (fstold(jt,i) + qf) - fsto(jt,i)
      end if
c
c.....Second case: When FSTOLD >= FSTCAP and QF <= 0.....................
```

```
      if ((fstold(jt,i) .ge. fstcap) .and. (qf .le. 0)) then
c
c       Add the net supply of water to the layer (mm)
        ct1 = fstold(jt,i) + qf
c
c       Calculate new canopy storage (mm) and drainage (mm)
        if (ct1 .ge. fstcap) then
          temp = exp(-bdr * ct1)
          fsto(jt,i) = - (log(bdr*cdr + temp) / bdr)
          fdr(jt,i) = fstold(jt,i) + qf - fsto(jt,i)
        else
          fsto(jt,i) = fstold(jt,i)
          fdr(jt,i) = 0
        end if
      end if
c
c.....Third case: When FSTOLD < FSTCAP.....
      if (fstold(jt,i) .lt. fstcap) then
c
c       Add the net supply of rain (no evapo.) (mm)
        fsto(jt,i) = fstold(jt,i) + fdrold(jt,i-1)
c       When FSTO < FSTCAP, EPF is reduced by the factor F1
        f1 = fsto(jt,i) / fstcap
        if (f1 .gt. 1) f1=1.
c       Calculate evaporation loss (mm)
        evd = evd * f1
c       New storage (mm):
        fsto(jt,i) = fsto(jt,i) - evd
        fdr(jt,i) = 0
        if (fsto(jt,i) .lt. 0) then
c         Adjust evaporation loss (add `negative' storage) (mm)
          evd = evd + fsto(jt,i)
          fsto(jt,i) = 0
        end if
      end if
      return
      end
```

subroutine TVARY

```
c
      logical valid,take,lgsai,trees,skewlg,newcpy,cponly,dbhlog,square
c
      include 'BLOCK/speci.main'
      include 'BLOCK/speci.canopy'
      include 'BLOCK/speci.lcpy'
      include 'BLOCK/speci.init'
      include 'BLOCK/spec.index'
      include 'BLOCK/speci.tvary'
c
c
      dimension pd(51,2),adjlai(10000),thcov(10000),tempy(50)
      INTEGER*4 i
c     double precision G05DEF, xmean, stdev,grmean,grsd
c
```

```
c.....
c    Estimate LAI of each Delaunay triangle.  Loop on triangles
c.....
     cwgap = 0.0
     do 10 jt=1,ntr
c    if (.not. valid(jt)) goto 10
c
c    Calculate (1) proportion of the surface elements generating throughfall (remove
c    stemflow surface elements) and (2) LAI starea = 0.0
     tharea = 0.0
c    Loop on trees forming the triangle
     do 20 i=1,3
     jj = itetr(jt,i)
     temp = (pnt(jj,4)**2 * triano(jt,i+5) * 0.5) * pnt(jj,6)
     starea = starea + temp
c
     diam = pnt(jj,3)*100
     satree = ((diam**2)*0.3797) - (0.9045*diam)
     if (satree .le. 0.0) satree = 0.000000001
     temp1 = satree * (triano(jt,i+5)/(2*pi))
     temp2 = pnt(jj,6)
     temp = temp1 - temp1*temp2
     tharea = tharea + temp
  20 continue
c
     thcov(jt) = triano(jt,5) - starea
     if (thcov(jt) .lt. 0.0) then
      xlai(jt) = 0.0
      thcov(jt) = 0.0
     else
      xlai(jt) = tharea / thcov(jt)
     endif
     cthar = cthar + tharea
     cthcov = cthcov + thcov(jt)
c
c.....
c    Compute the probability distribution of the intercepting layers & their surface area
c.....
c
c    First case: throughfall elements (triangle scale)
c
c    Adjust LAI to consider canopy elements angle distribution  Note- in the current model
c    version, the surfaces are assumed to fit a spherical distribution (see Campbell &
c    Norman,1989)
     adjlai(jt) = xlai(jt)/2
     if (adjlai(jt) .eq. 0.0) then
      wgap(jt) = 0.0
      npd = 1
      goto 47
     endif
c
     call PDIST (pd,npd,adjlai(jt),pat(1),jt)
     wgap(jt) = pd(1,2) * thcov(jt)
  47  continue
     cwgap = cwgap + wgap(jt)
     cump = 0
c    remove gap layer from the total number of variates
     nfola(jt) = npd - 1
```

```
      do 25 i=npd,2,-1
       j = i-1
       cump = cump + pd(i,2)
       fa(jt,j) = cump * thcov(jt)
   25  continue
      if (nfola(jt) .eq. 50) then
       do 23 iik = 1,nfola(jt)
        tempy(iik) = (fa(jt,iik))/cump
   23  continue
       jkk = 51
       do 24 mmk = 1, nfola(jt)
        jkk = jkk - 1
        fa(jt,mmk) = tempy(jkk)
   24  continue
      endif
c
c     goto next triangle
    10  continue
c
c.....
c     Second case: Stemflow elements (tree scale)
c.....
c
      do 30 i=1,ntree
       if (.not. take(i)) goto 30
c
c      calculate stem area index
c      2 choices: equal to LAI or provided as input data
       if (lgsai) then
        sai(i) = saiput
       else
        diam = pnt(i,3)*100
        satree = ((diam**2)*0.3797) - (0.9045*diam)
        if (satree .le. 0.0) satree = 0.000000001
        sai(i) = (satree/20.) / (pi*pnt(i,4)**2)
       endif
c      sai(i) = sai(i) - 1
       if (sai(i) .le. 0) then
        write(6,*) 'sai is smaller than 0...'
        goto 999
       endif
       stcov(i) = pnt(i,6) * covin(i)
       cstcov = cstcov + stcov(i)
c
       call PDIST (pd,npd,sai(i),pat(2),i)
       stgap(i) = pd(1,2) * stcov(i)
       cump = 0
c      remove gap layer from the number of stem layers
       nstla(i) = npd - 1
       do 35 ii=npd,2,-1
        j = ii-1
        cump = cump + pd(ii,2)
        sa(i,j) = cump * stcov(i)
   35  continue
c
c      Include trunk layer in the total number of stem layers
       nstla(i) = nstla(i) + 1
c     goto next tree
```

```
 30  continue
c
      strtio = cstcov/tocca
      tolai = cthar / cthcov
      xmlai = tolai* (tocca/totsa)
c
c     print triangle center x/y coordinates and leaf area index
      do 300 jt=1,ntr
c       if (valid(jt)) then
        xt = (pnt(itetr(jt,1),1) + pnt(itetr(jt,2),1) + pnt(itetr(jt,3),1)) / 3
        yt = (pnt(itetr(jt,1),2) + pnt(itetr(jt,2),2) + pnt(itetr(jt,3),2)) / 3
        tlai = (triano(jt,5)/triano(jt,3)) * xlai(jt)
c       endif
 300  continue
 900  format(4(i4,2x),3(4x,f7.3))
c
 999  return
      end
```

::

function xmatr2(tpbv)

::

```
c
      include 'BLOCK/spec.phys'
      include 'BLOCK/spec.index'
      include 'BLOCK/spec.smc'
c
c     Check on initial moisture contents w.r.t. allowable extreme values
c
      if(tpbv.ge.sr1)then
       xmatr2=0.0
       else
        if(tpbv.lt.smx(1))xmatr2=smy(1)
       endif
c
c      Linear interpolation of suction values between smx(20) and sr1 moisture contents
c
       smg(20)=(0.0-smy(20))/(sr1-smx(20))
c
c      Calculate suction values if moisture content lies between smx(20) and sr1
c
       if(tpbv.gt.smx(20).and.tpbv.lt.sr1) xmatr2=smy(20)+smg(20)*(tpbv-smx(20))
c
c     Calculate suctions from given moisture contents for within the suction moisture curve
c     range
c
       do 1 j=1,19
       if(tpbv.gt.smx(j).and.tpbv.le.smx(j+1))xmatr2=smy(j) +smg(j)*(tpbv-smx(j))
 1      continue
c
c      Convert to cms suction
c
       xmatr2=xmatr2*100.
       return
       end
```

COMMON BLOCKS

spec.char
```
    common/charac/note,name
```
spec.clock
```
    common/CLOCK/IMIN,IHOUR,IDAY,IMONTH,IYEAR,IROUT,ecum(500,5)
```
spec.com2
```
    common/COM2/ADEPTH,BDEPTH(6),hlen(5),yi(5,16),xi(5,16), depmax(5,16),
   &        cocor(5,4,2), sgarea, totar, totar2
```
spec.error
```
    common/error/everv(5),chsmv(5),soils(5),overs(5),cchsto,cpre, css, qqt, chfev, chsev,
   &        fpre,ffev,fsev,fwfre,fbfre, fthro, fstem, chthro, ftrfr, chwfre, chtrfr, chbfre
```
spec.geom
```
    common/geom/stonec(5),sumar(5,16),avwid(5,16),avdep(5,16,5), avele(5,0:16,5),
   &        avslp(5,16,5), avslln(5,16,5), shift(5), dist(5,16,5,3), sarea(5,16,5,3),
   &        avvol(5,16,5), roffst(5),avlen(5,16),asslp(5,16,5),dummy(5,16,5),asslln(5,16,5),
   &        xa(5,0:16),elev(5,0:20,5),nlimk(10),area(5),a1,a2
```
spec.index
```
    common/index/mno,kno,ni,ihr,it,jno,lrep,krep,isgno,jss,jx,js,nx,ns
```
spec.phys
```
    common/phys/pbv(5,16,5),smcvol(5,16,5),poros(5,16,5),pos(10), cmax(5,16,5),
   &        smcmax(5,16,5), conduc(5,16,5), poten(5,16,5), cmaxs(10,5,6), poross(10,5,6),
   &        nost
```
spec.water
```
    common/water/precip(500),flow(5,6),eflow(5),tflow(500),ptot(500), sflow(5,15,8,2),
   &        smerv(0:500,5), oflow(500,5),peror(5), evap(500),pnet,pef,pnr,q
```
speci.canopy
```
    common /cpy/grmean,grsd,triano(10000,8),pnt(5000,9),pat(5), tpa(5000),
   &        covin(10000), itetr(10000,3),isdead(1000), ntrel(15), nyear(15), itt, croang,
   &        dbhmax, cslope,cicept,zoi, tocca,ntree,ntr,dbhval,space,totpa,pi,totsa, aleng,
   &        hslope,hicept,ittlo,npnt,kmmax,ntint
```
speci.init
```
    common/init1/fstcap,bstcap,trscap,bdr,cdr,saiput
```
speci.lcpy
```
    common /lcpy/valid(10000),take(5000),square,lgsai,trees,newcpy, skewlg, cponly,
   &        dbhlog
```
speci.main
```
    common/main/time,tint,tstep,pr
```
speci.tess
```
    common/tessi/itemp(3,2),xpnt(3,3)
```